



Modeling of Disease through Discrete Time Models

R. Sivaraman*

Associate Professor, Department of Mathematics, D. G. Vaishnav College, Chennai, India.

Received: 26 July 2020

Revised: 28 Aug 2020

Accepted: 03 Oct 2020

*Address for Correspondence

R. Sivaraman

Associate Professor,
Department of Mathematics,
D. G. Vaishnav College, Chennai,
Tamil Nadu, India.
Email: rsivaraman1729@yahoo.co.in



This is an Open Access Journal / article distributed under the terms of the **Creative Commons Attribution License** (CC BY-NC-ND 3.0) which permits unrestricted use, distribution, and reproduction in any medium, provided the original work is properly cited. All rights reserved.

ABSTRACT

In the time of whole globe suffering due to Pandemic, it is inevitable to come up with good scientific measures and models to prevent the spread and control the diseases through all possible ways. Discrete Time model is one such scientific method used for controlling diseases. In this paper, we shall discuss methods of modeling disease through using a discrete time model. We achieve this by minimizing a Hamiltonian function containing square terms of both state and control variables. The formulation of the model was first presented and then the model was solved in particular case to illustrate the methods involved.

Keywords: State Variables, Control Variables, Objective Function, Optimal Values, Hamiltonian, Necessary Conditions

INTRODUCTION

For many populations, births and growth occur in regular times each year (or each cycle). Discrete time models or difference equations are well suited to describe the life histories of organisms with discrete reproduction and/or growth. We note that in discrete time models, the order of events within a time step is crucial, so one should keep this concept in mind when building a discrete model. See [1] for an epidemic which is discrete in time and space and in which the order of events is important. In an optimal control problem, we can adjust controls in a dynamic system to achieve a particular goal. The underlying system can have a variety of types of equations such as ordinary differential equations, partial differential equations, difference equations, stochastic differential equations or integro-difference equations. In this paper, we are considering only systems of equations which are discrete in time.

In control of a single difference equation, with discrete time steps, we denote $u = (u_0, u_1, \dots, u_{T-1})$ as the control variables vector and $x = (x_0, x_1, \dots, x_T)$ as the state variables vector. Given x_0 , the state function satisfies a particular

28300





R. Sivaraman

difference equation modeling the scenario. The control variables affects the state difference equation, $x_{k+1} = g(x_k, u_k, k)$ for $k = 0, 1, 2, \dots, T - 1$ with x_0 as given value. Both the control and the state variables usually affect the goal, which is called the objective function. We seek to find an optimal control and corresponding state variables that achieve the maximum (or minimum) of our objective function.

Description of the Model

Let's start with a simple example of optimal control of a discrete time model to illustrate the ideas. We need to minimize the following objective function subject to the constraints as given below:

$$\min_u \sum_{k=0}^2 \frac{1}{2} [x_k^2 + Bu_k^2] \quad (2.1)$$

subject to $x_{k+1} = x_k + u_k$ for $k = 0, 1, 2$ and $x_0 = 5$.

The state vector has 4 components, x_0, x_1, x_2, x_3 while the control vector has one fewer component, u_0, u_1, u_2 . Our objective is to minimize the square of the state terms and the square of the control terms. The coefficient B is a weight factor that gives the relative importance of the two terms in meeting the objective.

General Formulation

We now formulate a control problem in more generality. Given a control $u = (u_0, u_1, \dots, u_{T-1})$ and initial state x_0 , the state equation is given by the difference equation $x_{k+1} = g(x_k, u_k, k)$ for $k = 0, 1, 2, \dots, T - 1$. Note that the state vector has one more component than the control vector $x = (x_0, x_1, \dots, x_T)$.

We have the following objective function

$$J(u) = \phi(x_T) + \sum_{k=0}^{T-1} f(x_k, u_k, k) \quad (3.1)$$

The term $\phi(x_T)$, represents a type of 'salvage' term; for example, one may want the population to be large at the final time T . The objective function can be maximized or minimized over controls u . In the minimization case, the goal is to find an optimal control u^* such that $J(u^*) = \min_u J(u)$ (3.2)

(where the minimization is taken over a class of vectors with bounded components with bounds specified to fit the situation)

The necessary conditions, that an optimal control and corresponding state vectors must satisfy, can be derived similarly to the case of ordinary differential equations, using a generalization of Pontryagin's Maximum Principle [2]. To see more detail about the derivation of the necessary conditions, see the book by Lenhart and Workman [3]. The key idea is introducing the adjoint function to attach the difference equation to the objective function, resulting in the formation of a function called the Hamiltonian. This principle converts the problem of finding the control to optimize the objective function subject to the state difference equation with initial condition to finding the control to optimize Hamiltonian pointwise (with respect to the control variables).

We now have the Hamiltonian at each time step k , where our adjoint function is $\lambda = (\lambda_0, \lambda_1, \lambda_2, \dots, \lambda_T) : H_k = f(x_k, u_k, k) + \lambda_{k+1}g(x_k, u_k, k)$, for $k = 0, 1, \dots, T - 1$.

Notice the indexing on the adjoint; it is one step ahead of the other terms. The necessary condition states that the Hamiltonian is maximized at each step with respect to the control u_k at the optimal control vector u_k^* . The adjoint equations and corresponding final time conditions (transversality conditions) are also given. If we do not have any constraints on our control variables, then the necessary conditions are





R. Sivaraman

$$\lambda_k = \frac{\partial H_k}{\partial x_k} \quad (3.3)$$

$$\lambda_T = \phi'(x_T^*) \quad (3.4)$$

$$\frac{\partial H_k}{\partial u_k} = 0 \text{ at } u^* \quad (3.5)$$

We observe that the adjoint function has final time conditions while the state function has initial time conditions. Suppose that the control variables are bounded, which is quite usual in biological examples. That is, suppose $a \leq u_k \leq b$ for each k , then these bounds need to be imposed after you solve the optimality equation (3.5) $\frac{\partial H_k}{\partial u_k} = 0$ at u^*

for each component of the control variable at each time step. Thus it is computationally quite difficult to solve biological problems since we more restrictions and variables to solve.

Solving Sample Modeling Problem

We now consider a simple example to illustrate the solution technique for the proposed disease model.

Let us consider the objective function $\min_u \sum_{k=0}^2 \frac{1}{2} [x_k^2 + u_k^2]$ (4.1)

subject to $x_{k+1} = x_k + u_k$ for $k = 0, 1, 2$ and $x_0 = 5$.

At each time step, the control variable u_k is the input, that will result in the growth or decline of the state variable. What optimal control is expected? We are seeking to minimize the state variables and the size of control variables. To attain perfect modeling condition, we expect the optimal control to be negative or zero.

We begin with the Hamiltonian, $H_k = \frac{1}{2} [x_k^2 + u_k^2] + \lambda_{k+1} (x_k + u_k)$ (4.2)

From equations (3.3) to (3.5) and (4.2), our necessary conditions are:

$$\lambda_k = \frac{\partial H_k}{\partial x_k} = x_k + \lambda_{k+1} \text{ for } k=0,1,2 \quad (4.3)$$

$$\lambda_3 = 0 \quad (4.4)$$

$$\frac{\partial H_k}{\partial u_k} = 0 \Rightarrow u_k + \lambda_{k+1} = 0 \text{ at } u_k^* \quad (4.5)$$

Thus the optimal control variables (from (4.5)) satisfies $u_k = -\lambda_{k+1}$

Thus the constraint in equation (4.1) can be written as $x_{k+1} = x_k - \lambda_{k+1}$ (4.6) for $k = 0, 1, 2$.

The transversality condition is $\lambda_3 = 0$, since we do not have a salvage term, meaning there is no dependence on the state at the final time in the objective function.

Taking $k = 2$ in $x_{k+1} = x_k - \lambda_{k+1}$ we get $x_3 = x_2 - \lambda_3 = x_2 - 0 = x_2$. Thus, $x_3 = x_2$.

We now solve for the four variables $x_1, x_2, \lambda_1, \lambda_2$. From (4.6) taking $k = 0,1$ we have

$$x_1 = x_0 - \lambda_1 = 5 - \lambda_1 \quad (4.7)$$

$$x_2 = x_1 - \lambda_2 \quad (4.8)$$

Now taking $k = 1, 2$ in (4.3) we have

$$\lambda_1 = x_1 + \lambda_2 \quad (4.9)$$

$$\lambda_2 = x_2 \quad (4.10)$$





R. Sivaraman

Using (4.10) in (4.8) we get $x_1 = 2x_2$ (4.11)

Using (4.9) and (4.10) in (4.7) we get $2x_1 + x_2 = 5$ (4.12)

Now using (4.11) in (4.12), we get $x_2 = 1$. From this, we have $x_1 = 2x_2 = 2$, $x_3 = x_2 = 1$.

Hence, the optimal state variables are

$$x_1^* = 2, x_2^* = 1, x_3^* = 1 \quad (4.13)$$

From (4.9) and (4.10), we have $\lambda_1 = x_1 + x_2 = 3$ and $\lambda_2 = x_2 = 1$.

Now from (4.5) we have $u_0^* = -\lambda_1 = -3, u_1^* = -\lambda_2 = -1, u_2^* = -\lambda_3 = 0$

Hence, the optimal control variables are

$$u_0^* = -3, u_1^* = -1, u_2^* = 0 \quad (4.14)$$

Thus, we see in our sample model, only the control variables are making changes in the states. Moreover, the state variables and control variables obtained in (4.13) and (4.14) respectively ensure that the objective function in (4.1) attains minimum.

CONCLUSION

By considering two types of variables namely state and control, we have formulated the disease model in section 2. In section 3, we provided a generalized version of the same model. Our model achieves the optimal values by considering the Hamiltonian function. Using the necessary conditions, we can determine the optimal state variables as well as optimal control variables. To obtain perfect optimal scenario our optimal control variables should either be negative or zero, which means that we need not have to improve those variables further. In section 4, we considered a sample model to illustrate the ideas presented in sections 2 and 3. Through detailed computations we arrived at the conclusion that the optimal control variables (through (4.14)) are negative or zero. Hence this assures that the objective function attains minimum for our computed state and control variables.

In the case of using this model for biological problems, we can similarly solve for associated state and control variables to obtain optimal values, but the only problem that we may face in such situations, there may be hundreds of state and control variables to solve, which becomes computationally difficult. But by using sophisticated algorithms we can easily solve for objective functions including many variables. We note that careful formulation of objective function and constraints provides meaningful results.

REFERENCES

1. W. Ding, L. J. Gross, K. Langston, S. Lenhart and L. S. Real, Rabies in Raccoons: Optimal Control for a Discrete Time Model on a Spatial Grid, *J. of Biological Dynamics* 1(4), 2007, pp. 379-393.
2. L.S. Pontryagin, V.G. Boltyanskii, R.V. Gamkrelize, and E.F. Mishchenko, *The Mathematical Theory of Optimal Processes*, New York, Wiley, 1962.
3. S. Lenhart and J. Workman, *Optimal Control Applied to Biological Models*, Boca Raton, Chapman Hall/CRC, 2007.
4. L. J. S. Allen and D. A. Flores and R. K. Ratnayake and J. R. Herbold, Discrete-time deterministic and stochastic models for the spread of rabies, *Applied Mathematics and Computation*, 132 (2002), 132, pp. 271–292.
5. C. Castillo-Chavez and A. Yakubu, Discrete time S-I-S models with complex dynamics, *Nonlinear Analysis TMA*, 47 (2001), pp. 4753-4762.
6. M. Kot, *Elements of Mathematical Ecology*, Cambridge, MA 2001.





Various Call Signal and Body Posture in Red-vented Bulbul (*Pycnonotus cafer*) at Udaipur District, Rajasthan, India

Nadim Chishty^{1*}, Rehana Parveen², Narayan Lal Choudhary¹, Pritesh Patel¹ and Pushkar Kumawat¹

¹Wildlife, Limnology and Toxicology Research Laboratory, Department of Zoology, Government Meera Girl's College, MLSU, Udaipur, Rajasthan, India.

²Government Meera Girl's College, MLSU, Udaipur, Rajasthan, India.

Received: 27 Aug 2020

Revised: 30 Sep 2020

Accepted: 03 Oct 2020

*Address for Correspondence

Nadim Chishty

Wildlife, Limnology and Toxicology Research Laboratory,
Department of Zoology,
Government Meera Girl's College,
MLSU, Udaipur, Rajasthan, India.
Email :nadimchishty@gmail.com



This is an Open Access Journal / article distributed under the terms of the **Creative Commons Attribution License** (CC BY-NC-ND 3.0) which permits unrestricted use, distribution, and reproduction in any medium, provided the original work is properly cited. All rights reserved.

ABSTRACT

Vocal and body posture signals are important way of communication in birds among same species and as well as different species. The red vented bulbul produces various types of communication calls and body posture during various types of activity in breeding and non breeding season. Various call patterns were observed during study like- morning, resting, matting and threatening or alarm call produced by red vented bulbul. Morning call was a very complex with high amplitude. Resting call is generally performed by both male and female with simple signal composed of single phrase with multiple elements. Matting call is mostly recorded in breeding season. Threatening calls are occasionally produced when predator movements near by a roosting and nesting sites.

Keywords: communication call, amplitude, breeding season, red vented bulbul, predator.

INTRODUCTION

Diversity of vocalizations with explicit biological functions is produced by birds. These signals are either long and complex or short and straightforward, occurring in particular perspectives and can be illustrated in terms of frequency, duration and amplitude (Catchpole and Slater, 1995; Weary, 1996). To study the physical structure of a sound and to compare the acoustic characters of signals with each other sound spectrograph serves as a best method (McGregor and Ranft, 1994). Birds convey information to each other mainly in visual and vocal modalities. In birds, generally uses two types of communication patterns are frequently sighted; optical display and body posture are used when lack of vocalized signals (Murphy, 2006; Randler, 2007). The optic signals are established by specific movements of various body parts like- head, neck, feathers, tail; they are also enhanced by extravagant of plumaged

28304



**Nadim Chishty et al.,**

and colorful (Birkhead, 1991; Fitzpatrick, 1999; Randler, 2006). Most avian species use threat displays in conflict with conspecific/ heterospecific for showing when duration of resource partition and matting times (Birkhead, 1991). The movements of head region are generally sign of fighting and territorial behaviors among passerine birds (Marler, 1961).

These signals are act as a bridge to maintain the bond of the pair, family and flock members (Caine and Stevens, 1990). Communications between parents and nestlings & fledgling has been symbolized by a number of call signals like -offspring request for food from parents (Muller and Smith, 1978; Miller and Conover, 1983), warmth (Evans, 1992), and guarding from predators, nestlings or fledglings requesting for foods (Whittemore and Fraser, 1974; Nuechterlein, 1988), predator presence in the surroundings (Nuechterlein, 1988; Weary and Fraser, 1995). Among some Passerine birds showing variety of signals when leaving fledglings from nests for a first flight and sometimes these signals using by nestlings stage to requesting for food from parents (Armstrong, 1973; Bengtsson and Ryden, 1981; Robertson *et al.*, 1992; Clemmons, 1995a, b). A vocalization signals composed from single and multiple elements. In a spectrogram an elements is simply and continuous sounds, produced after a silent gap. Signal elements contain a particular gap between calls. Complex and multiple signals are generally made up by numerous distinct parts called phrases. Each phrases structure elements having wide ranges series of similar and dissimilar phrase (Catchpole and Slater, 1995; Bhatt *et al.*, 2000). In the present study provides details account of various communication call patterns of Red vented bulbul on the basis of their physical characters.

MATERIAL AND METHODS

The data were collected from city and rural areas of Udaipur district. In non- breeding season, coverage area was inspected twice a week but during breeding season intensity of observations was increased. Data were collected from January 2019 to December 2019 and timing of observation from 6.00 A.M. to 8.30 A.M. and from 5.00 P.M. to 6.30 P.M. daily. In breeding period more time was given for data collection. The behavior of *Pycnonotus cafer* was observed by using Olympus 8 x 40 DPS – I Binoculars. Simultaneously, video was recorded by using Sony Handy cam. For photography and video recording, Nikon P900, SLR camera of Canon 550 D with 18 – 135 mm lenses and SLR camera 60 D Canon with 150 – 500 mm lenses were used. With the help of the high precision camera and lenses, we observed the behavior and display of breeding birds without disturbing them. Recordings of Red-vented Bulbuls were made in their natural habitats. Various red vented bulbul calls recorded by using Sony CFS 1030S sound recorders and JVC MZ-500 microphones. Various communication calls were analyzed with the help of Avisoft SAS Lab Pro (version 4.1) software with a 16 bit high resolution and frequency range between 22.5 to 48 KHz.

RESULT AND DISCUSSION

Aggressive birds display fluffing of feathers, while submissive birds display oppressed crests and sleeked plumage. The Pendulum display is a highly ritualized display showing the bird's under tail spread out and is followed by its side-to-side movement. This is followed by the Agonistic call, which is used during overt attacks. Appeasement was displayed by the vertical raising of its bill towards the dominant bird. They often nest in close proximity to each other. While mating, they are with only one partner at all times. Courtship display consists of the male fluttering its wings over its head by spreading and slightly depressing its tail, along with the female lowering its head, depressing its crest, and quivering its spread wings. The female frequently moves its beak from side to another, while also twittering.

Different communication patterns amongst Red-vented bulbuls

Various communication patterns in Red vented bulbul following characteristic features were analyzed on the basis of minimum and maximum frequency, amplitude of frequencies, time interval, number of elements per phrases and types of phrases used to define physical characteristic of body.





Nadim Chishty et al.,

The following types of vocal signals were observed during the course of the study

Morning Calls

These types of calls were made by the birds in the early morning. These are complex vocalizations composed of high amplitude, with slight modulations in frequency. The calls were continuous after almost fixed duration. Some phrases were repeated again and again and were composed of 3 elements. The average minimum frequencies were recorded (1.6 ± 0.3) and maximum (3 kHz). The common durations of elements 0.2 to 0.3 seconds and average call interval was 0.63 ± 0.3 seconds (Fig. 1 and 2).

Resting Calls

This is a song-like vocalization produced by the bulbul especially during the resting period. Both male and female were observed using this type of vocalization. This is a simple signal composed of single phrase with multiple elements. A minimum of 4-5 types of elements were observed in their recordings. Duration of phrases was 7s. The vocalizations produced were of medium amplitude neither too low nor too high. The average minimum frequencies was (1.5 kHz) and maximum frequencies (2.6 kHz) was recorded. The average duration of elements 0.001 to 0.002 and average call interval was (9 ± 2 seconds) (Fig. 3 and 4)

Mating Calls

These types of calls are generally given during breeding season. Birds usually give them to attract their mates. The elaborations of calls or type of various songs birds can produce with the help of display of its maturity, intelligence and characteristic features of mate. The calls were soft, continuous, and low in amplitude, complex and were opposite sex oriented. In some birds, irregular phrase groups were observed while in others repetition of phrases was also seen. Some phrases were of narrow band with complex set of elements. The elements P1 to P5 were irregular. Sounds of frequency ranging between 1.3 - 3.5 KHz have been observed in bulbuls. The duration of the phrases was 0.9 ± 0.2 s and the interval between any two phrases was 0.7 ± 0.2 s. It was observed that first a low pitch sound is produced and after it continuous high pitch sound was produced by the bulbuls to attract their partners for mating. Complex phrases were recorded in them with 7-8 elements per phrase. (Fig. - 5 and 6)

Threatening Calls (Alarm Calls)

Two types of alarm calls were observed in Red Vented bulbuls.

Type I – Type I calls produces when the nearby presence of predator like- eagle, hawk, owl, mongoose and cats, then red vented bulbul produce Type I calls(composition of calls contains as twe...twe...twe...). Type I calls was composed high number of elements (Almost 7-8) with large number of frequencies (1 to 3.7 kHz). The average duration of type I calls was 0.1 ± 0.005 s with intervals of 0.3 ± 0.01 s and they produced treble voice. Two types of pattern were recorded during the study, generally individuals produced elements with almost equal temporal gaps, while in some cases red vented bulbul calls produces these elements in groups of 2 to 6 with larger inter-gaps (Fig. 7, 8 and 9)

Type II – Type II calls had a small frequency range (1 kHz) as compared to Type-I calls. The duration of calls were comparatively more, while rate of production was very lower than Type- I calls. These calls had a low pitch. The red vented bulbul produce type-II calls when their nestlings or fledglings were under the higher threats of predators or may be nearby location of predators (Fig. 7, 8, 9).

REFERENCES

1. Catchpole, C. K. and Slater, P. J. B. (1995). Bird song: Biological themes and variations (London: Cambridge University Press).





Nadim Chishty et al.,

2. Weary, D. M. (1996) How birds use frequency to recognize their songs; in Neuroethological studies of cognitive and perceptual processors (ed.s) C. F. Moss and S. Shettleworth (Boulder: Westview Press) pp 138–157.
3. McGregor, P. K., and Ranft, R. R. (1994). Review of software packages for sound analysis; *Bioacoustics*, Vol.6;pp 83–86.
4. Murphy, T.G. (2006). Predator-Elicited Visual Signal: Why The Turquoise-Browed Motmot Wag-Displays Its Racketed Tail. *Behavioural Ecology*, Vol.17;pp 547-553.
5. Randler, C. (2006). Is tail wagging in White Wagtails (*Motacilla alba*) an honest signal of vigilance? *Animal Behaviour*, Vol.71;pp1089-1093.
6. Randler, C. (2007). Observational and experimental evidence for the function of tail flicking in European Moorhen (*Gallinula chloropus*). *Ethology*, Vol. 113: 629-639
7. Birkhead, T. (1991). Behaviour. In: Brooke, M. and T. Birkhead (eds.). *The Cambridge Encyclopedia of Ornithology*, Cambridge University Press, USA, 362pp.
8. Fitzpatrick, S. (1999). Tail length in birds in relation to tail shape, general flight ecology and sexual selection. *Journal of Evolutionary Biology*, Vol. 12: pp49-60.
9. Marler, P. (1961). The evolution of visual communication, pp. 96-121. In: Blair, W.F (ed.). *Vertebrate Speciation*. University of Texas Press, Austin, xvi+642pp.
10. Caine, N. G. and Stevens, C. (1990). Evidence for a "monitoring call" in Red-bellied tamarins; *Am. J. Primatol.* Vol.22: pp 251–262.
11. Muller, R. E., and Smith, D. G., (1978). Parent-offspring interactions in zebra finches; *Auk*, Vol. 95: pp 485–495.
12. Miller, D. E., and Conover, M. R., (1983). Chick vocal patterns and non-vocal stimulation as factors instigating parental feeding behaviour in the Ring-billed gull; *Animal Behaviour*, Vol.31; PP145–151.
13. Evans, R. M., (1992). Embryonic and neonatal vocal elicitation of parental brooding and feeding responses in American white pelicans; *Anim. Behav.* Vol. 44;pp 667–675.
14. Whittemore, C. T., and Fraser, D., (1974). The Nursing and Suckling Behaviour Of Pigs II. Vocalization of The Sow In Relation To Suckling Behaviour And Milk Ejection. *Br. Vet. J.*, Vol. 130;pp346– 356.
15. Nuechterlein, G. L., (1988). Parent-young vocal communication in Western grebes. *Condor*, Vol. 90;pp 632–636.
16. Weary, D. M., and Fraser, D., (1995). Calling by domestic piglets: Reliable signals of need? *Animal Behavior*. Vol.50: pp 1047– 1055.
17. Armstrong, E. A., (1973). A study of bird song (New York: Dover).
18. Bengtsson, H., and Ryden, O., (1981). Development of parent-young interaction in a synchronously hatched broods of altricial birds. *Zoology Tier psychology*. Vol. 56: pp 255–272.
19. Robertson, R. J., Stutchbury, B. J., and Cohen, R. R. (1992) Tree Swallow (*Tachycineta bicolor*) in The birds of North America (eds). A Poole, P Stettenheim and F Gill Washington DC: *Academy of Natural Sciences*, Philadelphia and American Ornithologists Union) Vol. 11, pp 87–94.
20. Clemmons, J. R., (1995a). Development of a selective response to an adult vocalization in nesting Black-capped chickadees. *Behaviour*, Vol. 132: pp 1–20.
21. Clemmons, J. R., (1995b). Vocalizations and other stimuli that elicit gaping in nestling Black-capped Chickadees (*Parus atricapillus*). *Auk*, Vol. 112: pp 603–612.
22. Bhatt, D., Kumar, A., Singh, Y., and Payne, R. B., (2000). Territorial songs and calls in oriental magpie robin (*Copsychus saularis*). *Current Science Journal*, Vol. 78;pp722–728.

Table 1: Physical characteristics of different types call signals in the Red-vented bulbul.

Type of Call	Nature of Call	Minimum Frequency (KHz)	Maximum Frequency (KHz)	Range of Frequency (KHz)	Duration (s)	Interval (s)
Morning call	Complex	1.6	3.0	1.4	0.2-0.3	0.63 ± 0.3
Resting Call	Simple, resting type	1.5	2.6	1.1	0.7 ±0.02	9 ±2





Nadim Chishty et al.,

Alarm call- Type I	Fast, stereotyped	1.0	3.7	2.7	0.1 ±0.05	0.3±0.01
Alarm Call - Type II	Low pitched	1.0	2.0	1	2	1 ±.02
Mating Call	Continuous, complex	1.3	3.5	2.2	0.8 ±0.02	0.7±0.2

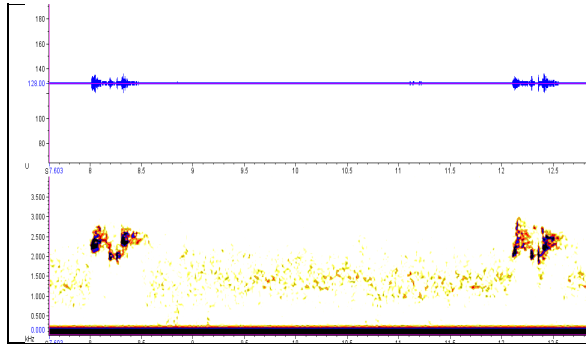


Figure 1. Physical characteristics and structure of vocalization produced in morning

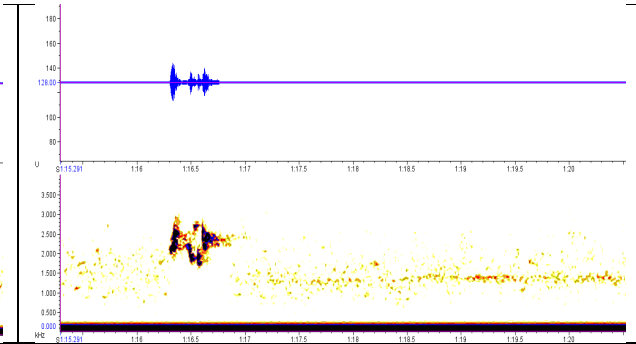


Figure 2. 1-Physical characteristics and structure of vocalization produced in morning by other adults

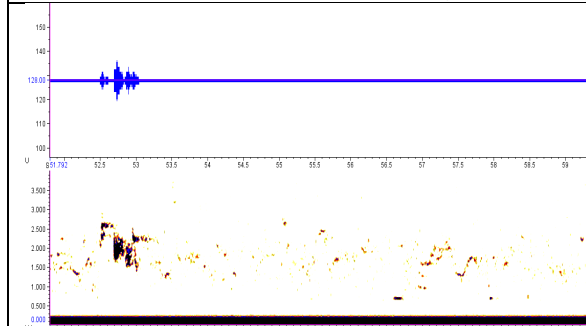


Figure 3. Physical characteristic and structure of vocalizations produced during resting time

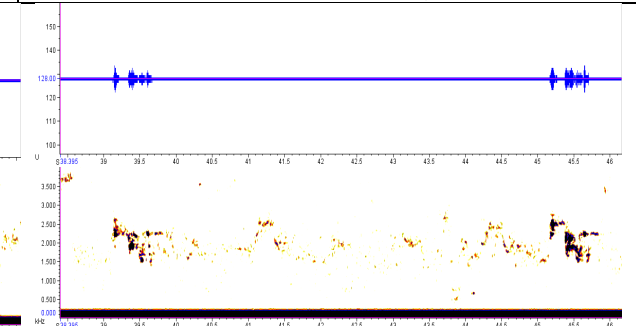


Figure 4. Physical characteristic and structure of vocalizations produced during resting time by another adults

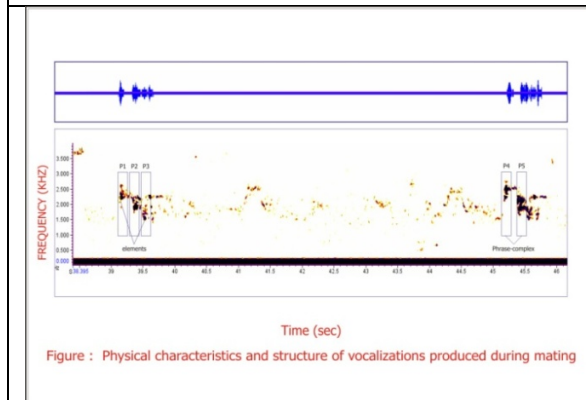


Figure : Physical characteristics and structure of vocalizations produced during mating

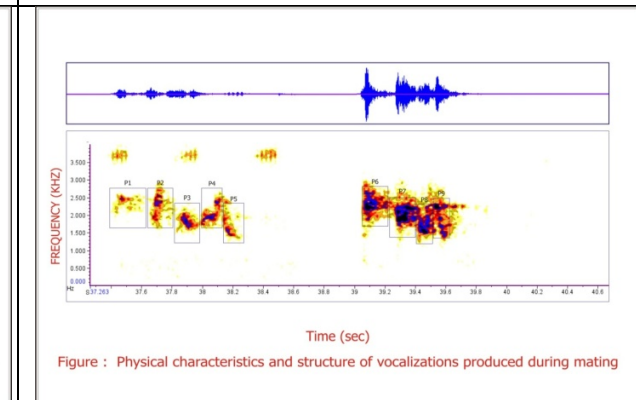


Figure : Physical characteristics and structure of vocalizations produced during mating

Figure 5- Physical characteristics and structure of vocalization produced during mating

Figure 6- - Physical characteristics and structure of vocalization produced during mating





Nadim Chishty et al.,

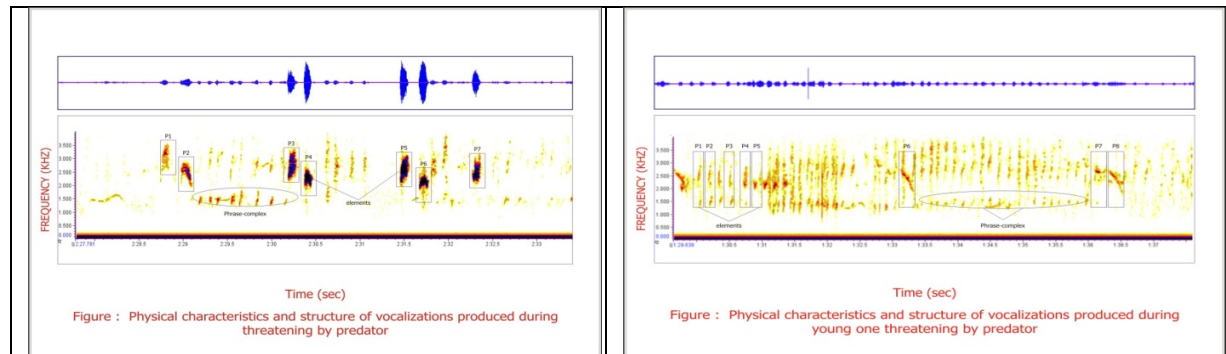


Figure 7. Physical characteristic and structure of vocalizations produced during threatening by predator.

Figure 8. Physical characteristics and structure of vocalizations produced during young one threatening by predator.

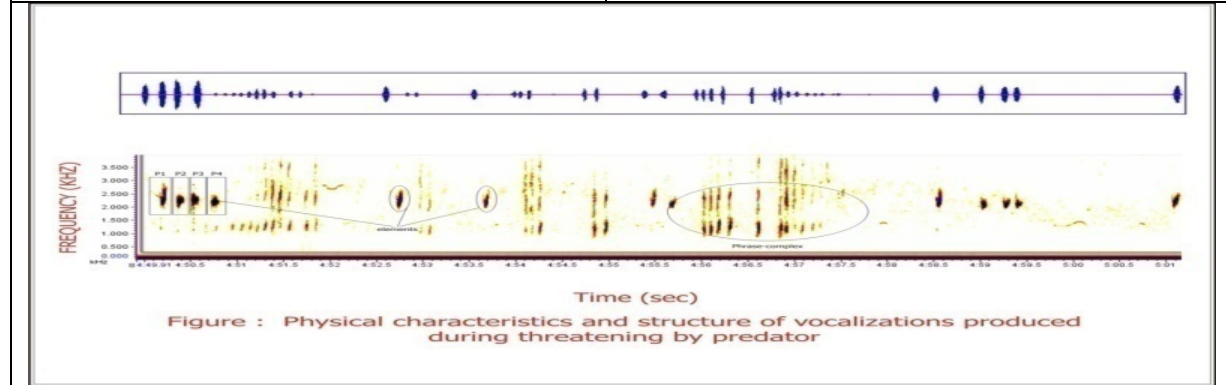


Figure 9. Physical characteristics and structure of vocalizations produced during threatening by predator.





Sensible Energy Meter

N.Vellachi^{1*}, VE.Jayanthi² and E.Chandrasekhar³

¹Assistant Professor, PSNA College of Engineering and Technology, Dindigul, Tamil Nadu, India.

²Professor, PSNA College of Engineering and Technology, Dindigul, Tamil Nadu, India.

³Zylog Systems, Chennai, Tamil Nadu, India.

Received: 18 Aug 2020

Revised: 20 Sep 2020

Accepted: 22 Oct 2020

*Address for Correspondence

N.Vellachi

Assistant Professor,

PSNA College of Engineering and Technology,

Dindigul, Tamil Nadu, India.

Email: vellachism@psnacet.edu.in



This is an Open Access Journal / article distributed under the terms of the **Creative Commons Attribution License** (CC BY-NC-ND 3.0) which permits unrestricted use, distribution, and reproduction in any medium, provided the original work is properly cited. All rights reserved.

ABSTRACT

Since today's energy meters have several drawbacks like 2 method communication, real time watching, energy tampered, etc. to cope up with these disadvantages, this planned work is employed to watch energy consumption at domestic level. Energy consumptions can be reduced and the units consumed can be monitored as well.. The target is to create the electrical appliances intelligent and supply comfort to shopper and to scale back power consumption in internet applications. Style and implementation of the project is especially supported Arduino UNO controller and IoT technology. If any meddling happens the controller can send the information to the server this project describes the conversion of load energy usage readings over the web. The Webpage utilizes the THINGSPEAK analytics to investigate the energy usage to relinquish additional elaborate description and mental image of the energy usage statistics. Wi-Fi unit performs IOT operation by causing energy knowledge of the load to the webpage which may be accessed through the channel ID of the device. The higher method is done to each single appliance to watch power consumed by that specific appliance. By doing this over consumption that's consumption on the far side specific limit will be simply known and tends to decide on an appropriate replacement for that specific appliance by another that consumes less power or to spot any fault in it.

Keywords: Wi-Fi, technology, energy, power, IOT

SENSIBLE ENERGY METER

The web of things conception permits us to attach the traditional day to day devices with every alternative over the web. The devices connected through IOT conception will be analyzed remotely. The IOT conception provides the fundamental infrastructure and opportunities to create a affiliation between the physical world and laptop primarily





Vellachi et al.,

based systems. The conception has been gaining importance with additional and additional wireless devices that are increasing quickly within the market. Hardware devices are connected with one another over the web. The extrasensory perception 8266 Wi-Fi module employed in the system provides the property with the web within the system. Now-a-days the demand for electricity is increasing at a relentless rate within the population and is being used for varied functions viz, agriculture, industries, unit functions, hospitals etc.,. So, it's changing into additional and additional difficult to handle the electricity maintenance and needs. Thus there is an on the spot demand to save lots of the maximum amount electricity as attainable because the demand from the newer generations of population for electricity is increasing Therefore on the basis of it the technology improvement is required. The planned system provides a technical twist to the traditional energy meters exploiting the IOT technology. Additionally there are alternative problems that we've to handle like power thievery that successively generate economic loss to the state. Monitoring, Optimized power usage and reduction of power wastage are the main objectives that lie ahead for a far better system.

Smart energy meter exploitation Wi-Fi system is meant supported for 3 major objectives. They are

1. To supply machine-driven load energy reading over an on the spot basis.
2. To use the electricity in associate degree optimized manner.
3. Scale back the ability wastage.

The system primarily can be classified depending on service ends in 2 ways like

1. Consumer side and 2. Service side

The data from the system is displayed on a webpage which may be accessed by the buyer. The system is meant on associate degree Arduino small controller. It will be structurally differentiated into 2 components viz., controller, circuit and a WLAN unit. The controller performs the fundamental calculations and processes the data. thievery detection circuit provides info regarding any further or thievery load energy reading and therefore the most vital role is compete by the Wi-Fi unit to send the data from the controller over the web. The Arduino controller is programmed on the Arduino computer code IDE (Integrated Development Environment) that could be a pre-requisite to work on the Arduino board. Its code is by-product of the C language.

Planned System

Within the planned technique, the buyer will manage their energy consumption by knowing their energy usage time to time. This technique not solely provides 2 method communications between utility and shopper however additionally provides alternative functions that are if the buyer fails to pay the electricity bill the energy offer would be impede from the utility facet and once the bill is paid the energy offer is reconnected. Another immense advantage of this method is that it notifies the buyer & utility at the event of the meter meddling. By this info the buyer & utility will management the meddling are scale back energy crises. The planned system offers a far better modeling for the event of associate degree intelligent sensible grid system with the assistance of user acknowledged distributed remote sensible meters interfaced during a distributed management structure motor-assisted superordinate management and knowledge Acquisition (SCADA) with PLC. so to avoid several methods associated with power systems, up the potency and eliminating the three-quarter losses and power thievery completely. The systems have several applications for optimising overall energy management inside the house hold shopper and industries, manage the load within the grid and forestall power demand peaks with associate degree interface between the sensible grid and customers.

- i.To the load through this sensing element (ACS712)
- ii.230V AC/12V DC Power offer module

The 12V power offer module provides power to the microcontroller (Arduino/Wemos), this sensing element (ACS712) and OLED show voltage is being perceived by voltage sensing element circuit and given to Arduino. The AC current passing through the load is perceived by this sensing element module (ACS712) and fed to the analog

28311





Vellachi et al.,

pins (A0,A1.....A5) of the Arduino board. Once the analog input is given to Arduino, the measuring of power/energy is finished by Arduino sketch. The calculated power and energy by arduino is showed on the user put in display module and sent to WLAN module.

OUTPUT AND RESULT

When devices are switched ON, the ability consumed by that specific load correspondingly shown on the {lcd|liquid crystal show|LCD|digital display, alphanumeric display} display and therefore the details are uploaded to THINGSPEAK via WI-FI module. Hardware outputs when different loads are switched on fig 3, fig 4 and fig 5. Three incandescent lamps(60W,60W.40W) were used as three loads whose Power Factor is equal to 1 and the LCD shows the power consumed by that particular lamp and the details are uploaded to THINGSPEAK .We used three Current sensor for three loads and one extra sensor for calculation of total power. THINGSPEAK is an IoT analytics platform service that allows you aggregate, visualize and analyze live data streams in the cloud .you can send datan to THINGSPEAK from you devices and create instant visualizations of live data and send alerts using webservices like twitter and twilo. THINGSPEAK details of our experiment is shown below.

CONCLUSION AND FUTURE WORK

Energy watching with use of IOT is an innovative application of web of things developed to observe each home appliances remotely over the cloud from anyplace within the world. Within the projected project current sensing element is employed to sense the present and show it on web exploitation IoT. The system updates the data in each ten to twenty seconds on the web exploitation public cloud THINGSPEAK. Within the gift system, energy load consumption is accessed utilizing Wi-Fi and it'll facilitate customers to avoid unwanted use of electricity. IoT system wherever a user will monitor energy consumption and pay the bill on-line is created. Currently we have a tendency to developed an energy meter that monitors power solely. In future we are going to expose projected system to develop an energy management system that takes the humidness, temperature, light illumintion into thought and consequently interface ARDUINO microcontroller for controlling power appliances like speed of fan strength instead of switched on and off.

REFERENCES

1. Darshan Iyer N, Dr. KA Radhakrishnan Rao, "IoT Based EnergyMeter Reading, Theft Detection & disconnection using PLC modem and Power optimization ",IRJET, (2015)
2. Garrab, A.; Bouallegue, A.; Ben Abdallah, "A new AMR approach for energy saving in Smart Grids using Smart Meter and partial Power Line Communication", IEEE First International Conference on RenewableEnergies and Vehicular Technology (REVET), pp. 263 – 269, march 2012
3. Internet of things (<http://en.wikipedia.org/wiki/Internet-of-Things>)
4. Landi, C.; Dipt. di Ing. dell'Inf., Seconda Univ. di Napoli, Aversa, Italy ; Merola, P. ; Ianniello, G, " ARM-based energy management system using smart meter and Web server", IEEE Instrumentation and Measurement Technology Conference Blinjiang, pp. 1 – 5, May 2011
5. Luís M. L. Oliveira, João Reis, Joel J. P. C. Rodrigues, Amaro F. de Sousa"IOT based Solution for Home Power Energy Monitoring andActuating" 978-1-4799-6649-3/15/\$31.00©2015IEEE.
6. Pooja D Talwar, Prof. S B Kulkarni " IoT Based energy meter reading" Volume 02, Issue 06; June - 2016 [ISSN: 2455-1457]
7. Thingspeak (www.Thingspeak.co.in)
8. (2008 Oct. 29) Specifications of LCD [Online] Available: <https://www.sparkfun.com/datasheets/LCD/ADM1602K-NSW-FBS-3.3v.pdf>





Vellachi et al.,

9. (2013 April 15) ArduinoUno (V2.3) [Online] Available: <https://www.arduino.cc/en/uploads/Main/ArduinoUnoManual23.pdf>
10. [10] (2014 March 19) ESP8266 Wi-Fi Module [Online]Available:
11. https://cdn-shop.adafruit.com/product-files/2471/0A-ESP8266_Datasheet_EN_v4.3.pdf

Table 1. Readings shown by the LCD display

Power consumed by load 1	45 W
Power consumed by load 2	57 W
Power consumed by load 3	61 W
Total power	169W

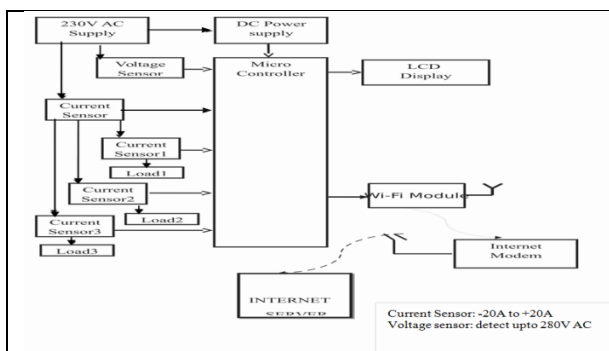


Fig. 1. Block Diagram of Planned Energy Measurement System

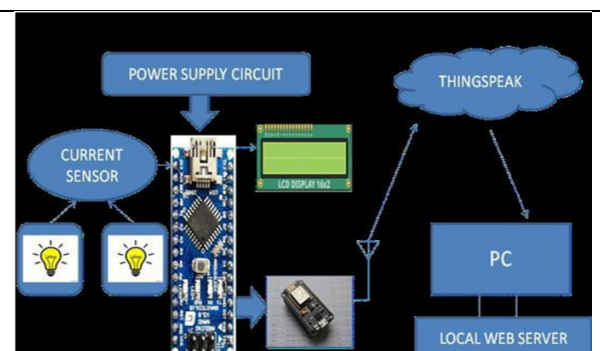


Fig. 2. DC Power offer module

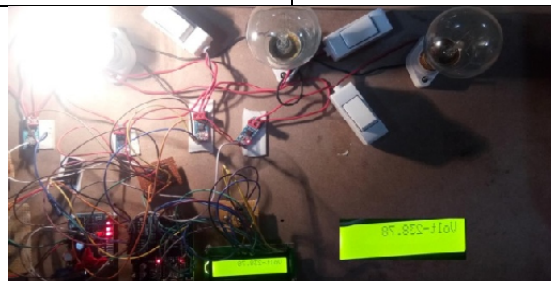


Fig. 3.



Fig. 4.



Fig. 5.

Hardware outputs when different loads are switched on fig 3, fig 4 and fig 5





Vellachi et al.,

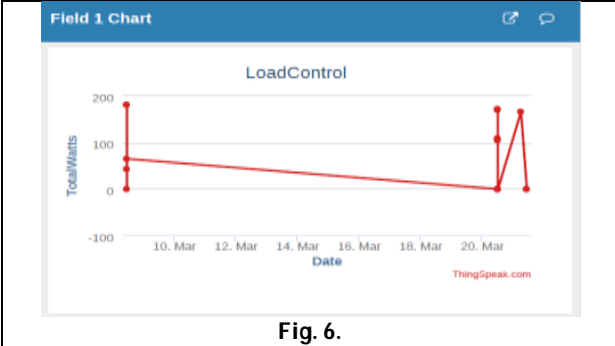


Fig. 6.

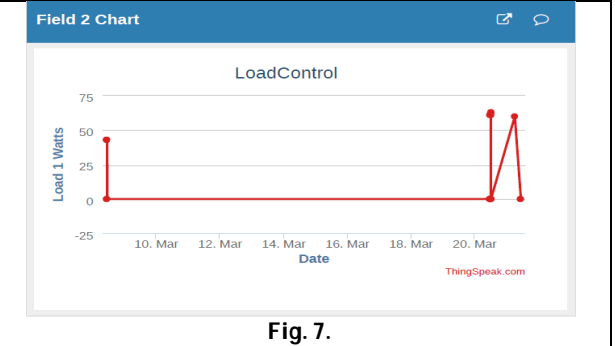


Fig. 7.

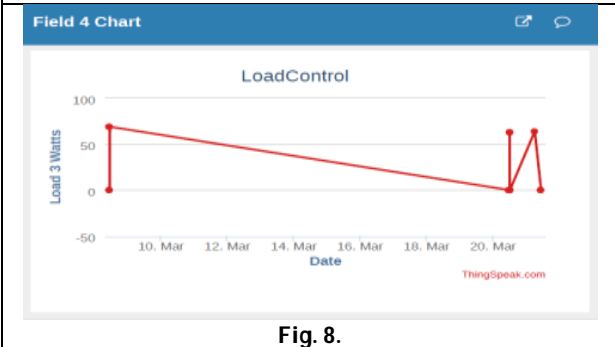


Fig. 8.

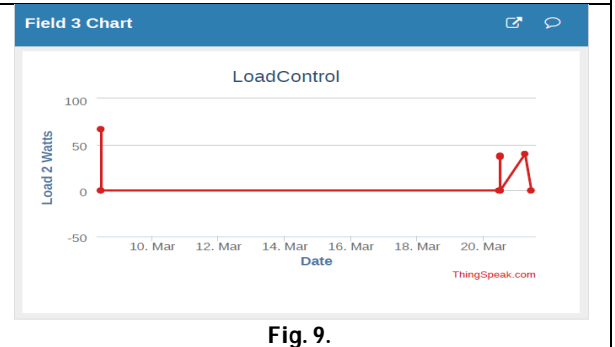


Fig. 9.

THINGSPEAK Data and Website Data for I) Many Loads Fig 6,7,8 and II) Total Power Fig 9





Are Mothers Shaping or Shaking the Lives of Daughters? A Study of Select Novels of Manju Kapur.

A.Visva Sangeetha¹ and A.Muthu Meena Losini^{2*}

¹Ph.D. Research Scholar, Madurai Kamaraj University, Madurai, Tamil Nadu, India.

Assistant Professor of English, PSNA College of Engineering and Technology, Dindigul, Tamil Nadu, India.

²Assistant Professor of English, Mother Teresa Women's University, Kodaikanal, Tamil Nadu, India.

Received: 10 Aug 2020

Revised: 12 Sep 2020

Accepted: 14 Oct 2020

*Address for Correspondence

A.Muthu Meena Losini

Assistant Professor of English,
Mother Teresa Women's University,
Kodaikanal, Tamil Nadu, India.
Email.id: minuarms@gmail.com



This is an Open Access Journal / article distributed under the terms of the **Creative Commons Attribution License** (CC BY-NC-ND 3.0) which permits unrestricted use, distribution, and reproduction in any medium, provided the original work is properly cited. All rights reserved.

ABSTRACT

Women undergo silent suffering as they do not find any solace at home when their mothers do not provide the necessary space for them to share their problems. The absence of a mother's empathy and sympathetic shoulders at home forces these women to look for sympathy outside which leads to deception. Women become susceptible and vulnerable to outside influences. The essence of a good relationship is a sense of belonging. When this quality of belongingness is found missing in the life of women, their future is devastated. Several promising lives go down the drain due to maternal apathy. Authoritative and autocratic attitude of mothers may spoil the individuality and personality of their daughters. They want their daughters to make the right choices –'right' in the sense; they must lead a socially acceptable life. With due respect to their tradition, religion, and caste, women should marry a person and can lead a happy life. This is what typical mothers expect from their daughters.

Keywords: Daughters, Family, Freedom, Identity, Loneliness, Marriage, Mother, Suffering.

In the novel *Difficult Daughter-Virmati*, the eldest of eleven children are always busy with work. But she is so keen to study. She looks after her weak mother who is harassed by childbirth. When Virmati's mother considers her daughter eligible for marriage she chooses Indrajit to get her daughter married. But this marriage is postponed due to the sudden demise of his father. Meanwhile, Professor Harish meets Virmati and she falls in love with him despite knowing that he is married. The professor has an illiterate wife and a daughter. Now, he finds an intellectual companion in the form of Virmati. They get married but she is not accepted by Harish's mother and his first wife Ganga. She tries to be friendly with his children but she is insulted. She loses all sense of identity. Due to the defiance of Virmati to her parents, she is not allowed to go near her father's dead body when he is killed in the riots.

28315



**Visva Sangeetha and Muthu Meena Losini**

Since her childhood, Virmati craves for her mother's love and support but when it seems it is impossible, her yearning for her mother's concern and sturdy support dies down. Thus, maternal isolation or estrangement leads to poor changes and sufferings in the life of Virmati. Virmati could never belong to her mother. Her pains, her pathetic life as a mistress, and then a second wife, all remained her distress. She could not share these pains with her mother. Moreover Kasturi, Virmati's mother never attempts to understand her daughter's difficulties. Mothers who do not try to understand their daughters are misleading the daughters to go astray which may bring bad consequences.

Manju Kapur in her novel *Home* presents Nisha who is torn between her innermost desires and family-oriented responsibilities and restrictions. It is a joint family saga, where a girl is never allowed to discuss her marital descendants. Love marriage is considered as a social sin and a symbol of shame whereas arranged marriage is viewed with the eyes of respect. Men in their family carry out the outside work and their wives are meant to play their role within the four walls. There are many implications and regulations in this family which are framed only for the women and they are expected to accept it without questioning. Mostly, it is a female who is carving such rules and is compelling another female to abide by it. The birth of Nisha brings luck to the family, but being the luckiest for others, she cannot bring it for herself. During her childhood, Nisha is physically exploited by her cousin, Vicky. Her intolerable sufferings, cries, and voice against these filthy fluctuations are not heard or understood by her mother Sona, and by others of her family. Even though the family realizes who the culprit of Nisha's sexual abuse is, they do not oust him or punish him but simply ensure that there is the distance between them and they make sure that their family dignity is saved.

Nisha undergoes this pain in the form of horrible nightmares and sleepless nights. Nisha, being an intellectual thinker and studious girl, loses her academic interest in her college life when she stays with her aunt Rupa. Due to the sexual harassment by her cousin Vicky, and the separation of Nisha from her mother make her feel insecure. The homely love and care are stolen from her as she is distanced by her aunt Rupa. After so many years, when she returns to her own home and meets her mother Sona, she is not received by her mother with great love and gratitude. Her mother, Sona, subordinates her into doing household chores. But Nisha nurtures her desire to lead a life of her own. She is not a silent rebel but she strongly put forward her inner urges loudly. After overcoming her core hardships in her life, facing so many disappointments at last she emerges as an independent financial woman without the help of anyone. This emancipation of Nisha from the border to the mainland amidst of the restrictions by her family cannot be underestimated. *A Married Woman* by Manju Kapur, carries the study of the life of Astha, she is brought up in a traditional family environment. As she is the only child of her parents, they concentrate on her education, her character, her health, and marriage. They monitor and guard Astha, during her childhood days as their precious treasure. But Astha dislikes to be monitored and this action of her parents make her be disturbed.

Particularly, Astha's mother tries to insist on the importance of her tradition, religious piety, and formal rituals of Hinduism. Always her mother concerns with Astha's good habits, tastes, and manners. Every mother has an unsuspecting fear of their daughter which Astha's mother has. This fear becomes a threat to the daughter instead of getting love from her mother. Astha expects a soft corner from her mother. But her mother is very much concerned about the marriage of her daughter without understanding Astha's expectations and desires. Astha's mother Sita gives the first and foremost priority to Astha's marriage and she believes that things must be done at the proper time, especially in marriage (AMW 20). Moreover, her mother insists Astha read shastras which can teach her the art of living. She advises Astha to pray to God for a good husband. And forced to go for a morning walk and pranayam. Perhaps this sort of motivation has affected the psychology of Astha very deeply. Contrary to her mother's wish, Astha begins to think that getting love is the only aim of this life. She falls in love at first sight with Bunty. She is overwhelmed by the feeling of love. She writes him letters but this correspondence does not last long. Her suspicious mother smells the truth. After knowing that, her daughter is in a relationship with a boy, she visits Bunty's family and complains Bunty's father that Bunty is distracting Astha. Bunty is asked to do nothing with Astha. Thus all Astha's fantasies end in tears.



**Visva Sangeetha and Muthu Meena Losini**

Despite Astha's mother's effort to confine Astha to be in the boundary of tradition, and culture Astha proves that she cannot be imprisoned. During the final year of her college, Astha meets Rohan, moreover, she has a physical relationship with him. To continue this relationship, Astha lies about her visits and doings to her mother. But all her desire to marry Rohan goes in vain when Rohan moves to Oxford for his further studies. After her marriage to Hemant, Astha's life was running very smoothly. The death of Astha's father makes her mother lean on the spiritual life. Though Astha compels her mother to be with her, Sita denies and tells Astha about the importance of spiritual life. Whenever Astha needs a mother's love and kind words, her mother fails to show it. This leads Astha to take wrong decisions and fills her life with frustration. Sita acts exactly like a traditional woman as she hands over the proceeds of their land are entrusted to Hemant. Sita thinks that the only man can deal with all the financial matters and she advises her daughter to pay more attention to Hemant's health and be a dedicated wife. Astha pleads for her rights but her feelings are undervalued. When her mother goes to Rishikesh she sells most of the stuff at home. Astha's desire to keep the books with her is denied and it is donated to a library. She is not considered by her mother even when their plot of land is sold.

Thus, When Astha could not find any solace and support from her mother and her husband, she moves for a lesbian relationship with Pipeelika. The woman becomes strong to do unexpected things in her life who silently suffers. In Manju Kapur's *The Immigrant* Nina's mother is also a typical Indian mother who gives importance to husband and family. And she wishes, her daughter to get married soon and should have a good family life. In the beginning, in Nina's childhood days, the mother-daughter are more like friends, sharing, caring, and supporting each other. After Nina's father's death, they were given no choice but to move to grandparents' house in Lucknow. Nina and her mother struggled, suppressed, and suffered for years. Meanwhile, Nina longs for true love and she has a relationship with Rahul. She is treated as a toy, abused, misused, and finally, she is thrown from the human phase. She is prey to Rahul who exploits her and squeezes her body as lemon and enjoys every moment with her. Her self-respect, at last, forced her to choose loneliness over compromise. She grieves within herself without disclosing her feelings to anyone. Her mother knows nothing about Nina's agony and joy. She thinks that Nina is a sweet girl and a virgin. Nina's mother never thinks to live independently after the death of her husband. She always needs support from her husband's family and she decides to be a slave for them.

When Ananda comes as a suitor for Nina, her mother feels very happy because she thinks that marrying an NRI is the best thing to lead a secure and stable life. Even though Nina does not find any spark in him, she is persuaded by her mother to marry Ananda and her mother insists Nina that her bright future lies in going abroad with Ananda. According to Nina's mother, her maternal duty is over by marrying off her daughter abroad. Nina's marriage to Ananda leaves her mother alone. The separation of a mother from her daughter is certainly a painful thing. This distance seems to be a curse. Nina's mother promises her daughter to visit Nina's house, but that does not happen. The death of her mother makes Nina's dreams shatter, to be in Halifax with her mother always. This distance and separation seem to be a curse when Nina hears about her mother's death but could not attend the funeral.

Nina's disappointment in her marriage life as Ananda is an impotent, her loneliness in Halifax, her frustrations, the loss of her mother's love and support, everything leads Nina to feel failure in life. Thus in *The Immigrant* Manju Kapur, portrays another mother-daughter relationship. Mothers in all her novels are the mouthpieces of the patriarchal system of India. The relationships between mothers and daughters are not at all smooth ones. They are full of love and care at one side and at the same time full of anger also. It can be explained as a complex and obscure relationship with many love-hate layers of feelings. Though Manju Kapur's protagonists are well educated and independent thinkers, without their mother's support and proper guidance, they face a lot of sufferings and failures. All of the major characters of her novels fall in love at first sight and lose their virginity before marriage where their search for their self-identity becomes the second thought. Despite getting education and freedom, Manju Kapur's protagonists could not blossom into new women in the real sense.





WORKS CITED

1. Ghosh, Arpita. "Women's Vulnerability to violence as portrayed in the novels of Manju Kapur." *Literary Insight* 4. (Jan 2013) :129-Print.
2. Gunjan. "*Difficult Daughters, A Married Woman and Home* of Manju Kapur: A saga of New Indian Women." *Emergence of New Woman Indian Writing in English*. Ed. Qamar Talat. New Delhi: Adhyayan Publishers & Distributors, 2012.91-116. Print.
3. Savio, G. Dominic and A. Visva Sangeetha, "Braving Barriers of Culture in Manju Kapur's *Difficult Daughters: A Study in Indian Culture*" in *The Atlantic Literary Review*.15.3(July-September 2014).49-59.Print.
4. Sharma, Ram. "Quest for Feminine Identity in Manju Kapur's Novel *Home*." *Post Colonial Indian English Literature*. Jaipur: Aavishkar Publishers & Distributors, 2012.66.Print.
5. Velmani, N. "Woman's Abnormal Relationship as an Antidote for Masculine Superiority: A study of Manju Kapur's Novels." *The Atlantic Criterion* 45.4(2010):17.Print.





***Cordia sebestena* Linn: Pharmacognostic Standardization and Phytochemical Studies of its Leaves**

Karthikeyan V^{1*}, Senniappan P¹, Janarthanan L¹ and Loganathan J²

¹Assistant Professor, Department of Pharmacognosy, Vinayaga Mission's College of Pharmacy, Salem, Tamil Nadu, India.

²Assistant Professor, Department of Pharmaceutical Chemistry, Vinayaga Mission's College of Pharmacy, VMRF(DU), Salem, Tamil Nadu, India.

Received: 17 Aug 2020

Revised: 19 Sep 2020

Accepted: 21 Oct 2020

*Address for Correspondence

Karthikeyan V

Assistant Professor,
Department of Pharmacognosy,
Vinayaga Mission's College of Pharmacy,
Salem, Tamil Nadu, India.
Email: karthikseera27@gmail.com



This is an Open Access Journal / article distributed under the terms of the **Creative Commons Attribution License** (CC BY-NC-ND 3.0) which permits unrestricted use, distribution, and reproduction in any medium, provided the original work is properly cited. All rights reserved.

ABSTRACT

Cordia sebestena is commonly known as Aloe wood, geranium tree, large leaf Geiger tree, orange geiger tree, scarlet cordial and sea trumpet. Leaves of this plant are traditionally used for gastrointestinal issues (decrease indigestion and increase appetite). It is used in treatment of urinary incontinence, malaria, catarrh, oedema, and venereal diseases. It is also used in horticultural industry. Micromorphology and physicochemical parameter of the leaves of *C.sebestena* were performed as per WHO and Pharmacopoeial methods. The leaves are large, 7inch long, stiff, dark green in colour and are rough and hairy and feel somewhat like sandpaper. Microscopic evaluation of leaves showed midrib appears as quiet large, circular body with short and broad adaxial hump. The midrib consists of a multi-stranded vascular system with complex arrangement. There is a wide ring of about 16 discrete vascular bundles and a central are of about 6 vascular bundles. Lamina is bifacial with distinction between adaxial and abaxial sides. The abaxial epidermis is stomatiferous. The trichomes have thick cylindrical solid cysolith at the base. Preliminary phytochemical screening of appropriate solvent extracts showed the presence of alkaloids, sterols, tannins, proteins and amino acids, flavonoids, terpenoids, saponin, carbohydrates and absence of glycosides and volatile and fixed oil. Microscopic analysis and other parameters were informative and provide valuable information in the authentication, standardization of *C.sebestena* leaves.

Keywords: *Cordia sebestena*, Boraginaceae, Aloe wood, Microscopical evaluation.





INTRODUCTION

Cordia sebestena is commonly known as Aloe wood, geranium tree, scarlet cordial and sea trumpet belongs to the family Boraginaceae [1]. *Cordia sebestena* is a small tree which grows up to be 25 feet tall and as 5-10 cm wide. Genus *Cordia* is shrubs or flowering trees comprising more than 300 species distributed in the tropical zones. It occurs in coastal forests and shrub lands in sand or limestone substrates [2]. *Cordia sebestena* has been used in Ayurvedic medicines for very long time for treating various ailments. Traditionally this plant is used in the treatment of gastrointestinal issues (decrease indigestion and increase appetite). It is used in treatment of urinary incontinence, respiratory disorders, inflammatory disorders, liver diseases, rheumatism, menstrual pain and venereal diseases [3 & 4]. Leaves used as emollient prepared from leaves used in the treatment of respiratory disorders such as bronchitis, cough, fever and influenza [5].

Taxonomical classification [6]

Kingdom : Plantae
Phylum : Magnoliophyta
Class : Magnoliopsida
Order : Lamiales
Family : Boraginaceae
Genus : *Cordia*
Species : *sebestena*

Vernacular names [7]

Bengali : Kamla buhal, Raktarag
Hindi : Lal lasora, bohar
Kannada : Challekendala
Tamil : Acchinaruvihli
Telugu : Virigi.

Various phytoconstituents has been reported in this plant such as meroterpenoid benzoquinones, meroterpenoid naphthoquinones, hydroquinones and terpenoid quinines [8 & 9]. As mentioned previous reports have been published regarding phytochemical and different therapeutic activities *in-vitro* and *in-vivo*. An investigation to inquire its pharmacognostic examination is unavoidable. The present work was aimed to lay down standards which could be useful to detect the authenticity of this therapeutically useful plant *Cordia sebestena* leaves to treat various illnesses.

MATERIALS AND METHODS

Chemicals

Ethyl alcohol, Formalin, Chloral hydrate, Acetic acid, Glycerin, Phloroglucinol, Toludine blue, Hydrochloric acid and all other chemicals used in this study were of analytical grade.

Collection and authentication of Plant

The leaves of the selected plant were collected from in and around Salem district, Tamilnadu with the help of local tribal and field botanist. It was authenticated by Dr. Dr. P. Jayaraman, Director of Plant Anatomy Research Institute (PARC), Chennai, Tamil Nadu, India.





Karthikeyan et al.,

Macroscopic analysis

Organoleptic characters such as colour, odour, taste, shape, size, surface characters, texture, etc were done [10].

Microscopic analysis

The samples of leaves were fixed in FAA [Formalin (5mL), Acetic acid (5mL), Ethyl alcohol (90mL)]. After one day of fixing, the specimens were dehydrated by t-butyl alcohol. Specimen Infiltration was done by paraffin wax (M.P-58-60°C) [11].

Sectioning

Specimens were sectioned by rotary microtome. The thickness of the sections were about 8-10 µm. The sections were de waxed and stained by using Toluidine blue. The staining results were remarkably good as the stain was a polychromatic stain. The dye impart pink color to the cellulose, lignified cells, mucilage and blue color to the protein bodies [12].

Leaf clearing

Paraffin embedded leaf was used for para-dermal sections. Another method was clearing leaf fragments by immersing in alcohol followed by treating with 5% sodium hydroxide. The material was made transparent due to loss of cellular contents.

Photomicrographs

Photographs were taken with help of Nikon lab-photo 2 microscopic Unit. Bright field and polarized light was used. The magnifications are indicated by the scale-bars in the photographs.

Quantitative Microscopy

Stomatal number, Stomatal index, Vein islet and Vein termination was determined as per standard method [13].

Physicochemical analysis

Total ash, acid insoluble ash, water soluble ash, loss on drying and extractive values were determined as per standard methods [14].

Preliminary phytochemical screening

Preliminary phytochemical screening of ethanolic and aqueous extract carried out to find out the presence of various phytoconstituents using standard procedure [15].

RESULTS

Macroscopy

The leaves are simple, alternate, ovate, thick and rough on the upper surface, often toothed on edges, to 9 inches long and 4½ inches wide. The texture of the leaves is somewhat like sandpaper (Fig 1).

Microscopy

Midrib

In cross sectional view of the leaf, the midrib appears as quiet large, circular body with short and broad adaxial hump. The abaxial part is more or less circular and even in outline. The midrib consists of a multi-stranded vascular system with complex arrangement (Fig. 2 & 3). The epidermis of midrib is thin and the epidermal cells are small, squarish and thick walled. The ground tissue includes outer, 100 µm wide thick walled (Collenchymatous) cells and inner compact, angular thin walled parenchyma cells. There is a wide ring of about 16 discrete vascular bundles and



**Karthikeyan et al.,**

a central are of about 6 vascular bundles. All the bundles are separated widely from each other with parenchymatous interfascicular regions. The bundles have wide, dense cluster of thick walled angular vessels and conical segment of phloem on the outer part. The medullary bundles have xylem strands oriented towards the adaxial side phloem on the abaxial part.

Lamina

The lateral vein of the lamina is prominent with central prominent cluster of xylem and phloem surrounded by wide, thick walled bundle sheath cells. The bundle sheath has thick vertical extensions both on the adaxial and abaxial sides (Fig.4). The lamina is 120 μ m thick. It is bifacial with distinction between adaxial and abaxial sides. The adaxial epidermis is large and vertically oblong. The cells are thick walled. It is 30 μ m thick. The abaxial epidermis is thin and the cells are narrowly cylindrical. The abaxial epidermis is stomatiferous (Fig.5).

Petiole

The petiole is vertically oblong in sectional view. It consists of thin epidermal layer, heterogeneous outer ground tissue and a wide ring of about 20 wedge shaped vascular bundles and a horizontal row of about 3 vascular bundles (Fig.6). All the bundles are collateral and possess wide, circular, thick walled vessels and thick mass of phloem elements situated on the outer ends of the vascular bundles. The vessels are up to 50 μ m in diameter. Microsphenoidal calcium oxalate crystals are abundant in the ground parenchyma of the petiole and mesophyll tissue of the leaf (Fig.7).

Stomata

Stomata are absent on the adaxial epidermis. The abaxial epidermis consists of slightly smaller cells with wavy anticlinal walls. Stomata are abundant on the abaxial epidermis. Stomata are actinocytic type (Fig.8 & 9). The stomata are 20 X 15 μ m in size.

Trichomes

Unicellular, unbranched, thick walled epidermal trichomes are commonly seen on the abaxial epidermis. The trichomes have thick cylindrical solid cystolith at the basal part of the trichome (Fig.10). The cystolith is 300 μ m long and 50 μ m thick.

Venation pattern

The lateral veins are thick and the vein-lets become gradually thin. The veins form reticulate venation with wide polygonal vein- islets (Fig. 11). Vein terminations are seen almost in all vein-islets. The terminations are thin, long, straight or slightly wavy. Non- glandular trichome and crystal masses are also seen in the vein-islets.

Quantitative Microscopy (Table 1)

Physio-chemical parameter (Table 2)

Preliminary Phytochemical Screening of leaves of *Cordia sebestena* Linn (Table 3)

DISCUSSION

Crude drug evaluation done for confirmation of its identity and determination of its quality and purity and also detect adulterated content. It is a qualitative evaluation based on the sensory and morphology profiles of crude drugs [16]. This present study is to serve as a tool for developing standards for authentication, quality and purity of *Cordia sebestena* leaf. Adulteration of crude drugs can cause serious health problems to consumers and pharmaceutical industries. The anatomical character is an important aid for the identification of plant drugs [17]. Microscopic evaluation is one of the simplest methods for the proper authentication of plant materials [18].



**Karthikeyan et al.,**

Microscopic evaluation of leaves showed the midrib appears as quiet large, circular body with short and broad adaxial hump. The midrib consists of a multi-stranded vascular system with complex arrangement. There is a wide ring of about 16 discrete vascular bundles and a central are of about 6 vascular bundles. Lamina is bifacial with distinction between adaxial and abaxial sides. Petiole consists of thin epidermal layer, heterogeneous outer ground tissue and a wide ring of about 20 wedge shaped vascular bundles and a horizontal row of about 3 vascular bundles.

Microsphenoidal calcium oxalate crystals are abundant in the ground parenchyma of the petiole and mesophyll tissue of the leaf. Stomata are abundant on the abaxial epidermis and actinocytic type. Unicellular, unbranched, thick walled cylindrical epidermal trichomes and thick solid cysolith at the base. The veins form reticulate venation with wide polygonal vein- islets. The terminations are thin, long, straight or slightly wavy. Non- glandular trichome and crystal masses are also seen in the vein-islets. Quantitative analytical microscopy is useful in measuring the cell contents of the crude drugs and help in their identification, characterization and standardization. A Pharmacognostical study on the root of *Cordia sebestena* was previously published [19]. No report available on therapeutically important leafy portion. The ash values are useful for detecting foreign inorganic matter. Acid insoluble ash gives information regarding the presence of inorganic dirt and dust [20 & 21]. Phytochemical evaluation and characterization of plant extract is an important tool in drug discovery [22]. Preliminary phytochemical screening of appropriate solvent extracts showed the presence of tannins, sterols, alkaloids, flavonoids, amino acids, terpenoids, carbohydrates and absence of glycosides and volatile and fixed oil.

CONCLUSION

Cordia sebestena has a wide array of therapeutically potential phytochemicals which could be useful for treatment of various diseases. The pharmacognostic features, physicochemical constants, preliminary phytochemical studies have been useful in deciding the identity, purity and strength of the plant material and also for fixing standards for this plant. This present study will certainly help to build a monograph of the plant in Herbal Pharmacopoeia.

Conflict of interest

We declare that we have no conflict of interest.

ACKNOWLEDGEMENT

The author extent their heartfelt thanks for Dr.P.Jayaraman, Director of Plant Anatomy Research Institute, Tambaram, Chennai for authentication and microscopical studies.

REFERENCES

1. Kirtikar KR, Basu RR. Indian Medicinal Plants. Dehradun, India: International Book Distributors, 2005.
2. Morton JF. A survey of medicinal plants of Curacao. Econ Bot 1968; 22: 87–102.
3. Duke JA. Duke's Handbook of Medicinal Plants of Latin America. Boca Raton: CRC Press, 2008.
4. Osho A, Otuechere CA, Adeosun CB, Oluwagbemi T, Atolani O. Phytochemical, sub-acute toxicity, and antibacterial evaluation of *Cordia sebestena* leaf extracts. Journal of Basic and Clinical Physiology and Pharmacology, 2015.
5. Grandtner MM, Chevrette J. Dictionary of Trees, South America: Nomenclature, Taxonomy and Ecology. Academic Press, Amsterdam: Elsevier, 2013.
6. Oza MJ, Kulkarni YA. Traditional uses, phytochemistry and pharmacology of the medicinal species of the genus *Cordia* (Boraginaceae). Journal of Pharmacy and Pharmacology, 2017; 69: 755–789.





Karthikeyan et al.,

7. Orient B. Indian Medicinal Plants: A Compendium of 500 Species, Arya Vaidya Sala (Kottakkal, India). Hyderabad: Orient Blackswan Publisher, 1993.
8. Thirupathi K, Sathesh Kumar S, Raju VS, Ravikummar B, Krishna DR, Krishna Mohan G. A review of medicinal plants of the genus *Cordia*: their chemistry and pharmacological uses. J Nat Remedies 2008; 8: 1–10.
9. Matias EF, Alves EF. The genus *Cordia*: botanists, ethno, chemical and pharmacological aspects. Rev Bras Farmacogn 2015; 25: 542–552.
10. Kokate CK, Gokhale SB, Purohit AP. Pharmacognosy. 32nd ed., New Delhi: Nirali Prakashan; 2005.
11. Asokan J. Botanical Micro Technique Principles and Practice. 1st edn, Chennai: Plant Anatomy Research Centre; 2007.
12. Johansen DA. Plant Microtechnique. Newyork: MC Graw hill; 1940, pp. 523.
13. Evan WC. Trease and Evans Pharmacognosy. 15th edn, London Saunders: Elsevier; 2002, pp. 563-70.
14. WHO. Quality control methods for medicinal plant materials. Geneva: World Health Organization; 1998.
15. Anonymous. The Indian Pharmacopoeia. Vol II, New Delhi: Ministry of Health and Family Welfare; 1996.
16. Karthikeyan V, Agrawal SK, Parthiban P, Nandhini SR. Multivitamin plant: pharmacognostical standardization and phytochemical profile of its leaves. *Journal of Pharmacy Research* 2014; 8(7): 910-915.
17. Periyanyagam K, Karthikeyan V. Pharmacognostical, SEM and XRF profile of the leaves of *Artocarpus heterophyllus* L. (Moraceae) -A contribution to combat the NTD. *Innovare Journal of Life sciences*, 2013; 1(1): 23-8.
18. Karthikeyan V, Balakrishnan BR, Senniappan P, Janarthanan L, Anandharaj G, Jaykar B. Pharmacognostical, phyto-physicochemical profile of the leaves of *Michelia champaca* Linn. *International Journal of Pharmacy and Pharmaceutical Research*, 2016; 7(1): 331-44.
19. Trivedi MH, Venkata Ramana K. Pharmacognostical and Preliminary Phytochemical Studies on *Cordia Sebestena* L. Root. *J. Global Trends Pharm Sci*, 2019; 10(1): 6001 – 6006.
20. Agrawal SK, Karthikeyan V. Quality assessment profile of the leaves of *Tecoma stans* L. *International Journal of Pharmaceutical Research*, 2014; 6(2): 94-99.
21. Karthikeyan V, Balakrishnan BR, Senniappan P, Janarthanan L, Anandharaj G, Jaykar B. Pharmacognostical, phyto-physicochemical profile of the leaves of *Michelia champaca* Linn. *International Journal of Pharmacy and Pharmaceutical Research*, 2016; 7(1): 331-44.
22. Aruna A, Nandhini SR, Karthikeyan V, Bose P, Vijayalakshmi K, Jegadeesh S. Insulin plant (*Costus pictus*) leaves: Pharmacognostical standardization and phytochemical evaluation. *American Journal of Pharmacy & Health Research* 2014; 2(8): 106-119.

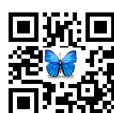
Table 1: Quantitative analytical microscopical parameters of the leaf of *Cordia sebestena*

S. No.	Parameters	Values obtained*
1	Stomatal number in upper epidermis	40.0 ± 1.68
2	Stomatal number in lower epidermis	32.13 ± 0.22
3	Stomatal index in upper epidermis	22.9 ± 1.05
4	Stomatal index in lower epidermis	25.2 ± 1.56
5	Vein islet number	11.67 ± 0.33
6	Vein termination number	17.0 ± 1.15

*mean of three readings ± SEM

Table 2: Physical parameters of *Cordia sebestena*

S. No	Parameters	Values*
1	Loss on drying	20
2	Extractive values	
	Ethanol	14.72 ± 0.12





Karthikeyan et al.,

	Methanol	12.13 ± 0.10
	Water	23.12 ± 0.73
3	Ash values	
	Total ash	21.83 ± 0.08
	Acid insoluble ash	7.55 ± 0.23
	Water soluble ash	6.0 ± 0.29

*mean of three readings ± SEM

Table 3: Preliminary Phytochemical Screening of Different Solvent Extracts

Tests	Ethanollic extract	Aqueous extract
Alkaloids		
Mayers Reagent	+	-
Dragendorffs reagent	+	-
Hagers reagent	+	-
Wagners reagent	+	-
Carbohydrates		
Molishch's Test	+	+
Fehlings Test	+	+
Benedicts Test	+	+
Glycosides		
General Test	-	-
Anthraquinone	-	-
Cardiac	-	-
Cyanogenetic	-	-
Coumarin	-	-
Phytosterols		
Salkowski Test	+	-
Libermann Burchard Test	+	-
Saponins	+	+
Tannins	+	+
Proteins & Free Amino Acid		
Millons test	+	+
Biuret test	+	+
Flavonoids		
Shinoda test	+	+
Alkaline Reagent test	+	+
Terpenoids	+	-
Fixed Oil	-	-



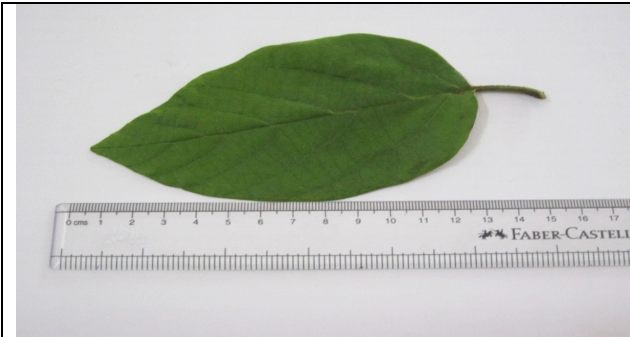


Fig 1: Leaves and flowers of *Cordia sebestena*

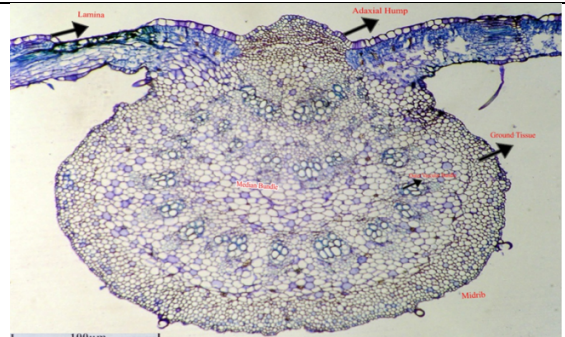


Fig.2 T.S of leaf through Midrib with Lamina

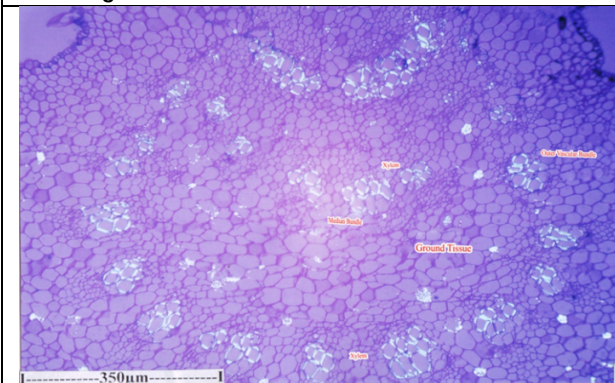


Fig 3: T.S of Midrib- Vascular Bundle

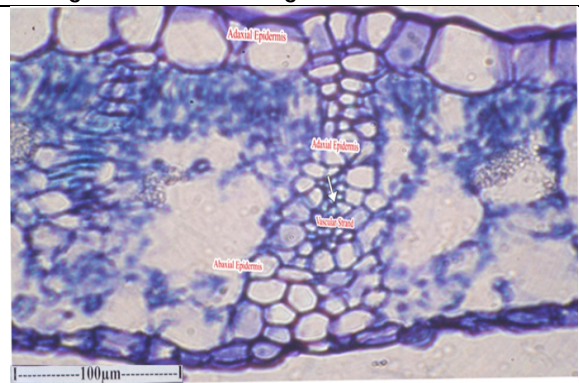


Fig 4: T.S of lamina through lateral vein



Fig 5: T.S of Lamina showing abaxial epidermis and spongy mesophyll tissue

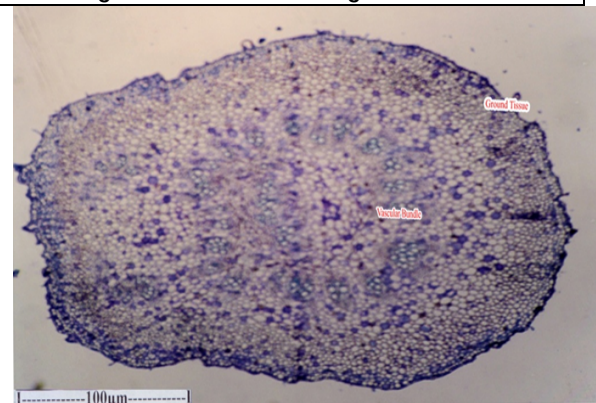


Fig 6: T.S of Petiole





Karthikeyan et al.,

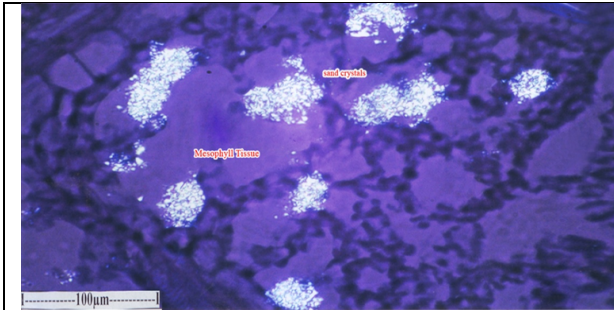


Fig 7: Sand Crystal in the mesophyll of Lamina-Enlarged

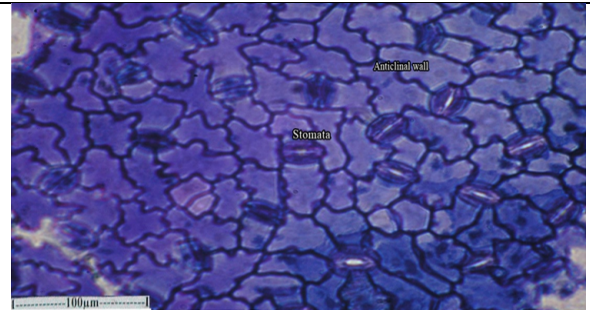


Fig 8: Actinocytic stomata in Abaxial Epidermis

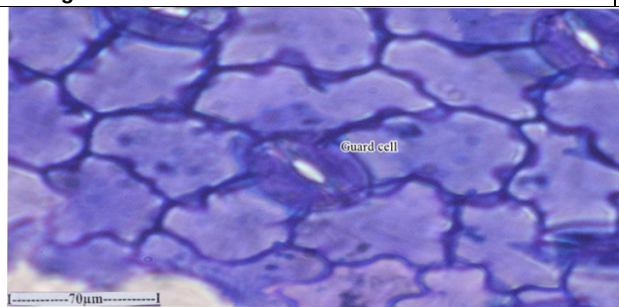


Fig 9: Actinocytic stomata in Abaxial Epidermis-Enlarged

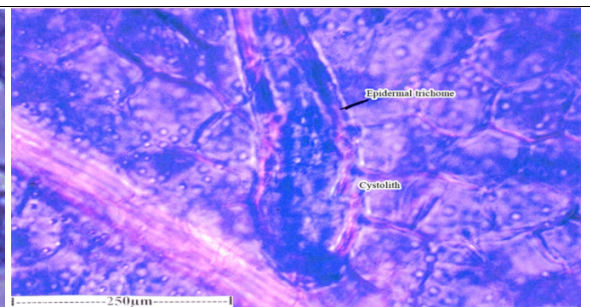


Fig 10: Cylindrical trichome with cystolith

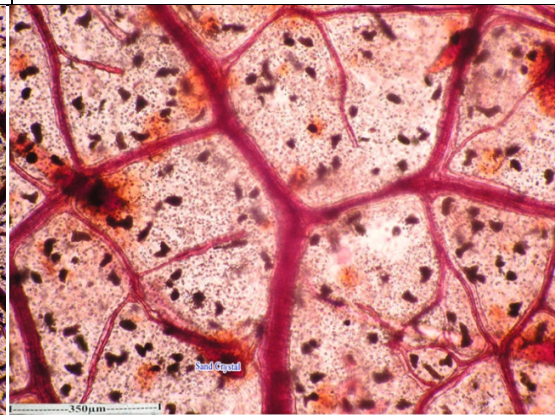
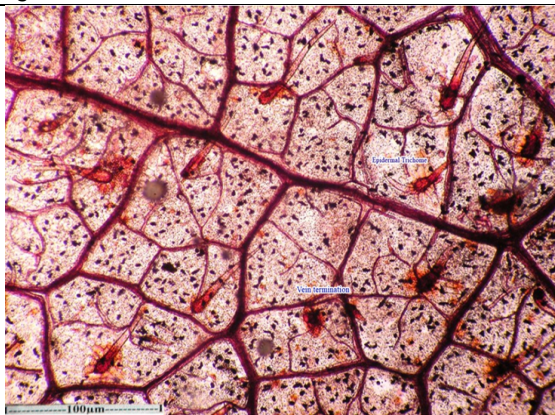


Fig 11: Paradermal section showing vein-islets and vein-termination





Development of a Prototype for Ion Beam Diagnostic

G.K.Sahu^{1*}, P.K. Rath¹, D.Das², H.Pai² and N.N.Deshmukh³

¹Centurion University of Technology and Management, Odisha, India.

²SINP, Kolkata, India.

³School of Sciences, Auro University, Surat, India.

Received: 16 Aug 2020

Revised: 18 Sep 2020

Accepted: 20 Oct 2020

*Address for Correspondence

G.K.Sahu

Centurion University of Technology and Management,

Odisha, India.

Email : gksahu@cutm.ac.in



This is an Open Access Journal / article distributed under the terms of the **Creative Commons Attribution License** (CC BY-NC-ND 3.0) which permits unrestricted use, distribution, and reproduction in any medium, provided the original work is properly cited. All rights reserved.

ABSTRACT

In the ion beam facility center like Accelerator the beam diagnostic components plays an important role. Especially in the low energy machine it is difficult to use the conventional diagnostic when the ion beam having low energy and the low intensity. The present paper describes a suitable method to manufacture a nondestructive beam diagnostic component. It will be use full for the low energy and low intensity beam. As the methodology is different than the conventional method like BPM it has a wide potential for the application of the same device as the detection purpose using suitable modification. The detail of the prototype has been explained.

Keywords: CN.MCP, mirror, grid, efficiency

INTRODUCTION

The diagnostic instruments play a very important role on a daily basis in an accelerator performance [1]. They are particularly paramount when new detectors/components are commissioned at the start-up or after a long shutdown. Besides that during the daily operation of the machine, these beam measurements inform the operator, if the machine is performing as per requirements or not and furthermore, these instruments will help him to find potential defects in the accelerator components. So the diagnostics tools are crucial. In one aspect they enable to control the particle beam and provide elaborate information concerning the stability and the quality of the particle beam delivered at the user-area. Beam instrumentation including diagnostics is the combines of the Science and engineering specially mechanical, electronic, including accelerator Physics for the improvement on the diagnostic equipment's which will be used to observe the size of beam profile with the needed tuning precision and thereby enhancing the performance of accelerators and their associated transfer lines. Although non-perturbative devices are preferred, the destructive solutions are also often used for the transfer lines and first turn diagnostics. A range of beam monitors are required for various stages of accelerator performance optimization and its later operation. A





number of different types of device exist for just such a purpose that come under the generic title Beam Position Monitor, or BPM. Thus the non-destructive measurements of beam position are essential for the effective running of any modern day accelerator. However for the low energy machines, they are very crucial. The attributes of non-destructive diagnostic methodologies towards the implementation of such a device has been discussed.

PROCESS AND RESULTS

The measurements of beam profiles using non-destructive or minimally-invasive techniques, where the instruments can be operated in real time, are much needed apparatus for accelerators. Moreover, in the high energy accelerators, especially storage rings, the non-destructive beam measurements are highly desirable to optimize the effect on the beam quality [2]. An increasing number of their applications encompass the varied aspects of experimental research and applied physics. So there is a need to develop a device that should be able to operate in two (low-energy and low-intensity) regimes as a non-destructive beam diagnostic component. The main part of the proposed prototype is the MCP (micro channel plates) these are very sensitive detectors which can emit secondary electron upon hitting by a primary electron or ion. The proposed prototype is very simple and explained below. The detection system, is a transmission type detector, based on the mechanism of secondary emission of electrons as mentioned above. With this system, the TOF (Time of flight) can be measured of better accuracy than the conventional systems. A schematic of the detection system has been shown in Fig.1.

The main components are the conversion foil for the generation of the secondary electron, and micro channel plate for detection. When an ion beam passes through the conversion foil of the detector, they knock out electrons, which move in the beam direction. These electrons are called secondary electrons. These electrons travel the equal lengths from starting point till detection point; therefore, the output timing signal of the detector is position-independent. Carbon foils with a thickness of 20–40 $\mu\text{g}/\text{cm}^2$ will be used as the conversion foil. The thickness of the foil is very important as the particle lose energy as it passage. The thickness of the foil should such that energy loss should be minimum. Once the secondary electrons come out of the foil it move towards the forward direction and come close to the electrostatic mirror. These mirror change the Primary direction of the electron and practically without changing its initial velocity. After that these electron will reach to the entrance of the MCP [3] plates, which will amplify and provide a fast rise time signal. This signal will be our start signal in case where use it as trigger. But in case of beam diagnostic as explained above the secondary electron from the MCP will strike a scintillating screen which will emit a flash of light when a charged particle/electron will strike it. These light will be generated at the location where the electron will strike. These flash will be pickup by a CCD camera and connected to a visual monitor for the visualization.

SUMMARY AND CONCLUSION

A clear picture with procedure has been explained for the fabrication of a beam diagnostic component using completely different approach for detection of a low energy/ low intensity ion beam. It is has a completely different approach compared to the conventional diagnostic. Here the proposed component is based on the secondary electron emission for the detection. The use of the same module for other purpose also explained as TOF [4] detectors.

REFERENCES

1. M. Gasior et al. In: CERN Accelerator School: Advanced Accelerator Physics Course. 2014, arXiv:1601.04907.
2. Kay Wittenburg. In: CERN Accelerator School on High Power Hadron Machines, arXiv:1303.6767.
3. https://www.hamamatsu.com/jp/en/product/optical-sensors/electron_ion-sensor/mcp/index.html





4. E. M. Kozulin et al. "The CORSET time-of-flight spectrometer for measuring binary products of nuclear reactions " *Instruments and Experimental Techniques* volume 51, article number: 44 (2008)

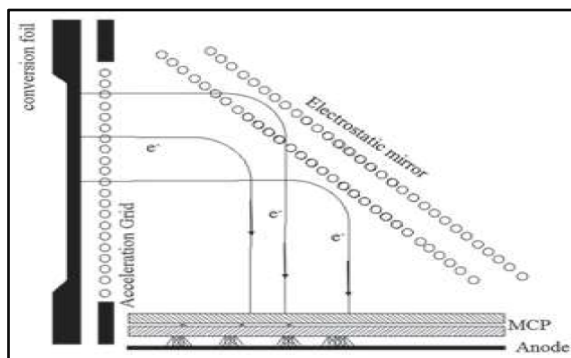


Fig. 1. Thorough schematic has presented for the beam diagnostic. The conversion foil is made up of $^{12}\text{C}/\text{Au}$. The grid and the mirror is clearly shown. The MCP assembly is down where the scintillating screen is there.





Clinical Characteristics of Novel Coronavirus and Its Impacts

R. Venkatesh^{1*}, L. Vadivel Kannan² and K. Jeyalakshmi³

¹Assistant Professor, Department of Physics, PSNA College of Engineering and Technology, Dindigul, Tamil Nadu, India.

²Assistant Professor, Department of Mechanical Engineering, PSNA College of Engineering and Technology, Dindigul, Tamil Nadu, India.

³Professor, Department of Physics, PSNA College of Engineering and Technology, Dindigul, Tamil Nadu, India.

Received: 28 Aug 2020

Revised: 30 Sep 2020

Accepted: 02 Nov 2020

*Address for Correspondence

R.Venkatesh

Assistant Professor, Department of Physics,
PSNA College of Engineering and Technology,
Dindigul, Tamil Nadu, India.

Email: lakatesh@gmail.com



This is an Open Access Journal / article distributed under the terms of the **Creative Commons Attribution License** (CC BY-NC-ND 3.0) which permits unrestricted use, distribution, and reproduction in any medium, provided the original work is properly cited. All rights reserved.

ABSTRACT

SARS-CoV2 is one of seven types of coronavirus, including the ones that cause severe diseases like Middle East respiratory syndrome (MERS) and sudden acute respiratory syndrome (SARS). The other coronaviruses cause most of the colds that affect us during the year but aren't a serious threat for otherwise healthy people. Human coronavirus (HCoV) infection causes respiratory diseases with mild to severe outcomes. In this scenario, they are predicting that India would go into recession affecting the unorganized sector and semi-skilled job holders losing their employment. It may also likely surface that at this time of eroding trust within and between countries with national leadership under pressure from growing societal unrest and economic confrontations between major powers. Many articles have been written in the medical field related to the COVID-19 outbreak that has surrounded the World and killed many people. The main objective of this paper is to discuss the positive and negative impacts of COVID-19 in a sociological perspective with special attention to economy, education, employment and environmental pollution (4E's). It must be opined that partial lockdown would be beneficial for the health of the total environment. Thus, the temporary lockdown mechanism should be treated as the environmental blessings instead of the ruthless curse globally.

Keywords: COVID-19, Viruses, SARS, MERS, Corona, 4E's



**Venkatesh et al.,**

INTRODUCTION

Life seems to give lots of lessons to us every moment, but we fail to comprehend unless we face a catastrophe and till, we try to understand the laws of nature, it is already too late. The current situation of the world is no less than a world war which has put everyone in a skeptical situation especially dealing with young and blank minds. COVID-19 is the disease caused by the new coronavirus that emerged in China in December 2019. COVID-19 appeared in Wuhan, a city in China, in December 2019. Although health officials are still tracing the exact source of this new coronavirus, early hypotheses thought it may be linked to a seafood market in Wuhan, China. Coronaviruses are a type of virus. There are many different kinds, and some cause disease. A newly identified coronavirus, SARS-CoV-2, has caused a worldwide pandemic of respiratory illness, called COVID-19. Coronaviruses are common in different animals. Rarely, an animal coronavirus can infect humans. There are many different kinds of coronaviruses. Some of them can cause colds or other mild respiratory (nose, throat, lung) illnesses. Other coronaviruses can cause more serious diseases, including severe acute respiratory syndrome (SARS) and Middle East respiratory syndrome (MERS). Coronaviruses are named for their appearance: Under the microscope, the viruses look like they are covered with pointed structures that surround them like a corona, or crown. As of now, researchers know that the new coronavirus is spread through droplets released into the air when an infected person coughs or sneezes. The droplets generally do not travel more than a few feet, and they fall to the ground in a few seconds — this is why physical distancing is effective in preventing the spread. Naturally, anyone would think of a pandemic situation in very negative terms due to its emotional, socio-economic, environmental, political and cultural factors. However, it is also positive due to certain factors that help to reintegrate and reorganize the social system as a whole.

Positive and Negative Impact of COVID 19

Positive impacts are relatively high and some impacts are short term and most others are long term. This situation depends on the early stage of COVID 19 and the shape could change due to several global socio-economic and political factors. So far, COVID-19 is in a rapid spread tendency in most countries, and there are no sufficient health and socioeconomic facilities, especially supply chain networks to address the need structure of the pandemic situation in these countries. When the Indian scenario is analyzed, the COVID19 impacts will be the most painful here when compared to other countries. The social system prevailing in India is not simple in terms of managing the pandemic situation. It is very clear that any society which has a high social disparity may have to face the most negative impacts. The negative impacts towards the family, communities, nations, regions and the world push them backward in any sector or socio-economic and political spheres. Several elements which cause negative impacts can be identified as illnesses or COVID-19, pandemic situation, deaths, social distancing, curfew and the lock-down of the entire functional mechanism of a single society and the global network in production, trade, supply chain networks, transportation, social networking and political network. Therefore, this paper has given similar attention to the negative impacts of COVID-19 at the local, regional and global contexts based on the situation during the pandemic period.

Coronavirus Genome Structure

COVID-19 is a spherical or pleomorphic enveloped particle containing single-stranded (positive-sense) RNA associated with a nucleoprotein within a capsid comprised of matrix protein. The envelope bears club-shaped glycoprotein projections. Some coronaviruses also contain a hemagglutinin-esterase protein. (Fig.1)

Comparison of SARS-CoV2 (COVID-19), SARS-CoV and MERS-CoV

Rarer strains that cause more severe complications include MERS-CoV, which causes Middle East respiratory syndrome (MERS), and SARS-CoV, the virus responsible for severe acute respiratory syndrome (SARS). In 2019, a dangerous new strain called SARS- CoV-2 started circulating, causing the disease COVID- 19. SARS-CoV-2 (COVID-19) binds to ACE2 (the angiotensin-converting enzyme 2) by its Spike and allows COVID-19 to enter and infect cells. In order for the virus to complete entry into the cell following this initial process, the spike protein has to be primed





by an enzyme called a protease. Similar to SARS-CoV, SARS-CoV-2 (COVID-19) uses a protease called TMPRSS2 to complete this process. In order to attach virus receptor (spike protein) to its cellular ligand (ACE2), activation by TMPRSS2 as a protease is needed (Fig.2).

Transmission of Virus

The research is available on how HCoV spreads from one person to the next. Coughing and sneezing without covering the mouth can disperse droplets into the air. Touching or shaking hands with a person who has the virus can pass the virus between individuals. Making contact with a surface or object that has the virus and then touching the nose, eyes, or mouth. Some animal corona viruses, such as feline corona virus (FCoV), may spread through contact with feces. However, it is unclear whether this also applies to human corona viruses. The National Institutes of Health (NIH) suggest that several groups of people have the highest risk of developing complications due to COVID-19. These groups include children, people aged 65 years or older and pregnant women.

Testing for COVID-19

The PCR based tests are widely used for the detection of viruses in human disease and are currently the most commonly used nucleic acid tests (NATs) performed in clinical laboratories. PCR instruments and techniques are in widespread use in both clinical and research laboratories and the basis of the tests is well known. The tests consist of nucleic acid extraction and purification from the human specimen using authorized extraction methods/instruments followed by real-time RT-PCR, where the RNA is reverse transcribed into cDNA and then amplified using the primer sets and detected using specific probes. PCR-based tests were the initial tests used, starting with the CDC 2019-Novel Coronavirus Real-Time RT-PCR Diagnostic Panel. These tests detect nucleic acid from SARS-CoV-2 in patients suspected to have COVID-19 infection.

Impacts of COVID 19

Economy

There is a big shift in the world economic market and the share market has witnessed crashes day by day. Factories, Restaurants, Pubs, Markets, Flights, Super Markets, Malls, Universities and Colleges etc. were shut down. Fear of corona virus has limited the movement of the individuals. People were not even going to buy the daily essentials and these all were somewhere impacting the economy of the world as a whole. The Organization for Economic Co-operation and Development (OECD) reveals that they have cut their expectation for global growth to 2.4% from 2.9%, and warns that it could fall as low as 1.5%. India faces a huge decline in government revenues and growth of the income for at least two quarters as the coronavirus hits economic activity of the country as a whole. A fall in investor sentiment impacts privatization plans, government and industry. The lockdown in India will have a sizeable impact on the economy mainly on consumption which is the biggest component of GDP. India's total electronic imports is equal to 45% that of China. For automotive parts and fertilizers China's share in India's import is more than 25%. Around 65 to 70% of active pharmaceutical ingredients and around 90% of certain mobile phones come from China to India.

Education

The COVID-19 pandemic has also had a severe impact on higher education as universities closed their premises and countries shut their borders in response to lockdown measures. Although higher education institutions were quick to replace face-to-face lectures with online learning, these closures affected learning and examinations as well as the safety and legal status of international students in their host country. Perhaps most importantly, the crisis raises questions about the value offered by a university education which includes networking and social opportunities as well as educational content. To remain relevant, universities will need to reinvent their learning environments so that digitalization expands and complements student-teacher and other relationships. Fig.3 shows the global monitoring school closures by COVID 19.





Employment

According to the early estimates, tens of millions of migrant workers were left unemployed in India by the end of March 2020 due to the lockdown (Al-Jazeera, 2020). Many of the migrant workers have returned to their villages, and many more are just waiting for the lockdown to be lifted. The national statistical office's (NSO's) report presented in SARVEKSHANA (Govt. of India, 2009) revealed that among regular salaried employees in the non-agriculture sector, nearly 71 per cent had no written job contract, and such proportion was higher among males than females. Around 54 per cent of regular salaried employees in the non-agriculture sector were not eligible for paid leave. Moreover, nearly half of them were not eligible for any social security benefit. Most of the recruitment got postponed due to COVID-19. Unemployment rate is expected to be increased due to this pandemic. In India, there is no recruitment in Govt. sector and fresh graduates fear withdrawal of their job offers from private sectors because of the current situation. The Centre for Monitoring Indian Economy's estimates on unemployment shot up from 8.4% in mid-March to 23% in early April and the urban unemployment rate to 30.9% (Educationasia.in). When the unemployment increases then the education gradually decreases as people struggle for food rather than education

Al-Jazeera. (2020, April 2). Hungry, desperate: India virus controls trap its migrant workers. Al-Jazeera. Time Educationasia.in 2020. The Impact of COVID-19 on Education and Education Sectors, Know here. Retrieved on May 25, 2020 from <https://educationasia.in/article/the-impactof-covid-19-on-education-and-education-sectors-knowhere>

Environmental Pollution

Covid-19 and its associated lockdown have given us a rare opportunity to step back and assess our impact on the environment. We are witnessing clean air, water and livable cities that we have demanded for so long precisely because we have been shut away. Thus, before we resume life as usual, we should make commitment to instill the principles of sustainable development in our social behavior, life style and public policy making to make our environment clean and sustainable.

CONCLUSION

This new corona virus outbreak has challenged the economic, medical and public health infrastructure of China and to some extent, of other countries especially, its neighbors. Time alone will tell how the virus will impact our lives here in India. More so, future outbreaks of viruses and pathogens of zoonotic origin are likely to continue. Therefore, apart from curbing this outbreak, efforts should be made to devise comprehensive measures to prevent future outbreaks of zoonotic origin. A global recession now seems inevitable. But how deep and long the downturn will be depending on the success of measures taken to prevent the spread of COVID-19, the effects of government policies to alleviate liquidity problems in SMEs and to support families under financial distress. It also depends upon how companies react and prepare for the re-start of economic activities. And, above all, it depends on how long the current lockdowns will last. The country is facing an extra ordinary challenging time in this financial year. India has to urgently find a way to cushion the demand side shocks induced by potential lockdowns and other ongoing containment measure. Further detailed statistical study may be undertaken to explore the impact of COVID-19 on education system and economy and environment of India.

REFERENCES

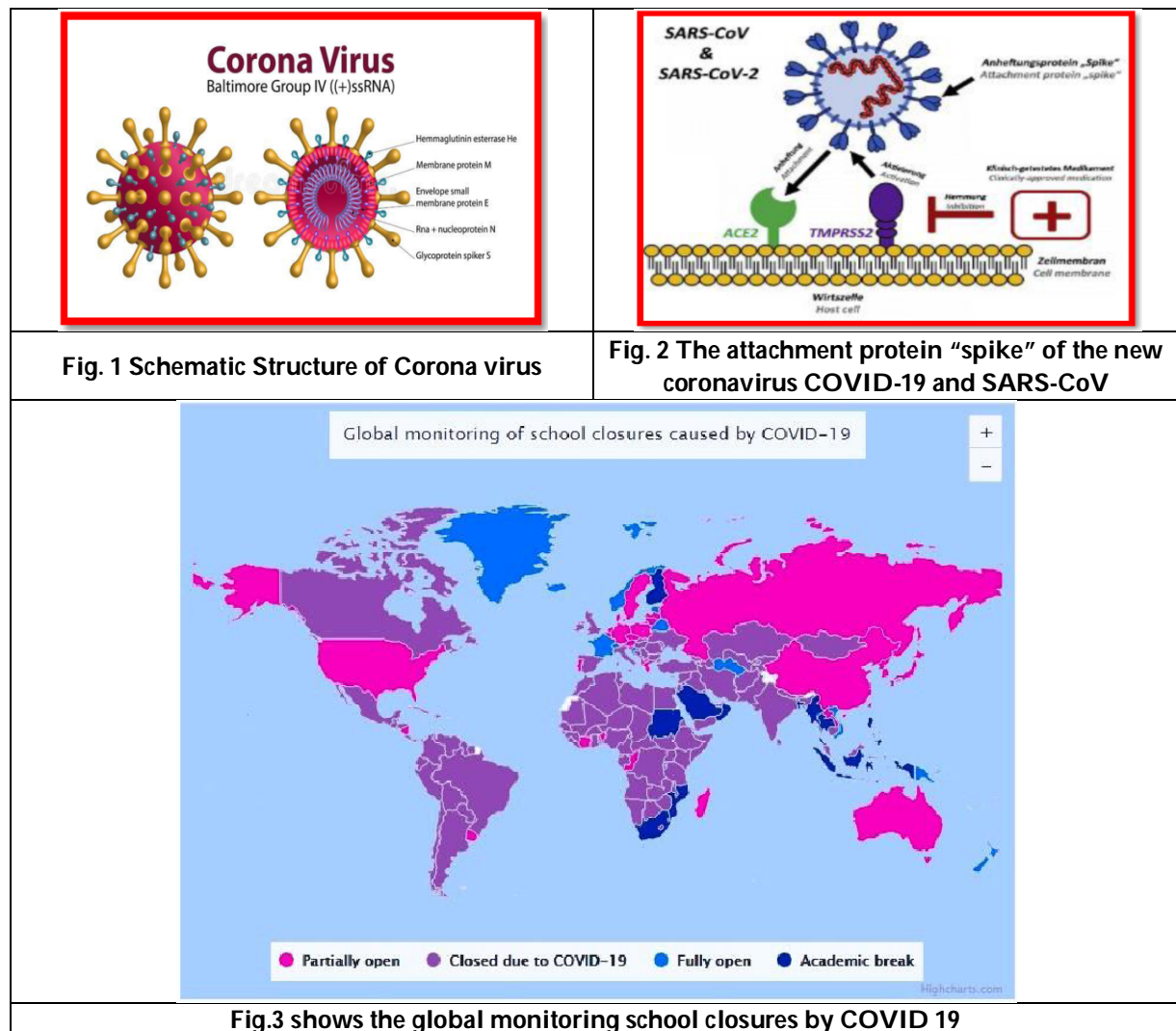
1. Coronavirinae in ViralZone. expasy.org/785 (accessed on 05 February 2019).
2. Subissi, L.; Posthuma, C.C.; Collet, A.; Zevenhoven-Dobbe, J.C.; Gorbalenya, A.E.; Decroly, E.; Snijder, E.J.; Canard, B.; Imbert, I. One severe acute respiratory syndrome coronavirus protein complex integrates processive RNA polymerase and exonuclease activities. *Proc. Natl. Acad. Sci. USA* 2014, 111, E3900–E3909.





Venkatesh et al.,

3. World Health Organization, nCoV Situation Report- 22 on 12 February, 2020. Source /coronaviruses /situation-reports/ 2019.
4. Armstrong J, Niemann H, Smeekens S, RottierP, Warren G. Sequence and topology of a model intracellular membrane protein, E1 glycoprotein, from a coronavirus. Nature, 1984; 308(5961): 751– 752.
5. <https://bfsi.economicstimes.indiatimes.com>.
6. Singhal, T. A Review of Coronavirus Disease-2019 (COVID-19). Indian J Pediatr 87, 281–286 (2020).
7. WHO. Novel coronavirus situation dashboard. Geneva, Switzerland: WHO, 2020.





An Introduction to Prime Topology along with the Concept of COVID-19 and Separation Axioms

Chinnadurai .V^{1*} and Sindhu M.P²

¹Department of Mathematics, Annamalai University, Annamalainagar, Tamil Nadu, India.

²Department of Mathematics, Karpagam College of Engineering, Coimbatore, Tamil Nadu, India.

Received: 14 Aug 2020

Revised: 18 Sep 2020

Accepted: 20 Oct 2020

*Address for Correspondence

Chinnadurai .V

Department of Mathematics,
Annamalai University,
Annamalainagar, Tamil Nadu, India.



This is an Open Access Journal / article distributed under the terms of the **Creative Commons Attribution License** (CC BY-NC-ND 3.0) which permits unrestricted use, distribution, and reproduction in any medium, provided the original work is properly cited. All rights reserved.

ABSTRACT

In this study, we introduce the notion of prime sets as one of the mathematical tools for dealing with the subsets of the universe set. We define prime topological spaces to study its related properties with illustrative examples. We compare a problem dealt with the concept of COVID-19 on prime topological spaces to the real-life result. We define a few separation axioms on this space and examine its relations among them with appropriate examples.

Keywords: Prime set (PS), prime topological space (PTS), prime interior, prime closure, prime subspace, prime neighbourhood, prime point, prime $T_{i=0,1,2}$ -spaces.

INTRODUCTION

Topology [1-5] is an extension of mathematics concerned with the properties of space conserved under endless distortions including elongating and twisting, but not scratching. It established the study of geometry and set theory by analyzing such concepts as space, dimension and transformation. It was designed by Henri Poincare at the end of the 19th century, and it became a major branch of mathematics in the middle of the 20th century. The topology defined on space and so called topological spaces (TSs). Separation axioms are the most attractive and remarkable thoughts in topology. Usually, it was denoted with the letter "T" after the German Trennungs axiom, which means "separation axioms". Nowadays, most of the researchers abundantly extended the study of topology in many fields. The different types of topologies are introduced in different types of sets such as fuzzy, intuitionistic, soft, rough, fine, ideal, neutrosophic [6, 7] etc., as well as widely spreads its application in medical diagnosis, decision making problem, multi-criteria decision making problem, COVID-19, etc.; The aim of this paper is to introduce the notion of a new set, namely PS, and to define a topology on this set, called PTS. Some basic theorems are stated and proved with suitable examples. The concept of COVID-19 on PTS is also discussed and compared to the real-life result. Additionally, the





Chinnadurai and Sindhu

separation axioms on such space are defined with perfect examples, also counterexamples are given. The following list reveals the presence of this paper. Few necessary definitions associated with TS are in division 2. In division 3, defined PTS, prime interior, prime closure, prime subspace and its properties are given with examples. In division 4, illustrated the problem of COVID-19 to compare its result with the result of the current situation. In division 5, the separation axioms on PTS is defined as prime $T_{i=0,1,2}$ -spaces and relations among them are examined with appropriate examples. In division 6, the conclusion is given to end up with some future work.

Preliminaries

In this division, some basic definitions correlated to TS are specified.

Definition

Let W be a set and $\tau \subseteq \mathcal{P}(W)$. Then τ is called a topology if it satisfies the following conditions

- (i) $\emptyset, W \in \tau$.
- (ii) the intersection of any finite number of members of τ belongs to τ .
- (iii) the union of any collection of members of τ belongs to τ .

Then the pair (W, τ) is called a topological space (TS).

Every member of τ is called open set. The complement of every open set is called a closed set and is denoted by C .

Definition

Let (W, τ) be a TS and let $R \subseteq W$. Then an interior of R is denoted by $\text{int}(R)$ and defined as the union of all open sets contained in R .

Definition

Let (W, τ) be a TS and let $R \subseteq W$. Then a closure of R is denoted by $\text{cl}(R)$ and defined as the intersection of all closed sets containing R .

Main Results

In this division, defined PTS, prime interior, prime closure, prime subspace and its properties are given with illustrative examples.

Definition

Let (W, τ) be a topological space (TS), where W is the universe and τ is a topology. Let K be a proper nonempty subset of W . Let R be a τ -open set, where $R \neq \emptyset, W$. Then the prime set (PS) over W is denoted by ζ and defined by $\zeta = \{K : K \cap R \neq \emptyset\}$.

Definition

Let (W, τ) be a TS. Let $PS(W)$ be the collection of prime sets over W and $\tau_p \subseteq \mathcal{P}(PS(W))$. Then τ_p is called a prime topology (PT) if it satisfies the following conditions

- (i) $\emptyset, W \in \tau_p$.
- (ii) the intersection of any finite number of members of τ_p belongs to τ_p .
- (iii) the union of any collection of members of τ_p belongs to τ_p .

Then the pair (W, τ_p) is called a prime topological space (PTS).





Chinnadurai and Sindhu

Every member of τ_p is called τ_p -prime open set (τ_p -POS). The complement of every τ_p -POS of W is called the τ_p -prime closed set (τ_p -PCS) of W and this collection is denoted by τ_p^* .

Remark

If $\tau_p = PS(W)$, they τ_p may or may not be a PT. This is illustrated in the following examples.

Example

Let $W = \{w_1, w_2, w_3\}$ with topology $\tau = \{\emptyset, W, \{w_1\}\}$.

Clearly, (W, τ) is a TS over W .

Then

$$\tau_p = \{\emptyset, W, \{w_1\}, \{w_1, w_2\}, \{w_1, w_3\}\} = PS(W)$$

and its members are τ_p -POS.

Thus (W, τ_p) is a PTS over W .

Then

$$\tau_p^* = \{\emptyset, W, \{w_2, w_3\}, \{w_3\}, \{w_2\}\}$$

and its members are τ_p -PCSs, whose complements are τ_p -POS.

Example 3.5 Let $W = \{w_1, w_2, w_3\}$ with topology $\tau = \{\emptyset, W, \{w_1\}, \{w_1, w_3\}\}$.

Clearly, (W, τ) is a TS over W .

Then

$$\tau_p = \{\emptyset, W, \{w_1\}, \{w_1, w_2\}, \{w_1, w_3\}, \{w_3\}, \{w_3, w_2\}\} = PS(W)$$

and its members are τ_p -Poss.

Also

$$\tau_p^* = \{\emptyset, W, \{w_2, w_3\}, \{w_3\}, \{w_2\}, \{w_1, w_2\}, \{w_1\}\}$$

and its members are τ_p -PCSs, whose complements are τ_p -Poss.

Here $\{w_1, w_2\}, \{w_3, w_2\} \in \tau_p$ but $\{w_1, w_2\} \cap \{w_3, w_2\} = \{w_2\} \notin \tau_p$.

Thus (W, τ_p) is not a PTS over W .

Remark

A PS can generate one or more PT.

Example

Consider Example 3.5.

The collection of PSs $PS(W)$ is

$$\{\{w_1\}, \{w_1, w_2\}, \{w_1, w_3\}, \{w_3\}, \{w_3, w_2\}\}.$$

Then its PT may have any one of the following

$$1\tau_p = \{\emptyset, W, \{w_1\}, \{w_1, w_2\}, \{w_1, w_3\}, \{w_3\}\}$$

$$2\tau_p = \{\emptyset, W, \{w_1\}, \{w_1, w_3\}, \{w_3\}, \{w_3, w_2\}\}.$$

Thus $(W, 1\tau_p)$ and $(W, 2\tau_p)$ are PTSs over W .





Definition

A PT τ_p is said to be a prime discrete topology if τ_p contains all the subsets of W .

Definition

A PT τ_p is said to be a prime indiscrete topology if τ_p contains only ϕ and W .

Proposition

Let $(W, 1\tau_p)$ and $(W, 2\tau_p)$ be two PTSs over W and let $1\tau_p \cap 2\tau_p = \{K \in PS(W) : M \in 1\tau_p \cap 2\tau_p\}$. Then $1\tau_p \cap 2\tau_p$ is also a PTS over W .

Proof. Let $(W, 1\tau_p)$ and $(W, 2\tau_p)$ be two PTSs over W .

(i) $\phi, W \in 1\tau_p \cap 2\tau_p$.

(ii) Let $K_1, K_2 \in 1\tau_p \cap 2\tau_p$.

Then $K_1, K_2 \in 1\tau_p$ and $K_1, K_2 \in 2\tau_p$.

$\Rightarrow K_1 \cap K_2 \in 1\tau_p$ and $K_1 \cap K_2 \in 2\tau_p$.

$\Rightarrow K_1 \cap K_2 \in 1\tau_p \cap 2\tau_p$.

(iii) Let $K_i \in 1\tau_p \cap 2\tau_p, i \in I$.

Then $K_i \in 1\tau_p$ and $K_i \in 2\tau_p, i \in I$.

$\Rightarrow \bigcup_{i \in I} K_i \in 1\tau_p$ and $\Rightarrow \bigcup_{i \in I} K_i \in 2\tau_p, i \in I$.

$\Rightarrow \bigcup_{i \in I} K_i \in 1\tau_p \cup 2\tau_p$.

Thus $1\tau_p \cap 2\tau_p$ is also a PTS over W .

Remark

The union of two PTs need not be a PT. The following example illustrates this remark.

Example

Let $W = \{w_1, w_2, w_3\}$ with topologies $1\tau = \{\phi, W, \{w_2\}\}$ and $2\tau = \{\phi, W, \{w_3\}\}$.

Clearly, $(W, 1\tau)$ and $(W, 2\tau)$ are two TSs over W .

Then

$1\tau_p = \{\phi, W, \{w_2\}, \{w_2, w_1\}, \{w_2, w_3\}\}$

and $2\tau_p = \{\phi, W, \{w_3\}, \{w_3, w_1\}, \{w_3, w_2\}\}$ are two PTs of $(W, 1\tau)$ and $(W, 2\tau)$, respectively.

Clearly, $1\tau_p \cup 2\tau_p = \{\phi, W, \{w_2\}, \{w_2, w_1\}, \{w_2, w_3\}, \{w_3\}, \{w_3, w_1\}\}$.

Thus $1\tau_p \cup 2\tau_p$ is not a PT, since $\{w_2, w_1\} \cap \{w_3, w_1\} = \{w_1\} \notin 1\tau_p \cup 2\tau_p$.

Hence the union of two PTs need not be a PT.

Proposition

Let K_1 and K_2 be two τ_p -POSSs over W . Then

(i) $(K_1 \cup K_2)^c = K_1^c \cap K_2^c$.

(ii) $(K_1 \cap K_2)^c = K_1^c \cup K_2^c$.

Proof. Straight forward.





Chinnadurai and Sindhu

Definition

Let (W, τ_p) be a PTS over W and let $R \subseteq W$. Then the prime interior of R is denoted by $p\text{-int}(R)$ and defined by $p\text{-int}(R) = \bigcup \{L : L \in \tau_p \text{ and } L \subseteq R\}$.

Clearly, it is the union of all τ_p -PO subsets of R .

Theorem

Let (W, τ_p) be a PTS over W and let $R, S \subseteq W$. Then

- (i) $p\text{-int}(R) \subseteq R$ and $p\text{-int}(R)$ is the largest τ_p -POS.
- (ii) $R \subseteq S \Rightarrow p\text{-int}(R) \subseteq p\text{-int}(S)$.
- (iii) $p\text{-int}(R)$ is an τ_p -POS.
- (iv) R is a τ_p -POS iff $p\text{-int}(R) = R$.
- (v) $p\text{-int}(p\text{-int}(R)) = p\text{-int}(R)$.
- (vi) $p\text{-int}(\phi) = \phi$ and $p\text{-int}(W) = W$.
- (vii) $p\text{-int}(R \cap S) = p\text{-int}(R) \cap p\text{-int}(S)$.
- (viii) $p\text{-int}(R \cup S) \subseteq p\text{-int}(R) \cup p\text{-int}(S)$.

Proof. Follows from Definition 3.14.

Definition

Let (W, τ_p) be a PTS over W and let $R \subseteq W$. Then the prime closure of R is denoted by $p\text{-cl}(R)$ and defined by $p\text{-cl}(R) = \bigcap \{L : L \in \tau_p^* \text{ and } L \supseteq R\}$.

Clearly, it is the intersection of all τ_p^* -PC supersets of R .

Theorem

Let (W, τ_p) be a PTS over W and let $R, S \subseteq W$. Then

- (i) $R \subseteq p\text{-cl}(R)$ and $p\text{-cl}(R)$ is the smallest τ_p^* -PCS.
- (ii) $R \subseteq S \Rightarrow p\text{-cl}(R) \subseteq p\text{-cl}(S)$.
- (iii) $p\text{-cl}(R)$ is an τ_p^* -PCS.
- (iv) R is a τ_p^* -PCS iff $p\text{-cl}(R) = R$.
- (v) $p\text{-cl}(p\text{-cl}(R)) = p\text{-cl}(R)$.
- (vi) $p\text{-cl}(\phi) = \phi$ and $p\text{-cl}(W) = W$.
- (vii) $p\text{-cl}(R \cup S) = p\text{-cl}(R) \cup p\text{-cl}(S)$.
- (viii) $p\text{-cl}(R \cap S) \subseteq p\text{-cl}(R) \cap p\text{-cl}(S)$.

Proof. Follows from Definition 3.16.

Example

Let $W = \{w_1, w_2, w_3\}$ with topology $\tau = \{\phi, W, \{w_1\}, \{w_1, w_3\}\}$.

Clearly, (W, τ) is a TS over W .

Then

$$\tau_p = \{\phi, W, \{w_1\}, \{w_1, w_3\}, \{w_3\}, \{w_3, w_2\}\}$$





Chinnadurai and Sindhu

is a collection of τ_p -POSSs.

Thus $(W, 2\tau_p)$ is a PTS over W .

Then

$$\tau_p^* = \{\phi, W, \{w_2, w_3\}, \{w_2\}, \{w_1, w_2\}, \{w_1\}\}$$

is a collection of τ_p^* -POSSs.

Here

$$p - \text{int}(\{w_2\}) = \phi ; p - \text{int}(\{w_1, w_3\}) = \{w_1, w_3\}$$

and

$$p - \text{cl}(\{w_2\}) = \{w_2\} ; p - \text{cl}(\{w_1, w_3\}) = W .$$

Theorem

Let (W, τ_p) be a PTS over W and let $R \subseteq W$. Then

(i) $(p - \text{int}(R))^c = p - \text{cl}(R^c)$.

(ii) $(p - \text{cl}(R))^c = p - \text{int}(R^c)$.

Proof. Follows from Definitions 3.14 and 3.16.

Definition

Let (W, τ_p) be a PTS over W where τ_p is a PT on W . Let $PS(W)$ be the collection of prime sets over W and $L \in PS(W)$ Suppose $\tau_{ps}(L) = \{L \cap K_i : K_i \in \tau_p\}$ and $\phi, W \in \tau_{ps}(L)$. Then $\tau_{ps}(L)$ forms also a topology on W . Thus $(W, \tau_{ps}(L))$ is a prime subspace topology of (W, τ_p) .

Example

Let $W = \{w_1, w_2, w_3\}$ with a topology $\tau = \{\phi, W, \{w_2\}, \{w_1, w_3\}\}$.

Clearly, (W, τ) is a TS over W .

The collection of PSSs $PS(W)$ is

$$\{\{w_1\}, \{w_2\}, \{w_3\}, \{w_1, w_2\}, \{w_1, w_3\}, \{w_2, w_3\}\} .$$

Then

$$\tau_p = \{\phi, W, \{w_1\}, \{w_2\}, \{w_1, w_2\}, \{w_2, w_3\}\} .$$

Thus (W, τ_p) is a PTS over W .

Let $L = \{w_1, w_3\}$.

Then

$$L \cap \phi = \phi , L \cap W = L , L \cap \{w_1\} = \{w_1\} , L \cap \{w_2\} = \phi , L \cap \{w_1, w_2\} = \{w_1\} , L \cap \{w_2, w_3\} = \{w_3\} .$$

Thus

$$\tau_{ps}(L) = \{\phi, W, \{w_1, w_3\}, \{w_1\}, \{w_3\}\}$$
 and $\tau_{ps}(L)$ is a PT on W .

Hence $(W, \tau_{ps}(L))$ is a prime subspace topology of (W, τ_p) .

The Concept of COVID-19 on PTS

In this division, the concept of COVID-19 is discussed on PTS and compared to the daily life situation of COVID-19 which spreads only through the person who is affected by it. This is illustrated in the following example.





Chinnadurai and Sindhu

Problem

Let $W = \{w_1, w_2, w_3\}$ be a set of sample people with a topology $\tau = \{\emptyset, W, \{w_1\}\}$ where w_1 is affected by COVID-19.

Clearly, (W, τ) is a TS over W .

The collection of PSs $PS(W)$ is

$$\{\{w_1\}, \{w_1, w_2\}, \{w_1, w_3\}\}.$$

Then the following PTs represents the possible ways w_1 to meet other people in W , say w_2 and w_3 , i.e, $W - \{w_1\}$.

$1\tau_p = \{\emptyset, W, \{w_1\}\}$, which indicates that w_1 does not meet others.

$2\tau_p = \{\emptyset, W, \{w_1\}, \{w_1, w_2\}\}$, which indicates that w_1 meets w_2 .

$3\tau_p = \{\emptyset, W, \{w_1\}, \{w_1, w_3\}\}$, which indicates that w_1 meets w_3 .

$4\tau_p = \{\emptyset, W, \{w_1\}, \{w_1, w_2\}, \{w_1, w_3\}\}$, which indicates that w_1 meets both w_2 and w_3 .

Thus $(W, 1\tau_p)$, $(W, 2\tau_p)$, $(W, 3\tau_p)$ and $(W, 4\tau_p)$ are PTSs over W .

Consider the PT $1\tau_p$.

Here

$$p - \text{int}(\{w_1\}) = \{w_1\}$$

$$p - \text{int}(\{w_2\}) = p - \text{int}(\{w_3\}) = \emptyset.$$

Thus w_1 is the only person who affected by COVID-19 among others in W .

Consider the PT $2\tau_p$.

Here

$$p - \text{int}(\{w_1\}) = \{w_1\}$$

$$p - \text{int}(\{w_2\}) = p - \text{int}(\{w_3\}) = \emptyset$$

$$p - \text{int}(\{w_1, w_2\}) = \{w_1, w_2\}.$$

Thus w_1 is affected by COVID-19. Also w_2 is affected by COVID-19, until w_1 meets w_2 .

Consider the PT $3\tau_p$.

Here

$$p - \text{int}(\{w_1\}) = \{w_1\}$$

$$p - \text{int}(\{w_2\}) = p - \text{int}(\{w_3\}) = \emptyset$$

$$p - \text{int}(\{w_1, w_3\}) = \{w_1, w_3\}.$$

Thus w_1 is affected by COVID-19. Also w_3 is affected by COVID-19, until w_1 meets w_3 .

Consider the PT $4\tau_p$.

Here

$$p - \text{int}(\{w_1\}) = \{w_1\}$$

$$p - \text{int}(\{w_2\}) = p - \text{int}(\{w_3\}) = \emptyset$$

$$p - \text{int}(\{w_1, w_2\}) = \{w_1, w_2\}$$

$$p - \text{int}(\{w_1, w_3\}) = \{w_1, w_3\}.$$

Thus w_1 is affected by COVID-19. Also w_2 and w_3 are affected by COVID-19, until w_1 meets both w_2 and w_3 .

Hence this problem concludes the same result while comparing to the current situation of COVID-19.





Chinnadurai and Sindhu

Separation Axioms on PTS

In this division, the separation axioms on PTS is defined as prime $T_{i=0,1,2}$ -spaces and relations among them are examined with appropriate examples.

Definition

Let (W, τ_p) be a PTS over W and $PS(W)$ be the collection of prime sets over W and $M, N \in PS(W)$. Then N is called a prime neighbourhood of M , if there exists a τ_p -OS K such that $M \subseteq K \subseteq N$.

Example

Let $W = \{w_1, w_2, w_3, w_4\}$ with a topology $\tau = \{\emptyset, W, \{w_2\}\}$.

Clearly, (W, τ) is a TS over W .

The collection of PSs $PS(W)$ is

$\{\{w_2\}, \{w_1, w_2\}, \{w_2, w_3\}, \{w_2, w_4\}, \{w_1, w_2, w_3\}, \{w_1, w_2, w_4\}, \{w_2, w_3, w_4\}\}$.

Then

$\tau_p = \{\emptyset, W, \{w_2\}, \{w_1, w_2\}, \{w_2, w_3, w_4\}\}$.

Thus (W, τ_p) is a PTS over W .

Here

$\{w_2\} \subseteq \{w_1, w_2\} \subseteq \{w_1, w_2, w_4\}$.

where

$\{w_2\}, \{w_1, w_2, w_4\} \in PS(W)$ and $\{w_1, w_2\} \in \tau_p$.

Hence $\{w_1, w_2, w_4\}$ is a prime neighborhood of $\{w_2\}$.

Definition

Let (W, τ_p) be a PTS over W . Then the singleton subset $\{w_{i \in I}\}$ of W which belongs to τ_p is said to be a prime point. Simply denoted by $w_{i \in I}$.

Example

Consider Example 5.2.

Here $\{w_2\}$ is the only singleton set belongs to τ_p .

This w_2 is a prime point.

Definition

Let (W, τ_p) be a PTS over W . Let w_i and w_j be two prime points over W . Then w_i and w_j are said to be distinct prime points if $w_i \cap w_j = \emptyset$.

Definition

Let (W, τ_p) be a PTS over W . Let w_i and w_j be two distinct prime points. Then (W, τ_p) is said to be prime T_0 -space, if there exists two τ_p -OSs G and H such that

$w_i \in G$; $w_j \cap H = \emptyset$ or

$w_j \in H$; $w_i \cap G = \emptyset$.





Chinnadurai and Sindhu

Definition

Let (W, τ_p) be a PTS over W . Let w_i and w_j be two distinct prime points. Then (W, τ_p) is said to be prime T_1 -space, if there exists two τ_p -OSs G and H such that

$$w_i \in G ; w_i \cap H = \phi \text{ and}$$

$$w_j \in H ; w_j \cap G = \phi .$$

Theorem

Every prime T_1 -space is a prime T_0 -space.

Proof. Follows from Definitions 5.6 and 5.7.

Remark

The converse of the above theorem is not true as shown in the following example.

Example

Let $W = \{w_1, w_2\}$ with a topology $\tau = \{\phi, W, \{w_1\}, \{w_2\}\}$.

Clearly, (W, τ) is a TS over W .

The collection of PSSs $PS(W)$ is

$$\{\{w_1\}, \{w_2\}, \{w_1, w_2\}\} .$$

Then

$$\tau_p = \{\phi, W, \{w_1\}, \{w_2\}\} .$$

Thus (W, τ_p) is a PTS over W .

Here w_1 and w_2 are two distinct prime points.

Thus

$$w_1 \in \{w_1, w_2\} ; w_1 \cap \{w_2\} = \phi \text{ but}$$

$$w_2 \in \{w_2\} ; w_2 \cap \{w_1, w_2\} = \{w_2\} \neq \phi .$$

Hence (W, τ_p) is a prime T_0 -space but not a prime T_1 -space.

Definition

Let (W, τ_p) be a PTS over W . Let w_i and w_j be two distinct prime points. Then (W, τ_p) is said to be prime T_2 -space, if there exists two τ_p -OSs G and H such that

$$w_i \in G, w_j \in H \text{ and } G \cap H = \phi .$$

Theorem

Every prime T_2 -space is a prime T_1 -space.

Proof. Follows from Definitions 5.7 and 5.11.

Remark

The converse of the above theorem is not true as shown in the following example.

Example

Let $W = \{w_1, w_2, w_3\}$ with a topology $\tau = \{\phi, W, \{w_2\}, \{w_1, w_3\}\}$.

Clearly, (W, τ) is a TS over W .

The collection of PSSs $PS(W)$ is

$$\{\{w_1\}, \{w_2\}, \{w_3\}, \{w_1, w_2\}, \{w_1, w_3\}, \{w_2, w_3\}\} .$$

Then





Chinnadurai and Sindhu

$$\tau_p = \{\emptyset, W, \{w_1\}, \{w_2\}, \{w_3\}, \{w_1, w_2\}, \{w_1, w_3\}, \{w_2, w_3\}\}.$$

Thus (W, τ_p) is a PTS over W .

Here

$$w_1 \in \{w_1, w_2\} ; w_1 \cap \{w_2, w_3\} = \emptyset \text{ and}$$

$$w_3 \in \{w_2, w_3\} ; w_3 \cap \{w_1, w_2\} = \emptyset .$$

But

$$\{w_1, w_2\} \cap \{w_2, w_3\} = \{w_2\} \neq \emptyset .$$

Hence (W, τ_p) is a prime T_1 -space but not a prime T_2 -space.

Theorem

Every prime T_2 -space is both prime T_1 -space and prime T_0 -space.

Proof. Follows from Definitions 5.6, 5.7 and 5.11.

Theorem 5.15 is illustrated in the following example.

Example

Let $W = \{w_1, w_2, w_3, w_4\}$ with a topology $\tau = \{\emptyset, W, \{w_1, w_3\}, \{w_2, w_4\}\}$.

Clearly, (W, τ) is a TS over W .

Thus $PS(W)$ contains all the subsets of W .

Then τ_p is a prime discrete topology and (W, τ_p) is a PTS over W .

Here

$$w_2 \in \{w_2, w_3\} ; w_2 \cap \{w_1, w_4\} = \emptyset \text{ and}$$

$$w_4 \in \{w_1, w_4\} ; w_4 \cap \{w_2, w_3\} = \emptyset .$$

Also

$$\{w_2, w_3\} \cap \{w_1, w_4\} = \emptyset .$$

Hence (W, τ_p) is a prime T_2 -space, a prime T_1 -space and a prime T_0 -space.

CONCLUSIONS

The aim of this paper is to introduce the notion of PS, and to define a topology, named as PTS. The notion of the prime interior, prime closure and prime subspace topology is also defined. Some basic theorems are stated and proved with suitable examples. Moreover, the problem of COVID-19 on PTS concludes the same result, while comparing to the current situation of COVID-19. The separation axioms on PTS is defined as prime $T_{i=0,1,2}$ -spaces, and relations among them are examined with appropriate examples. In future, this work may be extended to continuous mapping, continuous functions and open sets such as α -open sets, pre-open sets, β -open sets, etc.,

REFERENCES

1. Willard S., General Topology, Addison Wesley, London, 1970.
2. Sharma J. N., Topology, Krishna Prakasan Madir, Meerut (U. P), Fourth Edition, 1974-75.
3. Dugundji J., Topology, Allyn & Bacon Inc. Boston, 1996.
4. Aggarwal R. S., A Text Book on Topology, S Chand & Company Ltd, New Delhi, Second Edition, 1996.
5. James R., Munkers, Topology, Prentice Hall of India Private Ltd, New Delhi, Second Edition, 2000.
6. Chinnadurai, V., & Sindhu, M. P., A Novel Approach for Pairwise Separation axioms on Bi-Soft Topology Using Neutrosophic Sets and An Output Validation in Real Life Application. Neutrosophic Sets and Systems, 35, 435-463, 2020.
7. Chinnadurai, V., & Sindhu, M. P., Generalization of Level Sets in Neutrosophic Soft Sets and Points: A New Approach. Tathapi, 19(50), 54-81, 2020.





Analysis of Renal Stone Struvite Crystal and Evaluation of Antiurolithiatic Activity of Methanolic Leaf Extract of *Citrus maxima* Merr.

Surya.S¹, Naga krithika.N¹ and Priscilla Suresh^{2*}

¹Research Scholar, Department of Zoology, Bishop Heber College (Autonomous), Tiruchirappalli, Tamil Nadu, India.

²Head, Department of Zoology, Bishop Heber College (Autonomous), Tiruchirappalli, Tamil Nadu, India.

Received: 27 Aug 2020

Revised: 29 Sep 2020

Accepted: 31 Oct 2020

*Address for Correspondence

Priscilla Suresh

Head, Department of Zoology,
Bishop Heber College (Autonomous),
Tiruchirappalli, Tamil Nadu, India.
Email: priscisf@gmail.com



This is an Open Access Journal / article distributed under the terms of the **Creative Commons Attribution License** (CC BY-NC-ND 3.0) which permits unrestricted use, distribution, and reproduction in any medium, provided the original work is properly cited. All rights reserved.

ABSTRACT

The formation of urinary stones is known as urolithiasis. It is a serious debilitating problem throughout the world. Urinary stones have been found to contain calcium phosphate, calcium oxalate, uric acid and magnesium ammonium phosphate or struvite crystals. Struvite is a triple phosphate stone found more frequently in women. Urinary stones are characterized by high recurrence rate therefore requiring a preventive treatment by using the medicinal plants *Citrus maxima* leaves. The inhibitory effect of methanol extract of *Citrus maxima* leaves on the growth of struvite crystals were investigated. Struvite crystals were grown by the single diffusion gel growth technique. The weight of the formed struvite crystals were gradually reduced from 2.48 g to 0.23 g with increase in the concentration of ethanol extract of *Citrus maxima* leaves. Presence of bioactive compounds like Tannin, Phlobatannins, Alkaloids, Flavonoids, Saponins, Phenols, Steroids, Carbohydrates, Xanthoprotein, Leucoanthocyanin, Anthoquinines, Emodine, Terepenoids and Anthocyanins were confirmed by Preliminary phytochemical analysis of the rhizome extract. The struvite crystals are harvested and were characterized by Fourier Transform Infrared Spectroscopy (FTIR) to confirm the functional groups. The FTIR spectrum of harvested struvite crystals from various treatments showed shifts in bands, disappearance of existing and appearance of new peaks which indicated the activity of bioactive compounds in the extract. Results obtained are indicated that *Citrus maxima* leaves has the potential to inhibit the formation of struvite crystals.

Keywords: Urolithiasis, Struvite crystals, *Citrus maxima*, Fourier Transform Infrared Spectroscopy (FTIR).





Surya et al.,

INTRODUCTION

Urolithiasis is the formation of stones in the urinary tract. It majorly causes variable degrees of pain, bleeding, and may further leads to secondary infection. It is one among the third commonest afflictions found in humans (Selvam et al., 2001). The size and nature of crystals govern overall clinical manifestations of this complaint whereas urinary chemistry is one of the important factor in determining the type of crystals formed and the nature of macromolecules consisting of the surface of the crystals. Hence, the study of the urinary chemistry with respect to the stone-forming minerals provides a good indication of the risk of stone formation (Selvam et al., 2001). Recent decades have witnessed great advances in the surgical treatment of kidney stones. When stones were once treated with invasive open surgical techniques, in the present day almost all urinary calculi are treated either in a completely non invasive fashion with shockwave lithotripsy or in a less invasive endoscopic fashion with ureteroscopy or percutaneous nephrolithotomy (Pearle et al. 2005). While there are great advancements within the surgery of stone forming patients, efforts to stop the formation of kidney stones with medical therapy haven't experienced an equivalent rates of advance. Such a failure is disappointing. For these reasons, a proper understanding of the metabolic evaluation and medical management of a stone former is an important component of a complete urologic practice. Such techniques will often identify patient-specific factors which will be modified so as to scale back the danger for recurrent stone formation (Prezioso et al. 2007; Heilberg and Schor, 2006; Begun et al. 1997; Levy et al. 1995; Preminger, 1994; Pak et al. 1980).

Here in, we review the medical evaluation and therapy of stone formers. These chemicals are a part of the traditional diet and which are essential for the formation of bones and muscles. Once affected, the subsequent relapse rate is increased and the recurrence interval is shortened. The pharmacological treatment includes non-steroidal anti-inflammatory drugs, diuretics, Extra corporeal shock wave lithotripsy, percutaneous nephrolithotomy and ureteroscopy are the surgical treatment used to eliminate kidney stones. The treatment are costly, produce adverse effects include long term infertility and renal damage. As there are no satisfactory standard drugs in modern medicine, herbal remedies are proved to exert their effectiveness at kidney stone formation, the plant based therapy is used as adjunct therapy for better relief. *C. maxima* is taken into account as an easily recognized species thanks to variety of unable morphological characteristics, like huge leaves borne on broadly winged petioles, very large and fragrance flowers and large fruits with one embryo, while most of other Citrus species are polyembryonic (Uzun and Yesiloglu, 2012). Citrus peel is used as fodder at fisheries, raw material for traditional paper, activated carbon, cosmetic products and bio-ethanol production (Kim et al., 2008; Kim et al., 2007; Sharma et al., 2007). Likewise, volatile oil of citrus peel has been identified to exhibit antibacterial activity (Upadhyay et al., 2010; Palaka wong et al., 2010; Ayoola et al., 2008). *Citrus maxima*, the pomelo (also called pummelo or shaddock) within the Rutaceae (citrus family). Its scientific name is pomelo because it's the most important citrus. The closest in size to the present king of citrus fruits may be a grapefruit. Leaves, compound, appearing simple, having one leaflet, glandular, alternate, ovate, dotted, to elliptical, 5-20 cm long, 2- 12 cm wide and leathery. Petiole broadly winged to occasionally nearly wingless, up to 7 cm wide Orwa et al.(2009). Citrus is altogether |one amongst one in every of"> one among the foremost essential commercial fruit crops which are grown in all continents of the planet (Tao et al., 2008). This study will provide a multidisciplinary approach in characterizing urinary crystals grown in vitro and in vivo to help formulate prevention or dissolution strategies in controlling calcium urinary stone growth. This research focuses to find new alternative medicine methanol extracts of leaves of *Citrus maxima* for the treatment of urinary crystals.

MATERIAL AND METHODS

Collection of Plant Material

The leaves of *Citrus maxima* were collected in the month of September from Valparai, Tamil Nadu.





Preparation of Methanol Extracts

The leaves of *Citrus maxima* were washed in running water, cut into small pieces and then shade dried for a week at 35-40°C, after that it was grinded to a uniform powder of 40 mesh size (Doughari *et al.*, 2007). The methanol extracts were prepared by soaking 100 g of the dried powder plant materials in 1 L of methanol by using a soxhlet extractor for 10 hr continuously. The extracts were filtered through whatman filter paper No. 42 (125mm). The filtered extract was concentrated and dried by using a rotary evaporator under reduced pressure. The obtained residue 1.2 g (leaves) was used to prepare the series of (1%, 2%, 3%, 4% and 5%) methanol supernatant concentrations for *in vitro* studies (Table 1).

Growth and Characterization of Struvite Crystals

Glass test tubes were used as a crystallization apparatus and the single diffusion reaction technique was employed. One of the reactants, 0.5 M Ammonium dihydrogen phosphate (ADP), was mixed with sodium metasilicate solution the density of 1.04g/cm³ at pH9.4, so that the pH of the mixture was maintained at 6 and left undisturbed for 2-3 days. After gelation took place, the supernatant solution of 1 M Magnesium acetate was gently poured onto the set gel in various test tubes. After pouring on each supernatant solution, the test tubes were capped with airtight stopples. The experiments were conducted at room temperature (37°C). The grown struvite crystals were characterized using FTIR to verify the compound and structure of the grown crystal. FTIR was performed by Hitachi 570 FT-IR spectrophotometer technique to verify the proper formation of crystal and their purity.

Phytochemical Screening

Phytochemical screening for Tannin, Flavonoid, Terpenoid, Saponin, Phlobatanin, Steroid, Carbohydrate, Glycoside, Coumarin, Alkaloid, Protein, Emodin, Anthoquinone, Anthocyanine, Cardiac glycosides, Leucoanthocyanine, Phenol, Xanthoprotein were performed using standard procedures (Yadav M *et al.*, 2014).

Quantitative Phytochemical Analysis

Phytochemical analysis for alkaloid determination using Harborne (1973) method, Flavonoid determination by the method of Bohm and Kocipai Abyazan (1994) and Terpenoid Determination (Ferguson, 1956) were performed using standard procedures.

RESULTS

Phytochemical screening

The present study carried out on the leaves of *Citrus maxima* revealed the presence of medicinal active constituents. The phytochemical active compounds were qualitatively analyzed for leaves of *Citrus maxima*. Phytochemical compounds such as terpenoids, flavonoids, saponins, tannins, glycosides, coumarins, leucoanthocyanin, xanthoprotein are present in methanol extracts of leaves of *Citrus maxima*. phlobatanin, proteins, anthocyanins, cardiac glycosides and Phenols are absent. These eight compounds were present in methanol extracts of leaves of *Citrus maxima* (Table 2).

Quantitative analysis of active compounds in the methanolic leaf extract of *Citrus maxima*

The amount of phytochemicals which are found in the methanol extracts of leaves of *Citrus maxima* was quantitatively determined by standard procedures. Active compounds like Terpenoids, Flavonoids and Alkaloids are estimated quantitatively and the results are presented in the *Citrus maxima* leaves extract contained 0.623 g of alkaloids, 0.077 g of flavonoids, 0.29 g of terpenoids are found (Table 3).





Effect of the leaves of *Citrus maxima* on struvite crystals

Morphology of the harvested crystals after addition of leaves of *Citrus maxima* as shown in Fig. 3. The largest single struvite crystals having dimensions of 1.4cm was observed in Fig 3a. The sizes of the struvite crystals were reduced from 1.8 cm to 1.0cm at 1% concentration of extracts, 1.0 cm in 2%, 1.3 cm in 3%, 0.9cm in 4%, 0.9 cm in 5% and 0.9cm in fraction 14 were observed (Fig.3c-h). With an increase in the concentration of the leaves of *Citrus maxima* from 1% to 5% (v/v), the weight of the formed crystals were gradually reduced from 2.48 g to 0.23 g. The percentage of inhibition of Struvite crystals by the leaves of *Citrus maxima* are shown in (Table 4). In control there is 0% inhibition, In control+H₂O is 24%, In 1% is 51%, In 2% is 58.8%, In 3% is 57.8%, In 4% is 55.9%, In 5% is 74.5%, In Fraction14 is 66.7%. In the present work, Struvite crystals growth was reduced due to the inhibitory effect of the leaves of *Citrus maxima* under *in vitro* conditions.

Characterization of Struvite crystals

The FTIR spectra of Struvite crystals obtained in the presence and absence of the leaves of *C. maxima* are shown in Fig 5. In Fig 4(a), the peak at 2951 cm⁻¹ is due to the antisymmetric and symmetric stretching vibration of NH₄ units. The peak at 1604 cm⁻¹ is due to C=C group and the peak at 887cm⁻¹ is due to silicate ion. The band at 759cm⁻¹ is due to disulphide and (C-S) stretch the peak at 460 cm⁻¹ is due to ary sulfides (S-S) stretch. In Fig 4(b), the band at 2964 cm⁻¹ is due to the antisymmetric and symmetric stretching vibration of NH₄ units. The peak at 1606 cm⁻¹ is due to C=C group and the peak at 887 cm⁻¹ is due to silicate ion. The band at 760 cm⁻¹ is due to disulphide and (C-S) stretch and the peak at 460 cm⁻¹ is due to ary sulfides (S-S) stretch. In Fig. 4 (c), the band at 2374 cm⁻¹ is due to C-H stretch. The peak at 1605 cm⁻¹ is due to C=C group and the peak at 891 cm⁻¹ is due to silicate ion. The band at 760 cm⁻¹ is due to disulphide and (C-S) stretch and the peak at 460 cm⁻¹ is due to ary sulfides (S-S) stretch. In Fig 4(d), the band at 2372 cm⁻¹ is due to C-H stretch. The peak at 1676 cm⁻¹ is due to C=O group and the peak at 1435 cm⁻¹ is due to methyl C-H asymmetric and symmetric bend. The band at 1004 cm⁻¹ is due to Phosphate ion and C=O group and the peak at 759 cm⁻¹ is due to disulphide and (C-S) stretch. The peak at 460 cm⁻¹ is due to ary sulfides(S-S) stretch. In Fig 4(e), the band at 2356 cm⁻¹ is due to C-H stretch. The peak at 1679 cm⁻¹ is due to C=O group and the peak at 1435 cm⁻¹ is due to methyl C-H asymmetric and symmetric bend. The band at 892 cm⁻¹ is due to silicate ion and the peak at 571 cm⁻¹ is due to disulphide and (C-S) stretch. The peak at 440 cm⁻¹ is due to ary sulfides (S-S) stretch. In Fig 4(f), a band at and 2353 cm⁻¹ is due to C-H stretch. The peak at 1680 cm⁻¹ is due to C=O group and the peak at 1435 cm⁻¹ is due to methyl C-H asymmetric and symmetric bend. The band at 1002 cm⁻¹ is due to Phosphate ion and C=O group and the peak at 789 cm⁻¹ is due to disulphide and (C-S) stretch. In Fig 4(g), the band at and 2385 cm⁻¹ is due to C-H stretch. The peak at 1680 cm⁻¹ is due to C=O group and the peak at 1435 cm⁻¹ is due to methyl C-H asymmetric and symmetric bend. The band at 891 cm⁻¹ is due to silicate ion and the peak at 439 cm⁻¹ is due to ary sulfides(S-S) stretch. In Fig 4(h), the band at and 2367 cm⁻¹ is due to C-H stretch. The peak at 1603 cm⁻¹ is due to C=C group and the peak at 1434 cm⁻¹ is due to methyl C-H asymmetric and symmetric bend. The band at 988 cm⁻¹ is due to silicate ion and the peak at 459 cm⁻¹ is due to ary sulfides(S-S) stretch. Crystallization characterization of struvite crystals treated with the leaves of *Citrus maxima* was observed using FTIR techniques. In Control peak at 2951 cm⁻¹ is due to the antisymmetric and symmetric stretching vibration of NH₄ units. The peak at 1604 cm⁻¹ is due to C=C group. As there is increase in the inhibitory effect of struvite crystals when treated with the leaves of *Citrus maxima* at 5% methanolic extract, the band at 2951cm⁻¹ is shifted to 2385 cm⁻¹ is due to C-H stretch. The peak at 1604cm⁻¹ is shifted to 1680 cm⁻¹ is due to C=O group. The shifting further supports that the can promote the formation of triple phosphate crystals and reduce the nucleation rate of struvite crystals as compared with collected fractions.

DISCUSSION

The different kinds of phytochemicals have been found to possess a wide range of activities, which may help in protection against chronic diseases. For example, alkaloids protect against chronic diseases. Saponins protect against hypercholesterolemia and antibiotic properties. Steroids and terpenoids show the analgesic properties. The steroids and saponins were responsible for central nervous system activities (Gracelin et al., 2013). The most important of





Surya et al.,

alkaloids, saponins and tannins in various antibiotics used in treating common pathogenic strains has recently been reported by (Kubmarawa, 2007; Mensah, 2008) reports alkaloids in 12 leafy vegetables studied. The ethanolic and aqueous extracts showed the presence of flavonoids, carbohydrates, phenolic compounds and sterols were the major phytoconstituents. In the present study methanol extracts of leaves of *C.maxima* are screened for phytochemical analysis. Pragada et al. (2011) carried out then Preliminary work of phytochemical analysis and quantification of total phenols, in-vitro antioxidant and antibacterial activities of the hydro alcoholic (70% ethanol) extract of *Acalypha indica*. Ramamoorthy et al. (2011) screened the methanol extract of roots of *Gentiana kurroo*. As there is increase in the inhibitory effect of struvite crystals when treated with the leaves of *Citrus maxima* at 5% methanolic extract, the band at 2951cm⁻¹ is shifted to 2385 cm⁻¹ is due to C-H stretch. The peak at 1604cm⁻¹ is shifted to 1680 cm⁻¹ is due to C=O group. The shifting further supports that the can promote the formation of triple phosphate crystals and reduce the nucleation rate of struvite crystals as compared with collected fractions. This result mentioned that distilled water did not show any inhibitory activity with regard to crystal growth, where as the methanol extract of leaves of *C. maxima* possessed inhibitory activity due to the presence of bioorganic molecules diterpenes such as calcaratarins, sesquiterpenes such as shyobunone and coumarins such as herniarin. This study confirmed that the leaves of *C.maxima* methanolic extracts can promote the formation of hydroxyapatite crystals and treat urinary stone by inhibiting the formation of struvite crystals, a major component of calcium urinary stone. Presently, growth inhibition studies of Struvite crystals in the presence of some of the herbal extracts (Ahmed Bensatal and Ouahrani, 2008; Chauhan et al., 2009; Chauhan and Joshi, 2008) were attempted in literature. In the recent work, Struvite crystals growth was reduced due to the inhibitory effect of the leaves of *C.maxima* under in vitro conditions.

Citrus maxima leaves can exhibit antioxidant activity because of the presence of phytochemical such as alkaloids, terpenoids and flavonoids in the plant extract. *C. maxima* can proved to exhibit anti-microbial activity toward several microorganism strains. The factors which can affect the antimicrobial activity such as resistance of tested bacterial strains, variation of temperature of preparation condition and low concentration of phytochemical present in the plant extract (Naeem Hasan Khan, et al.,2018).In this study the presence of these active phytochemicals also showed inhibitory effect or anti urolithiatic activity towards struvite crystals that is kidney stone formation. Ragavendran et al. (2011) the functional groups of carboxylic acids, amines, amides, sulphur derivatives, polysaccharides, organic hydrocarbons, halogens that are responsible for various medicinal properties of *Aerva lanata*. Thangarajan Starlin et al. (2012), while analyzing the ethanolic extracts of *Ichnocarpus frutescens*, by FTIR, functional group components of amino acids, amides, amines, carboxylic acid, carbonyl compounds, organic hydrocarbons and halogens. The functional groups are observed in the extracts, OH group was found to be present uniformly only in the methanol extracts of all plants. As OH group has got the ability of forming hydrogen bonding capacity, presence of OH group particularly in methanol extract of leaves of *Citrus maxima* probably indicates the higher potential of methanol extract towards inhibitory activity against struvite crystals. the high level of antimicrobial activity of methanol extracts of leaf of all those four plants have been already demonstrated (Ashok kumar and Ramaswamy, 2013) together with low IC50 value (Ashok kumar and Ramaswamy, 2013). Crystallization characterization of struvite crystals treated with the leaves of *Citrus maxima* was observed using FTIR techniques. In Control peak at 2951 cm⁻¹ is due to the antisymmetric and symmetric stretching vibration of NH₄ units. The peak at 1604 cm⁻¹ is due to C=C group. As there is increase in the inhibitory effect of struvite crystals when treated with the leaves of *Citrus maxima*, the band at 2951cm⁻¹ is shifted to 2385 cm⁻¹ is due to C-H stretch. The peak at 1604cm⁻¹ is shifted to 1680 cm⁻¹ is due to C=O group. The shifting further supports that the can promote the formation of triple phosphate crystals and reduce the nucleation rate of struvite crystals as compared with collected fractions.

REFERENCES

1. Ashok kumar, R., and Ramaswamy, M. 2013. Comparative study on the antimicrobial activity of leaf extracts of four selected Indian medicinal plants against *Pseudomonas aeruginosa*, *Pseudomonas fluorescens*, *Penicillium chrysogenum* and *Penicillium restrictum*. Journal of Chemical, Biological and Physical Sciences. 3(2): 1376-1381.





Surya et al.,

2. Ashokkumar, R., and Ramaswamy, M. 2013. Determination of DPPH free radical scavenging oxidation effects of methanolic leaf extracts of some Indian medicinal plant species. *Journal of Chemical, Biological and Physical Sciences*. 3(2): 1273-1278.
3. Ayoola GA, Johnson OO, Adelowotan T, Aibinu IE, Adenipekun E, Adepoju AA, Bello-Coker HAB and Odugbemi TO (2008). Evaluation of the chemical constituents and the anti-microbial activity of the volatile oil of *Citrus reticulata* fruit (Tangerine fruit peel) from South West Nigeria. *Afr. J. Biotechnol.*, **7**(13): 2227-2231.
4. Beghalia, M. Ghalem, S. Allali, H. Belouatek, A. Marouf, A. 2007. Effect of herbal extracts of *Tetraclinis articulata* and *Chamaerops humilison* Calcium oxalate crystals *in vitro*. *Gomal J. Med. Sci.*, Vol. 5(2), pp. 55-58.
5. Begun, F.P., Foley, W.D., Peterson, A. and White, B. (1997) Patient evaluation laboratory and imaging studies, In: Resnick, M. (ed.). *The Urologic Clinics of North America, Urolithiasis*, Vol. 24, W.B. Saunders Company: Philadelphia, PA, pp. 97_116.
6. Boham, B.A. and Kocipai-Abyazan. R. Flavonoids and condensed tannins from leaves of *Vaccinium vaticulatum* and *V. calycinium*. *Pacific Science*, 48:458-463(1994)
7. Chauhan, C.K. and Joshi, M.J. 2008. Growth inhibition of Struvite crystals in the presence of juice of *Citrus medica* Linn. *Urol. Res.*, DOI: 10.1007/s00240-008-0154-4.
8. Ferguson, N.M. (1956). *A Text book of Pharmacognosy*. Mac Milan Company, New Delhi. pp. 191
9. Heilberg, I.P. and Schor, N. (2006) Renal stone disease: causes, evaluation, and medical treatment. *Arq Bras EndocrinolMetab* 50: 823_831.
10. Kim HG, Lim HA, Kim SY, Kang SS, Lee HY and Yun PY (2007). Development of functional Hanji added citrus peel. *J. Korea Tappi.*, **9**: 38-47.
11. Kim JY, Oh TH, Kim BJ, Kim SS, Lee NH and Hyun CG (2008). Chemical composition and anti-inflammatory effects of essential oil from *Faefugium japonicum* flower. *J. Oleo Sci.*, **57**: 623-628.
12. Levy, F.L., Adams-Huet, B. and Pak, C.Y.C. (1995) Ambulatory evaluation of nephrolithiasis: an update of a 1980 protocol. *Am J Med* 98: 50_59.
13. Lotan, Y., Cadeddu, J.A. and Pearle, M.S. (2005) International comparison of cost effectiveness of medical management strategies for nephrolithiasis. *Urol Res* 33: 223_230.
14. NaeemHasan Khan, Chin jiaQian, Nabila Perveen 2018. Phytochemical screening, antimicrobial and antioxidant activity determination of *Citrus maxima* peel.
15. Orwa et al. (2009) *Citrus maxima*. http://www.worldagroforestry.org/treedb/AFTPDFS/Citrus_maxima.PDF. Cited 1 Apr 2017.
16. Pak, C.Y.C., Britton, F., Peterson, R., Ward, D., Northcutt, C., Breslau, N.A. et al. (1980) Ambulatory evaluation of nephrolithiasis. Classification, clinical presentation and diagnostic criteria. *Am J Med* 69: 19_30
17. Palakawong C, Sophanodora P, Pisuchpen S and Phongpaichit S (2010). Anti-oxidant and anti-microbial activities of crude extracts from mangosteen (*Garcinia mangostana* L) parts and some essential oils. *Int. FoodRes. J.*, **17**: 583-589
18. Pearle, M.S., Calhoun, E.A. and Curhan, G.C., for the Urologic Disease of America Project (2005) Urologic Diseases in America Project: urolithiasis. *J Urol* 173: 848_857.
19. Preminger, G.M. (1994) Medical evaluation and treatment of nephrolithiasis. *SeminUrol* 12: 51.
20. Prezioso, D., Di Martino, M., Galasso, R. and Iapicca, G. (2007) Laboratory assessment. *UrolInt* 79(Suppl 1): 20_25.
21. Ragavendran, P., Sophia, D., Arul Raj, C., and Gopalakrishnan V.K., 2011. Functional group analysis of various extracts of *Aervalanata* (L.) by FTIR spectrum. *Pharmacology online*. 1, 358-364
22. Selvam, R. Kalaiselvi, P. Govindaraj, A. Balamurugan, V. and Satish Kumar, A.S. 2016. Effect of *Aervalanata* leaf extract and vediuppuchunnam on the urinary risk factors of calcium oxalate urolithiasis during experimental hyperoxaluria. *Pharmacol. Res.*, Vol. 43, pp. 89-93.
23. Sharma N, Kalra KL, Oberoi HS and Bansal S (2007). Optimization of fermentation parameters for production of ethanol from kin now waste and banana peels by simultaneous saccharification and fermentation. *Indian J. Microbiol.*, **47**: 310-316.
24. Tao N-guo, Liu Y-jin, Zhang J-hong, Zeng H-yan, Tang Y-fang and Zhang M-ling (2008). Chemical composition of essential oil from the peel of Satsuma mandarin. *Afr. J. Biotechnol.*, **7**: 1261-1264





Surya et al.,

25. Thangarajan Starlin, Paramasivam Ragavendran, Chinthamony Arul Raj, Palanisamy Chella Perumal and Velliur Kannappan Gopalakrishnan. 2012. Element and Functional Group Analysis of *Ichnocarpus frutescens* R. Br. (Apocynaceae). International Journal of Pharmacy and Pharmaceutical Sciences. 4(5): 343-345.
26. Upadhyay RK, Dwivedi P and Ahmad S (2010). screening of anti-bacterial activity of six plant essential oils against pathogenic bacterial strains. *Asian J. Med.Sci.*, 2: 152-158.
27. Uzun, A. and T. Yesiloglu, (2012). Genetic Diversity in Citrus. In: Genetic Diversity in Plants, Caliskan, M.(Ed.), InTech: 213-231
28. Yadav, J.K. Singhvi, A.N. and Sharma, N. 2014. Indigenous herbomineral drug calcury. *Med.Surg.* Vol.21, pp. 15-18.

Table 1: Supernatant solutions added to the set gels for struvite crystals.

Supernatant Solutions (SS) (Groups & Treatments)	Compositions
I (Control)	10 ml of 1 M magnesium acetate
II (Distilled water)	5 ml of 1 M magnesium acetate +5 ml of distilled water
III (1% methanol extract)	5 ml of 1 M magnesium acetate +5 ml of 1% of methanol extract of leaves of <i>Citrus maxima</i> separately
IV (2% methanol extract)	5 ml of 1 M magnesium acetate +5 ml of 2% of methanol extract of leaves of <i>Citrus maxima</i> separately
V (3% methanol extract)	5 ml of 1 M magnesium acetate +5 ml of 3% of methanol extract of leaves of <i>Citrus maxima</i> separately
VI (4% methanol extract)	5 ml of 1 M magnesium acetate +5 ml of 4% of methanol extract of leaves of <i>Citrus maxima</i> separately
VII (5% methanol extract)	5 ml of 1 M magnesium acetate 5 ml of 5% of methanol extract of leaves of <i>Citrus maxima</i> separately
VIII (Fraction 14 methanol extract)	5 ml of 1 M magnesium acetate +5 ml fraction 14 with methanol extract of leaves of <i>Citrus maxima</i> separately

Calculation of the percentage of inhibition (1%) was based on the formula:

$$1\% = [(TSI - TAI)] / TSI \times 100$$

TSI represents the number of crystals without inhibitors and TAI the number of crystals after addition of inhibitors (Beghalia et al., 2007).

Table 2: Qualitative phytochemical analysis of methanol extract of leaves of *Citrus maxima*

S.NO	Phytochemical constituents	Methanol extracts of leaves of <i>Citrus maxima</i>
1.	Terpenoids	+
2.	Flavonoids	+
3.	Saponins	+
4.	Tannins	+
5.	Steroids	-
6.	Glycosides	+
7.	Phlobatannins	-
8.	Proteins	-
9.	Coumarins	+
10.	Anthocyanins	-
11.	Leucoanthocyanin	+
12.	Cardiac glycosides	-
13.	Xanthoprotein	+
14.	Phenols	-





Table 3: Quantitative Phytochemical analysis

S. No	Bioactive Compounds	Wt. of the bioactive Compounds
1.	Alkaloids	0.6 g m
2.	Flavonoids	0.07 gm
3.	Terpenoids	0.29 gm

Table 4: Measurement and Percentage of inhibition of struvite crystals

CRYSTAL	GROUP	TREATMENT	PERCENTAGE OF INHIBITION	Mean (gm)±SD
Struvite	A	Control	0%	2.46±0.0623
	B	Control+ Dis H ₂ O	17.1%	2.06±0.0612
	C	Control+1% extracts	20.4%	1.93±0.0588
	D	Control+2% extracts	38%	1.53±0.0432
	E	Control+3% extracts	49%	1.24±0.0368
	F	Control+4% extracts	61.6%	0.93±0.0286
	G	Control+5%extracts	87.3%	0.31±0.0205
	H	Control+ fraction 14	82.8%	0.40±0.0326



Fig.1. Citrus maxima plant

Fig. 2. Citrus maxima leaf powder

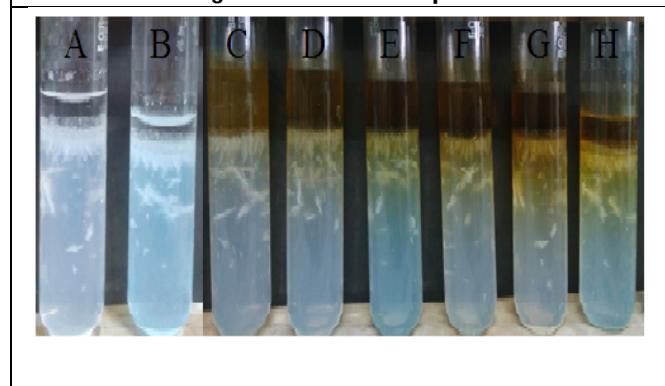


Fig.3.The effect of leaves of *Citrus maxima* on struvite crystals in the gel method (A) without any additive (B) with the distilled water (C) with the 1% extract (D) with the 2% extract (E) with the 3% extract (F) with the 4% extract (G) with the 5% extract (H) with the fraction 14 on 28th day.

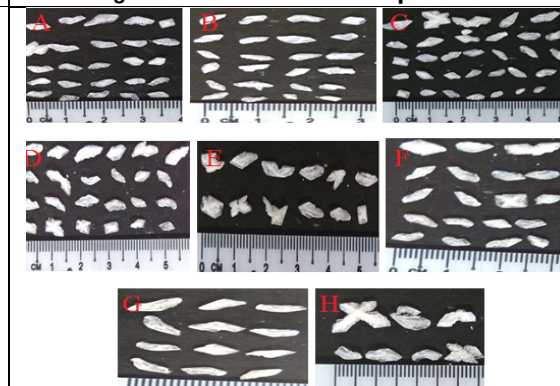


Fig.4. The measurement of struvite crystals obtained from leaves of *Citrus maxima* on struvite crystals in the gel method (A) without any additive (B) with the distilled water (C) with the 1% extract (D) with the 2% extract (E) with the 3% extract (F) with the 4% extract (G) with the 5% extract (H) with the fraction 14 on 28th day.





Surya et al.,

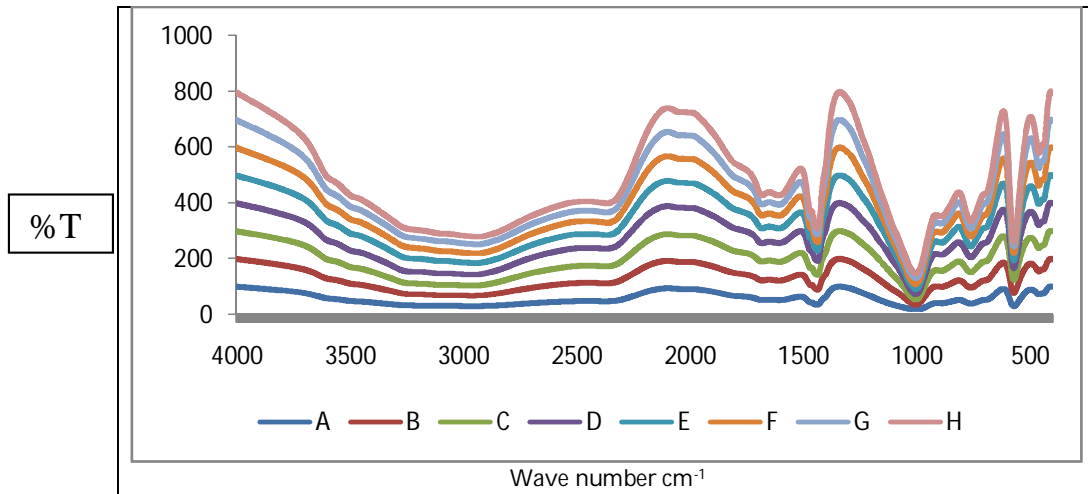


Fig.5. FTIR Characterization of Crystals comparing control and 5% of methanolic extract of *Citrus maxima*.





Signal Source Separation using PCA-ICA Method from Real Time Generated Signal

Sudhansu Kumar Samal^{1*}, Anjan Kumar Sahoo² and Anshuman Nayak³

¹Department of Electrical and Electronics Engineering, Centurion University of Technology and Management, Bhubaneswar, Odisha, India.

²Department of Electrical and Electronics Engineering, College of Engineering, Bhubaneswar, Odisha, India.

Received: 14 Aug 2020

Revised: 17 Sep 2020

Accepted: 20 Oct 2020

*Address for Correspondence

Sudhansu Kumar Samal

Department of Electrical and Electronics Engineering,
Centurion University of Technology and Management,
Bhubaneswar, Odisha, India
Email: sudhansu.samal@cutm.ac.in



This is an Open Access Journal / article distributed under the terms of the **Creative Commons Attribution License** (CC BY-NC-ND 3.0) which permits unrestricted use, distribution, and reproduction in any medium, provided the original work is properly cited. All rights reserved.

ABSTRACT

Partition of music/voice signals is a fascinating and troublesome issue. In this exploration work I have prepared a sound sign utilizing distinctive dynamic channel, assessed its range utilizing FFT calculation, additionally apply postpone work. Primary thought of applying channel is to expel the clamor and PCA-ICA has been utilized music/voice partition. As needs be, another partition calculation is actualized. The principle thought is to get familiar with a channel structure for every music signal in the blend, and afterward channel the signs by utilizing these models to recognize various signs. Test results show that a high as well as a fairly decent emotional sound quality. Smother vocals from ambient sounds in single-source tunes. Concealment performing voice from music backup is extremely valuable in numerous applications, for example, verses acknowledgment and arrangement, and music data recovery. Even though performing voice partition has been little explored. Our framework comprises of three phases. The performing voice identification stage segment and arranges a contribution to vocal and non-vocal bit. For vocal segments, the dominating pitch recognition stage distinguishes the pitch of the performing voice and afterward the concealment stage utilizes the recognized pitch to bunch the time-recurrence portions of the performing voice. Quantitative outcomes show that the framework plays out the concealment task effectively.

Keywords: ICA-PCA, echo, music signal separation, spectrum, reverb play, cancel vocals.





INTRODUCTION

Literature Review

Isolating voice and music from singing is a helpful innovation these days, as it has reasonable vocalist needs, song extraction utilizing defer work, invert capacity, channels and ICA parts. In particular, when individuals need to chime in with music without unique vocals, voice and music partition could process the first blend of sound and give us the music aide.

Contributions and novelties

There are many ways and algorithm to separate singing voice and music. For example, low-pass filtering is one way to achieve goal. The low-pass filtering could barely separate the singing voice from music. As for other complex algorithm, robust principal component analysis and predominant pitch detection are also achieved the separation of singing voice and music. This report is based on the simple rationale. Repetition is the basic of music and one big difference between the vocals and music is that the music. In this report, the algorithm based on analysis the structure of music is implemented to separate the singing voice and music. The core repeating music Background by cancelling the non-repeating elements. The idea is to find the repeating patterns in the audio and extract the original music signal. This algorithm shows its superiority since it does not depend on particular features of audio and not rely on complicate frameworks. This method can be potentially applied to any audio, as long as there exists the structure. Therefore, it advantages to fast, blind, and completely automatic.

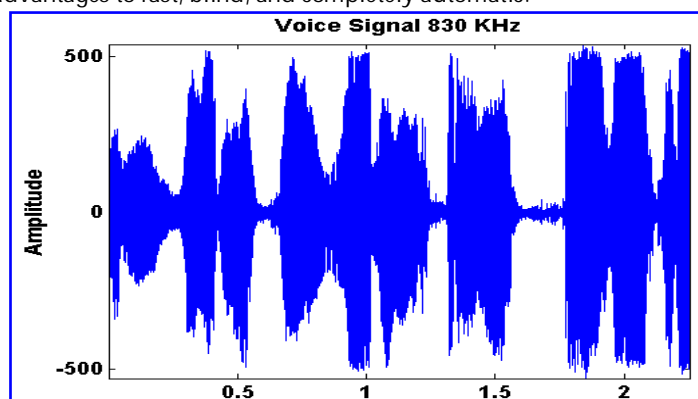


Figure 1. Generated Voice Signal

Paper layout

The rest of the paper is arranged as follows. Section 2 gives a working model of music and voice recognition system. Section 3 reviews the configuration principle component analysis and incremented component analysis and its application to recognize the music and voice algorithm. Section 4 provides the properties of the music algorithm used. Section 5 describes the result and Discussions about proposed approach used for modes estimation in power system. Section 6 gives the conclusion and future work related to present work.

Working Model

The Repeating Pattern in Music Background

The repeating pattern in music background and non-repeating pattern in voice from the wave plot of the signals. The signals of voice, music and mixture audio. In voice signal since the voice signal varies. In mixture signal, although it is made up with voice signal and music signal, we could still see the structures in it.





Sudhansu Kumar Samal et al.

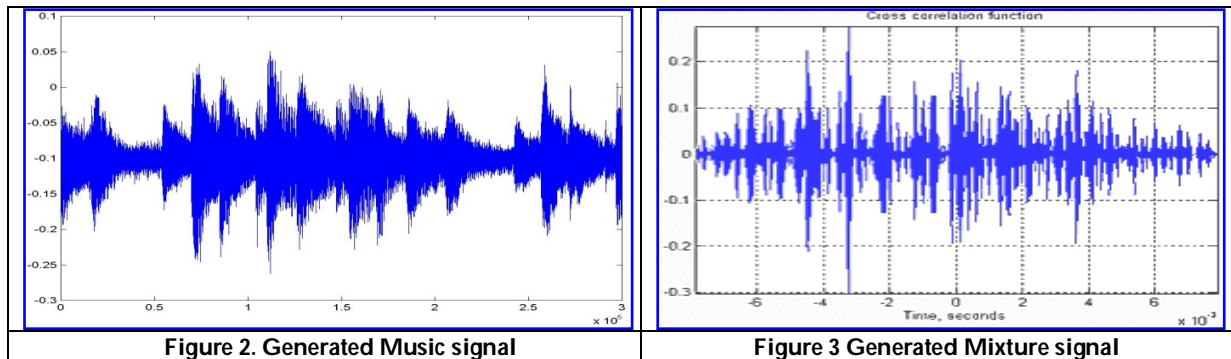


Figure 2. Generated Music signal

Figure 3 Generated Mixture signal

The Delay

A defer impact takes a sound sign in its most straightforward structure, and plays it back after a postpone time. This reverberation gadget, it is in any case known, produces a solitary duplicate of the information, which is deferred by a few microseconds to a few seconds anyplace. The utilization of criticism control, which takes the yield of the postponement and sends it back to the info, commonly in the wake of duplicating by an increase not exactly or equivalent to one, creates an all the more intriguing sound. This permits the sound to be rehashed and once more, bit by bit lessened with each progressive circle. Hypothetically, input can be utilized to create a sound that proceeds always, however eventually practically speaking the sound level will fall beneath that of the framework's sound processing range.

Audio Source Separation

People have a wonderful ability to expel from a discernible scene a visual wellspring of intrigue. This regular assignment can be completed progressively by the human cerebrum utilizing just the data obtained from a couple of sensors, for example, our ears. Envision the situation of going down with a companion on a bustling path. Our ears record an enormous exhibit of sound sources: traffic clamor, others talking, a companion visiting, and ringing phones. Partition of the sound source might be depicted as the issue of breaking down a genuine sound blend (sound-related scene) into singular sound things. The principle target of this report is the robotized examination utilizing a PC which catches a sound-related scene through various sensors.

Blind Source Separation

Blind source separation, unlike CASA and beam forming, is a statistical technique that draws inspiration neither from the functioning mechanism nor from the auditory scene geometry. Blind source separation systems can classify sound artifacts, simply by analyzing the audio sources' general statistical profile. There is no a priori knowledge available in blind separation regarding the exact statistical distributions of the source signals; no available information about the nature of the process by which the source signals were combined. Independent Component Analysis (ICA) is a special case of separating blind sources.

Butterworth filter

Filters are also used as the components of electronic circuits. The two main types of filters are active and passive filters based on the nature of the components used. Passive filters, including L, C and R, are made of passive components. In addition to passive components an active filter also contains one or more active components. Different L, C, and R combinations result in LC, RC, and some filters. Furthermore, these filters are categorized according to the spectrum of frequencies they attenuate. Four such classifications exist, namely Low Pass Filter (LPF), High Pass Filter (HPF), Band Pass Filter (BPF), and Band Reject Filter (BRF).





Sudhansu Kumar Samal et al.

Source Separation Algorithm

ICA/PCA Identification Approach

Independent Component Analysis (ICA)/Principal Component Analysis (PCA) is also extensively used for separating sound sources. ICA estimates source data from observed data that have an instantaneous or convoluted representation of the mixture only on the assumption that sources are statistically independent. ICA was previously used in combination with microphone arrays to separate a few (about 2–4) speech signals, since ICA requires the number of observations, i.e. microphones, to be equal to or greater than the number of sources. However, typical musical audio signals are recorded in stereo, and in most sections of the musical pieces more than two musical instrument sounds are performed. To understand ICA, let's discuss the famous problem with the cocktail party. Imagine where two people speak simultaneously in two different locations, using two microphones. The microphones give you two registered signals, which we could denote with $x_1(t)$ and $x_2(t)$ with x_1 and x_2 the signal amplitudes and the corresponding time index with 't'. Each of these signals recorded is a mixture (weighted sum) of the voice signals emitted by two speakers denoted by $s_1(t)$ and $s_2(t)$. BSS assumes linear blending and is expressed as linear equation.

$$x_1(t) = a_{11}s_1(t) + a_{12}s_2(t) \dots\dots\dots(1)$$

$$x_2(t) = a_{21}s_1(t) + a_{22}s_2(t) \dots\dots\dots(2)$$

The a_{11} , a_{12} , a_{21} and a_{22} parameters depend on the distance of microphones from the speakers and the response in the room. BSS shall measure the two speech signals $s_1(t)$ and $s_2(t)$ using only the recordings (mixes) or findings $x_1(t)$ and $x_2(t)$. We can write equation without loss of generality as blind source separation method.

$$x(t) = As(t) \dots\dots\dots(3)$$

ICA (Independent Component Analysis) uses the assumption of statistical independence between source signals to estimate the source and coefficients of the mixing matrix. The sources include ECG signals in our system, as well as different noise elements, such as white Gaussian noise, impulse, and flicker and Rayleigh noise. In ICA the detected signals are believed to be at least as similar as the sources.



Principal analysis of the elements. It is a way to identify data patterns, and to express the data in a way that highlights their similarities and differences. Number of dimensions reduced.

Role of Sound Recognition

The onset time estimation is an important role in instrument sound recognition. The aim of this task is to estimate the start time in the audio signal for each sound of the musical instrument. Different initial time prediction methods are proposed: based on a sharp rise in magnitude at the beginning time and based on a harmonic shift at the beginning time of the pitched sounds. These methods can recognize the initial time of audio signals with a simple rhythm, equally spaced rhythm, while the actual musical pieces sometimes have complex patterns of initiation.

Units

Tonality

Tone implies the unadulterated sinusoidal waveform, or a solitary symphonious of an occasional sign, without pitches. Music will in general comprise of a variety of tones, each with remarkable symphonious dispersion. Regardless of the kind of music or instruments [7, 8, 9], this example is steady. While in discourse the tonality of his voice is of extraordinary concern.





Sudhansu Kumar Samal et al.

Bandwidth

Discourse ordinarily has 90 percent of its capacity assembled at frequencies underneath 4 kHz (and constrained to 8 kHz), while music can reach out at 20 kHz through the maximum furthest reaches of the reaction of the ear. The greater part of the significant force in the music waveforms is commonly amassed at lower frequencies [8, 10].

Power distribution

The force circulation in the force unearthly scope of the discourse signal is not the same as the music signal; normally the intensity of discourse accumulate at low frequencies and falls quickly into the higher recurrence esteems without the DC esteem, though the music range doesn't have a specific shape and at times it incorporates DC.

Tonal duration

In discourse, the span of vowels is standard, after the syllabic rate. Music displays a more noteworthy variety in tone lengths, not being confined by the explanation procedure. In this manner tonal length would potentially be a decent discriminator.

Energy sequences

Reasonable speculation is that discourse follows an example of high-vitality voicing conditions joined by low-vitality conditions which are less inclined to be shown in the music envelope.

Equations

Ica Algorithm: Given; $x_1(t), x_2(t), x_3(t)$

Want to find: $s_1(t), s_2(t), s_3(t)$

$$x_1(t) = a_{11} s_1(t) + a_{12} s_2(t) + a_{13} s_3(t) \dots\dots\dots(4)$$

$$x_2(t) = a_{21} s_1(t) + a_{22} s_2(t) + a_{23} s_3(t) \Leftrightarrow X = AS \quad (4) \dots\dots\dots(5)$$

$$x_3(t) = a_{31} s_1(t) + a_{32} s_2(t) + a_{33} s_3(t) \dots\dots\dots(6)$$

PCA Algorithm: eigenvectors: 0.7352 0.6779

Given resulted principle components are **0.6779, 0.7352**.

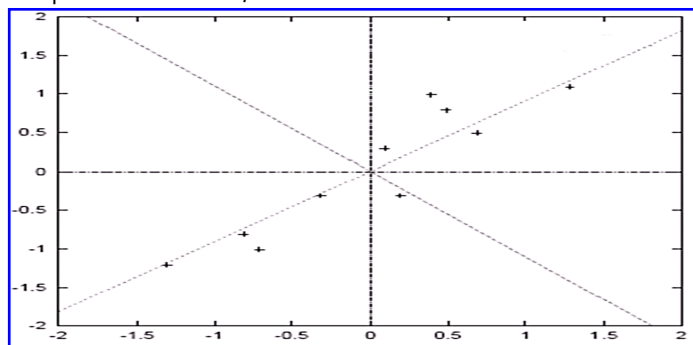


Figure 4. Eigen Vectors Distributions

Music Generation

Tone is the most significant part of sound in music. Two sorts of tone structures exist: a basic tone framed by a solitary sinusoidal waveform and a mind boggling tone produced by more than one consonant [11, 12]. The tone quality relies upon how little segments of non-consonant frequencies are. All old style melodic tones originate from a reverberation recurrence of the instrument's moving or frictional parts and a few tones originate from the reverberation tube with the exception of electronic music that creates its tone dependent on electromagnetic power.





Sudhansu Kumar Samal et al.

Partials are not a numerous of the major recurrence of any non-symphonious recurrence segments. Makers of instruments are trying to curtail partials. By creating wide band tones, covering every perceptible band [13], they attempt to make every single melodic sound built of just music with less-incomplete tones. Notwithstanding, all instruments normally create partials which are not amicably associated with the central recurrence. What's more, spectra with instruments have prompted another idea in the relationship of sound to clarify contrasts in tonal quality. This idea expects that the sound range of a given instrument is described by a specific symphonious structure, which would in a perfect world be the equivalent for each tone of the instrument.

MUSIC PROPERTIES USED

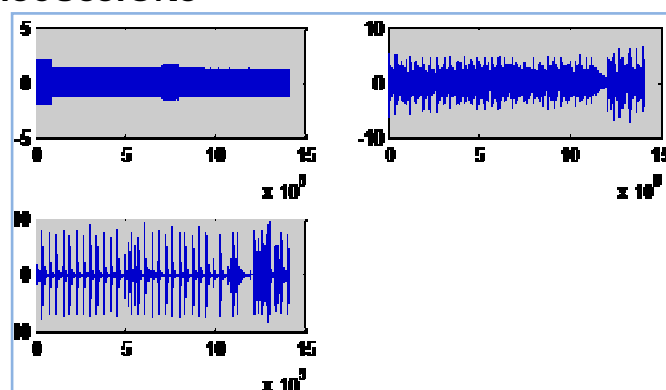
Music Range

It has double the discussion range transfer speed. The majority of the sign force in sound waveform (discourse or music) is commonly gathered at lower frequencies. The attributes of the music rely upon the sort of instruments played and its physical measurements. Artists and melodist separate the symphonious minor into eight sections, every one of which is called octave and every octave is isolated into seven sections (tones) [3]. Named as (Do, Re, Me, Fa, in this way, La and Se) or essentially (A, B, C, D, E, F, and G). This variety is rendered by recurrence of sound. A tempered size of various instruments. The primary octave tone (A1) has the fundamental recurrence of the main tone in every octave, implying that every first tone takes the decreased recurrence of the principal octave tone (for example $A = 2nA1$ or $Bn = 2nB1$). Each tone has its own recurrence in one octave and the instrument needs to create a tone around its specific recurrence. Taking a gander at the tempered scale, we note that at 4186 Hz, which the most noteworthy recurrence is utilized in human sound, the most elevated tone C8 is at. This implies instrument producers are attempting their best to tie music recurrence to the sound furthest reaches of the individual so as to accomplish solid accord [4, 5, 6]. The musical instruments in the real world cover more than an audible band (approx. 20 kHz).

Vocal Source Separation

A major problem experienced when conducting experiments on source separation is assessment of the separation efficiency of the individual sources. A good measure which describes the quality of source separation and which adheres well to auditory perception due to information loss in the analysis process is difficult to come up with. In our case, the performance problem is to some degree mitigated with an application that tries to extract the melody from the separate monophonic vocal track.

RESULTS AND DISCUSSIONS

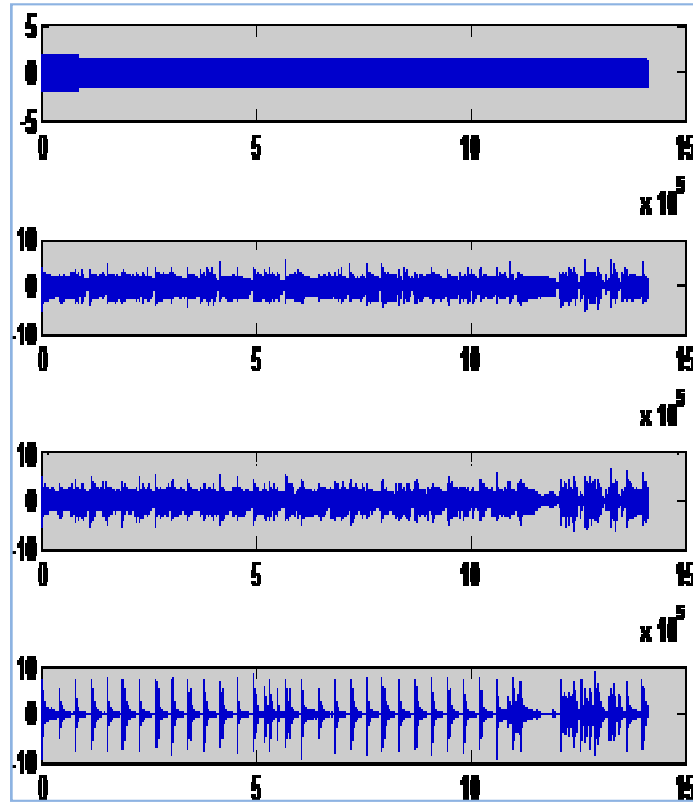


(a)





Sudhansu Kumar Samal et al.



(b)

Figure 5. Composite Musical Sounds a. Drum bass and b.guitar signals

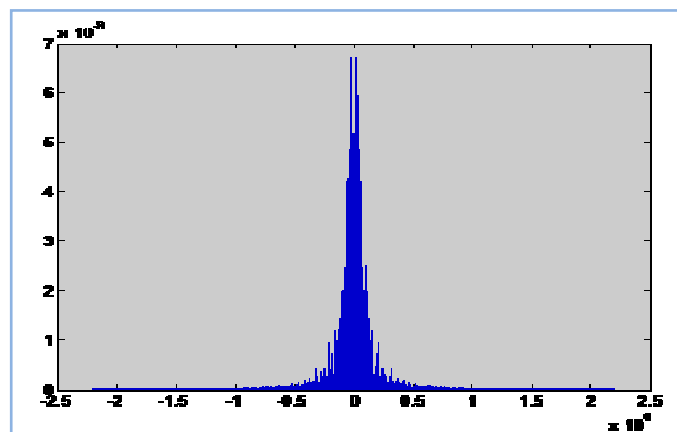


Figure 6. Road Music File Spectrums





Sudhansu Kumar Samal *et al.*

CONCLUSION AND FUTURE SCOPE

Outcome of the research

As a result, in recent day's music separation systems are getting more and more important. It is used in a lot of area. For example, some newer cellular phones include music separation that allows utterances such as "cell home". Our goal was to separate a complex audio mixture into each musical instrument sound, to develop a functional audio player, INTER, and to apply INTER to query-by-example music information retrieval. To achieve this, we focused on two aspects of sound source separation:

- (1) Separation of both harmonic and inharmonic musical instrument sounds and
- (2) Separation of complex musical audio signals.

Future Scope of the research

The research for the future leads to be focused on the large IEEE standard systems and also the adaptive filter should be properly tuned. Physical behavior of the simulation should be tested.

REFERENCES

1. Downie, J. Stephen. "Music information retrieval." Annual review of information science and technology 37, no. 1 (2003): 295-340.
2. Li, Yipeng, and DeLiang Wang. "Separation of singing voice from music accompaniment for monaural recordings." IEEE Transactions on Audio, Speech, and Language Processing 15, no. 4 (2007): 1475-1487.
3. Al-Shoshan, Abdullah I. "Speech and music classification and separation: a review." Journal of King Saud University-Engineering Sciences 19, no. 1 (2006): 95-132.
4. Bateman, W. Introduction to Computer Music. NeYork: John Wiley & Sons, (1984).
5. Pierce, J. R. The Science of Musical Sound. 3rd ed., York, USA: W.H. Freeman and Company, (1996).
6. Lerdahl, Fred, and Ray S. Jackendoff. A generative theory of tonal music. MIT press, (1996).
7. Stevens, Catherine, J. Wiles, M. Mozer, P. Smolensky, D. Touretsky, J. Elman, and A. S. Wcigend. "Representations of tonal music: A case study in the development of temporal relationship." In Proceedings of the 1993 Connectionist Models Summer School, pp. 228-235. Psychology Press, (1994).
8. Griffith, N. and Todd, P. M. Musical Networks. Bradford Books, Cambridge, MA, USA: The MIT Press, (1999).
9. Monelle, R. Linguistics and Semiotics in Music. Chur, Switzerland: Harwood Academic Publishers, (1992).
10. Feiten, Frank. "Ungvary.(1991)."Organization of sounds with neural nets "." In Proc. International Computer Music Conference. (1991).
11. Cook, N. A Guide to Musical Analysis. UK: Oxford University Press, (1987).
12. Laine, P. "Generating Musical Patterns Using Mutually Inhibited Artificial Neurons." Proceedings of the International Computer Music Conference, San Francisco, (1997).
13. Backus, J. The Acoustical Foundations of Music. 2nd ed., W.W. Scranton, Pennsylvania, U.S.A.: Norton & Company, (1977).





Agricultural Waste as a Sustainable Source for 2G-Bioethanol Production: Future Prospects and Challenges

Jyoti Gupta¹, Anjali Shukla², Kiransinh Rajput¹ and Rakeshkumar Panchal^{1*}

¹Department of Microbiology and Biotechnology, University School of Sciences, Gujarat University, Ahmedabad, Gujarat, India.

²Department of Botany, Bioinformatics, Climate change and Impacts Management, School of Science, Gujarat University, Ahmedabad, Gujarat, India.

Received: 25 Aug 2020

Revised: 27 Sep 2020

Accepted: 29 Oct 2020

*Address for Correspondence

Rakeshkumar Panchal

Department of Microbiology and Biotechnology,
University School of Sciences,
Gujarat University, Ahmedabad, Gujarat, India.
Email: rpanchal@gujaratuniversity.ac.in



This is an Open Access Journal / article distributed under the terms of the **Creative Commons Attribution License** (CC BY-NC-ND 3.0) which permits unrestricted use, distribution, and reproduction in any medium, provided the original work is properly cited. All rights reserved.

ABSTRACT

In a scenario with a growing population, increasing demand for energy and volatile prices of fossil fuel, there is a high incentive for the use of biofuels, especially those produced from waste material. For that reason, lignocellulosic substances such as agricultural wastes (wheat straw, corn straw, rice straw, sugarcane bagasse, etc.) are attractive feed stocks for bioethanol production. In 2014, the Ministry of New and Renewable Energy (MNRE), in association with the Indian Institute of Science, Bangalore, has estimated that about 500 million tons of agricultural and agro-industrial residues are being generated annually in the country. About 120-150 million tons of surplus agro-industrial and agriculture residues per year could be surplus for power generation. Bioethanol produced from agricultural waste has several challenges and limitations, i.e. biomass transport, handling and efficient pre-treatment methods for total delignification of lignocellulosic and also increase concentrations of fermentable sugars, ethanol production needs some new fermentation technologies to make the whole process cost-effective. Thereby improving the efficiency of the entire process is the main objective of this review. In this review, feedstock prospects, process technologies for bioethanol production from agricultural wastes, the current research and industrial developments are discussed.

Keywords: Lignocellulosic biomass (LCB), Pretreatment, Cellulase, Saccharification, Fermentation, *Saccharomyces cerevisiae*.



**Jyoti Gupta et al.,**

INTRODUCTION

Depriving fossil fuels are the primary energy sources worldwide. Fossil fuels are nonrenewable resources primarily responsible for the increased carbon dioxide (CO₂) level in the environment and associated climate changes [1]. Climate change and energy security are significant issues that need to be urgently addressed. Besides, the unbridled use of these fuels may harm the environment and cause several problems, such as air pollution, and unexpected changes in entire ecosystems. Therefore, renewable fuels come in handy to solve those problems. Declining the petroleum reservoir and its negative impacts on the environment have raised interest in exploring alternative resources for energy [2,3]. Wind, water, sun, biomass, geothermal heat can be renewable sources for the energy industry whereas fuel production and the chemical industry may depend on biomass as an alternative source in the near future [4]. Bioethanol is an important renewable fuel certainly obtained from agricultural wastes at comparatively low cost and can partly replace fossil-derived fuels. In the future, due to the impending exhaustion of fossil fuels, our world greatly requires biofuel replacement for oil. 2G bioethanol provided a clean source of energy and help provide higher income to farmers and prevent them from having to burn agricultural waste, which can be a chief source of air pollution. Bioethanol demand has increased owing to the growing environmental and social concerns [5]. DBT-ICT Centre for Energy Biosciences, funded by the Department of Biotechnology, Government of India, has developed a novel process for converting lignocellulosic biomass (LCB) to ethanol [6]. Likewise, with the prior approval from the Ministry of petroleum and natural gas, Bharat Petroleum Corporation Limited (BPCL), is all set to architect India's first 2G refinery producing bioethanol at the Bargarh district in Odisha [7]. Bioethanol can be produced from many different types of agricultural waste, including algae waste, vegetable and fruit waste, sugarcane bagasse, rice straw, wheat straw, etc. Lignocellulosic (cellulosic) biomass-derived ethanol is often termed as "second generation" or "2G," and the "first generation" or "1G" ethanol is derived from sugarcane, corn, wheat, and other starchy feedstocks [8]. The whole process of Production of 2nd generation ethanol from LCB is shown in Fig 1. This review highlights agricultural waste, its sources and various practices that include the processes undergone to produce 2nd generation ethanol economically. Therefore, the review aims to describe the overall process of bioethanol production viz., properties of bioethanol, various feedstocks used and their structures, phases of Production, different pre-treatment techniques adopted for biomass, merits and demerits thereof, cellulolytic indigenous microbes and mechanism of cellulase enzyme. Eventually, the article has attempted to address the various concerns that hamper the worthwhile bioethanol production and the remedial solutions thereof.

Potential agricultural waste as raw materials

Biomass refers to renewable organic materials, including agricultural products and agricultural wastes, wood and its wastes, animal wastes, urban wastes, aquatic plants, etc. [9]. Agricultural waste, otherwise termed agro-waste is involved food processing waste (only 20% of maize is canned and 80% is waste), animal waste (manure, animal carcasses), crop waste (corn stalks, sugarcane bagasse, drops and culls from fruits and vegetables) and hazardous and toxic agricultural waste (insecticides pesticides, and herbicides, etc.). Crop wastes are used as significant agricultural waste for the production of bioethanol in recent times. Lignocellulosic biomass (LCB) represents a promising resource for bioethanol production which is renewable. Not only an energy source, biomass is also a promising raw material for the Production of chemicals [10]. The amount of agro-waste biomass available for bioethanol production is summarized in Table 1. LCB relates to agricultural residues such as wheat straw, rice straw, bagasse, maize stover and residues from plants. These biomasses are the world's most valuable and sustainable raw materials and are the appealing feedstock for bioethanol extraction because their use as bioenergy raw materials does not deplete food and feed sources. In general, lignocellulosic material can be split into three primary parts: cellulose (30–50%), hemicellulose (15–35%) and lignin (10–20%) [11]. The transformation from LCB to ethanol has involved some pre-treatments followed by polysaccharide hydrolysis to simple sugars by yeast fermentation [12, 13, 14]. Cellulose, hemicellulose and lignin contents in Wheat straw, Corn stover, Rice straw, Sugarcane bagasse and Cotton stalk are shown in Table 2. Cellulose, which is a linear syndiotactic (alternating spatial arrangement of the side chains) polymer of glucose linked together by β -(1 \rightarrow 4)-glycosidic bonds, is the most abundant polymer on earth, has





Jyoti Gupta et al.,

many beneficial properties such as biocompatibility, stereo-regularity, hydrophilicity, and reactive hydroxyl groups [15]. Hemicellulose is a mixture composed of different polysaccharides, including straight and branched-chainones, to connect different numbers of acetyl and methyl. This polysaccharide has low degree of polymerization, and without crystalline regions, so it is relatively easily degraded into monosaccharides, such as arabinose, xylose, galactose, fructose, mannose, dextrose, or glucuronide. Lignin is a complex hydrophobic, cross-linked aromatic polymer that interferes with the hydrolysis process [16, 17].

Biomass pre-treatment overview

Pretreatment is the crucial step in the conversion of energy from lignocelluloses, which provide the separation or solubilization of the complex components of lignocellulose. And the choice of pre-treatment should consider the compatibility of feedstocks, enzymes and organisms. This process generally can be classified into physical, chemical, physical-chemical, biological methods and their combinations (Fig. 2). In general, physical and chemical pre-treatments results are relatively good, but the equipment requirement is strict and linked to severe pollution. The biological method consumes less energy and causes less pollution than other methods, but it is costly and needs a long time, and enzyme activities in lignocellulose decomposition are low [15]. Recent studies of different pre-treatment of agriculture wastes for bioethanol production are shown in Table 3. Based on the finding, even every single method has its advantage and disadvantages, but more research is needed to find an efficient combination of the existing methods. Besides, the pre-treatment efficiency can be enhanced by doing more research on either the mechanism or beneficial application of generated by-products. Although, the pre-treatment procedure should be optimized in terms of energy consumption efficiency and eco-friendly process [18]. The pretreatment process changes the microstructure, macrostructure, and chemical composition of lignocellulose. And it also alters the natural macromolecular structure of lignocellulose during decomposition to become susceptible to microbial degradation [19]. Lignin acts as a shield and interferes with hydrolysis by preventing access of cellulases and hemicellulases to cellulose and hemicelluloses fraction of the biomass, thereby resulting in extended reaction times to achieve a high conversion rate. Another obstacle in the enzymatic hydrolysis process is the irreversible adsorption of a large amount of the cellulase enzyme by lignin rendering it unavailable for further hydrolysis process. Therefore, degradation and removal of lignin is one of the most significant steps for the conversion of ethanol and is achieved by various pretreatment methods to enhance the process of enzymatic hydrolysis [20]. Based on the drawbacks of single pre-treatment methods, researchers have been trying to combine these methods to overcome the problems and increase efficiency. Since many years ago, many studies have been carried out by a combination of various pretreatment methods [21]. Some major problems in pre-treatment processes are summarized by Chen. Many problems still exist in each pre-treatment process, and it remains in the experimental stage [15].

Enzymatic hydrolysis

Saccharification (Hydrolysis) plays a major role, and it is an important step for bioethanol production, which mainly involves the production of fermentable sugars. During the hydrolysis process, the long chains of glucose molecules present in the cellulose are broken down to release the sugars for fermentation [22]. Enzymatic hydrolysis involves enzymes for the conversion of LCB into sugars. Enzymatic saccharification of cellulose is carried out by cellulases, a mixture of a large number of different cellulose hydrolyzing enzymes that act in synergy to hydrolyze both crystalline and amorphous domains of cellulose to fermentable sugars [23]. Cellulase and hemicellulase enzymes cleave the bonds of cellulose and hemicellulose, respectively. Cellulose contains glucan and hemicellulose has different sugar units such as mannan, xylan, glucan, galactan and arabinan. Cellulase enzymes involve endo and exoglucanase and β -glucosidases. Endoglucanase (endo 1,4-D glucan hydrolase or E.C. 3.2.1.4) attacks the low crystallinity regions of the cellulose fiber, exoglucanase (1,4-b-D glucan cellobiohydrolase or E.C. 3.2.1.91) removes the cellobiose units from the free chain ends and finally cellobiose units are hydrolyzed to glucose by β -glucosidase (E.C. 3.2.1.21) [24, 25]. The deficiency of β -glucosidase activity in enzyme increased the accumulation of cellobiose attributes towards product inhibition. Hence, the incorporation of the β -glucosidase enzyme with cellulase enzyme improved the product yield obtained from enzymatic hydrolysis of biomass [26, 27].





Jyoti Gupta et al.,

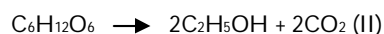
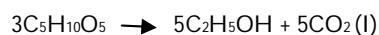
Both bacteria and fungi are known to produce cellulolytic enzymes blamable for the hydrolysis of LCB. Various reported genera, the most extensive study was on *Clostridium*, *Cellulomonas*, *Bacillus*, *Cellulovibrio*, *Thermomonospora*, and *Paenibacillus* sp. as per earlier reports [28]. *Trichoderma* and *Aspergillus* sp. are known as the model fungi among a variety of fungal organisms known for their potential to produce cellulases [29]. The process of enzymatic hydrolysis can be performed in both solid-state and submerged culture media. SSF has several economical and practical advantages over SmF as it is cheaper, less technology-oriented; thus, low energy requirements and the enzyme extraction and downstream processing are easier with limited solvent requirement and lower recovery cost than SmF [30].

Analytical-scale enzymatic saccharification: This technique utilizes a small number of biomass samples to screen a large number of samples and parameters. Various parameters tested during this process may involve a comparison of different LCF, different parts of plants, different pre-treatment techniques, and various environmental and cultural factors. Several different approaches used in analytical-scale enzymatic saccharification with or without pre-treatment are semi-automated, high-throughput (HTP), microtiter plate (MTP) and microwell plates (MWP) based methods [31].

Factors influence the process of enzymatic hydrolysis: Various nutritional and fermentation parameters affect enzyme production both under submerged as well as solid-state conditions. The fermentation medium must meet the nutritional requirements of the microorganism and thus need to be optimized for maximum enzyme production. The efficiency of the enzymatic saccharification depends on several factors such as reaction time, temperature, pH, sources of carbon, nitrogen and some growth factors, the type of pre-treatment of the substrate, enzymes and substrate concentrations and catalytic action of cellulolytic enzyme complex [32].

Production of ethanol

For ethanol production from the lignocellulose material, fermentation is the third important process in which ethanol is directly produced through the metabolic activities of a fermenting agent (i.e. microorganisms, usually either bacteria, yeast, or fungi). Theoretically, one kilogram of glucose and xylose may produce 0.49 kg of carbon dioxide and 0.51 kg of ethanol [33]. The equation for the conversion of glucose to ethanol and xylose to ethanol is shown below:



Yeasts involved in the fermentation process: Fermentation is the following step and requires the presence of microorganisms to degrade sugars into alcohols and other end products. Typically *S. cerevisiae* converts the sugars into ethanol under anaerobic conditions at a temperature of 30°C. In this pathway other by-products are also generated in the form of CO₂ and N-based compounds. *S. cerevisiae* is known as the most studied microorganism for the fermentation of lignocellulosic hydrolysate that ferment the glucose contained in hydrolysate while unable to ferment pentose sugar such as xylose. *S. cerevisiae* is a prevalent microorganism and provides a high yield of ethanol (12.0–17.0% w/v; 90% of the theoretical yield) from sugars [34]. Certain yeast strains such as *Pichia stipitis* (NRRL-Y-7124), *S. cerevisiae* (RL-11) and *Kluyveromyces fragilis* (Kf1) were reported as good ethanol producers from different types of sugars [35].

Fermentation Strategies: Ethanol fermentation is a biological process in which simple sugars are followed up on and used by microorganisms to change over them into ethanol and CO₂[32]. In Figure 3, various saccharification and fermentation bioprocess integrations have been reported. Out of the several strategies, separate hydrolysis fermentation (SHF) and simultaneous saccharification fermentation (SSF) are mostly used during the fermentation of hydrolysate obtained from lignocellulosic biomass. With regard to SHF, SSF is mostly preferred due to the ability of





Jyoti Gupta et al.,

the system to overcome the problem of product inhibition [36]. Previous study reported that *Saccharomyces cerevisiae* NGY10 obtained 49.77 ± 0.34 g/L bioethanol by SSF which is very high comparing to other yeast [37]. Simultaneous Saccharification & Co-Fermentation (SSCF), in which hexose and pentose co-fermentation is performed. In SSCF, in terms of operating pH and temperature, co-fermenting microorganisms must be compatible [38]. SSCF technology can reduce the overall cost of alcohol production and the inhibitory effects of xylose are also minimized [39]. In consolidated Bioprocessing, consolidated arises as the entire production process of biomass to biofuel is accomplished into a single reactor. During this process, microbes produce enzyme, which leads to disintegrate the biomass itself for the production of biofuel within the reactor [40, 41].

Worldwide Status of Bioethanol

The bioethanol market has grown considerably from less than a billion liters in 1975 to more than 65 billion liters in 2008 and could grow to exceed 125 billion liters by 2020 [42]. Also, the global biofuels supply since the year 2000 increased by a factor of 8% to contribute to 4% of the world's total transport fuels in 2015. [43]. According to International Energy Agency, the total worldwide demand for oil is estimated to rise by 1% per year especially due to the increasing demand for energy in developing countries like India (3.9% per year) and China (3.5% per year). Major contributors are industries such as aviation, marine transport and heavy freight, where biofuels are conceived as the only practical and low-carbon alternative. Also, the recent signing of an agreement by 191 countries to curb aviation pollution accentuates that there is a notable market future for continued biofuel adoption [44]. According to the Energy Independence and Security Act of 2007, the USA mandates the use of a minimum volume of biofuel in the transportation industry, but it does not compel biofuel production. The Environmental Protection Agency which oversees this act was essentially designed to increase the consumption of renewable fuel from 9 billion gallons in 2008 to 36 billion in 2022 [45]. EU Energy and Climate Change Package (CCP) 2009 outline the regulations for the use of transport-based biofuels [46]. Brazil is the world's largest exporter of bioethanol and also the 2nd largest producer after the USA. Brazil is one of the most developed nations in ethanol production with the blending requirement for ethanol recently between 18 and 27.5%, currently 27% [47]. According to India's National Policy on Biofuels (2018), as per the government's targets, biofuels would contribute 10 gigawatts (GW) of power by 2022. The policy seeks to achieve a 20% blending of ethanol with gasoline by 2030 [48]. The major goal for the country now is the amendment of the 2009 biofuel policy with the focus on the development and utilization of indigenous lignocellulosic feedstocks with a thrust on research and development for efficient production 2G biofuels and a blending mandate for both bioethanol and biodiesel [32].

CONCLUSION

Challenges and future prospects: Ethanol production by fermenting agriculture waste faces three challenges. All through the fermentation process, the temperature increases from about 30°C to 40°C. Meanwhile, the commercially available yeast strains are good at fermenting at 30°C; the fermenter has to be cooled down when the temperature increases, which increases the cost of ethanol production. Second, lignocellulose biomass (rice and wheat straw) has a mixture of hexose and pentose sugars. However, yeast can ferment glucose (a hexose sugar); it cannot ferment pentose sugar (xylose and arabinose) efficiently that makeup 30% of the composition. Lastly, the pre-treatment of lignocellulose (to breakdown the recalcitrant structure of the biomass) results in the production of three main inhibitors (furfural, 5-HMF, and acetic acid). These inhibitors diminish the fermentation performance of yeast, leading to reduced ethanol production. Again, biotechnological methods, including scientific frameworks and computational tools, are likely suitable candidates to solve these issues. Future cost-saving inclinations should include more productive biomass pre-treatment, improvement of explicit action and cellulase profitability, improvement of recombinant microorganisms for more notable coordination of the apparent multitude of sugars delivered during pre-treatment and hydrolysis action, and further advancement of the system for co-aging. The advancement of powerful and stable strains of microorganisms to convert cellulosic biomass into ethanol will undoubtedly make progressive research on hereditary and metabolic design conceivable. In recent years, using





Jyoti Gupta et al.,

metabolic engineering along with random mutagenesis techniques, advancement in terms of the enhancement of microorganism capabilities by adding/modifying traits such as reduced essential nutrient supplementation, hydrolysis of cellulose or hemicellulose, thermo-tolerance, and tolerance to inhibitors. Further, improving pre-treatment method and identifying metabolic pathways through genetic engineering for pentose fermentation, genomic sequencing, environmental genomics, and/or meta-genomic technologies may assist to make bioethanol production more economical, practical, and commercially feasible.

DECLARATION

Ethics approval and consent to participate

Not applicable

Consent for publication

Not applicable

Availability of data and material

Not applicable

Competing Interests

All the authors approve that they have no conflicting interests, which may seem to have affected the research documented in this paper.

Funding

No funding was sourced.

Authors Contribution

JG and AS performed major contribution in writing the manuscript. RP and KR was associated in supervising, advising positioning and structuring the manuscript. All authors read and approved the final manuscript.

Acknowledgements

The authors are thankful to the authorities of Gujarat University, Ahmedabad, Gujarat, India.

Study Involving Plants

As per the local and national guidelines and legislation and the required or appropriate permissions and/or licenses for the study.

REFERENCES

1. Saravanan, A.P., Mathimani, T., Deviram, G., Rajendran, K., and Pugazhendhi, A. Biofuel policy in India: a review of policy barriers in sustainable marketing of biofuel. *Journal of cleaner Production*. 2018;193:734-747.
2. Bhatia, L., Johri, S., and Ahmad, R. An economic and ecological perspective of ethanol production from renewable agro waste: a review. *Amb Express*. 2012;2(1):1-19.
3. Mussatto, S.I.A closer look at the developments and impact of biofuels in transport and environment; what are the next steps? *Biofuel Research Journal*, 2016;3(1):331-331.
4. Lynd L.R, Wang M.Q.A product-nonspecific framework for evaluating the potential of biomass-based products to displace fossil fuels. *Journal of Industrial Ecology*. 2003;7 (3-4):17-32.





Jyoti Gupta et al.,

5. Akbarian- Saravi, N., Mobini, M., and Rabbani, M. Development of a comprehensive decision support tool for strategic and tactical planning of a sustainable bioethanol supply chain: Real case study, discussions and policy implications. *Journal of Cleaner Production*. 2020;244:118871.
6. Sreekumar, A., Shastri, Y., Wadekar, P., Patil, M., Lali, A. Life cycle assessment of ethanol production in a rice-straw-based biorefinery in India. *Clean Technologies and Environmental Policy*. 2020; 22(2):409-22.
7. Haldar, D., and Purkait, M.K. Lignocellulosic conversion into value-added products: A review. *Process Biochemistry*. 2020;89:110-133.
8. Jordan, D.B., Bowman, M.J., Braker, J.D., Dien, B.S., Hector, R.E., Lee, C.C., Mertens, J. A., Wagschal, K. Plant cell walls to ethanol. *Biochem J*. 2012;442(2):241–252.
9. Chen, H.Z. *Biomass science and technology*. Beijing: Chemical Press. 2008.
10. Werpy, T. and Petersen, G. *Top value-added chemicals from Biomass*. National Renewable Energy Laboratory. 2004.
11. Gírio, F.M., Fonseca, C., Carvalheiro, F., Duarte, LC., Marques, S., Bogel- Łukasik, R. Hemicelluloses for fuel ethanol: a review. *Bioresource technology*. 2010;1;101(13):4775-800.
12. Srivastava, A.K., Agrawal, P., Rahiman, A. Delignification of rice husk and Production of bioethanol. *International Journal of Innovative Research in Science, Engineering and Technology*. 2014;3(3):10187-94.
13. Gnansounou, E. and Dauriat, A. Ethanol Fuel from Biomass: A Review. *Journal of Scientific and Industrial Research*. 2005;64:809-821.
14. Murphy, J.D., McKarty, K. Ethanol Production from Energy Crops and Wastes for Use as a Transport Fuel in Ireland. *Applied Energy*, 2012;82:148-166.
15. Chen, H., Liu, J., Chang, X., Chen, D., Xue, Y., Liu, and Han, S. A review on the pretreatment of lignocellulose for high-value chemicals. *Fuel Processing Technology*. 2017;160:196-206.
16. Karimi, K., & Taherzadeh, M. J. A critical review of analytical methods in pretreatment of lignocelluloses: composition, imaging, and crystallinity. *Bioresource technology*, 2016;200:1008-1018.
17. Shishir PS.C., Gregg T.B., Michael E.H., & Bruce E.D. Deconstruction of Lignocellulosic Biomass to Fuels and Chemicals. *Annual Review of Chemical and Biomolecular Engineering*. 2011;2(1).
18. Rezaia, S., Oryani, B., Cho, J., Talaiekhosani, A., Sabbagh, F., Hashemi, B., Rupani, PF., Mohammadi, AA. Different pre-treatment technologies of lignocellulosic biomass for bioethanol production: An overview. *Energy*. 2020;29:117457.
19. An, Y.X., Zong, M.H., Wu, H., Li, N. Pretreatment of lignocellulosic biomass with renewable cholinium ionic liquids: Biomass fractionation, enzymatic digestion and ionic liquid reuse. *Bioresource technology*. 2015;192:165-71.
20. Prasad, S., Singh, A., Joshi, HC. Ethanol as an alternative fuel from agricultural, industrial and urban residues. *Resour Conserv Recycl*. 2007;50:1–39.
21. Shirkavand, E., Baroutian, S., Gapes, DJ., Young, BR. Combination of fungal and physicochemical processes for lignocellulosic biomass pre-treatment- A review. *Renew Sustain Energy Rev*. 2016; 54:217-34.
22. Niju, S., M. Swathika, and M. Balajii. "Pre-treatment of lignocellulosic sugarcane leaves and tops for bioethanol production." *Lignocellulosic Biomass to Liquid Biofuels*. Academic Press. 2020:301-324.
23. Van, D.J.S., Pletschke, B.I., A review of lignocellulose bioconversion using enzymatic hydrolysis and synergistic cooperation between enzymes-factors affecting enzymes, conversion and synergy. *Biotechnol Adv*. 2012;30:1458–1480.
24. Banerjee S, Mudliar S, Sen R, Giri B, Satpute D, Chakrabarti T, et al. Commercializing lignocellulosic bioethanol: technology bottlenecks and possible remedies. *Biofuels, Bioproducts and Biorefining*. 2010;4:77-93.
25. Taherzadeh, M.J., Karimi, K. Enzyme-based hydrolysis processes for ethanol from lignocellulosic materials: a review. *Bioresources*. 2007;2(4):707-38.
26. Chen, C.H., Yao, J.Y., Yang, B., Lee, H.L., Yuan, S.F., Hsieh, H.Y., & Liang, P.H.. Engineer multi-functional cellulase/xylanase/β-glucosidase with improved efficacy to degrade rice straw. *Bioresource Technology Reports*. 2019;5:170-177.





Jyoti Gupta et al.,

27. Xia, Y., Yang, L., & Xia, L. High-level production of a fungal β -glucosidase with application potentials in the cost-effective production of *Trichoderma reesei* cellulase. *Process biochemistry*. 2018;70:55-60.
28. Sukumaran R.K., Singhanian R.R., Pandey A. Microbial cellulases— production, applications and challenges. *J Sci Ind Res*. 2005;64:832–844
29. Srivastava, N., Srivastava, M., Mishra, P. K., Gupta, V. K., Molina, G., Rodriguez-Couto, S., & Ramteke, P. W. (2018). Applications of fungal cellulases in biofuel production: advances and limitations. *Renewable and Sustainable Energy Reviews*, 82, 2379-2386.
30. Pandey, A., and Radhakrishnan, S., The Production of glucoamylase by *Aspergillus niger* NCIM 1245. *Proc Biochem*. 1993;28:305.
31. Berlin, A., Maximenko, V., Bura, R., Kang, K.Y., Gilkes, N., Saddler, J. A rapid microassay to evaluate enzymatic hydrolysis of lignocellulosic substrates. *Biotechnol Bioeng*. 2006;93:880–886.
32. Sharma, A., & Aggarwal, N.K. *Water Hyacinth: A Potential Lignocellulosic Biomass for Bioethanol*. Springer. 2020.
33. Singh, A.P., Sharma, Y.C., Mustafi, N.N., & Agarwal, A.K. *Alternative Fuels and Their Utilization Strategies in Internal Combustion Engines*. Springer Singapore. 2020.
34. Kumar S, Singh S. P., Mishra IM, Adhikari D.K. Recent advances in production of bioethanol from lignocellulosic biomass. *Chem Eng Technol* 2009;32:517–526
35. S.I. Mussato, E.M.S. Machado, L.M. Carneiro, J.A. Teixeira, Sugar metabolism and ethanol production by different yeast strains from coffee industry wastes hydrolysates,
 - a. *Appl. Energy* 92:2012;763–768.
36. D. Dahnum, S.O. Tasum, E. Triwahyuni, M. Nurdin, H. Abimanyu, Comparison of SHF and SSF processes using enzyme and dry yeast for optimization of bioethanol production from empty fruit bunch, *Ener. Procedia* 68:2015;107–116.
37. Ajay Kumar Pandey., Mohit Kumar., Sonam Kumari., Priya Kumari., Farnaz Yusuf., Shaik Jakeer., Sumera Naz., Piyush Chandna., Ishita Bhatnagar and., Naseem A. Gaur. Evaluation of divergent yeast genera for fermentation-associated stresses and identification of a robust sugarcane distillery waste isolate *Saccharomyces cerevisiae* NGY10 for lignocellulosic ethanol production in SHF and SSF. *Biotechnol Biofuels*. 2019;12:40.
38. Talebnia, F., Karakashev, D. and Angelidaki, I. Production of bioethanol from wheat straw: an overview on pretreatment, hydrolysis and fermentation. *Bioresour Technol*. 2010;101(13):4744–4753.
39. Zhang, J., Lynd, L.R. Ethanol production from paper sludge by simultaneous saccharification and co-fermentation using recombinant xylose-fermenting microorganisms. *Biotechnol. Bioeng*. 2010;107:235-244.
40. N. Singh, A.S. Mathur, R.P. Gupta, C.J. Barrow, D. Tuli, M. Puri, Enhanced cellulosic ethanol production via consolidated bioprocessing by *Clostridium thermocellum* ATCC 31924*, *Bioresour. Technol*. 250 (2018) 860–867.
41. F. Xin, W. Dong, W. Zhang, J. Ma, M. Jiang. Biobutanol production from crystalline cellulose through consolidated bioprocessing. *Trends Biotechnol*. 37(2):2019;167–180.
42. Demirbas A. Producing and using bioethanol as an automotive fuel. *Energy Sour Part B* 2007;2:391–401.
43. Renewable Energy Network 21 (REN21) Global status report. REN21, Paris, France. 2016.
44. Innovation Outlook: Advanced Liquid Biofuels International Renewable Energy Agency (IRENA). Abu Dhabi, UAE. 2016.
45. Bramcourt K. The renewable fuel standard (RFS). In: Brief: congressional research service. Washington, DC, USA, 2016;7–5700.
46. Araujo, K., Mahajan, D., Kerr, R., Silva, M. Global biofuels at the crossroads: an overview of technical, policy, and investment complexities in the sustainability of biofuel development agriculture. 2017. <https://doi.org/10.3390/agriculture7040032>
47. US Department of Agriculture (USDA), Brazil Biofuels Annual. GAIN report number BR 16009. Brazilian law 13.263/2016. USDA, Washington DC, USA. 2016.
48. Prasad, S., Kumar, S., Sheetal, K.R., & Venkatramanan, V. Global Climate Change and Biofuels Policy: Indian Perspectives. In *Global Climate Change and Environmental Policy* Springer, Singapore. 2020;207-226.
49. Singh, R., Srivastava, M., Shukla, A. Environmental sustainability of bioethanol production from rice straw in India: a review. *Renewable and Sustainable Energy Reviews*. 2016; 54:202-16.



**Jyoti Gupta et al.,**

50. Singh, J. and Gu, S. Biomass conversion to energy in India – a critique. *Renew Sustain Energy Rev.* 2010;14:1367–78.
51. Khan, Z., Dwivedi, A.K. Fermentation of Biomass for Production of Ethanol: A Review *Universal Journal of Environmental Research and Technology.* 2013;3:1-13.
52. Daud, Z., Mohd Hatta, M.Z., Mohd Kassim, A.S. and Mohd Aripin, A. Analysis of the chemical composition and fiber morphology of pineapple (*Ananas comosus*) leaves in Malaysia. *J Appl Sci.* 2014;14(12):1355–1358.
53. Saini, J. K., Saini, R., & Tewari, L. Lignocellulosic agriculture wastes as biomass feedstocks for second-generation bioethanol production: concepts and recent developments. *3 Biotech.* 2015;5(4), 337-353.
54. Ayeni, A.O. Valorization of Biomass to Value-Added Commodities.
55. Liu, Y., Guo, L., Wang, L., Zhan, W., & Zhou, H. Irradiation pre-treatment facilitates the achievement of high total sugars concentration from lignocellulose biomass. *Bioresource technology.* 2017;232, 270-277.
56. Álvarez, A., Cachero, S., González-Sánchez, C., Montejo-Bernardo, J., Pizarro, C., & Bueno, J. L. Novel method for holocellulose analysis of non-woody biomass wastes. *Carbohydrate polymers.* 2018;189, 250-256.
57. Hassan, S.S., Williams, G.A., & Jaiswal, A.K. Emerging technologies for the pre-treatment of lignocellulosic biomass. *Bioresource Technology.* 018;262, 310-318.
58. Serna, L.D., Alzate, C.O., & Alzate, C.C. Supercritical fluids as a green technology for the pre-treatment of lignocellulosic biomass. *Bioresource technology,* 2016;199, 113-120.
59. Kim, H., Ahn, Y., & Kwak, S.Y. Comparing the influence of acetate and chloride anions on the structure of ionic liquid pretreated lignocellulosic biomass. *Biomass and Bioenergy.* 2016;93, 243-253.
60. Molaverdi, M., Karimi, K., Mirmohamadsadeghi, S. Improvement of dry simultaneous saccharification and fermentation of rice straw to high concentration ethanol by sodium carbonate pre-treatment. *Energy.* 2019; 167:654-60.
61. Yuan, Z., Li, G. and Hegg, E.L. Enhancement of sugar recovery and ethanol production from wheat straw through alkaline pre-extraction followed by steam pre-treatment. *Bioresour Technol.* 2018;266:194-202.
62. Nosratpour, M.J., Karimi, K., Sadeghi, M. Improvement of ethanol and biogas production from sugarcane bagasse using sodium alkaline pre-treatments. *J Environ Manag.* 2018; 226:329-39.
63. de Carvalho, D.M., de Queiroz, J.H., & Colodette, J.L. Assessment of alkaline pre-treatment for the Production of bioethanol from eucalyptus, sugarcane bagasse and sugarcane straw. *Industrial Crops and Products.* 2016;94:932-941.
64. Zhu, S., Huang, W., Huang, W., Wang, K., Chen, Q. and Wu, Y. Pre-treatment of rice straw for ethanol production by a two-step process using dilute sulfuric acid and sulfomethylation reagent. *Appl Energy.* 2015;154:190-6.
65. Yu, J., Xu, Z., Liu, L., Chen, S., Wang, S. and Jin, M. Process integration for ethanol production from corn and corn stover as mixed substrates. *Bioresour Technol.* 2019;279:10-6.
66. Jaisamut, K., Paulova, L., Patakova, P., Kotúcová, S. and Rychtera, M. Effect of sodium sulfite on acid pre-treatment of wheat straw with respect to its final conversion to ethanol. *Biomass Bioenergy.* 2016; 95:1e7.
67. Nasirpour, N., Mousavi, S. M. RSM based optimization of PEG assisted ionic liquid pretreatment of sugarcane bagasse for enhanced bioethanol production: effect of process parameters. *Biomass Bioenergy.* 2018; 116:89-98.
68. Kumar, A.K., Parikh, B.S., Shah, E., Liu, L.Z. and Cotta, M. A. Cellulosic ethanol production from green solvent-pretreated rice straw. *Biocataly Agri Biotech.* 2016; 7:14-23.
69. Zhao, Z., Chen, X., Ali, M.F., Abdeltawab, A.A., Yakout, S.M. and Yu, G. Pretreatment of wheat straw using basic ethanolamine-based deep eutectic solvents for improving enzymatic hydrolysis. *Bioresour Technol.* 2018; 263:325-33.
70. Dimos, K., Paschos, T., Louloudi, A., Kalogiannis, K.G., Lappas, A. A., Papayannakos, N., & Mamma, D. Effect of various pretreatment methods on bioethanol production from cotton stalks. *Fermentation.* 2019;5(1):5.
71. Yuan, Z., Wen, Y., Kapu, N.S. and Beatson, R. Evaluation of an organosolv-based biorefinery process to fractionate wheat straw into ethanol and co-products. *Ind Crop Prod.* 2018; 121:294-302.





Jyoti Gupta et al.,

72. Katsimpouras, C., Zacharopoulou, M., Matsakas, L., Rova, U., Christakopoulos, P., Topakas, E. Sequential high gravity ethanol fermentation and anaerobic digestion of steam explosion and organosolv pretreated corn stover. *Bioresour Technol.* 2017; 244:1129-36.
73. Gurgel, L.V.A., Pimenta, M.T.B., Curvelo, A.A. Ethanol- water organosolv delignification of liquid hot water (LHW) pretreated sugarcane bagasse enhanced by higher pressure carbon dioxide (HPeCO₂). *Ind Crop Prod.* 2016; 94:942-50.
74. Huang, C., Wu, X., Huang, Y., Lai, C., Li, X. and Yong, Q. Prewashing enhances the liquid hot water pre-treatment efficiency of waste wheat straw with high free ash content. *Bioresour Technol.* 2016; 219:583-8.
75. Wu, X., Zhang, J., Xu, E., Liu, Y., Cheng, Y., Addy, M., Zhou, W., Griffith, R., Chen, P. and Ruan, R. Microbial hydrolysis and fermentation of rice straw for ethanol production. *Fuel.* 2016;180:679-86.
76. Fonseca, B.G., Mateo, S., Moya, A.J., Roberto, I. C. Biotreatment optimization of rice straw hydrolyzates for ethanolic fermentation with *Scheffersomyces stipitis*. *Biomass Bioenergy.* 2018; 112:19-28.
77. García-Torreiro, M., Lopez-Abelairas, M., Lu-Chau, T. A. and Lema, J. M. Fungal pre-treatment of agricultural residues for bioethanol production. *Ind Crop Prod.* 2016;89:486-92.
78. Arora, A., Priya, S., Sharma, P., Sharma, S. and Nain, L. Evaluating biological pre-treatment as a feasible methodology for ethanol production from paddy straw. *Biocataly Agri Biotech.* 2016; 8:66-72.
79. Akhtar, N., Goyal, D. and Goyal, A. preS. Rezania et al. Characterization of microwave-alkali-acid treated rice straw for optimization of ethanol production via simultaneous saccharification and fermentation (SSF). *Energy* 2020;199:117457 13.
80. Banoth, C., Sunkar, B., Tondamanati, P. R., & Bhukya, B. Improved physicochemical pre-treatment and enzymatic hydrolysis of rice straw for bioethanol production by yeast fermentation. *3 Biotech.* 2017;7(5):334.
81. Hilares, R.T., Kamoei, D.V., Ahmed, M.A., da Silva, S.S., Han, J. I., & dos Santos, J. C. A new approach for bioethanol production from sugarcane bagasse using hydrodynamic cavitation assisted-pretreatment and column reactors. *Ultrasonics sonochemistry.* 2018;43: 219-226.
82. Qiu, J., Tian, D., Shen, F., Hu, J., Zeng, Y., Yang, G. & Zhang, J. Bioethanol production from wheat straw by phosphoric acid plus hydrogen peroxide (PHP) pre-treatment via simultaneous saccharification and fermentation (SSF) at high solid loadings. *Bioresource technology.* 2018;268:355-362.
83. Yuan, Z., Wen, Y. and Li, G. Production of bioethanol and value added compounds from wheat straw through combined alkaline/alkaline-peroxide pre-treatment. *Bioresour Technol.* 2018; 259:228-36.
84. Wang, Z., Wu, G. and Jonsson, L. J. Effects of impregnation of softwood with sulfuric acid and sulfur dioxide on chemical and physical characteristics, enzymatic digestibility, and fermentability. *Bioresour Technol.* 2018;247:200–208.
85. Yuan, W., Gong, Z., Wang, G., Zhou, W., Liu, Y., Wang, X., & Zhao, M. Alkaline organosolv pre-treatment of corn stover for enhancing the enzymatic digestibility. *Bioresource technology.* 2018;265:464-470.

Table 1. Amount of agro-waste biomass available for bioethanol production (Million Tons)

Country	Rice Straw	Wheat Straw	Corn Straw	Sugarcane Bagasse	Literature Source
India	126.6	78,000 metric tonnes	18,000 metric tonnes	2,76,250 metric tonnes	[49,50]
Africa	20.90	5.34	0.00	11.73	[51]
Asia	667.60	145.20	33.90	74.88	[51]
Europe	3.90	132.59	28.61	0.01	[51]
America	37.20	62.64	140.86	87.62	[51]
Oceania	1.70	8.57	0.24	6.49	[51]



Jyoti Gupta *et al.*,**Table 2. Cellulose, hemicellulose and lignin contents in common agricultural residues and waste**

Agricultural Residues And Waste	Cellulose % (w/w)	Hemicellulose % (w/w)	Lignin % (w/w)	References
FOOD CROPS				
Pineapple leaves fiber (PALF)	66.2	19.5	4.2	[52]
Wheat straw	37–41	27–32	13–15	[53]
Corn cob	40.3–45	28.7–35	15–16.6	[54]
Corn stalk	22.82	43.01	15.59	[54]
Corn stover	51.2	30.7	14.4	[54]
Barley straw	36.0–43.0	24.0–33.0	6.3–13.1	[3], [55]
Barley hull	34.0	36.0	13.8–19.0	[3]
Extracted olive pomace	19	22	40.0	[56]
Rice straw	29.2–38.1	23.0–31.1	17.0–26.4	[57], [3]
Rice husks	28.7–40.0	12.0–29.3	15.4–26.0	[3], [58]
Sugarcane bagasse	31.9–43.4	12.2–25.5	23.1–27.6	[3]
NON-FOOD CROPS				
Cotton stalk	67	16	13	[59]
Hazel branches	30.8	15.9	19.9	[55]
Miscanthus	35.0–40.0	16.0–20.0	20.0–25.0	[3]
Tobacco chops	22.0–30.0	15.0–20.0	15.0–25.0	[3]

Table 3. Recent studies of different pre-treatment of agriculture wastes for bioethanol production

Raw material	Pre-treatment type	Pre-treatment Condition	Reducing Sugars %	Deligni- fication Rate (%)	Fermentation condition	Bioethanol Yield (g/L)	Literature Source
ALKALINE PRE-TREATMENT							
Rice straw	Na ₂ CO ₃	93 °C, 3-10 h	77.4 g/L	54.5-62.7	37 °C; 120 h	83.1	[60]
Wheat straw	Na ₂ CO ₃ (11%)	75° C; 10-85min	Xylose: 85.7%	70.4	30 °C; 96 h	65	[61]
Wheat straw	NaOH/H ₂ O ₂	50° C, 3e15 h	61.9 g/L	60	37 °C; 96 h	31.1	[61]
Sugarcane bagasse	Na ₂ CO ₃ (5%)	140° C; 1 h	Glucose: 97.6%	40-59	37° C, 72 h	7.27	[62]
Sugarcane bagasse	NaOH (15%)	175 °C; 1.5 h	5.29 g/L	22-90	37° C; 10 h	8.8	[63]
ACID PRE-TREATMENT							
Rice straw	H ₂ SO ₄	100° C; 2 h	14 g/L	92	30 °C; 72 h	40.6	[64]
Corn and Corn Stover	H ₂ SO ₄	160 °C; 10 min	184.4 g/L	NA	30 °C; 96 h	99.3	[65]
Wheat straw	H ₂ SO ₄ and Na ₂ SO ₃	180° C; 30 min	NA	21	48 h	17.25 g/g	[66]
IL (Ionic Liquid) PRE-TREATMENT							
Sugarcane bagasse	BMIMCl; PEG	154.6 °C; 60 min and 5 (%w/ w) of PEG	62%	NA	30 °C; 15h	84%	[67]





Jyoti Gupta et al.,

ORGANIC SOLVENT PRE-TREATMENT							
Rice straw	Choline chloride-based solvent	60-121°C 30 min-12 h	Xylose: 88	57.273.6	37 °C; 72 h	36.7 g/L	[68]
wheat straw	Eutectic solvents	70 °C, 9 h	Glucose: 79.7	71.4	50 °C; 72h	89.8%	[69]
Cotton Stalks	Organosolv	80 °C, 1 h	NA	81	30 h.	52%	[70]
STEAM EXPLOSION PRE-TREATMENT							
Wheat straw	-	151° C; 16 min	Glucose: 59.3 Xylose: 55.7	20.8	33 °C, 96 h	55 g/L	[71]
Corn Stover	-	200° C; 10 min	84.7%	NA	50 °C, 72 h	78.3%	[72]
HYDROTHERMAL PRE-TREATMENT							
Rrice straw	-	40-180° C; 5-20 min	71.8	NA	50 °C; 72 h	-	[59]
Sugarcane bagasse	-	180° C; 20 min	Glucose: 69	77.0	50 °C; 72 h.	-	[73]
wheat straw	-	180 °C; 40 min	Cellulose: 84.15	23.52	50 °C; 48 h.	-	[74]
Corn stover	-	180 °C; 4 min	Glucose: 89 Xylose: 134	52.6	62 °C; 72 h	-	[59]
BIOLOGICAL PRETREATMENT							
Rice straw	T. reesei Aq-5b and T. viride NSW-XM	28 °C; 2e4 days	22.74 g/L	NA	30 °C; 48 h	2.17	[75]
Rice straw	Saccharomyces cerevisiae	25 °C; 30 min	NA	NA	30 °C; 24 h	0.24	[76]
Wheat straw	Corn Stover White- rot fungus Irpex lacteus	121 °C; 20 min	11.5%	Straw 45.8	50 °C; 94 h	Straw:12.5	[77]
Paddy straw	Trametes Hirsute MTCC 136	30° C	52.91 g/L	71.34	50 °C; 24 h	0.86	[78]
COMBINED PRE-TREATMENTS							
Rice straw	Steam explosion And KOH	170 °C for 10 min, sequentially treated with 2% (w/v) KOH	58.70 ± 1.5 2 g/L	-	-	26.12 ± 1.24 g/L	[79]
Wheat straw	Phosphoric acid p hydrogen peroxide (PHP)	40.2° C; 2.9 h H ₃ PO ₄ (85%, w/w) H ₂ O ₂ (30%, w/w)	NA	70.8	38 °C; 96 h	15.5 g	[80]
Wheat straw	Alkaline + steam explosion	151 °C; 16 min	Glucose:5 9.3% Xylose:55. 7%	20.8	50 °C; 72 h	54.5 g/L	[81]





Jyoti Gupta et al.,

Sugarcane bagasse	Liquid hot water p disk milling	121° C; 1 h 47	Glucose: 0.392 g/g Xylose: 0.132 g/g	NA	50 °C; 72 h	79.6%	[82]
Corn Stover	Alkaline organosolv	20- 100 °C; 0.5- 3.0 h	29.5 g/L	NA	NA	0.5 g/g	[83]

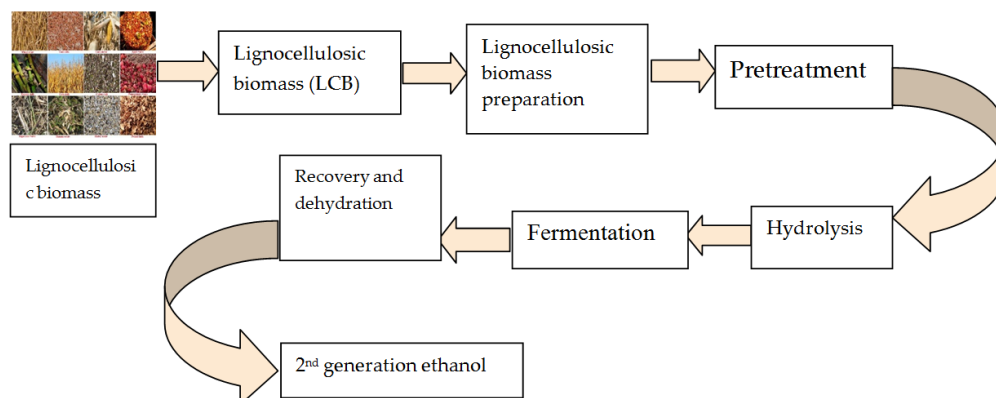


Figure 1. Production of 2nd generation ethanol from LCB

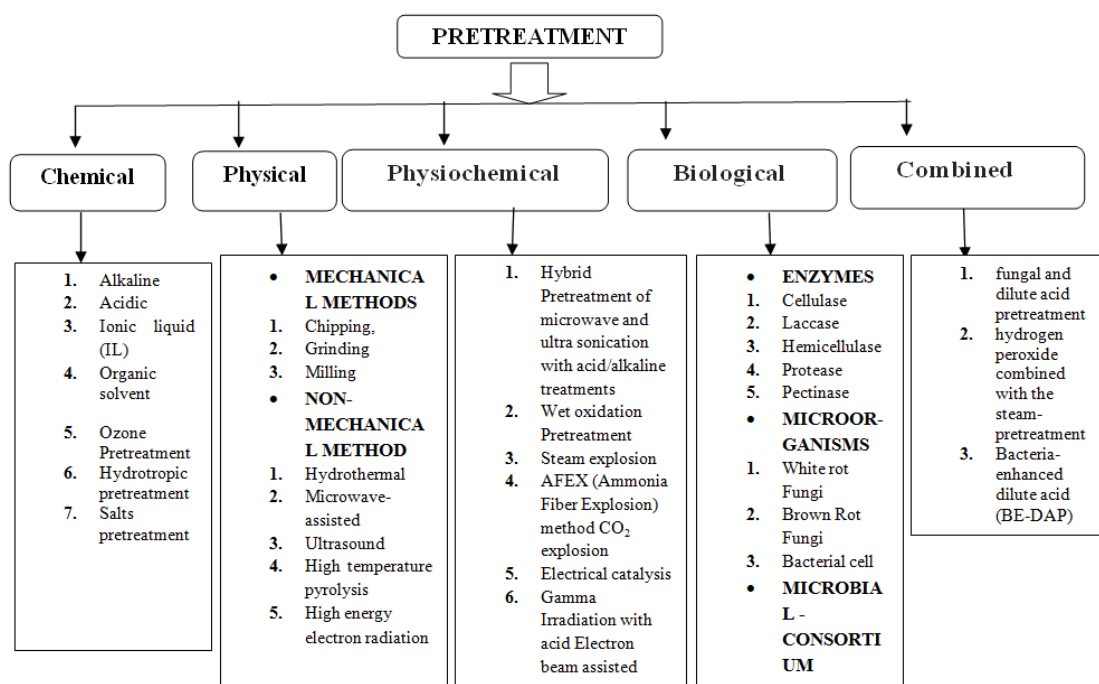


Figure 2. Different types of Pre-treatment methods for agricultural waste



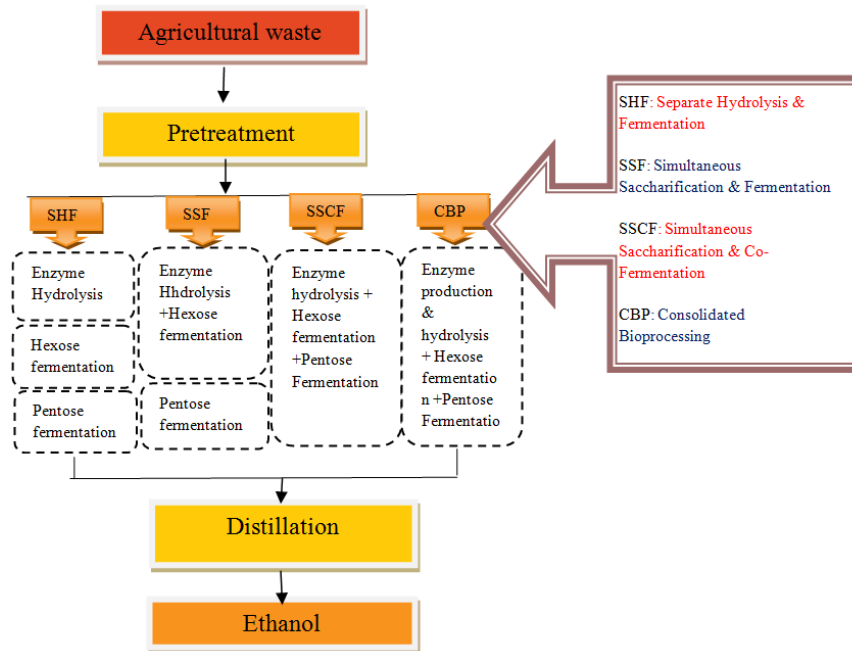


Figure 3. Process configurations for the conversion of agricultural waste to bioethanol





Stirling's Numbers and Matrices

R. Sivaraman*

Associate Professor, Department of Mathematics, D. G. Vaishnav College, Chennai, Tamil Nadu, India

Received: 25 July 2020

Revised: 27 Aug 2020

Accepted: 03 Oct 2020

*Address for Correspondence

R. Sivaraman

Associate Professor,
Department of Mathematics,
D. G. Vaishnav College,
Chennai, Tamil Nadu, India
Email: rsivaraman1729@yahoo.co.in



This is an Open Access Journal / article distributed under the terms of the **Creative Commons Attribution License** (CC BY-NC-ND 3.0) which permits unrestricted use, distribution, and reproduction in any medium, provided the original work is properly cited. All rights reserved.

ABSTRACT

Among several class of interesting family of numbers that were used for counting problems, Stirling's numbers of first kind and second kind play significant role. These numbers occur in various unexpected situations. In this paper, we introduce two kinds of Stirling's numbers and prove their recurrence relations. We connect these numbers through matrices and determine the inverse of such matrices through a fascinating theorem which is proved by combining both kinds of Stirling's numbers.

Keywords: Stirling's Numbers of First and Second Kinds, Recurrence Relation, Diagonal Matrices, Lower Triangular Matrices, Inverse of a Matrix.

INTRODUCTION

Stirling's numbers were named after Scottish mathematician James Stirling. While Stirling's numbers of first kind were connected with number of disjoint cycle factorizations of permutations in symmetric groups, Stirling's numbers of second kind were related to counting number of partitions of a given finite set in to disjoint parts. In this paper, we discuss the recurrence relations of Stirling's numbers of both kinds and relate these numbers as entries of matrices to determine interesting properties.

Definition

Stirling's Numbers of First Kind

The number of permutations in S_m whose disjoint cycle factorizations consists of exactly n cycles is defined to be the Stirling's Number of the First Kind denoted by $s(m, n)$. In $s(m, n)$ we note that $1 \leq n \leq m$.

The Stirling's numbers of first kind satisfies the recurrence relation





R. Sivaraman

$$s(m + 1, n) = s(m, n - 1) + m s(m, n) \quad (2.1)$$

Further by definition of Stirling’s numbers of first kind, we note that $s(m, 1) = (m - 1)!$ and $s(m, m) = 1$. For proof of recurrence relation (2.1) and these two results see [4] by the corresponding author.

Stirling’s Numbers of Second Kind

The number of partitions of a set with m elements using n non-empty disjoint subsets is defined as the Stirling’s numbers of second kind denoted by $S(m, n)$ or $\left\{ \begin{matrix} m \\ n \end{matrix} \right\}$. We notice that $1 \leq n \leq m$.

Theorem 1

The Stirling’s numbers of second kind satisfies the recurrence relation

$$S(m + 1, n) = S(m, n - 1) + n S(m, n) \quad (2.2)$$

Proof: The n - block partitions of $T = \{1, 2, 3, \dots, m, m + 1\}$ can be divided in to two types, those for which $m + 1$ is alone in its block and those for which it is not so. We now count the partitions of T for which $m + 1$ is alone in its block. If $\{m + 1\}$ is a block of the partition, then the remaining m elements of T can be partitioned in to $n - 1$ blocks in $S(m, n - 1)$ ways.

If $m + 1$ is not isolated, then removing $m + 1$ from its block produces an n - part partition of $\{1, 2, 3, \dots, m\}$ say $A_1 \cup A_2 \cup A_3 \cup \dots \cup A_n$. Now, this same partition would arise if $m + 1$ has been removed from any one of the blocks $A_i, 1 \leq i \leq n$. That is, to each n - part partition of $\{1, 2, 3, \dots, m\}$ there correspond n different n - part partitions of T of the second type. Hence, there are exactly $n S(m, n)$ partitions of T in which $m + 1$ shares its block with at least one other integer. Thus combining these types, we get equation (2.2). This completes the proof.

Matrices whose entries are Stirling’s numbers

Let us define two types of $n \times n$ matrices whose entries are Stirling’s numbers of first and second kinds respectively as follows:

Let F_n be a $n \times n$ matrix whose (i, j) th entry is Stirling’s number of first kind $s(i, j)$ for $1 \leq i, j \leq n$ and 0 otherwise since $s(i, j) = 0$ if $i < j$. Thus, using Figure 1, F_n for $n = 2, 3, 4, 5$ are respectively given by

$$F_2 = \begin{pmatrix} 1 & 0 \\ 1 & 1 \end{pmatrix}, F_3 = \begin{pmatrix} 1 & 0 & 0 \\ 1 & 1 & 0 \\ 2 & 3 & 1 \end{pmatrix}, F_4 = \begin{pmatrix} 1 & 0 & 0 & 0 \\ 1 & 1 & 0 & 0 \\ 2 & 3 & 1 & 0 \\ 6 & 11 & 6 & 1 \end{pmatrix}, F_5 = \begin{pmatrix} 1 & 0 & 0 & 0 & 0 \\ 1 & 1 & 0 & 0 & 0 \\ 2 & 3 & 1 & 0 & 0 \\ 6 & 11 & 6 & 1 & 0 \\ 24 & 50 & 35 & 10 & 1 \end{pmatrix} \quad (3.1)$$

From these matrices we notice that by definition F_n is a lower triangular matrix for each n . Moreover, by expanding through first row, it is easy to see that $|F_2| = |F_3| = |F_4| = |F_5| = \dots = 1$. That is, each square matrix of the form F_n which is a lower triangular matrix whose non-zero entries are Stirling’s numbers of first kind all have determinant value 1.





R. Sivaraman

Let S_n be a $n \times n$ matrix whose (i, j) th entry is Stirling's number of second kind $S(i, j)$ for $1 \leq i, j \leq n$ and 0 otherwise since $S(i, j) = 0$ if $i < j$. Thus, using Figure 2, S_n for $n = 2, 3, 4, 5$ are respectively given by

$$S_2 = \begin{pmatrix} 1 & 0 \\ 1 & 1 \end{pmatrix}, S_3 = \begin{pmatrix} 1 & 0 & 0 \\ 1 & 1 & 0 \\ 1 & 3 & 1 \end{pmatrix}, S_4 = \begin{pmatrix} 1 & 0 & 0 & 0 \\ 1 & 1 & 0 & 0 \\ 1 & 3 & 1 & 0 \\ 1 & 7 & 6 & 1 \end{pmatrix}, S_5 = \begin{pmatrix} 1 & 0 & 0 & 0 & 0 \\ 1 & 1 & 0 & 0 & 0 \\ 1 & 3 & 1 & 0 & 0 \\ 1 & 7 & 6 & 1 & 0 \\ 1 & 15 & 25 & 10 & 1 \end{pmatrix} \quad (3.2)$$

From these matrices we notice that by definition S_n is a lower triangular matrix for each n . Moreover, by expanding through first row, it is easy to see that $|S_2| = |S_3| = |S_4| = |S_5| = \dots = 1$. That is, each square matrix of the form S_n which is a lower triangular matrix whose non-zero entries are Stirling's numbers of second kind, all have determinant value 1.

Diagonal Matrices

Let D_n be a $n \times n$ diagonal matrix (that is, the non-diagonal entries are all zero) whose diagonal entries are defined by $a_{ii} = (-1)^i$ for $1 \leq i \leq n$. That is, D_n is a $n \times n$ diagonal matrix whose diagonal entries are $-1, 1, -1, 1, -1, 1, \dots, (-1)^n$. The first few diagonal matrices of these kind were shown below:

$$D_2 = \begin{pmatrix} -1 & 0 \\ 0 & 1 \end{pmatrix}, D_3 = \begin{pmatrix} -1 & 0 & 0 \\ 0 & 1 & 0 \\ 0 & 0 & -1 \end{pmatrix}, D_4 = \begin{pmatrix} -1 & 0 & 0 & 0 \\ 0 & 1 & 0 & 0 \\ 0 & 0 & -1 & 0 \\ 0 & 0 & 0 & 1 \end{pmatrix}, D_5 = \begin{pmatrix} -1 & 0 & 0 & 0 & 0 \\ 0 & 1 & 0 & 0 & 0 \\ 0 & 0 & -1 & 0 & 0 \\ 0 & 0 & 0 & 1 & 0 \\ 0 & 0 & 0 & 0 & -1 \end{pmatrix} \quad (3.3)$$

Computing Inverse

We now use the diagonal matrices D_n to determine inverse of the matrices F_n and S_n defined in (3.1) and (3.2) respectively. As a basic clue, let us consider an example with $n = 4$.

First, let us calculate the matrix $P_4 = D_4 S_4 D_4$. From (3.2) and (3.3), we get

$$P_4 = D_4 S_4 D_4 = \begin{pmatrix} -1 & 0 & 0 & 0 \\ 0 & 1 & 0 & 0 \\ 0 & 0 & -1 & 0 \\ 0 & 0 & 0 & 1 \end{pmatrix} \times \begin{pmatrix} 1 & 0 & 0 & 0 \\ 1 & 1 & 0 & 0 \\ 1 & 3 & 1 & 0 \\ 1 & 7 & 6 & 1 \end{pmatrix} \times \begin{pmatrix} -1 & 0 & 0 & 0 \\ 0 & 1 & 0 & 0 \\ 0 & 0 & -1 & 0 \\ 0 & 0 & 0 & 1 \end{pmatrix} = \begin{pmatrix} -1 & 0 & 0 & 0 \\ 0 & 1 & 0 & 0 \\ 0 & 0 & -1 & 0 \\ 0 & 0 & 0 & 1 \end{pmatrix} \times \begin{pmatrix} -1 & 0 & 0 & 0 \\ -1 & 1 & 0 & 0 \\ -1 & 3 & -1 & 0 \\ -1 & 7 & -6 & 1 \end{pmatrix} = \begin{pmatrix} 1 & 0 & 0 & 0 \\ -1 & 1 & 0 & 0 \\ 1 & -3 & 1 & 0 \\ -1 & 7 & -6 & 1 \end{pmatrix} \quad (4.1)$$

If we now consider the product of F_4 and P_4 , we get

$$F_4 \times P_4 = \begin{pmatrix} 1 & 0 & 0 & 0 \\ 1 & 1 & 0 & 0 \\ 2 & 3 & 1 & 0 \\ 6 & 11 & 6 & 1 \end{pmatrix} \times \begin{pmatrix} 1 & 0 & 0 & 0 \\ -1 & 1 & 0 & 0 \\ 1 & -3 & 1 & 0 \\ -1 & 7 & -6 & 1 \end{pmatrix} = \begin{pmatrix} 1 & 0 & 0 & 0 \\ 0 & 1 & 0 & 0 \\ 0 & 0 & 1 & 0 \\ 0 & 0 & 0 & 1 \end{pmatrix} = I_4 \quad (4.2) \text{ where } I_4 \text{ is the unit matrix of order 4. Thus we see}$$

that $P_4 = F_4^{-1}$ (4.3).

Similarly, let us now calculate the matrix $Q_4 = D_4 F_4 D_4$. From (3.1) and (3.3) we get





R. Sivaraman

$$Q_4 = D_4 F_4 D_4 = \begin{pmatrix} -1 & 0 & 0 & 0 \\ 0 & 1 & 0 & 0 \\ 0 & 0 & -1 & 0 \\ 0 & 0 & 0 & 1 \end{pmatrix} \times \begin{pmatrix} 1 & 0 & 0 & 0 \\ 1 & 1 & 0 & 0 \\ 2 & 3 & 1 & 0 \\ 6 & 11 & 6 & 1 \end{pmatrix} \times \begin{pmatrix} -1 & 0 & 0 & 0 \\ 0 & 1 & 0 & 0 \\ 0 & 0 & -1 & 0 \\ 0 & 0 & 0 & 1 \end{pmatrix} = \begin{pmatrix} -1 & 0 & 0 & 0 \\ 0 & 1 & 0 & 0 \\ 0 & 0 & -1 & 0 \\ 0 & 0 & 0 & 1 \end{pmatrix} \times \begin{pmatrix} -1 & 0 & 0 & 0 \\ -1 & 1 & 0 & 0 \\ -2 & 3 & -1 & 0 \\ -6 & 11 & -6 & 1 \end{pmatrix} = \begin{pmatrix} 1 & 0 & 0 & 0 \\ -1 & 1 & 0 & 0 \\ 2 & -3 & 1 & 0 \\ -6 & 11 & -6 & 1 \end{pmatrix} \quad (4.4)$$

If we now consider the product of S_4 and Q_4 we get

$$S_4 \times Q_4 = \begin{pmatrix} 1 & 0 & 0 & 0 \\ 1 & 1 & 0 & 0 \\ 1 & 3 & 1 & 0 \\ 1 & 7 & 6 & 1 \end{pmatrix} \times \begin{pmatrix} 1 & 0 & 0 & 0 \\ -1 & 1 & 0 & 0 \\ 2 & -3 & 1 & 0 \\ -6 & 11 & -6 & 1 \end{pmatrix} = \begin{pmatrix} 1 & 0 & 0 & 0 \\ 0 & 1 & 0 & 0 \\ 0 & 0 & 1 & 0 \\ 0 & 0 & 0 & 1 \end{pmatrix} = I_4 \quad (4.5) \text{ where } I_4 \text{ is the unit matrix of order 4.}$$

Thus we see that $Q_4 = S_4^{-1}$ (4.6).

In fact equations (4.3) and (4.6) are not just true for the case $n = 4$ but for any natural number n . We prove this important concept through the following theorem.

Theorem 2

Let $F_n = (s(i, j))$ and $S_n = (S(i, j))$ be $n \times n$ matrices of Stirling's numbers of first and second kinds respectively. Let D_n be a $n \times n$ diagonal matrix such that $a_{ii} = (-1)^i, 1 \leq i \leq n$. Then $F_n^{-1} = D_n S_n D_n$ (4.7) and $S_n^{-1} = D_n F_n D_n$ (4.8)

Proof: First we observe that by definition of the diagonal matrix D_n , the diagonal entries of D_n^2 will also be a diagonal matrix whose diagonal entries are $a_{ii}^2 = (-1)^{2i} = 1$ for all $1 \leq i \leq n$. Thus, $D_n^2 = I_n$ where I_n is a unit matrix of order n . From this it follows that $D_n = D_n^{-1}$.

Thus, if we consider (4.8) and take inverse (which will exist since $|F_n| = |S_n| = 1, |D_n| = \pm 1$) on either side, we get

$$S_n^{-1} = D_n F_n D_n \text{ if and only if } (S_n^{-1})^{-1} = (D_n F_n D_n)^{-1} \text{ if and only if } S_n = D_n^{-1} F_n^{-1} D_n^{-1}.$$

$$S_n = D_n^{-1} F_n^{-1} D_n^{-1} \text{ if and only if } D_n S_n D_n = D_n (D_n^{-1} F_n^{-1} D_n^{-1}) D_n = F_n^{-1} \text{ which is (4.7).}$$

Thus, we have shown that equations (4.7) and (4.8) are equivalent, in the sense that if we prove one, we get the other subsequently. So to prove the theorem it is enough to prove just (4.8).

To prove (4.8), we need to show that $S_n \times Q_n = I_n$ (4.9) where $Q_n = D_n F_n D_n$.

We now notice that multiplying any $n \times n$ matrix A by D_n the (i, j) th entry of AD_n is given by $(-1)^j a_{ij}$ which is a_{ij} if j is even and $-a_{ij}$ if j is odd. Thus pre and post multiplying A by D_n sprinkles a checkerboard pattern of alternating minus signs among its entries as the way we obtained Q_4 in (4.4). Since $S_n \times Q_n = S_n D_n F_n D_n$ to prove

$$(4.9) \text{ it is enough to show that } \sum_{k=1}^n (-1)^{k+j} S(i, k) s(k, j) = \delta_{ij}, \quad 1 \leq i, j \leq n \quad (4.10).$$

We note that $\delta_{ij} = 1$ if $i = j$ and 0 otherwise. If we prove (4.10) then that implies (4.9) which in turn implies (4.8).

Also (by Figure 1) we know that $s(i, n) = 0, 1 \leq i < n$. Hence the only non-zero entry in the last column of Q_n is $s(n, n) = 1$. Similarly since $S(i, n) = 0, 1 \leq i < n$ the only non-zero entry in the last column of S_n is $S(n, n) = 1$





R. Sivaraman

. From these observations, we can make two conclusions. The first conclusion is that the last column of $S_n \times Q_n$ is equal to the last column of the unit matrix of order n namely I_n . But this fact establishes equation (4.10) for $j = n$. The second conclusion is the fact that the leading $(n - 1) \times (n - 1)$ principal sub-matrix of $S_n \times Q_n$ is $S_{n-1} \times Q_{n-1}$.

We now try to prove that the entries in the first $(n - 1)$ columns of the n th row of $S_n \times Q_n$ are all zero. That is, we will prove that

$$\sum_{k=1}^n (-1)^{k+j} S(n, k) s(k, j) = 0, \quad 1 \leq j < n \quad (4.11)$$

Now by the relation of falling factorial $x^{(k)} = x(x - 1)(x - 2) \cdots (x - k + 1)$ and Stirling's numbers of first kind we have

$$x^{(k)} = x^k - s(k, k - 1)x^{k-1} + s(k, k - 2)x^{k-2} + \cdots + (-1)^{k+j} s(k, j)x^j + \cdots + (-1)^{k-1} s(k, 1)x \quad (4.12)$$

Now multiplying both sides of (4.12) by $S(n, k)$ and summing up values of k from 1 to n we get

$$\begin{aligned} \sum_{k=1}^n S(n, k)x^{(k)} &= \sum_{k=1}^n S(n, k)x^k - \sum_{k=1}^n S(n, k)s(k, k - 1)x^{k-1} + \sum_{k=1}^n S(n, k)s(k, k - 2)x^{k-2} + \cdots \\ &+ \sum_{k=1}^n (-1)^{k+j} S(n, k)s(k, j)x^j + \cdots + \sum_{k=1}^n (-1)^{k-1} S(n, k)s(k, 1)x \end{aligned}$$

But we know that for any positive integer k , $x^n = \sum_{k=1}^n S(n, k)x^{(k)}$ (4.13)

Hence using (4.13) in last equation, we get

$$\begin{aligned} x^n &= \sum_{k=1}^n S(n, k)x^k - \sum_{k=1}^n S(n, k)s(k, k - 1)x^{k-1} + \sum_{k=1}^n S(n, k)s(k, k - 2)x^{k-2} \\ &+ \cdots + \sum_{k=1}^n (-1)^{k+j} S(n, k)s(k, j)x^j + \cdots + \sum_{k=1}^n (-1)^{k-1} S(n, k)s(k, 1)x \end{aligned}$$

Now equating coefficients of x^j on both sides of the previous equation, we have

$$\sum_{k=1}^n (-1)^{k+j} S(n, k)s(k, j) = 0$$

proving (4.11) and hence (4.10) which eventually proves (4.8). This completes the proof.

CONCLUSION

After introducing the Stirling's numbers of first and second kinds in sections 2.1 and 2.2, through theorem 1, we proved the recurrence relation for Stirling's numbers of second kind which enabled us to produce the entries of such numbers in Figure 2. In section 3, we defined the matrices F_n, S_n which are lower triangular matrices whose entries are Stirling's numbers of first and second kinds respectively. We also noticed that the determinant of the matrices F_n, S_n is always 1. Using the diagonal matrices D_n defined in section 3.3, we computed the inverse of the matrices F_n and S_n . In particular, through theorem 2, we proved that $F_n^{-1} = D_n S_n D_n$ as well as $S_n^{-1} = D_n F_n D_n$. This paper thus establishes a wonderful relationship between, the Stirling's numbers of first and second kinds through the matrices F_n and S_n .





R. Sivaraman

REFERENCES

1. V.S.Adamchik, On Stirling Numbers and Euler Sums, J. Comput. Appl. Math.79, 119-130, 1997.
2. K.S. Kölbig, The complete Bell polynomials for certain arguments in terms of Stirling numbers of the first kind. J. Comput. Appl. Math. 51 (1994) 113-116.
3. H.S. Wilf, The asymptotic behaviour of the Stirling numbers of the first kind. Journal of Combinatorial Theory, Series A, 64, 344-349, 1993.
4. R. Sivaraman, Stirling's Numbers and Harmonic Numbers, Indian Journal of Natural Sciences, Accepted, To be Published in October 2020 issue.
5. T. Mansour, Combinatorics of Set Partitions, CRC Press, 2013.
6. R.P. Stanley, Enumerative Combinatorics, Volume 1, Cambridge University Press, 1997.
7. D. I.A. Cohen, Basic Techniques of Combinatorial Theory, John Wiley & Sons, 1978.

	n	1	2	3	4	5	6	7		n	1	2	3	4	5	6	7
m																	
1		1									1						
2		1	1								1	1					
3		2	3	1							1	3	1				
4		6	11	6	1						1	7	6	1			
5		24	50	35	10	1					1	15	25	10	1		
6		120	274	225	85	15	1				1	31	90	65	15	1	
7		720	1764	1624	735	175	21	1			1	63	301	350	140	21	1
							

Figure 1: Stirling's numbers of first kind

Figure 2: Stirling's numbers of second kind





Production of a Herbal Wine from *Aloe vera* Gel and its Antimicrobial Activity

Ruffina.D^{1*}, John Bastin.T.M.M², Ramanathan.K¹ and Sudhakar.S¹

¹PG and Research Department of Microbiology, Thanthai Hans Roever College, Perambalur, Tamil Nadu, India.

²PG and Research Department of Biotechnology, Thanthai Hans Roever College, Perambalur, Tamil Nadu, India.

Received: 02 Sep 2020

Revised: 04 Oct 2020

Accepted: 06 Nov 2020

*Address for Correspondence

Ruffina.D

Assistant Professor,

PG and Research Department of Microbiology,

Thanthai Hans Roever College (Autonomous),

Perambalur, Tamil Nadu, India.

Email: ruffina86@gmail.com



This is an Open Access Journal / article distributed under the terms of the **Creative Commons Attribution License** (CC BY-NC-ND 3.0) which permits unrestricted use, distribution, and reproduction in any medium, provided the original work is properly cited. All rights reserved.

ABSTRACT

The present study focused on investigating the alternatives of beneficial herbs and their ingredients for enhancing the potentiality and functionality of *Aloe vera* wine. In this work, we have developed the process for the production of *Aloe vera* and Pineapple wine. We found that the optimum concentration of *Aloe vera* to water weight by volume of 1:3 the highest quantity of alcohol was obtained. If the appropriate quantity of pineapple is added with *Aloe vera*, it produces the large quantity of alcohol in the wine. The antibacterial potential and bactericidal activity were found against common pathogens with potential effect. From these results, we found that the herbal wine used as a food with antimicrobial potential against various pathogens. From this work, we concluded that, *Aloe vera* Juice can be used as a healthy and nourishing food which has the potential antimicrobial activity. This study could be helpful for formulating new antimicrobial drugs in future.

Keywords: *Aloe vera* gel, herbal wine, antimicrobial activity, bactericidal activity

INTRODUCTION

Aloe vera is an important medicinal herb used for the treatment of various infections such as antimicrobial, anti-inflammatory and immune boosting properties [1]. The potent antimicrobial activity of gel and leaf of *Aloe vera* against a wide range of bacteria and fungi [2]. *Aloe vera* gel and green and black tea extracts have physicochemical, microbial and sensorial properties of fresh cut oranges and it have significant differences in terms of quality

28383



**Ruffina et al.,**

parameters were observed. The weight loss was increased with time but the coating treatment especially with 100% *Aloe vera* had significant effect on the prevention of weight loss [3]. *Aloe vera* gel contains a blend of carbohydrates, glycoprotein as well as a variety of nutrients, vitamins and minerals and has antimicrobial, anti-fungal and anti-oxidant properties [4]. *Aloe vera* contains potentially active constituents including vitamins, enzymes, minerals, sugars, lignin, saponins, salicylic acids and amino acids. It has Antiulcer, Antidiabetic, Antihypercholestermic, Antioxidative Effect, Antibacterial activity, Antiviral activity and Antifungal activity. *Aloe vera* could be used in various conditions like Mild to moderate burns, Erythema, Genital herpes, Seborrheic dermatitis, Psoriasis vulgaris, Skin moisturizer, Type 2 diabetes, Oral lichen planus infections, Angina pectoris, Ulcerative colitis, UV-induced erythema, Kidney stones and Alveolar osteitis [5]. The gel of *Aloe vera* was used to treat stomach ailments, gastrointestinal problems, skin disease, constipation, radiation injury, inflammatory effect, healing wounds and burns, ulcer and diabetes and *Aloe vera* products are mainly for cosmetic, pharmaceutical, nutraceuticals and food industries. *Aloe vera* gel act against the selected pathogens *Bacillus subtilis*, *Salmonella typhi*, *Escherichia coli*, *Staphylococcus aureus*, *Proteus vulgaris*, *Aspergillus fumigatus*, *Candida albicans* and *Penicillium* sps [6]. The antibacterial activity of wine due to its essential biological function which has been verified under various experimental conditions. Wine serves as a base for medicinal preparations compounded with a range of herbs adapted to treat various disorders [7]. Wine has one of the functional fermented foods and it exhibits protective effect against bacterial food infections [8] [9]. The wine exhibited bactericidal activity against common food borne pathogens such as *Salmonella typhimurium*, *Staphylococcus aureus* and *Escherichia coli*. However, its bactericidal effect was much faster in case of *Salmonella* as compared to other pathogens [10].

MATERIALS AND METHODS

Extraction and Processing of Aloe Gel

Aloe vera leaves were collected from Perambalur region and the inner part of the fresh leaf which contains colourless gel extracted by hand filleting method was used for the production of wine. The lower one inch of the leaf base, the tapering point (2-4 inches) of the leaf top and the short sharp spines located along the leaf margins were removed by a sharp knife. The knife was then, inserted into the mucilage layer below the green rind followed by the removal of top and bottom rinds. The gel was then blended in a mixer after adding cane sugar to adjust the TTS to 20 % and then supplemented pH was adjusted to 4.75 to make it favourable for the yeast growth, using citric acid.

Inoculum Preparation

Twenty five ml of sterilized Glucose yeast Broth dispensed in 100ml flask was inoculated with loopful culture of *Saccharomyces cerevisiae*. The flask incubated at 30°C on a rotary shaker (150 rpm) for overnight the cell were separated by centrifugation 10.000 rpm and these were washed twice and resuspended in normal saline to give a concentration of 10 cells /ml which was used as a pre-inoculum. The inoculums was prepared by transferring 10ml of the pre-inoculum to 250 ml conical flask having 100 ml of *Aloe vera* juice supplemented with 5% sucrose and incubating overnight as a shake culture at 30°C.

Fermentation

Aloe vera gel supplemented with cane sugar with pH 4.75 was subjected to batch fermentation. After completion of fermentation, the wine was clarified by repeated siphoning which was carried four times with a sedimentation period of 3 days between each siphoning and analyzed for various constituents including Total Soluble Solids, total acids, content and various elements including in it.





Maturation of wine and antibacterial efficacy

Ageing of *Aloe vera* wine was done for one year in an oak wood barrel the container were Filled upto the prime and analyzed for various components after one year of ageing. The antibacterial efficacy of prepared wines against various pathogens was assessed by the presence or absence of zone of inhibition.

RESULTS AND DISCUSSION

The antibacterial efficacy of prepared wines against *S.typhimurium*, *S.aureus* and *E.coli*, the common food borne pathogens, was assessed by the presence or absence of inhibition zones by MIC and MBC values and time kill curves. To investigate the antibacterial efficacy of the *Aloe vera* based herbal wines against known pathogenic organisms like *S.typhimurium*, *S.aureus* and *E.coli* bacterial growth inhibition zones were observed for both the wines by well diffusion assay. The recorded size of zone inhibition against the pathogens by prepared wines and their controls. It was observed that both the wines showed remarkably higher efficacy of inhibition in comparison to respective controls like 10% ethanol and herbal extracts. Average zone sizes with Aloe-ginger wine against the three organisms measured about 12.3 and 11.0 mm respectively making wine slightly more efficacious in terms of its antibacterial activity as compared to its counterpart. Wine had the highest antibacterial against *S. typhimurium* and *E. coli* while Aloe-ginger wine worked best against *S. aureus*. Table 2 represents the characteristic features of aloe wine such as appearance, colour, sugar, body, flavor, astringency, aroma and general quality. Table 3 represents the presence of phytochemicals such as tannins, flavonoids, alkaloids, saponins, glycosides, terpenoides, polysaccharides and free amino acids.

CONCLUSION

In the preparation of *Aloe vera* juice, we found that the optimum concentration of *Aloe vera* to water weight by volume of 1:3 at this concentration the highest volume of alcohol was obtained. We observed that the tasting of wine has clarity, color, body and overall quality of each sample of *Aloe vera* are not significant difference at $\alpha = 0.05$ but there were significant difference in aroma and flavor. In the yellow colour of *Aloe vera* wines, it was found that the optimum ratio of *Aloe vera* to water is 1:3. The suitable amount of added pineapple is 33.3 gram/litre of water with 250 gram of *Aloe vera* flash because it gave the highest concentration of alcohol in the wine. The result of tasting by adding pineapple, we found that color and flavor of two sample are no significant difference at $\alpha = 0.05$. Most of panelists like sweet wines with low percentage of alcohol. *Aloe vera* wine with added pineapple was more acceptable than the one without added pineapple. From these observations, we concluded that *Aloe vera* herbal wine can be used as a healthy and nutritional food which has the potential antimicrobial activity. These results could be possible to formulate and identify the composition of new compounds in the antimicrobial drugs in future.

REFERENCES

1. Supreet Jain, Nirav Rathod, Ravleen Nagi, Jaideep Sur, Afshan Laheji, Naveen Gupta, Priyanka Agrawal, and Swati Prasad (2016) Antibacterial Effect of *Aloe Vera* Gel against Oral Pathogens: An In-vitro Study. J Clin Diagn Res. 10(11): ZC41–ZC44.
2. Agarry, Olaleye, Machael (2005) Comparative antimicrobial activities of *Aloe vera* gel and leaf Afr.J.Biotechnol. 4: 1413-1414.
3. Mohsen Radi, Elham Firouzi, Hamidreza Akhavan and Sedigheh Amir (2017) Effect of Gelatin based Edible coatings incorporated with *Aloe vera* and Black and Green Tea extracts on the shelf life of fresh cut oranges. *Journal of Food Quality*. (1):1-10
4. Kazhal Sajadi and Samira Bahramian. (2015) Antifungal Effect of *Aloe Vera* Gel on *Penicillium Citrinum* in Culture Media and UF Cheese. *International Journal of Food Engineering*. 1: (1)





Ruffina et al.,

5. Bhuvana K.B, Hema N.G, Rajesh T Patil. (2014) Review on *Aloe vera*. International Journal of Advanced Research 2 (3):677-691.
6. Renisheya Joy Jeba Malar T, Johnson M, Nancy Beaulah S , Laju R S , Anupriya G, Renola Joy Jeba Ethal (2012) Anti-Bacterial and Antifungal Activity of Aloe Vera Gel Extract. International Journal of Biomedical and Advance Research 3 (03) : 184-187
7. Sheth NK, Wisniewski TR, Franson TR. Survival of enteric pathogens in common beverages: an in vitro study. American Journal of Gastroenterology. 83:658-660.
8. Soni SK, Bansal N, Soni R. (2009) Standardization of conditions for fermentation and maturation of wine from Amla International Journal of Home Science (Emblica officinalis). Natural Product Radiance 8:436-444.
9. Bellido-Blasco JB, Arnedo-Pena A, Cordero-Cutillas E, Canos-Cabedo M, Herrero-Carot C, Safont-Adsuara L.. (2002) The protective effect of alcoholic beverages on the occurrence of a Salmonella food-borne outbreak. Epidemiology 13:228-230
10. Neetika Trivedi, Praveen Rishi, Sanjeev Kumar Soni (2015) Antibacterial activity of prepared *Aloe vera* based herbal wines against common food-borne pathogens and probiotic strains, International Journal of Home Science 1(2): 91-99.

Table 1: Antimicrobial activity of *Aloe vera* aqueous extract

Bacteria / Fungi	50% of Aloe aqueous extract	75% of Aloe aqueous extract
<i>Staphylococci</i>	18.8	21.0
<i>E.coli</i>	12.66	13.5
<i>Aspergillus niger</i>	5.5	8.0
<i>Aspergillus flavus</i>	6.0	9.0

Table 2: Evaluation card of Aloe wine by five tasters

Characteristics	Max score	Score by tasters				
		I	II	III	IV	V
Appearance	2.0	2.0	2.0	2.0	2.0	2.0
Colour	2.0	2.0	1.5	2.0	2.0	2.0
Bou	2.0	1.5	2.0	2.0	2.0	2.0
Acescent	2.0	2.0	1.5	2.0	2.0	2.0
Total acid	2.0	2.0	2.0	2.0	1.0	1.5
Sugar	1.0	0.5	1.0	0.5	1.0	1.0
Body	1.0	1.0	1.0	1.0	1.0	1.0
Flavor	2.0	2.0	1.5	2.0	1.0	2.0
Astringency	2.0	2.0	2.0	2.0	2.0	1.5
Aroma	2.0	1.5	2.0	2.0	2.0	2.0
General quality	2.0	2.0	2.0	2.0	2.0	2.0
Total	20.0	19.0	18.5	18.5	18.0	18.0





Ruffina et al.,

Table 3: Phytochemical profile of *Aloe vera* based herbal wine

Phytochemical analysis	Aloe wine
Tannins	+
Flavonoids	+
Alkaloids	+
Saponins	+
Glycosides	+
Terpenoides	+
Polysaccharides	+
Free amino acids	+



Fig 1: *Aloe vera* herbal wine

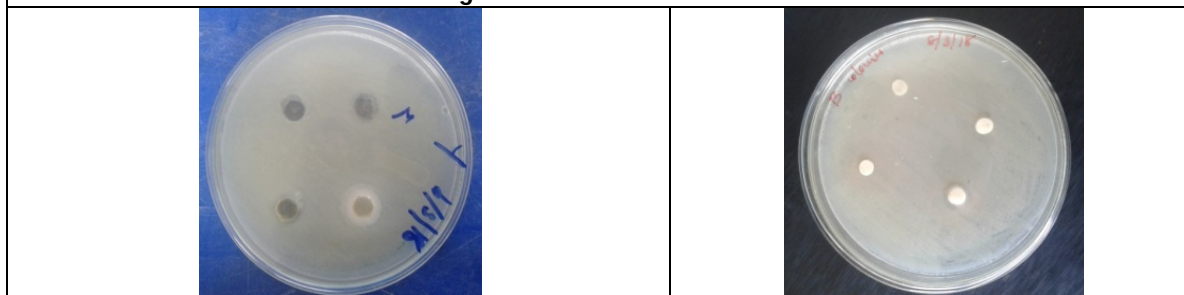


Fig 2: Antimicrobial activity of *Aloe vera* in *E.Coli*.

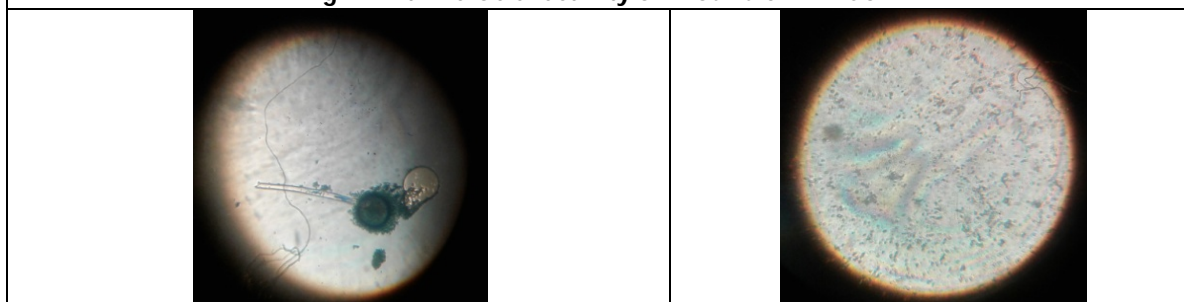


Fig 3: Antimicrobial activity of *Aloe vera* in fungal plates

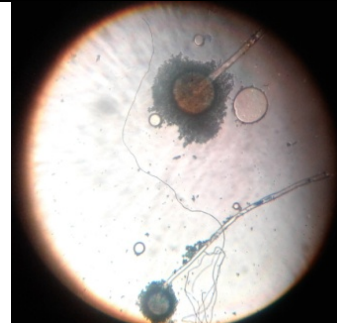




Ruffina et al.,

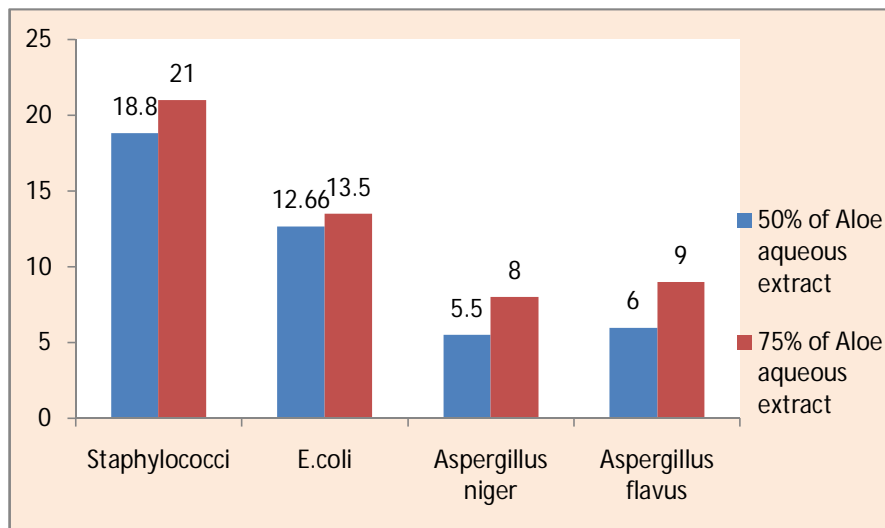


Aspergillus niger



Aspergillus falavous

Fig 4: Antimicrobial activity of *Aloe vera* in fungal plates



Graph 1: Antimicrobial activity of *Aloe vera* extract base on zone of inhibition





An Overview of Slope Monitoring Techniques in Opencast Mines

Arun Kumar Sahoo* and Jitendra Pramanik

Centurion University of Technology and Management, Odisha, India.

Received: 26 Aug 2020

Revised: 28 Sep 2020

Accepted: 31 Oct 2020

*Address for Correspondence

Arun Kumar Sahoo

Centurion University of Technology and Management,
Odisha, India.

Email: arunkumar.sahoo@cutm.ac.in



This is an Open Access Journal / article distributed under the terms of the **Creative Commons Attribution License** (CC BY-NC-ND 3.0) which permits unrestricted use, distribution, and reproduction in any medium, provided the original work is properly cited. All rights reserved.

ABSTRACT

In opencast mining, slope stability plays a vital role towards the operational safety. A slope failure imparts greater loss to both economy and human life. To ensure proper management and mitigation of the stability problems it is necessary to provide accurate slope designs and constant and accurate slope monitoring procedures. Several techniques have been employed to assess the slope stability in opencast mines. This paper aims at reviewing the different slope monitoring strategies currently in use along with its limitations.

Keywords: Slope stability, Slope monitoring techniques

INTRODUCTION

The fast raise in open cast mining with enhanced mechanization has significantly enhanced the production of minerals. Because of this rapid development, the risks of slope failure and dump failure have also increased in open cast mines day by day. The sudden failure of slopes can inflict heavy casualties and damages in several ways. In Indian mining, there is no clear protocol that is devised for slope designs to make mining operation safe and productive and need for it is growing day by day. Mostly the mines slopes are designed with engineered factor so as to recover maximum ore at optimum cost and safety. However, with unexpected seismic activities and weather conditions along with unknown geological structures can trigger sudden slope failures even in the most robustly designed slopes. To avoid such situations, systematic monitoring with pre-warming system and periodic examinations have been made for safety of mine workers.

In past, several devices have been used to monitor the slopes in open pit mines. The aim is to identify the slope movements before the failure occurs so as to minimize the damage as low as possible. The devices which allowed remote measurement and monitoring of slopes are found to be most effective. Mostly two methods are used for slope monitoring (a) Conventional method where technicians manually monitor by the geo-technical sensors in the field; and (b) Automated sensing methods like Slope Stability Radar (SSR), Light Detection and Ranging (LiDAR), Ground



**Arun Kumar Sahoo and Jitendra Pramanik**

Based Synthetic Aperture Radar Interferometry (GB-InSAR), monitoring by sensing through Artificial Neural Networks (ANN) and so on. The use of WSN in both opencast and UG mines can also provide data of different physical factors. The accumulated data can be further processed using different data analytics techniques.

Related Works

Recently, various methods have been implemented for slope monitoring. In many countries like USA, Japan, Hong Kong, Malaysia have been using GIS to map the soil slopes [1-3] and it has been found to be very effective in identifying the areas which are susceptible to slope bust. With satellite image analysis vital information about vegetation, geology, landscape & land usage is collected [4]. In GIS, it is not possible to collect any information of motion which is pressed within the rock and soil. It only gives information about horizontal surface motion using which topographical slope failures can be detected [5].

SAR is an instrument which use microwave signals that are capable to detect EM waves that echo from earth surface. It can be used for both short range and log range slope monitoring. With limitations in data processing and parameter interpretation, SAR has not found the popularity it promised [6]. Another technology known as TLS which is used to gather surface data over wide range & environmental conditions. By monitoring the change in slope surface using TLS, landslide hazards are avoided [7-8]. However, there is no standard to assess the accuracy and precision of TLS. Slope monitoring using GPS is most common method in practice in mining industries. It measures the slope stability through displacements. For the purpose of survey physical Structures are placed on ground which cover a slope area as point of reference. There coordinates are being determined at periodic intervals. Through studying the rate of change of point the types of displacements with its characteristics are assessed. The information coming out the survey results of GPS give magnitude of slope progress for a particular site [9-10].

Type of slope failures

The slope failures are considered to be most hazardous of natural calamities that occurs around the globe. The types of slope failures are normally controlled, by water content, foundation strength & material properties. The most of the common slope failures, are plane, wedge, toppling, rock fall & rotational. The below table -1 shows the mass movement classification based on process type and material.

Factors Affecting Slope Stability

Slope failures occurs when the downward movements of material due to gravity & shear stress exceed the shear strength. There can be several factors that influences the shear stress which initiates the slope failure. The table 2 put forwards a concise description of various factors affecting slope failures.

Different slope monitoring system in opencast mines

The rock excavation can initiate the deformation in the rock mass which can be closely monitored to prevent the accident which will be occurred due to unstable conditions. At time of designing safe and efficient the mining operations rock mass properties, geological structure and ground water conditions should be taken into consideration. The factor of safety is playing the major role for controlling the damage of machinery and loss of life due to movement of rock mass and slope failure. When considering factor of safety there is a requirement of cost control. Steepen pit walls minimize and reduce the operational cost by minimizing waste removal. Mines use benches and berms to arrest falling material, control blasting practices to lessen unnecessary fracturing, and deal with ground water to help stabilize the slopes. However, unidentified geological structures, unexpected weather conditions, or seismic activities can instigate well-designed slopes to fail. Due to this uncertainty regular visual inspections and systematic monitoring should be applied to provide early warning signs of failures [11].

A slope monitoring system is determined the slope movement with sub millimeter precision. It is the process for saving a whole mine against all possible dangerous movements of soil and rocks and provide early warning before



**Arun Kumar Sahoo and Jitendra Pramanik**

the failure occur. In exact accuracy of measurement of slope deformation and wall movements can be helpful to provide the early warning. A slope monitoring system should be able to detect all types of slope deformations covering an area or an entire open pit. This condition is important to give suitable preventive measurements. Furthermore, only a continuous measurement which means 24 hours in a day, which can withstand all weather conditions, provide a full slope stability protection. It is the important point for the data collected to be analyzed and interpreted correctly. Any wrong interpretation could lead to poor decision making. Communication of false data must be avoided, because it may result in wrong or unnecessary alarms in the mine.

Monitoring methods can be categorized into four types

- Visual monitoring
- Surface monitoring
- Subsurface monitoring
- Remote monitoring

Visual monitoring

In this monitoring process a geotechnical engineer checks visually the area prone to failure or any danger on a daily basis which is the primary step of slope monitoring. It can be calculated the changes in slope with comparing the previous measurement. Not only the geotechnical engineer is responsible for checking the stability of slope those who are working there they will be held responsible for the inspection for safe and stable working. After visual inspection all have to report about changes in slope.

Surface monitoring

Any changes that occur in the surface will be monitored by this monitoring method by using these instruments like global positioning system and total station which is primarily used for surveying. In surveying the changes in position can be calculated.

Subsurface monitoring

For measuring the type, size, and rate of the slope deformation, determine shear zones, monitor groundwater conditions, rock electric characteristics or seismicity of the area the subsurface monitoring is necessary. Inclined meters, borehole extensometers, piezometers, and geophysical methods are the mainly used for subsurface monitoring techniques.

Remote monitoring

There is no need of physical contact for measuring the displacements. In remote monitoring method changes can be measured from a certain distance. Light Detection and Ranging (LIDAR), Interferometry of Synthetic Aperture Radar (InSAR), Time Domain Reflectometry or Slope Stability Radar (SSR) are the principal remote monitoring methods which are discussed one by one in below.

Time Domain Reflectometry (TDR)

TDR is the electrical method for measuring the slope stability. This method has many advantages as follows

- Installation cost is low
- Longer lifetime
- Remote data collection
- Continuous monitoring is possible

The disadvantages are

- For proper measurement it requires surface devices
- Proper cementing
- No indication of direction of discontinuities orientation





Arun Kumar Sahoo and Jitendra Pramanik

Photogrammetry

In this monitoring method the photographs of the mine are captured from two different locations for getting the line of sight from each place. Photos are captured by the help of drones, cameras, helicopters etc. These photos are used to produce 3D image of the mine which give the details about the fault, folds, cracks etc. it is done in repeated manner at a regular interval and comparing the images the changes or movements or displacements can be assessed.

Light Detection and Ranging (LIDAR)

With LIDAR 3-D laser scanning is carried out and terrestrial laser scanning and an air borne scanning can also be done. A cloud of points is the result of scanning. And this cloud of points indicates the slope surface in 3D. There are many advantages of this equipment such as

- Measuring a wide variety of materials,
- Measurement with High Resolution & Quality,
- Providing measurement at unreachable places,
- Battery operated, fast response

It has one big disadvantage

- Early warning system not available

Interferometry of Synthetic Aperture Radar (InSAR)

InSAR measures slope displacements using satellites. By Collecting Satellites signals a device creates an image. Main advantages are

- High accuracy on a big surface

There are many disadvantages such as

- Measurements are get easily affected by weather conditions
- Impossible to execute long slope monitoring

Slope Stability Radar (SSR)

SSR is a Ground-based radar which uses a remote sensing technology that utilizes the phase-change interferometry to quantify a surface deformation of a slope over time. It can remotely assess a surface deformation of a slope from a stationary platform without reflectors or prisms. This system scans a region of a slope and divides an area into pixels. An amount of movement can be computed for each pixel and compared with an amount of movement from the previous scan. With the use of ground-based radar slope deformation in the range of sub millimeter can be collected in a matter of few minutes which don't get affected by weather conditions

CONCLUSION

With change in the stress levels influences the wall movements and deformation in open pit mines. Unprecedented movement / deformation and increase stress level can result slope failure. Different methods are employed to monitor the slope stability there by to provide an early warning system. More studies deemed essential to develop and refine the existing technologies to improve the safety and production in open pit mines.

REFERENCES

1. Ayalew, L., Yamagishi, H., Marui, H., Kanno, T., 2005. Landslides in Sado Island of Japan: Part I. Case studies, monitoring techniques and environmental considerations. Eng. Geol. 81 (4), 419–431.





Arun Kumar Sahoo and Jitendra Pramanik

2. Dai, F.C., Lee, C.F., 2002. Landslide characteristics and slope instability modeling using GIS, Lantau Island, Hong Kong. *Geomorphology* 42 (3–4), 213–228.
3. Pradhan, B., 2010. Remote sensing and GIS-based landslide hazard analysis and cross-validation using multivariate logistic regression model on three test areas in Malaysia. *Adv. Space Res.* 45 (10), 1244–1256.
4. H.Z.M., Zahidi, I.M., Bakar, S.A., 2010. Development of landslide susceptibility map utilizing remote sensing and Geographic Information Systems (GIS). *Disaster Prev. Manag.* 19 (1), 59–69
5. Jongmans, D., Garambois, S.P., 2007. Geophysical investigation of landslides: a review. *Bull. Soc. geol. France* 178 (2), 101–112.
6. Colesanti, C., Wasowski, J., 2006. Investigating landslides with space borne Synthetic Aperture Radar (SAR) interferometry. *Eng. Geol.* 88 (3–4), 173–199.
7. Akib, W.A.A.W.M., Tahar, K.N., Ahmad, A., 2012. Slope gradient analysis at different resolution using terrestrial laser scanner. In: *Proceedings – 2012 IEEE 8th International Colloquium on Signal Processing and its Applications (CSPA)*. pp. 169–173.
8. Luzi, G., Noferini, L., Mecatti, D., Macaluso, G., Pieraccini, M., Atzeni, C., Schaffhauser, A., Fromm, R., Nagler, T., 2009. Using a ground-based SAR interferometer and a terrestrial laser scanner to monitor a snow covered slope: results from an experimental data collection in Tyrol (Austria). *IEEE T. Geosci. Remote* 47 (2), 382–393.
9. Othman, Z., Wan, A.W.A., Anuar, A., 2011. Evaluating the performance of GPS survey methods for landslide monitoring at hillside residential area: Static vs rapid static. In: *7th IEEE International Colloquium on Signal Processing and Its Applications (CSPA 2011)*. pp. 453–459
10. Kondo, H., Sugiyama, A., Cannon, M.E., 1996. Precise carrier phase GPS and its application to real-time landslide detection. *1996 IEEE Digital Signal Processing Applications (TENCON 096)*, vol. 2, pp. 906–911.
11. Upasna P. Chandarana¹, Moe Momayez², Keith W. Taylor .MONITORING AND PREDICTING SLOPE INSTABILITY: A REVIEW OF CURRENT PRACTICES FROM A MINING PERSPECTIVE. *IJRET: International Journal of Research in Engineering and Technology* eISSN: 2319-1163 | pISSN: 2321-7308.

Table 1. Mass Movement classification based on process type and material.

Process Type	Type of Material		
	Topple	Rock Topple	Debris topple
Fall	Rock Fall	Debris fall	Earth fall
Slide	Rockslide	Debris Slide	Earth Slide
Flow	Rock flow	Debris flow	Earth flow
Spread	Rock spread	Debris spread	Earth spread
Complex	Rock avalanche	Flow slide	Slump-earth flow

Table 2. Factors Affecting Slope stability

Parameters Name	Description
Ground water	The accumulation of excess ground water inflicts increased upthrusts and affect the slope stability adversely. At places, where the confining stress has been reduced, the decrease in compressive strengths happens due to the effect of water pressure in the rock pores.
Mining Method and machinery	Surface mining operations depends on the design of the steep pit slope. The unstable pit slope is playing a major role for large scale failure. Mining machinery which is used for excavation piles the excavated material on the benches. That gives rise to a surcharge load on the slope and pulls the slope downward.
Geological Structure	Geological structures like joints and discontinuities, faults, amount and angle of dip is





Arun Kumar Sahoo and Jitendra Pramanik

	affected the stability of the slope which is dependent on the shear strength available along the surface. Presence of Joints and bedding planes develop weakness of the surface.
Slope Geometry	The fundamental slope design parameters are bench height, slope angle & surface failure area. With increase in bench height and slope angle, the slope stability decreases.
Lithology	Slopes pit with alluvium or weathered rocks have low shearing strength, which is reduced even further when water gets into it. These types of slopes should be flattered.
Cohesion	It is measure in pascal and its attributed as resistance force per unit area. Soil cohesion values comes in the range of KPa & in case of rocks its is 100 times higher than soils. Higher the value of cohesion, more stable will be the slope.
Dynamic Forces	Shear stress is increased with blast vibrations. Blasting influences the max attainable bench face angles. Poor blasting can significantly affect the slope stability. Smooth blasting techniques are found to be good for smaller slopes. For larger slopes, back break and blast damage have little effect on the slope angle.
Time	The time for which the slope has to stand after excavation also considered towards the slope stability.
Internal Friction Angle	In reaction to a shearing stress when a slope failure occurs, the angle between normal force & resultant force gives a measure of angle of internal friction. Particle size its structure affects the angle of internal friction.
Old Workings	Old working acting as network of ground water flow are unstable and can get collapsed very easily when subjected to any loads.





Pharmacognostic Standardization and Phytochemical Studies of *Physalis minima* Leaves

Senniappan P^{1*}, Karthikeyan V¹, Janarthanan L¹, Loganathan J² and Sathiyabalan G³

¹Assistant Professor, Department of Pharmacognosy, Vinayaga Mission's College of Pharmacy, VMRF(DU), Salem, Tamil Nadu, India.

²Assistant Professor, Department of Pharmaceutical Chemistry, Vinayaga Mission's College of Pharmacy, VMRF(DU), Salem, Tamil Nadu, India.

³Assistant Professor, Department of Pharmacognosy, College of Pharmacy, Madurai Medical College, Madurai, Tamil Nadu, India.

Received: 27 Sep 2020

Revised: 29 Oct 2020

Accepted: 03 Nov 2020

*Address for Correspondence

Senniappan P

Assistant Professor, Department of Pharmacognosy,
Vinayaga Mission's College of Pharmacy, VMRF (DU),
Salem, Tamil Nadu, India.

Email: senniappan1979@gmail.com



This is an Open Access Journal / article distributed under the terms of the **Creative Commons Attribution License** (CC BY-NC-ND 3.0) which permits unrestricted use, distribution, and reproduction in any medium, provided the original work is properly cited. All rights reserved.

ABSTRACT

Physalis minima L. (Family: Solanaceae) is a perennial herb which commonly known as Native gooseberry and wild cape gooseberry. *Physalis minima* have been used in Indian traditional medicinal system for very long time for treating various disorders and in folk remedies used to relieve pain. Micro morphology and physicochemical parameter of the leaves of *P.minima* were performed as per WHO and Pharmacopoeial methods. Leaves are soft and smooth, with entire or jagged margins, 2.5–12 cm long. Microscopic evaluation of leaves showed the midrib has a long erect adaxial cone and the abaxial part is wide, thick and semi circular. The ground tissue has three or four layers of wide, compactly arranged parenchymatous cells. The vascular system consists of a single large centrally placed bicollateral vascular bundle and the vascular bundle has dense mass of xylem elements which are wide, angular and thick walled. Lamina is bifacial in nature with thin walled cylindrical epidermal cells. Calcium oxalate crystals are fairly abundant in mesophyll cells of the leaf. The crystals are druses which are spherical bodies with spiny surface. Preliminary phytochemical screening of appropriate solvent extracts showed the presence of alkaloids, sterols, tannins, proteins and amino acids, flavonoids, terpenoids, saponin, carbohydrates and absence of glycosides and volatile and fixed oil. Microscopic analysis and other parameters were informative and provide valuable information in the authentication, standardization of *P.minima* leaves.

Keywords: *Physalis minima*, Solanaceae, Native gooseberry, Microscopical evaluation.





INTRODUCTION

Physalis minima L. is a species of perennial herbs belonging to the Solanaceae family. It is commonly known as Native gooseberry, wild Cape gooseberry and pygmy ground cherry [1]. It is a pan-tropical annual herb 20–50 cm high at its maturity. This plant widely distributed throughout India and other Southasian countries [2]. *Physalis minima* have been used in Indian traditional medicinal system for very long time for treating various disorders [3]. Traditionally this plant is used in folk remedies used to relieve pain. This plant is reported for its diuretic, laxative and anti-inflammatory activities [4 & 5].

Taxonomical classification [6]

Kingdom	: Plantae
Subkingdom	: Viridiplantae
Infrakingdom	: Streptophyta
Superdivision	: Embryophyta
Division	: Tracheophyta
Subdivision	: Spermatophytina
Class	: Magnoliopsida
Superorder	: Asteranae
Order	: Solanales
Family	: Solanaceae
Genus	: <i>Physalis</i>
Species	: <i>minima</i>

Vernacular names [7]

English	: Native gooseberry, wild cape gooseberry and pygmy groundcherry
Sanskrit	: Tankari
Kannada	: Bandula
Hindi	: Tulatipati
Mah.	: Tan – mori
Telugu	: Kupante; Budamakaya
Tamil	: Siruthakkali, sodakkuthakkali
Bengali	: Bantipariya; Bantepari
Punjabi	: Kaknaj

Various phytoconstituents has been reported in this plant such as steroidal lactons Physalin A, Physalin B and Withaphysalins A & B belong to the withanolide group [8 & 9]. As mentioned previous reports have been published regarding phytochemical and different therapeutic activities *in-vitro* and *in-vivo*. An investigation to inquire its pharmacognostic examination is unavoidable. The present work was aimed to lay down standards which could be useful to detect the authenticity of this therapeutically useful plant *Physalis minima* leaves to treat various illnesses.

MATERIALS AND METHODS

Chemicals: Ethyl alcohol, Formalin, Chloral hydrate, Acetic acid, Glycerin, Phloroglucinol, Toludine blue, Hydrochloric acid and all other chemicals used in this study were of analytical grade.





Collection and authentication of Plant: The leaves of the selected plant were collected from in and around Salem district, Tamilnadu with the help of local tribal and field botanist. It was authenticated by Dr. P. Jayaraman, Director of Plant Anatomy Research Institute (PARC), Chennai, Tamil Nadu, India.

Macroscopic analysis: Organoleptic characters such as colour, odour, taste, shape, size, surface characters, texture, etc were done [10].

Microscopic analysis: The samples of leaves were fixed in FAA [Formalin (5mL), Acetic acid (5mL), Ethyl alcohol (90mL)]. After one day of fixing, the specimens were dehydrated by t-butyl alcohol. Specimen Infiltration was done by paraffin wax (M.P-58-60°C) [11].

Sectioning: Specimens were sectioned by rotary microtome. The thickness of the sections were about 8-10 μ m. The sections were de waxed and stained by using Toluidine blue. The staining results were remarkably good as the stain was a polychromatic stain. The dye impart pink color to the cellulose, lignified cells, mucilage and blue color to the protein bodies [12].

Leaf clearing: Paraffin embedded leaf was used for para-dermal sections. Another method was clearing leaf fragments by immersing in alcohol followed by treating with 5% sodium hydroxide. The material was made transparent due to loss of cellular contents.

Photomicrographs: Photographs were taken with help of Nikon lab-photo 2 microscopic Unit. Bright field and polarized light was used. The magnifications are indicated by the scale-bars in the photographs.

Quantitative Microscopy: Stomatal number, Stomatal index, Vein islet and Vein termination was determined as per standard methods [13].

Physicochemical analysis: Total ash, acid insoluble ash, water soluble ash, loss on drying and extractive values was determined as per standard methods [14].

Preliminary phytochemical screening: Preliminary phytochemical screening of ethanolic and aqueous extract carried out to find out the presence of various phytoconstituents using standard procedure [15].

RESULTS

Macroscopy: Leaves are soft and smooth, with entire or jagged margins, 2.5–12 cm long. Cream to yellowish flowers are followed by edible yellowish fruit encapsulated in papery cover which turns straw brown and drops to the ground when the fruit is fully ripe. The fruit has a pleasant cherry-tomato like flavor when fully ripe (Fig 1).

Leaf Morphology

Colour	: Green
Odour	: Characteristic
Taste	: Slightly bitter and Characteristic
Size	: 3-8cm in length and 1.5-4.1cm width
Shape	: Ovate
Apex	: Acute
Margin	: Shallowly toothed or lobed margin
Base	: Asymmetrical base
Texture	: More or less pubescent,
Extra Feature	: Midrib and veins are prominent on lower surface, reticulate venation.





Microscopy

Midrib: The midrib has a long erect adaxial cone and the abaxial part is wide, thick and semi circular. The midrib is 650 μ m in thickness. The adaxial cone is 200 μ m in height and 150 μ m in thickness. The abaxial part is 550 μ m wide (Fig 2). The midrib consists of a thin epidermal layer of cells of irregular shape and size. The ground tissue has three or four layers of wide, compactly arranged parenchymatous cells (Fig 3 & 4).

Vascular Bundle: The vascular system consists of a single large centrally placed bicollateral vascular bundle and the vascular bundle has dense mass of xylem elements which are wide, angular and thick walled (Fig 5). The xylem elements are up to 50 μ m wide and phloem elements on both upper and lower parts of the xylem strand. The phloem is thin layer of small angular compact cells. The adaxial phloem and abaxial phloem are similar in shape and size.

Lateral Vein: The lateral vein is flat on the adaxial side and semi circular on the abaxial side. It is 210 μ m thick and 200 μ m wide. The lateral vein consists of a thick vertical block of xylem and small unit of phloem. The vascular strand is surrounded by thick walled, wide parenchymatous cells (Fig 3).

Lamina: The lamina is soft and tender. It is bifacial (Dorsiventral leaf) nature with thin walled cylindrical epidermal cells. There is a single horizontal band of cylindrical palisade cells are compactly arranged on the adaxial part and three or four layers of spherical lobed, less compactly arranged spongy parenchymatous cells in lamina (Fig 6).

Crystal Distribution: Calcium oxalate crystals are fairly abundant in mesophyll cells of the leaf. The crystals are druses which are spherical bodies with spiny surface. The calcium oxalate druses are random in distribution and they occur in ordinary unmodified cells (Fig 7).

Quantitative Microscopy (Table 1)

Physio-chemical parameter (Table 2)

Preliminary Phytochemical Screening of leaves of *Physalis minima* Linn (Table 3)

DISCUSSION

Crude drug evaluation done for confirmation of its identity and determination of its quality and purity and also detect adulterated content. It is a qualitative evaluation based on the sensory and morphology profiles of crude drugs [16]. This present study is to serve as a tool for developing standards for authentication, quality and purity of *Physalis minima* leaf. Adulteration of crude drugs can cause serious health problems to consumers and pharmaceutical industries. The anatomical character is an important aid for the identification of plant drugs [17]. Microscopic evaluation is one of the simplest methods for the proper authentication of plant materials [18]. Microscopic evaluation of leaves showed the midrib has a long erect adaxial cone and the abaxial part is wide, thick and semi circular. The midrib consists of a thin epidermal layer of cells of irregular shape and size. The ground tissue has three or four layers of wide, compactly arranged parenchymatous cells. The vascular system consists of a single large centrally placed bicollateral vascular bundle and the vascular bundle has dense mass of xylem elements which are wide, angular and thick walled. Lamina is bifacial in nature with thin walled cylindrical epidermal cells. Calcium oxalate crystals are fairly abundant in mesophyll cells of the leaf. The crystals are druses which are spherical bodies with spiny surface. Quantitative analytical microscopy is useful in measuring the cell contents of the crude drugs and help in their identification, characterization and standardization. The ash values are useful for detecting foreign inorganic matter. Acid insoluble ash gives information regarding the presence of inorganic dirt and dust [19 & 20]. Phytochemical evaluation and characterization of plant extract is an important tool in drug discovery [21]. Preliminary phytochemical screening of appropriate solvent extracts showed the presence of tannins, sterols, alkaloids, flavonoids, amino acids, terpenoids, carbohydrates and absence of glycosides and volatile and fixed oil.





CONCLUSION

Physalis minima have a wide range of therapeutically active compounds which could be useful for treatment of various ailments. The pharmacognostic features, physicochemical constants, preliminary phytochemical studies have been useful in deciding the identity, purity and strength of the plant material and also for fixing standards for this plant. This present study will certainly help to build a monograph of the plant in Herbal Pharmacopoeia.

Conflict of interest statement

We declare that we have no conflict of interest.

ACKNOWLEDGEMENT

The author extend their heartfelt thanks for Dr.P.Jayaraman, Director of Plant Anatomy Research Institute, Tambaram, Chennai for authentication and microscopical studies.

REFERENCES

1. Nathiya M, Dorcus D. Preliminary phytochemical and anti-bacterial studies on *Physalis minima* Linn. International Journal of Current Sciences, 2012: 24-30.
2. Anand TJ, Liakhat Ali SK, Sudhir M, Manjula RR, Jaya Sravani P, Saraswathi Devi L. Phyto chemical investigation and evaluation of analgesic activity of *Physalis minima*. World Journal of Pharmacy and Pharmaceutial Sciences, 2012; 3(10): 471 -478.
3. Karpagasundari C, Kulothungan S. Free radical scavenging activity of *Physalis minima* Linn. leaf extract (PMLE). Journal of Medicinal Plants Studies, 2014; 2(4): 59-64.
4. Patel T, Shah K, Jiwan K, Shrivastava N. Study on the antibacterial potential of *Physalis mimima* Linn. Indian Journal of Pharmaceutical Sciences, 2011: 111-115.
5. Tammu J, Venkata Ramana K, Thalla S, Narasimha raju B. Diuretics activity of methanolic extract of *Physalis minima* leaves. Der Pharmacia Lettre, 2012; 4(6): 1832-34.
6. Chopra RN, Nayar SL, Chopra IC. Glossary Indian Med. Plants, CSIR, New Delhi; 1956: p-192.
7. Kirtikar KR, Basu BD. Indian Medicinal Plants, Lalit Mohan Basu; Allahabad; Vol.3, 1935: p-1766-1768.
8. Sinha SC, Ali A, Bagchi A, Sahai M, Ray AB. Physalindicanols, new biogenic Precursors of C₂₈-steroidal lactones from *Physalis minima* var.indica. Planta medica, 1987; 55-57.
9. Glotter E, Kirson I, Abraham A, Sethi PD, Sankara Subramanian S. Steroidal constituents of *Physalis minima* (Solanaceae). J.C.S. Perkin J, 1975; 1370-74.
10. Kokate CK, Gokhale SB, Purohit AP. Pharmacognosy. 32nd ed., New Delhi: Nirali Prakashan; 2005.
11. Asokan J. Botanical Micro Technique Principles and Practice. 1st edn, Chennai: Plant Anatomy Research Centre; 2007.
12. Johansen DA. Plant Microtechnique. Newyork: MC Graw hill; 1940, pp. 523.
13. Evan WC. Trease and Evans Pharmacognosy. 15th edn, London Saunders: Elsevier; 2002, pp. 563-70.
14. WHO. Quality control methods for medicinal plant materials. Geneva: World Health Organization; 1998.
15. Anonymous. The Indian Pharmacopoeia. Vol II, New Delhi: Ministry of Health and Family Welfare; 1996.
16. Periyannayagam K, Karthikeyan V. Pharmacognostical, SEM and XRF profile of the leaves of *Artocarpus heterophyllus* L. (Moraceae) - A contribution to combat the NTD. Innovare Journal of Life sciences, 2013; 1(1): 23-8.
17. Karthikeyan V, Agrawal SK, Parthiban P, Nandhini SR. Multivitamin plant: pharmacognostical standardization and phytochemical profile of its leaves. Journal of Pharmacy Research, 2014; 8(7): 910-915.
18. Agrawal SK, Karthikeyan V. Quality assessment profile of the leaves of *Tecoma stans* L. International Journal of Pharmaceutical Research, 2014; 6(2): 94-99.



Senniappan *et al.*,

19. Karthikeyan V, Karthikeyan J. *Citrus aurantium* (Bitter Orange): A Review of its Traditional Uses, Phytochemistry and Pharmacology. International Journal of Drug Discovery and Herbal Research, 2014; 4(4): 766-772.
20. Aruna A, Nandhini SR, Karthikeyan V, Bose P, Vijayalakshmi K, Jegadeesh S. Insulin plant (*Costus pictus*) leaves: Pharmacognostical standardization and phytochemical evaluation. American Journal of Pharmacy & Health Research, 2014; 2(8): 106-119.
21. Karthikeyan V, Balakrishnan BR, Senniappan P, Janarthanan L, Anandharaj G, Jaykar B. Pharmacognostical, phyto-physicochemical profile of the leaves of *Michelia champaca* Linn. International Journal of Pharmacy and Pharmaceutical Research, 2016; 7(1); 331-44.

Quantitative Microscopy

Table 1: Quantitative analytical microscopical parameters of the leaf of *Physalis minima*

S. No.	Parameters	Values obtained*
1	Stomatal number in upper epidermis	36.34 ± 1.38
2	Stomatal number in lower epidermis	27.13 ± 0.22
3	Stomatal index in upper epidermis	19.9 ± 1.34
4	Stomatal index in lower epidermis	22.2 ± 1.43
5	Vein islet number	10.67 ± 0.36
6	Vein termination number	15.0 ± 1.17

*mean of three readings ± SEM

Table 2: Physical parameters of *Physalis minima*

S. No	Parameters	Values *
1	Loss on drying	18
2	Extractive values	
	Ethanol	13.72 ± 0.15
	Methanol	10.13 ± 0.12
	Water	17.15 ± 0.77
3	Ash values	
	Total ash	20.53 ± 0.06
	Acid insoluble ash	6.93 ± 0.42
	Water soluble ash	5.27 ± 0.22

*mean of three readings ± SEM

Preliminary Phytochemical Screening of leaves of *Physalis minima* Linn

Table 3: Preliminary Phytochemical Screening of Different Solvent Extracts

Tests	Ethanollic extract	Aqueous extract
Alkaloids		
Mayer's Reagent	+	-
Dragendorff's reagent	+	-
Hager's reagent	+	-
Wagner's reagent	+	-
Carbohydrates		
Molishch's Test	+	+





Senniappan et al.,

Fehlings Test	+	+
Benedicts Test	+	+
Glycosides		
General Test	-	-
Anthraquinone	-	-
Cardiac	-	-
Cyanogenetic	-	-
Coumarin	-	-
Phytosterols		
Salkowski Test	+	-
Liebermann Burchard Test	+	-
Saponins	+	+
Tannins	+	+
Proteins & Free Amino Acid		
Millons test	+	+
Biuret test	+	+
Flavonoids		
Shinoda test	+	+
Alkaline Reagent test	+	+
Terpenoids	+	-
Fixed Oil	-	-
Volatile oil	-	-



Figure 1: Leaves of *Physalis minima*

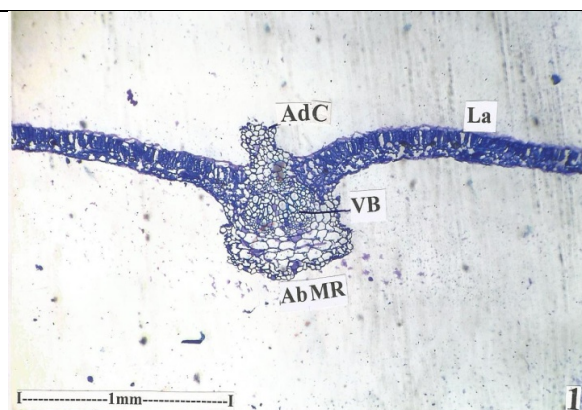


Figure 2: TS of Leaf through Midrib (AbMR: Abaxial Midrib, AdC: Adaxial Cone, La: Lamina, VB: Vascular Bundle)





Senniappan et al.,

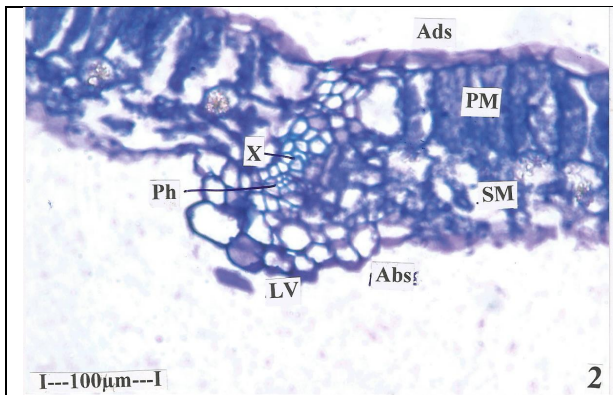


Figure 3:T.S of lateral vein of leaf of *Physalis minima* Linn (Abs:Abaxial side, Ads:Adaxial side, Ph;Phloem, PM:Palisade Mesophyll, LV:Lateral Vein, SM: Spongy Mesophyll, X:Xylem)

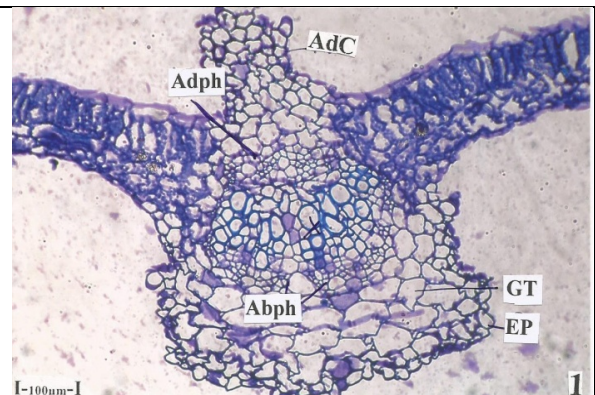


Figure 4:T.S of Midrib-enlarged (Abph:Abaxial phloem, AdC:Adaxial Cone, Adph: Adaxial phloem, Ep:Epidermis, GT:Ground Tissue)

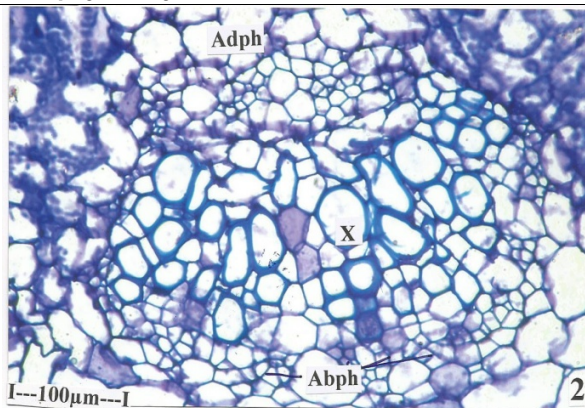


Figure 5: Vascular Bundle of the Midrib (Abph:Abaxial phloem, Adph: Adaxial phloem, X:Xylem)



Figure 6: T.S of Lamina (AbE:Abaxial Epidermis, AdE:Adaxial Epidermis, PM:Palisade Mesophyll, SM: Spongy Mesophyll)

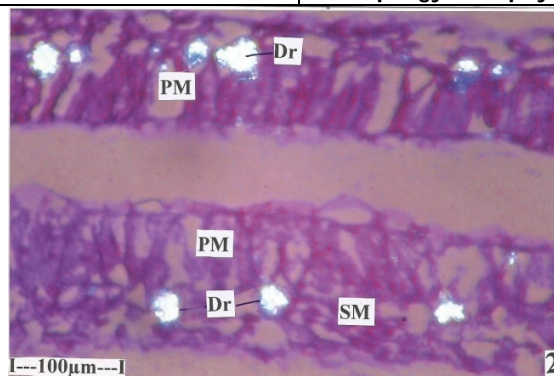


Figure 7:T.S of Lamina crystal distribution as seen under Polarized Microscope (Dr:Druses, PM:Palisade Mesophyll, SM: Spongy Mesophyll)





One-Pot Synthesis, Spectral Characterization, Antibacterial, Antifungal Studies of New Schiff Base Fe(III) Complex

C. Veeravel*, K. Rajasekar, S. Balasubramanian and R. Selvarani

PG and Research Department of Chemistry, Government Arts College (Affiliated to Bharathidasan University), Ariyalur, Tamil Nadu, India.

Received: 28 Aug 2020

Revised: 30 Sep 2020

Accepted: 04 Nov 2020

*Address for Correspondence

C. Veeravel

PG and Research Department of Chemistry,
Government Arts College (Affiliated to Bharathidasan University),
Ariyalur, Tamil Nadu, India.
Email: cveeravel.ml@gmail.com



This is an Open Access Journal / article distributed under the terms of the **Creative Commons Attribution License** (CC BY-NC-ND 3.0) which permits unrestricted use, distribution, and reproduction in any medium, provided the original work is properly cited. All rights reserved.

ABSTRACT

New Fe(III) complex have been synthesized by the reaction of sodium oxalate ion and Schiff base ligands (E-N-((E)-3-phenylallylidene)aniline derived from (2E)-3-Phenylprop-2-enal and Benzenamine. The complex is soluble in DMF and DMSO; low molar conductance values indicate that they are non-electrolytes. Elemental analyses suggest that the complex have 1:1 stoichiometry of the type $[\text{Fe}_2(\text{C}_{15}\text{H}_{13}\text{N})_4(\text{C}_2\text{O}_4)_3]$. Structural and spectroscopic properties have been studied on the basis of FT-IR and Far-IR spectra mass and electronic spectra. Magnetic moment and electronic spectra (diffused reflectance spectral studies) reveal that the octahedral geometry of the prepared complex. The complex and Schiff base showed relatively high antibacterial activity against *E. coli*, *S. aureus*, *B. subtilis*, and *P. auriginosa*. Also good antifungal activities against *A. Niger* and *C. Albicans* have been found compared to its free ligands.

Keywords: (E-N-((E)-3-phenylallylidene) aniline, (2E)-3-Phenylprop-2-enal, Benzenamine, antibacterial, antifungal.

INTRODUCTION

Schiff base ligands derived from an aldehyde and amine, and their transition metal complexes have been widely used in many organic transformations. Schiff base ligands are able to coordinate many different metals and to stabilize them in various oxidation states [1-2]. Furthermore, Schiff base complexes have been used as drugs and they have a wide variety of antimicrobial activities against bacteria and fungi [3-4]. Papers dealing with immobilizations of these complex within mesoporous supports have been extensively studied [5,6]. Iron is the most abundant transition metal for both plants and animals, and it plays an important role in cellular metabolism, enzyme catalysis,



**Veeravel et al.,**

and as an oxygen carrier in hemoglobin and also a cofactor in many enzymatic reactions [7]. However, the imbalance of iron in a human body induces the occurrence of many diseases such as anaemia, liver and kidney damages, diabetes and heart diseases [8-10]. In addition, the discrimination of Fe^{2+} from Fe^{3+} is very important in order to understand the biological functions regulated by iron, because their ferrous / ferric states are one of the important redox pairs in biology systems [11–18]. Therefore, developing sensors capable of determining both Fe^{2+} and Fe^{3+} is very valuable and still regarded as a challenge. We have chosen the metal easily available in the market with low price and the many more chemical products well bio-active in the field.

MATERIALS AND METHODS

All the reagents were of AnalaR grade used as such without further purification. Aniline, cinnamaldehyde, sodium oxalate, Ferric nitrate were of AnalaR grade. Solvents such as methanol and ethanol were used as such without further purification. The elemental analysis of the complex were carried out using (Thermo Finnegan make, Flash EA1112 series) CHNS(O) analyser instrument. The molar conductance of 10^{-3} M complex in acetonitrile was conducted using Systronic Conductivity Bridge at 300C. Absorption spectra of the Schiff base and Fe(III) complex were obtained by solid state spectra (DRS-method) using JASCO model No:V-650 make UV-VIS spectrophotometer in the range of 200-800nm. The IR-spectra of Schiff base and its metal complexes were recorded in the range of 4000-400 cm^{-1} , using KBr pellet technique by Perkin Elmer spectrum, ONE-NO17-1159 Spectrometer.

Antimicrobial assay

The newly synthesized compound were screened for their antibacterial and antifungal activity against four bacterial strains namely *Escherichia coli* (MTCC 732), *Staphylococcus aureus* (MTCC 3160), *Bacillus subtilis* (MTCC 441) and *Pseudomonas aeruginos* (MTCC 1035) and *Candida Albicans* (MTCC 183), *Aspergillus niger* (MTCC 10180) for fungal strains were obtained from Microbial type culture collection (MTCC) at the institute of Microbial Technology (IMTECH), Chandigarh, India. The discs measuring 6.0 mm in diameter were punched from Whatman No.1 filter paper. Petri plates were prepared by pouring 30 ml of Nutrient agar (NA) medium and Potato dextrose agar (PDA) medium. The plates were incubated at 37 °C for 24 h for the bacteria and 48 hr. for fungal strains. Each sample was tested in triplicate. The discs of each concentration were placed in nutrient agar medium inoculated with fresh bacterial strains separately. Each disc was added 100 μ l of test samples, standard drug as Chloramphenicol (10 mg/ml distilled water) for bacteria and Fluconazole (10 mg/ml distilled) for fungi separately. The antimicrobial potential of test compound was determined on the basis of mean diameter of zone of inhibition around the disc in millimetres. The zones of inhibition of the tested microorganisms by the samples were measured using a millimetre scale. The values are given in the table.

Synthesis of Schiff base

A solution of Benzenamine 0.462g (4.9 mmole) in 10 ml ethanol, 0.668g (5.05 mmole) of (2E)-3-phenylprop-2-enol in 10 ml Diethyl ether was mixed in a beaker, add a 15 ml water as a catalyst. The whole mixture was stirred 10 min at room temperature. The pale yellow precipitated powder was formed and then the reaction mixture was filtered, washed with water, dried in desiccators, kept in an airtight glass container. The Schiff base is soluble in ethanol [19-21].

Synthesis of Metal Complexes

2.0g (4.9mm) Iron was dissolved in 25ml ethanol and the ligand of Schiff base 2. 0523g (9.9) dissolved in ethanol in other hand the anionic ligand of oxalate 0.9950g (3.9) soluble in 35ml water. These two ligand mixtures was mixed with in metal ion solution and well stirred at room temperature in 20 min with 15 ml water used as catalyst. The green shade-seaweed colour precipitate was formed and the reaction mixture was filtered and dried.





RESULT AND DISCUSSIONS

Elemental analysis and Molar Conductance: The Schiff base and its complex are colored solid, soluble in common organic solvents such as DMSO, ethanol and methanol but insoluble in water. The analytical data show that 1:1 metal to ligand ratio in Fe(III) complex. Lower values of molar conductance indicate that complexes are nonelectrolytes [22]. The analytical and physical data of ligand and its complex are given in Table-1 & 2

Mass spectrum of Schiff base: The ESI mass spectrum fragmentation of Schiff base shows the m/z value at 207 indicating the formula and molecular weight of them, the other two m/z values of 115 and 89 indicating the fragment of $C_9H_8^+$ and $C_6H_7N^-$ [23].

IR spectrum: To study the binding modes of ligand towards metal ion, IR spectral data of Schiff base ligand compared with the complex. The IR spectrum of free Schiff base ligand shows a peak of azomethine group $-CH=N$ at 1621 cm^{-1} , which is shifted to a higher frequency in the Fe(III) complex at 1628 cm^{-1} indicates that azomethine nitrogen coordinate to the metal ion. This increase in IR stretching frequency occurs due to increase in electron density during coordination. A broad band at 3053 cm^{-1} is assigned to hydrogen bonded aromatic C-H in the spectrum of the ligand which is appeared in metal complexes shows the 3055 cm^{-1} involvement of aromatic ring involve in the coordination of metal complex. This is further confirmed by the shifting of C=C, C-C, C-H, C-N stretching band 1953 cm^{-1} , 2979 cm^{-1} , 3456 cm^{-1} and 1300 cm^{-1} respectively shifted to higher/lower frequency at 1970 cm^{-1} , 2890 cm^{-1} , 3425 cm^{-1} and 1312 cm^{-1} in the complex. The very weak band which is absent in ligand but present in metal complexes are in the ranges $481, 354-353\text{ cm}^{-1}$ assigned to stretching frequencies of $\nu(M-N)$ and $\nu(M-O)$ bands [24]. The very lower and weak frequency at 160 cm^{-1} present in the IR spectra shows the M-M bond present in the complex (Fe-Fe) which is absent in Schiff base indicating the binuclear and bridging nature of the structure [25].

Electronic Spectra: The electronic absorption spectra of metal complex were recorded in DMSO in the range 200-800 nm. The electronic spectrum of Fe(III) complex shows bands at 687, 505, 419 and 363nm corresponding to the ${}^6A_{1g} \rightarrow {}^4T_{1g}$, ${}^6A_{1g} \rightarrow {}^4T_{1g}(G)$ and ${}^6A_{1g} \rightarrow {}^4E_g(G)$ transitions respectively, indicates octahedral geometry around Fe(III) ion [26].

Antimicrobial activities: The synthesized ligand and the complex were tested *in-vitro* antimicrobial activity against bacteria (*Staphylococcus aureus*, *Bacillus subtilis* and *Escherichia coli* and *Pseudomonas auriginosa*) and fungi (*Aspergillus Niger* and *Candida albicans*). The inhibition zone values in diameter (mm) was investigated and summarized in Table.3. A comparative study of inhibition zone diameter (mm) values of the Schiff base ligand and the complex indicates that the metal complex exhibit higher antimicrobial activity than the free Schiff base ligand. Such increased activity of the complex can be explained on the basis of Tweedy's chelation theory [27].

CONCLUSION

In summary, a new transition metal complex based on Schiff base ligand have been successfully synthesized under eco-friendly conditions. The Schiff base ligand ((E)-N-((E)-3-phenylallylidene) aniline) and its Fe(III) complex successfully synthesized and characterized. The deprotonated monodentate Schiff base ligand coordinated to the metal(III) ion via the azomethine nitrogen. An octahedral geometry has been proposed for the metal(III) complex based on the electronic spectra. The complex formed are neutral with no free anions outside the coordination sphere. The metal (II) complex exhibited better antibacterial properties than the parent Schiff base ligand under the same experimental conditions. It can also be deduced from this study that the antibacterial growth inhibition ability of the synthesized compound increased with increasing.





REFERENCES

- Katarzyna, Brodowska Elżbieta, Lodyga-Chruscinska, (2014)– *Institute of General Food Chemistry*,68(2): 129–134.
- Nabil Ramadan Bader, (2010) *Rasayan J.Chem*, 3(4): 660-670.
- Balachandran Unni Nair, (2000) *Biochimica et Biophysica Acta* 1475: 157-162.
- A. Datta, N. K. Karan, S. Mitra, G. Rosair, Z. Naturforsch. (2002), 576, 999. Available online through, <http://jpr solutions.info>.
- T. Joseph, M. Hartmann, S. Ernst, S.B. Halligudi, (2004) *J. Mol. Catal. A: Chem.* 207: 129–135.
- Sujandi, E.A. Prasetyanto, D.-S. Han, S.-C. Lee, S.-E. Park, (2009) *Catal. Today* 141: 374–377.
- P. Aisen, M. Wessling-Resnick, E.A. Leibold, (1999) *Iron metabolism*, *Curr. Opin. Chem. Biol.* 3: 200–206.
- E.L. Que, D.W. Domaille, C.J. Chang, (2008) *Metals in neurobiology: probing their chemistry and biology with molecular imaging*, *Chem. Rev.* 108: 1517–1549.
- J.R. Burdo, (2003) J.R. Connor, *Brain iron uptake and homeostatic mechanisms: An overview*, *Biometals* 16: 63–75.
- J.A. Lee, G.H. Eom, H.M. Park, J.H. Lee, H. Song, C.S. Hong, S. Yoon, C. Kim, (2012) *Bull. Korean Chem. Soc.* 33: 3625.
- J. Zhan, L. Wen, F. Miao, D. Tian, X. Zhu, H. Li, (2012) *New J. Chem.* 36: 656–661.
- S.L. Hu, N.F. She, G.D. Yin, H.Z. Guo, A.X. Wu, C.L. Yang, (2007) *Tetrahedron Lett.* 48: 1591–1594.
- Y. Xiang, A. Tong, (2006) *Org. Lett.* 8 1549–1552.
- J. Mao, L.N. Wang, W. Dou, X.L. Tang, Y. Yan, W.S. Liu, (2007) *Org. Lett.* 9: 4567–4570.
- X.B. Zhang, G. Cheng, W.J. Zhang, G.L. Shen, R.Q. Yu, (2007) *Talanta* 71: 171–177.
- O. Oter, K. Ertekin, C. Kirilmis, M. Koca, M. Ahmedzade, (2007) *Sens. Actuators B* 122 :450–456.
- G.E. Tumambac, C.M. Rosencrance, C. Wolf, (2004) *Tetrahedron* 60: 11293–11297.
- Magdy shebl, (2009) *Journal of coordination chemistry*, 62(19).
- Awoyinka, O.A., Balogun I.O. and Ogunnow, A.A. (2007) *J. Med. Plant Res*, 1: 63-95.
- NCCLS. (1993) National Committee for Clinical Laboratory Standards. Performance standards for antimicrobial disc susceptibility tests. PA: NCCLS Publications 25.
- Xavier A. and Srividhya N., (2014) *IOSR Journal of Applied Chemistry*, 7(11): 06-15.
- Prakash Gouda Avaji and Sangamesh Amarappa Patil, (2009) *Journal of Enzyme Inhibition and Medicinal Chemistry*, 24(1): 140–150.
- Maria C. DAntonio, Alejandra Wladimirsky, Daniel Palacios, Liliana Coggiolaa, Ana C. González-Baró, Enrique J. Baran, Roberto C. Mercader (2009) *J. Braz. Chem. Soc.* 20(3).
- Vineetha C. M., Nishana Shoukath and Rajendraprasad Y, (2013) *International Journal of Advances in Pharmacy, Biology and Chemistry*, 2(2).
- V. Koteswara Rao V, S. Subba Reddy S, Satheesh Krishna .B, Reddi Mohan Naidu B, Naga Raju C. & S.K. Ghosh S. K, (2010) *Green Chemistry Letters and Reviews.* 3(3): 217-223.
- Akram A. Mohammed, (2007) *Raf. Jour. Sci.*, 18(2): 37-45.
- A. P. Thakare, P. R. Mandlik, (2017) *Indian Journal of Advances in Chemical Science* 5(4) :318-323.

Table 1: Analytical Data

Elemental Analysis						
S.No	Complex/Ligand	%C	%H	% N	%O	% Metal
1	(C ₁₅ H ₁₃ N)	86.83 (86.20)	6.27 (5.90)	6.75 (6.00)	-	-
2	[Fe ₂ (C ₁₅ H ₁₃ N) ₄ (C ₂ O ₄) ₃]	58.97 (59.20)	3.87 (04.10)	04.17(04.25)	14.29 (15.21)	08.31 (09.12)

Theoretical values are given in parenthesis





Table 2: Physical and spectral data

S.No	Sample	Color	MP (°C)	Molar Conductance (Ohm ¹ cm ² mo ⁻¹)	μ _{eff} (BM)	λ _{max} (nm)	yield
1	(C ₁₅ H ₁₃ N)	Pale yellow	125	20.00	-	261 388	71.42
2	[Fe ₂ (C ₁₅ H ₁₃ N) ₄ (C ₂ O ₄) ₃]	Green shade-seaweed	160	08.33	5.8	363 419 505 687	91.60

Table 3: Bio-potential activities of the Schiff base and complex

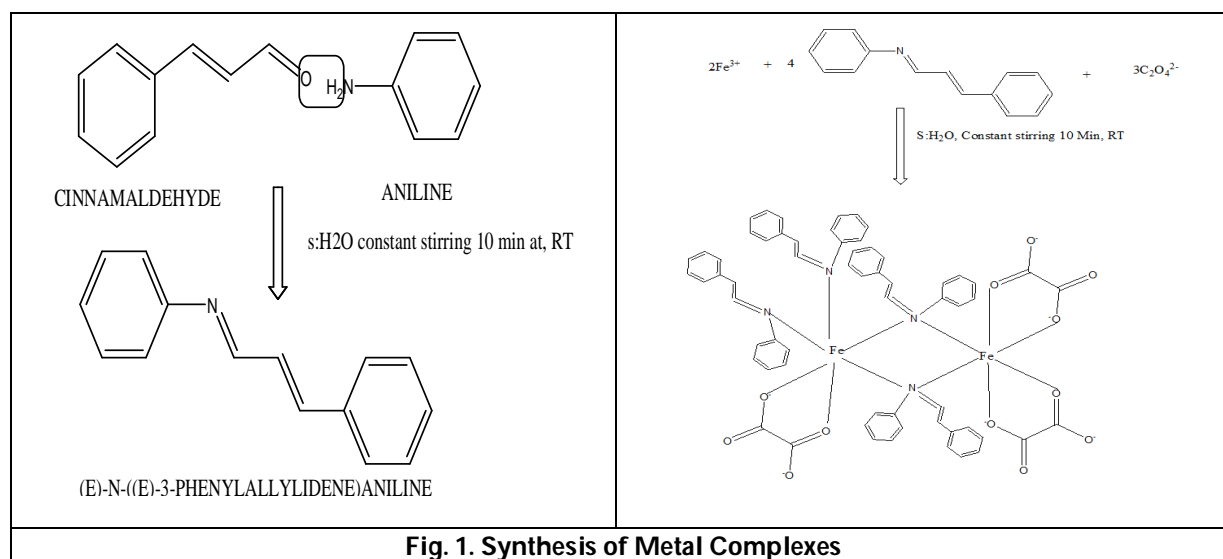
Sample dose (100μl)	<i>E. coli</i> (mm)	<i>S. aureus</i> (mm)	<i>B. subtilis</i> (mm)	<i>P.aeruginos</i> (mm)	<i>C. Albicans</i> (mm)	<i>A.Niger</i> (mm)
Std	15.6	14.8	14.3	14.6	13.6	13.3
CV	09.0	08.6	07.6	08.4	07.1	06.8
V4	10.3	10.0	08.8	09.3	08.4	07.6

Standard : Chloramphenicol & Fluconazole

Control : DMSO

CV : Schiff base

V4 : [Fe₂(C₁₅H₁₃N)₄(C₂O₄)₃]





Isolation and Biochemical Composition of the Filamentous Algae Collected from Tamil Nadu

Swetha.G¹, Vasugi.V¹, Sandhya.P² and Jegan.G^{3*}

¹Department of Biotechnology, Apollo Arts and Science College, Poonamallee, Chennai, Tamil Nadu, India.

²Assistant Professor and Head, Department of Biotechnology, Apollo Arts and Science College, Poonamallee, Chennai, Tamil Nadu, India.

³Assistant Professor, Department of Biotechnology, Apollo Arts and Science College, Poonamallee, Chennai, Tamil Nadu, India.

Received: 01 Sep 2020

Revised: 03 Oct 2020

Accepted: 05 Nov 2020

*Address for Correspondence

Jegan.G

Assistant Professor,
Department of Biotechnology,
Apollo Arts and Science College,
Poonamallee, Chennai,
Tamil Nadu, India.
Email: jeganbgl@gmail.com



This is an Open Access Journal / article distributed under the terms of the **Creative Commons Attribution License** (CC BY-NC-ND 3.0) which permits unrestricted use, distribution, and reproduction in any medium, provided the original work is properly cited. All rights reserved.

ABSTRACT

The combustion of fossil fuels to increase the atmospheric pollution due to greenhouse gases which leads to climate change and global warming. Therefore, the production of biofuel from biological sources is way to reducing the emission of greenhouse gases. Among this green algae are the most diverse group of algae including various filamentous genera and species. In this study the filamentous algal biomass were collected from agriculture tube well reservoir at different sites of Tamil Nadu namely Vadugapalayam Site 1, Vadugapalayam Site 2 Cuddalore District and Namachivayapuram Site 3, Thiruvallur Dist. Tamil Nadu, India. These samples were subjected to morphological identification and found that different species of filamentous algae were dominated in these three regions of collection sites. Pure algal cells were isolated and cultured in the laboratory. Then the remaining of these three sites algal biomass were dried separately and analyzed for pigments and biochemical constituents and which showed good results. Also these three algal biomass were accumulated more lipids but compare to these three samples high lipid content was found in the sample B which was collected from Vadugapalayam Site 2. Therefore, these filamentous algal lipids can be used for the production of biofuels.

Keywords: Agriculture tube well reservoir, Filamentous algae, Biomass, Pigments, Lipid



**Swetha et al.,**

INTRODUCTION

Bioenergy production is the most important to reduce greenhouse gas emissions and used as biofuel instead of fossil fuels (Goldemberg, J., 2000). Algae are plant-like living microorganisms that can able to make food their own by photosynthesis using of sunlight. Algae are the best sources for the production of biodiesel (Shay E.G., 1993). Biodiesel production from algae is the way of alternate sources of energy and microalgae are better for the production of biodiesel because it contain more oil content when compared to macroalgae. Microalgae can grow fast and easy to cultivate rather than terrestrial crops (Shay, 1993; Wagner, 2007). The filamentous algae are otherwise called as pond scum or pond mosses which are showing like thread, high greenish masses and float on the surface of water. It can be form thick mats in static water or long and rope like strands in flowing waters (Hesham R. Lotfy et al., 2014). These filamentous algae were tending to form clumps or floating mats attach to surfaces but not like a microalgae (Lawton *et al.*, 2013). The filamentous algae are single cells and they visible chains and form threads like filaments. They are primary producers and also which are used as a bioindicators in aquatic ecosystem (Bellinger and Sigeo, 2010; Schneider and Lindstrøm, 2011; Schneider et al., 2013). Monitor of water quality using filamentous algae has various advantages such as easily available to collect from the environment, it can be growth and accumulate pollutants, easily identify both microscopic and macroscopic and also distributed wide and easy to comparison (Karez et al., 2004; Bellinger and Sigeo, 2010). It can be produce various biochemical compounds at different aquatic ecosystems (Bellinger and Sigeo, 2010; Çelekli *et al.*, 2016a). Hillebrand (1983) reported that filamentous algae are dominating the different environmental changes. The Cyanobacteria are the largest group of photosynthetic microorganism and ability to fix the atmospheric nitrogen and carbon compounds. They are used widely in food industry and some biotechnological applications (Fatma *et al.*, 1994; Rastogi and Sinha, 2009; Thajuddin and Subramanian, 2005; Venkataraman and Becker, 1985). It is also used for heavy metal removal from polluted waters through the process biosorption or bioaccumulation (karna et al., 1999). Cyanobacteria has the promising group of organisms from which isolated biochemical active natural compounds and some species of cyanobacteria such as Anabaena, Nostoc, Oscillatoric and spirulina has the potential to produce secondary metabolites (shalaby *et al.*, 2010). Cyanobacteria has potential to produce different types of amino acids and hormonal substances and sugars which are involved in the soil texture by acting as chelating agents for heavy metals and may possibly stimulate heterotrophic bacterial growth and act as plant growth promoting substances (Misra and Kaushik, 1989). In this investigation was carried out the production of biochemical compound from filamentous algae which are collected from different places of Tamil Nadu, India.

MATERIALS AND METHODS

Sample Collection

The fresh water algal samples were collected randomly from agriculture tube well reservoir at three different places such as Vadugapalayam Site 1, Vadugapalayam Site 2 Panruti, Cuddalore Dist. Tamil Nadu, India and Namachivayapuram Site 3, Thiruvallur Dist. Tamil Nadu, India (Fig. 1). These three sites of collected biomass were named as sample A (Vadugapalayam Site 1 Fig. 1A), sample B (Vadugapalayam Site 2 Fig. 1B) and Sample C (Namachivayapuram Site 3 Fig. 1C). These samples were collected in winter season in the month of December 2019 and the wet and dry weights of the algal biomass were recorded. These three samples were subjected to isolated pure cells and cultured. The remaining biomass were dried separately at room temperature and analysed for Pigments and Biochemical compositions.

Microscopic identification of the algae

Microscopic identification of collected algal cells were made based on the previous reports by various scientists using of phase contrast microscope (Barry H. Rosen (1990); Desikachary, 1959; Gour Gopal Satpati and Ruma Pal, 2016; Philipose, 1967; Yuvaraj Sampathkumar and Elumalai. S, 2018).





Swetha et al.,

Isolation and Purification of algal cells

The collected three fresh water filamentous algal samples were brought to the laboratory and subjected to isolate pure cells using the techniques like plating, serial dilution and inoculated into the 100ml conical flask contain BG11 medium. The inoculated algal samples were kept for incubation under light intensity of 120 $\mu\text{mol photons/m}^2/\text{s}^{-1}$ on 12:12 h Light/Dark with room temperature and monitored every day for their growth. During the growth period a drop of the algae containing liquid is placed upon a slide for examination of pure algal cells under the phase contrast microscope and photograph was recorded. Finally the dominated pure cells were isolated from each collection sites and these cultures were maintained in Biotechnology laboratory at Apollo Arts and Science College, Poonamallee, Chennai, Tamil Nadu, India. On the other hand the remained three sites algal biomasses were examined for following analysis.

Estimation of Pigments

The pigments of *Chlorophyll 'a'* and *Chlorophyll b'* were examined against the three sites filamentous algae based on Jeffery and Humphrey (1975) and β -carotene was determined by Shaish et al., 1992 using spectrophotometer.

Biochemical Composition

The collected three sites algal biomass were subjected to analyze Total Protein, Carbohydrate and Lipid based on the method followed by Lowry et al., 1951, Dubois et al., 1956 and Bligh and Dyer et al., 1959.

RESULTS AND DISCUSSION

Biomass Analysis

The filamentous algal samples were collected randomly from agriculture tube well reservoir at three different areas namely Vadugapalayam Site 1, Vadugapalayam Site 2 Panruti, Cuddalore Dist. and Namachivayapuram Site 3, Thiruvallur Dist. Tamil Nadu, India. The wet and dry weights of the collected three filamentous algal biomass were recorded and the results were shown in the Table: 1 and Fig. 2 and Fig. 3. In overall dry weight of sample A was showed high rate (77.40g) when compared to sample B (14.25g) and sample C (10.35g) (Fig. 4). Overall Wet weight also observed huge in sample A (312.85g) followed by sample B (211.50g) and sample C (175.25g) (Fig. 4). Moreover dominated pure algal cells were isolated in each collected sites, cultured (Fig. 5) and maintained separately in biotechnology laboratory at Apollo Arts and Science College, Poonamallee, Chennai, Tamil Nadu, India. The remaining biomasses were investigated against pigments and biochemical analysis such as Carbohydrates, protein and lipids.

Microscopic Identification and Isolation

Microscopic identification was made on the collected algal cells and which was confirmed that the presence of filamentous algae in these three regions of collection sites namely Vadugapalayam Site 1, Vadugapalayam Site 2 Panruti, Cuddalore Dist. and Namachivayapuram Site 3, Thiruvallur Dist. Tamil Nadu, India. The dominant species of pure algal cell was isolated in each collection site and microscopic photographs were recorded (figure 5). The figure 5 was shows that the isolated dominant species at Vadugapalayam Site 1 (I), Vadugapalayam Site 2 (II) and Namachivayapuram Site 3 (III). The collection sites were found different species of filamentous algae but not same species because of their morphological characters like size, shape of the cell, branch or unbranch etc.

Pigments Analysis

The *Chlorophyll a*, *Chlorophyll b* and β - Carotene contents were determined in the filamentous algal sample A, sample B and sample C (Table: 2 and Fig: 6, 7 and 8). The results were obtained that the sample C has showed high rate of *Chlorophyll a*, *Chlorophyll b* and β - Carotene (32 $\mu\text{g/ml}^{-1}$ /24 $\mu\text{g/ml}^{-1}$ /86 mg/ml) when compared to sample A (21 $\mu\text{g/ml}^{-1}$ /16 $\mu\text{g/ml}^{-1}$ /54 mg/ml) and Sample B (17 $\mu\text{g/ml}^{-1}$ /11 $\mu\text{g/ml}^{-1}$ /27 mg/ml).





Swetha et al.,

Biochemical composition of the three Filamentous algal biomass

Carbohydrate : These three filamentous algal samples were examined for carbohydrate estimation and showed that sample A was obtained 23.65mg/g, sample B was showed 48.27mg/g and sample C was found 37.21 mg/g (Table: 3 and Fig. 9). In this study showed that the carbohydrate content was accumulated more in the sample B while comparing with sample A and sample C (Table: 3 Fig: 9) and the sample C has showed high carbohydrate content followed by sample A.

Protein: The total amount of protein content of the collected three filamentous algal samples were estimated and expressed in mg/g⁻¹. The Sample A was found 19.61 mg/ g⁻¹, sample B was obtained 16.58 mg/ g⁻¹ and sample C was showed 12.61 mg/ g⁻¹ (Table: 3 and Fig.10). These results were confirmed that protein rate was high in the sample A when compared to sample B and Sample C (Table: 3 and Fig.10). The least amount of protein was observed in sample C while comparing with sample A and sample B.

Lipid : The total lipid content were estimated from the three samples of filamentous algal biomass and obtained sample A 15.30 mg/g, sample B 38.41 mg/g and sample C 23.57 mg/g (Table: 3 and Fig.11). This result were revealed that high amount of lipid was found in sample B when compared to both sample A and sample C (Fig.11). Moreover the sample C was showed high lipid content when compared to sample A.

DISCUSSION

The production of biomass is important for the energy sources (Kulkarni and Dalai, 2006). The large scale production of biomass energy could be feasible for the improvement of economical, social and environment (UNDP, 2008; Turkenburg, 2000). Many bioactive compounds such as pigments, proteins, PUFAs, sterols, enzymes and vitamins are produced by the microalgae and cyanobacteria (de Jesus Raposo et al., 2013). These kinds of bioactive compounds have to be use for the human and animal food and feed stock (Hemaiswarya et al., 2011). In this study the waste filamentous algal biomass were collected from three different places of agriculture tube well reservoir and dry weight were measured in which the sample A (Vadugapalayam Site 1) showed high amount of biomass followed by sample B (Vadugapalayam Site 2) and sample C (Namachivayapuram Site 3). These three sites were identified as filamentous algae are dominated but found that different species. These algal biomasses were used for the production of bioactive compounds. *Chlorophyll* is a green photosynthetic pigment which is found in plants, algae, and cyanobacteria. Usually the chlorophylls are naturally attractive green colored pigments but it was very vulnerable to oxygen, weak acid and light reported by the Cubas et al., 2008. Carotenoids are organic compounds which are occurring in chloroplasts and chromoplasts. The pigments such as chlorophylls and carotenoids are the part of the photosynthesis phenomenon (Anon, 2014). Therefore, *Chlorophyll a*, *Chlorophyll b* and β - Carotene contents were examined in these filamentous algae which are proved good results and which obtained that the sample C have the high rate of *Chlorophyll a*, *Chlorophyll b* and β - Carotenes when compared to sample A and sample B. Safonova and Reisser (2005) suggested that the growth of some cyanobacteria promoting and inhibiting effect of carbohydrates secreted as extracellular substances. Carbohydrates is one of biochemicals which was determined in this study that the carbohydrate content was accumulated more in the sample B while comparing with sample A and sample C. Some species of cyanobacteria like *Spirulina* sp., *Nostoc* sp. and *Anabaena* sp. has the high protein and fiber content which are used as food (Anusuya et al., 1981; Anupama, 2000). In the experiment of Protein content was determined in different ratios in these three samples in which the algal sample from Vadugapalayam Site 1 was obtained huge protein and slightest amount of proteins were obtained at Vadugapalayam Site 2 and Namachivayapuram Site 3. Algae consist between 2 and 40% of total lipid and oil by their weight of biomass (Wagner, 2007). The researcher of Schneider, 2006 and Haag, 2007 reported that the microalgae can also be used as feed for livestock. According to the chemical composition of algal biomass can able to produce different biofuel compounds such as bioethanol, biodiesel, biomethane, biohydrogen, biobutanol, jetfuel etc, (Chinnasamy et al.,

28411



**Swetha et al.,**

2012). Based on these reports this experiment was also extracted high amount of lipids from the three filamentous algae which are collected from three different sites for the production of biofuels. In which the more lipid content was obtained in the area of Vadugapalayam Site 2 and least amount of lipids was found in Namachivayapuram Site 3 and Vadugapalayam Site 1. These lipids can be used for the production of biofuels after the process of transesterification. Finally this experiment was confirmed that the production of renewable energy from the collected waste algal biomass from the agriculture tube well reservoir is one of the best for future.

CONCLUSION

This research was concludes that the waste filamentous algal biomasses from agriculture tube well reservoir are easily available in different environmental conditions with high amount of biomass and these algal biomass can be used for the production of biodiesel. The Biofuel productions from these selected potential filamentous algal species are eco-friendly and cost effective not only that which is also used for the waste water treatment in many industries.

ACKNOWLEDGEMENTS

Authors acknowledge sincere thanks to the Chairman, Vice-Chairman, Secretary, Principal, Vice-Principal and the Department of Biotechnology, Apollo Arts and Science College, Poonamallee, Chennai – 602 105, Tamil Nadu, India.

REFERENCES

1. Anon, 2014. Advances in Biorefineries: Biomass and Waste Supply Chain Exploitation. Elsevier Science.
2. Anupama, P. R. (2000), Value added food: single cell protein. *Biotechnol. Advan.*, 18: 459–479.
3. Anusuya, D. M.; Subbulakshmi, G.; Madhavi, D. M. and Venkataraman, L. V. (1981), Studies on the proteins of mass cultivated blue green alga (*Spirulina platensis*). *J. Agri. Food Chem.*, 29: 522 – 525.
4. Barry H. Rosen. Microalgae Identification for Aquaculture. Florida Aqua Farms, 1990.
5. Bellingier, E.G., Sigeo, D.C., 2010. Freshwater Algae. Identification and use as bioindicators. The first edition. John Wiley & Sons, Ltd. UK, pp. 271.
6. Blight, E.G. and W.J. Dyer. 1959. A rapid method of total lipid extraction and purification. *Can. J. Biochem. Physiol.* 37: 911-917.
7. Çelekli, A., Arslanargun, H., Soysal, Ç., Gültekin, E., Bozkurt, H., 2016a. Biochemical responses of filamentous algae in different aquatic ecosystems in South East Turkey and associated water quality parameters. *Ecotox. Environ. Safe.* 133, 403–412.
8. Chinnasamy,S.,Rao,P.H.,Bhaskar,S.,Rengasamy,R.,andSingh,M.(2012).“Algae: a novel biomass feed stock for biofuels,” in *Microbial Biotechnology: Energy and Environment*, ed.R. Arora (Walling ford: CAB International), 224–239.
9. Cubas, C., Lobo, M.G., Gonza´lez, M., 2008. Optimization of the extraction of chlorophylls in green beans (*Phaseolus vulgaris* L.) by N, N-dimethylformamide using response surface methodology. *J. Food Compos. Anal.* 21, 125–133.
10. Dayananda C, Sarada R, Bhattacharya S, Ravishankar GA (2005). Effect of media and culture conditions on growth and hydrocarbon production by *Botryococcus braunii*. *Process Biochem.* 40:3125-3131.
11. De Jesus Raposo, M.F., de Morais, R.M., de Morais, A.M., 2013. Health applications of bioactive compounds from marine microalgae. *Life Sci.* 10, 479–486.
12. Desikachary, T.V., 1959. Cyanophyta. *Indian Council of Agricultural Research*, New Delhi, 700.
13. Dubois, M., K. A. Gilles, J. K. Hamilton, P. A. Robers and F. S. Smith. 1956. Colorimetric method for the determination of sugars and related substances. *Anal. Chem.* 18: 50-356.





14. Energy Assessment, Preface UNDP (2008). United Nations Development Programme, New York, USA, pp: 219-272. Am. J. Biochem. Biotech. 4 (3):250-254.
15. Fatma, T.; Sarada, R. and Venkataraman, L. V. (1994), Evaluation of selected strains of *Spirulina* for their constituents. *Phykos*, 33: 89 – 97.
16. Goldemberg J (2000). World Energy Assessment, Preface. United Nations Development Programme, New York, NY, USA.
17. Gour Gopal Satpati and Ruma Pal. New and rare records of filamentous green algae from Indian Sundarbans Biosphere Reserve. 2016, 7 (2): 159- 175.
18. Haag AL (2007). Algae bloom again. *Nature* 447(31): 520-521. Hossain ABMS, Salleh A (2008). Biodiesel fuel production from algae as renewable source of energy. *Am. J. Biochem. Biotechnol.* 4(3):250-254.
19. Hemaiswarya, S., Raja, R., Kumar, R.R., Ganesan, V., Anbazhagan, C., 2011. Microalgae: a sustainable feed source for aquaculture. *World J. Microbiol. Biotechnol.* 27, 1737–1746.
20. Hesham R. Lotfy, Martha N. Amputu and Celestine Raidron (2014). Determination of optimum growth conditions and biodiesel production from filamentous algae. 8(6): 344-349.
21. Hillebrand, H. (1983). Development and dynamics of floating clusters of filamentous algae. In R.G. Wetzel (ed.), *Periphyton of Freshwater Ecosystems* (pp.31-39). Springer Netherlands, DOI: 10.1007/978-94-009-7293-3_7.
22. Jeffrey, S.W., Humphrey, G.F.: New spectrophotometric equations for determining chlorophyll a, b, c 1 and c 2 in higher plants, algae and natural phytoplankton. – *Biochem. Physiol. Pflanz.* 167: 191-194, 1975.
23. Karez, R., Engelbert, S., Kraufvelin, P., Pedersen, M.F., Sommer, U., 2004. Biomass response and changes in composition of ephemeral macroalgal assemblages along an experimental gradient of nutrient enrichment. *Aquat. Bot.* 78, 103–117.
24. Karna, R. R.; Uma, L.; Subramanian, G. and Mohan, P. M. (1999), Biosorption of toxic metal ions by alkali extracted biomass of a marine cyanobacterium *Phormidium valderianum* BDU 30501. *World J. Microbiol. Biotechnol.*, 15: 729 – 732.
25. Kulkarni MG, Dalai AK (2006). Waste cooking oil-an economical source for biodiesel: A review. *Ind. Eng. Chem. Res.* 45: 2901-2913.
26. Lawton, R. J., de Nys, R., & Paul, N. A. (2013). Selecting Reliable and Robust Freshwater Macroalgae for Biomass Applications. *PLoS ONE*, 8(5), 1-7.
27. Lowry, O. H., N. J. Rosebrough, A. L. Farr and R. J. Randall. 1951. Protein measurement with folin phenol reagent. *J. Bio. Chem.* 193: 265-275.
28. Misra, S. and Kaushik, B. D. (1989), Growth promoting substances of cyanobacteria. II. Detection of amino acids, sugars and auxins. *Proc. Indian Natn. Sci. Acad.*, B 55: 499 – 504.
29. Philipose, M.T., 1967. Chlorococcales, Indian Council of Agricultural Research, New Delhi, 1-365.
30. Rastogi, R. P. and Sinha, R. P. (2009), Biotechnological and industrial significance of cyanobacterial secondary metabolites. *Biotechnol. Adv.*, 27: 521 – 539.
31. Safonova, E. and Reisser, W. (2005), Growth promoting and inhibiting effects of extracellular substances of soil microalgae and cyanobacteria on *Escherichia coli* and *Micrococcus luteus*. *Phycol. Res.*, 53: 189 – 193.
32. Schneider D (2006). Grow your own? Would the wide spread adoption of biomass-derived transportation fuels really help the environment. *Am. Sci.* 94:408-409.
33. Schneider, S.C., Kahlert, M., Kelly, M.G., 2013. Interactions between pH and nutrients on benthic algae in streams and consequences for ecological status assessment and species richness patterns. *Sci. Total Environ.* 444, 73–84.
34. Schneider, S.C., Lindstrøm, E.A., 2011. The periphyton in dextrotrophic status PIT: a new eutrophication metric based on non-diatomaceous benthic algae in Nordic rivers. *Hydrobiologia* 665, 143–155.
35. Shaish A, Ben-amotz A, Avron M. Biosynthesis of β -carotene in *Dunaliella*. *Method Enzymol.* 1992;213:439–444. doi: 10.1016/0076-6879(92)13145-N. [CrossRef] [Google Scholar]
36. Shalaby EA, Shanab SMM, Singh V. Salt stress enhancement of antioxidant and antiviral efficiency of *Spirulina plantensis*. *J Med plants Res* 2010; 4: 2622-32.
37. Shay EG (1993). Diesel fuel from vegetable oils: Status and opportunities. *Biomass Bioenergy* 4:227-242.





Swetha et al.,

38. Thajuddin, N. and Subramanian, G. (2005), Cyanobacterial biodiversity and potential applications in biotechnology. *Curr. Sci.*, 89: 47 – 57.

39. Turkenburg WC (2000). Renewable energy technologies. In: Goldemberg, J. (Ed). World

40. Venkataraman, L. V. and Becker, E. W. (1985), Biotechnology and Utilization of Algae – The Indian Experience. Dept. Sci. Technol. New Delhi, India and CFTRI, Mysore, India. 257 pp.

41. Wagner L (2007). Biodiesel from Algae oil. Research report, MORA associates from www.fao.org/uploads.

42. Yuvaraj Sampathkumar and Elumalai S 2018. Isolation, Physiochemical Characterization and Cultivation of Salt Tolerant Microalgal Species from Marakkanam Salt Pan, Tamil Nadu, India

Table: 1. The Wet and Dry weight of the collected filamentous algal biomass.

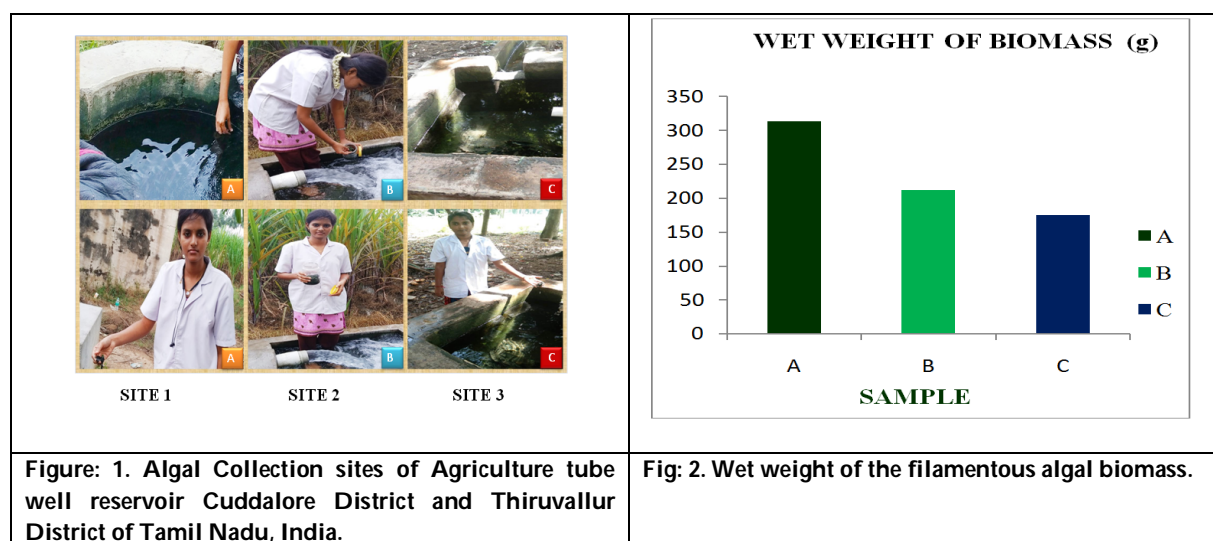
SAMPLE	WET WEIGHT (g)	DRYWEIGHT (g)
A	312.85	77.4
B	211.5	14.25
C	175.25	10.35

Table: 2. The Pigment analysis of the three filamentous algal samples.

Sample	Chlorophyll a $\mu\text{g/ml}^{-1}$	Chlorophyll b $\mu\text{g/ml}^{-1}$	β - Carotene mg/ml
A	21	16	54
B	17	11	27
C	32	24	86

Table: 3. The Biochemical compositions of the three algal samples.

Sample	Carbohydrate mg/ g ⁻¹	Protein mg/ g ⁻¹	Lipid mg/g
A	23.65	19.61	15.3
B	48.27	16.58	38.41
C	37.21	12.61	23.57





Swetha et al.,

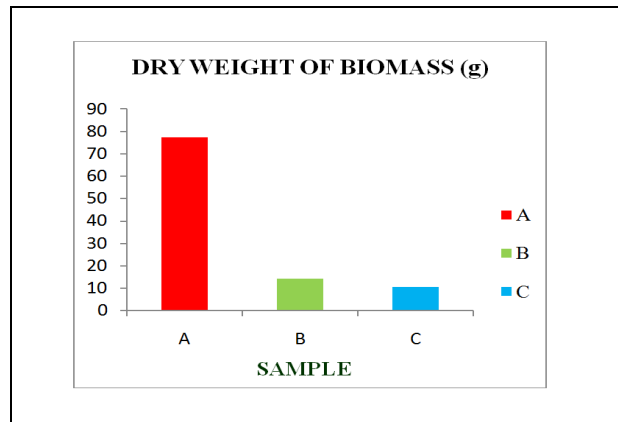


Fig. 3. Dry weight of the filamentous algal biomass.

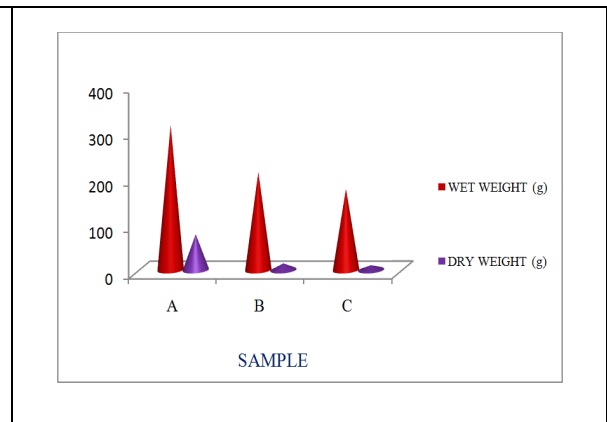


Fig. 4. Overall wet and dry weight of the filamentous algal biomass.

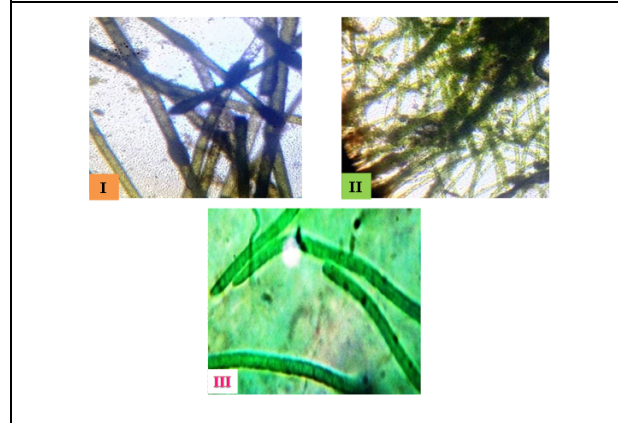


Fig. 5. Microscopic identification of filamentous algae from the three collection sites.

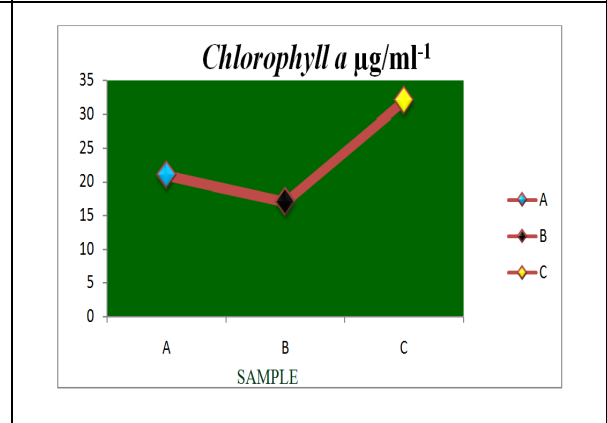


Fig. 6. The Chlorophyll a content of the three filamentous algae.

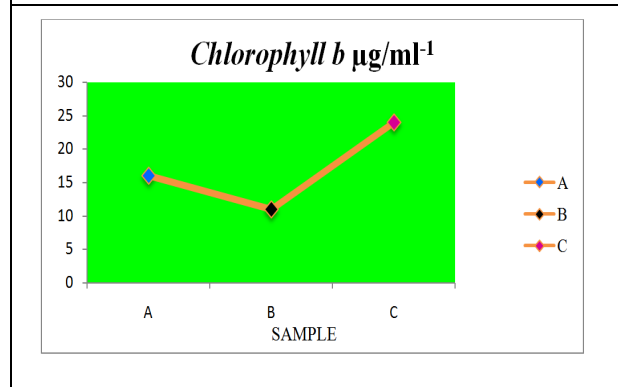


Fig. 7. The Chlorophyll b content of the three filamentous algae.

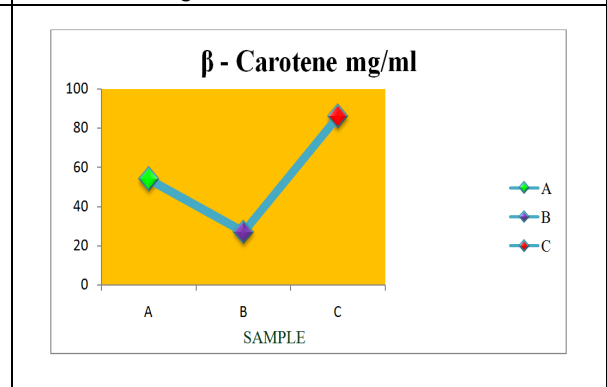


Fig. 8. The beta-Carotene content of the three filamentous algae.



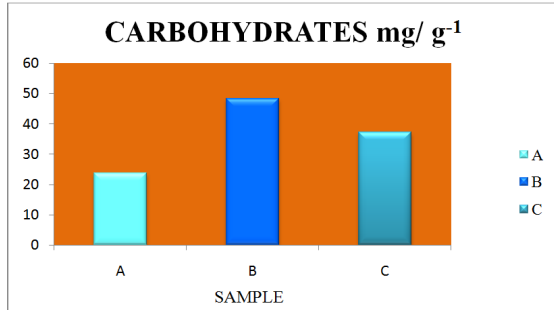


Fig: 9. The Quantity of Carbohydrates from the three filamentous algal samples.

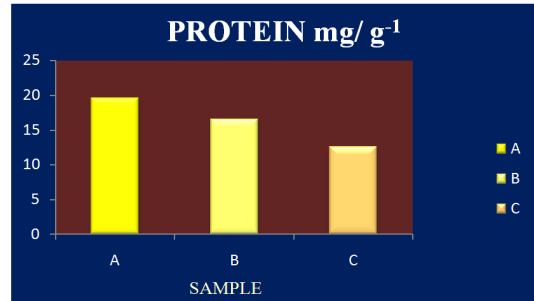


Fig: 10. The Protein content of the three filamentous algal samples.

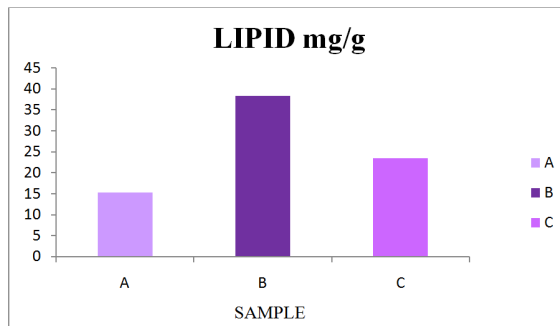


Fig: 11. The Lipid contents of the three filamentous algal samples.





Adaptive LMS-Filtering to Remove the Outliers from the Power System using Dymola

Sudhansu Kumar Samal^{1*}, Anshuman Nayak² and Anjan Kumar Sahoo¹

¹Department of Electrical and Electronics Engineering, Centurion University of Technology and Management, Bhubaneswar Odisha, India.

²Department of Electrical and Electronics Engineering, College of Engineering, Bhubaneswar Odisha, India

Received: 15 Aug 2020

Revised: 17 Sep 2020

Accepted: 20 Oct 2020

*Address for Correspondence

Sudhansu Kumar Samal

Department of Electrical and Electronics Engineering,
Centurion University of Technology and Management,
Bhubaneswar Odisha, India.

Email : sudhansu.samal@cutm.ac.in



This is an Open Access Journal / article distributed under the terms of the **Creative Commons Attribution License** (CC BY-NC-ND 3.0) which permits unrestricted use, distribution, and reproduction in any medium, provided the original work is properly cited. All rights reserved.

ABSTRACT

A sifting approach that totally denoises the sign just as maximal reduced the data conveyed by the sign is suggesting in this paper. This proposed approach can be utilized for both ring down, surrounding, and testing signals. It can likewise work all the more definitely in the nearness of both Additive White Gaussian Clamor (AWGN) and Additive Shaded Gaussian Commotion (ACGN). It can likewise work for both little and huge frameworks. It can work for both fixed and non-fixed signs. It is important to keep up the deliberate sign from the phas or estimation unit (PMU) commotion free for viable and precise mode estimation. Yet, because of quality exceptions, the higher request sounds just as undesirable spikes get declined in the sign. Using a Versatile Least Methods Squares (LMS) these spikes and higher request recurrence parts can be from a sign without smoothing the information. The rest of the clamor segments are then changed over into exceptionally related ACGN. The recreation can be done by utilizing Modelica language and 3d Dassault dymola stage for executing the materialness of the proposed approach with WSCC-9BUS-PQLoad.

Keywords: Supply chain management, Sustainability, Hybrid method, Automobile Industry, Sustainability Assessment





INTRODUCTION

Literature Review

Wide-territory interconnected territorial force systems give an improved designation and productive usage of dispersed force assets of various territories. In any case, these interconnected frameworks are affected by region motions (IAOs) when exposed to stack shedding, line blackout, and issue. These motions may prompt flimsiness in the interconnected frameworks [1, 2, 3]. Thus, it is important to screen the dynamical conduct of the interconnected force frameworks and furthermore to balance out such wavering modes. Little Sign Soundness Investigation (SSSA), utilizes the state conditions to gauge the AIOs by linearizing the framework however this methodology bombs when there is an enormous unsettling influence, though a non-direct methodology utilizes the numerical methods(off-line) to fathom the dynamic differential-mathematical conditions [4,5]. In any case, these non-direct methodologies have constraints because of substantial computational weight, huge computational time, and mistakes in parameter estimation. Henceforth, it is important to recognize the IAO modes legitimately from the deliberate sign utilizing on-line approaches [6, 7].

Contributions and Novelities

In this paper, Dymola was chosen as the setting for demonstrating and reenactment. Contrasted with other Modelica conditions, Dymola is easier to use and has solver proficiency that permits enormous frameworks to be reenacted quicker. It causes clients to make a graphical portrayal of physical structures that are helpful in power framework systems implementation. Likewise, models in Dymola can be traded to the FMU design which another programming (for example Simulink) can see, which means co-recreation and trade of information with other reproduction instruments can be figured out [10].

Paper Layout

The rest of the paper is arranged as follows. Section 2 gives a review on the effect of outliers in power system signal with problem occurring in power system with the proper signal model. Section 3 reviews the configuration of adaptive LMS filtering approach. Section 4 describes the result and Discussions about proposed approach used for modes estimation in power system. Section 5 gives a conclusion to the paper.

Problem Formulation

Power Signal Representation

The sign considered for introducing the force framework model can be communicated as far as exponentially damped sinusoids. We considered the genuine force for example $p(n)$ streaming in the tie-lines of the WSCC-9Bus-PQLoad [9,10].

The power system signal model can be expressed as:

$$p(n) = \sum_{k=1}^K a_k e^{b_k n} \cos(n\omega_k + \phi_k)$$

where frequencies $\{\omega_k\}$ and amplitudes $\{a_k\}$ are deterministic amounts. The stages $\{\phi_k\}$ are uncorrelated irregular factors, which are consistently circulated over $(0, 2\pi)$, where $\{b_k n\}$ is the constriction factor and K is the all out number of sinusoids. On the off chance that the sinusoids are affected by an AWGN succession for example $w(n)$ with zero-mean and change.

The signal with noise components can be represented as:

$$P(n) = p(n) + w(n) = \sum_{j=1}^L \alpha_j e^{\beta_j n} + w(n)$$





Effect of Outliers in Power System

The building of automated, interconnected regional electric power networks results generation of diverse and Complex outlier data in the power system. Major causes of outlier are as follows.

- I. **Signal Acquisition Capability:** The limited potentiality of the sensors and WAMSs.
- II. **Power System Failures:** The power system failures such as transmission line outage, faults in the transmission lines.
- III. **Human Influences:** The involvement of the human in the signal measurement and control process may lead to the production of outlier data signal measurement. In some power system activities such as outage control, handling of contingencies, the human intervention is necessary. Besides, the collection of data also requires human interference. Nevertheless, for a single out-of-scale measurement, the sample means of the estimation can be affected when the data sequence includes the outliers.

Removal of Outlier using Adaptive Filtering

Adaptive-Filter Structure

The flexible divert can be completed in different structures or recognize. The choice of the structure can affect the computational multifaceted nature (a proportion of calculating exercises per pattern) of the technique and moreover the crucial number of accentuations to achieve a perfect show level. Essentially, there are two huge classes of flexible automated channel recognize, perceived by the sort of the inspiration response:

- I. Finite-term drive response (FIR) channel
- II. Infinite-term drive response (IIR) channels.

FIR channels are commonly realized with non-recursive structures, while IIR channels utilize recursive recognition. Adaptable FIR channel recognizes: The most for the most part used flexible FIR channel structure is the transversal channel, in like manner called tapped delay line, which completes an every one of the zero trade work with a canonic direct structure affirmation without input. For this affirmation, the yield signal $y(k)$ is a straight mix of the channel coefficients, that yields a quadratic mean-square bumble ($MSE = E[|e(k)|^2]$) work with a unique perfect plan.

Noise Cancellation Using Least Mean Squares (LMS) Algorithms [9]

In the standard and normalized assortments of the LMS flexible channel, coefficients for the altering channel rise up out of the mean square bungle between the perfect sign and the yield signal from the dark system. Using the sign data estimation changes the mean square screw up figuring by using the sign of the data to change the channel coefficients. Exactly when the bungle is certain, the new coefficients are the past coefficients notwithstanding the slip-up expanded by the movement size μ . If the mix-up is negative, the new coefficients are again the past coefficients less the screw up copied by μ note the sign change. Exactly when the data is zero, the new coefficients are identical to the past set. In vector structure, the sign information LMS calculation is given as:

$$w(n+1) = w(n) + \mu e(n) \text{sgn}[x(n)]$$

$$\text{sgn}[x(n)] = \begin{cases} 1, & x(n) > 0 \\ 0, & x(n) = 0 \\ -1, & x(n) < 0 \end{cases}$$





Sudhansu Kumar Samal et al.,

with vector w containing the loads applied to the channel coefficients and vector x containing the information data. $e(k)$ (equal to wanted sign separated sign) is the mistake at time k and is the amount the LMS calculation tries to limit. μ is the progression size. Figure 1 describes the adaptive filtering to remove the outliers.

As you indicate μ littler, the rectification to the channel loads gets littler for each example and the LMS mistake falls all the more gradually. Bigger μ changes the loads more for each progression so the mistake falls all the more quickly, yet the subsequent blunder doesn't move toward the perfect arrangement as intently. To guarantee great combination rate and dependability, select μ inside the accompanying down to earth limits with vector w containing the loads applied to the channel coefficients and vector x containing the information data. $e(k)$ (equal to wanted sign separated sign) is the mistake at time k and is the amount the LMS calculation tries to limit. μ is the progression size. As you indicate μ littler, the rectification to the channel loads gets littler for each example and the LMS mistake falls all the more gradually. Bigger μ changes the loads more for each progression so the mistake falls all the more quickly, yet the subsequent blunder doesn't move toward the perfect arrangement's intently. To guarantee great combination rate and dependability, select μ inside the accompanying down to earth limits.

$$0 < \mu < \frac{1}{N\{\text{Inputs Signal Power}\}}$$

RESULTS AND DISCUSSION

Test signal Corresponding to Inter-Area Mode

The simulation is carried out considering a test signal with a frequency=0.4Hz, magnitude=1 and attenuate on factor=-0.07. Figure 2(a) and Figure 2(b) show the test signal for inter-area mode with SNRs=10dB and 30dB.

Test Signal Analogous to Local-Area Oscillating Mode

The simulation is carried out with a test signal for a frequency=1.5Hz, Attenuation factor=-0.1, and magnitude=1. Figure 3(a) and Figure 3(b) show the test signal for local-area mode with SNRs=10dB and 30dB.

WSCC_9Bus_PQLoad

Figure 4 describes the modeling of WSCC_9Bus system with PQ load using Dymola and modelica language

Model Scripting using Modelica for WSCC_9Bus_PQLoad [10]

Path: ModPowerSystems.PhasorSinglePhase.Examples.ReferenceGrids.WSCC_9Bus_PQLoad

Filename: declaration window

Uses: Modelica (version="3.2.2"), Complex (version="3.2.2"), Modelica Services (version="3.2.2")

model WSCC_9Bus_PQLoad

ModPowerSystems.PhasorSinglePhase.Connections.BusBar BUS2(Vnom=18e3)

equation

connect(GEN1.Pin1, BUS1.Pin1) annotation (Line(points={{4,-58},{4,-52}}));

connect(TR14.Pin1, BUS1.Pin1) annotation (Line(points={{4,-44},{4,-52}}));

connect(TR14.Pin2, BUS4.Pin1)

annotation (Line(points={{4,-24},{4,-20},{4,-17.2149},{3,-17.2149}}));

connect(LINE96.Pin2, BUS6.Pin1)

annotation (Line(points={{46,40},{46,40},{46,22}}));

connect(LINE96.Pin1, BUS9.Pin1)

annotation (Line(points={{46,60},{46,90},{48,90}}));





Sudhansu Kumar Samal et al.,

```

connect(LINE78.Pin1, BUS7.Pin1)
annotation (Line(points={{-26,94},{-40,94},{-40,80},{-35.6764,80}}));
connect(LINE78.Pin2, BUS8.Pin1)
annotation (Line(points={{-6,94},{4,94},{4,78}}));
connect(LINE78.Pin1, BUS8.Pin1)
annotation (Line(points={{2,72},{2,72},{2,78},{4,78}}));
connect(LINE75.Pin2, BUS5.Pin1)
annotation (Line(points={{-24,38},{-24,38},{-24,26}}));
connect(LINE75.Pin1, BUS7.Pin1)
annotation (Line(points={{-24,58},{-35,58},{-35, 80},{35.6764,80}}));
connect(LINE75.Pin1, BUS5.Pin1)
annotation (Line(points={{-48,20},{-24,20},{-24,26}}));
connect(LINE54.Pin1, BUS5.Pin1)
annotation (Line(points={{-24,14},{-24,20},{-24,26}}));
connect(LINE54.Pin2, BUS4.Pin1)
annotation (Line(points={{-24,-6},{-6,-6},{-6,-17.2149},{3,-17.2149}}));
connect(GEN2.Pin1, BUS2.Pin1)
annotation (Line(points={{-96,80},{-86,80},{-86,80},{-74.1269,80}}));
connect(TR27.Pin1, BUS2.Pin1)
annotation (Line(points={{-60,75},{-72,75},{-72,80},{-74.1269,80}}));
connect(TR27.Pin2, BUS7.Pin1)
annotation (Line(points={{-38,75},{-38,73.9642},{-35.6764,73.9642},
{-35.6764,80}}));
connect(LINE66.Pin1, BUS6.Pin1)
annotation (Line(points={{62,4},{46,4},{46,22}}));
connect(TR39.Pin2, BUS9.Pin1)
annotation (Line(points={{68,80},{58,80},{58,90},{48,90}}));
connect(TR39.Pin1, BUS3.Pin1)
annotation (Line(points={{88,80},{102,80},{102,82},{102,90},{98,90}}));
connect(GEN3.Pin1, BUS3.Pin1)
annotation (Line(points={{132,80},{116,80},{116, 90},{98,90}}));
connect(LINE89.Pin2, BUS9.Pin1)
annotation (Line(points={{36,94},{48,94},{48,90}}));
connect(LINE89.Pin1, BUS8.Pin1)
annotation (Line(points={{16,94},{4,94},{4,78}}));
connect(LINE64.Pin1, BUS6.Pin1)
annotation (Line(points={{20,14},{46,14},{46,22}}));
connect(LINE64.Pin2, BUS4.Pin1)
annotation (Line(points={{20,-6},{4,-6},{4,-17.2149},{3,-17.2149}}));
connect(LINE78.Pin1, TR27.Pin2)
annotation (Line(points={{-26,94},{ 40,94},{40,75},{38,75}}, color={0,0,0});
annotation (Diagram(coordinateSystem(preserveAspectRatio=false, extent={{160, 80},{160,114}}), Icon(coordinateSystem(
extent={{-160,-80},{160,100}})));
end WSCC_9Bus_PQLoad;

```





CONCLUSION AND FUTURE SCOPE

Outcome of the research

Adaptive filtering with LMS is a new outlier removal technique to filter the signal from unwanted communication noises to improve the estimation method, has been proposed in this paper and it works on the Modelica and 3D Dymola software platform using adaptive filtering which to achieve the robust real-time estimation of modes in different real-time noisy conditions. The efficacy of the proposed algorithm is also provided using large WSCC_9Bus_PQLoad loading conditions.

Limitation of the work

Adaptive filtering with LMS provides the filtration approach to the signal obtained from the real-time power signal, which is very crucial to maintain the information contained in the signal. Much more filtration may cause toward misleading of the estimation of proper estimation of that. It needs proper tuning of the signal and initial weight section of the adaptive filtering is also a difficult task.

Future Scope of the research

The research for the future leads to be focused on the large IEEE standard systems and also the adaptive filter should be properly tuned. Physical behavior of the simulation should be tested.

REFERENCES

1. Rogers, Graham. "Power system structure and oscillations." In Power system oscillations, pp. 101-119. Springer, Boston, MA, (2000).
2. Kokai, Yutaka, Fumio Masuda, Satoshi Horiike, and Yasuji Sekine. "Recent development in open systems for EMS/SCADA." International Journal of Electrical Power & Energy Systems 20, no. 2 (1998): 111-123.
3. Bose, Anjan. "Smart transmission grid applications and their supporting infrastructure." IEEE Transactions on Smart Grid 1, no. 1 (2010): 11-19.
4. Taylor, Carson W., Dennis C. Erickson, Kenneth E. Martin, Robert E. Wilson, and Vaithianathan Venkatasubramanian. "WACS-wide-area stability and voltage control system: R&D and online demonstration." Proceedings of the IEEE 93, no. 5 (2005): 892-906.
5. Phadke, Arun G., and B. I. Tianshu. "Phasor measurement units, WAMS, and their applications in protection and control of power systems." Journal of Modern Power Systems and Clean Energy 6, no. 4 (2018): 619-629.
6. Benmouyal, Gabriel, E. O. Schweitzer, and Armando Guzmán. "Synchronized phasor measurement in protective relays for protection, control, and analysis of electric power systems." (2004): 814-820.
7. Kundur, Prabha, John Paserba, VenkatAjjrapu, Göran Andersson, Anjan Bose, Claudio Canizares, Nikos Hatziargyriou et al. "Definition and classification of power system stability IEEE/CIGRE joint task force on stability terms and definitions." IEEE transactions on Power Systems 19, no. 3 (2004): 1387-1401.
8. Samal, Sudhansu Kumar, and Bidyadhar Subudhi. "New signal subspace approach to estimate the inter-area oscillatory modes in power system using TLS-ESPRIT algorithm." IET Generation, Transmission & Distribution 13, no. 18 (2019): 4123-4140.
9. Wies, R. W., A. Balasubramanian, and J. W. Pierre. "Adaptive filtering techniques for estimating electromechanical modes in power systems." In 2007 IEEE Power Engineering Society General Meeting, pp. 1-8. IEEE, (2007).
10. Modelica association. Modelica language specification, version 3.3. 2012-05-09.



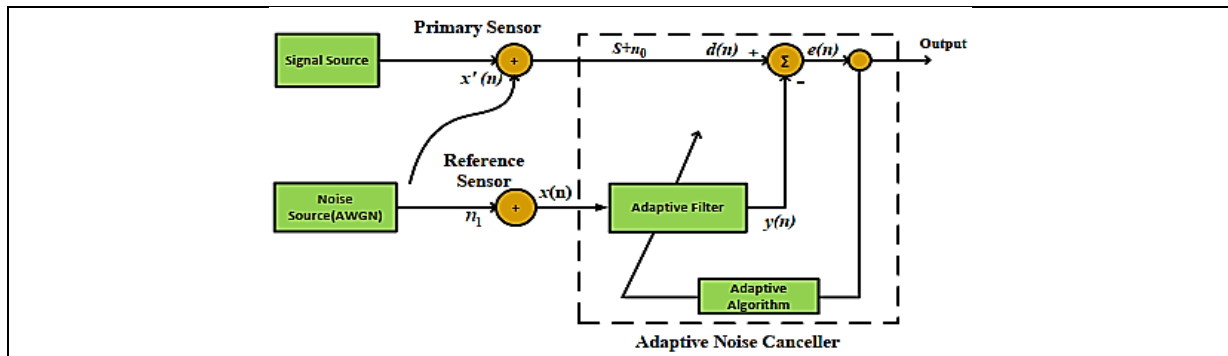


Figure 1. Block Diagram of Adaptive Filtering Estimation Approach

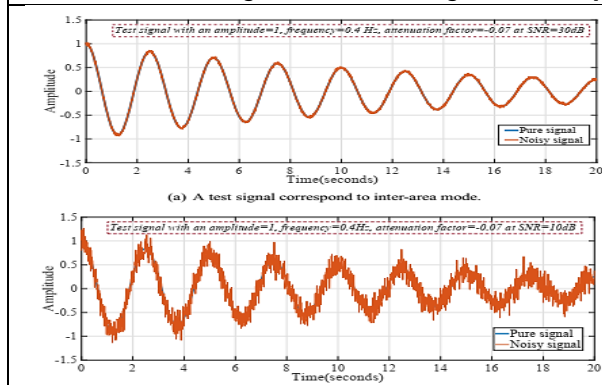


Figure 2. Test Signals for Inter-Area Oscillating Modes in Power System using SNR 10dB and 30dB

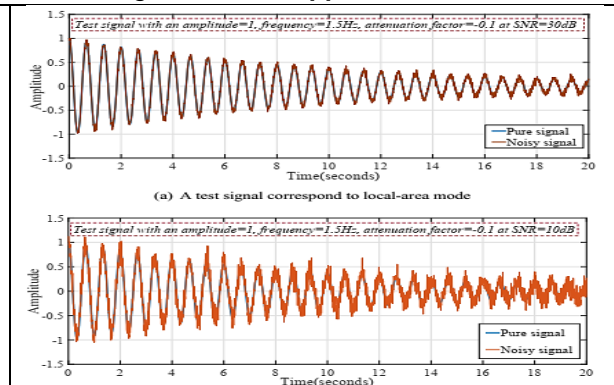


Figure 3. Test Signals for Local-Area Oscillating Modes in Power System using SNR 10dB and 30dB

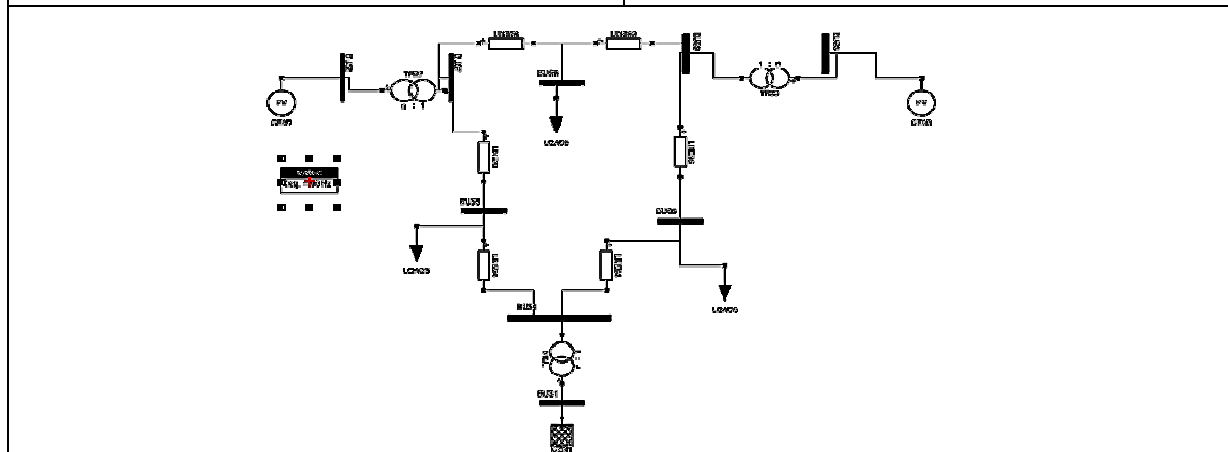


Figure 4. Modeling of WSCC_9Bus_PQLoad using 3DS Dymola modelica platform





Pharmacognostic Standardization and Phytochemical Studies of *Coelogyne breviscapa* Lindl Leaves

Janarthanan L^{1*}, Karthikeyan V¹, Senniappan P¹ and Loganathan J²

¹Assistant Professor, Department of Pharmacognosy, Vinayaga Mission's College of Pharmacy, VMRF(DU), Salem, Tamil Nadu, India.

²Assistant Professor, Department of Pharmaceutical Chemistry, Vinayaga Mission's College of Pharmacy, VMRF(DU), Salem, Tamil Nadu, India.

Received: 03 Sep 2020

Revised: 05 Oct 2020

Accepted: 07 Nov 2020

*Address for Correspondence

Janarthanan L

Assistant Professor,

Department of Pharmacognosy,

Vinayaga Mission's College of Pharmacy, VMRF(DU),

Salem, Tamil Nadu, India.

Email: jana_loganathan@yahoo.co.in



This is an Open Access Journal / article distributed under the terms of the **Creative Commons Attribution License** (CC BY-NC-ND 3.0) which permits unrestricted use, distribution, and reproduction in any medium, provided the original work is properly cited. All rights reserved.

ABSTRACT

Coelogyne breviscapa Lindl.(Family: Orchidaceae) is a perennial herb which commonly known as short-inflorescence *Coelogyne* and Short-Stem *Coelogyne*. *Coelogyne* is a genus of over 200 sympodial epiphytes and distributed across India, China, Indonesia and the Fiji islands, Sumatra and the Himalayas. Micromorphology and physicochemical parameter of the leaves of *C.breviscapa* were performed as per WHO and Pharmacopoeial methods. Microscopic evaluation of leaves showed the midrib bundle is small and collateral. It consist of a group of wide angular cluster of xylem elements and a prominent unit of phloem elements located on the abaxial part of the xylem strand. The lamina consists of thin adaxial epidermis. The epidermal cells are narrow rectangle and have thick cuticle. The abaxial epidermis is slightly larger rectangular and have thick cuticle. Mucilaginous cells are also found along the hypodermal layer of the abaxial epidermis and median area of the lamina. Collateral vascular bundles of large and small sizes are seen in the median part of the lamina. Preliminary phytochemical screening of appropriate solvent extracts showed the presence of alkaloids, sterols, tannins, proteins and amino acids, flavonoids, terpenoids, saponin, carbohydrates and absence of glycosides and volatile and fixed oil. Microscopic analysis and other parameters were informative and provide valuable information in the authentication, standardization of *Coelogyne breviscapa* Lindl leaves.

Keywords: *Coelogyne breviscapa* Lindl, Orchidaceae, Short-Stem *Coelogyne*, Microscopical evaluation.





Janarthanan et al.,

INTRODUCTION

Coelogyne breviscapa Lindl. is a species of perennial herbs belonging to the Solanaceae family. It is commonly known as Native gooseberry, wild Cape gooseberry and pygmy ground cherry [1]. *Coelogyne* is a genus of over 200 sympodial epiphytes and distributed across India, China, Indonesia, Sumatra and the Himalayas [2]. *Coelogyne breviscapa* Lindl have been used in Indian traditional medicinal system for very long time for treating various disorders [3]. This plant is reported for its antibacterial [4], antifungal [5] and antioxidant activities [6 & 7].

Taxonomical classification [8]

Kingdom	: Plantae
Clade (Unranked)	: Angiosperms
Clade (Unranked)	: Eudicots
Clade (Unranked)	: Monocotyledones
Division	: Magnoliophyta
Class	: Liliopsida
Super order	: Coelogyneinae
Order	: Asparagales
Family	: Orchidaceae
Genus	: <i>Coelogyne</i>
Species	: <i>breviscapa</i>

Vernacular names [9]

Common Name	: The Short-Inflorescence <i>Coelogyne</i> , Short-Stem <i>Coelogyne</i>
Botanical Name	: <i>Coelogyne breviscapa</i> Lindl
Tamil Name	: Orilai Thamarai

As mentioned previous reports have been published regarding phytochemical and different therapeutic activities *in-vitro* and *in-vivo*. An investigation to inquire its pharmacognostic examination is unavoidable. The present work was aimed to lay down standards which could be useful to detect the authenticity of this therapeutically useful plant *Coelogyne breviscapa* Lindl leaves to treat various illnesses.

MATERIALS AND METHODS

Chemicals: Ethyl alcohol, Formalin, Chloral hydrate, Acetic acid, Glycerin, Phloroglucinol, Toluidine blue, Hydrochloric acid and all other chemicals used in this study were of analytical grade.

Collection and authentication of Plant: The leaves of the selected plant were collected from in and around Salem district, Tamil Nadu with the help of local tribal and field botanist. It was authenticated by Dr. P. Jayaraman, Director of Plant Anatomy Research Institute (PARC), Chennai, Tamil Nadu, India.

Macroscopic analysis: Organoleptic characters such as colour, odour, taste, shape, size, surface characters, texture, etc were done [10].





Janarthanan *et al.*,

Microscopic analysis: The samples of leaves were fixed in FAA [Formalin (5mL), Acetic acid (5mL), Ethyl alcohol (90mL)]. After one day of fixing, the specimens were dehydrated by t-butyl alcohol. Specimen Infiltration was done by paraffin wax (M.P-58-60°C) [11].

Sectioning: Specimens were sectioned by rotary microtome. The thickness of the sections were about 8-10 µm. The sections were de waxed and stained by using Toluidine blue. The staining results were remarkably good as the stain was a polychromatic stain. The dye impart pink color to the cellulose, lignified cells, mucilage and blue color to the protein bodies [12].

Leaf clearing: Paraffin embedded leaf was used for para-dermal sections. Another method was clearing leaf fragments by immersing in alcohol followed by treating with 5% sodium hydroxide. The material was made transparent due to loss of cellular contents.

Photomicrographs: Photographs were taken with help of Nikon lab-photo 2 microscopic Unit. Bright field and polarized light was used. The magnifications are indicated by the scale-bars in the photographs.

Quantitative Microscopy: Stomatal number, Stomatal index, Vein islet and Vein termination was determined as per standard methods [13].

Physicochemical analysis: Total ash, acid insoluble ash, water soluble ash, loss on drying and extractive values was determined as per standard methods [14].

Preliminary phytochemical screening: Preliminary phytochemical screening of ethanolic and aqueous extract carried out to find out the presence of various phyto constituents using standard procedure [15].

RESULTS

Macroscopy

Leaf Morphology [Figure 1]

Habitat: Found in southern India and Sri Lanka in montane forests on tree branches and on rocks in grasslands at elevations of 1800 to 2000 meters as a miniature to small sized, cool growing epiphyte or lithophyte.

Flowers: Inflorescence bears 4 to 8 flowers, simultaneously opening, white in colour of 25 mm size with persistent floral bracts of size 20-25 mm.

Flowering time: March – April

Leaves: Narrowly 2 per ovate pseudo bulbs that are reddish brown in colour of size 5 cm X 1.5 cm

Apex: Tapering towards apex floral bracts 2-3 x 1 cm, lanceolate, acute; dorsal sepal 13 x 4 mm, oblong-lanceolate, acute, 5-veined;

Base: Acute, 3-veined; lip 12 x 7-8 mm, 3-lobed, middle ovate.

Petiole: 10-24.5 by 3.4 mm. Blade lanceolate to linear lanceolate, plicate, top acute.



**Janarthanan et al.,**

Margin: 1 to 2 linear oblong leaves of 15 cm X 1.5 cm each, acute; dorsal sepal 13 x 4 mm, oblong-lanceolate, acute, 5-veined; lateral sepals 11.5 x 3.5-4.1 mm, oblong-lanceolate, acute, 5-veined; petals 11 x 2-2.5 mm, linear, acute, 3-veined; lip 12 x 7-8 mm, 3-lobed, middle ovate.

Microscopy

The leaf is uniformly smooth on either side. It is deeply grooved along the median part of the lamina (Fig 2 & 3) beneath the median groove occurs the midrib vascular bundle. The midrib bundle is small and collateral. It consist of a group of wide angular cluster of xylem elements and a prominent unit of phloem elements located on the abaxial part of the xylem strand (Fig 4). The vascular bundle is surrounded by sclerenchyma cells which are highly thick walled and narrow lumened. The lamina in the midrib is 250 μ m thick. The lamina consists of thin adaxial epidermis. The epidermal cells are narrow rectangle and have thick cuticle. The abaxial epidermis is slightly larger rectangular and have thick cuticle. On the adaxial and abaxial sides occurs sub-epidermal cells, which are large squarish and thin walled and these cells are filled with dense mucilage. Mucilaginous cells are also found along the hypodermal layer of the abaxial epidermis. The mucilaginous cells are also found in the median area of the lamina (Fig 5). The lamina is 430 μ m thick. Collateral vascular bundles of large and small sizes are seen in the median part of the lamina. These bundles have vertical rows of small angular compact xylem elements and duster of phloem elements. These lateral vein bundles have a thin cap of sclerenchyma cells on the phloem cells (Fig 5).

Leaf margin: The leaf margin is flat on the adaxial side and slightly curved on the abaxial side. The extreme margin is thick and conical. The leaf margin is 90 μ m thick. The end of the margin has very thick cuticle. The mesophyll tissue consist of 5 or 6 layers of vertically oblong compact cells occur along the sub-epidermal cells as well as in the median zone of the lamina. Small circular vascular bundles of lateral veins occur in horizontal row of the lamina (Fig 6).

Distribution of calcium oxalate crystals: Small crystal with 4 or more petal like lobes are abundant in the mesophyll tissue of the lamina. The crystals have small dark spot in the center (Fig 7 & 8). Crystals are about 5 μ m in diameter. The crystal bearing cells are normal unmodified cells.

Quantitative Microscopy (Table 1)

Physio-chemical parameter (Table 2)

Preliminary Phytochemical Screening of leaves of *Coelogyne breviscapa* Lindl (Table 3)

DISCUSSION

Crude drug evaluation done for confirmation of its identity and determination of its quality and purity and also detect adulterated content. It is a qualitative evaluation based on the sensory and morphology profiles of crude drugs [16]. This present study is to serve as a tool for developing standards for authentication, quality and purity of *Coelogyne breviscapa* Lindl leaf. Adulteration of crude drugs can cause serious health problems to consumers and pharmaceutical industries. The anatomical character is an important aid for the identification of plant drugs [17]. Microscopic evaluation is one of the simplest methods for the proper authentication of plant materials [18]. Microscopic evaluation of leaves showed the midrib bundle is small and collateral. It consist of a group of wide angular cluster of xylem elements and a prominent unit of phloem elements located on the abaxial part of the xylem strand. The lamina consists of thin adaxial epidermis. The epidermal cells are narrow rectangle and have thick cuticle. The abaxial epidermis is slightly larger rectangular and have thick cuticle. Mucilaginous cells are also found along the hypodermal layer of the abaxial epidermis and median area of the lamina. Collateral vascular bundles of large and small sizes are seen in the median part of the lamina. Quantitative analytical microscopy is useful in measuring the cell contents of the crude drugs and help in their identification, characterization and standardization. The ash values are useful for detecting foreign inorganic matter. Acid insoluble ash gives information regarding the





presence of inorganic dirt and dust [19 & 20]. Pharmacognostical study on the leaves of *C.cristata* was previously reported [21]. Phytochemical evaluation and characterization of plant extract is an important tool in drug discovery [22]. Preliminary phytochemical screening of appropriate solvent extracts showed the presence of tannins, sterols, alkaloids, flavonoids, amino acids, terpenoids, carbohydrates and absence of glycosides and volatile and fixed oil.

CONCLUSION

Coelogyne breviscapa Lindl have a wide range of therapeutically active compounds which could be useful for treatment of various ailments. The pharmacognostic features, physicochemical constants, preliminary phytochemical studies have been useful in deciding the identity, purity and strength of the plant material and also for fixing standards for this plant. This present study will certainly help to build a monograph of the plant in Herbal Pharmacopoeia.

Conflict of interest statement: We declare that we have no conflict of interest.

ACKNOWLEDGEMENT

The author extend their heartfelt thanks for Dr.P.Jayaraman, Director of Plant Anatomy Research Institute, Tambaram, Chennai for authentication and microscopical studies.

REFERENCES

1. Yoga Narasimhan, S.N.2000.Medicinal Plants of India. Vo1.II.Tamil Nadu. Regional Research Intitute, Bangalore, India. P.715.
2. Henry, A.N; Kumari, G.R. and Chitra, V. 1987. Flora of Tamil Nadu, India. Vol.3 Botanical Survey of India, Southern Circle, Coimbatore, India. PP-258.
3. Gamble, J.S 1935. Flora of The Presidency of Madras. Vol. I, II, & III. Botanical Survey of India, Calcutta, India.
4. Ranjitha MC, Akarsh S, Prashith Kekuda TR, Darshini SM and Vidya P., Antibacterial Activity of Some Plants of Karnataka, India. Journal of Pharmacognosy and Phytochemistry 2016; 5(4): 95-99.
5. Shweta S.D, Sudeshna C.S, Rashmi K, Vrushala P.S, Prashith Kekuda T.R Antifungal efficacy of some epiphytic orchids of Karnataka, India. Sch J Agric Vet Sci 2015; 2(3B):266-269.
6. Parveen S, Mahmood R. Folklore Medicinal Orchids from South India: The Potential source of Antioxidants. Asian Journal of Pharmaceutical and Clinical Research, Vol. 11, no. 6, June 2018, pp. 194-198.
7. Clayton, D. (2002). The Genus Coelogyne: A Synopsis. Natural History Publication, Borneo. 316 pp.
8. Chopra RN, Nayar SL, Chopra IC. Glossary Indian Med. Plants, CSIR, New Delhi; 1956: p-192.
9. Kirtikar KR, Basu BD. Indian Medicinal Plants, Lalit Mohan Basu; Allahabad; Vol.3, 1935: p-1766-1768.
10. Kokate CK, Gokhale SB, Purohit AP. Pharmacognosy. 32nd ed., New Delhi: Nirali Prakashan; 2005.
11. Asokan J. Botanical Micro Technique Principles and Practice. 1st edn, Chennai: Plant Anatomy Research Centre; 2007.
12. Johansen DA. Plant Microtechnique. Newyork: MC Graw hill; 1940, pp. 523.
13. Evan WC. Trease and Evans Pharmacognosy. 15th edn, London Saunders: Elsevier; 2002, pp. 563-70.
14. WHO. Quality control methods for medicinal plant materials. Geneva: World Health Organization; 1998.
15. Anonymous. The Indian Pharmacopoeia. Vol II, New Delhi: Ministry of Health and Family Welfare; 1996.
16. Periyanyagam K, Karthikeyan V. Pharmacognostical, SEM and XRF profile of the leaves of *Artocarpus heterophyllus* L. (Moraceae) - A contribution to combat the NTD. Innovare Journal of Life sciences, 2013; 1(1): 23-8.
17. Agrawal SK, Karthikeyan V. Quality assessment profile of the leaves of *Tecoma stans* L. International Journal of Pharmaceutical Research, 2014; 6(2): 94-99.





Janarthanan et al.,

18. Karthikeyan V, Agrawal SK, Parthiban P, Nandhini SR. Multivitamin plant: pharmacognostical standardization and phytochemical profile of its leaves. *Journal of Pharmacy Research*, 2014; 8(7): 910-915.
19. Karthikeyan V, Karthikeyan J. *Citrus aurantium* (Bitter Orange): A Review of its Traditional Uses, Phytochemistry and Pharmacology. *International Journal of Drug Discovery and Herbal Research*, 2014; 4(4): 766-772.
20. Aruna A, Nandhini SR, Karthikeyan V, Bose P, Vijayalakshmi K, Jegadeesh S. Insulin plant (*Costus pictus*) leaves: Pharmacognostical standardization and phytochemical evaluation. *American Journal of Pharmacy & Health Research*, 2014; 2(8): 106-119.
21. Sharma C, Irshad S, Khatoon S, Arya KR. Pharmacognostical evaluation of Indian folk-traditional plants *Coelogyne cristata* and *Pholidota articulata* used for healing fractures. *Indian Journal of Experimental Biology*, 2017; 55: 622-627.
22. Karthikeyan V, Balakrishnan BR, Senniappan P, Janarthanan L, Anandharaj G, Jaykar B. Pharmacognostical, phyto-physicochemical profile of the leaves of *Michelia champaca* Linn. *International Journal of Pharmacy and Pharmaceutical Research*, 2016; 7(1): 331-44.

Quantitative Microscopy

Table 1: Quantitative analytical microscopical parameters of the leaf of *Coelogyne breviscapa* Lindl

S. No.	Parameters	Values obtained*
1	Stomatal number in upper epidermis	32.14 ± 1.25
2	Stomatal number in lower epidermis	23.10 ± 0.39
3	Stomatal index in upper epidermis	15.84 ± 1.23
4	Stomatal index in lower epidermis	17.23 ± 1.72
5	Vein islet number	8.27 ± 0.51
6	Vein termination number	12.12 ± 1.09

*mean of three readings ± SEM

Table 2: Physical parameters of *Coelogyne breviscapa* Lindl

S. No	Parameters	Values *
1	Loss on drying	17
2	Extractive values	
	Ethanol	15.82 ± 0.12
	Methanol	12.27 ± 0.09
	Water	19.71 ± 0.43
3	Ash values	
	Total ash	22.49 ± 0.05
	Acid insoluble ash	7.82 ± 0.83
	Water soluble ash	6.72 ± 0.14

*mean of three readings ± SEM





Preliminary Phytochemical Screening of leaves of *Coelogyne breviscapa* Lindl

Table 3: Preliminary Phytochemical Screening of Different Solvent Extracts

Tests	Ethanolic extract	Aqueous extract
Alkaloids		
Mayers Reagent	+	-
Dragendorffs reagent	+	-
Hagers reagent	+	-
Wagners reagent	+	-
Carbohydrates		
Molishch's Test	+	+
Fehlings Test	+	+
Benedicts Test	+	+
Glycosides		
General Test	-	-
Anthraquinone	-	-
Cardiac	-	-
Cyanogenetic	-	-
Coumarin	-	-
Phytosterols		
Salkowski Test	+	-
Liebermann Burchard Test	+	-
Saponins	+	+
Tannins	+	+
Proteins & Free Amino Acid		
Millons test	+	+
Biuret test	+	+
Flavonoids		
Shinoda test	+	+
Alkaline Reagent test	+	+
Terpenoids	+	-
Fixed Oil	-	-
Volatile oil	-	-



Figure 1: Habit and Habitat of *Coelogyne breviscapa* Lindl

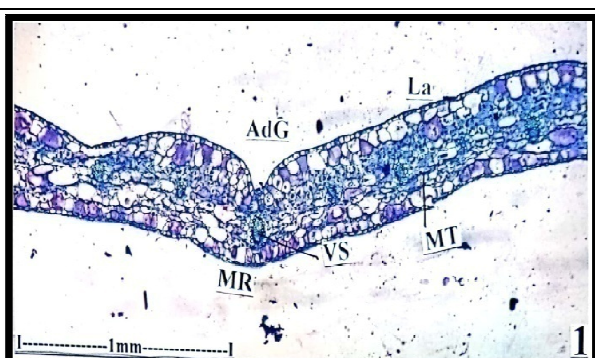


Figure 2: T.S of Lamina through Midrib (AdG – Adoxial Groove; La – Lamina; MT – Mesophyll tissue; MR – Mid Rib; VS – Vascular Strand)



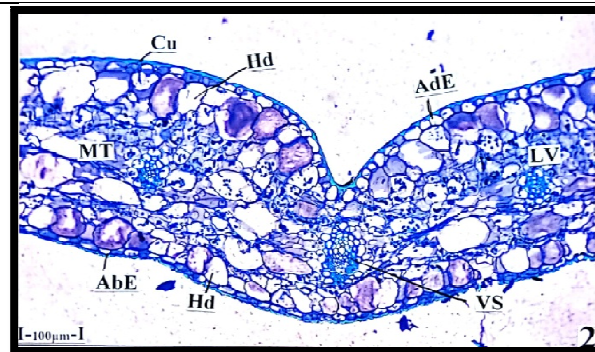


Figure 3: T.S of Midrib with Adaxial groove and Midrib Vascular Bundle (AbE – Abaxial Epidermis; AdE – Adaxial Epidermis; Cu – Cuticle; Hd – Hypodermis; LV – Lateral Vein; MT – Mesophyll tissue; VS – Vascular Strand)

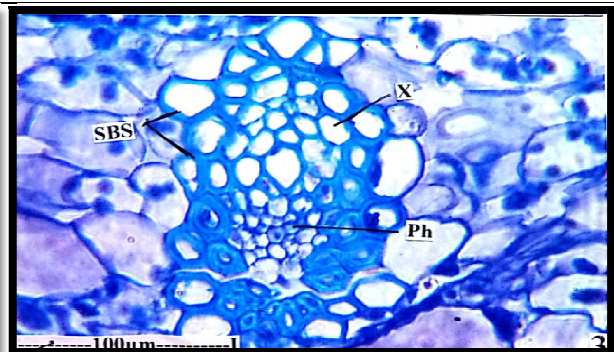


Figure 4: Midrib vascular bundle – Enlarged (Ph – Phloem; SBS – Sclerenchymatous Bundle Sheath; X – Xylem)

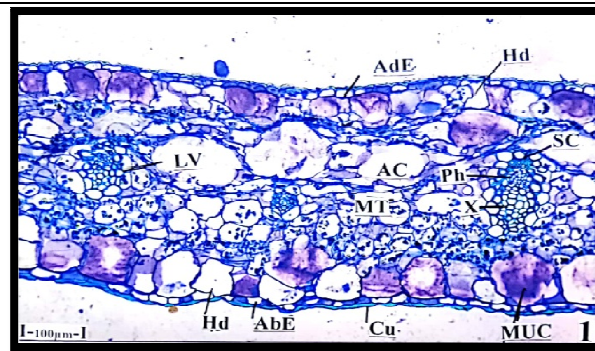


Figure 5: T.S of Lamina (AbE – Abaxial Epidermis; AdE – Adaxial Epidermis; AC – Air Chamber; Cu – Cuticle; Hd – Hypodermis; LV – Lateral Vein; MT – Mesophyll tissue; MUC – Mucilage cell; Ph – Phloem; SC – Sclerenchyma Cell)

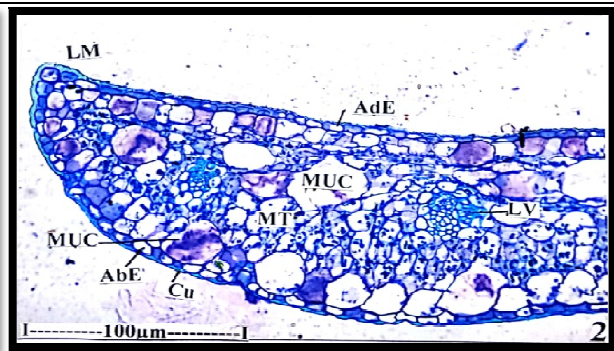


Figure 6: T.S of marginal part of the lamina (AbE – Abaxial Epidermis; AdE – Adaxial Epidermis; Cu – Cuticle; LV – Lateral Vein; MT – Mesophyll tissue; MUC – Mucilage cell; LM – Leaf Margin)

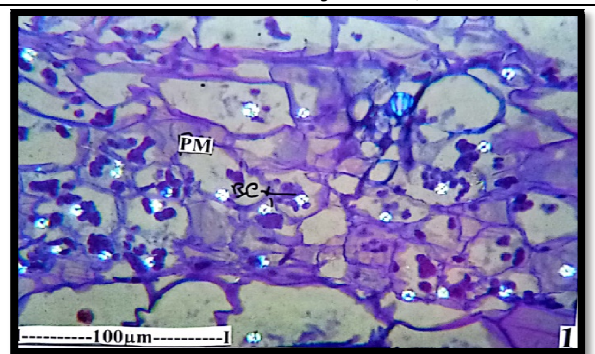


Figure 7: Rosette crystals found in the leaf mesophyll (PM – Palisade Mesophyll; RCr – Rosette Crystal)

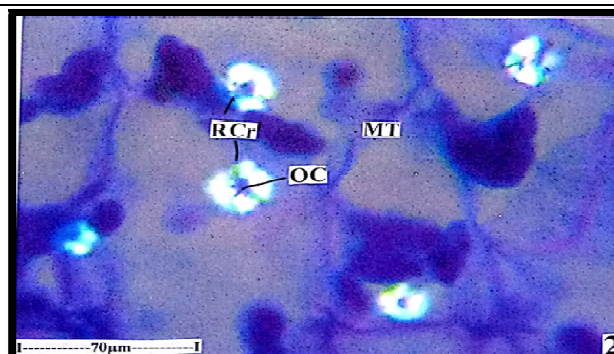


Figure 8: Rosette Crystals – Enlarged (MT – Mesophyll tissue; OC – Organic Compound; RCr – Rosette Crystal)





RESEARCH ARTICLE

In-vitro Hepatoprotective Activity of *Notonia grandiflora* Wall. On Ethanol-Induced Oxidative Damage in HEPG2 CellsMeera Paul^{1*}, R.Sanilkumar² and Sabu M.C¹¹Mookambika College of Pharmaceutical Sciences and Research, Muvattupuzha, Kerala, India.²Department of Pharmacy, Annamalai University, Annamalai Nagar, Tamil Nadu, India.

Received: 06 Sep 2020

Revised: 08 Oct 2020

Accepted: 10 Nov 2020

Address for Correspondence*Meera Paul**Mookambika College of Pharmaceutical Sciences and Research,
Muvattupuzha, Kerala, India.

Email : meera5paul@gmail.com



This is an Open Access Journal / article distributed under the terms of the **Creative Commons Attribution License** (CC BY-NC-ND 3.0) which permits unrestricted use, distribution, and reproduction in any medium, provided the original work is properly cited. All rights reserved.

ABSTRACT

The aim of this study was to investigate the in-vitro hepatoprotective activity of solvent extracts of *Notonia grandiflora* Wall. on HEPG2 cell line. The hexane, ethyl acetate, ethanol and water extracts of aerial parts of *Notonia grandiflora* were used in this study. The different extracts of *Notonia grandiflora* were assessed for their hepatoprotective activity on human liver hepatocellular carcinoma (HEPG2) cell line against ethanol as a liver damage inducing agent by quantifying the release of lactate dehydrogenase (LDH) in the medium. Elevated levels of LDH indicates liver damage. The cytotoxicity study was conducted for the ethylacetate extract of *Notonia grandiflora* (EANG) using MTT assay to determine the CTC₅₀ value. 6.25–100 µg/ml concentration of extracts were selected for the hepatoprotective study in HEPG2 cell lines. The extract, EANG exhibited significant protection against ethanol induced cytotoxicity and the activity was comparable with that of the standard Silymarin. The maximum protection was observed to be 75.72% at dose 12.5 µg/ml. The study revealed that the ethylacetate extract of *Notonia grandiflora* had shown significant hepatoprotective activity against ethanol-induced cytotoxicity assay.

Keywords: *Notonia grandiflora*, ethanol, HEPG2, MTT, Hepatoprotective activity, Silymarin.**INTRODUCTION**

Drugs derived from natural products have the ability to affect body systems. The World Health Organization estimated that 80% of the population of developing countries relies on traditional medicines, for their primary health care needs [1]. Medicinal plants play a crucial role in the discovery of novel drugs [2]. In spite of tremendous scientific advancement within the field of hepatology in recent year, liver diseases constitute a major cause of morbidity and mortality among all the fatal diseases. Jaundice and hepatitis are two major hepatic disorders that account for a high mortality [3]. A number of hepatotoxins such as viruses, bacteria, chemicals, free radicals, excess consumption of alcohol, xenobiotics, food additives and pollutants are prone to injure the liver and these are the

28432



**Meera Paul et al.,**

major risk factors which lead to the manifestation of various liver disorders such as hepatitis, cirrhosis and alcoholic liver diseases [4]. Exposure of the liver to the free radicals, mainly the reactive oxygen species (ROS) and reactive nitrogen species (RNS), derived from some xenobiotic and drugs leads to oxidative stress, which is recognized to be a major factor responsible for liver laceration or be involved in the pathogenesis of liver disorder. The oxygen centered free radicals (ROS) and other reactive nitrogen species (RNS), which are continuously produced, resulting in cell death or tissue damage [5]. This oxidation damage caused by free radical is linked to pathogenesis of many chronic degenerative diseases like cancer, diabetes, neurodegenerative diseases, atherosclerosis, cirrhosis, malaria and acquired immune deficiency syndrome. Therefore, antioxidants may play a role in inhibiting the liver injury induced during cell damage and are recommended for liver disorders [3]. Despite tremendous advances in modern medicine, there are no effective and reliable drugs that stimulate hepatic function, offer complete protection to the organ, or aid in regenerating hepatic cells. Additionally, most of the drugs can induce adverse or side effects. Thus, it is necessary to identify alternative pharmaceuticals for the treatment of hepatic diseases, with the aim of these agents being more effective, reliable and less toxic [6]. It is estimated that about 80% of the population of developing countries depends on traditional medicines, mostly plant drugs and for their primary health-care needs. But, only a small proportion of hepatoprotective plants used in traditional medicine are pharmacologically evaluated for their safety and efficacy, and many are yet to be investigated [7]. Therefore, there is an urgent need for identification of such plants for scientific pharmacological investigation. *Notonia grandiflora* Wall. is a perennial succulent genus of Asteraceae-Senecioneae commonly known as "large flower-Kleinia". Traditionally, the plant is named as Muyal Kadhu (Tamil). It is commonly found on bare, exposed slopes and rocks of deciduous forests from plains to 1400m [8]. The plant has been found to possess pharmacological activities as antioxidant, analgesic and antinociceptive, anti-inflammatory [9], antimicrobial, antibacterial, antifungal, and antipyretic [10]. It really is utilized by the tribal as traditionally in the treatment of joints pains, ear ache [11], to get relief from gastric complaints [12], for pimples and as a remedy for hydrophobia, used in the treatment of urinary disorders, infection, stones, diuretic, oedema [13], for scabies and skin eruptions [14], wounds including sores and ulcers and in the treatment of scorpion bite [15]. The present study is an attempt to evaluate scientifically and through experimental manipulations the hepatoprotective activity of *Notonia grandiflora*.

MATERIALS AND METHODS

Collection and Identification of plant material

The fresh aerial parts (stems and leaves) of *Notonia grandiflora* was collected from Tirunelveli district of Tamil Nadu, India. The identification and authentication of plant was done by Dr. V. Chelladurai, Research Officer (Botany), Central Council of Research in Ayurveda and Siddha, Government Siddha Medical College, Palayamkottai, Tamilnadu, India.

Preparation of extract

Fresh aerial parts collected was washed under running tap water, air dried and powdered. About 50g of coarsely powdered plant materials (50g/250ml) were extracted in a Soxhlet extractor for 8 hours, sequentially with hexane, ethyl acetate, ethanol and water. The temperature of the extract was maintained (25°C- 100°C) on an electric heating mantle with thermostat control. The extracts were then concentrated by a rotary evaporator under 40°C and low pressure and finally dried to a constant weight. Dried extracts were kept at 20°C in air tight containers until further test were carried out.

Phytochemical analysis

The extracts were subjected to chemical tests for detection of various phytoconstituents such as saponins, steroid / triterpenoidal, flavonoidal compounds, glycosides, alkaloids, phenolics, and tannins [16,17].



**Meera Paul et al.,****Total phenolic content (TPC) determination**

Folin-Ciocalteu method was used for the determination of the total phenolic content of the plant extracts using gallic acid as an internal standard with slight modification [18]. 2.5 mL of Folin-Ciocalteu phenol reagent was added to 1 ml of the extract (1 mg/ml) and were mixed. After 5 min, 4 mL of 7.5% Na₂CO₃ solution was added to the mixture and made up to the mark with distilled water. The mixture was incubated in the dark for 90 mins at room temperature. Standard gallic acid solutions of concentrations 100,200,400,800, and 1000 µg/mL were also prepared in same manner. The absorbance's of the plant extracts and gallic acid standard solutions were measured at 750 nm against the reagent blank using UV/Visible spectrophotometer (UV-1800, Shimadzu, Japan). The total phenolic content was determined from the calibration curve and expressed as milligram of gallic acid equivalent (GAE) per gram of the extracts. All the sample determinations were carried out in triplicate.

Determination of total flavonoid content (TFC)

Aluminium chloride colorimetric method was used for the determination of the total flavonoid content[19].Each plant extracts (2ml, 0.3 mg/mL) in methanol were mixed with 0.1 mL of 10% aluminium chloride hexahydrate, 0.1 mL of 1 M potassium acetate and 2.8 mL of deionized water. The absorbance of the reaction mixture was determined spectrophotometrically at 415 nm, after 40 minutes of incubation at room temperature. A set of standard solutions of quercetin of concentrations 100, 80, 60, 40 and 20 µg/ml were prepared in the same manner as described for the extracts. The absorbance's of the extracts and standard solutions were measured against the reagent blank at 415 nm with a UV/Visible spectrophotometer. The total flavonoid content was determined from the calibration curve and expressed as milligram of quercetin equivalent (QE) per gram of extracts. The total flavonoid content in the extracts and standards were carried out in triplicates.

Cell culture

HEPG2 (Human Hepatic Cells) cells was procured from National Centre for Cell Sciences (NCCS), Pune, India and maintained Dulbecco's modified Eagles medium, DMEM (Sigma aldrich, USA). The cell line was cultured with DMEM supplemented with 10% FBS, L-glutamine, sodium bicarbonate (Merck, Germany) and antibiotic solution containing: Penicillin (100U/ml), Streptomycin (100µg/ml), and Amphotericin B (2.5µg/ml) in 25 cm² tissue culture flask. The cultured cell lines were maintained at a temperature of 37°C in a humidified 5% CO₂ incubator (NBS Eppendorf, Germany)[20]. The viability of cells was evaluated by a direct observation of cells using an Inverted phase contrast microscope.

In vitro cytotoxicity assay

The CTC₅₀ (50% cytotoxic concentration) was evaluated by estimating mitochondrial synthesis using MTT assay.

Determination of in vitro cytotoxic activity**Cells seeding in 96 well plate**

Two days old confluent monolayer of cells were trypsinized and the cells were suspended in 10% growth medium, 100µl cell suspension (5x10³ cells/well) was seeded in 96 well tissue culture plate and incubated at a temperature of 37°C in a humidified 5% CO₂ incubator.

Preparation of compound stock

1mg of ethylacetate extract was weighed and dissolved in 1mL DMEM using a cyclomixer and the sample solution was filtered through 0.22 µm Millipore syringe filter to ensure the sterility.

Hepatotoxicity evaluation

After 24 hours the growth medium was removed, freshly prepared plant extract in DMEM were five times serially diluted by two-fold dilution (100µg, 50µg, 25µg, 12.5µg, 6.25µg in 500µl of DMEM) and each concentration of 100µl





Meera Paul et al.,

were added in triplicates to the respective wells and incubated at a temperature of 37°C in a humidified 5% CO₂ incubator. Non treated control cells were also maintained at 37°C.

Hepatotoxicity assay by direct microscopic observation

Entire plate was observed after 24 hours of treatment in an inverted phase contrast tissue culture microscope (Olympus CKX41 with Optika Pro5 CCD camera) and microscopic observation were recorded as images. Changes in the morphology of the cells (such as rounding or shrinking of cells, granulation and vacuolization in the cytoplasm of the cells) were considered as indicators of cytotoxicity.

Hepatotoxicity Assay by MTT Method

In 3 ml PBS, 15 mg of MTT (Sigma, M-5655) was reconstituted until completely dissolved and was sterilized by filter sterilization. After the incubation period of 24 hours, the sample content in wells were removed. Then 30µl of reconstituted MTT solution was added to all test and control wells. The plate was gently shaken, then incubated for 4 hours at a temperature of 37°C in a humidified 5% CO₂ incubator. After the incubation period, the supernatant was removed and added 100µl of MTT Solubilization Solution. Then the wells were mixed gently by pipetting up and down in order to solubilize the formazan crystals. The absorbance values were measured by microplate reader at a wavelength of 540 nm. The percentage growth inhibition was calculated using the following formula: % Growth inhibition = (Mean OD of normal control – Mean OD of test group/ Mean OD of Normal control) × 100. A dose-response curve was generated using % growth inhibition on Y axis and the extract concentration (µg/ml) on X-axis. The CTC₅₀ (50% cytotoxic concentration) value is calculated from dose-response curve.

Assessment of hepatoprotective activity of *Notonia grandiflora in vitro*

The hepatoprotective activity of *Notonia grandiflora* was evaluated using well maintained HEPG2 cells. Hepatotoxicity was induced by ethanol (100 mM) and silymarin was used as a standard positive control. The choice of concentrations of EANG and standard was based on the results of the MTT assay. The experimental groups were carried out in triplicate as follows:

- Group I Dimethyl sulfoxide (DMSO) control: The cells were treated with 100 µl of serum-free culture medium containing DMSO (0.3% v/v) for 24 hrs.
- Group II (toxin treatment): The cells were treated with 100 µl of serum-free culture medium containing 100mM ethanol for 24 hrs.
- Group III (silymarin treatment): The cells were treated with 100 µl of serum-free culture medium containing 100 mM ethanol with silymarin at a concentration of 6.25,12.5,25, and 50 µg/ml for 24 hrs.
- Group IV (EANG treatment): The cells were treated with 100 µl of serum-free culture medium containing 100 mM ethanol with EANG at a concentration of 6.25,12.5,25,50 and 100µg/ml for 24 hrs. Later, cell viability, and lactate dehydrogenase (LDH) leakage assays were performed for all groups according to the standard methods.

The absorbance values were measured at a wavelength of 540 nm using microplate reader. The percentage of growth inhibition was calculated using the formula:

% of viability =	$\frac{\text{Mean OD Samples} \times 100}{\text{Mean OD of control group}}$
------------------	---

Measurement of LDH activities

After attaining sufficient growth of HEPG2 cells, ethanol (40%) was added to induce toxicity and incubated for one hour. LDH release assay was performed with cell free supernatant collected from tissue culture plates induced with ethanol was exposed to different concentrations of sample (EANG) such as 6.25 µg/ml,12.5µg/ml, 25µg/ml, 50µg/ml and 100µg/ml. To this, added 2.7ml potassium phosphate buffer, 0.1ml 6mM NADH solution, and 0.1ml sodium



**Meera Paul et al.,**

pyruvate solution. The decrease of OD was measured at 340nm in a spectrophotometer, thermo stated at 250 °C. Prepared a blank solution by adding enzyme dilution buffer instead of sample. Untreated control and ethanol induced cells were also maintained [23]. Lactate dehydrogenase activity can be calculated by using the formula [23], Activity of LDH (U/ml) = $[(Abs - Ab0) \times 3 (ml) \times df] \div [6.2 \times 0.1 (ml)]$

RESULTS AND DISCUSSION

The present study revealed that the various extracts of *Notonia grandiflora* contained alkaloids, glycosides, flavonoids, phenols, saponins, steroids, tannins and reducing sugars (Table -1). Compared to all other solvent extracts, ethylacetate extract had higher number of secondary metabolites such as alkaloids, terpenoids, steroids, tannins, flavonoids, phenols, carbohydrates and glycosides with high degree of precipitation (++) .

Quantitative analysis of phytochemical substances

The highest total phenolic content (65.41±0.21mg GAE/g dry wt.) and flavonoid content (73.9±0.17mg QE/g dry wt.) was recorded in ethyl acetate extract of *Notonia grandiflora* where as the contents obtained from ethanolic extract was the least (Table-2). The flavonoidal and phenolic compounds play an important role in culminating the oxidative stress produced by reactive oxygen species and hydroxyl radicals generated in alcohol metabolism [22].

In vitro cytotoxicity assay

From the above four extracts, ethylacetate extract was selected for the determination of *in vitro* cytotoxicity and cytoprotective effect, as it contains highest phenolic and flavonoid content. The percentage cell viability with respect to the normal control (NC) cell lines (HEPG2) at different concentrations of EANG were determined (Fig.2.).The NC cells showed 100% cell viability. The ethylacetate extracts of *Notonia grandiflora* at concentration 100 µg/mL, 50 µg/mL, 25 µg/mL and 12.5 µg/mL and 6.25 µg/mL showed 77.67%, 83.18%, 89.20%, 91.56% and 95.27% cell viability, respectively. The inhibitory concentration 50% value of EANG was found to be 249.025 µg/mL (Calculated using ED50 PLUS V1.0 Software). In MTT assay, the cell viability was >75% up to a concentration of 100µg/ml. Thus, EANG showed less cytotoxic effect to hepatic cells due to the presence of phytochemicals. Therefore, these extract concentrations were selected to further evaluate the cytoprotective activity against ethanol-induced cell damage.

Morphological changes

The morphological changes observed in HEPG2 cells are shown in Fig. 3. (a– g). Cells exposed to 100 mM of ethanol reduced the normal morphology of HEPG2 cells and cell adhesion capacity in comparison with the control. Most of the cells exposed to ethanol lost their typical morphology and appeared smaller in size (Fig.3.(b)). But HEPG2 exposed to increasing concentrations of various extracts of *Notonia grandiflora* for 24 h prior to ethanol exposure significantly restore their original morphology in a concentration-dependent manner (Fig.3. (c–g)).

Cytoprotective effect of ethylacetate extract (EA) of *Notonia grandiflora* in HEPG2 cells

The exposure of HEPG2 cells to 100mM ethanol-induced significant cell death. The cell viability was almost half of control after 24 h exposure (42.58 ±0.09). Following pre-treatment of cells with various concentrations (6.25–100 µg/ml) of EANG, exposure to 100mM ethanol did not drastically affect the cell viability. The result of cell viability is depicted in Table 3. The ethylacetate extract exhibited significant protection against ethanol induced cytotoxicity and the activity was comparable with that of the standard Silymarin. The maximum protection was observed to be 75.72% at dose 12.5 µg/ml. Increase in the cell viability percentage of HEPG2 cells pretreated with extracts indicates that the cells get boosted up upon treatment with extract and does not allow oxidation to take place upon intoxication with ethanol.





Meera Paul et al.,

Effect of ethyl acetate extract (EA) of *Notonia grandiflora* on LDH leakage in EtOH-induced HEPG2 cells

The content of LDH in the supernatant exhibits the degree of cell membrane damage [24]. EtOH treatment at a concentration of 100 mM for 24 h significantly increased the leakage of LDH from the HEPG2 cells compared with untreated cells (Fig.4). Treatment with EANG at 6.25, 12.5, 25, 50 and 100 µg/mL significantly reduced the elevated level of these enzymes in ethanol treated groups indicating the hepatoprotective activity of the extract. In particular, 12.5 µg/mL of EANG treatment adjusted the LDH level to near-normal levels. The extracts protected the cell membrane integrity from EtOH-induced cell membrane damage. This result may be related to the free radical scavenging capability of EANG. The result of LDH corresponds to MTT assay data. The percentage cell viability as well as the reduction in the elevated LDH levels in ethanol treated groups was maximum with EANG at 12.5 µg/mL.

CONCLUSION

Ethanol induces production of reactive oxygen species (ROS), leading to huge oxidative stress which causes liver injury [25]. The results suggest the presence of antioxidant principles such as flavonoids and phenolic compounds present in the extract which strengthens antioxidant defense in cells and thus minimizing the chances of production of free radicals. The present study reveals the hepatoprotective activity of ethylacetate extract of *Notonia grandiflora*, by *in vitro* analysis on HEPG2 cells against ethanol induced toxicity which was proven by MTT assay and LDH leakage assay. Thus, it can be concluded that *Notonia grandiflora* may be a promising hepatoprotective agent and this activity may be due to its antioxidant activity.

REFERENCES

1. Martins Ekor. The growing use of herbal medicines: issues relating to adverse reactions and challenges in monitoring safety. *Front Pharmacol.* 2013; 4: 177.
2. Anees A. et al. Role of Natural Products in Drug Discovery Process. *IJDDR.* 2014; 6 (2): 172-204.
3. Tukappa NK et al. Cytotoxicity and hepatoprotective attributes of methanolic extract of *Rumex vesicarius* L. *Biol. Res.* 2015; 48:19.
4. Haniadka et al. Ginger Protects the Liver against the Toxic Effects of Xenobiotic Compounds: Preclinical Observations, *J Nutr Food Sci.* 2013; 3:5.
5. Pablo Muriel. Role of free radicals in liver diseases. *Hepato Int.* 2009 Dec; 3(4): 526–536.
6. Eduardo Madrigal-Santillán. Review of natural products with hepatoprotective effects. *World J Gastroenterol.* 2014; 20(40): 14787-14804.
7. Praneetha et al. *In vitro* hepatoprotective effect of *Echinochloa colona* on ethanol-induced oxidative damage in HEPG2 cells. *Asian J Pharm Clin Res.* 2017; 10: 259-261.
8. Khare C.P. *Indian Medicinal Plants: An Illustrated Dictionary*, New York. 2007.
9. Bose N.J.J, Mehalingam P. Antinociceptive and Anti-Inflammatory activities of leaf extracts of ethnomedicinal plant. *Acta Hort.* 2014; 1023:117-22.
10. Vanijajiva O et al. *Kleinia grandiflora* (Asteraceae: Senecioneae), a species and genus newly discovered in Thailand. *Phytotaxa* 2014; 159 (1): 017–022.
11. Basha M. et al. Diversity of ethnomedicinal plants used by Malayali tribals in Yelagiri hills of Eastern ghats, Tamilnadu, India. *Asian J. Plant Sci. Res.* 2013; 3(6): 29-45.
12. Ayyanar, M, Ignacimuthu S. Traditional Knowledge of Kanitribals in Kouthalai of Tirunelveli hills, Tamil Nadu, India. *J. Ethno-pharmacol.* 2005; 102: 246-255.
13. Sharma A.J, Naresh C. Pharmacognostical Studies of *Bryophyllum pinnatum* (Lam.) Kurz. *Phcog J.* 2014; 6: 20-6.
14. Ganesan K, Xu B. Ethnobotanical studies on folkloric medicinal plants in Nainamalai, Namakkal District, Tamil Nadu, India. *Trends Phytochem. Res.* 2017; 1(3): 153-68.





Meera Paul et al.,

15. Maharajan M.J, Janakiraman N. Floristic Diversity and Medicinal importance of South Vagaikulam region Tirunelveli, Tamil Nadu, South India. JMHE.2015;1:125-29.
16. Farnsworth NR. Biological and phytochemical screening of plants. Indian J Pharm Sci. 1966; 55:225-86.
17. Amita Pandey, Shalini Tripathi. Concept of standardization, extraction and pre- phytochemical screening strategies for herbal drug, J Pharmacogn Phytochem. 2014; 2 (5): 115-119.
18. Singleton V *Let al.* Analysis of total phenols and other oxidation substrates and antioxidants by means of folin-ciocalteu reagent. Methods Enzymol. 1999; 299: 152-178.
19. Jin-Yuarn Lin, Ching-Yin Tang. Determination of total phenolic and flavonoid contents in selected fruits and vegetables, as well as their stimulatory effects on mouse splenocyte proliferation. Food Chemistry. 2007; 101: 140-147.
20. Neethu Cyril *et al.* Assessment of antioxidant, antibacterial and anti-proliferative (lung cancer cell line A549) activities of green synthesized silver nanoparticles from *Derris trifoliata*. Toxicol Res (Camb). 2019; 8(2): 297-308.
21. Reena *et al.* Synthesis Characterisation and Application of Manganese Complex with Dafone and Methanol. IJRASET.2020; 8:722-733.
22. Praneetha Pet *et al.* *In vitro* and *In vivo* hepatoprotective studies on methanolic extract of aerial parts of *Ludwigiahysosopifolia* G. Don Exell. Phcog Mag.2018; 14:546-53.
23. Kanakarajan Vijayakumari Pratheeshet *et al.* Study on the Anti-Cancer Activity of *Tylophora indica* Leaf Extracts on Human Colorectal Cancer Cells. IJPPR.2014; 6(2); 355-361.
24. Xingxing Sheet *et al.* *In vitro* antioxidant and protective effects of corn peptides on ethanol-induced damage in HEPG2 cells. Food Agric Immunol.2016;27:99-110.
25. Sha Liet *et al.* The Role of Oxidative Stress and Antioxidants in Liver Diseases. Int J Mol Sci. 2015; 16(11): 26087-26124.

Table 1 Test for Phytoconstituents for different extract of *Notonia grandiflora*

Test for various secondary metabolites	n-Hexane extract	Ethylacetate extract	Ethanol extract	Aqueous extract
Test for alkaloids	±	±	+	±
Test for tannins	+	++	++	+
Test for flavonoids	++	++	+	+
Test for steroids	+	++	++	+
Test for terpenoids	+	++	++	+
Test for carbo-hydrates	±	+	++	++
Test for glycosides	±	++	+	+
Test for oils and fats	-	±	±	-
Test for saponins	±	±	+	+
Test for proteins and amino acids	-	++	++	++
Test for phenols	+	++	+	+

Where; + Positive, ++ Strong positive, ± Trace, - Negative





Meera Paul et al.,

Table 2: Quantitative analyses of phytochemical substances present in different extracts of *Notonia grandiflora*

Solvents	Total phenolics (mg GAE/g)	Total flavonoids (mg QE/g)
Hexane	25.62± 0.25	62.73±0.30
Ethyl acetate	65.41±0.21	73.9±0.17
Ethanol	11.35±0.31	34.92±0.58
Aqueous	15.61±0.15	48.3±0.51

Values are means of three analyses of the extract ± standard deviation (n=3) GAE: Gallic acid equivalent, QE: Quercetin equivalent

Table 3: *In vitro* hepatoprotective activity of EANG using HEPG2 cell lines

Groups	%Cell viability
Group I (control)	
Normal control	100.00
Group II (toxin treatment)	
100 mM ethanol	42.58 ±0.09
Group III silymarin treatment	
100 mM ethanol + silymarin (6.25 µg/ml)	65.99±0.43
100 mM ethanol + silymarin (12.5 µg/ml)	84.35±0.46
100 mM ethanol + silymarin (25 µg/ml)	95.08±1.17
100 mM ethanol + silymarin (50 µg/ml)	96.38±0.44
Group IV (EANG treatment)	
100 mM ethanol + EANG (6.25 µg/ml)	61.65±0.41
100 mM ethanol + EANG (12.5 µg/ml)	75.72±0.61
100 mM ethanol + EANG (25 µg/ml)	66.21±0.21
100 mM ethanol + EANG (50 µg/ml)	50.40±0.30
100 mM ethanol + EANG (100 µg/ml)	46.66±0.35

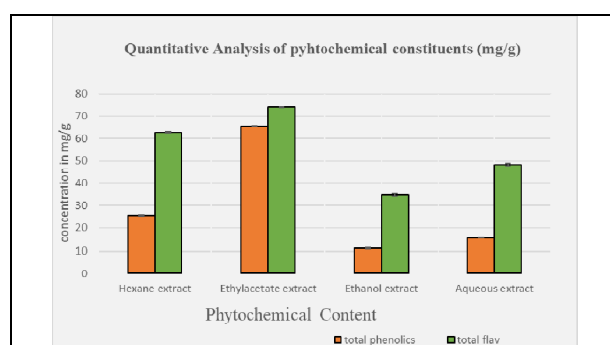


Figure 1: Total Phenolic and Flavonoid content of different extracts

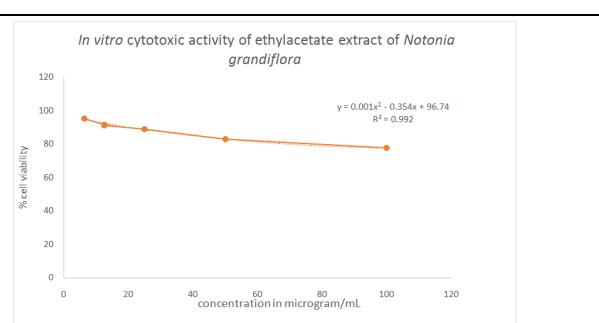


Fig. 2: *In vitro* cytotoxic activity of ethylacetate extract of *Notonia grandiflora*





Meera Paul et al.,

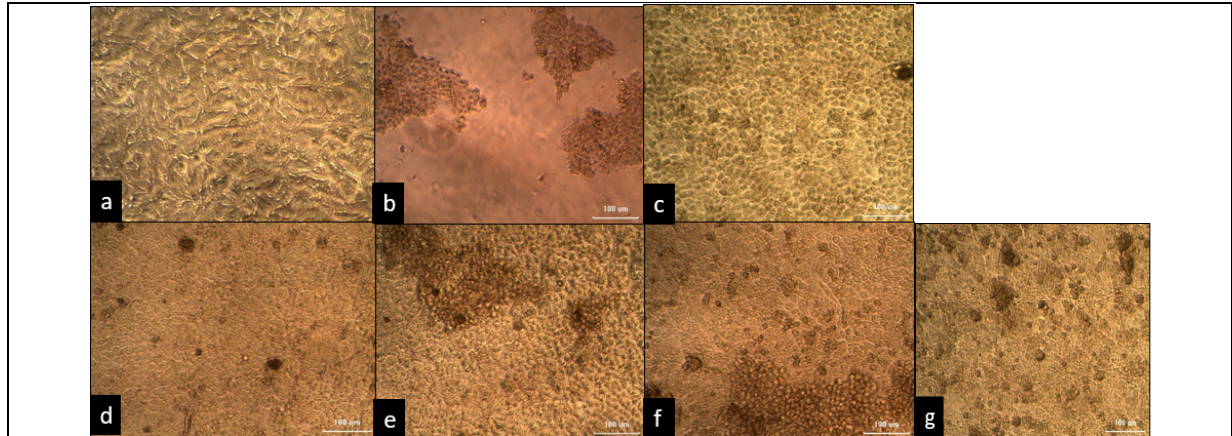


Fig.3. a: Normal control cells. The HEPG2 cells pretreated with Dulbecco's Modified Eagles Medium showing normal cells surface architecture ($\times 40$); Fig.3b: Ethanol treated. Ethanol induced toxicity to hepatic cells (HEPG2) showed detachment of cells from the surface of plate, rounding up of cells and alteration in cellular meshwork indicating cytotoxicity and necrosis ($\times 40$), Fig.3.c: Protection of HEPG2 pre-treated EANG at concentration 6.25 $\mu\text{g/mL}$, Fig.3d protection of HEPG2 pre-treated with EANG at concentration 12.5 $\mu\text{g/mL}$ Fig.3(e) protection of HEPG2 pretreated with EANG at concentration 25 $\mu\text{g/mL}$, Fig.3(f) protection of HEPG2 pretreated with EANG at concentration 50 $\mu\text{g/mL}$, Fig.3(g) protection of HEPG2 pretreated with EANG at concentration 100 $\mu\text{g/mL}$.

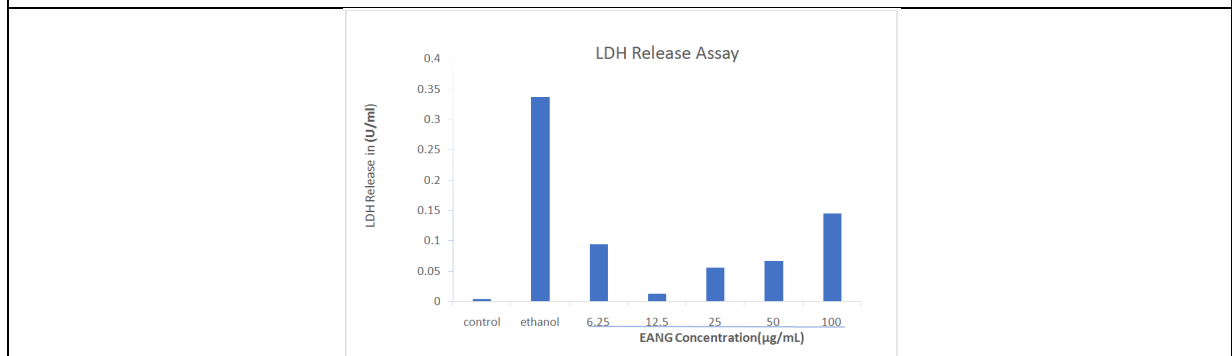


Fig.4. Effect of EANG on LDH in EtOH-induced HEPG2 cells.





Soft Template Mediated Approach towards PbS Nanoparticles and Application

Ashish Kumar Sahoo*

Centurion University of Technology and Management, Odisha, India

Received: 28 July 2020

Revised: 30 Aug 2020

Accepted: 31 Oct 2020

*Address for Correspondence

Ashish Kumar Sahoo

Centurion University of Technology and Management,
Odisha, India

Email: ashish.sahoo@cutm.ac.in



This is an Open Access Journal / article distributed under the terms of the **Creative Commons Attribution License** (CC BY-NC-ND 3.0) which permits unrestricted use, distribution, and reproduction in any medium, provided the original work is properly cited. All rights reserved.

ABSTRACT

In present work we report the single step wet chemical synthesis of PbS nanoparticles at low temperatures under reflux condition. PbS nanomaterials were synthesized via wet-chemical synthesis from lead (II) nitrate, sodium sulphide and water as a solvent where, SDS and EDTA was used as the templating agents in temperature range of 50° C, 70° C and 90° C. The as synthesized nanoparticle is characterized by powder x-ray diffraction, scanning electron microscopy, and Fourier transforms infrared spectroscopy. By basing upon the possible mechanism for the formation of the numerous nanostructures of PbS in this system is described. The as synthesized PbS nanoparticles were characterized by XRD which shows the cubic lattice phase of PbS. SEM manifests monodispersed particle with irregular phase and also shows that the particle size increased with rise in temperature. From the FT-IR analysis it is attested that there exists the presence of O-H bending, C-C, C-N and C-H stretching vibration. Lead II sulphide nanoparticles have vast application in many fields like as LEDs, telecommunications, solar absorber, photographs, detectors, optical switches, and optical amplification and are also using as the gas sensing agent in the solid-state sensors. These have several industrial applications, which include transistors, photoconductive cells, high temperature lubricants, infrared detectors.

Keywords: lead sulphide, nanomaterials, photocatalytic study, photosensitization

INTRODUCTION

Nanomaterials have build up prominence in technological advancements for their tunable physicochemical characteristics like as melting point, wettability, electrical and thermal conductivity, catalytic activity, light absorption and scattering resulting in enhanced performance over their bulk counterparts [1-4]. These materials have designed and already being used in many commercial products like as sunscreen lotion, tires, sensors, computer

28441



**Ashish Kumar Sahoo**

chips, cosmetics, sporting goods, strain resistant clothing, nanowires for junction less transistors, catalysis and they are utilized in medicines for the purpose of diagnosis, imaging and drug delivery [5]. According to Sigel, Nanomaterials are confidential as Zero dimensional spheres and clusters, one dimensional nanofiber, nanowires and nanorods, two dimensional nanofilms, nanoplates and networks, three dimensional nanostructures [6]. Recently, because of the vast application in distinct field, semiconducting materials are acquiring gigantic consideration. These are the solid crystalline substances, having electrical conductivity greater than insulators and less than the superior conductors. The resistivity of semiconductors varies in wide limits, i.e., 10^{-4} to 10^4 ohm-metre and reduced to a very pronounced extent with an increase in temperature. Its conducting possessions may be altered in encouraging ways by introducing impurities (“doping”) into the crystal structure. The most typical and extensively employed semiconductors are silicon, germanium, gallium and arsenide. However, there are countless compound semiconductors, which are composed of two or more elements, gallium arsenide (GaAs), gallium phosphide (GaP), mercury indium telluride (HgIn_2Te_4) etc. Basically, the semiconductors are classified into two types, namely intrinsic semiconductor or pure semiconductor and extrinsic semiconductor or doped semiconductor [7]. All semiconductors can be classified either as direct gap semiconductors with a valence band maximum or a conduction band minimum occurring at the same point in the Brillouin zone, or as indirect gap semiconductors in which these extreme occur at different points in the Brillouin zone [8]. The optical properties of direct gap semiconductors differ immensely from those of indirect gap semiconductors [9]. Semiconductors are employed in the manufacture of various kinds of electronic devices, including diodes, transistors, and integrated circuits. Such devices have wide application because of their compactness, reliability, power efficiency, and low cost [10]. As discrete components, they have found use in power devices, optical sensors, and light emitters, including solid state lasers. They are, and will be in the foreseeable future, the key elements for the majority of electronic systems, serving communications, signal processing, computing, and control applications in both the consumer and industrial markets [11].

There have been substantial experimental and theoretical studies of optical responses of semiconductor nanoparticles, as they have a wealth of quantum phenomena and manifest quirky size dependent materials features over the few decades [12-14]. Dispersion of semiconductor nanoparticles in an optically transparent matrix will have various application including nonlinear properties and luminescence. The electronic and optical properties of II-VI compound semiconductor nanoparticles [15]. The electronic and optical features of II-VI compound semiconductor nanoparticles have been immensely explored in view of vast variety applications. By coinage the particle size, dramatic modifications of their electronic and optical properties take place due to the three-dimensional quantum confinement of electrons and holes when the size of the particle approaches the Bohr radius of an exciton (Kukushkin et al 2011; Yadav et al 2010). Semiconductors with widely tunable energy band gap are considered to be the materials for next generation flat panel displays, photovoltaic optoelectronic devices, laser, sensors, photonic band gap devices, etc. Artificially obtained semiconductor structures with reduced dimensions present a large variety of new interesting properties in comparison to the bulk material and open new ways in the engineering of semiconductors. Further, by the dwindling of dimension to one-dimensional and quasi-zero-dimensional structures leads to large intensification of their optical features. The alteration of electronic structure, the optical and other properties, of doped semiconductor nanoparticles, is an interesting area of research. There are endeavouring not only to look over the static equilibrium possessions of the doped nanoparticles but also the charge dynamics in nanoparticles.

Among different semiconducting materials lead sulphide (PbS) is an supreme and incomparable binary semiconductor material. The size controlled PbS nanocrystals can be potentially used in preparing optical switches solid-state laser, solar cells, solar absorbers, photographs, lasers, LED devices, telecommunications, detectors, optical switches, optical amplification, electro-luminescent devices such as light emitting diodes [16,17]. Because of its direct band gap of 0.41 eV PbS nanocrystals are in interest and its exciton Bohr radius of 18nm at room temperature [18]. Therefore, when crystal sizes are smaller than the Bohr radius, such a small bandgap and a large exciton Bohr radius make it as an engrossing system for studying the effect of size confinement. PbS nanoparticles can also manifest multiple exciton generation (MEG), in which the impact of a single photon produces two or more no of excitons [17].



**Ashish Kumar Sahoo**

This phenomenon has raised the possibility of quantum dot based solar cells with photo-conversion efficiency of as much as 66% [17]. Different morphologies can play roles in properties. They include nanocrystals, nanorods, nanotubes, nanocubes, star shapes, dendrites, and flower-like crystal [10]. All can be prepared by different methods such as hydrothermal and solvothermal, vacuum deposition, electrochemical deposition, pulsed laser deposition, microwave radiation, sonochemical, photochemical, chemical bath deposition (CBD), γ -ray irradiation, successive ionic layer adsorption reaction (SILAR), and spray pyrolysis [10]. By changing the size and shape from bulk material to nanoparticles, it is possible to change the optical band gap from 0.41 eV to the values up to 5.2 eV. Therefore, it is possible to build optical sensors with adjustable features [19]. By adopting different methods the sizes of the nanoparticles have been modified. PbS nanoparticles prepared by the ionomer powder with H₂S and it furnishes a divergent way for the synthesis of PbS semiconductor nanoparticles in a polymer matrix [20]. By adopting polymer matrix as the template, one-dimensional PbS nanocrystals in the shape of nanorods has been synthesized [21]. Cheon and co-worker [22-24] together have made tetrapod and branched nanocrystals of PbS from single source predecessor X(S₂CNEt₂), where X=Pb, Cd, Mn. By employing the surfactant of C₁₂E₉ as the soft template, other groups [25] have successfully synthesized PbS nanobelts (width 50-120 nm and length ~ 3 μ m) in a reverse micelle system. The research is on the way for the synthesis and utilization of low dimensional nanostructure [26-28]. PbS nanowires with uniform diameter (30nm and 60nm) has been successfully counterfeited by electrochemical deposition with sulfuric and oxalic anodic alumina membranes [29]. PbS nanowires are incorporated in mesoporous silica [30] and also within mica channel [31]. The report has been done [30] for the template-assisted deposition of PbS nanowires with uniform diameter (~5 nm). There is also an important route for the synthesis of nanowires at low temperature and that is hydrothermal synthesis [32]. By adopting solvothermal approach, using precursors Pb(NO₃)₂, 2,2-azobisisobutyronitrile (AIBN) at 110-150 °C, closed PbS nanorods are synthesized lead sulphide (PbS) nanowires array with different shapes have been presented.

Wet chemical synthesis emerged in contrast to conventional and solid-state synthesis procedures of compounds and materials. By using precursor at proper experimental condition, this chemical synthesis deals with chemical reaction in the solution phase. For the synthesis process there are no general rules, that means each of the synthesis method are divergent from each other. 2D nanomaterials are prepared by using these synthesis strategies. Wet chemical synthesis offers a high degree of controllability and reproducibility for the fabrication of 2D nanomaterials. The foremost wet-chemical synthesis routes for 2D nanomaterials are solvothermal synthesis, template synthesis, interface-mediated synthesis, hot injection and self-assembly. The wet-chemical synthesis routes fine tuning of reaction conditions (temperature, concentration of substrate and also additive or surfactant, pH etc.) which gives the desired nanomaterial.

EXPERIMENTAL DETAILS

Chemicals used

Lead nitrate Pb(NO₃)₂, Sodium dodecyl sulphate (SDS); (NaC₁₂H₂₅SO₄), Sodium Sulphide (Na₂S), Ethylenediaminetetraacetic acid (EDTA), Hydrazine (N₂O₄), Pb(NO₃)₂, SDS and Na₂S were purchased from Aldrich company and EDTA and Hydrazine were bought from NICE company, all chemicals were used without any further purification, Distilled water is

Synthetic Method Adopted

Synthesis of PbS nanoparticles

The synthesis of PbS nanoparticle was executed by using the following procedure.

By using EDTA: In a round bottom flask 50 mL of water was taken and 5 g of EDTA (ethylenediamine tetraacetic acid) was added to it. A magnetic bead was put into the flask, then it was stirred in a magnetic stirrer. In the second step 3 Mmol (0.99 g) lead nitrate Pb (NO₃)₂ was added to the above solution and dissolved by constant stirring. After,

28443



**Ashish Kumar Sahoo**

3 Mmol sodium sulphide was added to the above solution. A dark grey colour solution was seen. After that a reflux condenser was attached to the round bottom flask. The reaction was carried out at temperature of 50 °C for about 4h with RPM 300. After completion of 4h stirring, a light grey coloured precipitation was formed, it was filtered with a Buchner funnel provided with suction pump. The precipitation was washed for several times with hot water and kept for oven dry for about 7h. The same procedure was repeated at 70 °C and 90 °C.

By using SDS

In this procedure, 30 mL of distilled water was taken in a beaker then about 3 Mmol (0.99) of lead nitrate ($\text{PbNO}_3)_2$ was added and then 5 g of EDTA was added to it. It was dissolved by constant stirring with the help of a magnetic bead. After, 20 mL of water was taken in another beaker and 10 times CMC of SDS (0.545 g) was added with a constant stirring for about 30 min. Now the solution prepared in the second step was added to the first beaker. After this 3 mM (0.243 g) of Na_2S was added to the first beaker with continuous stirring. Now the white colour solution turned into dark grey. The reaction was carried out for 4 h at temperature 50 °C with RPM 300. The same method of preparation was carried out at temperature 70 °C and 90 °C. After 4h of stirring the mixture was filtered and washed for several times with hot water and kept for oven dry for about 8 h.

Synthesis of ZnS nanoparticles

In overall synthesis purpose, the typical procedure included addition of 2 mmol of SDS (0.554 g) to 50 mL of distilled water taken in a 100 mL of round bottom flask. A magnetic bead was put into the flask and was allowed for constant stirring for 3 minutes at 200 RPM. Then to the solution 3mmol of $\text{Zn}(\text{NO}_3)_2$ (0.89 g) was added and was allowed to mix thoroughly. After 2 minutes of stirring 8 mL of acetone was added to the solution. About 3 ml of CS_2 added to the mixture and the mixture was allowed to stir thoroughly and just after few seconds of mixing 2 ml of hydrazine was added and as result white colored solution was obtained. A reflux condenser was then attached to the round bottom flask and the set up was placed on a hot plate provided with magnetic stirrer. Overall reaction process was carried out for 3 hours with temperature 50 °C with 200 RPM. Upon continuous stirring for 3 hours a white precipitation was obtained and was filtered using Buchner funnel provided with solution pump. The precipitate was washed several times followed by drying in oven for 2 hours in 60 °C. The obtained powder was then taken for further characterization. The same process was repeated under temperatures 70 °C and 90 °C respectively keeping other experimental parameters same.

The same experiment was repeated using EDTA as complexing agent as follows. In a typical procedure included addition of 2 mmol of SDS (0.554 g) to 30 ml of distilled water taken in a 100 ml of round bottom flask. A magnetic bead was put into the flask and was allowed for constant stirring for 20 minutes at 200 RPM. After 20 minutes of stirring 8 ml of acetone was added to the solution and 3 ml of CS_2 added to the mixture and the mixture was allowed to stir thoroughly. In a separate beaker an equimolar solution of $\text{Zn}(\text{NO}_3)_2$ (0.89 g) and EDTA(0.87 g) was prepared with 20 ml of distilled water. This solution was stirred another for 15 minutes. The prepared ZnS nanoparticles is triturated with some amount of PbS to study the photocatalytic effect.

RESULT AND DISCUSSION**XRD**

The structure was scrutinized with the help of an X-ray diffractometer. The scanning regions of the diffraction angle (2θ) were 20°-70° and Cu-K α radiations were used to collect the spectrum. The diffraction peaks of PbS nanoparticle were detected at 26.85°, 31.20°, 43.85°, 52.62°, 54.75°, 63.80°, 69.90°, 72.50° are ascribed to 111, 200, 220, 311, 222, 400, 331 and 420 planes respectively. The peaks are indicated to the polycrystalline nature having a cubic lattice phase. The dominant and intense peak (200) at 31.20°. Average crystalline size can be calculated from the XRD pattern using the well known Debye-Scherrer formula given in the equation,





Ashish Kumar Sahoo

$$D = K\lambda / (\beta \cos \theta)$$

Where, K is the shape factor= 0.96

β , is full width at half maxima [FWHM] of the highest peak in radian.

$\lambda = 1.5 \text{ \AA}$, θ is the angle at the top of the highest peak

The crystalline size of the products obtained from XRD is given below.

FTIR

The figure displays the FT-IR spectrum in the range 4000-600 cm^{-1} and resolution of 2 cm^{-1} PbS powder synthesized at 90° C indicating formation and vibrational characteristics. The characteristic band at 3435 cm^{-1} corresponds to the vibration mode of water (OH group) indicating the presence of small amount of water adsorbed in the sample [33]. The band at 1631 cm^{-1} is due to -OH bending of water [34]. The band at 1050 cm^{-1} , 1170 cm^{-1} and 2950 cm^{-1} is due to C-C, C-N and C-H stretching vibration, which indicates the presence of EDTA. The band at 879 cm^{-1} is attributed to the Pb-S stretching vibration [35].

Study of Morphology

The SEM analysis of the sample has been shown in figure 53. From the figure, it can be scrutinized that nanostructures with different morphology is obtained by the variation of temperatures. Based on the results, the below mechanism was postulated. EDTA and SDS were taken as templating agent also acts as a complexing agent, binds with Pb^{2+} and forms a complex [30]. In this process the release and availability of Pb^{2+} was reduced for which the reaction is slowed down favouring crystallisation and separating the growth step from the nucleation step [31-33]. So Pb^{2+} ions from Pb-EDTA and PbS-SDS complex are released slowly and react with S^{2-} ions of Na_2S . At lower temperatures (50° C and 70° C), there is slow releasing of Pb^{2+} ions from the complex which reduces the speed of reaction. Hence, the formation of PbS become slow and the growth on the nucleating centre is less, so that the size of the particle is lesser. When the reaction temperature increased to 90° C, the complex becomes unstable and nearly breaks to generate higher concentration of Pb^{2+} ions in the solution leading to faster growth of PbS nanocrystals to bigger particles. Here monodispersed particles are observed with irregular shapes. So, the observed crystalline size of PbS nanoparticles are 75, 90 and 115 nm at temperatures of 50° C, 70° C and 90° C respectively.

PHOTOCATALYTIC ACTIVITY

Determination of Dye degradation efficiency

Lead sulphide itself did not show any activity for degradation of dye, when tested for photocatalytic activity for a radiation period of 3 hour. But when it mixed with ZnS it enhances the photocatalytic activity of ZnS for a radiation period of 3 hours. The photocatalytic degradation of methyl orange (MO) was carried out in order to evaluate the photocatalytic activity of the as prepared PbS-ZnS nanoparticles. 10 mg of prepared samples was dispersed in 50 mL of an aqueous solution of MO with an initial concentration of 10 mg/L. The above mixture was first stirred for 30 minutes in the dark to ensure that the adsorption-desorption equilibrium was reach. Then, the photocatalytic degradation reaction was carried out under the irradiation of sun light. At every 10 min interval during sunlight irradiation, 3 mL of the suspension was collected and subsequently centrifuged. The degraded solution supernatants were measured using a colorimeter by using blue-green filter.

- It was observed that in the absence of any catalyst/PbS/ in dark there was no photodegradation took place even for 3 hours.
- The degradation patterns for methyl orange is as shown in figure according to which a degradation of around 70% was achieved for a time period of 180 minutes.
- However, the degradation efficiency of the sample ZnS triturated with PbS was found to be about 78% for the same time period (180 minutes), which demonstrate the photosensitizing effect of PbS for ZnS.





CONCLUSION

We have prepared the PbS nanoparticles by adopting soft template mediated approach at low temperature, then it was characterized by XRD, it shows cubic lattice phase and in SEM, monodispersed particles with irregular shapes was observed. Thereafter, when tested for photocatalytic activity for degradation of dye it did not show any activity. However, when triturated with ZnS nanoparticles, it enhances the photocatalytic activity of ZnS by 25 to 30 percent for radiation periods of 3 hour.

REFERENCES

1. A. Sanchez, S. Recillas, X. Font, E. Casals, E. Gonzalez and V. Puentes, *TrAC, Trends Anal. Chem.*, 2011, 30, 507–516.
2. J Tian, J Xu, F Zhu, T Lu, C Su, G Ouyang - *Journal of Chromatography A*, 2013
3. L. Jacak, P. Hawrylak and A Wojs, *Quantum Dots*, Springer, Berlin Heidelberg New York, 1997.
4. J. H. Davis, *Physics of Low Dimensional Structures*, Cambridge, 1998.
5. The Max Tishler Laboratory for Organic Chemistry, Department of Chemistry, Tufts University, 62 Talbot Avenue, Medford, Massachusetts 02155
6. AM Morales, CM Lieber - *Science*, 1998 - science.sciencemag.org
7. M. Brust, M. Walker, D. Bethell, D. J. Schiffrin, and R. Whyman, *J. Chem. Soc., Chem. Commun* 7, 801 (1994)
8. Weck, M.: *Werkzeugmaschinen und Fertigungssysteme 2: Konstruktion und Berechnung*. Springer, Berlin (1997)
9. P.J. Vikesland, K.R. Wigginton, Nanomaterial enabled biosensor for pathogen monitoring - A Review, *Environ. Sci. Technol.* 44(10) (2010) 3656-3669.
10. C.A. Martínez Bonilla, V.V. Kouznetso, "Green" quantum dots: Basics, green synthesis and nanotechnological applications, *Green Nanotechnology-Overview and Further Prospects*, Chapter 7, IntechOpen, 2016, pp.174-192.
11. S. Sarma, B.M. Mothudi, M.S. Dhlamini, Observed coexistence of memristive, memcapacitive and meminductive characteristics in polyvinyl alcohol/cadmium sulphide nanocomposites, *J. Mater. Sci. Mater. Electron.* 27 (2016) 4551-4558.
12. Sandro Carraraa, Davide Sacchettoa, Marie-Agnès Doucey, Camilla Baj-Rossi Giovanni De Micheli, Yusuf Leblebici, Memristve-biosensor: A new detection method by using nanofabricated memristors, *Sens. Actuator B* 171-172 (2012) 449-457.
13. B. Das, J. Devi, P. Kalita, P. Datta, Memristive, memcapacitive and meminductive behavior of single and co-doped cadmium selenide nanocomposites under different doping environment, *J. Mater. Sci. Mater Electron.* 29 (2017) 546-557.
14. B. Ibarlucea, T.F. Akbar, K. Kim, T. Rim, Chang-Ki Baek, Ultrasensitive detection of Ebola matrix protein in a memristor mode, *Jour. Nano Res.* 11(2) (2018) 1057-1068.
15. A. Shivashankarappa, Study on biological synthesis of cadmium sulphide nanoparticles by *Bacillus licheniformis* and its antimicrobial properties against food
16. Introduced on graphene by oxygen gas". *Journal of American Chemical Society*.
17. Eftekhari, A.; Jafarkhani, P. (2013). "Curly Graphene with Specious Interlayers Displaying
18. Superior Capacity for Hydrogen Storage". *Journal of Physical Chemistry*.
19. M.A. Walling, J.A. Novak, J.R.E. Shepard, Quantum dots for live cell and in vivo imaging, *Int. J. Mol. Sci.* 10 (2009) 441-491.
20. Yamada, Y.; Yasuda, H.; Murota, K.; Nakamura, M.; Sodesawa, T.; Sato, S. (2013). "Analysis
21. of heat-treated graphite oxide by X-ray photoelectron spectroscopy". *Journal of Material*
22. A.H. Souici, N. Keghouche, J.A. Delaire, H. Remita, A. Etcheberry, M. Mostafavi Structural and optical properties of PbS Nanoparticles synthesized by the radiolytic method, *J. Phys. Chem. C* 113 (2009) 8050–8057.





Ashish Kumar Sahoo

23. Chemical Sciences Division and Computer Science and Mathematics Division and 3Center for
24. Nanophase Materials Sciences, Oak Ridge National Laboratory, Oak Ridge, Tennessee
25. 37831Jiang et al., Journal of Chemical Physics.
26. C. Kittel, *Solid State Physics*, Hoboken, NJ: John Wiley and Sons, Inc., 1996.
27. R. Saito, G. Dresselhaus, and M. S. Dresselhaus, *Physical Properties of Carbon Nanotubes*,
28. Nature Nanotechnology 7,562–566 (2012) doi:10.1038/nnano.2012.118.
29. Nehru L C, Swaminathan V and Sanjeeviraja C 2012 *American.J.Mat.Sci.* 2(2) 6
30. A. Alyamani, , & O. M Lemine,. (2012). FE-SEM characterization of some nanomaterial. In V.
31. Scientific Reports ISSN (online): 2045-2322 Scientific Report 2,Article number: 613 (30 august 2012)doi:10.1038/srep00613
32. Nature Nanotechnology 7,562–566 (2012) doi:10.1038/nnano.2012.118.
33. Sharma K, Sharma R and Das H L 2008 *Chalcogenide letter* 5 153
34. Nehru L C, Swaminathan V and Sanjeeviraja C 2012 *American.J.Mat.Sci.* 2(2) 6
35. V. F. Nesterenko, *Dynamics of Heterogeneous Materials* (Springer, 2001).

Table 1. The crystalline size of the products obtained from XRD

Sl.No.	Temperatures	Size of crystalline
01	50° C	35 nm
02	70° C	42 nm
03	90° C	62 nm

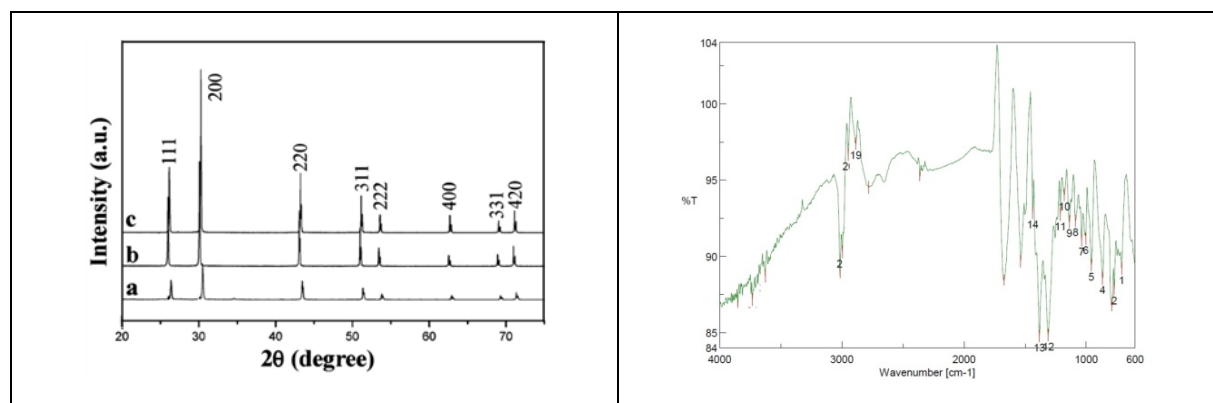


Figure 1. XRD patterns of the sample synthesized in presence of EDTA at (a) 50 °C, (b) 70 °C and (c) 90 °C

Figure 2. FTIR of thus synthesized sample of PbS at 90 °C

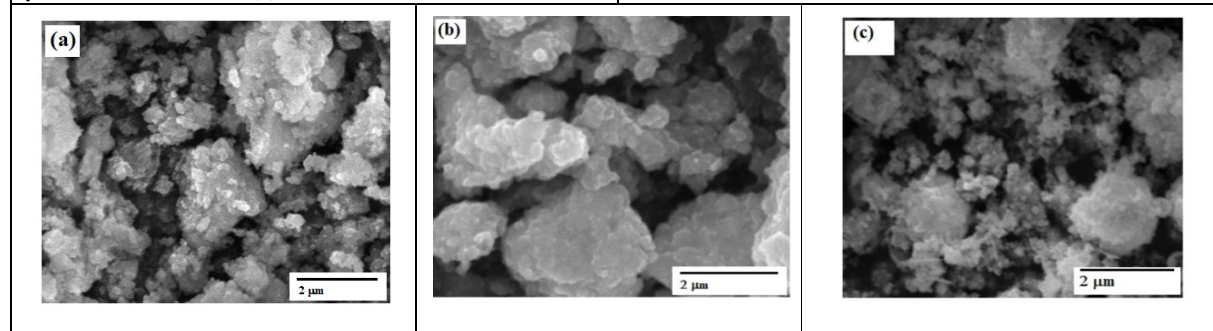


Figure 3. SEM images of PbS synthesized under reflux condition at (a) 50 °C (b) 70 °C and (c) 90 °C





Ashish Kumar Sahoo

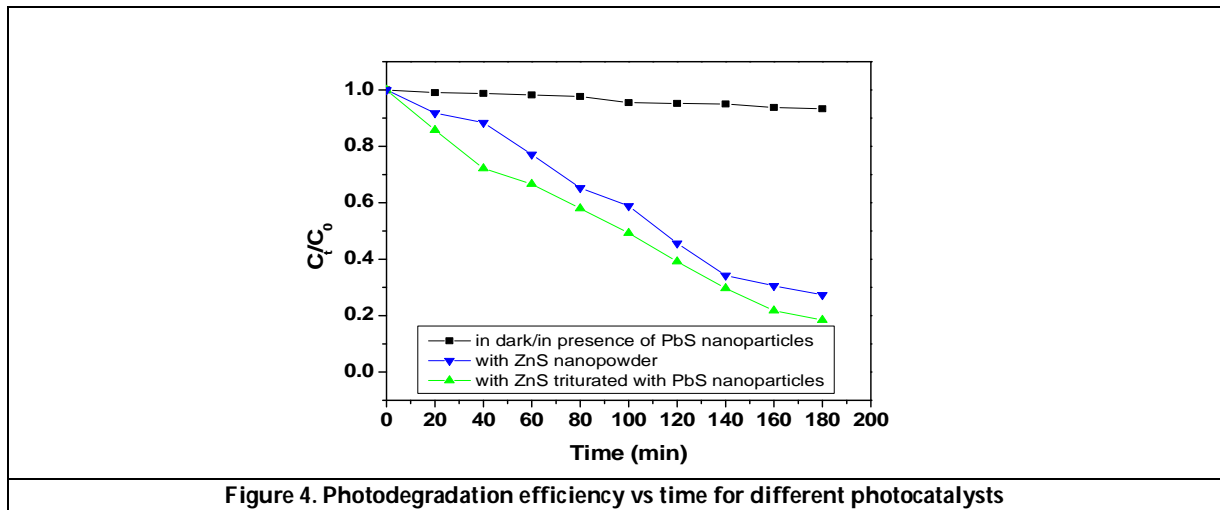


Figure 4. Photodegradation efficiency vs time for different photocatalysts





Phytochemical Evaluation and Antioxidant Activity of Selected Medicinal Plant *Terminalia bellerica*

P. Venkatachalam^{1*} and C.V Chittibabu²

¹Ph.D Research Scholar, Department of Plant Biology and Plant Biotechnology, Presidency College (Autonomous), Chennai, Tamil Nadu, India.

²Associate Professor, Department of Plant Biology and Plant Biotechnology, Presidency College (Autonomous), Chennai, Tamil Nadu, India.

Received: 14 Sep 2020

Revised: 16 Oct 2020

Accepted: 18 Nov 2020

*Address for Correspondence

P. Venkatachalam

Ph.D Research Scholar, Department of Plant Biology and Plant Biotechnology,
Presidency College (Autonomous),
Chennai, Tamil Nadu, India.
Email: Pvchalam55@gmail.com



This is an Open Access Journal / article distributed under the terms of the **Creative Commons Attribution License** (CC BY-NC-ND 3.0) which permits unrestricted use, distribution, and reproduction in any medium, provided the original work is properly cited. All rights reserved.

ABSTRACT

The present study was analyzing the phytochemical profile and antioxidant activity of *Terminalia bellerica*. The leaves powder was successively extracted with various solvents namely, ethanol, chloroform, acetone, ethyl acetate and benzene phytochemical analysis clearly showed in the presence of flavonoids, tannin triterpenoids, saponins, sterols, alkaloids and carbohydrates. After preliminary screening the plant materials high levels phytochemical compound present in the methanolic *Terminalia bellerica* leaf extract. Very important aspect all plants have antioxidant activates that antioxidant activity diseases curable compound hence our study focused the methanolic extract by standard qualitative analysis and the *invitro* antioxidant activity was evaluated by standard methods determination of total antioxidant capacity 1.1-diphenyl-2-picrylhydrazyl (DPPH) radical scavenging activity Antioxidant activity Nitric oxide potential. The analyses revealed that the methanol extract of *Terminalia bellerica* was able to efficiently scavenge the free radicals in a dose dependant manner. The results were compared with the standard antioxidant ascorbic acid. Thus, further research may be warranted to study active compounds of *Terminalia bellerica* that confer the antioxidant activity. The findings presented here might have implications in the population disease prevention and medicinal research field.

Keywords: *Terminalia bellerica*, Antioxidant activity, *Invitro*, Phytochemical.



**Venkatachalam and Chittibabu****INTRODUCTION**

Plants produce wide scope of bioactive compound and to establish a rich wellspring of methods. The old Ayurvedic, Unani and Siddha frameworks of medication depend on the mending capacity of plants. In various locales of the world, plant determined restorative frameworks stay significant in the treatment of different infections. Man has since quite a while plants as a wellspring of promptly accessible and inventive medications (Day C, 1990). It is assessed that at some rate 75% of the total population depends significantly on plant drugs materials (Weragoda, 1980). Plants have been a significant source of medicine with characteristics for a enormous many years. Plants are utilized therapeutically in various nations, and they are the source of numerous strong and incredible medications. mainly on normal cures, for example, spices for their set of experiences, they have been utilized mainstream people medication (Adikha *et al.*, 2014). The *Terminalia bellerica* Roxb. (Combretaceae) is one of the elements of ayurvedic laxative medicament of 'Triphala' accessible in the Indian market for the treatment of Dyspepsia, looseness of the bowels, and diarrhea, aggravation of the small digestive system billiousness, tooting, liver infection and disease (Sharma *et al.*, 2005). Artificially, the presence of β -sitosterol, gallic corrosive, ellagic corrosive, galactose, ethyl gallate, chebulagic corrosive, mannitol, glucose, galactose, fructose and rhamnose in the product of *Terminalia bellerica* have likewise been accounted for (Row and Murty, 1970). It is uncontrollably circulated all through the world particularly Indian subcontinent, Sri Lanka, Pakistan, Nepal and South East Asia. *T. bellerica* is utilized in customary medication because of the wide range of pharmacological exercises related with the naturally dynamic optional metabolites present in this plant. Assortment of phytochemicals is separated from different pieces of the plant which incorporate alkaloid, coumarin, flavones, steroids, lignans, tannins, glycosides, terpenoid, saponin and so forth (Abraham *et al.*, 2014). Medicines pointed toward upgrading b-cell capacity and diminishing insulin obstruction is key role to improving metabolic control and impeding the improvement of diabetic confusions. Fluid concentrates of the bark or products of *T. bellerica* have additionally been utilized for an assortment of afflictions in people, including the runs, leucoderma, feebleness, bronchitis, cold, cholera, respiratory plot contaminations, pallor, hemorrhoids, eye diseases, as a cerebrum tonic and as a diuretic to eliminate kidney stones (Chopra *et al.*, 1956; Sharma *et al.*, 2001). Ayurvedic cure is generally drilled in India with an expected 85 % of Indians actually utilizing rough plant arrangements for the treatment of a wide assortment of sicknesses and illnesses (Kamboj, 2000). A large number of the professionally prescribed medications presently advanced for a wide assortment of afflictions were initially confined from plants or potentially are semi-manufactured analogs of plant inferred synthetic substances. It has been assessed that around 25 % of all physician endorsed medicates right now being used are of plant starting point (Walsh, 2003; Newman and Cragg, 2007). Moreover, roughly 75% of new anticancer medications utilized somewhere in the range of 1981 and 2006 were gotten from plant mixes (Newman and Cragg, 2007).

Lately, in vitro approaches have been utilized as an effective apparatus for micropropagation of trees and it demonstrated that tissue culture innovation is reasonable for enormous scope spread of trees in brief timeframe (Pena and Seguin, 2001). Nonetheless, in vitro hard-headedness, culture pollution, slow development reaction and phenolic exudation have made a snag for laborers managing woody trees (Rai *et al.*, 2010). Nonetheless, seeds have low suitability and because of hard seedcoat show helpless germination. It is a tall deciduous tree found all through enormous pieces of India, besides in dry locales. It likewise happens in Nepal, Sri Lanka, Southeast Asia, and Malaysia. Aside from filling in as nourishment for silkworms, this plant has a few drug esteems. Furthermore, the natural product skin (pericarp) of *T. bellerica* comprises the ayurvedic drug 'vibhitaki'. Business misuse of this plant is hampered by the deficiency of prevalent plants, essentially because of the troubles experienced in proliferating this species utilizing the customary technique for uniting and the helpless establishing capacity of vegetative cuttings. Home grown meds have gotten a lot of consideration as wellsprings of lead mixes since they are considered as tried and true and moderately ok for both human use and climate neighborly (Fazly-Bazzaz *et al.*, 2005). They are likewise modest, effectively accessible and reasonable. Regular items, either as unadulterated mixes or as normalized plant removes, give limitless occasions to new medication drives in view of the unequalled accessibility of compound variety. Plants produce wide cluster of bioactive standards and comprise a rich wellspring of meds. Natural





Venkatachalam and Chittibabu

medications are set up from an assortment of plant materials as leaves, stems, roots, bark and so forth they for the most part contain organically dynamic fixings and are utilized basically for treating mellow or constant infirmities. In India 45,000 plant species have been recognized and out of which 15-20 thousand plants are of acceptable restorative worth. As per World Health Organization (WHO) gauges, over 80% of the individuals in agricultural nations rely upon the customary medication for their essential wellbeing needs. It is commonly assessed that more than 6000 conventional plants in India are being used society and natural medication, speaking to about 75% of the therapeutic requirements of the Third World nations (Kumudhavalli *et al.*, 2010). These days numerous medication opposition has created because of the aimless utilization of business antimicrobial medications generally utilized in the treatment of irresistible illnesses. Furthermore, issues are here and there related with unfavorable consequences for the host including excessive touchiness, insusceptible concealment and hypersensitive response; this circumstance constrained researchers to look for new antimicrobial substances. There is an expansion in the quantity of irresistible illnesses, incorporating bacterial diseases with different degrees of medication obstruction. Right around 50,000 individuals are kicking the bucket worldwide consistently in view of irresistible sicknesses. The proceeded with advancement of irresistible sicknesses and the improvement of obstruction by microorganisms to existing drugs have prompted the heightening of the quest for new novel leads, against contagious, parasitic, bacterial, and viral diseases (Gibbons, 2004).

MATERIALS AND METHODS

Collection and identification of plant materials

The leaf of a healthy plant *Terminalia bellerica* was collected from local areas of near to Kalvarayan Hills, Arasampattu, Tamil Nadu, India then plant dried and powder prepared at Department of Plant Biology and Plant Biotechnology, Presidency College (Autonomous) Chennai-600005, Tamil Nadu, India.

Preparation of plant extracts

These leaves were washed with distilled water to eliminate the adhering dust particles. They were dried in the shaded place. The dried leaf were powdered, weighed and stored in clean containers (Tamizhazhagan *et al.*, 2017). Five gram of dried plant powder was extracted for 4-5 hrs of (150ml) polar, non polar and dipolar solvent (ethanol, methanol, acetone, ether, chloroform etc.) By hot continuous per location method in a Soxhlet apparatus. After the effective extraction, solvent were concentrated using a rotary flash evaporator and water was removed by evaporated to dryness on a hot water bath to yield a soxhlet crude extract.

Photochemical analysis

The phytochemical analysis of the plant was carried out by standard methods provided by Odebiyi and Ramstard, 1978 and Waterman (1993). Test for tannins, Test for saponins (frothing test), Test for Flavonoids, Salkowski's for test steroids, Fehling's test for glycosides, Test for alkaloids. Were analysed methonolic extract (Tamizhazhagan *et al.*, 2017).

Antioxidant assay

The antioxidant activity of the plant extracts was tested using two methods, ferric thiocyanate FTC and thiobarbituric acid TBA methods. The FTC method was used to measure the amount of peroxide at the beginning of the lipid peroxidation in which peroxide reacts with ferrous chloride and form ferric ion. The ferric ion then combines with ammonium thiocyanate and produce ferric thiocyanate. The substance is red in colour. The thicker the colour was the higher the absorbance (Ramrajan *et al.*, 2017). Whereas the TBA methods measure free radicals present after peroxide oxidation (Tamizhazhagan *et al.*, 2017a).



**Venkatachalam and Chittibabu****DPPH radical scavenging activity**

The free radical scavenging activity by different plant extracts was done according to the method reported by (Gyamfi *et al.*, 2002) 3cv. 50µL of the plant extract in methanol yielding 100µg/ml respectively in each reaction was added with 1ml of 0.1mM DPPH in methanol solution and 450 µl of 50 mM Tris - HCl buffer (pH 7.4). Methanol (50µl) only was used as control of experiment. After 30 min of incubation at room temperature the reduction of the DPPH free radical was measured reading the absorbance at 517 nm. L - Ascorbic acid and BHT are used as controls. The percent inhibition was calculated from the following equation % Inhibition = (Absorbance of control – Absorbance of test sample / Absorbance of control) 100 (Tamizhazhagan *et al.*, 2017a).

In vitro nitric oxide radical (NO) Scavenging assay

Nitric Oxide created from sodium nitroprusside SNP was estimated by the technique for (Marocci *et al.*, 1994). Quickly the response blend 5.0 ml containing SNP 5 mM in phosphate cradled saline (pH 7.3) with or without the plant remove at various fixations was hatched at 25°C for 180 min before noticeable polychromatic light source 25W tungsten light. The nitric oxide revolutionary in this way created interfaced with oxygen to deliver the nitrite particle which was examined at 30 min stretches by blending 1.0 ml of the brooding combination with an equivalent measure of Griess reagent (1% sulfanilamide in 5% phosphoric corrosive and 0.1% Naphthylethylene Diamine Dihydrochloride). The absorbance of the chromophore (purple azo color) framed during the diazotisation of nitrite particles with sulphanilamide and resulting coupling with Naphthylethylene Diamine Dihydrochloride was estimated at 546 nm. The nitrite generated in the presence or absence of the plant extract was estimated using a standard curve based on sodium nitrite solutions of known concentrations. Each experiment was carried out at least three times and the data presented as an average of three independent determinations (Tamizhazhagan *et al.*, 2017a).

RESULTS AND DISCUSSION

The phytochemical evaluation is best methods of qualitative analysis (Figure.1) of secondary metabolites. The secondary metabolites structure Alkaloid present in the ethyl acetate extracts, flavonoid are present in the metabolic extract and ethyl acetate solvents and also indicate benzene solvent presence in smaller amount. Terpenoids trace amount present in metabolic extract and also phenol compound all solvent present in the plant extracts it may regulate the forging substance. Results show on (Table 1). The protein presence of methanol and ethyl acetate solvents the phytosteroids present the same. The identifying of secondary metabolites has various examinations much potential of methanolic extracts compared to others. Hence this attempt has clearly monitored various test methanolic extracts high-quality active compound them. There are numerous reports that diverse plant parts, for example, bark, leaves, strip, seed, stem, may conceivably have antimicrobial property (Ahmad *et al.*, 2011, Ekundyo *et al.*, 2011, Chandra *et al.*, 2012). The majority of the restorative and sweet-smelling plants and substances are rich sources in antibacterial mixes which can be a choice to battle bacterial illnesses. The Combretaceae is a huge group of plants, the most generally happening genera of which are Combretum and Terminalia (Hutchings *et al.*, 1996), both broadly utilized in conventional medication. The sort Terminalia is broadly conveyed and is known as a rich wellspring of optional metabolites (Mahato *et al.*, (1992); Garcez *et al.*, (2003); Cao *et al.*, (2010) and flavonones and chalcones (Garcez *et al.*, (2006).

The total antioxidant level was highly presented in the *Terminalia bellerica* plants extracts compared with other standard solutions fractions were analyzed three have good activity against standard BHT (Figure 2). The DPPH free extreme compound has been generally used to test the free revolutionary searching capacity of different food tests; the cancer prevention agent present kills the DPPH by the exchange of an electron or hydrogen molecule. The decrease limit of DPPH could be controlled by shading changes from purple to yellow by perusing at 517 nm (Figure 3). The methanolic concentrate of *Terminalia bellerica* showed H-benefactor movement in our investigation. The DPPH revolutionary rummaging action of removed material was recognized and contrasted and standard cancer prevention agent - Vitamin C. The concentrate of *Terminalia bellerica* tried against DPPH stable revolutionaries



**Venkatachalam and Chittibabu**

spectrophotometrically which uncovers that the extremist rummaging movement of *Terminalia bellerica* methanol remove had fantastic cell reinforcement limit by expanded with the expanding convergence of the concentrate (Figure 2). The methanolic concentrate of *Terminalia bellerica* viably diminished the age of nitric oxide from sodium nitroprusside. *Terminalia bellerica* methanol separate demonstrated nitric oxide rummaging action at the centralization of 10 µg/ml while the standard nutrient C was indicated 50 µg/ml (Figure 4). At a convergence of 100 µg/ml of methanol extricate, the level of hindrance was discovered to be 78%. In any case, the rummaging action of ascorbic corrosive at a similar fixation was 85.02%. The methanol concentrate of *Terminalia bellerica* was found at the centralization of 50 µg/ml. Searching of Nitric Oxide revolutionary depends on the age of nitric oxide from sodium nitroprusside in cradled saline, which responds with oxygen to deliver nitrite particles that can be estimated by utilizing Griess reagent. The absorbance of the chromophore was measured at 546 nm in the presence of the extract. *Terminalia bellerica* extract proved to decrease in amount of nitrite generated from the decomposition of sodium nitroprusside in vitro.

Methanol extract recorded maximum percentage of NO activity of 84.11% at the concentration 50 µg/ml. The macrophage-interceded inflammatory reaction assumes a critical part in the movement of atherosclerosis. In atherosclerotic sores, macrophages discharge favorable to inflammatory cytokines, receptive oxygen species (ROS), and grid metalloproteinases (MMPs) (Libby, 2002; Galis *et al.*, 1994). ROS overproduction is related with the creation of numerous inflammatory go between and a scope of inflammation-related illnesses (Mittal *et al.*, 2014). Glucosides, tannins, galliacid, ellagic corrosive, ethyl gallate, gallylglucose, chebulanic corrosive are accepted to be for the most part answerable for its wide helpful activities. It is utilized as cell reinforcement, antimicrobial, antidiarrheal, anticancer, antidiabetic, antihypertensive and hepatoprotective specialist (Saraswathi *et al.*, 2012). The key dynamic specialists in such nanoparticles union were estimated to be polyphenols, flavonoids, diminishing sugars, sterols, fundamental oils, starch, cellulose, gelatins, gums, pitches, lectins, and so forth these biomaterials go about as decreasing specialists just as covering specialists in the blend of silver nanoparticles (Gangula *et al.*, 2011). In traditional Indian Ayurvedic medicine, *T. bellirica* fruit is used in the popular Indian herbal rasayana treatment triphala. *T. bellirica* is used to protect the liver, reduce high cholesterol, and treat digestive as well as respiratory disorders (Latha and Daisy 2011). Plants produce wide array of bioactive principles and constitute a rich source of medicines (Badrul Alam, 2011). *Terminalia bellirica* is a deciduous tree that is common in Southeast Asia. In traditional Indian Ayurvedic medicine, the fruit of *Terminalia bellirica* is extensively used as a folk medicine for the treatments of diabetes, hypertension, and rheumatism (Modak *et al.*, 2007).

CONCLUSION

The qualitative analysis of secondary metabolites characterization and isolation of the bio active chemical components possessed by these traditional medicinal plants. In addition to those pharmaceutical properties of *Terminalia bellirica* reported in the literature this research showed that leaves of this plant may possess considerable antioxidant activities compared to the rest of the medicinal plants as well as BHA and ascorbic acid (as positive controls). Thus, further research may be warranted to study active compounds of *Terminalia bellirica* that confer the antioxidant activity. The findings presented here might have implications in the population disease prevention field. The present study leads to the further research in the way of isolation and identification of the activity compound from the selected plants using chromatographic and spectroscopic techniques, and also a method developed researcher and pharmaceutical to help new drug synthesis and develops.

ACKNOWLEDGMENT

The authors express sincere thanks to the head of the Department of Plant Biology and Plant Biotechnology, Presidency College (Autonomous) Chennai-600005, Tamil Nadu, India for the facilities provided to carry out this research work.





Venkatachalam and Chittibabu

REFERENCES

- Day C (1990) Hypoglycaemic compounds from plants. In New Anti-Diabetic Drugs, pp. 267–278 [CJ Bailey and PR Flatt, editors]. London: Smith-Gordon.
- Weragoda PB (1980) Some questions about the future of traditional medicine in developing countries. J Ethnopharmacol 2, 193–194.
- Adlkha, M., Bhargava, A., Kapoor, R., Sharma, L. N., & Singh, C. (2014). Ayurvedic medicinal plant *Shorea robusta* (shala). Innovare Journal of Ayurvedic Sciences, 2(4), 18-21.
- Row, J. R., & Murty, P. S. (1970). Chemical examination of *Terminalia bellirica* Roxb. Indian Journal of Chemistry, 8, 1047-1048.
- Abraham, A., Mathew, L. and Samuel, S. (2014). Pharmacognostic studies of the fruits of *Terminalia bellirica* (Gaertn.) Roxb. J Pharm Phytochem. 3:45-52.
- Chopra R, Nayar S & Chopra I (1956). Glossary of Indian Medicinal Plants, pp. 241–242. New Delhi: Council of Scientific and Industrial Research.
- Sharma HK, Chhange L & Dolui AK (2001) Traditional medicinal plants in Mizoram, India. Fitoterapia 72, 146–161.
- Kamboj, V.P. (2000). Herbal medicine. Current Science. 78:35-39.
- Walsh, G. (2003). Biopharmaceuticals: Biochemistry and Biotechnology, 3rd edition. Wiley, Chinchester.
- Newman, D.J. and Cragg, G.M. (2007). Natural products as sources of new drugs over the last 25 years. J Nat Prod.70:461-477.
- Pena L, Seguin A (2001) Recent advances in the genetic transformation of trees. Trends Biotechnol 19:500–506
- Rai MK, Asthana P, Jaiswal VS, Jaiswal U (2010) Biotechnological advances in guava (*Psidium guajava* L.): recent developments and prospects for further research. Trees Struct Funct 24:1–12
- Fazly-Bazzaz, Karamadin MK and Shokoheizadeh HR (2005). In vitro antibacterial activity of Rheum ribes extract obtained from various plant parts against clinical isolates of Gram negative pathogens. Iranian J Pharm, 2:87-91.
- Kumudhavalli MV, Vyas M and Jaykar B (2010). Phytochemical and pharmacological evaluation of the plant fruit of *Terminalia bellirica* Roxb. Int J Pharm Life Sci ,1: 1-11.
- Gibbons S. (2004). Anti-staphylococcal plant natural products. Nat Prod Rep 21: 263-277.
- Tamizhazhagan, V. Pugazhendy K, Sakthidasan V, Jayanthi C (2017). "Preliminary screening of phytochemical evaluation selected plant of *Pisonia alba*." International Journal of Biological Research 2.4, 63-66.
- Odebiyi EO, Ramstard AH, (1978). Investigation photochemical screening and antimicrobial screening of extracts of *Tetracarpidium conophorum* J Chem Soc. Nig, 26:1
- Waterman PG (1993). Methods in plant Biochemistry, 8(2).
- Gyamfi, M.A., Yonamine, M. and Aniya Y., 2002. Free radical scavenging action of medicinal herbs from Ghana *Thonningia sanguine* on experimentally induced liver injuries. Gen. Pharmacol., 32, 661-667.
- Marcocci, L., Maguire, J.J., Droy-Lefaix, M.T., Packer, L., 1994. The nitric oxide scavenging properties of *Ginkgo biloba* extract EGb761. Biochem. Biophys. Res. Commun., 201, 748-755.
- Libby, P(2002). Inflammation in atherosclerosis. Nature, 420, 868–874.
- Galis, Z.S.; Sukhova, G.K.; Lark, M.W.; Libby, P (1994). Increased expression of matrix metalloproteinases and matrix degrading activity in vulnerable regions of human atherosclerotic plaques. J.Clin. Investig. 94, 2493–2503.
- Mittal, M.; Siddiqui, M.R.; Tran, K.; Reddy, S.P.; Malik, A.B (2014). Reactive oxygen species in inflammation and tissue injury. Antioxid. Redox Signal, 20, 1126–1167.
- Saraswathi M N, Karthikeyan M, Kannan M and Rajasekar S (2012). *Terminalia bellirica* Roxb.-A phytopharmacological review, Int J Pharm Biomed Res, 3(1), 96-99.
- Tamizhazhagan, V. Pugazhendy K, Sakthidasan V, Jayanthi C (2017a). Antioxidant properties of *Pisonia alba* plant leaf extract. International Journal of Zoology and Applied Biosciences, 2(6), 311-314.
- Gangula A, Podila R, Ramkrishna M, Karanam L, Janardhana C, Rao AM (2011) Catalytic reduction of 4-nitrophenol using biogenic gold and silver nanoparticles derived from *Breynia rhamnoides*. Langmuir 27:15268–15274.





Venkatachalam and Chittibabu

27. Latha R, Daisy P (2011). Insulin-secretagogue, antihyperlipidemic and other protective effects of gallic acid isolated from *Terminalia bellirica* Roxb. In streptozotocin-induced diabetic rats. Chem Biol Interact 189:112–118.
28. Ramrajan K., Ramakrishnan N, Tamizhazhagan V and Bhuvanewari M (2017). *In vitro* screening and characterization of biosurfactant from marine *streptomyces* sp. European Journal of Pharmaceutical and Medical Research, 4(1), 531-534.
29. Badrul Alam (2011). Antioxidant, Antimicrobial and Toxicity studies of the Different Fractions of Fruits of *Terminalia bellirica* Roxb. Global Journal of Pharmacology. 5(1):07-17.
30. Modak, M, Dixit, P, Londhe, J, Ghaskadbi, S, Devasagayam, T.P. (2007). Indian herbs and herbal drugs used for the treatment of diabetes. J. Clin. Biochem. Nutr, 40, 163–173.

Table 1. Phytochemical screening of plant extract of *Terminalia bellerica*

S.No	Phyto constituents	Methanol	Ethyl acetate	Acetone	Benzene
1	Alkaloids	N	p	p	N
2	Flavonoids	p	pp	p	p
3	Saponins	pp	N	N	N
4	Steroids	p	p	N	N
5	Tannins	p	N	p	N
6	Terpenoids	p	N	N	N
7	Tri-terpenoids	p	N	pp	p

"p" indicate presence "pp" strongly presence "N" absence.

<p>Figure 1. Preliminary screening of <i>Terminalia bellerica</i> plant extract</p>	<p>Figure 2. <i>Terminalia bellerica</i> methanolic plant extracts shows total antioxidant activity.</p>
<p>Figure 3. <i>Terminalia bellerica</i> methanolic plant extracts shows DPPH Scavenging activity.</p>	<p>Figure 4. <i>Terminalia bellerica</i> methanolic plant extracts shows Nitric Oxide Radical Scavenging Activity.</p>





RESEARCH ARTICLE

Performance Analysis of Variable Compression Ratio Diesel Engine using Kusum Biodiesel

Manas Ranjan Padhi*

Centurion University of Technology and Management, Odisha, India.

Received: 07 Sep 2020

Revised: 09 Oct 2020

Accepted: 11 Nov 2020

*Address for Correspondence

Manas Ranjan Padhi

Centurion University of Technology and Management,
Odisha, India.

Email: manas.padhi@cutm.ac.in



This is an Open Access Journal / article distributed under the terms of the **Creative Commons Attribution License** (CC BY-NC-ND 3.0) which permits unrestricted use, distribution, and reproduction in any medium, provided the original work is properly cited. All rights reserved.

ABSTRACT

The alternate energy sources are required to fulfil for the future prosperity. Among different alternative fuels, biodiesel is regarded as a key source as a substitution fuel for internal combustion engine which has similar properties with diesel. India has a great scope for the production of biodiesel from nonedible oil seeds due to abundance of vegetable plants. Raw vegetable oils can be used directly or blended with diesel to run diesel engines. However the engine modification is a challenge for its usability aspect. In the present work, attempt has been made to prepare biodiesel from Kusum oil and run a variable compression ratio diesel engine without any engine modification. The performance results obtained are within acceptable limits.

Keywords: Diesel engine, Performance, Transesterification, Biodiesel, Blends

INTRODUCTION

Biodiesel can be produced both edible and non-edible seed like sunflower, rapeseed, palm, rubber seed etc. many vegetable oil are edible in nature, continuous use of this oil causes lack of food supply. With the increase in consumption rate, it has been seen that the total consumption of fossil fuels globally is 10million tons per day. These fuels are present in limited quantity and there is a possibility of an energy supply collapse in near future. Again the use of these fuels causes environmental problems as it emits harmful gases. Hence it is very necessary to find an alternative source for fossil fuel which can be obtained from biomass (from plant and animal fats). Now a day to overcome all these problems biodiesel become one of the most interesting alternatives because biodiesel are biodegradable, non-polluting and has very similar physical properties with biodiesel. Biodiesel can be produce from nonedible oils. The use of edible oil to produce biodiesel in India is not feasible because of their high cost and India is deficient in edible oils [1]. From the economy point of view nonedible oils can be used as best source for biodiesel production. The nonedible oils such as mahua, jatropa, karanja, castor, neem etc are generally used to produce

28456



**Manas Ranjan Padhi**

biodiesel as these oils are easily found and has low cost. Kusum is indigenous plant in India and can easily found in all over India. The properties of Kusum oil are preferably good over the other oils and are close to that of the diesel. From safety and storage point of view Kusum biodiesel is good as its fire and flash points are higher as complex to diesel. Hence Kusum oil is used as the raw material for biodiesel production. Transesterification is the common process to produce biodiesel from oils. However sometimes esterification is also follow to get better and purified biodiesel. Esterification is the reaction between the oil and alcohol in the presence of acid catalyst to produce glycerol and methyl ester. The esterified oil we get here is pure than crude Kusum oil. Transesterification is the reaction between the esterified oil with alcohol in the presence of alkali catalyst to produce glycerol and ester. The ester we get has molecular weight one-third less than the crude Kusum oil ratio was taken to get low viscosity. Generally methanol and ethanol is widely used for transesterification. In this study, Kusum oil methyl ester was prepared by using alkali catalyst as potassium hydroxide by transesterification process. Here KOH is used for transesterification due to their low cost and large availability. Although ester is a major product, glycerol is also collected because of its industrial uses. The esterification and transesterification reaction time is the controlling factor in determining the yield of methyl ester. Here the upper methyl ester obtained was washed several times with de-sterilized water and filtered to remove impurities. Then the water washed biodiesel was heated to remove any remain water. Kusum biodiesel was mixed with conventional diesel to produce different blends such as B10, B20 and B30. The prepared biodiesel was then tested in IC engine and performance parameters were compared with engine using conventional diesel. Mahalingam et al., [2] did their search on emission analysis by mixing alcohol with mahua oil and reported a reduction in CO, HC and NO_x. Arunkumar et al., [3] experimentally investigated the performance of diesel engine using castor biodiesel and obtained favourable results. They emphasised on more cultivation on castor plant which could lead to employability as well as a new source for diesel engine fuel. Ismail et al. [4] studied the production of castor biodiesel from crude castor oil through transesterification method. In this process they carried out the transesterification method under different proportions of reactant. The optimum condition for base catalysed transesterification of castor oil was found to be 1:4.5 of oil to methanol ratio and 0.005:1 of potassium hydroxide to oil ratio. Bajpai and Das [5] carried out their experimental work on running engine with alkyl esters of Jatropha, Karanja and castor. They found lower blends of higher alkyl esters giving the performance result close to diesel oil. Ogunkunle and Ahmed [6] carried out their research on optimizing the biodiesel production from sand apple which is widely cultivated in Africa and subsequent its use in diesel engine to run. They obtained good result on engine performance with no modification in engine. Saheb et al., [7] carried out their experimental work on enhancement of engine performance by blending Mahua oil with diesel. Pradhan et al. [8] obtained biodiesel from mahua seed by pyrolysis process for using in diesel engine.

MATERIALS AND METHOD

The Kusum trees are fast growing and can grow easily in any kind of soils. Hence these trees are shown all over the India and easy to collect Kusum seeds and oil directly. The biodiesel was obtained from two steps i.e. the first step is the acid catalysed esterification with the acid H₂SO₄ as catalyst and second step is the base catalysed transesterification with the base KOH as catalyst. In this study, the Kusum oil was converted to Kusum biodiesel by the two step transesterification process. Here in the first step the free fatty acid (FFA) in the Kusum oil was converted into methyl ester by acid-catalysed esterification and the second step was the base-catalysed transesterification using potassium hydroxide as catalyst. The esterification was carried out to reduce the FFA of the oil. In the first step the temperature was maintained about 60-64°C with 200ml methanol and 10gm of concentrated H₂SO₄. After 3hour of heating process, excess alcohol with impurities was removed after pouring the product into a separating funnel. After removing the impurities from the lower layer, the upper layer methyl ester was collected from the separating funnel for the base transesterification process. In the transesterification process, 10gm of KOH was dissolved in 200ml of methanol then poured in the flask. The mixture was heated at constant temperature about 62°C and stirred continuously for 3hour. After 3hour of heating the mixture was poured into a separating funnel for about 12hour where two layers were formed. The upper layer contained methyl ester and the lower layer contained glycerol, extra



**Manas Ranjan Padhi**

methanol, catalyst and other by products were removed. The upper layer of methyl ester or biodiesel was collected and washed several times with de-sterilized water until the washing water become neutral. The biodiesel layer was filtered to remove impurities and then heated up to 100°C to remove any remaining water. The Kusum biodiesel was tightly sealed and kept for storage. Different blends of Kusum biodiesel such as B10, B20 and B30 were prepared by blending with diesel. For example, in a B10 Kusum biodiesel, there is a composition of 10% Kusum biodiesel and 90% diesel. The biodiesel blends were then tested in variable compression ratio engine shown in Figure 1, where there is a provision to change the compression ratio by changing clearance volume of the engine cylinder. The engine was started and run idle for 10 minutes. Now the compression ratio of the engine is set at 18. Then Kusum biodiesel of B10 blend was poured in fuel tank and the engine was run with no load condition. The load was increased to 2kg by means of variac. Important performance parameters of the engine such as Brake Power (BP), Brake Thermal Efficiency (BTE) and Specific Fuel Consumption (SFC) were obtained from a computer integrated with VCR engine. Gradually the engine load was increased to 4, 6 and 10 kg and corresponding values of performance parameters were recorded. This procedure was followed for B20 and B30 blend of Kusum biodiesel.

RESULT AND DISCUSSION

The performance comparison of VCR engine using different blends of Kusum biodiesel and conventional diesel was shown in Table: 1-3 and graphs were plotted accordingly. From Figure 2, it is observed that there is a decrease in brake power output for biodiesel blends B10, B20 and B30 in comparison to conventional diesel. This may be due to lower energy content per volume of Kusum biodiesel. However for higher loads, there is no significant reduction in brake power. The decrement in power output is only less than 4% though the engine is run with biodiesel blend of 30%. This shows that Kusum is suitable to be used as biodiesel. From Figure 3, there is increasing trends of specific fuel consumption as the blending percentage of Kusum biodiesel increases. The increment percentages for B10, B20 and B30 in comparison to conventional biodiesel are 34.28%, 37.14%, 41.42% respectively at a constant load of 2kg. The increase in specific fuel consumption (SFC) of biodiesel especially for higher blends is due to the reason that the Calorific Value (CV) of Kusum biodiesel is less as compared to convention diesel fuel. However, at higher loads this increment is limited to within 15%. From Table-3 and Figure-4, the break thermal efficiency (BTE) of different Kusum biodiesel blends is observed to be slightly less as compared to conventional diesel at different loads. The decrements in the values of brake thermal efficiencies for Kusum blends B10, B20 and B30 in comparison to conventional diesel are 1.07%, 1.98% and 2.78% respectively at constant compression ratio of 18. The decrement for a higher load of 10 kg is limited to only 3% which proposes Kusum biodiesel for running a diesel engine without any damage.

CONCLUSION

The biodiesel obtained from Kusum oil has good inherent properties and most of its properties are similar with diesel fuel. The performance parameters of the variable compression ratio diesel engine was analysed at a fixed compression ratio of 18 and compared when the engine was running with same operating conditions. From the above result it can be stated that the Kusum biodiesel can be used as an alternative fuel to run a diesel engine without any engine modification. The reduction in performance parameters is limited to 5% for a biodiesel of 30 % blending, which is acceptable. Hence Kusum oil is a good replacement for conventional diesel fuel at lower blends.

REFERENCES

1. Amita Nakarmi and Susan Joshi, "A Study on Castor Oil and Its Conversion into Biodiesel by Transesterification Method", Nepal Journal of Science and Technology, Vol. 15, 45-52, 2014.
2. Mahalingam, Y. Devarajan, S. Radhakrishnan, S. Vellaiyan, B. Nagappan, "Emissions analysis on mahua oil biodiesel and higher alcohol blends in diesel engine", Alexandria Engineering Journal, Vol. 57, 2627-2631, 2018.





Manas Ranjan Padhi

3. M. Arunkumar , M. Kannan, G. Murali , “Experimental studies on engine performance and emission characteristics using castor biodiesel as fuel in CI engine”, “Renewable Energy”, Vol. 131, 737-744, 2019.
4. S. Ismail, S. A. Abu, R. Rezaur and H. Sinin, “Biodiesel Production from Castor Oil and Its Application in Diesel Engine”, ASEAN Journal on Science and Technology for Development, Vol. 31(2), 2014.
5. Sanjay Bajpai and Lalit Mohan Das, “ Experimental Investigations of an IC Engine Operating with alkyl esters of Jatropha, Karanja and Castor Seed Oil, Energy Procedia, Vol. 54, 701-714, 2014.
6. OyetolaOgunkunle, Noor A. Ahmed, “Performance Evaluation of a Diesel Engine using Blends of Optimized Yields of Sand apple (ParinariPolyandra) Oil biodiesel”, Renewable Energy, Vol. 134, 1320-1331, 2019.
7. ShaikHimamSaheb, Govardhana Reddy, KumramAnusha, “Performance Test on Diesel Engine Using Mahua Oil & Diesel Blends”, International Journal of Advanced Research in Mechanical Engineering & Technology, Vol. 1, 2015.
8. DebalaxmiPradhan, HarisankarBendu, R.K. Singh, S. Murugan, “Mahua seed pyrolysis oil blends as an alternative fuel for light-duty diesel engines”, Energy, 1-13, 2016.

Table 1: Break Power (BP) of conventional diesel and different Kusum biodiesel blends

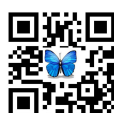
Load (Kg)	BP (kW) Diesel	BP (kW) B10	BP (kW) B20	BP (kW) B30
2	0.71	0.59	0.54	0.51
4	1.17	1.12	1.1	1.08
6	1.78	1.74	1.71	1.7
8	2.33	2.31	2.28	2.26
10	2.72	2.68	2.65	2.62

Table 2: Specific Fuel Consumption (SFC) of diesel and different Kusum biodiesel blends

Load(kg)	SFC (kg/kWh) Diesel	SFC (kg/kWh) B10	SFC (kg/kWh) B20	SFC (kg/kWh) B30
2	0.7	0.94	0.96	0.99
4	0.51	0.57	0.59	0.62
6	0.39	0.4	0.41	0.43
8	0.34	0.35	0.37	0.39
10	0.3	0.32	0.35	0.37

Table 3: Brake Thermal Efficiency (BTE) of conventional diesel and different Kusum biodiesel blends

Load (kg)	□bth	□bth	□bth	□bth
2	12.48	10.56	10.32	10.12
4	16.84	16.3	15.65	15.4
6	21.92	21.62	21.41	21.24
8	25.08	24.8	24.49	24.21
10	28.75	28.44	28.18	27.95





Manas Ranjan Padhi

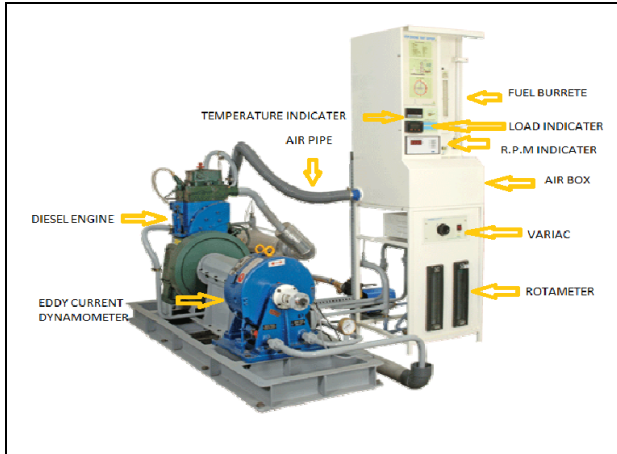


Figure 1: Variable Compression Ratio Engine

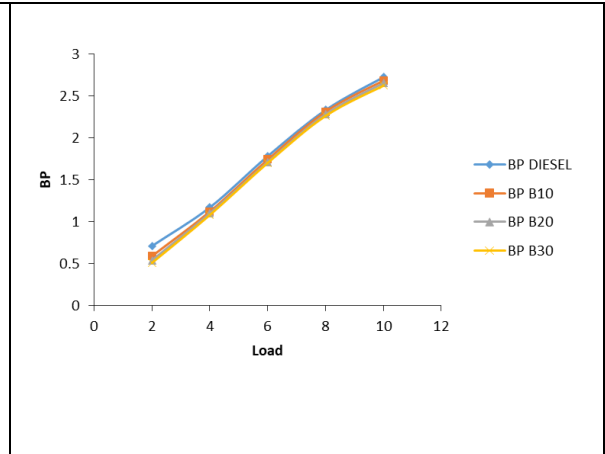


Figure 2: Break Power Vs Load of different biodiesel blends of Kusum

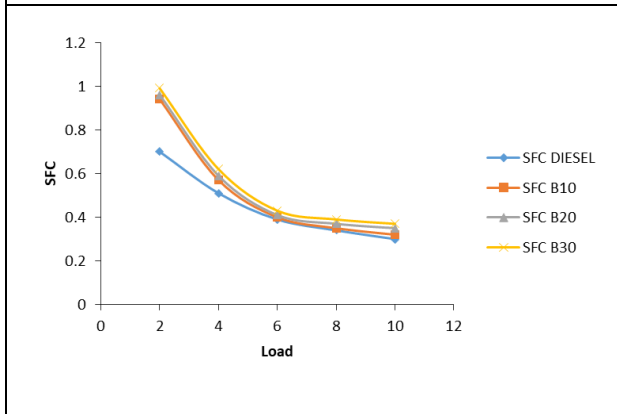


Figure 3: SFC Vs load of different biodiesel blends of Kusum

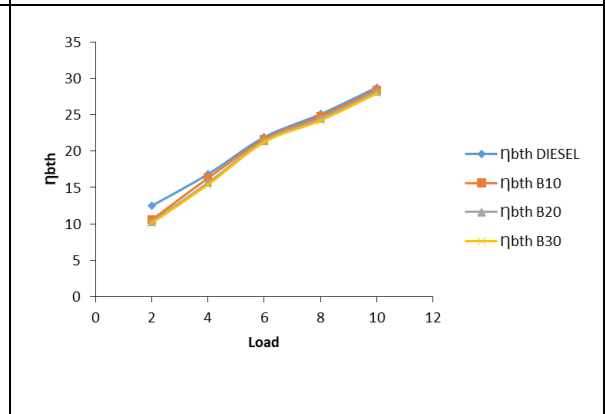


Figure 4: BTE Vs. load of different biodiesel blends of Kusum





Effect of Myofascial Release on Flexibility

Sam Thamburaj.A^{1*}, Prabhakaradoss.D¹, Rajan Samuel.A¹, Murali Sankar.KSI² and Arul.B³

¹Vinayaka Mission's College of Physiotherapy, Vinayaka Mission's Research Foundation (Deemed to be University), Salem, Tamil Nadu, India.

²School of Physiotherapy, Vinayaka Mission's Research Foundation (Deemed to be University), Puducherry, India.

³Department of Pharmacy Practice, Vinayaka Mission's College of Pharmacy, Vinayaka Mission's Research Foundation (Deemed to be University), Salem, Tamil Nadu, India.

Received: 08 Sep 2020

Revised: 10 Oct 2020

Accepted: 13 Nov 2020

*Address for Correspondence

Sam Thamburaj. A

Vinayaka Mission's College of Physiotherapy,

Vinayaka Mission's Research Foundation (Deemed to be University),

Salem, Tamil Nadu, India.

Email: samsy4u@gmail.com



This is an Open Access Journal / article distributed under the terms of the **Creative Commons Attribution License** (CC BY-NC-ND 3.0) which permits unrestricted use, distribution, and reproduction in any medium, provided the original work is properly cited. All rights reserved.

ABSTRACT

The purpose of the study is to evaluate the effect of Myofascial release on flexibility. Twenty college-level athletes between the age group of 18 and 22 yrs at Vinayaka Missions Research Foundation – Deemed to be University, Salem who had below-average joint range-of-motion (specifically a sit and reach the score of 13.5 inches [34.3 cm] or less were selected using simple random sampling technique and were further divided into two equal groups randomly. Pretest measurements of flexibility were collected using sit and reach test. After the pretest assessment, the experimental group received myofascial release along with their warm-up exercises and the Control group received warm-up alone for 2 weeks and on the 14th day, post-test measurements of flexibility were collected similarly to that of pretest measurement. The results were in the favor of the Experimental group who received Myofascial therapy additionally along with the warm-up exercises in improving the flexibility of the athletes.

Keywords: Myofascial release, Warm-up exercises, Flexibility.

INTRODUCTION

Flexibility is needed for the relatively easy performance of everyday and sporting activities. Flexibility is perhaps the most overlooked aspect of fitness for both the general public and athletes alike. It's a highly adaptable part of fitness and at any age, one can reap the benefits of flexibility. Enhanced flexibility may boost performance, muscle strength, agility, stamina and decrease the chance of injury. They have to use the maximum length of the muscle to





Sam Thamburaj et al.,

demonstrate power and energy to reach optimum performance. If the muscles and fascia are tight, they may not be able to provide the explosiveness required for a particular movement. Fascia is the network of connective tissue fibers that lie just below the surface of our skin and may look like a web or sweater of a spider. Fascia is highly structured into a mesh formulation of tubules filled with water and has the function of connecting, stabilizing, enclosing, and building a space to separate muscles and internal organs. Through damage, inflammation, or discomfort, fascia appears to get irritated leading to increased development of scar tissue and underneath it causes restraint of soft tissues. Fascia can form abnormal crosslinks and have changes in the ground substance viscosity, changing from a gel to a more solid-state[1]. If the fascia is restricted at the time of trauma, the forces cannot be dispersed properly and areas of the body are then subjected to an intolerable impact. The forces do not have to be enormous; a person who just does not have enough "give" can be severely injured. This begins to explain the sports and performance injuries that reoccur despite extensive therapy and strengthening and flexibility programs. An athlete with fascial restrictions will not efficiently absorb the shocks of continued activity. The body then absorbs too much pressure in too small an area, and during the performance, the body keeps "breaking down. Active passive stretching (more generally called just active stretching) has been used for years without doubt by physios, fitness trainers, coaches, and athletes to boost flexibility.

Myofascial therapy can be characterized as "the assistance of mechanical, neural and psycho physiological versatile potential as interfaced by the myofascial framework" [2]. In the latest decade, self-myofascial release (SMR) has become a certainly ordinary technique to upgrade regular methodologies for treating the sensitive tissue[3]. In a self-myofascial release, subjects utilize their body weight on a myofascial foam roller to load pressure on the delicate tissues. The subjects can alter positions and utilize the rollers to avoid certain areas of the body and treat the myofascial restrictions[4,5]. Self Myofascial Release (SMFR) Therapy is an approach designed to help minimize restrictive barriers or adhesions between muscles and fascial tissue layers[6]. As of late picking up prominence, myofascial release utilizes sustained, hand-on pressure in the fascial restrictions. MFR lengthens and hydrates the tissue, lessening the pull of affected tissue. It is estimated that supported weight enables delicate tissue bonds to scatter in which the bundles are remedied from a packaged situation into a straighter arrangement along the characteristic lines of the muscle filaments[7]. The musculoskeletal system which permits competent movement could be restricted by the restrictions in the fascia. Myofascial release releases the restrictions and Myofascial trigger points and expands the scope of movement (ROM) and muscle work restoring physical action[8]. To achieve peak performance and to have the winning edge the athletes must utilize the full length of the muscle to exhibit power and ability to change positions faster with balance and control. Hence there is an acute need to find an effective way of improving the flexibility thereby improving his explosive power.

MATERIALS AND METHODS

Study design: Randomized control trial with an experimental group and a control group.

Inclusion criteria

- All the college level athletes belonging to the constituent colleges of Vinayaka Mission's Research Foundation – Deemed to be University, Salem
- Subjects who had below-average joint range-of-motion (specifically a sit and reach a score of 13.5 inches [34.3 cm] or less were only included.
- Subjects between the age group of 18 and 22 years were only included.
- Subjects with Medical fitness for participation in sports from a recognized Government doctor were only included.





Exclusion criteria

- Athletes belonging to the off-campus of Vinayaka Mission's Research Foundation – Deemed to be University, Salem were excluded.
- Athletes with recent injuries were excluded.

Study population

All the college level athletes between the age group of 18 and 22 years at Vinayaka Missions Research Foundation – Deemed to be University, Salem who had below-average joint range-of-motion (specifically a sit and reach a score of 13.5 inches [34.3 cm] or less will form the population of this study). All the psychologically and medically fit athletes belonging to both genders without any other associated problem will be the population of the study.

Number of Samples and Method of Selection: 20 samples were selected using Simple Random Sampling and were further divided into two equal groups.

Type of sample: Human Volunteers (Athletes)

Materials used for the study

1. Sit And Reach Box
2. A Cylindrical Foam Roller (6" Circumference And 36" Long)

Procedure

The control group performed the warm-up practices which included 10 powerful activities that advanced from moderate to high intensity. Subjects played out every unique exercise for a period of 13 min, rested around 10 sec, and again did the same exercise for 13 min as they got back to the starting point. Subjects were ceaselessly trained to keep up the appropriate posture during the warm-up exercises. This protocol was intended to be like warm-up protocols ordinarily used to prepare sportspersons for the performance.

1. High-knee walk. While walking, lift knee towards the chest, raise the body on toes, and swing alternate arms.
2. Straight-leg march. While walking with the two arms reached out before the body, lift one extended leg towards the hands and bring back to the starting position before performing with the other leg.
3. Hand walk. With hands and feet on the ground with knees extended, walk feet towards hands while keeping knees extended then walk hands forward while keeping knees extended.
4. Lunge walks. Lunge forward with alternate legs while keeping trunk vertical.
5. Backward lunge. Move backward by arriving every leg as far back as you could.
6. High-knee skip. While skipping, insist height, high knee lift, and arm swing.
7. Lateral shuffle. Move laterally rapidly without crossing feet.
8. Backpedal. While holding feet under hips, make small steps to move backward quickly.
9. Heel-ups. Quickly kick heels towards buttocks while moving forward.
10. High-knee run. Stress knee lift and arm swing while at the same time moving forward rapidly.

The experimental group performed the self-myofascial release along with their routine warm-up exercises. The subjects administered self-myofascial release on gluteus maximus, hamstrings, calves, thoracolumbar fascia, latissimus dorsi, and rhomboid muscles. The subjects rolled the foam roller from the top of the every chosen muscle to its base and afterward got back to the beginning position and rehearsed this activity for 2 min on every chosen muscle. The members sat with the roller underneath their proximal thighs/calves making it comfortable to roll on the hamstrings and the calves. Taking support for balance with their hands they moved distally and proximally on each muscle. To roll the gluteus maximus, the erector spinae of the lumbar and thoracic spine, thoracolumbar fascia, and



**Sam Thamburaj et al.,**

rhomboids, the subjects were made to lie supine with arms crossed with the foam roller under every chosen muscle/fascia. The subjects rolled the foam caudally and cranially.

Data Analysis

The collected data from both the groups in the sit and reach test were analyzed using a paired 't' test and independent 't' test (Table No. 1).

RESULTS AND DISCUSSION

20 samples were selected using simple random sampling and they were allotted into two equal groups randomly. The first group received Warm up exercises and the second group received Myofascial release along with the warm up exercises. The analysis of the collected data using paired "t" test for 9 degrees of freedom at 95% confident level have revealed that both Warmup and Myofascial release with Warm up were significantly effective in improving the flexibility of the athletes. The analysis of the collected data using independent "t" test for 18 degrees of freedom at 95% confident level have revealed that Myofascial release with Warm up was significantly more effective than warmup exercises alone in improving the flexibility in athletes. For a warm-up, stretching is commonly performed following a short aerobic workout, which hoists the internal heat level, diminishes muscle solidness, and builds flexibility[9]. Active stretching delivered the more prominent addition in the flexibility, and the increase was kept up about a month after the finish of the preparation[10].

The motivation behind the deep myofascial release is to release restrictions (barriers) inside the more profound layers of fascia. This is cultivated by a stretching of the musculo elastic segments of the fascia, alongside the crosslinks, and changing the consistency of the ground substance of fascia. Repeated pressure put on the delicate tissue of the body because of abuse or the immobility will cause unusual crosslinking and scaring to develop in the fascia. As a result, of these unusual changes, the mobility and range of motion will get affected. The Self myofascial release will break out the crosslinks and scar tissue, restoring the fascia to its gel-like state [1]. When the fascia is in a more gel-like state, delicate tissue consistence increases permitting for more increased ROM [11]. The expansion in the Range of motion is due to the alteration in the thixotropic property of the fascia [12]. Release, in MFR idea, is the tissue unwinding, which follows the proper use of weight on the tissue. The restrictions "give way" or melts under the utilization of the load [13]. Myofascial release is one of the numerous strategies used to build mobility in a joint or arrangement of joints and improve athletic performance[14].

CONCLUSION

The results of the study make us conclude that Myofascial release with warmup is significantly more effective than warmup exercises alone in improving flexibility in athletes.

ACKNOWLEDGEMENT

The authors acknowledge Vinayaka Mission's College of Physiotherapy, Vinayaka Mission's Research Foundation (Deemed to be University), Salem for providing the facilities to carry out the research.

REFERENCES

1. Stone JA. Myofascial release. Int J Athl Ther Train. 2000;5(4):34–5.
2. Manheim CJ. The Myofascial Release Manual. SLACK Incorporated; 2008. 1 p.
3. Boyle M. Foam rolling. Training and Conditioning Magazine. Momentum Media Sports Publishing. 2006;





Sam Thamburaj et al.,

4. Castiglione A. Self-Myofascial Release Therapy and Athletes. *ALO SMR Ther.* 2010;
5. Curran PF, Fiore RD, Crisco JJ. A comparison of the pressure exerted on soft tissue by 2 myofascial rollers. *J Sport Rehabil.* 2008 Nov;17(4):432–42.
6. Barnes JF. *Pediatric Myofascial Release.* 1991.
7. Russell A. Self-Myofascial Release Techniques [Internet]. 2002 [cited 2020 Sep 24].
8. Mauntel T, Clark M, Padua D. Effectiveness of Myofascial Release Therapies on Physical Performance Measurements: A Systematic Review. *Athl Train Sport Heal Care.* 2014 Jul 1;6:189–96.
9. Gillette TM, Holland GJ, Vincent WJ, Loy SF. Relationship of Body Core Temperature and Warm-up to Knee Range of Motion. *J Orthop Sport Phys Ther [Internet].* 1991 Mar 1;13(3):126–31.
10. Meroni R, Cerri CG, Lanzarini C, Barindelli G, Morte G Della, Gessaga V, et al. Comparison of Active Stretching Technique and Static Stretching Technique on Hamstring Flexibility. *Clin J Sport Med [Internet].* 2010;20(1).
11. Barnes M. The basic science of myofascial release: Morphologic change in connective tissue. *J Bodyw Move Ther.* 1997;1:231–8.
12. Paolini J. Review of Myofascial Release as an Effective Massage Therapy Technique. *Athl Ther Today.* 2009 Sep 1;14:30–4.
13. Shah S, Bhalara A. Myofascial release. *Inter J Heal Sci Res.* 2012;2(2):69–77.
14. Peacock CA, Krein DD, Silver TA, Sanders GJ, VON Carlowitz K-PA. An Acute Bout of Self-Myofascial Release in the Form of Foam Rolling Improves Performance Testing. *Int J Exerc Sci [Internet].* 2014 Jul 1;7(3):202–11.

Table. 1. Sit and reach test data with paired 't' test and independent 't' test

Test	Variable	"t" calculated value	"t" table value
Paired "t" test Warm-up exercises	Flexibility	8.32	2.26
Paired "t" test Myofascial release	Flexibility	21.31	2.26
Independent "t" test	Flexibility	11.86	2.09

"t" calculated value > than "t" table value

Significant at 5% level





Effect of Matrix Rhythm Therapy on Pain and Disability of Patients with Adhesive Capsulitis

Rajan Samuel A*, Sam Thamburaj A and Prabhakaradoss D

Vinayaka Mission's College of Physiotherapy, Vinayaka Mission's Research Foundation (Deemed to be University), Salem, Tamil Nadu, India.

Received: 08 Sep 2020

Revised: 10 Oct 2020

Accepted: 13 Nov 2020

*Address for Correspondence

Rajan Samuel A

Vinayaka Mission's College of Physiotherapy,
Vinayaka Mission's Research Foundation (Deemed to be University),
Salem, Tamil Nadu, India.
Email: rajanmpt@yahoo.co.in



This is an Open Access Journal / article distributed under the terms of the **Creative Commons Attribution License** (CC BY-NC-ND 3.0) which permits unrestricted use, distribution, and reproduction in any medium, provided the original work is properly cited. All rights reserved.

ABSTRACT

The purpose of the study is to evaluate the effect of Matrix Rhythm Therapy on pain and disability of patients with Adhesive capsulitis. Thirty samples with unilateral primary adhesive capsulitis in the second clinical stage i.e frozen stage between the age group of 45-55 years were selected randomly and divided into two equal groups randomly. The pretest measurement of pain and disability was done using the shoulder pain and disability index for both the groups. After the pretest assessment, the experimental group received Matrix rhythm therapy and conventional physiotherapy treatment and the control group received conventional physiotherapy treatment alone for 3 weeks and on the 21st day, post-test measurement of pain and disability was done using Shoulder pain and disability index in a similar fashion as that of pretest measurement. The results of the study favored the experimental group who received Matrix rhythm therapy additionally along with conventional physiotherapy treatment in the reduction of pain and disability of patients with adhesive capsulitis.

Keywords: Matrix Rhythm Therapy; Adhesive Capsulitis; Pain; Disability; Frozen Shoulder; Musculoskeletal Physiotherapy.

INTRODUCTION

Frozen shoulder or adhesive capsulitis is a very common clinical situation characterized by pain and gradual restriction of shoulder motion mostly presenting with unknown etiology. Frozen shoulder is reported to affect 2% to 5% of the general population[1-3]. The pathophysiology of frozen shoulder involves diffuse inflammatory synovitis with subsequent adherence of the capsule and a loss of normal axillary pouch and joint volume, which in turn leads to a noteworthy loss of motion of the shoulder joint. The contracture of the capsule is thought to result from the

28466



**Rajan Samuel et al.,**

adhesion of the capsular surfaces or fibroblastic proliferation in response to cytokine production. The capsule of the shoulder is thickened in adhesive capsulitis and a mild chronic inflammatory infiltrate and fibrosis maybe present. Adhesive capsulitis, primarily a fibrosing condition affecting the capsule (fibrous bag around a joint) of the shoulder joint has been stated in many of the modern work, such as that of Bunker. This causes tightness of the coracohumeral ligament (one of the ligaments attaching the shoulder to the humerus) which in turn leads to restriction of passive movement of the shoulder especially the external rotation [4]. The definitive treatment for frozen shoulder remains unclear even though many interventions have been studied including active/passive range of motion (ROM) exercises, stretching, soft tissue mobilization, myofascial release, proprioceptive neuromuscular facilitation techniques, ultrasound, electrical stimulation, ice packs, and joint mobilization techniques [5]. Matrix Rhythm Therapy was postulated by Dr. Ulrich G. Randoll which works on the principle of that all tissues in the body vibrate/oscillate with a frequency of 8 to 12 Hz which maintains the normal physiologic function of the body and any disturbance such as injury, inflammation, trauma interrupts the rhythm which causes further loss of function and pain in the body[6,7]. Matrix Rhythm Therapy (MRT) provides Vibromassage and activates and rebalances specific vibration in skeletal muscles and the nervous system. The oscillating rhythm produced by it maximizes lymphatic venous perfusion of the extracellular space in which the anti-edematous effects originate [8–10]. Studies are needed to investigate the principles and broader applications of matrix rhythm therapy as less number of research studies are available to demonstrate the effect of matrix rhythm therapy in the treatment of adhesive capsulitis. Hence understanding the effect of matrix rhythm therapy in the management of pain and disability of patients with adhesive capsulitis is essential and needs to be researched. The primary aim of this study is to find the effectiveness of matrix rhythm therapy on adhesive capsulitis with respect to pain and disability.

MATERIALS AND METHODS

This study is a randomized control trial with an experimental group and a control group. Thirty samples with unilateral primary adhesive capsulitis in the second clinical stage i.e frozen stage between the age group of 45 -55 years were selected randomly and divided into two equal groups randomly. Subjects who have Diabetes Mellitus & Allergic skin conditions and Post operated cases at the shoulder were excluded from the study. Subjects satisfying the inclusion criteria and attending to outpatient physiotherapy departments in Salem city were only selected. All the subjects were explained about the purpose of the study. Subjects who gave written informed consent were only included for the study. Both the groups underwent a pretest assessment of pain and disability using the shoulder pain and disability index. Pretest measurement was done in the following fashion using the shoulder pain and disability index. The Shoulder Pain and Disability Index (SPADI) consist of two aspects i.e. pain and disability and is a self-administered questionnaire. The pain component had five questions relating to the severity of pain in various situations. The disability component had eight questions aimed to assess the degree of difficulty with various activities that require the use of upper-extremity. The SPADI takes 5 to 10 minutes for a patient to complete and is the only reliable and valid region-specific measure for the shoulder. Subjects were instructed to place a mark on a 10cm visual analog scale for each question. The pain dimension ranged from 'no pain at all' to 'worst pain imaginable', and those for the disability ranged from 'no difficulty' to 'so difficult it required help'. The total score was derived by averaging the scores of both components of the questionnaire. After the pre-test assessment was over, Group I (Experimental group) received Matrix rhythm therapy and conventional physiotherapy treatment for a period of 3 weeks. Matrix rhythm therapy was given with subjects lying down on the couch comfortably as instructed by the therapist. The area to be treated was exposed and the powder was applied over it in order to avoid the friction caused by the Matrix Rhythm Therapy probe. Matrix Rhythm Therapy was applied through longitudinal stroking into the soft tissues with the help of firm pressure on the probe. Matrix Rhythm Therapy was given for a period of 75 minutes which included the paraspinal region and around the anterior, posterior, medial and lateral aspects of the shoulder region. Subjects were treated for 15 minutes on either side of the vertebral column and in the following four positions 15 minutes to each position.



**Rajan Samuel et al.,**

- A. Supine position with the arm abducted to the available range and Matrix Rhythm Therapy was applied around the anterior aspect of the shoulder region
- B. Supine position with the arm abducted to the available range and Matrix Rhythm Therapy was applied on the medial aspect of humerus including the axillary region
- C. Side-lying –Side-lying with armrest over the body and Matrix Rhythm Therapy applied to the lateral aspect of the shoulder region).
- D. Prone lying with the arm abducted to the available range and Matrix Rhythm Therapy applied to the posterior aspect of the shoulder region including neck and upper back region.

Matrix Rhythm therapy was given for 2 days a week for 3 weeks. Conventional therapy included Short wave diathermy for 15 minutes once in a day for the first 1 week and active and passive mobilization and strengthening exercises for 6 days in a week for 3 weeks. The subjects were taught to perform active exercises to the shoulder joint, wand exercises, pendulum exercises, and isometric exercises. Subjects belonging to Group II received conventional physiotherapy alone for a period of 3 weeks in a similar fashion as that of Group I. Both the groups underwent post-test assessment for pain and disability using the shoulder pain and disability index similar to that of pretest measurement after a period of 3 weeks of treatment in a similar fashion and were recorded in a separate pro forma maintained for each individual subject. A pilot study was done two months before the main study with six subjects to know the feasibility of the study. The collected data were subjected to statistical analysis. Shapiro-Wilk test was used to find the normality of the data and results showed that data is normally distributed. The data were analyzed using the 't' test to test the hypothesis.

RESULTS

The results of the study were derived from the statistical analysis using the paired t-test for the experimental and control group and from the statistical analysis using an independent t-test between the experimental group and control group. The results of the statistical analysis are represented in table No.1, 2 & 3. Statistical analysis using a paired t-test with 14 degrees of freedom and 99% confidence limit revealed that there is a significant reduction in pain and disability in both the experimental group (Group I) which received Matrix rhythm therapy and Conventional physiotherapy and Control group (Group II) which received Conventional physiotherapy alone. (Table 1 & 2). Statistical analysis using an independent t-test with 28 degrees of freedom and 99% confidence limit revealed that there is a significant difference in the reduction of pain and disability in favour of the experimental group (Group I) which received Matrix rhythm therapy and Conventional physiotherapy than the Control group (Group II) which received Conventional physiotherapy alone.(Table 3).

The following results were obtained after subjecting the data to statistical analysis

1. There was a statistically significant reduction in pain and disability for the subjects with Adhesive Capsulitis in the experimental group (Group I) treated with Matrix rhythm therapy and Conventional physiotherapy.
2. There was a statistically significant reduction in pain and disability for the subjects with Adhesive Capsulitis in the control group (Group II) treated with Conventional physiotherapy alone.
3. There was a statistically significant difference in the reduction of pain and disability for the subjects with Adhesive Capsulitis in the experimental group (Group I) treated with Matrix rhythm therapy and Conventional physiotherapy than the subjects with Adhesive Capsulitis in the control group (Group II) treated with Conventional physiotherapy alone.





DISCUSSION

The results of this study indicate that matrix rhythm therapy is effective in decreasing pain and disability of shoulder in subjects with Adhesive Capsulitis. Matrix Rhythm Therapy allows the cell metabolism of the tissue to be reactivated with depth-effective rhythmical micro-extensions and the contracted areas of the musculature will be inductively relaxed (circulation>oxygen> ATP>dissolution of the tension) [7]. Matrix Rhythm therapy is known to improve microcirculation within the tissues which gives the basis of the enhanced removal of metabolic waste products, to reduce edema, and to improve the extensibility of soft tissues through research. Jager et al did a study with 80 patients and assessed the effect of Matrix rhythm therapy on pain level, sleep patterns, and flexibility of the spine in patients with low back pain. The results of the study demonstrated that the application of Matrix rhythm therapy is more effective in reducing pain and increasing flexibility when compared with conservative therapy[11]. Randoll and Hennig et al reported a significant improvement in 65 patients with low back pain applied with Matrix rhythm therapy over six sessions within a week [12]. This study clearly demonstrates the positive effects of Matrix rhythm therapy in the reduction of pain and disability in patients with Adhesive capsulitis when compared with the control group who did not receive Matrix rhythm therapy with Shoulder Pain and Disability Index (SPADI) as an outcome measure. The study results are in line with the following studies done in a similar population. Varun Naik et al concluded that Matrix rhythm therapy is effective in treating Frozen shoulder in terms of pain and range of motion and it showed positive results in reducing 30% of pain and increased shoulder range of motion with just one sitting of treatment [13]. Vijay et al summarized that the combination of Matrix Rhythm Therapy and Physiotherapy intervention have a beneficial long term effect on physical health, functional outcome, and satisfaction of patient with frozen shoulder [14].

CONCLUSION

The results of the study make us conclude that Matrix rhythm therapy and conventional physiotherapy treatment provides better results than conventional physiotherapy treatment for the reduction of pain and disability in subjects with adhesive capsulitis. Hence Matrix rhythm therapy gives exclusive benefits in the reduction of pain and disability in subjects with adhesive capsulitis.

ACKNOWLEDGEMENT

The authors are grateful to the authorities of Vinayaka Mission's College of Physiotherapy, Vinayaka Mission's Research Foundation (Deemed to be University), Salem for their encouragement and support to complete this study. We extend our sincere thanks to Dr. S. Sathish Kumar PhD, Assistant Professor cum Statistician, Vinayaka Mission's Medical College and Hospital, Karaikal for his valuable guidance in Statistical analysis.

REFERENCES

1. Davies G, Ellenbecker T. Focused exercise aids shoulder hypomobility. *Biomechanics*. 1999;6:77–81.
2. Bridgman JF. Periarthritis of the shoulder and diabetes mellitus. *Ann Rheum Dis* [Internet]. 1972 Jan;31(1):69–71.
3. Lundberg BJ. The frozen shoulder. Clinical and radiographical observations. The effect of manipulation under general anesthesia. Structure and glycosaminoglycan content of the joint capsule. Local bone metabolism. *Acta Orthop Scand Suppl*. 1969;119:1–59.
4. Barua SK, Chowdhury MZA. Phonophoresis in Adhesive Capsulitis (Frozen Shoulder). *Chattagram Maa-O-Shishu Hosp Med Coll J*. 2014;13(1):60–4.
5. Hannafin JA, Chiaia TA. Adhesive capsulitis. A treatment approach. *Clin Orthop Relat Res*. 2000 Mar;(372):95–109.





Rajan Samuel et al.,

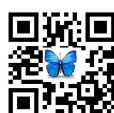
6. Randoll U. Matrix-Rhythm-Therapy: Utilizing the entrainment effect to optimize body performance and tissue regeneration in chronic diseases.
7. Randoll UG, Hennig FF. Matrix-Rhythm-Therapy Cell-Biological Basics, Theory and Practice. *pt_Zeitschrift für Physiother.* 2009;61:1–6.
8. Randoll U, Hennig F. Matrix-Rhythm-Therapy basics theory and practice. *Z Physiother.* 9AD:61:1–6.
9. Randoll U, Hennig F. Coherent Rhythms (Timing Frequencies) in Biological Systems as a Basis for the Matrix-Rhythm-Therapy [Internet]. 2003 [cited 2020 Sep 20].
10. Randoll U, Hennig F. Vibrations and their Indication in Sport Injuries [Internet]. <http://www.marhythesystems.de/en/research-and-practical-experience/publications>. 2003 [cited 2020 Sep 20]. p. 1–8.
11. Jäger A, Chan D. The effect of Matrix Rhythm Therapy on back pain patients. In: 2nd National Physiotherapy and Rehabilitation Congress. 2009. p. 132.
12. Randoll UG, Hennig FF. A new approach for the treatment of low back pain: Matrixrhythm-therapy. *Osteologie.* 2001;(Suppl):66.
13. Naik V, Bhagwat S, Pathania T, Bootwala F. Effectiveness of matrix rhythm therapy in frozen shoulder with respect to ROM and pain- An experimental study. 2018;4(1):73–6.
14. Bhartiya V, Darade S, Bhagwat S, Roy M. Effect of matrix rhythm therapy (MRT) combined with physiotherapy intervention in frozen shoulder – a case report. *VIMS J Physiother Case Reports.* 2017;2(1):72–7.

Table No. 1. Experimental Group descriptive statistics with the comparison

Experimental Group					
Variable	Group	Range	Mean ± SD	t-test	P-value
Pain	Pre	58 – 76	68.40 ± 4.97	22.895	0.0001
	Post	36 – 50	43.60 ± 4.35		
Disability	Pre	58.75 – 76.25	68.21 ± 4.74	26.276	0.0001
	Post	37.50 – 48.75	42.83 ± 3.55		
Total Score	Pre	58.46 – 73.84	68.25 ± 3.69	35.154	0.00101
	Post	37.69 – 46.15	43.12 ± 2.82		

Table No 2. Control Group descriptive statistics with the comparison

Control Group					
Variable	Group	Range	Mean ± SD	t-test	P-value
Pain	Pre	58 – 70	65.33 ± 4.25	11.297	0.0001
	Post	50 – 64	57.91 ± 4.92		
Disability	Pre	60 – 75	69.25 ± 4.14	11.611	0.0001
	Post	53.75 – 70	62.00 ± 4.21		
Total Score	Pre	59.23 – 72.30	67.74 ± 3.15	14.269	0.0001
	Post	53.07 – 63.84	60.40 ± 2.92		





Rajan Samuel et al.,

Table No. 3. Pre and Post Group descriptive statistics with the comparison

Variable	Group	Mean ± SD	T	P-value
Pain	Experimental Pre	68.40 ± 4.97	1.686	0.114
	Control Pre	65.33 ± 4.25		
	Experimental Post	43.60 ± 4.35	-10.149	0.0001
	Control Post	57.91 ± 4.92		
Disability	Experimental Pre	68.21 ± 4.74	-0.740	0.471
	Control Pre	69.25 ± 4.14		
	Experimental Post	42.83 ± 3.55	-12.758	0.0001
	Control Post	62.00 ± 4.21		
Total Score	Experimental Pre	68.25 ± 3.69	0.402	0.694
	Control Pre	67.74 ± 3.15		
	Experimental Post	43.12 ± 2.82	-16.163	0.0001
	Control Post	60.40 ± 2.92		





Impacts of Structural and Optical Properties of FeWO₄ Nanoparticles in the Photocatalytic Degradation of Rhodamine-B Dye under Solar Light.

Tamilarasi and K.Balakrishnan*

AVVM Sri Pushpam College (Autonomous), Poondi, Thanjavur, Tamil Nadu, India.

Received: 08 Sep 2020

Revised: 10 Oct 2020

Accepted: 13 Nov 2020

*Address for Correspondence

K.Balakrishnan

Associate Professor, Department of Chemistry,
A.V.V.M Sri Pushpam College (Autonomous),
Poondi, Thanjavur, Tamil Nadu, India
Email: professorsorbavvm63@gmail.com



This is an Open Access Journal / article distributed under the terms of the **Creative Commons Attribution License** (CC BY-NC-ND 3.0) which permits unrestricted use, distribution, and reproduction in any medium, provided the original work is properly cited. All rights reserved.

ABSTRACT

In this work, the ferric tungstate (FeWO₄) nanoparticles were victoriously developed by simple chemical co-precipitation technique. The structural orientation of the material was were characterized by X-ray diffraction (XRD), optical properties was studied by UV-visible diffuse reflectance spectroscopy (UV-vis-DRS), metal-ligand bonding nature in the prepared nano crystals were found by Fourier transform infrared spectroscopy (FT-IR), surface morphological analysis and elemental analysis were carried out by field emission scanning electron microscopy (FE-SEM), energy dispersive X-ray spectroscopy (EDX), and elemental colour mapping (ECM) techniques. The photocatalytic degradation of Rhodamine-B (RhB) was for FeWO₄ nanoparticles are scrutinized by altering various parameters under sunlight.

Keywords: Sunlight, Rhodamine-B, Hetero-Fenton photocatalyst, co-precipitation method

INTRODUCTION

Application of solar energy as a clean and renewable energy has received a lot of attentions in photodegradation of environment pollutants [1–6]. The textile dyeing industry consumes large quantities of water at its different steps of dyeing and finishing, among other processes. Then non-biodegradable nature of dyes and their stability toward light and oxidizing agents complicate the selection of a suitable method for their removal. Moreover, toxicity bioassays have demonstrated that most of them are toxic [7–12]. Therefore, a current critical issue for the scientific community is to develop and improve treatment technologies and produces to remove those pollutants from the aqueous medium, improving water quality and enhancing its possible reuse. Since the 90s an increasing number of chemical processes are being modified attending to environmental criteria and taking into account several principles of the green chemical [13]. Advanced oxidation processes (AOPs) have been proven to be one of the most effective technologies to treat a wide variety of recalcitrant pollutants in wastewater. As one of the most promising AOPs,



**Tamilarasi and Balakrishnan**

heterogeneous photo-Fenton processes has attracted considerable interest because it can generate highly oxidizing $\cdot\text{OH}$ radicals for non-selective oxidation of organic pollutants [14–18]. In recent years, metal tungstates have been on the focus of intensive research due to their high application potential in various fields such as photoluminescence, optical fibers, scintillator materials, humidity sensors, magnetic properties and catalysis [19–22]. As one of the important families of inorganic materials, FeWO_4 has been proven to display significant magnetic and optical properties [23, 24]. Metal tungstate (MWO_4 ; M = Ni, Fe, Ba, Bi) is one of the narrow band gap semiconductor to exploit new photocatalysts with visible light driven photocatalytic ability [25, 26]. Among these FeWO_4 has been found to possess interesting physical properties such as ferroelectric piezoelectricity, pyroelectricity, catalytic behaviour and a nonlinear dielectric susceptibility [27]. Therefore, in this paper, a novel FeWO_4 nanocatalyst was prepared by simple co-precipitation method and test their photocatalytic activity for the degradation of organic pollutants like Rhodamine-B (Rh-B) under natural sunlight irradiation in the presence of H_2O_2 . The nanocatalyst characterized by XRD, FT-IR, FE-SEM, EDX, elemental colour mapping and UV-vis-DRS analysis.

MATERIALS AND METHODS

Double distilled water was used for all dilution and sample preparation of Rhodamine-B (C.I. 45170) was obtained from HiMedia Chemical, ferric chloride (FeCl_3), sodium tungstate ($\text{Na}_2\text{WO}_4 \cdot 2\text{H}_2\text{O}$) from A.R, sodium hydroxide (NaOH) from Merck, ethanol ($\text{C}_2\text{H}_5\text{OH}$) and sulfuric acid (H_2SO_4) from Qualigens were used as received. The pH of the solution was adjusted H_2SO_4 or NaOH .

Synthesis of iron tungstate (FeWO_4)

0.8246 g of sodium tungstate ($\text{Na}_2\text{WO}_4 \cdot 2\text{H}_2\text{O}$) in 25 mL distilled water was added drop wise into 1.623 g ferric chloride (FeCl_3). The above mixture was maintained at 80 °C under continuous stirring a brown precipitate was formed by adding sodium hydroxide solution to this mixture its pH adjusted to 7–8 on further stirring for 4 h. The colour of the precipitate filtration and washing with distilled water and ethanol several times. The sample was filtered and dried in oven at 80 °C for 2 h. Then it was calcined in muffle furnace at 550 °C for 6 h.

Photocatalytic activity

For all the solar photoreacting experiment 50 mL of dye solution containing appropriate quantity of the FeWO_4 suspension was used. The suspension was stirred for 30 min in the dark and then irradiated. The solution and dark dye was continuously aerated by a pump to provide oxygen and for complete mixing of reaction medium sample for analysis were 2–3 mL extracted through pipette every 10 min and centrifuged immediately separate the catalyst. The centrifugate (1 mL) was diluted to 10 mL and its absorbance was measured 553 nm using UV-vis spectrophotometer to determine the concentration of dye from the concentration of dye during the degradation process, percentage of dye remaining was determined. Heterogeneous photocatalytic degradation of Rh-B on iron immobilized catalyst was reported to follow *pseudo*-first order kinetics. At low initial dye concentration, the rate expression is given by $d[C]/dt = k'[C]$ where k' is the *pseudo*-first order rate constant. The dye was adsorbed on the catalyst surface and adsorption-desorption equilibrium was reached in 10 min after adsorption, the equilibrium concentration of the solution was determined and taken as the initial dye concentration (C_0) for kinetic analysis. At $C = C_0$, $t = 0$, $\ln(C_0/C) = k't$, where C_0 is the equilibrium concentration of dye and C is the concentration at time t . *pseudo*-First order rate constant k' was determined from the plot of $\ln(C_0/C)$ versus t .

Solar experiment

All solar photocatalytic experiment were carried out in a open space on sunny days of summer under clear skies between 11 a.m and 2 p.m. Solar light intensity was measured for every 10 min and the average light intensity over the duration of each experiment was calculated of the sensor was always set at the position of maximum intensity. The intensity of solar light was measured using LT Lutron LX -10/A digital Lux meter. The intensity of solar light (1250×100 Lux) was nearly constant during the experiments.





Characterization of photocatalyst

X-Ray diffraction pattern was recorded on the Equinox-1000 model X-ray diffractometer from analytical instruments operated at a voltage of 30 kV and a current of 30 mA with $\text{CuK}\alpha$ (1.54056 Å). FT-IR spectrum was recorded using Shimadzu IRAffinity-1 spectrometer in KBr pellet. About 5 mg of sample was mixed with 50 mg of IR grade KBr, ground and pressed using hydraulic press under a pressure of 15 tons into wafer of 13 mm diameter. This pellet was used to record the infrared spectra in the range of 4000–400 cm^{-1} . The spectrum was recorded as percentage transmittance against wave number. FE-SEM images were taken using on Carlzeiss-Specification EV018 scanning electron microscope. Samples were mounted on a carbon platform placed in the scanning electron microscope for taking images at various magnifications. EDX (Bruker-X-Flash X130) and elemental colour mapping were performed at different points of the surface in order to minimize any possible anomalies arising from the heterogeneous nature of the analyzed surface. Most elements were detected with the concentration in the order of 0.1%. The UV-DRS spectrum was recorded by using the instrument Jasco the Model No. V-670. Ultraviolet and visible light absorbance spectra were measured over a range of 200–700 nm with a Shimadzu UV-1650PC recording spectrometer using a quartz cell with 10 mm optical path length.

RESULT AND DISCUSSION

XRD analysis

X-ray diffraction (XRD) patterns shown in Fig. 1. The peaks at 15.4, 18.6, 23.7, 24.9, 30.3, 31.2, 36.12, 38.08, 41.09, 43.9, 45.1, 49.8, 51.2, 53.2, 61.2, 65.1 and 67.5° are assigned to (010), (100), (011), (110), (111), (020), (002), (200), (102), (112), (211), (022), (130), (221), (113), (132) and (041) planes of monoclinic FeWO_4 (JCPDS Card File No. 71-2390) [28,29]. The average crystalline size is 35 nm.

FT-IR spectrum

The FT-IR spectrum of the prepared FeWO_4 nanorods was shown in Fig. 2. The peak adsorbed at 3479–2361 cm^{-1} corresponds to the O–H bending vibration. The band observed at 564 cm^{-1} corresponds to the Fe–O stretching vibration and the band at 782 cm^{-1} corresponds to the W–O lattice vibration [30].

FE-SEM, EDX with elemental colour mapping

The surface morphology of the sample was measured by FE-SEM. The FE-SEM images of FeWO_4 at different magnifications are shown in Fig. 3. A large number of FeWO_4 nanorods formed under the current synthesis condition. The structure of the FeWO_4 nanorods was further investigated by EDX and elemental colour mapping observation. The EDX recorded from the selected area is shown in Fig. 4, which reveals the presence of Fe, W and O in the catalyst. Confirm the colour mapping (Fig. 5) the different colour area indicates Fe, W and O in bulk of FeWO_4 nanocatalyst.

UV-vis-DRS

Fig. 6 represents the UV-vis absorption spectrum and T_{auc} plot of $[\text{FR}(\text{h}\nu)]^2$ Vs $\text{h}\nu$ (eV) for FeWO_4 nanocatalyst. The UV-vis absorption spectrum of FeWO_4 exhibits the absorption in the visible region as shown in Fig. 6. The band absorption around 340 nm attributing to the excitation of electron from the valence band to conduction band [31]. Kubelka-Munk plot for FeWO_4 are shown in Fig. 7. The optical band gap energy of FeWO_4 was found to be 2.46 eV respectively.

Photocatalytic activity

The photocatalytic activities of FeWO_4 on the degradation of Rhodamine-B (Rh-B) under various conditions have been discussed. Structure and UV spectrum of the dye is given in Fig. 8.





Primary analysis

The photocatalytic activity of the FeWO_4 was evaluated by the degradation of Rh-B under solar light. Controlled experiments under different reaction conditions were carried out and the results are discussed in Fig. 9. From the results, it is clear that the dye is resistant to direct photolysis by solar light (curve a). There is no appreciable decrease in the concentration of dye occurred when it is treated with FeWO_4 /dark (curve b). In the presence of FeWO_4 dye is irradiated with solar light only 12% of dye concentration decreased (curve c). The dye on irradiation with sunlight in the presence of H_2O_2 a small decrease in dye concentration was observed (curve d). There is a decrease in concentration of dye occurred when it is treated with dye/ FeWO_4 / H_2O_2 /dark (curve e). Curve f is heterogeneous-Fenton type reaction (dye/ FeWO_4 / H_2O_2 /solar), 88% degradation was observed at the time of 90 min.

Effect of pH

Solution pH plays a vital role in photocatalytic degradation. The effect of pH ranges from 3–9 was studied and the results are shown in Fig. 10. The maximum percentage of degradation (88%) was observed at pH 7 (90 min). Above pH 7 the degradation efficiency decreases. The higher efficiency at pH 7 may be due to the maximum adsorption of Rh-B by the catalyst at this pH. The surface charge of the catalyst becomes negative at pH above 7, and as a consequence, the electrostatic attraction between dye (anion) and negatively charged catalyst becomes weak, resulting in decreased adsorption [32]. Hence pH 7 is considered to be an optimum pH for this reaction.

Effect of H_2O_2 dosage

Hydrogen peroxide concentration is an important parameters for the degradation of the dye in the heterogeneous photo-Fenton reaction (Fig. 11) illustrates degradation efficiency of Rh-B at variation of H_2O_2 amount also effects the rate of reaction and therefore, the dye degradation rate was studied in the range from 5–20 mmol of H_2O_2 increasing rate constant from 0.012 to 0.024 min^{-1} (30 min). Further increases H_2O_2 above 20 mmol the rate constant is decreases. It was due to the scavenging effect of excess H_2O_2 which could be expressed with eqns. 1 and 2 [33]. Hence, 20 mmol H_2O_2 is the optimum level for the Rh-B mineralization.



Effect of catalyst loading

The study of degradation rate with different amount of catalysts is important to find out the minimum amount of catalyst required for maximum dye removal. Hence it is required to optimize the dose of catalyst for the effective mineralization of Rh-B. The experiment was carried out by varying catalyst concentration from 0.5 to 2 g L^{-1} . The increase of catalyst weight from 0.5 to 1.0 g L^{-1} increases the rate of degradation from 0.005 to 0.019 min^{-1} at the time of 30 min (Fig. 12). Further increase of catalyst amount above 1 g L^{-1} the rate constant is decreases. This is due to impairment in light penetration with increasing catalyst dose. The increased catalyst dose increases the turbidity of the solution thus blocking the light and causing scattering [34]. The optimum catalyst dosage of 1 g L^{-1} .

Effect of dye concentration

Fig. 13 shows the effect of dye concentration on the degradation of Rh-B. The photodegradation rate of Rh-B decreases from 0.062 to 0.007 min^{-1} with increase of dye concentration from 1 to 6×10^{-4} M. The results shows that dye degradation rate decreases by increases of dye concentration. This is because of higher dye concentration i) decreases the path length of photon entering dye solution and ii) absorb significant amount of UV light rather than the catalyst [35].





Long-term stability

Stability is the key role for the recycled application of photocatalyst. The stability of the catalyst was tested for multiple runs. Almost all the five runs gave <95% degradation was observed. This shows that the catalyst (Fig. 14) is stable and reusable for multiple runs and also it can be used for industrial applications widely.

Mechanism

Based on the results above, a possible mechanism for FeWO₄ as heterogeneous catalyst for the degradation of Rhodamine B is proposed. Mainly the redox cycle of Fe³⁺/Fe²⁺ on the surface of the FePO₄ was initiated by the addition of H₂O₂, similar the process occurred in homogeneous Fenton system (eqns 3 and 4).



Finally, the Rh B molecules attacked into CO₂ and H₂O by the generated •OH radicals on the surface of the catalyst while the catalyst itself was restored to the original state.



CONCLUSION

The hetero-fenton (FeWO₄) nano photocatalyst was prepared successfully and their structural and morphological natures were studied by XRD and FE-SEM instruments. The average crystallite size and optical bandgap was calculated as 35nm and 2.46 eV respectively. The obtained bandgap value confirms that the prepared material was active in visible region of the solar spectrum. The mineralization of Rhodamine-B (RhB) dye was done using the synthesized photocatalyst material and 97% of efficiency is achieved within 90 minutes of irradiation. To optimize the various parameters those are highly influence the photocatalytic activity, different initial concentrations of the dye, various catalyst load, different H₂O₂ dosage and different pH values are maintained and studied thoroughly. The overall obtained experimental results have been concluded that the prepared FeWO₄ nanoparticles are highly suitable for the remediation of wastewater under direct sunlight irradiation.

REFERENCES

1. J Lu, C Xu, J Dai, J Li, Y Wang, Y Lin, P Li. Improved UV photoresponse of ZnO nanorod arrays by resonant coupling with surface plasmons of Al nanoparticles. *Nanoscale*. 2015; 7(8):3396-403.
2. MH Habibi, AH Habibi, M Zendehtel, M Habibi. Dye-sensitized solar cell characteristics of nanocomposite zinc ferrite working electrode: Effect of composite precursors and titania as a blocking layer on photovoltaic performance. *Spectrochimica Acta Part A: Molecular and Biomolecular Spectroscopy*. 2013; 110, 226-32.
3. Z., Han, L., Liao, Y., Wu, H., Pan, S., Shen, & J. Chen,. Synthesis and photocatalytic application of oriented hierarchical ZnO flower-rod architectures. *Journal of hazardous materials*, (2012), 217, 100-106.
4. M. H., Habibi, & A. H. Habibi. Nanostructure composite ZnFe₂O₄-FeFe₂O₄-ZnO immobilized on glass: Photocatalytic activity for degradation of an azo textile dye F3B. *Journal of Industrial and Engineering Chemistry*, (2014), 20(1), 68-73.
5. Eskizeybek, V., Sarı, F., Gülce, H., Gülce, A., & Avcı, A. (2012). Preparation of the new polyaniline/ZnO nanocomposite and its photocatalytic activity for degradation of methylene blue and malachite green dyes under UV and natural sun lights irradiations. *Applied Catalysis B: Environmental*, 119, 197-206.
6. M.H. Habibi, B. Karimi, M. Zendendel, M. Habibi, Fabrication, characterization of two nano-composite CuO-ZnO working electrodes for dye-sensitized solar cell. *Spectrochim. Acta A* 116 (2013) 374-380.
7. N.M. Mahmoodi, M. Arami, Bulk phase degradation of Acid Red 14 by nanophotocatalysis using immobilized titanium (IV) oxide nanoparticles. *J. Photochem. Photobiol. A* 182 (2006) 60-66.
8. N.M. Mahmoodi, M. Arami, Numerical finite volume modeling of dye decolorization using immobilized titania nanophotocatalysis. *Chem. Eng. J.* 146 (2009) 189-193.





Tamilarasi and Balakrishnan

9. N.M. Mahmoodi, M. Arami, Modeling and sensitivity analysis of dyes adsorption onto natural adsorbent from colored textile wastewater, *J. Appl. Polym. Sci.* 109 (2008) 4043–4048.
10. N.M. Mahmoodi, M. Arami, N.Y. Limaee, N.S. Tabrizi, Decolorization and aromatic ring degradation kinetics of Direct Red 80 by UV oxidation in the presence of hydrogen peroxide utilizing TiO₂ as a photocatalyst. *Chem. Eng. J.* 112 (2005) 191-196.
11. M. Arami, N.Y. Limaee, N.M. Mahmoodi, Degradation and toxicity reduction of textile wastewater using immobilized titania nanophotocatalysis. *Chemosphere* 65 (2006) 999–2006.
12. M. Arami, N.Y. Limaee, N.M. Mahmoodi, Evaluation of the adsorption kinetics and equilibrium for the potential removal of acid dyes using a biosorbent. *Chem. Eng. J.* 139 (2008) 2–10.
13. P.T. Anatas, J.C. Warner, Principles of green chemistry. *Green chemistry: Theory and practice*, Oxford University Press, Oxford, 1998.
14. E. Brillias, I. Sires, M.A. Oturan, Electro-Fenton process and related electrochemical technologies based on Fenton's reaction chemistry. *Chem. Rev.* 109 (2009) 6570–6631.
15. X.Q. Wang, C.P. Liu, Y. Yuan, F.B. Li, Arsenite oxidation and removal driven by a bio-electro-Fenton process under neutral pH conditions. *J. Hazard Mater.* 275 (2014) 200–209.
16. C. Walling, Degradation of methyl orange using Fenton catalytic reaction. *Acc. Chem. Res.* 8 (1975) 125–131.
17. J.W. Jang, J.W. Park, Iron oxide nanotube layer fabricated with electrostatic anodization for heterogeneous Fenton like reaction, *J. Hazard. Mater.* 273 (2014) 1–6.
18. X.J. Yang, X.M. Xu, J. Xu, Y.F. Han, Iron oxychloride (FeOCl): an efficient Fenton-like catalyst for producing hydroxyl radicals in degradation of organic contaminants. *J. Am. Chem. Soc.* 135 (2013) 16058–16061.
19. Q. Zhan, W.T. Yao, X. Chen, L. Zhu, Y. Fu, G. Zhang, L. Sheng, S.H. Yu, Microwave-assisted controlled synthesis of monodisperse pyrite microspherulites. *Cryst. Growth Des.* 7 (2007) 1423–1431.
20. F. Amano, K. Nogami, R. Abe, B. Ohtani, Preparation and characterization of bismuth tungstate polycrystalline flake-ball particles for photocatalytic reactions. *J. Phys. Chem. C* 112 (2008) 9320–9326.
21. X. Guo, J. Yang, Y. Deng, H. Wei, D. Zhao, Hydrothermal synthesis and photoluminescence of hierarchical lead tungstate superstructures: effects of reaction temperature and surfactants. *Eur. J. Inorg. Chem.* (2010) 1736–1742.
22. X.J. Dai, Y.S. Luo, W.D. Zhang, S.Y. Fu, Facile hydrothermal synthesis and photocatalytic activity of bismuth tungstate hierarchical hollow spheres with an ultrahigh surface area. *Dalton Trans.* 29 (2010) 3426–3432.
23. W. Hu, Y. Zhao, Z. Liu, C.W. Dunnill, D.H. Gregory, Y. Zhu, Nanostructural evolution: from one-dimensional tungsten oxide nanowires to three-dimensional ferberite flowers. *Chem. Mater.* 20 (2008) 5657–5665.
24. Y.X. Zhou, H.B. Yao, Q. Zhang, J.Y. Gong, S.J. Liu, S.H. Yu, Hierarchical FeWO₄ microcrystals: solvothermal synthesis and their photocatalytic and magnetic properties. *Inorg. Chem.* 48 (2009) 1082–1090.
25. H. Fu, C. Pan, L. Zhang, Y. Zhu, Synthesis, characterization and photocatalytic properties of nanosized Bi₂WO₆, PbWO₄ and ZnWO₄ catalysts. *Mater. Res. Bull.* 42 (2007) 696–706.
26. A. Ankita, A. Rakshit, A. Mamta, Non-TiO₂ Based Photocatalysts for Remediation of Hazardous Organic Pollutants under Green Technology-Present Status: A Review. *Acta Chem. Pharm. Ind.* 3 (2013) 268–276.
27. T. Monitini, N. Gombac, A. Hameed, L. Felisari, G. Adami, P. Fornasiero, Different catalytic behavior of amorphous and crystalline cobalt tungstate for electrochemical water oxidation. *Chem. Phys. Lett.* 498 (2012) 113–119.
28. Y.X. Zhou, H.B. Yao, S. Zhang, J.Y. Gong, S.I. Liu, S.H. Yu, Hierarchical FeWO₄ microcrystals: solvothermal synthesis and their photocatalytic and magnetic properties. *Inorg. Chem.* 48 (2009) 1082–1090.
29. Z.G. Chen, H. Ma, J.X. Xia, J. Zeng, S. Yin, L. Xu, H.M. Li, Facile microwave-assisted ionic liquid synthesis of sphere-like BiOBr hollow and porous nanostructures with enhanced photocatalytic performance. *Ceram. Int.* 42 (2016) 8997–9003.
30. B. Jansi Rani, G. Ravi, R. Yuvakkumar, M. Praveenkumar, S. Ravichandran, P.M. Mareeswaran, S.I. Hong, Bi₂WO₆ and FeWO₄ nanocatalysts for the electrochemical water oxidation process, *ACS Omega* 4 (2019) 5241–5253.
31. F. Yu, L. Cao, J. Huang, J. Wu, Effects of pH on the microstructures and optical property of FeWO₄ nanocrystallites prepared via hydrothermal method. *Ceramic Int.* 39 (2013) 4133–4138.





Tamilarasi and Balakrishnan

32. K. Gowthami, B. Krishnakumar, Abilio J.F.N. Sobral, G. Thirunarayanan, M. Swaminathan, R. Siranjeevi, T. Rajachandrasekar, I. Muthuvel, Fabrication of Hybrid Fe₂V₄O₁₃/ZnO Heterostructure for Effective Mineralization of Aqueous Methyl Orange Solution. *J. Cluster Sci.* (2019), 1-11.
33. J.Y. Feng, X.J. Xu, P.L. Yue, H.Y. Zhu, G.Q. Lu, Aligned α-FeOOH nanorods anchored on a graphene oxide-carbon nanotubes aerogel can serve as an effective Fenton-like oxidation catalyst. *Water Res.* 37 (2003) 3776–3784.
34. G. Bandekar, N.S. Rajurkar, I.S. Mulla, U.P. Mulik, D.P. Amalnerkar, P.V. Adhyapak, Synthesis, characterization and photocatalytic activity of PVP stabilized ZnO and modified ZnO nanostructures. *Appl. Nanosci.* 4 (2014) 199–208.
35. A. Balcha, O.P. Yadav, T. Dey, Photocatalytic degradation of methylene blue dye by zinc oxide nanoparticles obtained from precipitation and sol-gel methods. *Environ. Sci. Pollut. Res. Int.* 23 (2016) 25485–25493.

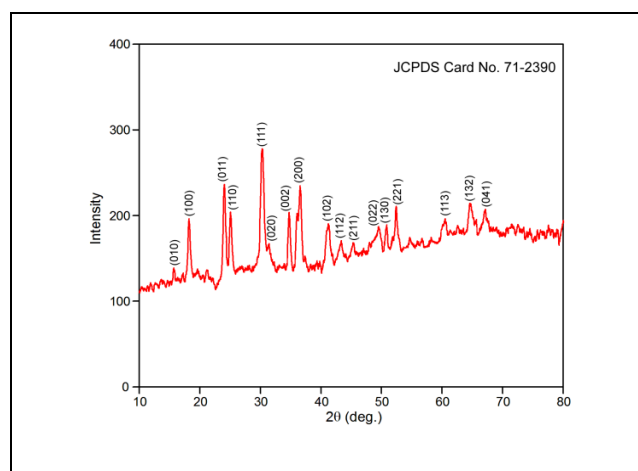


Fig. 1 XRD pattern of FeWO₄

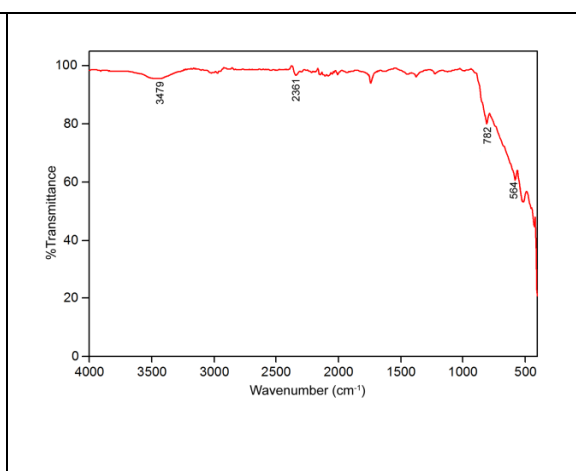


Fig. 2 FT-IR spectrum of FeWO₄

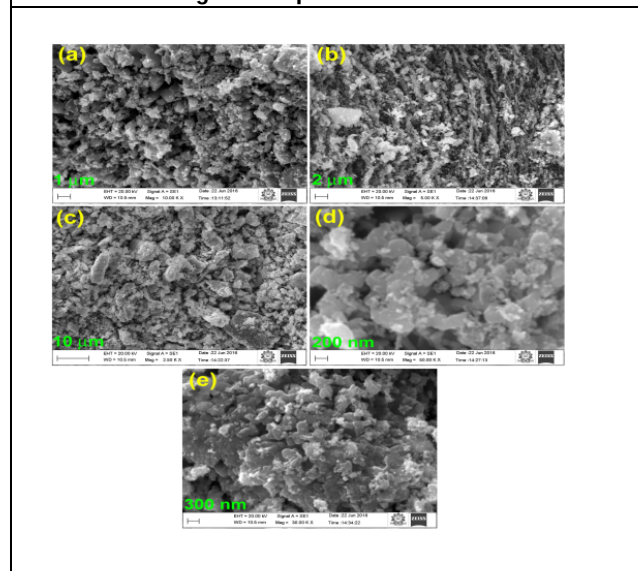


Fig. 3. FE-SEM images of FeWO₄: a) 1 μm, b) 2 μm, c) 10 μm, d) 200 nm and e) 200

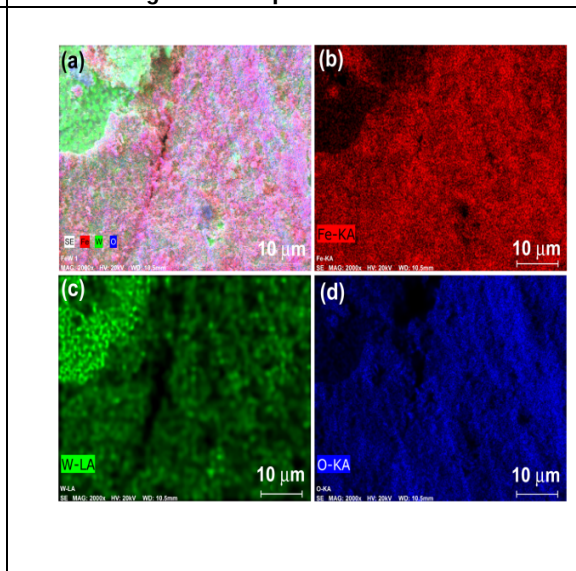


Fig. 4 Elemental colour mapping images of FeWO₄: a) FeWO₄ composition, b) Fe, c) W and d) O





Tamilarasi and Balakrishnan

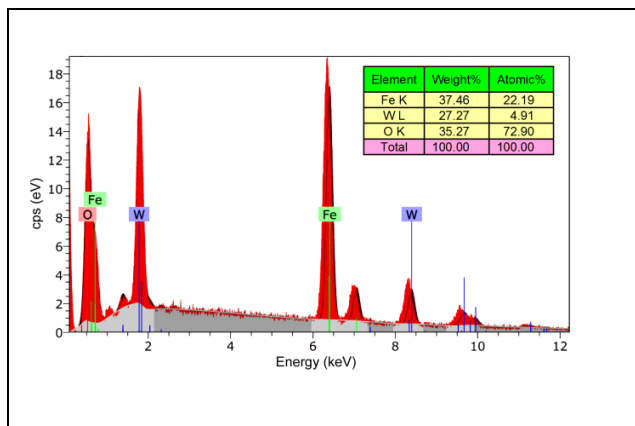


Fig. 5 EDX of FeWO₄

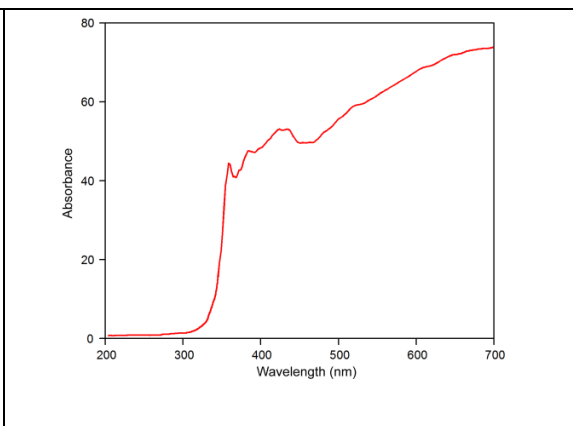


Fig. 6. UV-DRS of FeWO₄

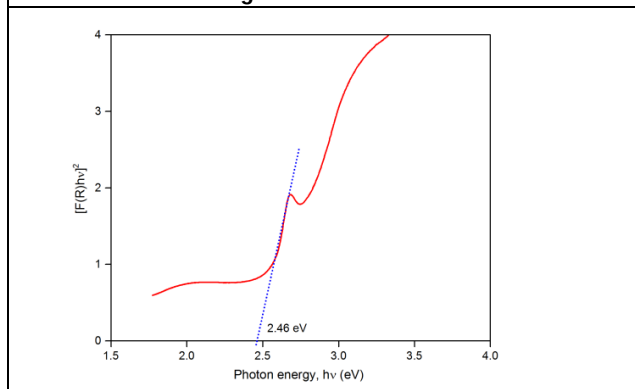


Fig. 7. Tauc plot of FeWO₄

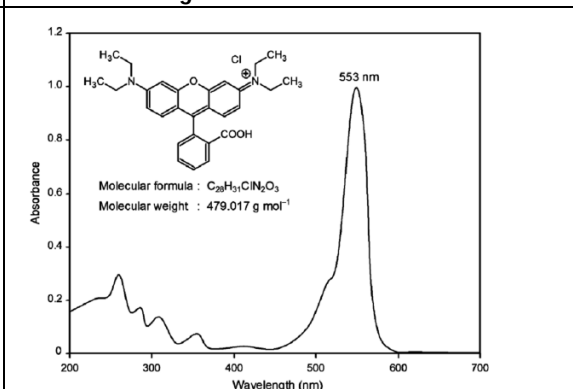


Fig. 8 Structure of Rh-B and its absorption spectrum, Absorbance maximum at 553 nm

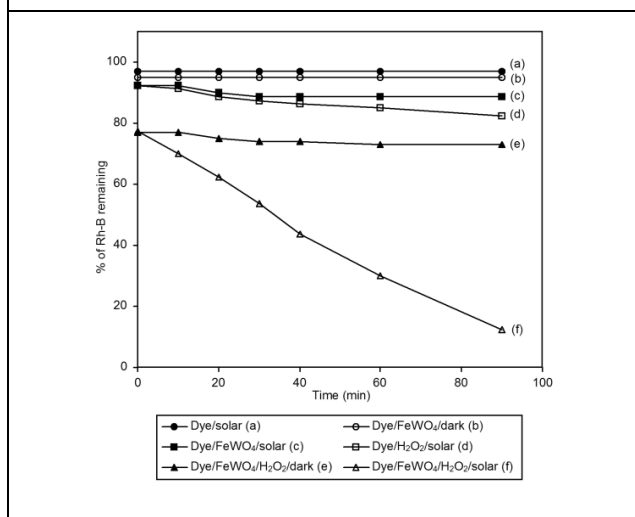


Fig. 9. Primary analysis of Rh-B under solar light. [Rh-B] = 5×10⁻⁴ M, catalyst suspended = 1 g L⁻¹, H₂O₂ = 10 mmol, airflow rate = 8.1 mL s⁻¹, pH 7, I_{solar} = 1250×100±100 lux.

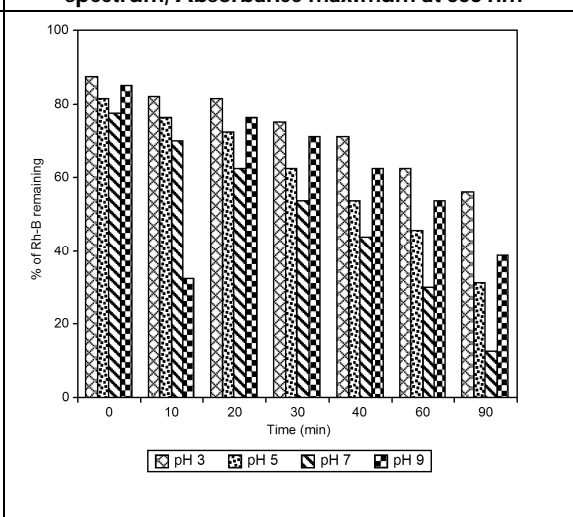


Fig. 10. Effect of pH. [Rh-B] = 5×10⁻⁴ M, catalyst suspended = 1 g L⁻¹, H₂O₂ = 10 mmol, airflow rate = 8.1 mL s⁻¹, irradiation time = 30 min, I_{solar} = 1250×100±100 lux.





Tamilarasi and Balakrishnan

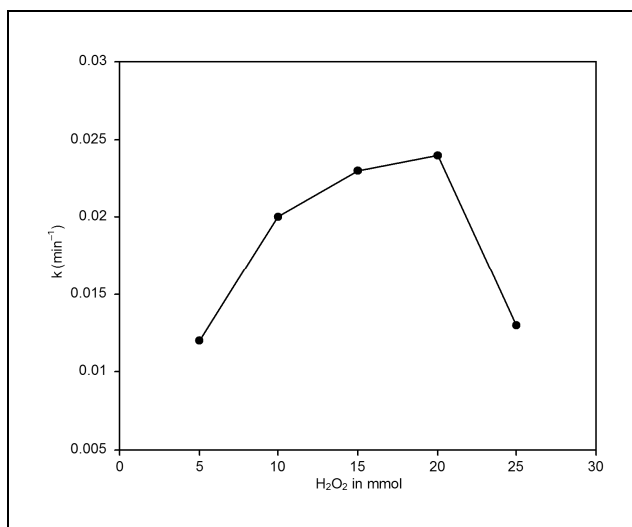


Fig. 11. Effect of H₂O₂ dosage. [Rh-B] = 5×10⁻⁴ M, catalyst suspended = 1 g L⁻¹, airflow rate = 8.1 mL s⁻¹, pH 7, irradiation time = 30 min, I_{solar} = 1250×100±100 lux.

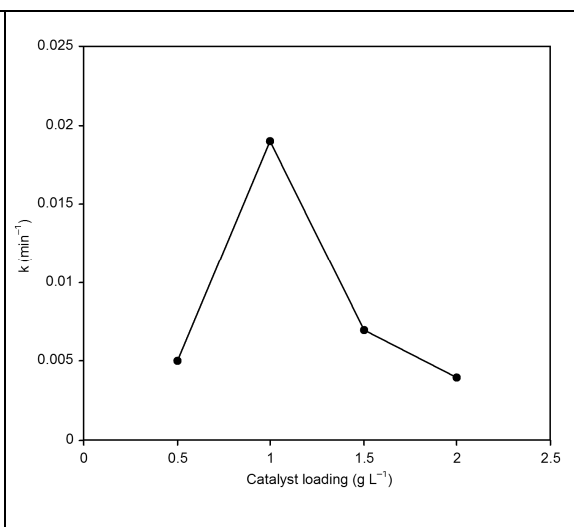


Fig. 12. Effect of catalyst loading. [Rh-B] = 5×10⁻⁴ M, H₂O₂ = 20 mmol, airflow rate = 8.1 mL s⁻¹, pH 7, irradiation time = 30 min, I_{solar} = 1250×100±100 lux.

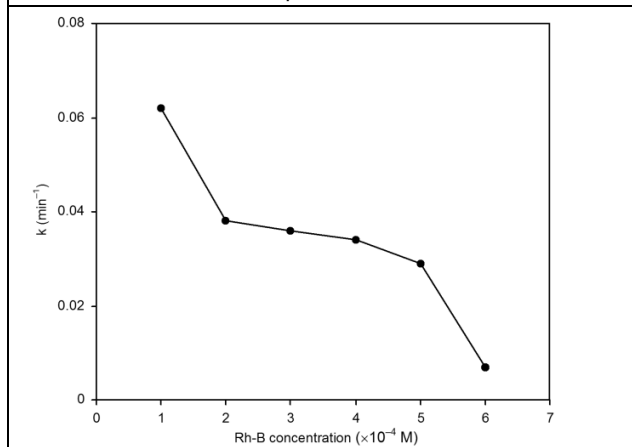


Fig. 13. Effect of dye concentration. Catalyst suspended = 1 g L⁻¹, H₂O₂ = 20 mmol, airflow rate = 8.1 mL s⁻¹, pH 7, irradiation time = 20 min, I_{solar} = 1250×100±100 lux.

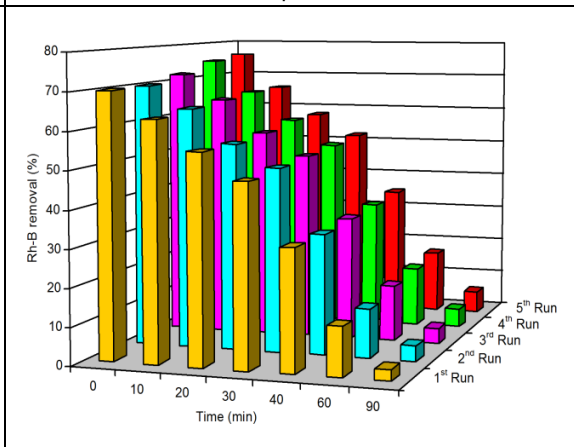


Fig. 14. Long-term stability. [Rh-B] = 5×10⁻⁴ M, catalyst suspended = 1 g L⁻¹, H₂O₂ = 20 mmol, airflow rate = 8.1 mL s⁻¹, pH 7, irradiation time = 90 min, I_{solar} = 1250×100±100 lux.





Utilization of Plastic Waste for Paver Blocks

Monalisha Pani* and Chiranjeeb Prasad Mohanty

Centurion University of Technology and Management, Odisha, India.

Received: 12 Sep 2020

Revised: 14 Oct 2020

Accepted: 16 Nov 2020

*Address for Correspondence

Monalisha Pani

Centurion University of Technology and Management,
Odisha, India.

Email: monalisha.pani@cutm.ac.in



This is an Open Access Journal / article distributed under the terms of the **Creative Commons Attribution License** (CC BY-NC-ND 3.0) which permits unrestricted use, distribution, and reproduction in any medium, provided the original work is properly cited. All rights reserved.

ABSTRACT

Concrete is the common material used for erection purpose in the high-society. Using misspend of plastic material for manufacturing of concrete, reduces plastic pollution as well as wastage of plastic from municipal areas. The blocks are normally available in the form of rectangular shape and has more or less same size as the bricks. But now a days various shapes are also available. Recently the shape of the block has improved from non-interlocking to interlocking and it can be used in construction of roads and pavements. As the rate of humiliation of plastic waste is increasing, we can use these waste plastic into a new innovative form by making Paver blocks out of the waste plastics. This article, presents the experimentation and finding of the project based on use of waste plastic to new productive resource.

Keywords: Concrete, plastic, construction, shapes, material.

INTRODUCTION

Paver block is an adaptable, restrained appearance, serviceable, and avaricious and it need little or no continuance if it is properly constructed and designed [1]. Almost all concrete blocks are designed in India. But the two main scope of treats fail occasionally due to excessive surface wear, and variability in the strength of block. The most common of pattern of the Paver block is herringbone pattern. This pattern is the most common and well-built paving bond as it provides intermesh quality, so that it can be used for manufacturing a well alternative for carriage way and road surfacing. The favored kind of specimen is stretcher bond and basket weave design. Squander plastic materials are used to totally put back the conventional cement which is used for binding purpose in blocks of concrete paving to ameliorate crave engineering properties of paving blocks for road pavement and other purposes also [1]. Melted LDPE are blends with fine aggregate and coarse aggregate to construct paving blocks for road pavement purposes [2]. Plastic is a synthetic material having molecular structure built up chiefly or completely from a large number of similar units bonded together, such as polyethylene, PVC, nylon, etc., that can be moulded into shape while soft, and then set into an inflexible or slightly elastic form[3]. Plastic might be obtained by reprocessing with respect to waste management [4]. If the plastics are not reprocessed then that leads to the major cause of environment pollution as



**Monalisha Pani and Chiranjeeb Prasad Mohanty**

they do not combine and get decomposed in the soil [3]. This create prodigious hassle in percolation process and proves to be toxicant which is inimical for environment as well as for all living beings. After burning and melting of waste plastic materials the Paver block is designed [2]. In this process, plastic bottles and polythene are accumulated and then smouldered [4]. After that the burnt particles are kept in low temperature to cool down in a close chamber and then converted into the liquid state and then stockpiled and combine with other additive materials for manufacturing of plastic Paver blocks.

MATERIAL SELECTION WITH ITS PROPERTIES

For re-designing of plastic Paver blocks various materials such as geosynthetic aggregate, stone dust, cement, water, com-mixture, ceramic waste and waste plastic materials from municipal area has been used.

Plastic waste: Plastic is the general material which is term for wide range of synthetic or semi synthetic organic formless solid material obtained from oil and natural gas. For this project, plastic waste was collected from the surrounding locality for making the Paver block [1]. Then after it is converted into brittle form as well as the liquid form.

Quarry dust: Quarry dust is a byproduct of the crushing process which is a vigorous material to use as aggregate for concreting purpose, especially as fine aggregates. In quarrying method, first the rocks are crushed into various sizes; during the process the dust generated is called quarry dust and it is formed as waste material. In this project crushed sand is shorter than 4.75 mm, which is generated from rock using the state of crushing. Generation of quarry fineness is a significance of removal.

Coarse Aggregate: Coarse aggregate is the portion of the concrete which is made up of the large stone implants in the mix. The aggregate may be of fine sand and coarse gravel and in this project work the aggregate were obtained very easily and sectionally. For checking out the crushed stone it should have first screening. As per the IS:383-1970 sieve, the aggregate which has been screened through 12mm sieve and hold on 10mm sieve is the specific size of the aggregate that has been obtained [2].

Ceramic Waste: Ceramic waste can be used in the concrete for improving its strength and durability factors also. It can be used as a partial replacement of cement or as a partial replacement of fine aggregate or sand as a supplementary addition that has to reach different properties of concrete [2]. The ejection of those squander requires broader area. So it is very arduous to discover the use of ceramic waste manufacture.

Admixture: Polycarboxylate super plasticizer are also added for concrete manufacturing process because it affords excellent control over initial and final setting times. Retarding admixtures has also been used because of it effects on high temperature and to avoid complications when unavoidable delays between mixing and placing occur.

Concrete Mix Design

Concrete mix design is the process of finding the appropriate proportion or ratio of materials such as cement, fine aggregate, coarse aggregate and water to achieve the target strength in structures. It involves various steps, calculations and laboratory testing to find right mix proportion. In this project, M20 grade concrete has been used to form design mix concrete as per by IS456-2000. It has been used for both ordinary and plastic pavement blocks [3]. As per M20 grade concrete, the water cement ratio was taken 0.5 for ordinary concrete and for plastic Paver block no moisture was added [2]. Three square dummy container was prepared for casting of blocks. The volume of each carried 0.00206 cubic meter and then the quantities of materials essential per cubic meter was decided by IS method.





Monalisha Pani and Chiranjeeb Prasad Mohanty

RESULTS AND DISCUSSION

From this finding it is observed that by adding 5% of misused plasticizer a minute divergence of compressiveness has occurred. From this experiment it has been noticed that the compressiveness utility of concrete blend reduced with inclusion of squander plasticizer eminently 5% of squander plastics. So we can append squander plastics in blocks of concrete that may act as a source of help to restate blocks of concrete with the help of plastic.

CONCLUSION

Plastic is a revolutionary substance for redesigning in construction purpose. This project succeeds in highlighting the use of plastic waste as a productive resource. Plastic Paver block is a high-yielding way of discarded plastic waste and it proves to have better results in strength wise. It can be used for light traffic road or footpath. For manufacturing of plastic Paver block, less amount of time is required. It is cost effective as in comparison to concrete Paver block. Observation from the above feature indicates that, aggregate cement can be replaced by plastics to design the Paver blocks. We can use squander with concrete mix design of cement for the erection of walkway. The resistance of concrete cement is equivalent with normal concrete cement. The best alternate gratified squander plasticizers has been set to 5% for surface blocks and 3% for rock hard blocks. However through this project and the analysis done, it highlights the usage of waste material like plastic can be recycled in to a useful product like plastic pavement blocks which are less brittle and more elastic in nature than blocks of concrete pavements.

REFERENCES

1. S. Vanitha, V. Natrajan and M. Praba. Utilization of waste plastics as a partial replacement of coarse aggregate in concrete paver blocks, Indian Journal of Science and Technology, June 2015.
2. Jeevan Ghuge, Saurabh Surale, Dr. B.M. Patil, S B Bhutekar .Utilization of waste plastic in manufacturing of paver blocks, International Research Journal of Engineering and Technology (IRJET), April 2019.
3. B. Shanmugavalli, K.Gowtham, P. JebaNaIwin, B. Eswara Moorthy. Reuse of plastic waste in paver blocks. International Journal of Engineering Research & Technology (IJERT) ISSN: 2278-0181, February-2017.
4. Mohan D.M.S1, Vignesh.J2, Iyyappan.P3, C.Suresh. Utilization of plastic bags in pavement blocks. International Journal of Pure and Applied Mathematics 1407-1415, 2018.
5. 1Sarang ShashikantPawar, 2Shubhankar AnantBujone. Use of Fly ash and Plastic in Paver Block. International Research Journal of Engineering and Technology (IRJET), e-ISSN: 2395-0056, Nov -2017.
6. Prakash Hanchinal1, Raju Jakkappannavar2, Shivan and Rathod3, Sunil Mayachari4.Paver blocks using waste plastic. International Journal of Technical Innovation in Modern Engineering & Science (IJTIMES), e-ISSN: 2455-2585, April-2019.
7. 1Ambrish Narayan Pandey, 2Abhishek Yadav, 3Durgesh Chaudhary, 4Nageshwar, 5Vijay Kumar Srivastava. Waste Plastic Used In Paving Block: A Research, ISSN:2279-543x, March 2019.
8. A.Panimayam1, P.Chinnadurai2, R.Anuradha*, K.Pradeesh4, A.Umar Jaffer4.Utilisation of Waste Plastics as a Replacement of Coarse aggregate in Paver Blocks. International Journal of Chem Tech Research, ISSN (Online):2455-9555, 2017.
9. Dinesh.S 1, Dinesh.A 2, Kirubakaran.K 3.Utilization of waste plastic in manufacturing of bricks and paver blocks. ISSN 0973-4562, 17May 2016.
10. R.jayasankar1, S.Dinesh2, k.mohamedshalmanparishee3, j.sriram4, m.mohamed, bashith5. Effective use of waste plastic as manufacturing of paver block. International Journal of Advanced Research in Basic Engineering Sciences and Technology (IJARBEST).





Monalisha Pani and Chiranjeeb Prasad Mohanty

Table-1(Properties and observations of materials)

Cement	Properties of cement		Observations
		Specific gravity	
	Consistency		34%
	Fineness		10
	Initial fixture time		25 minute
	Final fixture time		540 minute
Quarry dust	Specific gravity		1.99
	Categorized section		Soil of zonell
	Fineness modulus		1.95
	Water absorption		1.75
Coarse aggregate	Specific gravity	20 mm	2.36
		10 mm	2.59
	Water absorption	20 mm	4.1
		10 mm	3.1

Table-2 (Compressive Strength Test Report M 20 Grade Paver Block)

Sl no	Waste plastic in %age	7 days compressive strength N/mm ²	14 days compressive strength N/mm ²	28 days compressive strength N/mm ²
1	0%	9.6	16.6	25.8
2	2%	9.2	15.8	25.5
3	4%	8.9	15	26.3
4	6%	8	13.8	22
5	8%	5.4	12.9	16
6	10%	4	8	13





Assessment of Antioxidant Activity of Garcinol Derived from *Garcinia xanthochymus* Hook. f.

Gogoi Nabajyoti^{1*}, Gogoi Ankur², Neog Bijoy³ and Baruah Dibyojyoti³

¹Centre for Biotechnology and Bioinformatics, Dibrugarh University, Dibrugarh, Assam, India.

²Regional Medical Research Center, NE, ICMR, Dibrugarh, Assam, India.

³Plant Molecular Biology Laboratory, Department of Life Sciences, Dibrugarh University, Dibrugarh, Assam, India.

Received: 13 Sep 2020

Revised: 15 Oct 2020

Accepted: 16 Nov 2020

*Address for Correspondence

Gogoi Nabajyoti

Centre for Biotechnology and Bioinformatics,

Dibrugarh University,

Dibrugarh, Assam, India.

Email: gogoinabajyoti24@gmail.com / ORCID id: <https://orcid.org/0000-0001-5625-5596>



This is an Open Access Journal / article distributed under the terms of the **Creative Commons Attribution License** (CC BY-NC-ND 3.0) which permits unrestricted use, distribution, and reproduction in any medium, provided the original work is properly cited. All rights reserved.

ABSTRACT

The present investigation was designed to evaluate the antioxidant activity of Garcinol extracted from *Garcinia xanthochymus*. The crude extract of *G. xanthochymus* was subjected in column chromatography and elucidated with graduated polar solvents to achieve separated fractions. Out of 24 fractions, 7 fractions showed antioxidant activity at *in vitro* models which were evaluated by determined the IC₅₀. Fraction 1 showed highest antioxidant in all models, and its structure was elucidated with NMR spectrum and FTIR, found as Garcinol. Results revealed that the known polyisoprenylated benzophenone (Garcinol) was first reported in *G. xanthochymus* which exhibited antioxidant activity in DPPH, ABTS and NO models.

Keywords: Antioxidant, *Garcinia*, Garcinol, NMR

INTRODUCTION

Garcinia species has been known to be a rich source of bioactive compounds of oxygenated and prenylated phenol derivatives such as prenylated xanthenes, polyisoprenylated benzophenones, bioflavonoids and triterpenoids [1, 2, 3]. Many bioactive chemicals such as xanthenes, benzophenone, and flavonoids have been isolated from the fruits, leaves, and stem of *Garcinia mangostana*. The medicinal properties of plants can be attributed to a larger extent to xanthenes, the most bioactive constituents [4]. *Garcinia parvifolia* is recognized as a rich source of xanthone and xanthonoid natural products with high pharmaceutical and medicinal potential [5]. Many authors have recommended the antioxidant activity of garcinol in both *in vitro* as well as *in vivo* models. It has significant





Gogoi Nabajyoti et al.,

anticancer activity in both cell line and animal models. Among this *Garcinia* genus, *Garcinia xanthochymus* is a crucial species contributes significant antioxidant activity with high content of polyphenols [6]. Therefore in the present investigation designed such as way to isolate most antioxidant fraction from this species and elucidated its chemical structure.

MATERIALS AND METHODS

Chemicals: The analytic grade methanol, HPLC grade (Hexane, Ethyl acetate, ethanol, methanol), Silica gel (mesh size, 60-120), TLC plate were purchased from the mark Millipore.

Collection of plant and preparation of crude extract: A fresh fruit of *Garcinia xanthochymus* was collected and rind was separated from the fruits and dried in an oven by maintaining the temperature 25-30°C. It was powered by Mixer Grinder. The 10gm of powder sequentially soaked into the 80% methanol for the 48 hours in shaking condition in room temperature in Shaker incubator (Certomat®BS1, Germany). The extract was then filtered with Whatman No. 1 paper and concentrated in Rotary evaporator (IKA-RB10, IKA, Germany) under pressure. The concentrated extract was taken for the column chromatography.

Column chromatography: Concentrated extract (5gm) was then mixed (adsorbed) with the silica gel (60-120 mesh). The glass column was then packed with the silica gel and initially washed with the hexane for suitable flowing of the mobile phase. Then, the extract which was adsorbed with the silica gel was put in the column and eluted by increasing the polarity with the solvent mixer (100% hexane, hexane: ethyl acetate, ethyl acetate: methanol, and 100% methanol). The same fractions were collected and chromatographically (TLC) similar fractions were collected, concentrated and evaluated the antioxidant activity with DPPH, ABTS and NO model.

Antioxidant activity of the fraction: Eluted fragments were then subjected to evaluate the free radical scavenging activity in three different *in vitro* models; viz. DPPH, ABTS, NO. The experiment was carried out to determine the IC₅₀ of the active fragment by standard protocol [7, 8]. Briefly, the several concentration of fraction was subjected into the antioxidant system and evaluated the 50% inhibition by the fractions. The IC₅₀ was determined for each fraction by plotting the regression curve, in X-axis concentration of eluting fragment and in Y-axis inhibition of eluting fragments in the antioxidant system, in the curve we can calculate the X value, where Y=50. The most potent antioxidant fraction was then subjected to FTIR, NMR for structural conformation.

Thin layer chromatography: Thin Layer Chromatography (TLC) is a solid-liquid type in which the two phases are present, a solid (stationary phase) and a liquid (mobile phase). Solid phases, most commonly used in chromatography are silica gel (SiO₂ x H₂O) and alumina (Al₂O₃ x H₂O). In our experiments, TLC was done to identify the same fraction initially and finally to understand the purity of the highest antioxidant activity fraction. TLC was done in Merck Millipore TLC silica gel plate. Different ratios of the solvent system were used as mobile phase in the experiment.

FTIR analysis: FTIR analysis was done in BRUKER (Vertex70, US), to understand the presence of the functional group in the most active fraction.

Nuclear Magnetic Resonance (NMR) analysis: Proton NMR analysis was carried in AVANCE III 500 MHz FT-NMR Spectrometer (BRUKER, Switzerland) at NEIST, Jorhat in hire basis. In the NMR analysis, the chloroform was used as a solvent.





RESULTS

Fraction isolation: Column chromatography of methanolic extract of *Garcinia xanthochymus* gave a total 24 fractions. The same fraction was collected by TLC using a suitable solvent system (Hexane: Ethyl acetate in different ratio) and total 7 similar fractions were concentrated and further used for the antioxidant activity. Elucidate solvent system and amount of the particular fraction was listed in Table 1. The amount of isolated fractions by the different solvent system, found that the highest amount of isolated fraction was found the fraction 7, elucidated with the 100% methanol and the lowest amount was found in the fraction no 4, elucidated with the 8:2(v/v) ratio of ethyl acetate and methanol only.

Antioxidant activity: All the fractions were subjected to evaluate the antioxidant activity. The antioxidant activity was carried out in the three *in vitro* assays, viz. DPPH, ABTS, and NO. The IC₅₀ was calculated for each fraction, which is listed in Table 2. The fractions activities in the antioxidant models revealed that the least IC₅₀ was shown by fraction 1, considered as the most potent antioxidant fraction in all models. Physical properties of the fraction 1 were yellow in color; needle crystal with melting temperature 709.15°C was recorded.

Structure preparation: Fraction 1 was again purified by extracting by hexane and ethyl acetate, and subjected to the TLC, FTIR, and NMR for structure preparation.

TLC analysis: The fraction 1 was elucidated with the Hexane: Ethyl acetate (7:3) and 20mg was obtained which showed the single spot in TLC (Fig 2), the TLC solvent system Hexane: Ethyl acetate (5:5). The purified fraction was subjected to spectroscopic analysis such as FTIR and NMR.

FTIR analysis: The FTIR analysis of the fraction 1 help to analyzed the functional group present in the particular compound. The fingerprints of the FTIR assumed the containing high molecular weight functional groups (Fig 3).

NMR- analysis: The fingerprint of proton (Fig 4) gave the following data [¹H NMR (CDCl₃)] 6.95 (1H, dd, J 9.0 and 2.0 Hz), 6.91 (1H, d, J 2.0 Hz), 6.60 (1H, d, J 9.0 Hz), 4.96, 5.06, 5.10 (1H each, t, J 5.0 Hz), 4.40 (d, J 15.0 Hz), 2.80–1.46 (m, 12H, methylene and methyne), 1.78, 1.74, 1.69, 1.62, 1.59, 1.56, 1.21, 1.05 (3H each). From the data it can be said that presence of three aromatic protons in 3,4-dihydroxybenzoyl group, three isopropylidene group, one isoprenyl group and two saturated carbon. The data from the ¹H- NMR the fraction has been identified as Garcinol (Fig 5) [9].

DISCUSSION

It was observed *Garcinia xanthochymus* exhibited the highest antioxidant activity in all three models. So, this methanolic extract was further subjected to the separation of fraction or compounds using the Column chromatography. The earlier observation was revealed the presence of many bioactive compounds in the *Garcinia xanthochymus*. Methanolic extract of this species have two new benzophenones, guttiferone H and gamboginone [10], many prenylated xanthones [11, 12, 13] has been reported. In other species also many bioactive benzophenone are also reported [14, 15, 16, 17, 18] with significant amount of antioxidant activity. In the present study, the polyprenylated benzophenones (garcinol) was isolated, as Clusiaceae family containing benzophenones [19], and most of the benzophenones reported from genus *Garcinia* are polyisoprenylated structural group [20] supported the present investigation. The presence of garcinol in the *Garcinia* species was first reported by Krishnamurthy *et al.* [21] from the fruit rind of *G. indica*, fruits of *G. cambogia* and stem bark of *G. huillensis* [22, 23], also supported the present investigation. We also found that the fraction 1, later identified as garcinol have the highest antioxidant activity with very less IC₅₀ values compare to the other fractions could be responsible for the antioxidant activity. The present



**Gogoi Nabajyoti et al.,**

observation supported by Ito *et al.* [24] observation that garcinol, isogarcinol, guttiferone H and E, gambogenone, xanthochymol, cycloxanthochymol, isoxanthochymol and aristophenones exhibited significant antioxidant activity against DPPH radicals, among which garcinol showed nearly three times more activity than the standard DL-tocopherol [25]. Others observation of antioxidant activity of garcinol was reported by Yamagusi *et al.*, [26] at *in vitro* model such as DPPH, H₂O₂ and superoxide ion model and *in vivo* model using animal stomach. Antioxidant activities of garcinol in different models were observed by Sang *et al.* [27] and Liao *et al* [28] supported the present findings.

CONCLUSION

The present investigation revealed that the garcinol is mainly responsible for the higher antioxidant activity exhibited by *Garcinia xanthochymus*. It containing in very less amount in the fruit *i.e.* out of 5gm of crude extract 150mg of Garcinol is reported in the present study. It can be also concluded that polyisoprenylated benzophenones (garcinol) have diverse pharmacological properties can be synthetically modified to produce new and active molecules for future drug development and treatments for many diseases.

ACKNOWLEDGEMENTS

The authors express sincere gratitude to ICMR, New Delhi for financial support (No. 59/14/2011/BMS/TRM, dt.25.03.2015).

REFERENCES

1. Babu, V., Ali, S. M., Sultana, S. and Ilyas, M. (1988) A biflavonoid from *Garcinia nervosa* Phytochemistry 27(10):3332-3335
2. de Oliveira, C. M., Porto, A. L., Bittrich, V. and Marsaioli, A. J. (1999) Two polyisoprenylated benzophenones from the floral resins of three *Clusia* species Phytochemistry 50(6):1073-1079
3. Nyemba, A. M., Mpondo, T. N., Connolly, J. D. and Rycroft, D. S. (1990) Cycloartane derivatives from *Garcinia lucida* Phytochemistry 29(3):994-997
4. Pedraza-Chaverri, J., Cárdenas-Rodríguez, N., Orozco-Ibarra, M. and Pérez-Rojas, J. M. (2008) Medicinal properties of mangosteen (*Garcinia mangostana*) Food and Chemical Toxicology 46(10):3227-3239
5. Xu, G., Feng, C., Zhou, Y., Han, Q. B., Qiao, C. F., Huang, S. X., Chang, D.C., Zhao, Q.S., Luo, K.Q. and Xu, H.X. (2008) Bioassay and ultraperformance liquid chromatography/mass spectrometry guided isolation of apoptosis-inducing benzophenones and xanthone from the pericarp of *Garcinia yunnanensis* Hu. Journal of Agricultural and Food Chemistry 56(23):11144-11150
6. Gogoi, N., Gogoi, A., Neog, B. (2015). Free radical scavenging activities of *Garcinia xanthochymus* hook. F. and *Garcinia lanceaefolia* roxb. using various in vitro assay models. Asian Journal of Pharmacology and Clinical Research, 8(3), 138-141.
7. Brand-Williams, W., Cuvelier, M. E. and Erset, C. L. W. T. (1995) Use of a free radical method to evaluate antioxidant activity LWT-Food Science and Technology 28(1): 25-30
8. Bondet, V., Brand-Williams, W. and Berset, C. (1997) Kinetics and mechanisms of antioxidant activity using the DPPH free radical method LWT-Food Science and Technology 30: 609-615
9. Sang, S., Pan, M. H., Cheng, X., Bai, N., Stark, R. E., Rosen, R. T. *et al.* (2001) Chemical studies on antioxidant mechanism of Garcinol: analysis of radical reaction products of Garcinol and their antitumor activities Tetrahedron 57(50):9931-9938
10. Lin, K. W., Huang, A. M., Yang, S. C., Weng, J. R., Hour, T. C., Pu, Y. S. and Lin, C.N. (2012) Cytotoxic and antioxidant constituents from *Garcinia subelliptica* Food Chemistry 135(2):851-859



**Gogoi Nabajyoti et al.,**

11. Chanmahasathien, W., Li, Y., Satake, M., Oshima, Y., Ruangrunsi, N. and Ohizumi, Y. (2003) Prenylated xanthenes with NGF-potentiating activity from *Garcinia xanthochymus* Phytochemistry 64(5):981-986
12. Chen, Y., Zhong, F., He, H., Hu, Y., Zhu, D. and Yang, G. (2008) Structure elucidation and NMR spectral assignment of five new xanthenes from the bark of *Garcinia xanthochymus*. Magnetic Resonance in Chemistry 46(12):1180-1184
13. Chen, Y., Fan, H., Yang, G. Z., Jiang, Y., Zhong, F. F. and He, H. W. (2010) Prenylated xanthenes from the bark of *Garcinia xanthochymus* and their 1, 1-diphenyl-2-picrylhydrazyl (DPPH) radical scavenging activities. Molecules 15(10):7438-7449
14. Wu, C. C., Weng, J. R., Won, S. J. and Lin, C. N. (2005) Constituents of the Pericarp of *Garcinia subelliptica*. Journal of natural products 68(7):1125-1127
15. Masullo, M., Bassarello, C., Suzuki, H., Pizza, C. and Piacente, S. (2008) Polyisoprenylated benzophenones and an unusual polyisoprenylated tetracyclic xanthone from the fruits of *Garcinia cambogia*. Journal of Agricultural and Food Chemistry 56(13):5205-5210
16. Chen, J. J., Ting, C. W., Hwang, T. L. and Chen, I. S. (2009) Benzophenone derivatives from the fruits of *Garcinia multiflora* and their anti-inflammatory activity. Journal of Natural Products 72(2): 253-258
17. Zhang, Y., Song, Z., Hao, J., Qiu, S. and Xu, Z. (2010) Two new prenylated xanthenes and a new prenylated tetrahydroxanthone from the pericarp of *Garcinia mangostana*. Fitoterapia 81(6):595-599
18. Stark, T. D., Salger, M., Frank, O., Balemba, O. B., Wakamatsu, J. and Hofmann, T. (2015) Antioxidative compounds from *Garcinia buchananii* stem bark. Journal of natural products 78(2):234-240
19. Acuna, U. M., Jancovski, N. and Kennelly, E. J. (2009) Polyisoprenylated benzophenones from Clusiaceae: potential drugs and lead compounds. Current topics in Medicinal Chemistry 9(16): 1560-1580
20. Wu, S. B., Long, C. and Kennelly, E. J. (2014) Structural diversity and bioactivities of natural benzophenones. Natural product reports 31(9):1158-1174
21. Krishnamurthy, N., Lewis, Y. S. and Ravindranath, B. (1981) On the structures of Garcinol, isogarcinol and camboginol. Tetrahedron Letters 22(8):793-796
22. Bakana, P., Claeys, M., Totté, J., Pieters, L. A., Van Hoof, L., Van Den Berghe, D. A. and Vlie-tinck, A. J. (1987) Structure and chemotherapeutical activity of a polyisoprenylated benzophenone from the stem bark of *Garcinia huillensis*. Journal of Ethnopharmacology 21(1): 75-84
23. Masullo, M., Bassarello, C., Bifulco, G. and Piacente, S. (2010) Polyisoprenylated benzophenone derivatives from the fruits of *Garcinia cambogia* and their absolute configuration by quantum chemical circular dichroism calculations. Tetrahedron 66(1):139-145
24. Ito, C., Itoigawa, M., Miyamoto, Y., Onoda, S., Rao, K. S., Mukainaka, T., Tokuda, H., Nishino, H. and Furukawa, H. (2003). Polyprenylated benzophenones from *Garcinia assigu* and their potential cancer chemopreventive activities. Journal of Natural Products 66(2):206-209
25. Baggett, S., Protiva, P., Mazzola, E. P., Yang, H., Ressler, E. T., Basile, M. J. and Kennelly, E. J. (2005) Bioactive Benzophenones from *Garcinia xanthochymus* Fruits. Journal of Natural Products 68(3):354-360
26. Yamaguchi, F., Saito, M., Ariga, T., Yoshimura, Y. and Nakazawa, H. (2000) Free radical scavenging activity and antiulcer activity of Garcinol from *Garcinia indica* fruit rind. Journal of Agricultural and Food Chemistry 48(6):2320-2325
27. Sang, S., Liao, C. H., Pan, M. H., Rosen, R. T., Lin-Shiau, S. Y., Lin, J. K. and Ho, C. T. (2002) Chemical studies on antioxidant mechanism of Garcinol: analysis of radical reaction products of Garcinol with peroxy radicals and their antitumor activities. Tetrahedron 58(51):10095-10102
28. Liao, C. H., Ho, C. T. and Lin, J. K. (2005) Effects of Garcinol on free radical generation and NO-production in embryonic rat cortical neurons and astrocytes. Biochemical and Biophysical Research Communications 329(4):1306-1314





Gogoi Nabajyoti et al.,

Table 1. The amount of isolated fraction from the *G. xanthochymus* fruit extract, and the elucidated solvent system

Fraction code	Elucidated solvent system (v/v)	Fraction amount
1	Hexane: Ethyl acetate (7:3)	150mg
2	Hexane: Ethyl acetate(5:5)	300mg
3	Hexane: Ethyl acetate (2:8)	250mg
4	Ethyl acetate: Methanol (8:2)	180mg
5	Ethyl acetate: Methanol (3:7)	250mg
6	Ethyl acetate: Methanol(5:5)	185mg
7	100% Methanol	200mg

Table 2. The antioxidant activity of the isolated fraction from the *G. xanthochymus* fruit extract, value is expressed in mean±SEM of three replicates, IC₅₀= sample concentration exhibit 50% inhibition of free radicals at *in vitro* assay

Fraction code	DPPH(IC ₅₀ , µg/mL)	ABTS (IC ₅₀ ,µg/mL)	NO (IC ₅₀ µg/mL)
1	15.29± 0.20	1.26±0.06	433.06±1.63
2	43.58±1.72	70.01± 0.19	749.23± 1.24
3	65.37±0.83	8.34± 0.09	570.05± 0.98
4	820.36± 2.73	108.76± 0.87	1586.65±3.39
5	304.92± 3.46	108.04± 0.70	NO ACTIVITY
6	1583.65± 1.45	607.81± 3.161	NO ACTIVITY
7	1251.34± 5.69	350.30± 2.25	NO ACTIVITY

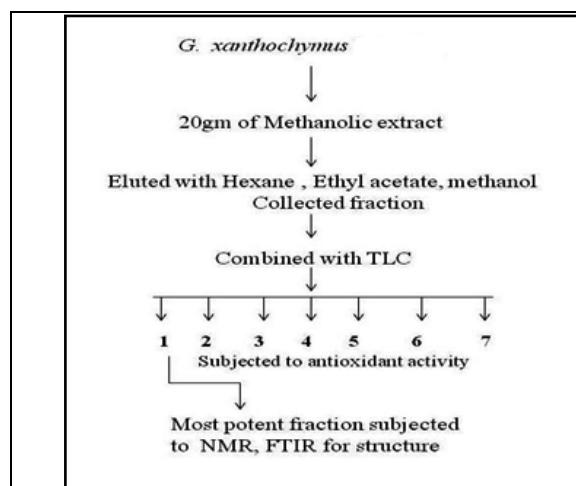


Fig 1 Pictorial representation of isolation of active principle compounds from the crude rind extract of *G. xanthochymus*

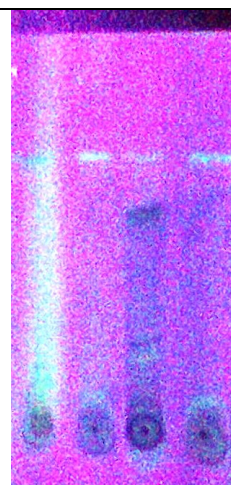


Fig 2 TLC analysis showing the single spot in UV-light, R_f = 0.38





Gogoi Nabajyoti et al.,

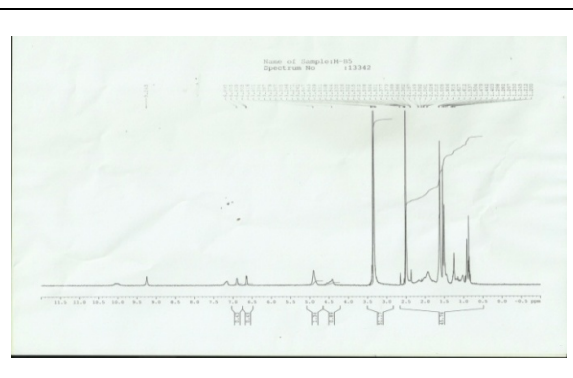
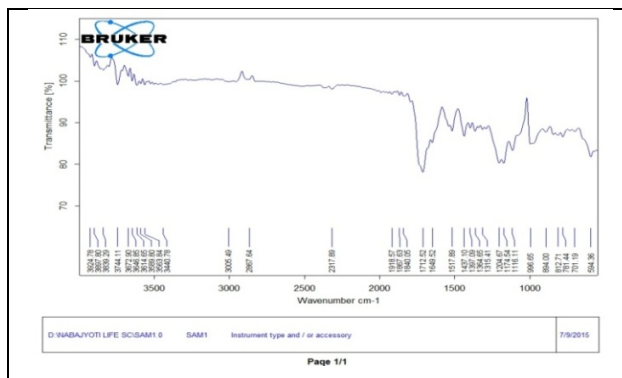


Fig 3 FTIR Spectrum of fraction 1 isolated from the methanol extract of *G. xanthochymus*

Fig 4 Proton NMR spectrum of fraction 1 isolated from the methanolic extract of *G. xanthochymus*

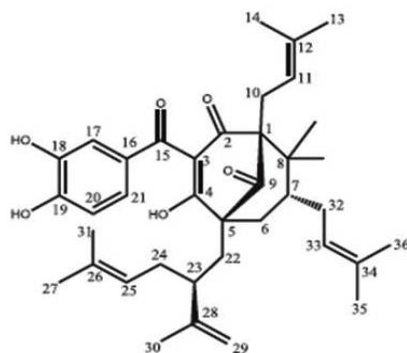


Fig 5 Structure of Garcinol, referred with the position of a proton in NMR [9].





A Review on Multi Dimensional uses of *Bauhinia variegata* Plant

Somalika Pradhan*

Centurion University of Technology and Management, Odisha, India.

Received: 10 Sep 2020

Revised: 14 Oct 2020

Accepted: 16 Nov 2020

*Address for Correspondence

Somalika Pradhan

Centurion University of Technology and Management,
Odisha, India.

Email: somalika.pradhan@cutm.ac.in



This is an Open Access Journal / article distributed under the terms of the **Creative Commons Attribution License** (CC BY-NC-ND 3.0) which permits unrestricted use, distribution, and reproduction in any medium, provided the original work is properly cited. All rights reserved.

ABSTRACT

Bauhinia variegata Linn is a well-known medium size plant belonging to the family Leguminosae plant and commonly known as cows Paw. *Bauhinia variegata* mostly used in traditional medicine for variety purposes of human health. The different parts of these plants like stem, bark, leaves, bud and flowers are widely rich in various phytochemicals which have been used since ancient times as a traditional medicine for diseases like diabetes, dysentery, piles, diabetes and skin diseases etc. It has numerous medicinal values and is rich in phytochemicals like tannin, flavonoids, terpenoids and kaempferol etc. Modern studies confirmed that *Bauhinia variegata* used as an anti-diabetic, anti-oxidant, anti-inflammatory and anti-carcinogenic purpose. This review shows a detailed survey on study of phytochemical, pharmacological and anti-microbial effect and also medicinal uses of *Bauhinia variegata*.

Keywords: *Bauhinia variegata*, Anti – oxidant, Phytochemical effect, Anti-microbial effect

INTRODUCTION

Plant species maintain our biodiversity and our ecosystem. Various plants on our planet have very much medicinal and pharmacological value. Since ancient age it has been concluded that various diseases are curable by using plant products, as plant are a source of high range of secondary metabolites. *Bauhinia variegata* is a species of flowering plant that belongs to the family Fabaceae and kingdom Plantae. Commonly this plant is known as mountain ebony. This plant has 10 to 12 cm long and broad leaves with the bright pink colour flowers of 8 to 12 cm in diameter. Contrary to synthetic drugs, antimicrobials of plant origin are not associated with many side effects and have an enormous therapeutic potential to treat many infectious diseases.



**Somalika Pradhan****Taxonomy of *Bauhinia variegata***

Kingdom	Plantae
Division	Tracheophyta
Class	Magnoliopsida
Family	Fabaceae
Genus	<i>Bauhinia</i>
Species	<i>Bauhinia variegata</i>

This plant is called kanchar in Hindi. It was planted in roadside, park and garden in most of the warm or tropical regions. It consists of About 200 to 300 species of medium sized which remain leafless in the month of February to April and after that period flowering of tree starts [2]. This plant has the ability to restore nitrogen so it can degrade soil particles. As synthetic drugs or medicine have some side effects so people want to use medicine which is coming from natural products obtained from plant [2]. It has been estimated that the active compounds used for medicine about 50% is from natural products. This plant is a source of high number of secondary metabolites which have medicinal value and gives importance to human health [1]. The various parts of *Bauhinia variegata* like bark, stem, seed, leaves, flowers and roots have been used for its high range of medicinal value. So, diseases like Dysentery, Diarrhea, Piles, Diabetic and other stomach disorders were cured by using these plant products. And also, it acts as antidote against snake bite [2]. The phytochemical screening showed that Variegate contained different phytochemicals which are required for the treatment of different kinds of pathologies. This plant has a great number of pharmacological properties and studies showed that Bauhinia Variegate exerted anticancer, antimicrobial, anti-inflammatory, antiulcer etc.

Traditional uses of *Bauhinia variegata* plant

In Medicines it has a great contribution to the environment. *Bauhinia variegata* is a medicinal plant as it has some similar properties as conventional drug. So all parts of the tree are used in traditional medicines and also in Ayurveda for the treatment of a wide variety of different health disorders. Bauhinia tree parts have many more healing properties due to the presence of various kinds of phytochemicals in it. It has anti-bacterial, anti-fungal, anti-malarial, cytotoxic, fever reducing and thyroid hormone regulating properties. The extensive use of *Bauhinia variegata* in treating glandular diseases, leprosy, intestinal worms, tumours, wounds, ulcers, inflammations, scrofula, proptosis, haemorrhoids, haemoptysis, cough, menorrhagia and bleeding disordersis found in Ayurveda. For treating diseases related to lymphatic system and glands the *Bauhinia variegata* is considered to be best. *Bauhinia variegata* is a medicinal tree and used in India for the treatment of various diseases. The leaves consist of a high amount of reducing monosaccharide and give good nutrition to the Tasar silkworm for its healthy growth and development. The root acts as an antidote to snake poison. The extract of flowers is used to treat many stomach disorders like diarrhea, dysentery etc. The dried buds also have many more contributions towards human health and it has been used for the treatment of dysentery, worms' piles, Wound healing or tumors [2].

Phytochemical Analysis

The main constituents or chemicals of *Bauhinia variegata* are as follows:

Aerial part

Phytochemical studies showed that non woody aerial part consists of, ombuin, Triterpene, Kaempferglycopyranoside ol-7, 4-dimethyle ether-3-o- β -D-2 glycopyranoside, Kaempferol 3-o- β -D-2 glycopyranoside, isorhamnetin 3-o- β -D-2 glycopyranoside [1].



**Somalika Pradhan****Stem and stem bark**

Bauhinia variegata stem and stem bark extract has contain sterols, Glycosides, Reducing sugars and nitrogenous substances on preliminary phytochemical analysis. The main chemical compound which is isolated from the bark of *B.vareigata* are quercitroside, Isoquercitroside, Rutosidemycetol glycoside and Kaempferol glycoside Bauhini one is one of the new phenanthraquinone isolated from *B.variegata* (Fig.1).

Seed

Seeds have protein, Oleic acid which consist of fatty acid, Linoleic acid and stearic acid. One organic solvent has been used for its extraction. This extraction gives 15% of light yellow colour fatty oil. Phytochemical analysis shows the presence of all-important amino acids like Valine leucine, Isoleucine, Lysine methionine and Phenylalanine and some other amino acids are also found like aspartic acid, Glutamic acid, Glycine and Tyrosine (Fig.2).

Leaves

Heptatriacontane-12, 13-diol and doletracont-15-en-9-ol have been extracted from leaves of *B. variegata*. Leaves which are long chain organic compounds. The leaves have high content of ascorbic acid and reducing monosaccharide and also contain tannins, sterol etc. Structures of the new organic compound have been analyzed by spectral studies. Transmission electron microscopy study of leaves confirmed the presence of insulin like protein in chloroplast. So the presence of this protein in leaves may indicates its involvement in carbohydrate metabolism (Fig.3).

Buds: Phytochemicals found in buds are α -Alanine, Aspartic acid, Glutamic acid and Glycine appeared in early stages. Oxalo acetic acid, Phosphoenol Pyruvic acid and α -Keto Glutaric acid have been found in later stages (Fig.4).

Flowers: The pale violet colour flowers of *B.Variegata* contain following phytochemicals i.e. Rutoside, Quercitroside, Isoquercitroside, Kaempferol-3-glucoside, Myricetolglycoside, Ascorbic, Aspartic octadecanoic acid, Ketoacid, Aminoacid, Tannins, Peonidin-3-glucoside, Peonidine-3 diglucoside, 3-galactoside and 3-rhamnoglucoside of Kaempferol (Fig.5).

Pharmacological Studies

The Pharmacological study of *Bauhinia variegata* shows that this plant exerted many kinds of biological effects towards human health.

Antioxidant effects

B.variegata plant has been broadly used in Indian tradition for its high range of medicinal value that can cure various human ailments [4]. *B. Variegata* plant extracts were taken for their antioxidant properties. Basically, the smallest antioxidant effect was found in organic solvent chloroform and in another two organic solvent it shows medium range value i.e. in methanol and in hexane it shows medium range activity as compared to standard quercetin [3]. Phytoconstituents that are found from *Bauhinia variegata* like beta-sitosterol and oleic acid is examined to reduce the hyperlipidemic states [4]. *Bauhinia variegata* bark fraction with methanol concluded for antioxidant.[3] some results have been found that it has a numerous and significant antioxidant effect [4]. The potential of antioxidant effect of this plant may be due to its richness in phenolic and flavonoids compounds [4]. Morley there was a significant correlation between antioxidant effect and total content of phenolic and flavonoids compounds [3]. The experimental investigation of the stem with methanol give the isolation of four biochemicals which have significant biological activities. The four phytoconstituents are kaempferol, Beta-sitosterol, Lupeol and quercetin [4].

Anticancer effects

B. variegata plant extract with ethanol solvent shows anticarcinogenic effect. It was help to protect liver from the cytotoxic effect of a carcinogenic compound .i.e. diethyl nitrosamine [3] extract of stem bark of this plant in methanol



**Somalika Pradhan**

also shows anticancer activity using two protocol at a dose of 500 and 1000mg/kg bw in skin papilloma model against 7, 12-dimethyle Benz anthracene and croton oil induced in mice [2]. The result was effective i.e. tumor yield found to be reduced and also tumor burden was found to be reduced [3].

Antimicrobial activity

Antimicrobial activity against four organisms (*Staphylococcus aureus*, *Bacillus subtilis*, *Klebsiella Pneumonia* and *Escherichia coli*) were investigated. It has been concluded that plant extracts were more effective against gram positive bacteria compared to gram negative bacteria [3]. *Bauhinia variegata* plant aqueous and methanolic extract of stem bark shows its antimicrobial activity against the above organisms [2]. The chloroform and methanolic fractions of this plants were found to be active against *Staphylococcus aureus*, *Bacillus subtilis* and *Klebsiella Pneumonia* [3]. The antimicrobial effect of *Bauhinia variegata* plant leaf extract also analyze against gram positive species staphylococcus and gram negative species *Escherichia coli* [3]. Leave extract in alcohol shows maximum antimicrobial effect compared to other two solvents extract i.e. chloroform and ether [3].

Anti-diabetic Effect

Anti-diabetic effect of *Bauhinia variegata* can be studied from its leaves and stem extract. Leaves of this plant consist protein which is similar to insulin so it has been used as an anti-diabetic agent [1]. Leaves of *B. variegata* with methanol shows the antidiabetic effect and hypoglycemic effect. *Bauhinia* plant extract has taken for alloxan induced diabetic model. Aqueous and organic solvent extract of this plant with hexane and ethanol in alloxan induced diabetes model in rats caused reduced glucose, triglycerides, total cholesterol and lipid cholesterol level [2].

Immunomodulatory activity

The isolated compound of *B.variegata* stem bark were screened for their possible immune-modulatory activity [1].The etholic extract of stem bark of *B.variegata* found to show immunomodulatory action on primary and secondary antibody responses. Phagocytic index and percentage of neutrophil adhesion increases at the doses of 250 and 500mg/kg [2]. The isolated compound of *B.variegata* stem bark with acetone and water showed significant activity of immunomodulatory [1].

Hepatoprotective Activity

This activity is caused by its ability to inhibit the free radicals that are produced from the metabolism of toxic substances like acetaminophen, ethanol and carbon tetrachloride etc [1]. With a dose of 150 to 200 mg of ethanolic extract of the stem bark of *Bauhinia variegata* induced in Sprague rats confirm she patoprotective activity against tetrachloride. After this it has been found that this Hepatoprotective activity decreases the level of total lipids and increases the level of total protein in it [2].

Wound healing activity

Two model i.e. excision and incision wound model in rats were used to give the idea of wound healing effect of this plant with ethanolic and aqueous extract of root of *Bauhinia variegata* at a dose of 200 and 400mg/kg bw [3]. Both the solvent extract of root *B.variegata* produced significant wound healing activity which was comparable to standard wound model [2].

CONCLUSIONS

It has been concluded that from this review analysis, *Bauhinia variegata* plant is belonging to medicinal plant for its numerous pharmacological activities. This literature confirmed that *Bauhinia variegata* plant contain different phytochemicals which are responsible for various activities. This plant has been used as a medicine for different diseases like diarrhea, dysentery, ulcer and skin diseases etc.





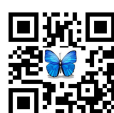
Somalika Pradhan

REFERENCES

1. Kanchan Lata Singh, D. K. Singh and Vinay Kumar Singh, Multidimensional Uses of Medicinal Plant Kachnar (*Bauhinia variegata* Linn.), *AJPCT*, 4(2),pp-058-072, ISSN: 2321 –2748, 2016.
2. SyedaShahana et.al. A Brief Review on *Bauhinia variegata*: Phytochemistry, Antidiabetic and Antioxidant potential, *Am. J. PharmTech Res.* 2017; 7(1).
3. Sahu G, Gupta PK, A Review on *Bauhinia variegata* Linn, *IRJP* 2012, 3 (1), ISSN 2230 – 8407.
4. Ali Esmail Al-Snafi, The Pharmacological Importance of *Bauhinia variegata*. A Review, *International Journal of Pharma Sciences and Research (IJPSR)*, ISSN : 0975-9492 Vol 4 No 12 Dec 2013.
5. Amita Mishra,1 Amit Kumar Sharma,1 Shashank Kumar,1 Ajit K. Saxena,2 and Abhay K. Pandey1, *Bauhinia variegata* Leaf Extracts Exhibit Considerable Antibacterial, Antioxidant, and Anticancer Activities, *BioMed Research International* Volume 2013, Article ID 915436, 10 pages.
6. Shilpa Gautam, *Bauhinia variegata* Linn: All Purpose Utility and Medicinal Tree, Botany Division, Forest Research Institute.
7. Pragati Khare , Kamal Kishore , Dinesh Kumar Sharma , Historical aspects, Medicinal uses, Phytochemistry and Pharmacological review of *Bauhinia variegata*, *Asian Journal of Pharmacy and Pharmacology* 2018; 4(5): 546-562.
8. TilahunTolossa Jima1 and Moa Megersa, Ethnobotanical Study of Medicinal Plants Used to Treat Human Diseases in Berbere District, Bale Zone of Oromia Regional State, South East Ethiopia, *Evidence-Based Complementary and Alternative Medicine* Volume 2018, Article ID 8602945, 16 pages.
9. S. S. Sawhney, M. Amin Mir*, Sandeep Kumar, Phytochemical Screening and Antioxidant properties of *Bauhinia variegata*, *International Journal of Research in Phytochemistry & Pharmacology*, ISSN: 2231-010X.
10. Rajat Singh1 , R.K.Bachheti1 , Shiva Saraswat2 & Santosh Kumar Singh*, Assessment of Phytochemical and Biological Potentials of *Bauhinia variegata* L, *International Journal of Pharmaceutical Research* 2012, Volume 4, ISSN 0975-2366.

Table-1: Table shows reported activity and model used

<i>Bauhinia variegata</i> effect	Parts used	Medium used	Model used
Antioxidant effect	Leaf, Bark and Root	Aqueous/Organic	Oxygen radical absorbance capacity
Anti-Microbial	Leaf, Stem bark	Aqueous/Organic	Against bacterial strain
Anti-inflammatory	Leaf, Stem bark and root	Aqueous/Organic	Carrageenan induced hind paw edema
Anti-cancer	Stem, bark	organic	DMBA and croton oil induced skin carcinogenesis in mice.
Anti-diabetic	Leaf and Stem bark	Aqueous/Organic	Glucose induced diabetes
Wound healing	Root and Seed	Aqueous/Organic	excision and incision wound model
Hepatoprotective	Stem bark	Organic	CCl ₄ induced hepatotoxicity





Somalika Pradhan

<p>Fig.1. Stem and stem bark</p>	<p>Fig.2. Seed</p>	<p>Fig.3. Leaves</p>
<p>Fig.4. Buds</p>	<p>Fig.5. Flowers</p>	<p>Fig.6. Kaempferol</p>
<p>Fig.7. Isoquercitide</p>	<p>Fig.8. Tyrosine</p>	<p>Fig.9. Alanine</p>
<p>Fig.10. Tannin</p>		<p>Fig.11. kaempferol-3-glucoside</p>





Biochemical Constituents of Microalgae and Filamentous Algae Collected from Chennai

Vijayalakshmi R¹, KokilaV¹, Deebiga S¹ and Jegan G^{2*}

¹Department of Biotechnology, Apollo Arts and Science College, Poonamallee, Chennai, Tamil Nadu, India.

²Assistant professor, Department of Biotechnology, Apollo Arts and Science College, Poonamallee, Chennai, Tamil Nadu, India.

Received: 11 Sep 2020

Revised: 14 Oct 2020

Accepted: 17 Nov 2020

*Address for Correspondence

Jegan G

Assistant professor, Department of Biotechnology,
Apollo Arts and Science College,
Poonamallee, Chennai,
Tamil Nadu, India.

Email: jeganbgl@gmail.com



This is an Open Access Journal / article distributed under the terms of the **Creative Commons Attribution License** (CC BY-NC-ND 3.0) which permits unrestricted use, distribution, and reproduction in any medium, provided the original work is properly cited. All rights reserved.

ABSTRACT

The production of energy from renewable resources is main challenge for science due to increasing of more population. The use of energy from fossil fuels which leads to increase the atmospheric pollution and global warming due to their high concentration of CO₂. Therefore algae are the best source for the production of renewable energy especially biofuel. In this present study fresh water samples were collected from inside of the Tamil Nadu Horticulture Management Institute, Madhavaram, and around the petroleum industries at Manali, Chennai, Tamil Nadu, India. These water samples were confirmed that the presence of algae and which was isolated and identified as microalgae and filamentous algae. The both microalgal and filamentous algal biomass were collected and wet and dry weight was measured. The biochemical compounds of carbohydrates, protein and lipid were analyzed in this collected algal biomass and which the results were showed that the microalgae produced more contents of biochemicals compared to filamentous algae. In particularly the lipids from these microalgae and filamentous algae can be used as biofuel instead of fossil fuels. Therefore, these algal strains are also potential strains for the production of biodiesel and which are cost effective and eco-friendly. Moreover these algal biomasses are also used for industrial waste water treatment and pharmaceutical industry.

Keywords: Biomass, Microalgae, Filamentous algae, Pigments, Lipid.



Vijayalakshmi *et al.*,

INTRODUCTION

The increasing of more population in the world leads to the demands of energy for their living. In particularly the use of energy from fossil fuels which are increasing atmospheric pollution and cause global warming and climate change in the environment. Therefore many researchers are finding alternative fuels instead of fossil fuels from biological resources. New technologies are ongoing all over the world to develop a liquid fuels from renewable resources especially from biomass (Bull, 1999). Biodiesel is the feasible alternative sources of energy for transport because of they are renewable, biodegradable and non-toxic (Lamers, 2009). Biodiesel produced from different sources such as waste cooking oil, oil crops and animal fats but it cannot be satisfy due to small quantities which are demand for the use of transport fuels. Therefore Algae are the best resources for the production of biodiesel when compared to other oil producing microorganism (Falkowski and Raven, 1997). Unicellular algae are the potential feed stock for the production of biodiesel (Demirbas, 2009; Pienkos, 2009). Microalgae and cyanobacteria are the diverse group of microorganisms which is living in different environmental habitats like freshwater, brackish water, marine and hyper saline conditions with the various temperature, pH and availability of nutrients (Falkowski and Raven, 1997). These algae are easy to cultivate with small nutrients and contain high lipid content and cost effective. Microalgae are the sunlight dependant cell factories which are convert the carbon dioxide into biofuels, foods, feeds, and valuable bioactive compounds (Walter *et al.*, 2005). Moreover microalgae are the constant sources of biofuels production (Qin, 2005; Chisti, 2007; Chisti & Yan, 2011). Based on previous reports were confirming that microalgae consisting of high quality of nutrition, more lipids content and fatty acid profiles (Brown *et al.*, 1997; Brown, 2004; Reitan *et al.*, 1997; Volkman *et al.*, 1980, 1989, 1991). Moreover cyanobacteria have also the potential sources of renewable fuels, fine chemicals and biofertilizers (Lem N.W and Glck B.R 1985). Rastogi and Sinha 2009 reported that the Cyanobacteria have store food materials and these are the sources of the pigments, vitamins, proteins and lipids. Cyanobacteria are also used as bioremediation and pollution control agents because which are eco-friendly and produce more biomass which is used as feed for animals, food industries, pharmacy industries and biotechnological applications (Madhumathi, V, *et al* 2011; Thajuddin, N. and Subramanian, G. 2005 and Venkataramanan, L. V. 1994). The present research was studied that the pure algal cell isolation, identification, and biochemical composition of the microalgae and filamentous algae collected from different sites of Chennai, Tamil Nadu, India.

MATERIAL AND METHODS

Collection Area: Fresh water sample collection was chosen randomly in two different places of Chennai, namely Tamil Nadu Horticulture Management Institute, Madhavaram and around the petroleum industries, Manali, Chennai, Tamil Nadu, India. The pond water (Fig. 1A-B) and stagnant water containing filamentous algae (Fig. 1C) were collected from inside of the Tamil Nadu Horticulture Management Institute, Madhavaram and outlet water samples were collected around the petroleum industries (Fig. 2 D-G) at manali, Chennai. In which filamentous algal biomass was collected separately and stored in laboratory. The collection was carried out during the month of September 2019. The figure A and B shows the collection site of pond water at inside of the Tamil Nadu Horticulture Management Institute, Madhavaram, the figure C shows the filamentous algal collection site at inside of the Tamil Nadu Horticulture Management Institute, Madhavaram and the figure D – G shows the collection sites of around petroleum industries, Manali, Chennai, Tamil Nadu, India. The collected water samples were found green in color so it confirmed that algal growth was found to be rich (Fig. A-G). The water samples were centrifuged at 8000rpm for 10mins and the pellet was collected. The wet weight of biomass including microalgae and filamentous algae were recorded and kept in oven to dry. Finally the dried biomass of microalgal consortia and filamentous algal consortia were collected and analyzed dry weight and used for further biochemical compositions.

Microscopic identification of algae: The microscopic identification of collected microalgal and filamentous algal cells were studied based on the previous reports of various researchers using phase contrast microscope (Barry H. Rosen (1990); Desikachary, 1959; Gour Gopal Satpati and Ruma Pal, 2016; Philipose, 1967; Yuvaraj Sampathkumar



**Vijayalakshmi et al.,**

and Elumalai. S, 2018). Microscopic identification was confirmed that the presence of microalgae and filamentous algae in the collected water samples.

Isolation of Pure algal Strains: The collected water samples were instantly transported to the laboratory and these samples were subjected to isolate pure algal strains using the media BBM for microalgae and BG11 for filamentous algae by the method of agar plate techniques. Before start inoculation the BBM and BG11 media were autoclaved at 121°C for 15 min. Cultures were made by inoculating 50 mL onto Petri plates containing BBM and BG11 with 1.5% (w/v) of bacteriological agar. Algal strains were inoculated in the media and kept for incubation under light intensity of 120 $\mu\text{mol photons/m}^2/\text{s}^{-1}$ on 12:12 h Light/Dark with room temperature. The purities of the algal cultures were ensured by repeated plating and regular observation under a phase contrast microscope. The pure microalgal and filamentous algal strains were isolated and these strains are growing in the Department of Biotechnology laboratory at Apollo Arts and Science College, Poonamallee, Chennai, Tamil Nadu, India.

Pigments analysis: The pigments of '*Chlorophyll a* and *Chlorophyll b*' of consortium biomass including microalgae and filamentous algae were estimated by the method of Jeffery and Humphrey 1975 and the β -carotenes were determined by Shaish *et al.*, 1992 using spectrophotometrically.

Biochemical Composition of the Consortium Biomass: The collected biomass of the microalgal consortium and filamentous algal consortium were subjected to analyze the Carbohydrate, Protein and Lipid based on the method followed by Dubois *et al.*, 1956, Lowry *et al.*, 1951 and Bligh and Dyer *et al.*, 1959.

RESULTS AND DISCUSSION

The biomass of microalgal consortia and filamentous algal consortia were collected from fresh water bodies at inside of the Tamil Nadu Horticulture Management Institute, Madhavaram and around the petroleum industries, Manali, Chennai. These both biomasses were collected in two different places with different sites. The collected algal biomasses were estimated its wet and dry weights and the results were shown in the Table: 1. The wet weight of microalgae biomass was obtained 386g and wet weight of filamentous algae biomass was obtained 453g (Table:1 and Fig. 3). The filamentous algae were accumulated high amount (57 g) of dry biomass when compared to microalgal dry biomass (48 g) (Table: 1 and Fig. 4). The overall wet weight and dry weights were showing in the figure 5.

Identification of Microalgae and Filamentous algae: The microscopic identification was carried out and which was confirmed that the presence of microalgae and filamentous algae based on their Habitats, cell size, shape, single cell or multicellular, filament or non filament, branch or unbranch etc., The below figure 6 was showing the microalgal cells (A-C) and filamentous algal cell (D-G) in which pure algal cells were isolated and these cultures were maintained in the laboratory of biotechnology at Apollo Arts and Science college, poonamallee, Chennai.

Pigments Analysis: The pigments such as *Chlorophyll a*, *Chlorophyll b* and β - Carotene contents of the microalgae and filamentous algal consortium were analyzed and the result were showed excellent in microalgae (27 $\mu\text{g/ml}^{-1}$ /18 $\mu\text{g/ml}^{-1}$ /36 mg/ml) while compare to filamentous algae (19 $\mu\text{g/ml}^{-1}$ /14 $\mu\text{g/ml}^{-1}$ /20 mg/ml). The results were shown in the Table: 2 and the Figure 7 was showing of *Chlorophyll a*, figure 8 was showing of *Chlorophyll b* and figure 9 was showing of β - Carotene.

Biochemical Constituents: The biochemical Constituents such as Carbohydrates, Proteins and Lipid were analyzed and the results were showed that the microalgal biomass was produced more contents of the biochemicals when compared to filamentous algal biomass (Table: 3 and Figure: 10, 11, and 12).



**Vijayalakshmi et al.,**

Carbohydrate: Carbohydrate content of microalgal consortium was shown 33.22 mg/g⁻¹ and filamentous algal consortium was shown 26.30 mg/g⁻¹. In the results high amount of carbohydrates was accumulated in microalgae followed by filamentous algae (Table: 3 and Fig. 10).

Protein: The more protein content was showed in microalgae when compared to filamentous algae that is microalgae 21.26 mg/ g⁻¹ and filamentous algae 17.43 mg/ g⁻¹ (Table: 3 and Fig. 11). This was showed that not much difference in between microalgae and filamentous algae.

Lipid: Lipid content were estimated from the both microalgae and filamentous algal biomass which the result obtained that high yield of lipid in microalgae (42.26 mg/g) followed by filamentous algae (31.20 mg/g). The amount of lipid content of microalgae and filamentous algae was shown in the Table: 3 and Fig. 12

DISCUSSION

The microalgae and filamentous algae biomass were collected from different places of Chennai (Madhavaram and Manali), Tamil Nadu, India. The collected both algal biomass were examined to isolate different dominated pure algal strains and the remaining microalgal and filamentous algal consortium biomass were subjected to biochemical analysis for the production of biodiesel. Microalgae can able to produce the varieties of value added by products such as pigments, carbohydrates, proteins and lipids (Minhas AK *et al.*, 2016). Cyanobacteria also contain pigments such as chlorophylls (responsible for green color), Phycocyanin (responsible for blue-green color) (Whitton and Potts 2000) and carotenoids which are non-toxic and used as coloring agent in food industries (Bauernfeind, 1981). The pigments of *Chlorophyll a*, *Chlorophyll b* and β - Carotene were evaluated in this collected microalgae and filamentous algal samples and which was showed that microalgae contains high value of pigments followed by filamentous algae. Many species of microalgae were described that contains huge amount of carbohydrates, proteins, lipids and bioactive compounds (Sathasivam, R. *et al.*, 2017) According to the previous report in this study also proved that more contents of carbohydrate, protein and lipids were isolated in the microalgal biomass. Cyanobacteria are ability to secrete biochemicals such as carbohydrate, protein and lipids extracellularly and also their potential role in metal removal in food and package industries (Shah *et al.*, 2000). In this investigation the filamentous algal biomass were showed good results of biochemical compounds but not more than microalgae. Biofuel production from microalgae is considered as a good opportunity due to their consisting of more lipid content, fast growth, easy to cultivate biomass with less water (Andersen, 2005). Some examples of microalgal strains such as *Chlorella vulgaris*, *Tetraselmis* sp., *Scenedesmus* and *Spirulina* sp. and their lipids were used as biofuel production (Becker, 1995). Li *et al.*, (2008) was reported that the microalgal biomass is producing biodiesel which was collected from the triglycerides by the reaction of transesterification. Based on the previous report in this research also lipid was isolated from the microalgal consortia and which showed high amount of lipids when compared to filamentous algae. These lipids can be used for the production of biofuel from the triglycerides after the transesterification process. Many scientist were reported that some species of cyanobacteria can able to produce more lipid and fatty acid compounds under the effect of light, temperature and salinity (Liu *et al.*, 2005; Maslova *et al.*, 2004; Rezanka *et al.*, 2003; Rosales *et al.*, 2005). In this study also proved that the more lipid content were accumulated from the filamentous algal consortium and which are used as biodiesel through the process of transesterification. Therefore these both microalgal consortium and filamentous algal consortium were yield high amounts of lipids and which can able to use for the production of biodiesel in future.

CONCLUSION

The conclusion of the study is the waste microalgal and filamentous algal biomass is easily available with large quantity in various places including different industrial surroundings. These algal biomasses are the best source of





Vijayalakshmi et al.,

large scale biodiesel production and not only that which are also used for waste water treatment, animals feed, food industries, pharmacy industries and many biotechnological applications. The use of microalgae and filamentous algae are eco-friendly and cost effective at present and future.

ACKNOWLEDGEMENTS

Authors acknowledge sincere thanks to the Chairman, Vice-Chairman, Secretary, Principal, Vice Principal and Head of the Department of Biotechnology, Apollo Arts and Science College, Poonamallee, Chennai – 602105. Also we thank to the Tamil Nadu Horticulture Institute, Madhavaram, Chennai.

REFERENCES

1. Andersen, R.A. 2005. Algal Culturing Technique. Elsevier Academic Press, UK.
2. Barry H. Rosen. Microalgae Identification for Aquaculture. Florida Aqua Farms, 1990.
3. Bauernfeind JC (1981) Carotenoids as colorants and Vitamins A Precursors. London: Academic Press.
4. Becker, E.W. 1995. Microalgae Biotechnology and Microbiology. New York: Cambridge University Press.
5. Blight, E.G. and W.J. Dyer. 1959. A rapid method of total lipid extraction and purification. Can. J. Biochem. Physiol. 37: 911-917.
6. Brown, M.R. 2004. Nutritional value of microalgae for aquaculture, <http://www.google.co.th/uant.mx/publication/mariculture/vi/pdf/A19.pdf>, retrieved 27 December 2004.
7. Brown, M.R., S.W. Jeffrey, J.K. Volkman & G.A. Dunstan. 1997. Nutritional properties of microalgae for mariculture. *Aquaculture* 151: 315-331.
8. Bull, T. E.1999. Science., 285, 1209.
9. Chisti, Y & J. Yan 2011. Energy from algae: Current status and future trends Algal biofuels - A status report. *Applied Energy* 88: 3277-3279.
10. Chisti, Y. 2007. Biodiesel from microalgae. *Biotechnology Advances* 25: 294-306.
11. D. Soletto, L. Binaghi, A. Lodi, J.C.M. Carvalho, A. Converti, Batch and fed-batch cultivations of *Spirulina platensis* using ammonium sulphate and urea as nitrogen sources, (n.d.). doi: <https://doi.org/10.1016/j.aquaculture.2004.10.005>.
12. Demirbas A. 2009 Production of Biodiesel from Algae Oils. Energy Sources Part a-Recovery Utilization and Environmental Effects 31:163-168. DOI: 10.1080/15567030701521775.
13. Desikachary, T.V., 1959. Cyanophyta. *Indian Council of Agricultural Research*, New Delhi, 700.
14. Dubois, M., K. A. Gilles, J. K. Hamilton, P. A. Robers and F. S. Smith. 1956. Colorimetric method for the determination of sugars and related substances. *Anal. Chem.* 18: 50-356.
15. Falkowski, P. G. and Raven, J. A. 1997. Aquatic photosynthesis. Malden, MA: Blackwell Science.
16. Gour Gopal Satpati and Ruma Pal. New and rare records of filamentous green algae from Indian Sundarbans Biosphere Reserve. 2016, 7 (2): 159- 175.
17. Jeffrey, S.W., Humphrey, G.F.: New spectrophotometric equations for determining chlorophyll a, b, c 1 and c 2 in higher plants, algae and natural phytoplankton. – *Biochem. Physiol. Pflanz.* 167: 191-194, 1975.
18. Lamers, A. 2009. Algae oils from small scale low input water remediation site as feedstock for biodiesel conversion, Guelph. *Engineering Journal.*, 2 : 24-38.
19. Lem N.W, Glck B.R 1985.. *Biotechnol.Adv.* 3: 195-208
20. Li Q., Du W., Liu D.H. 2008 Perspectives of microbial oils for biodiesel production. *Applied Microbiology and Biotechnology* 80:749-756. DOI: 10.1007/s00253-008-1625-9.
21. Liu, X. J.; Jiang, Y. and Chen, F. (2005), Fatty acid profile of the edible filamentous cyanobacterium *Nostoc flagelliforme* at different temperatures and developmental stages in liquid suspension culture. *Process Biochem.*, 40: 371 – 377.





Vijayalakshmi et al.,

22. Lowry, O. H., N. J. Rosebrough, A. L. Farr and R. J. Randall. 1951. Protein measurement with folin phenol reagent. *J. Bio. Chem.* 193: 265-275.
23. Madhumathi, V, Deepa, P, Jeyachandren, S, Manoharan C and Vijayakumar S, 2011. Water Lake. *IJMR*, 2(3) 213-216.
24. Maslova, I. P.; Mouradyan, E. A.; Lapina, S. S.; Klyachko–Gurvich, G. L. and Los, D. A. (2004), Lipid fatty acid composition and thermophilicity of cyanobacteria. *Russian J. Plant Physiol.*, 51: 353 – 360.
25. Mata TM, Martins AA, Caetano NS. Microalgae for biodiesel production and other applications: A review. *Renew. Sust. Energ. Rev.* 2010; 14: 217-232.
26. Minhas AK, Hodgson P, Barrow CJ, Adholeya A. A review on the assessment of stress conditions for simultaneous production of microalgal lipids and carotenoids. *Front Microbiol.* 2016; 7: 1-19.
27. Philipose, M.T., 1967. Chlorococcales, Indian Council of Agricultural Research, New Delhi, 1-365.
28. Pienkos P.T., Darzins A. 2009 The promise and challenges of microalgal-derived biofuels. *Biofuels, Bioproducts & Biorefining-Biofpr* 3:431-440. DOI: 10.1002/bbb.159.
29. Qin, J.G. 2005. Bio-hydrocarbon from algae: Impacts of temperature, light and salinity on algae growth. A report for the Rural Industries Research and Development Corporation. Australia. RIRDC Publication No, 05/025.
30. R. Sathasivam, R. Radhakrishnan, A. Hashem, E.F. Abd Allah, Microalgae metabolites: a rich source for food and medicine, *Saudi J. Biol. Sci.* (2017), <http://dx.doi.org/10.1016/j.sjbs.2017.11.003>.
31. Rastogi, R.P. and Sinha, R.P. 2009. Biotechnological and industrial significance of cyanobacterial secondary metabolites. *Biotech. Adv.* 27: 521-539.
32. Reitan, K.I, J.R. Rainuzzo., G. Øie & Y. Olsen. 1997. "A review of the nutritional effects of algae in marine fish larvae". *Aquaculture.* 155:207-221.
33. Rezanka, T.; Viden, I.; Go, J. V.; Dor, I. and Dembitsky, V. M. (2003), Polar lipids and fatty acids of three wild cyanobacterial strains of the genus *Chroococcidiopsis*. *Folia Microbiol.* 48: 781 – 786.
34. Rodolfi, L.; Zittelli, G.C.; Bassi, N.; Padovani, G.; Biondi, N.; Bonini, G.; Tredici, M.R. Microalgae for oil: Strain selection, induction of lipid synthesis and outdoor mass cultivation in a low-cost photobioreactor. *Biotechnol. Bioeng.* 2009, 102, 100–112.
35. Rosales, N.; Ortega, J.; Mora, R. and Morales, E. (2005), Influence of salinity on the growth and biochemical composition of the cyanobacterium *Synechococcus* sp. *Ciencias marinas*, 31: 349 – 355.
36. Shah, V.; Ray, A.; Garg, N. and Madamwar, D. (2000), Characterization of the extracellular polysaccharides produced by the marine cyanobacterium *Cyanothece* ATCC 51142 and its exploitation toward metal removal from solutions. *Curr. Microbiol.*, 40: 274 – 278.
37. Shaish A, Ben-amotz A, Avron M. Biosynthesis of β -carotene in *Dunaliella*. *Method Enzymol.* 1992; 213:439–444. doi: 10.1016/0076-6879(92)13145-N. [CrossRef] [Google Scholar]
38. Stephenson, P.G.; Moore, C.M.; Terry, M.J.; Zubkov, M.V.; Bibby, T.S. Improving photosynthesis for algal biofuels: Toward a green revolution. *Trends Biotechnol.* 2011, 29, 615–623.
39. Thajuddin, N. and Subramanian, G. (2005). *Curr. Sci.*, 89: 47 – 57
40. Venkataramanan, L. V. 1994. (University of Malaysia, Kualalumpur), pp. 103-112.
41. Volkman, J.K. 1991. Fatty acids from Microalgae of the genus *Pavlova*. *Phytochem.* 30(6): 1855 - 1859.
42. Volkman, J.K., G. Eglinton & E.D.S. Corner. 1980. Sterol and fatty acids of the marine diatom *Biddulphia sinensis*. *Phytochem.* 19:1809-1813.
43. Volkman, J.K., S.W. Jeffrey, P.D. Nichols., G.I. Rogers & C.D. Garland. 1989. Fatty acid and lipid composition of 10 species of microalgae used in mariculture. *J. Exp.Mar. Biol. Ecol.* 128: 219-240.
44. Walter, T. L., Purton, S., Becker, D. K and Collect, C. 2005. Microalgae as bioreactor. *Plant cell rep.*, 24: 629- 641.
45. Whitton, B. A. & Potts, M. [Eds.] 2000. *The Ecology of Cyanobacteria: Their Diversity in Time and Space*. Kluwer Academic Publisher, Dordrecht, The Netherlands, 669 pp.
46. Yuvaraj Sampathkumar and Elumalai S 2018. Isolation, Physiochemical Characterization And Cultivation Of Salt Tolerant Microalgal Species From Marakkanam Salt Pan, Tamil Nadu, India.





Table 1: Wet and Dry Weight of microalgal and filamentous algal biomass

Sample	Wet Weight (g)	Dry Weight (g)
Microalgae Consortium	386	48
Filamentous algal Consortium	453	57

Table 2: Pigments analysis of the microalgal and filamentous algal biomass

Sample	Chlorophyll a $\mu\text{g/ml}^{-1}$	Chlorophyll b $\mu\text{g/ml}^{-1}$	β - Carotene mg/ml
Microalgae	27	18	36
Filamentous algae	19	14	20

Table 3: Biochemical Constituents of the Microalgae and Filamentous algae

Sample	Carbohydrates mg/ g ⁻¹	Protein mg/ g ⁻¹	Lipid mg/g
Microalgae	33.22	21.26	42.26
Filamentous algae	26.30	17.43	31.20



Fig. 1: A-C Algal Collection sites of Tamil Nadu Horticulture Management Institute, Madhavaram, Chennai.

Fig. 2: D - G Algal Collection sites of around petroleum industries, Manali, Chennai.

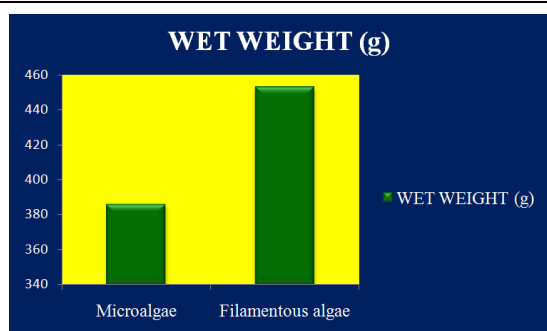


Fig. 3: The Wet weight of the collected microalgal and filamentous algal biomass.

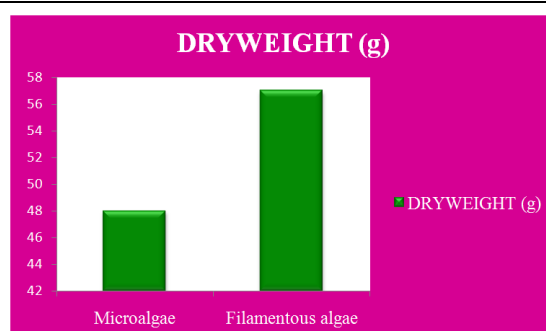


Fig. 4: The Dry weight of the collected microalgal and filamentous algal biomass.





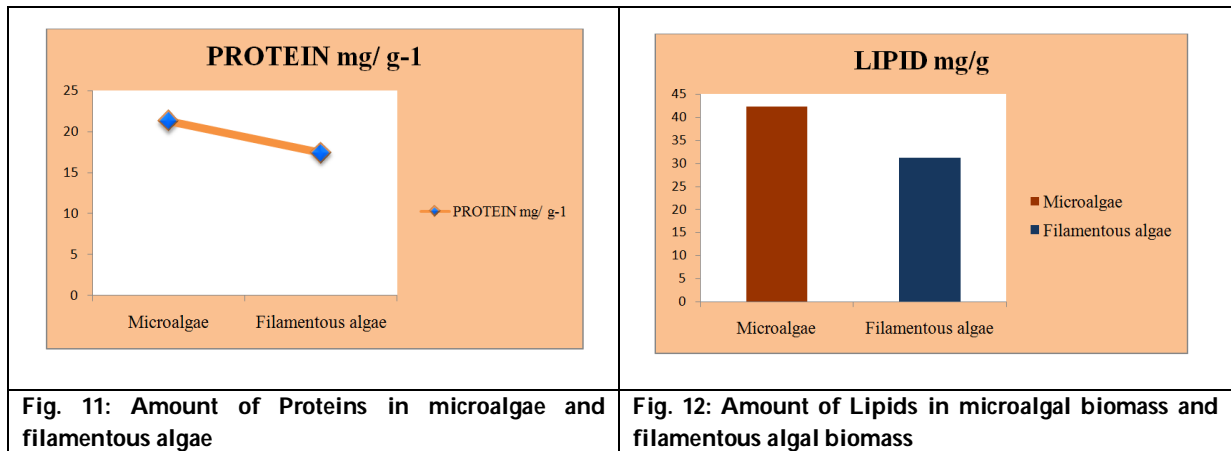
Vijayalakshmi et al.,

<table border="1"> <caption>Data for Fig. 5: Overall Wet and Dry weight</caption> <thead> <tr> <th>Category</th> <th>Wet Weight (g)</th> <th>Dry Weight (g)</th> </tr> </thead> <tbody> <tr> <td>Microalgae</td> <td>~380</td> <td>~50</td> </tr> <tr> <td>Filamentous algae</td> <td>~450</td> <td>~60</td> </tr> </tbody> </table>	Category	Wet Weight (g)	Dry Weight (g)	Microalgae	~380	~50	Filamentous algae	~450	~60				
Category	Wet Weight (g)	Dry Weight (g)											
Microalgae	~380	~50											
Filamentous algae	~450	~60											
<p>Fig. 5: The Overall Wet and Dry weight of the collected microalgal and filamentous algal biomass.</p>	<p>Fig. 6: Microscopic identification of Microalgae and Filamentous algae (A-C Microalgae and D-G filamentous algae)</p>												
<table border="1"> <caption>Data for Fig. 7: Chlorophyll a content</caption> <thead> <tr> <th>Category</th> <th>Chlorophyll a (µg/ml)</th> </tr> </thead> <tbody> <tr> <td>Microalgae</td> <td>~27</td> </tr> <tr> <td>Filamentous algae</td> <td>~19</td> </tr> </tbody> </table>	Category	Chlorophyll a (µg/ml)	Microalgae	~27	Filamentous algae	~19	<table border="1"> <caption>Data for Fig. 8: Chlorophyll b content</caption> <thead> <tr> <th>Category</th> <th>Chlorophyll b (µg/ml)</th> </tr> </thead> <tbody> <tr> <td>Microalgae</td> <td>~18</td> </tr> <tr> <td>Filamentous algae</td> <td>~14</td> </tr> </tbody> </table>	Category	Chlorophyll b (µg/ml)	Microalgae	~18	Filamentous algae	~14
Category	Chlorophyll a (µg/ml)												
Microalgae	~27												
Filamentous algae	~19												
Category	Chlorophyll b (µg/ml)												
Microalgae	~18												
Filamentous algae	~14												
<p>Fig. 7: Chlorophyll a content of the collected microalgae and filamentous algae</p>	<p>Fig. 8: Chlorophyll b content of the collected microalgae and filamentous algae</p>												
<table border="1"> <caption>Data for Fig. 9: beta-Carotene content</caption> <thead> <tr> <th>Category</th> <th>beta-Carotene (mg/ml)</th> </tr> </thead> <tbody> <tr> <td>Microalgae</td> <td>~38</td> </tr> <tr> <td>Filamentous algae</td> <td>~22</td> </tr> </tbody> </table>	Category	beta-Carotene (mg/ml)	Microalgae	~38	Filamentous algae	~22	<table border="1"> <caption>Data for Fig. 10: Carbohydrates content</caption> <thead> <tr> <th>Category</th> <th>Carbohydrates (mg/g)</th> </tr> </thead> <tbody> <tr> <td>Microalgae</td> <td>~33</td> </tr> <tr> <td>Filamentous algae</td> <td>~26</td> </tr> </tbody> </table>	Category	Carbohydrates (mg/g)	Microalgae	~33	Filamentous algae	~26
Category	beta-Carotene (mg/ml)												
Microalgae	~38												
Filamentous algae	~22												
Category	Carbohydrates (mg/g)												
Microalgae	~33												
Filamentous algae	~26												
<p>Fig. 9: beta - Carotene contents of the collected microalgae and filamentous algae</p>	<p>Fig. 10: Amount of Carbohydrates in microalgae and filamentous algae</p>												





Vijayalakshmi et al.,





RESEARCH ARTICLE

Development of Analytical Method and Validation for Nadolol in Pure and Pharmaceutical Formulations using UV-Spectrophotometry and Spectrofluorimetry using Sodium Hydroxide

Anandha Jothi.D¹, Arun.R² and Anton Smith.A^{3*}

¹Department of Pharmaceutical Analysis, JSS College of Pharmacy, Ooty, Tamil Nadu, India.

²Department of Pharmacy, Karpagam University, Coimbatore, Tamil Nadu, India.

³Department of Pharmacy, Annamalai University, Annamalai Nagar, Tamil Nadu, India.

Received: 10 Sep 2020

Revised: 13 Oct 2020

Accepted: 17 Nov 2020

*Address for Correspondence

A.Anton Smith,

Associate Professor, Department of Pharmacy,
Annamalai University, Annamalai Nagar,
Tamil Nadu-608002.

E-Mail: auantonsmith@yahoo.co.in.



This is an Open Access Journal / article distributed under the terms of the **Creative Commons Attribution License** (CC BY-NC-ND 3.0) which permits unrestricted use, distribution, and reproduction in any medium, provided the original work is properly cited. All rights reserved.

ABSTRACT

Development of analytical methods is in need for the estimation of drugs in pure and different pharmaceutical formulations. A simple, sensitive, rapid, accurate, precise and economic Spectrophotometric and Spectrofluorimetric method were developed and validated for Nadolol in pure and Pharmaceutical formulations. The wave length (λ_{max}) used for the estimation of Nadolol is 267nm by Spectrophotometry, excitation (λ_{Ex})-267nm and emission (λ_{Em})-305nm by Spectrofluorimetry. Linear correlation was obtained between absorbance and concentration of Nadolol in the concentration ranges of 5-40 μ g/ml with R^2 value 0.992 by Spectrophotometry and linear correlation was obtained between intensity of fluorescence and concentration of Nadolol in the concentration ranges of 1-5 μ g/ml with R^2 value 0.989 by Spectrofluorimetry in 0.1 N NaOH. The linearity of the calibration curve was validated by the high values of correlation coefficient of regression. LOD and LOQ values for Nadolol were found to be 9.11 μ g/ml and 27.62 μ g/ml by Spectrophotometry and 0.76 μ g/ml and 2.33 μ g/ml by Spectrofluorimetry. Among the two developed methods Spectrofluorimetric method is highly sensitive than the spectrophotometric method. These methods are simple and suitable for the determination of Nadolol in pure and Pharmaceutical preparations.

Key words: Nadolol, Spectrophotometry, Spectrofluorimetry, Determination



**Anandha Jothi et al.,**

INTRODUCTION

Nadolol, chemically is (2R,3S)-5-(((2R)-3-tert-butylaminol-2-hydroxypropyl]oxy) - 1, 2, 3, 4-tetrahydro naphthalene-2,3-diol (Figure 1) is a non-selective β -blocker which is official in BP[1]and USP[2] used in the treatment of high blood pressure and chest pain. It has a preference for beta-1 receptors, which are predominantly located in the heart, there by inhibiting the effects of catechol amines and causing a decrease in heart rate and blood pressure, inhibition of beta-2 receptors, which are mainly located in the bronchial smooth muscles of the airways leads to airway constriction similar to that seen in Asthma. Review of literature reveals that only few methods like UV[3-5], Colorimetry [6,7], Fluorimetry [8-10], HPLC [5,11-12], Biological fluids using HPLC [13], UHPLC–MS [14],and LC-MS [15] were developed for the determination of Nadolol in pure and Pharmaceutical preparation.

MATERIALS

Instruments

Absorption spectral measurements were carried out with a Systronics 2202 UV-Visible spectrophotometry, fluorescence spectra measurements were carried out with a Perkin Elmer LS 55 Spectrofluorimetry, for sonication Branson 2510 Sonicator was used.

Chemicals

Nadolol tablets (40mg) were procured from WalmartPharmacy 2051 Strachan Road S., Medicine Hat T1B OG4 from Canada. Hydrochloric acid was of AR grade from Nice Pharmaceuticals Pvt. Ltd., and in house produced distilled water was used. Nadolol working standard was obtained as gift sample from Biophore, Hyderabad, Telungana.

METHODS

Preparation of stock solution

25mg of Nadolol was accurately weighed and transferred to 25ml volumetric flask. About 10ml of 0.1N NaOH was added, vortexed for about 5min. The volume was made up to 25 ml and mixed well with 0.1 N NaOH to obtain a final concentration of 1mg/ml.

Determination of Absorbance maxima and Fluorescence maxima

An appropriate aliquot portion of 2 ml of Nadolol from standard stock solution of Nadolol was transferred to 100ml volumetric flask, mixed with 0.1N NaOH and the volume was made up to 100ml with 0.1N NaOH to obtain the concentration 20 μ g/ml of Nadolol. Drug solutions were scanned in Spectrophotometry and Spectrofluorimetry to determine the absorbance maxima and based on absorbance maxima, emission maxima was determined. Drug solutions were further diluted necessarily and scanned in Spectrophotometry and Spectrofluorimetry to determine the absorbance maxima and based on absorbance maxima, emission maxima was determined.

Validation of the proposed method

The proposed method was validated according to the International Conference on Harmonization (ICH) guidelines [17].

Linearity and range

Spectrophotometry

An appropriate aliquot portion of 0.5, 1, 2, 3 and 4ml of Nadolol from standard stock solution of Nadolol were transferred to 100ml volumetric flask, mixed with 0.1N NaOH and the volumes were made up to 100ml with 0.1N



**Anandha Jothi et al.,**

NaOH to obtain concentrations 5, 10, 20, 30 and 40 µg/ml of Nadolol. The absorbance of all the resulting solutions was measured at 267nm. The calibration curve was constructed by plotting drug concentration versus absorbance obtained.

Spectrofluorimetry

An appropriate aliquot portion of 1, 2, 3, 4 and 5ml of Nadolol from standard stock solution of Nadolol were transferred to 100ml volumetric flask, mixed with 0.1N NaOH and the volumes were made up to 100ml with 0.1N NaOH to obtain the concentrations 1, 2, 3, 4 and 5 µg/ml of Nadolol. The fluorescence of the resulting solutions with 0.1N NaOH was measured at Excitation (λ_{Ex})- 267nm, Emission (λ_{Em})-305nm.

Precision

Spectrophotometry

10 tablets were weighed accurately and crushed into fine powder using glass mortar and pestle. An accurately weighed quantity of tablet powder equivalent to 25mg of Nadolol transferred into to 25ml volumetric flask. 10ml of 0.1N NaOH was added and sonicated for 5 minutes, the volume was made upto 25ml with 0.1N NaOH, mixed well and filtered it. From the filtrate 1ml of the solution was pipetted out and transferred into 25ml of volumetric flask and the volume was made upto 25ml with 0.1N NaOH. The absorbance of resulting solution was measured at 267nm.

Spectrofluorimetry

10 tablets were weighed accurately and crushed into fine powder using glass mortar and pestle. An accurately weighed quantity of tablet powder equivalent to 25mg of Nadolol transferred in 25ml volumetric flask. 10ml of 0.1N NaOH was added and sonicated for 5 minutes. The volume was made upto 25ml with 0.1N NaOH and filtered. From the filtrate 1ml of solution was pipetted out and transferred into 100ml of volumetric flask and the volume was made upto 100ml with 0.1N NaOH. From the above solution 2ml was pipetted out and transferred into 10ml volumetric flask and made up the volume up to 10ml with 0.1N NaOH. The fluorescence intensity of the resulting solution was measured at excitation (λ_{Ex})-267nm, emission (λ_{Em})- 305nm using 0.1 N NaOH as solvent blank.

Accuracy

Preparation of stock solution

The first step is preparation of stock solution (500mg of pure drug of Nadolol was dissolved in 25ml of 0.1N NaOH)

Spectrophotometry & Spectrofluorimetry

206 mg of tablet powder weighed accurately (equivalent to 40 mg of Nadolol) and transferred into three different 25ml volumetric flask. 10ml of 0.1N NaOH was added and 1ml (50%), 2 ml (100%) and 3ml (150%) of the stock solution was added which contains 20mg/ml of Nadolol. The solution was sonicated for 3 minutes, made up the volume up to 25ml with 0.1N NaOH. The resulting solutions was filtered separately and from the filtrate 1ml of the solution was pipette out and transferred to 100ml volumetric flask and made up the volume up to 100ml with 0.1N NaOH. It was repeated for three times of different weighing at each level so that 9 different weighing was performed. For Spectrophotometry the absorbance of all the resulting solution was measured at 267nm and for Spectrofluorimetry the intensity of fluorescence of all the resulting solutions was measured at excitation (λ_{Ex})-267nm and emission(λ_{Em})-305nm using 0.1N NaOH as solvent blank.

Limit of detection

The detection limit of an individual analytical procedure is the lowest amount of analyte in a sample which can be detected but not necessarily quantitated as an exact value. Detection limit (DL) may be expressed as:



**Anandha Jothi et al.,**

$$DL = \frac{3.3\sigma}{S}$$

where, σ = the standard deviation of the response

S = the slope of the calibration curve

The slope 'S' is estimated from the calibration curve of the analyte. The estimation of σ was carried out using calibration curve.

Limit of quantitation

The quantitation limit of an individual analytical procedure is the lowest analyte in a sample which can be quantitatively determined with suitable precision and accuracy. The Quantitation limit is a parameter of quantitative assays for low levels of compounds in sample matrices, and is used particularly for the determination of impurities or degraded products.

$$QL = \frac{10\sigma}{S}$$

Ruggedness

Ruggedness is a measure of reproducibility of test results under normal, expected operational conditions from laboratory to laboratory and from analyst to analyst. Ruggedness is determined by the analysis of aliquots by different analyst. 30 μ g/ml and 3 μ g/ml solutions were prepared and analyzed using spectrophotometer and spectrofluorimeter respectively.

Robustness

The robustness of an analytical procedures is a measure of its capacity to remain unaffected by small, but deliberate variations in method parameters and provides an indication of its reliability during normal usage. It was carried out by changing the wavelength by one nm at 266nm and 268nm for spectrophotometry and emission wavelength at 299nm and 301nm respectively.

RESULTS AND DISCUSSION

Determination of absorption maximum

An absorbance maximum was determined in spectrophotometry by taking 20 μ g/ml Nadolol drug which is dissolved in 0.1 N NaOH and scanned from 200-400nm using UV-Visible Spectrophotometer. The absorption spectra was presented in Figure 2 It was found that two λ_{max} (220nm and 267nm) was identified in the spectra. Among that 267nm was used for further analysis because 267 nm shows highest absorbing character and produce incremental absorbance while increasing concentration where as at 220nm does not shows significant increment compare to 267nm.

Determination of emission maxima

Absorbance maxima was determined in spectrofluorimetry by taking 3 μ g/ml Nadolol drug which is dissolved in 0.1N NaOH and excitation maxima was fixed at 267nm. Since the wavelength shows highest absorbance the emission spectra was scanned from 280-500nm. The emission spectrum was presented in Figure 3. It was found that emission maxima 305nm was identified in the spectra.





Linearity and range

Spectrophotometry

Calibration standards for Nadolol covering range of 5-40 µg/ml were prepared in serial dilutions that were made with 0.1N NaOH. The absorbance of all resulting concentrations was measured at 267nm. The graph between the concentration and absorbance was plotted. The regression equation was found to be $y = 0.020x - 0.004$. The correlation coefficient (R^2) of the standard curve was found to be 0.992. The obtained data are presented in Table 1 and the calibration graph is presented in Figure 4 respectively.

Spectrofluorimetry

Calibration standards for Nadolol covering range of 1 to 5 µg/ml were prepared in serial dilutions that were made with 0.1N NaOH. The intensity of fluorescence of all resulting concentrations was measured at excitation (λ_{Ex})-267nm and emission (λ_{Em})-305nm. The graph between the concentration and absorbance was plotted. The regression equation was found to be $y = 107.7x + 33.34$. The correlation coefficient (R^2) of the standard curve was found to be 0.998. The obtained data are presented in table 2 and the calibration graph is presented in Figure 5 respectively.

Precision

The method was carried out as described. The results were presented in Table 3 and 4 for spectrophotometry and spectrofluorimetry respectively. The values obtained in the repeatability (precision) shows that there is no significant difference in the precision value. Hence that developed method can be used to analyze the Nadolol in tablet formulation. There is no evidence of interference of excitation with Nadolol. The mean precision value was found to be $100.25 \pm 0.207\%$. The value was obtained from 100 to 100.6% by spectrophotometric method. The mean precision value was found to be $100.5 \pm 0.9011\%$. The value was obtained from 99.12 to 101.52 % by spectrofluorimetric method.

Accuracy

The method was carried out as described. The results were presented in Table 5 and 6 for spectrophotometry and spectrofluorimetry respectively. The values obtained in the reproducibility (accuracy) shows that there is no significant difference in the value. Hence that developed method can be used to analyze the Nadolol in tablet formulation. The percentage recovery was found to be $100.02 \pm 0.701\%$. The value was obtained from 99 to 100.15 % by spectrophotometric method. The percentage recovery was found to be $100.01 \pm 0.714\%$. The value was obtained from 99.1 to 101.15% by spectrofluorimetric method.

LOD and LOQ

The LOD was found to be 9.11 µg/ml and the LOQ concentration was found to be 27.62 µg/ml with 0.1 N NaOH by spectrophotometric method. The LOD was found to be 0.76 µg/ml and the LOQ concentration was found to be 2.33 µg/ml with 0.1 N NaOH by spectrofluorimetric method.

Ruggedness

Ruggedness data is presented in Table 7 by spectrophotometric and spectrofluorometric methods.

Robustness

There is no significant difference in absorbance and fluorescence observed when the minor changes like one nanometer difference in spectrophotometer and spectrofluorometer.

Validation profile

Performing replicate analysis of the standard solutions was used to assess the accuracy and precision and reproducibility of the proposed methods. The selected concentration within the calibration range was prepared in 0.1 NaOH and analyzed with the relevant calibration curves to determine the intra-day and inter-day variability. The



**Anandha Jothi et al.,**

intra-day and inter-day precision were determined. Validation profile of Nadolol with 0.1N NaOH is presented in Table 8 by Spectrophotometric and spectrofluorimetric methods.

CONCLUSION

Spectrophotometric and Spectrofluorimetric method for quantifying Nadolol in pure and formulation has been developed and validated. The developed method is precise, accurate and linear over the concentration range from 5 – 40 µg/ml and 1 – 5 µg/ml for Spectrophotometric and Spectrofluorimetric method respectively. The precision was found to be $100.25 \pm 0.207\%$ and $100.5 \pm 0.9011\%$ for Spectrophotometry and Spectrofluorimetry respectively. The percentage of drug recovered $100.02 \pm 0.701\%$ and $100.01 \pm 0.741\%$ for Spectrophotometric and Spectrofluorimetric method respectively. The LOD and LOQ were found to be $9.11\mu\text{g/ml}$ and $27.62\mu\text{g/ml}$ for Spectrophotometry and LOD and LOQ were found to be $0.76\mu\text{g/ml}$ and $2.33\mu\text{g/ml}$ for Spectrofluorimetry with 0.1 N NaOH. Among the two developed methods Spectrofluorimetric method is highly sensitive than the spectrophotometric method. These methods are simple and suitable for the determination of Nadolol in pure and Pharmaceutical preparations

REFERENCES

1. British Pharmacopoeia, The Department of Health and Social Services and Public Safety, British Pharmacopoeial Commission; 2008;2:1504.
2. United States Pharmacopeia and National Formulary (USP 30-NF 25). Rockville, MD: United States Pharmacopeia Convention; 2007;2:2694.
3. Olajire A, Olakunle SI, Olaniyi AA. A new spectrophotometric method for the determination of Nadolol. J Iran Chem Soc 2006;3(3):277-84.
4. Vijayalakshmi R, Naga Sri Ramya, Dhanaraju M. Method development for quantification of oxidation complexes of Nadolol and Resveratrol by visible spectrophotometry. Int J Pharm Pharm Sci 2014;7(1):304-07.
5. Camila T, Pedro LG, Fabio PG, Erika RMKH, Maria IRMS. Quantitative Determination of Nadolol in Tablets by High-Performance Liquid chromatography and UV-Derivative Spectrophotometry. Anal Lett 2008; 41(3):424-36.
6. Eugene Ivashkiv. Colorimetric determination of Nadolol in Tablets. J Pharm Sci 1978; 67(7): 1024-1025.
7. Amin AS, Ragab GH, Saleh H. Colorimetric determination of beta blockers in pharmaceutical formulations. J Pharm Biomed Anal 2002;30(4):1347-53.
8. Eugene I. Fluorimetric determination of Nadolol in human serum and urine. J Pharm Sci 1977; 66(8):1168-1172.
9. Akanksha, Arun R, Anton Smith A. Development of analytical method and validation for Nadolol in pure and pharmaceutical formulations using UV-spectrophotometry and spectrofluorimetry using Hydrochloric acid. J Global Pharma Technol 2019; 11(6): 1-9.
10. Veeramanikandan.V, Arun R, Anton Smith A. Development of Analytical Method and Validation of Nadolol in Pure and Pharmaceutical Formulations using UV-Spectrophotometry and Spectrofluorimetry, Int J Pharm Sci Res 2020; 11(6): 2962-2968.
11. Perlman S, Szyper M, Kirschbaum JJ. High-performance liquid chromatographic analysis of nadolol and bendroflumethiazide combination tablet formulations. J Pharm Sci 1984;73(4) :259-61.
12. Bhupendra R. Patel, Joel JK, Raymond BP. High-pressure liquid chromatography of nadolol and other β -adrenergic blocking drugs. J Pharm Sci 1981;70(3):336-38.
13. Chandana, Manepalli. Method development and validation for simultaneous estimation of Nadolol and Bendroflumethiazide in pharmaceutical dosage form by using RP-HPLC method. J Pharm Sci 2012;4(1):216-227.
14. Srinivas NR, Shyu WC, Shah VR, Campbell DA, Barbhaiya RH. High-performance liquid chromatographic assay for the quantitation of nadolol in human plasma using fluorescence detection. Biomed Chromatogr 1995;9(2):75-79.





Anandha Jothi et al.,

15. Magdalena O, Katarzyna D, Waldemar B, Barbara Ć, Maciej S, Grzegorz S, Juliusz, Witold D. Radiodegradation of nadolol in the solid state and identification of its radiolysis products by UHPLC–MS method. ChemPap 2018;72(2):349–357.
16. Alaa A, Salem Ibrahim WasfiSalama S, Al-Nassib M, Allawy MN, Al-Katheeri. Determination of Some β -Blockers and β 2-Agonists in Plasma and Urine Using Liquid Chromatography–tandem Mass Spectrometry and Solid Phase Extraction. JChromatogrSci 2017;55(8):846–856.
17. International Conference on Harmonization of Technical Requirements for Registration of Pharmaceuticals for Human Use. Validation of Analytical Procedures: Text and Methodology, Q2 (R1), 2005.

Table 1:Linearity and range of Nadolol

S. No.	Concentration(μ g/ml)	Absorbance(nm)
1.	5	0.131
2.	10	0.167
3.	20	0.381
4.	30	0.601
5.	40	0.810

Table 2:Linearity and range of Nadolol

S.NO.	Concentration(μ g/ml)	Intensity of fluorescence(nm)
1.	1	147.12
2.	2	247.56
3.	3	344.06
4.	4	468.7
5.	5	575.19

Table 3: Precision study of Nadololby Spectrophotometry

S. No.	Weight of the tablet powder(mg)	Absorbance	Drug content present(mg)	Percentage found (%)
1	206.05	0.845	40.2	100.5
2	206.02	0.844	40.1	100.2
3	206.04	0.841	40	100
4	206.03	0.846	40.25	100.6
5	206.01	0.842	40.05	100.1
6	206.04	0.843	40.06	100.15
MEAN				100.25
S.D				0.207
RSD				0.002

The mean precision value was found to be $100.25 \pm 0.207\%$. The value was obtained from 100 to 100.6% by spectrophotometric method.

Table 4: Precision study of Nadololby Spectrofluorometry

S. No.	Weight of the tablet powder(mg)	Intensity of fluorescence	Drug content present(mg)	Percentage found (%)
1	206.01	290	39.65	99.12
2	206.04	296	40.47	101.17
3	206.02	295	40.33	100.8
4	206.01	297	40.61	101.52





Anandha Jothi et al.,

5	206.05	292	39.92	99.8
6	206.03	295	40.33	100.8
Mean				100.5
S.D				0.9011
RSD				0.0089

The mean precision value was found to be $100.5 \pm 0.9011\%$. The value was obtained from 99.12 to 101.52 % by spectrofluorimetric method.

Table 5: Accuracy study of Nadolol by Spectrophotometry

S.No.	Percentage level	Sample weight (mg)	Drug in the tablet powder (mg)	Pure drug added (mg)	Total drug content (mg)	Absorbance	Amount found (mg)	Amount Recovered	Percentage recovery (%)
1	50	206.26	40	20	60	0.402	60.1	20.1	100.5
2	50	206.46	40	20	60	0.400	59.8	19.8	99
3	50	206.14	40	20	60	0.402	60.1	20.1	100.5
4	100	206.26	40	40	80	0.535	79.98	39.98	99.1
5	100	206.45	40	40	80	0.538	80.36	40.36	100.9
6	100	206.16	40	40	80	0.536	80.06	40.06	100.15
7	150	206.75	40	60	100	0.672	100.47	60.47	100.7
8	150	206.72	40	60	100	0.678	100.5	60.5	100.8
9	150	206.52	40	60	100	0.671	100.19	60.19	100.3
MEAN									100.2
SD									0.701
RSD									0.0069

The percentage recovery was found to be $100.02 \pm 0.701\%$. The value was obtained from 99 to 100.15 % by spectrophotometric method.

Table 6: Accuracy study of Nadolol by Spectrofluorometry

S. No.	Percentage level	Sample weight (mg)	Drug in the tablet powder (mg)	Pure drug added (mg)	Total drug content (mg)	Intensity of fluorescence	Amount found (mg)	Amount Recovered	Percentage recovery (%)
1	50	206.26	40	20	60	250.67	60.02	20.02	100.1
2	50	206.26	40	20	60	250	59.86	19.86	99.3
3	50	206.45	40	20	60	251	60.10	20.1	100.5
4	100	206.18	40	40	80	335	80.21	40.21	100.5
5	100	206.59	40	40	80	336	80.46	40.46	101.15
6	100	206.25	40	40	80	334	79.99	39.99	99.97
7	150	206.21	40	60	100	415	99.46	59.46	99.1
8	150	206.13	40	60	100	417.28	99.48	49.48	99.13
9	150	206.56	40	60	100	419.8	100.24	60.24	100.4
MEAN									100.01
SD									0.741
RSD									0.0073

The percentage recovery was found to be $100.01 \pm 0.714\%$. The value was obtained from 99.1 to 101.15% by spectrofluorimetric method.





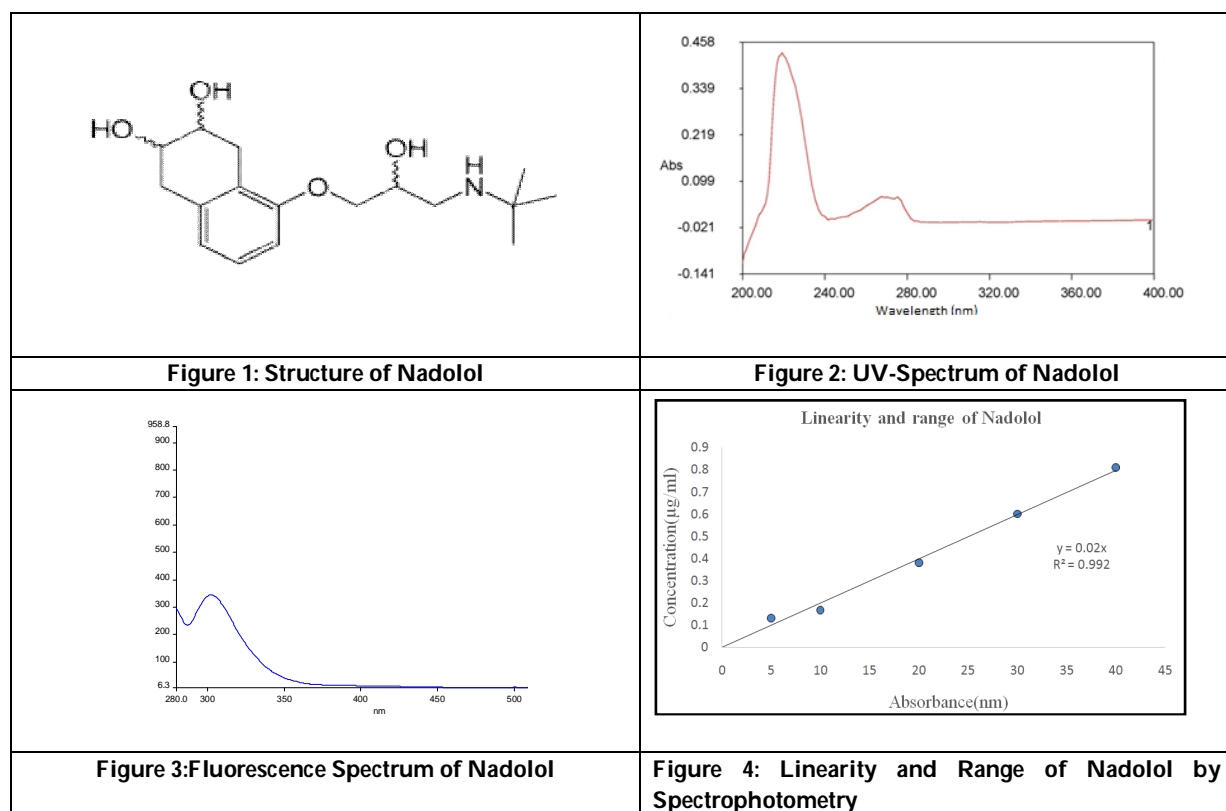
Anandha Jothi et al.,

Table 7: Ruggedness of Nadolol

S. NO	Analyst -1	Analyst-2
Absorbance at 267nm		
1	0.601	0.603
2	0.602	0.604
3	0.601	0.602
Intensity of fluorescence		
1	344.21	347.38
2	347.95	345.42
3	347.57	346.85

Table 8 : Validation profile of Nadolol

Parameters	Spectrophotometer	Spectrofluorometer
Linearity range (ug/ml)	5-40	1-5
Precision (%)	100.25±0.207	100.5 ± 0.9011
Accuracy (%)	100.02±0.701	100.01 ± 0.741
50%	100±0.866	99.96±0.818
100%	100.05±0.009	100.54±0.589
150%	99.99±1.041	99.54±0.74
LOD(µg/ml)	9.11	0.76
LOQ(µg/ml)	27.62	2.33





Anandha Jothi et al.,

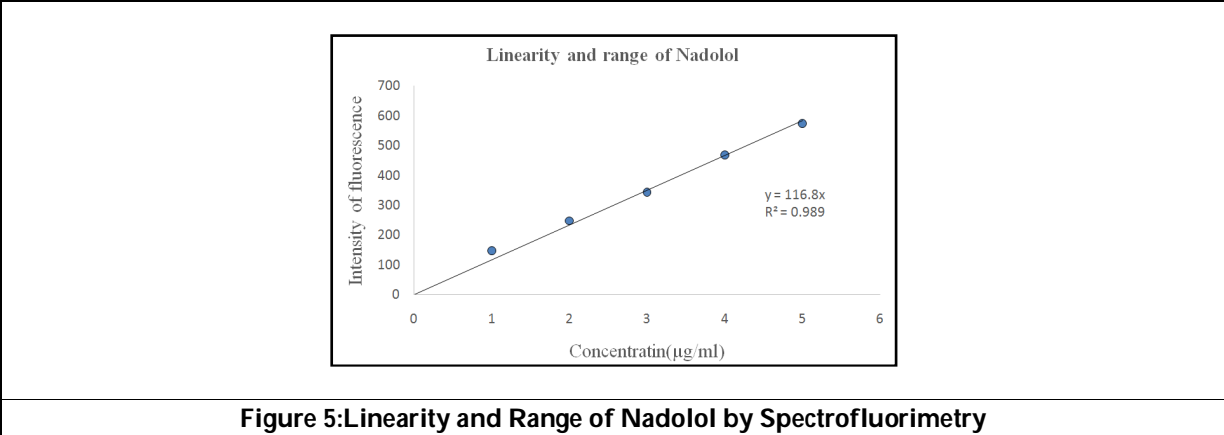


Figure 5:Linearity and Range of Nadolol by Spectrofluorimetry





Haematological Assessment of Some Fishes of Pradhanpat Waterfall, Deogarh, Odisha - A Review

Sagarika Mishra* and Siba Prasad Parida

Department of Zoology, School of Applied Sciences, Centurion University of Technology and Management, Odisha, India.

Received: 05 Sep 2020

Revised: 07 Oct 2020

Accepted: 09 Nov 2020

*Address for Correspondence

Sagarika Mishra

Department of Zoology, School of Applied Sciences,
Centurion University of Technology and Management,
Odisha, India.

Email: lect.sagarikamishra77@gmail.com



This is an Open Access Journal / article distributed under the terms of the **Creative Commons Attribution License** (CC BY-NC-ND 3.0) which permits unrestricted use, distribution, and reproduction in any medium, provided the original work is properly cited. All rights reserved.

ABSTRACT

Fish hematology plays an important role as a good indicator of health of aquatic ecosystem. The fish gives a valuable effort in malnutrition and fighting hunger bearing long chain Omega-3 fatty acid, iodine, vitamin-D and calcium. Taking this into consideration the haematological profile of Pradhanpat waterfall reservoir is studied during present investigation. The reservoir spread over area about 300 acre areas. The present findings indicate that the reservoir is blessed with diverse fish fauna including economically important edible fishes. The water quality of the reservoir is suitable for fish culture.

Keywords: Fish fauna, hematology, Pradhanpat waterfall reservoir, and review.

INTRODUCTION

Out of the 10 incarnations (Avatars) of lord Vishnu one of its is massy (Sanskrit-fish) for the purpose of saves the world from flood. A little fish caught by the first man saint Manu which later forms a giant size as lord Vishnu. For medical and biological research the most important species is fish is used in laboratory. The analysis of gene expression by the use of zebra fish as a model. Fish is a key structure reveals the idea about genetics, behavior, evolution and physiology of aquatic first vertebrates having gills throughout life and acquires half position out of total number of vertebrates. The haematological work of Indian fish was first published (Dhar, 1948) and he first done haematological work morphologically in air breathing fish *Ophiocephalus punctatus* as erythrocytes corpuscles, leucocytes count and clotting time. The morphology and fragility of erythrocytes in *Heteropneustes fossils* reported (Banerjee, 1956).



**Sagarika Mishra and Siba Prasad Parida**

The blood parameters of three Indian major carps *Labeo calbasu*, *Catla catla* and *Cirrhinus mrigala* studied (Das, 1958). The haematological study of *Hilsa ilisha* from river hoogly reported (Pilay, 1958). The study of total leucocytes count in blood of fish reported (Smirnova, 1965). The analysis of sex related blood parameters in air breathing fish *Anabas testudineus* reported (Banerjee, 1966). The routine examination in fish haematocrit value play a vital role in haematological status reported (Houston and De wilde, 1968). In *Channa punctatus* and *Heteropneustes fossilis*, the research work on erythrocytes, leucocytes, blood clotting time, hemoglobin contents and the degeneration of erythrocytes reported (Srivastav, 1967). The haematological constituents of fishes are affected by the seasonal variation (Giomski et al., 1992 and Dabrowski, 1998). After the evolution of amphibians fishes of fresh water are the most threatened group of vertebrates and the extinction rate is high in higher vertebrates globally (Bruton, 1995). The main cause of reduction of fish species are habitat degradation, introduction of exotic species, pollution, globalization, climate change (Gibbs, 2000). In national level the India acquired 17 mega biodiversity in world from which freshwater mega diversity acquire 9th position (Mittermeier et al., 1997). As per the view of global assessment of fresh water fishes is greater than the inland water area (Balian et al., 2008). About 1027 species of fresh water fishes found in India divided into primary, secondary and alien fresh water fishes (Dudgeon et al., 2005; Pattnaik, 2007). About 186 fish species found in Odisha in different fresh water bodies having 11 orders, 33 families, 96 genera. Among them the highest species found in order of *Cypriniformes* and family of *Cyprinidae* (Havagiappa et al., 2018).

Effect of Physico-Chemical Factors on Haematology of Fishes

Hesser(1960) investigate the use of haematological parameters in fish and its study indicate the status of fish health and physiological changes in different environmental conditions like pollution, metals, hypoxia, anesthetics, season, acclimation (Blaxhall,1972; Ogbulie and Okpokwasili,1999; Alwan et al., 2009). The fish animal protein is suitable for socio-economically important for society which harmfully affected from pesticides use in agriculture deposited in different water bodies involved in food chain of fishes (Anees,1975). Neutrophill is present in fish blood first investigated by Jordan and speidal (1924, 1929).The blood sugar and fish activity reported by Gray and Hall (1930). The study of blood in carp and trout reported (Field et al., 1943). The study of plasma erythrocyte in *Channa punctatus* and *Notopterus notopterus* reported (Saxena and Sharma, 1978). It is necessary to do more research work required on fish hematology due to major source of animal protein obtained from fish. The blood component of fish varies depending on physico-chemical of the environment due to intimate contact of the environment (Saravanan et al., 2010). The physico-chemical change in organism is influenced by the blood (Parma et al., 2007; Ololade and Oginni, 2010). Basing on stress condition and environmental factors changes occur in different blood parameters deals with ecotoxicological study (Golovina, 1996). In fish hematology stress is an important factor which is influenced by both biotic and a biotic factors of environment. Abiotic factors like water temperature, pH, and oxygen concentration water pollutants, pesticides, insecticides (Meier et al., 1983; Labeloet et al., 2001). Biotic factors like predators, parasitic invasions or strong competition with other organisms, human anthropogenic activities influence the stress on fish (Witeska, 2005).

Fluctuation of immune systems in blood parameters of fish due to stress condition results increase in volume and counting of erythrocytes reported by (Wendelaarbonga, 1997) and decrease in leucocytes count reported by (Ellsaesser and clem, 1986).When hypothalamus stimulates inhibits the activation of neuroendocrine system, changes in metabolic and physiological condition found in stress condition of fish (Wedemeyer et al.,1990; Lowe and Davison, 2005). The endocrine system of fish secretes stress hormones, cortisol and catecholamines into the blood controlled by central nervous system (Randall and perry,1992).The stress condition in fish vary from species to species (pottinger et al.,1994). The changes in fish haematological parameters found from species to species due to stress, age, season, water pollutants, and physico-chemical characteristics of water, sexual maturity, species, and health condition. Now normal levels of blood parameters are found in variety of teleosts (Darvish et al., 2009; Satheesh Kumar et al., 2012). Haematological indices plays a vital role to watch the physiological and pathological changes(Rambhaskar and rao 1986;Xiaoyun et al.,2009) and the indices diagnose the health condition of fish(De pedro et al.,2005).Basing on handling hypoxic stress vary the concentration of cortisol, glucose, cholesterol and other components (Skjervold et al.,2001). Under stress condition sympathetic activation are indicated by the levels of



**Sagarika Mishra and Siba Prasad Parida**

cortisol and glucose (Lermen et al., 2004). Biochemical parameters of fish hematology are influenced by ecological factors like feeding regime and stocking density (Coz-rakovac et al., 2005). The fresh water becomes polluted due to deposition of untreated waste, dumping of industrial waste; pesticides from agricultural fields causes stress on fishes results obtain physiological changes (Heath, 1991). The hematology, physico- chemical biochemical, oxygen consumption reveals the idea about toxicity of pollutants (Wepener, 1997). Cyanide is more harmful toxic sensitive to fish than humans (Ingles, 1982). The introduction on haematological indices studied by Hesser(1960).Due to acclimation fish haematological indices affected studied in species *Clarias gariepinus* (Ezerie et al., 2004; Gabriel et al., 2004).To govern the physiological changes in fishes is obtained by the study of blood (Iwama et al., 1976; Chakrabarty and Banerjee 1988). Due to direct contact of fish to environment is influenced by ecological factors like water quality, oxygen, temperature, salinity causes sensitive to haematological parameters (Leamaster et al., 1990; Luskovav 1997, Sheikh and Ahmed 2016). Human population facing health hazard by consuming the fish present in metal pollutants fresh water (Marr and Creaser, 1983; Gutenmann et al., 1988).

The valuable haematological parameters detection in fish caused by the effect of environment on fish (Musa and Onoregie, 1999). Fish blood parameters are highly sensitive to chemical, physical, and environmental factors (Akinrotimi et al., 2013). Fish hematology is affected by the human anthropogenic activities (Rechardson et al., 1995; Popper et al., 2003; Hastings 2008, Popper and Hastings 2009). The glucose-corticoid hormone secretes cortisol through blood stream into the tissue when the fish in stressful condition (Stormhofel and Bartke, 1998). A gene level estimation reveals the idea about physiological stress tolerance obtained by the combination of m-rna with cortisol (Wendelaar bonga,1997).The haematological parameters vary from season to season not to conform the actual baseline data on hematology (Leard et al.,1998). Fish blood parameters are directly or indirectly influence by the sex, size, season, age of fish (Bhagat and Banerjee, 1986). Depending on environmental factors only the haematological parameters is the mirror image of health condition of fish (Alkinson and Judd, 1978) and to identify help in study of stress indicator (Blaxhall, 1972).

The feeding habits, pathological status, environmental stress reflects on physiological response are obtained by the study of haematological parameters of fish (Svobdodova et al., 1986). For fish cultivation it needs to identify the haematological parameters by the study of haematocrit, erythrocytes count and hemoglobin concentration for better productivity (Bhasar and rao, 1990). From the available information the study of haematological parameters is well studied in marine species (Johnson, 1968). In Asia, the edible mudfish *Clarias batrachus* locally named as magur widely distributed in different fresh water bodies of India also available in other Asian countries (Mollahhfa et al., 1990). To diagnose the fish disease due to variation in haematological indices this reflects on fish blood. Evaluation of haematological parameters plays a vital role in function of physiological, biochemical, nutritional, health status influence by different age, sexual maturity, ecological and environmental factor (Blaxhall pc 1972, Patriche et al., 2011, Radu et al.,2009). Due to pollution, global warming, globalization changes occur in haematological parameters of fish (Pamila et al., 1991, Bhat and Farswan 1992, Varadraj et al., 1993, Gupta et al., 1995, Srivastav et al., 1996, Kumar et al., 1999, Nair 2000, Kumari and Pandey 2002, Paulose 2002, Das and Bhattacharya 2002, Svobodova et al., 2003, Yaji and Auta 2007, Ramesh and Saravanan 2008, Jafferli and Rani 2009). To evaluate the haematological parameters for diagnosing the physiological mechanisms pollutants affect the water quality this reflects on fish blood (Van vuren, 1986).

Blood is highly sensitive to external and internal environment causes physico chemical changes which reflect on blood components (Wilson and Taylor, 1993). Physical, chemical and environmental factors are highly sensitive to haematological parameters of fish (Lebedeva et al.,1998; Vosyline 1999), study of nutritional effects on haematological study(Rehulka 2000), infectious diseases (Rehulka 2002), Pollutants(Rehulka 2002). Stress responders are detected by the study of erythrocytes (Rainza-paiva et al., 2000; Oneal and weirich, 2001).To what extent a blood damaged and trace out of many diseases can be studied by evaluating the haematological parameters (Onyeyili et al., 1992, Togun et al., 2007). Healthy fish is identified by the study of very good blood composition (Issac et al., 2013). When the fish is in contact with toxic agent it reflects on fish blood (Olafedehan et al., 2010). The current status of



**Sagarika Mishra and Siba Prasad Parida**

physiological condition studied by the change in haematological parameters of fish (Togun et al., 2007). Depending on feeding habit the Asian indigenous, tropical catfish is *Clarias gariepinus* have high growth rate, omnivorous, high resistance to handling and stress the clarias species is found in different fresh water bodies of India (Olaifa et al., 2003; Eyo and Eyetie 2004; Akinsanya and Otubanjo 2006; Ogundiran et al., 2009). Basing on the biological status and time period spend with toxicants the changes in haematological parameters reflect on blood (Brungs, 1977). So fishes play a key role in environment as a bio-indicator (Nussey et al., 1995; Kock et al., 1996; Borkovic et al., 2008; Kim et al., 2008). For laboratory experiments of fish normal acclimation period is 7 and during this period symptoms of disease trace out for easy separation of healthy species take as experimental view (Heath, 1987). Depending on direct contact with aquatic environment and poikilothermic there is found variation in haematological parameters due to environmental factors, water temperature, oxygen content, pH and also changes seasonally (Atamanalp and Yanik, 2003). Basing on stocking, feeding and water quality studying by evaluation of haematological parameters for better health management (Rehulka et al., 2004; Tavares-dias et al., 2005). The haematological parameters of fish are variable due to intimate contact of phyco-chemical changes of environment which direct reflect on blood causes changes in fish physiology and plays a key role in environmental impacts upon fish (Romestand et al., 1983; Adams et al., 1993; Chen et al., 1995; Houston et al., 1997). Some factors like diet, temperature, pH, photoperiod, reproductive cycle influence the haematological indices (Sandness et al., 1988; Kavadias et al., 1996; Svoboda et al., 2001), stress, pollution, size, seasonal variations (Clarks et al., 1979; Barham et al., 1980; Ranzani-paiva et al., 2004).

Intake of Heavy Metals through Food in Fish

On entering the food accumulations of heavy metals occurring in different organs of fish and maternally transmit to next generation maternally. Depending on concentration of heavy metals, physiological, ecological and environmental influence the haematological parameters (Milda, 1992). The presence of harmful organic and inorganic chemicals in different fresh water bodies directly or indirectly influenced the fish health to obtain less production in piscine revolution. The 20th inorganic element Arsenic is toxic to fishes create health hazard (Shaw et al., 2007). Fish population is destroyed by pollutants, domestic waste, industrial effluents, manmade anthropogenic activities and heavy metals present in water (Zaki et al., 2009). Due to direct contact with the aquatic environment any change directly reflect on blood affected by heavy metals causes change in physiologically and biochemically found in tissue and blood of fish (Base and Rani, 2003). The metal pollutants and functional status of the oxygen carrying capacity of blood can be identified by evaluating the haematological parameters of fishes (Shah and Altindag, 2004). Under the influence of toxicant to diagnose the structural and functional status of fish can be evaluate by the study of haematological parameters (Adhikari et al., 2004). The measurement of hemoglobin by cyanmethemoglobin used (Barker and silvertorn 1976). The measurement of serum proteins by the modified biuret method, arid end point assay described (Lawrence 1986).

The contaminants heavy metals is highly influence the fish population to decreases its quality (Farombi et al., 2007). Basing on potentiality, the heavy metals chromium affects greater on fish population (Shuhaimi-othman et al., 2010). When the fish exposed to chromium changes physiologically like quick opercular movement, gulping for air due to respiratory rate impairment, darkening of body, sudden and quick movement seen initially reveals the idea about quality of pollution (Sentamilselvan et al., 2015). The United States Environment Agency proved that out of 18 hazardous air pollutants (HAPs) chromium is highly toxic widely present having several oxidation states (Ho yu et al., 2014). Depending on high solubility, mobility, toxicity not only affects the health but also the environment (Xu and Wang, 2012). Due to bioaccumulation and non-biodegradable characteristics the living organisms are affected by chromium and fish population on growth and survival (Mishra and Mohanty, 2008). The heavy metal arsenic is regulated by preventing toxic wastes discharge into the fresh water bodies and its effects on fish after exposed to 96 hours (Kumar and Banerjee, 2012). The gills are blocked causes difficulty in breathing; blood vessels are damaged to obtain vascular collapse in gills due to effect of arsenic (Sorenson 1991). Arsenic trioxides are deposited in the organ kidney, liver, tissue (Adhikari et al., 2004). The high tolerance toxic species gibel carp is widely distributed (Aliko et al., 2018).





Haematology and Toxicity

Blood is the mirror image of any disturbance in haematological indices in fishes that is affected by harmful toxic agents from environment, human anthropogenic activities. When the exposed to mercury the RBC count, Hb and HCT values decreases in *Anabas testudineus* (Panigrahi, 1977). The study of hemoglobin concentration and RBC count is greatly affected by metal toxicants (Qayyam et al., 1976). In fresh water teleosts, the erythropenia causes increase in hemolytic anemia and hemoglobin content and haematocrit value decreases (Srivastav and mishra, 1979) and also investigated the occurrence of immature erythrocytes in peripheral circulation on exposed to lead. In fresh water fishes hemoglobin and haematocrit values increases responsible for polycythemia when lymphocytes decrease on subjected to copper, nitrate, chromium and cobalt toxicity. Blood is greatly affected by Copper in teleosts *Colisa fasciatus* (Mishra and Srivastav, 1980). In *Channa punctatus* the RBC count and haematocrit increases in water when subjected to mercury chloride. In *Anabas testudineus* the blood parameters varies on exposure to titanium effluent (Nair et al., 1984). When *Heteropneustes fossilis* is subjected to zinc the hemoglobin content, RBC count, PCV decreased (Goel and Kalpana, 1985).

The toxicants NaCl cause stress symptoms in blood of *Channa punctatus* (Dheer et al., 1986). Van vuren (1986) investigate the food is affected by various toxins causes Hemoglobin content and MCV decreases. The leukocytes is affected by poisonous heavy metal studied (Banerjee and Verma, 1987) but on exposure to HgCl₂ the lymphocytes number increases. On exposure of sublethal conc. of lead nitrate the fish *Clarius batrachus* facing the problem hypoglycemic, hypocalcaemia and anemic. The *Cyprinus carpio* when exposed to cadmium nitrate and mercuric chloride the hemoglobin content, haematocrit values erythrocyte count decreases (Beena and Vishwaranjan, 1987). When the dogfish exposed to toxicants causes swells of erythrocytes (Tort et al, 1987). When the *Carassius carassius* exposed to lead the RBC count, haematocrit hemoglobin percentage and MCHC decreased. When the *Heteropneustes fossilis* exposed to manganese the leucocytes increases reported (Garg et al., 1989). The pollutants cadmium causes biphasic response in *Channa punctatus* (Dabowska, 1989). The *Channa punctatus* secretes mucus when exposed to mercuric chloride and zinc sulphate (Khillare and Sonwane, 1990) in *Channa gachua*.

When the fish *Oreochromis* sp. exposed to cadmium the mcv and mch of blood increases Ruparelia et al., (1992). When the fish *Oreochromis mossambius* is subjected to pulp mill effluent and paper the mcv and MCH increases (Varaharaj et al., 1993). When the *Channa punctatus* and *Heteropneustes fossilis* is subjected to cadmium chloride the body secretes excess mucus, opercular movement increases, swim erratically, jerky movements, spiral movement reported (Verma et al., 1992). When the *Labeo rohita* exposed to cadmium the hemoglobin contents, haematocrit, RBC counts decreases (Mukherjee and Sinha, 1993). A high energy is produced when the haematological constituent is affected by stressors is reported (Murad et al., 1993). When *Channa punctatus* is subjected to cadmium causes decrease in hemoglobin conc. PCV and total erythrocyte count reported (Shastry and Gupta, 1994). *Oreochromous mossambius* is subjected to copper the hemoglobin content; PCV value decreases (Sampath et al., 1998). The *Channa punctatus* is subjected to copper and chromium the leucocytes count increases (Singh 1995). The highly toxic pollutants cadmium creates harmful effects on fishes mainly found in mines area (Dojlido, 1995). The cadmium is quickly absorbed and concentrated in the bodies of fish (Houston and Keen, 1984).

Blood as Biological Indicator Unit

The haematological parameters play a key role as bioindicator for the estimation of fish health and impact of environment upon fish (Neff 1985, Adams 1990, Wendellarbonga 1997). Blood plays a vital role in monitoring physiological health status of fishes. The haematological work of Indian fish published (Dhar, 1948) and the first haematological work in air breathing fish *Ophiocephalus punctatus* as erythrocytes corpuscles, leucocytes count and clotting time. The morphology and fragility reported (Banerjee, 1956; 1957). In routine examination haematocrit value play as a key role in haematological status of fishes reported (Houston and De Wilde, 1968). In *Channa punctatus* and *Heteropneustes fossilis* the research work on erythrocytes, leucocytes, blood clotting time, haemoglobin contents and de generation of erythrocytes reported (Srivstava, 1967). The haematological constituent of fishes is greatly affected by the seasonal variation (Giomski et al., 1992) and Dabrowski (1998). The influence of stressors,



**Sagarika Mishra and Siba Prasad Parida**

deficiencies, metabolic disorders are reflects on blood of fishes cause changes haematological parameters (Bahmani et al., 2001). The fish health is detected by the analysis of blood biochemistry (De pedro et al., 2005), exogenous factors like management (Svobodova et al., 2008), diseases (Chen et al., 2004) responsible for variation in blood composition. The haematological parameter varies depending upon quality of water, temperature, food sources, and physiological status. (Iqbal et al.,1997). Fish blood is the mirror image of physiological status of fish, sex, size, season and age and any disturbances in physico – chemical parameters that influences the blood parameters (Venkaeshwaslu , 2011).The sex, size and age of fishes are affected by the changes in protein, cholesterol and glucose level of blood (Dharan and Singh, 2008). Due to the movement and seasonal variation there is a change in the values of blood parameters (Pandey et al. 1993). The toxic agents and microbes are directly affects the haematological indices of fishes (Parveen et al. 2011). Any disturbances detected in fishes of different age groups and habitat physico – chemically reflects on blood (Kocobatmazve and Ekingen, 1978). Due to the impact of environmental stressor upon fish causes variation in haemaological parameters reflects on fish blood. (Shah and Altindag, 2005), malnutrition (Caillas and Smith, 1977), gender (Collazos et al. 1998), Seasonal differences and breeding (Cech and Wohlsachlag, 1981).

Now days due anthropogenic activities by human increases the pollutants of fresh water influence the fish population that creates harmful hazards to fish population (Gutenmann et al., 1988). Blood constituents in fish play a key role in watching health status of fish (Bhaskar and rao, 1984; Schuett et al., 1997). The ecological factors water, temperature influence the haematological indices like haematocrit, hemoglobin concentration and erythrocyte count (Graham, 1997). A very well activity of fish depends upon the well blood constituents of fishes. Blood maintains the homeostasis of the body because fish is a poikilothermic animal (Issac et al., 2013). Seasonal factors in influence blood cell constituents like immune depression are recorded in the fish when the temperature is low observed in cold season (Avtalion, 1988). Evaluation of haematological parameters gives idea about substantial diagnostic information and standard reference values of fishes (Oryan et al., 2008). Haematological parameters clinically play a major role used as a health indicator (Schutt et al., 1997). The protein globulin is the major constituents in the plasma of fish blood. The study of haematological and blood biochemical in relation to age record the routine haematological methods using the fish blood (Blaxhall and Daisley, 1973). From the available literature and own experiences to know the fish species physiologically by the study of hematology indicate the fish welfare , health, condition of aquatic environment (Audin et al., 1997; Ivanc et al., 1997). A haematological index varies in circadian (daily) and circannual (seasonal) is recorded (Ivanc et al., 1985). By the determination of haemogram to evaluate the total RBC count ,total WBC count PCV, Hb, erythrocyte indices (MCV, MCHC, MCH), white blood cell differential count and the evaluation of stained peripheral blood film (Campbell, 2004). The study of haematological parameters is essential in the field of fish cultivation (Bhaskar and Rao, 1990). The haematological parameters is not constant due to malnutrition (Ighwela et al., 2012), gender (Collazos et al., 1998), seasonal differences and breathing efficiency (Pradhan et al., 2012), environmental stress (Singh and Tendon, 2009), fish size (Gracia et al., 1992).

CONCLUSION

The study of haematological analysis is related to healthy fish increase in fish cultivation consumption human population. The ecological, environmental factors and human anthropogenic activities directly or indirectly influence the fish population. Ichthyologist diagnoses the fish disease from the analysis of haematological parameters of fishes. The erythrocytes are responsible for dissolved oxygen carrying capacity. The investigation work on fish hematology reveals the idea about selection of healthy fish from unhealthy fish for more production. Thus it needs more research work on fish hematology.





REFERENCES

- Mishra, S.K. , Sarkar, U. K., Gupta, B.K., Trivedi , S.P. , Dubey, V. K, Pal, A, (2011) Patterns of freshwater fish diversity threats and issues of fisheries management in an unexplored tributary of the Ganges basin , Northern India . Journal of Ecophysiology and occupational health, vol.(11), 149-159.
- Chandra, K. , Gopi, K.C. , Rao, D.V., Valamathi, K, Alfred J.R.B, (2017), Current status of fresh water faunal diversity in India . Zoological Survey of India , Freshwater Biological Regional Centre , Hyderabad – 48) , Vol. (6), 1-624
- Mogalekar, S.H, Canciyal J. (2018] Fresh water fishes of Odisha Journal of Fisheries, Vol. (6), 587 – 598,
- Gupta, A., Kumar A. (2015), Haematological studies of some edible fresh water fishes of ncr region. World Journal of Pharmacy and Pharmaceutical Science, Vol.4 (6), 1467 – 1479.
- Vasanth, A., Chokki, P.V., Kumar, C.C, (2018), Haematological responses in the fresh water fish *Anabas testudineus*, Bloch 1972, exposed to sublethal concentration of acid range 7. Journal of Global Bioscience, vol .7(8), 5536-5549.
- Kandeepan, C.(2014) Effect of stress on haematological parameters of air breathing loach *Lepidocephalus thermalis*, International Journal of Current Research and Academic Review, Vol. 2(8) , 309-322.
- Kaur Y, Tyagi A (2017), Baseline studies on selected haematological parameters of Indian major carps, exotic carps and catfishes. Journal of Fisheries and Life sciences, Vol 2(2), 60-67.
- Adeymo, K, (2005), Haematological and histopathological effects of cassava mill effluents in *Clarias gariepinus*. African Journal of Biomedical Research, Vol-8,179-183.
- Akinrotmi, O.A, Vedeme, B, Agokei, E.O, (2010), Effects of acclimation on haematological parameters of *Tilapia guineensis*. Biology Science World Journal), Vol 5(4), 1597-6343.
- Kulkarni, R.S. (2015) Hematology of fresh water fish, *Notopterus notopterus* in relation to physico-chemical characteristics of the water. (International Letters of Natural Sciences), Vol. 40, 19-23.
- Parrino, V., Capello, T., Costa, G., Cannava, C., Sanfilippo and Fasulo, S. (2018). Comparative study of hematology of two teleosts fish *Mugil cephalus* and *Carrasius auratus* from different environments and feeding habits. The European Zoological Journal), vol. 85(1), 193- 199.
- Arnaudova, D. , Tomova, E. (2008) Selected haematological indices of freshwater fish from studenkladenetsh reservoir. Bulgarian Journal of Agricultural Science, Vol. 14(2), 244-250.
- George, A. , Akinotomi, O.A., Nwokoma, U.K. (2017) Haematological changes in African catfish *Carias gariepinus* to mixture of atrazine and metalachlor in the laboratory. Journal of fisheries sciences, Vol. 11(3), 048-054.
- Witeska, M., Lugowska, K., Kendera, E. (2016) Reference values of haematological parameters for juvenile *Cyprinus carpio*, (Bulletin of European association of fish pathologist), Vol. 36(4), 169.
- Arthanari, M., Kumar, S. , Palan, D., (2015) Assessment of the haematological and serum biochemical parameters of three commercially important freshwater fishes in river Cauvery, Velur, Namakkal District, Tamil Nadu , India. International Journals of Fisheries and Aquatic studies, Vol. 4(1), 155-159.
- Langer, S., Sharma, J. and Kant, K.R. (2013) Seasonal variation in haematological parameters of hill stream fish, *Garra gotyla gotyla* from Jhajjar stream of Jammu region, India. International journal of Fisheries and Aquacultures Sciences, Vol. 3(1), 63-70.
- Chauhan, J., Rao, S.N. (2018) Seasonal changes in the heamatology of the fresh water fish, *Clarias batrachus* of terai region of Uttarakhand. International Journal of Development Research, Vol.8 (3), 19493 – 19497.
- Adeymo, O.K. (2007) Haematological profile of *Clarias gariepinus*, Burchell 1822 exposed to lead. Turkish Journal of Fisheries and Aquatic Sciences, Vol. 7, 163 – 169.
- Etim, N.N., Williams, M. E., Akabio, U., Offiong, E.E.A. (2014) Haematological parameters and factor affecting their value. Science and Education Centre of North America, Vol.2 (1), 37-47.
- Abalaka, E.S. (2013), Evaluation of the haematology and bio chemistry of *Clarias gariepinus* as biomarkers of environment pollution in tiga dam, Nigeria. Brazilian Archives of Biology and Technology, an International Journal, Vol 56(3), 371-376.





Sagarika Mishra and Siba Prasad Parida

21. Gabriel, U. U., Ezeri .G N.O., Opabunmi O. O., (2004) Influence of sex, source, health status and acclimation on the hematology of *Clarias gariepinus*. African Journal of Biotechnology, Vol 3 (9), 463-467.
22. Duman, S., Sahan, A., (2017) Determination of some haematological parameters and non-specific immune responses in *Garrarufa* living in Kangal baliki ceramic thermal hot spring and to pardic stream. Journal of Aquaculture Engineering and Fisheries Research, vol.3 (3), 108 -115.
23. Karim, B., Yousria, G. and Wyllia. K. (2019) Influence of total length sex seasonal variation on haematological parameters in *Cyprinus carpio*, pisces Cyprinidae in lake Tonga, Algeria , Biodiversity Journal , Vol .10 (4). 593-600.
24. Acharya, G ., Mohanty, P. K., (2014) Comparative haematological and serum biochemical analysis of catfish, *Clarias batrachus*, Linnaeus 1756 and *Heteropneustes fossilis*, Bloch 794 with respect to sex. Journal of Entomology and Zoology Studies, Vol 2(6), 191-197.
25. Vosyliene, M.Z. (1992), the effect of heavy metal on haematological indices of fish. Acta Zoologica Lituanica Journal, Vol. 9(2), 76-82.
26. Manikandan, .S, R. , Sukumaran, M., Muthukumaravel, K., Ramya, P., Rajeswari, K., (2013) Haematological studies of fresh water catfish, *mystus vittatus* , exposed to sodium arsenate. International Journal of Pure and Applied Zoology, Vol .1(4), 310-314.
27. Eng, H. H, and Kottelat, M. (2008) the identity of *Clarias batrachus* , Linnaeus 1758 with the designation of a neotype. Zoological journal of the Linnaean Society, Vol. 15(3), 725-732.
28. Madhavan, P., Elumalai, K., (2016) Effect of chlorium on haematological parameters in catfish, *Clarius bataracius* 1758. International journal of advanced research in Biological Science, Vol. 3(5), 62 -70.
29. Pichhode, M., Ggaherwal, S. , (2019) Toxicological effect of Arsenic trioxides exposure on haematological profile in catfish *Clarius batarachus*., International Journal of Current Research and Review , Vol. 11 (16).
30. Vajargah, M.F., Faggio, C., Hedayati, A. (2019) Effect of long term exposure of silver nano particles on growing indices , haematological and biochemical parameters and gonad histology of male gold fish *Carassius auratus gibelio*. Microscopy Research and technique, Wiley, Vol.5.
31. Arya, P., Chauhan, R.S., Nazir I. (2018) Evaluation of haematological and biochemical parameters in fingerlings of Indian major carp *Labeo rohita* fed with nutraceuticals timulin. The Pharma Innovation Journal), Vol. 7(1), 565 – 568.
32. Malathi, K., Kannathasun, A., Rajendran, K. (2012) Comparative haematological studies on freshwater fishes *Channa striatus*. International Journal of Pharmaceutical Chemical and Biological Sciences), vol.2 (4), 644-648.
33. Adeymo, O.K. , Adedeji, O.B., Ofor, C.C. (2010) Blood lead level as biomarker of environmental lead pollution in feral and cultured African catfish *Clarius gariepinus* . African Journals Online, Vol.31 (2), 139 – 147.
34. Jawad, L. A., Al-mukhtarm, A and Ahmed, H.K. (2004), The relationship between haemotocrit and some biological parameters of Indian shad, *Tenualosa ilisha* . Animal biodiversity and conservation, Vol. 27(2), 47 -52.
35. Etim, N. (2014) Haematological parameters and factors affecting their values. Agricultural science, Vol. 2(1), 37-47.
36. Luska, V. (1998), Factors affecting haematological indices in free living fish population. ActaVeterinaria Brno, Vol. 67, 249- 255.
37. Firouzbakhsh, F., Abedi, Z., Rahmani ,H., Khaleshi, M.K., (2013), A comparative study of some factors in male and female *Caspian kutum rutilus frisii kutum* brood stock from the southern basin of the Caspian Sea. Turkish Journal of Veterinary and Animal Sciences, Vol. 37, 320-325.
38. Collazos, M.E., Ortega, E., Barigge, C. (1998) Sseasonal variation in haematological parameters of male and female *Tinca tinca* .Kluwer Academic publisher, Vol. 183 , 165- 168.
39. Motlagh, S.P., Zarejabad, A.M., Nsrabadi, R.G., Ahmadifar, E. Molae, M.(2012) Hematology, morphology and blood cells characteristics of male and female siamese fighting fish , *Betta splendens*. Comparative Clinical Pathology, Vol. 21(1), 15-21.
40. Samuel, V.K., Pascal, L.F., Tennyson, S., Pandeewari, M. , Dhinamala, K., Persis, D., Raven, R., (2018) Haematological studies of *Anabas testudineus* on exposure to aquatic toxicants of bucking ham canal , Chennai ,



**Sagarika Mishra and Siba Prasad Parida**

- Tamil Nadu , India. International Journal of Fisheries and Aquatic Studies, Dhaka University J. boil. Sci praxis veterinaria, Vol.6(4), 55-59.
41. Hasan, M., Mamun, A.A., Rabbane, M. D.G (2012) Haematological profile of Thai and indigenous male and female air breathing climbing perch. Dhaka university journal of Biological Sciences, Vol. 21(1), 67- 77.
 42. Val, A.L. (2000) Organic phosphates in red blood cells of fish. Comparative Biochemistry and Physiology, Vol. 125, 417- 435.
 43. Parrino, V., Capello, T., Costa, J.G., Cannava, C., Sanfilippo, M., Fazio, F. (2018) Comparative study of hematology of two teleosts fish *Mugil cephalus* and *Carassius auratus* from different environment and feeding habits. The European Zoological Journal, Vol. 85 (1), 193 -199.
 44. Kandari, M.S., Nautiyal, N., Rauthan, G. (2018) Study on monthly variation in haematological and chemical parameters of three Indian major carps under semi – intensive polyculture practice. International Journal of Fisheries and Aquatic Research, Vol. 3(3), 5-60.
 45. Invanc, A., Haskovic, E. , Jeremic, S., Dekiel, R. (2005) Haematological evaluation of welfare and health of fish, Bangladesh Journal Fisheries Research, Vol. 53(3), 191-202.
 46. Pradhan, S.C., Patra, A.K., Pal, A. (2014) Haematological and plasma chemistry of India major carp, *Labeo rohita*. Journal of Applied Ichthyology, Vol. 30, 48 -54..
 47. Sardar, M., Khan, M.A.H.N.A, Alam, M. and Rashid, M. (2000) Cell types in the peripheral blood of walking catfish *Clarias batarachus*. Bangladesh Journal of Fisheries Research, Vol. 4(2), 157-164.
 48. Lin Hui, C. Sung, W.T. (2003) the distribution of mitochondria rich cells in gills of air breathing fishes. Physiological and Biochemical Zoology, Vol. 76(2), 215 -228.
 49. Roberts, T.R. (1975) Geographical distribution of African freshwater fishes. Zoological Journal of Linnean Society, Vol. 57(4), 249-319.
 50. Burton, M.J.N. (1979) the food and feeding behaviour of *Clarias gariepinus* in lake sibaya South Africa. The transactions of the Zoological Society of London, Vol. 35(1), 47-114.
 51. Teuguis, G.G. (1979) Taxonomy phylogeny and biogeography of catfishes. Journal of Natural History, Vol. 9, 9-34.
 52. Teugels, G.G., Adriaens, D. (2003) Taxonomy and phylogeny of claridae. Journal of Natural History, Vol. 11, 465-487.
 53. Teugels, G.G. (1982) Preliminary results of a morphological study of African species of the subgenus *Clarias*. Journal of Natural History, Vol. 16(3), 439-464.
 54. Kelvin, K.P. (1993), *Clarias batu* a new species of catfish from pulautioman, peninsular Malaysia. The Raffles Bulletin of Zoology, Vol. 6 (6), 157 -167.
 55. Mahajan, C.L., Dheer, J.S. (1979) Seasonal variation in the blood constituents of an air breathing fish, *Channa punctatus*, Journal of Fish Biology, Vol. 14(4) , 413-417.





RESEARCH ARTICLE

Correlation between Blood Glucose, HbA1c and Serum Lipid Levels in Non-Insulin Dependent Diabetes Mellitus (NIDDM) Patients

Gopika R^{1*}, Senthilkumar G¹, Karthy E.S² and Panneerselvam A¹

¹A.V.V.M Sri Pushpam College (Autonomous), (Affiliated to Bharathidasan University, Tiruchirappalli – 620024), Poondi, Thanjavur, Tamil Nadu, India.

²AWECARE, Analytical and Research Laboratories, Thindal, Erode, Tamil Nadu, India.

Received: 13 Sep 2020

Revised: 16 Oct 2020

Accepted: 18 Nov 2020

*Address for Correspondence

Gopika R

A.V.V.M Sri Pushpam College (Autonomous),

Poondi, Thanjavur, Tamil Nadu, India.

Email: gopikaraj2010@gmail.com



This is an Open Access Journal / article distributed under the terms of the **Creative Commons Attribution License** (CC BY-NC-ND 3.0) which permits unrestricted use, distribution, and reproduction in any medium, provided the original work is properly cited. All rights reserved.

ABSTRACT

Diabetes mellitus (DM), or simply diabetes, is a group of metabolic diseases in which a person has high blood glucose, either because the body does not produce enough insulin, or because cells do not respond to the insulin that is produced. Conventionally, diabetes has been divided into three types namely: Type 1 DM or insulin-dependent diabetes mellitus (IDDM) in which body fails to produce insulin, and presently requires the person to inject insulin or wear an insulin pump. This is also termed as "juvenile diabetes". Type 2 DM or noninsulin-dependent diabetes mellitus (NIDDM), results from insulin resistance, a condition in which cells fail to use insulin properly, with or without an absolute insulin deficiency. This type was previously referred to as or "adult-onset diabetes". Study aimed to observe the lipid profile in type 2 diabetes mellitus patients and to find out the correlation between glycated haemoglobin (HbA1c) and lipid profile in type 2 diabetes mellitus patients. This study was a cross sectional study conducted on 1000 samples from diabetic and Non diabetic patients. Detailed history and examination were done in all patients. The fasting blood glucose (FBG) levels, HbA1C levels and serum lipid levels were performed and then correlated fasting blood glucose level with HbA1c levels and FBG and HbA1c with serum lipid levels. There was a significant positive correlation between FBG and HbA1c, and FBG and HbA1c with serum cholesterol and serum triglycerides level and negative correlation with serum HDL-cholesterol levels.

Keywords: Diabetes Mellitus (DM), Fasting Blood Glucose (FBG), Glycosylated Haemoglobin (HbA1c), Serum Cholesterol, Serum Triglycerides, Serum HDL-Cholesterol.



**Gopika et al.,**

INTRODUCTION

Diabetes mellitus (DM) is commonest endocrine disorder that affects more than 100 million people worldwide (6% population). It is caused by deficiency or ineffective production of insulin by pancreas which results in increase or decrease in concentrations of glucose in the blood. It is found to damage many of body systems particularly blood vessels, eyes, kidney, heart and nerves (Ismail., 2009). Diabetes mellitus has been classified into two types i.e. insulin dependent Diabetes mellitus (IDDM, Type I) and non-insulin dependent diabetes mellitus (NIDDM, Type II). Type I diabetes is an autoimmune disease characterized by a local inflammatory reaction in and around islets that is followed by selective destruction of insulin secreting cells whereas Type II diabetes is characterized by peripheral insulin resistance and impaired insulin secretion (Arora *et al.*, 2009). The presence of DM shows increased risk of many complications such as cardiovascular diseases, peripheral vascular diseases, stroke, neuropathy, renal failure, retinopathy, blindness, amputations etc. It is estimated that 439 million people would have type 2 DM by the year 2030. The incidence of type 2 DM varies substantially from one geographical region to the other as a result of environmental and lifestyle risk factors (Zimmet and Alberti., 2001). It is predicted that the prevalence of DM in adults of which type 2 DM is becoming prominent will increase in the next two decades and much of the increase will occur in developing countries where the majority of patients are aged between 45 and 64 years (Wild *et al.*, 2004). Dyslipidemia in diabetes commonly manifests as raised low-density lipoprotein cholesterol (LDL-C), decreased high-density lipoprotein cholesterol (HDL-C) levels, or elevated triglyceride (TGL) levels. Furthermore, data from the United Kingdom Prospective Diabetes Study suggest that both decreased HDL-C and elevated LDL-C predict CVD in diabetes. All national and international guidelines recommend aggressive management of lipids in this population (Sarat Chandra *et al.*, 2014). Glycated haemoglobin (HbA1c) is a routinely used marker for long-term glycaemic control. Apart from functioning as an indicator for the mean blood glucose level, HbA1c also predicts the risk for the development of diabetic complications in diabetes patients. This study was undertaken to correlate between fasting blood glucose level, HbA1c level and serum lipid levels in type 2 diabetes mellitus.

MATERIALS AND METHODS

The evaluated clinical and laboratory findings in 1000 samples from diabetic and Non diabetic patients at G.G. Clinical Laboratory and Arya Diabetic Centre, Tamil Nadu, India. Detailed history and examination were done in all patients. Sample collection and preparation of Fasting blood samples were collected into labelled centrifuge tubes, after an 8–12 h overnight fast, Postprandial samples were collected after meals (1 ½ - 2 hours) from the subjects by vein puncture. The blood samples were centrifuged at 2000 rpm for 10 min using a desktop centrifuge and the serum separated and kept in labelled sample bottles at –70°C until further analysis. The serum glucose (Fasting & Post Prandial) (Aziz S and Hsiang YH., 1983), Lipid Profile and HbA1c was analysed using standard Protocol (Niederau *et al.*, 1998). The sera were analyzed for FBG, PPBG, HbA1c and Lipid Profile using an autoanalyzer (Roche Modular P-800, Germany).

Statistical analysis

Statistical comparisons of various biochemical parameters were performed by one-way analysis of variance (ANOVA), and the groups means were compared by Dunnett test. The results were considered statistically significant if the values are $p < 0.05$

RESULTS

A total number of 1000 of patients were enrolled in our study, out of which 586 (58.6%) were male and 414 (41.4 %) were female and maximum were in the age group of 45 – 55 years (Table 1).



**Gopika et al.,**

Fasting Blood Glucose varied from 71 mg/dl to 328 mg/dl with a mean level of 115.12 mg/dl \pm 32.59 mg/dl and Postprandial Blood Glucose varied from 92 mg/dl to 422 mg/dl with a mean level of 191.70 mg/dl \pm 46.03 mg/dl. HbA1c level varied from 5.1 % to 14.9 % with a mean level of 8.27 % \pm 1.57 %. The correlation of Fasting blood glucose, Postprandial glucose and HbA1c level in different group of diabetic shows that patients in Normal had FBG 94.03 \pm 9.78 mg/dl, PPBG 162.4 \pm 17.34 mg/dl and HbA1c level of 7.26 \pm 0.61 %. Patients in Under Controlled group had FBG 124.0 \pm 10.7 mg/dl, PPBG 209.2 \pm 33.3 mg/dl and HbA1c level of 8.88 \pm 1.15 %. In Borderline and Unhealthy Controlled groups had 169.29 \pm 13.36 mg/dl, 260.4 \pm 26.92 mg/dl and HbA1c level 10.66 \pm 0.89 %, 224.11 \pm 33.75, 311.61 \pm 37.79 mg/dl and HbA1c level 12.25 \pm 0.83 % respectively (Table 2).

In these 1000 Patients Serum Cholesterol level varied from 119 mg/dl to 298 mg/dl with a mean level of 197.86 \pm 22.14 mg/dl and Serum Triglycerides varied from 70 mg/dl to 192 mg/dl with a mean level of 131.34 \pm 20.25 mg/dl and Serum HDL Cholesterol varied from 20 mg/dl to 97 mg/dl with a mean level of 51.51 \pm 8.87 mg/dl and LDL Cholesterol level varied from 70.6 mg/dl to 210 mg/dl with a mean level of 120.08 \pm 21.17 mg/dl and VLDL Cholesterol level varied from 12.6 mg/dl to 38.4 mg/dl with a mean level of 26.29 \pm 4.05 mg/dl. The correlation of Lipid Profile in different groups of diabetics shows that patient in Normal had Serum Total Cholesterol (TC) 191.71 + 20.62 mg/dl, Serum Triglycerides (TGL) 122.74 + 16.8 mg/dl, HDL Cholesterol (HDL – C) 52.64 + 9.39 mg/dl and LDL Cholesterol (LDL – C) 114.52 + 19.48 mg/dl. Patients in under controlled group had TC 198.79 + 17.02 mg/dl, TGL 138.37 + 19.17 mg/dl, HDL – C 50.55 + 7.75 mg/dl and LDL – C 120.56 + 17.11 mg/dl. In Borderline and Unhealthy Controlled groups had TC 217.19 + 20.73 mg/dl, TGL 148.12 + 15.36 mg/dl, HDL – C 49.18 + 8.88 mg/dl and LDL – C 138.3 + 19.73 mg/dl, TC 232.80 + 27.81 mg/dl, TGL 160.80 + 10.77 mg/dl, HDL – C 48.42 + 4.85 mg/dl and LDL – C 152.22 + 28.46 mg/dl respectively (Table 3).

There was just significant correlation between FBG and serum cholesterol ($r=0.53$, $P < 0.05$) and also just significant correlation between FBG and serum triglycerides level ($r= 0.22$, $P < 0.05$). Correlation between FBG and serum HDL-cholesterol was highly significant ($r= -0.08$, $P < 0.001$) but correlation was negative. There was significant correlation between HbA1c and serum cholesterol ($r= 0.383$, $P < 0.02$) and between HbA1c and serum triglycerides ($r= 0.097$, $p < 0.04$). HbA1c and serum HDL-cholesterol show significant negative correlation ($r = -0.04$, $P < 0.01$) (Table4).

DISCUSSION

In patients with diabetes, many studies have clearly established that complications are mainly due to chronic hyperglycemia that exerts its injurious to health effects through several mechanisms: dyslipidemia, platelet activation, and altered endothelial metabolism. Both lipid profile and diabetes have been shown to be the important predictors for metabolic disturbances including dyslipidemia, hypertension, cardiovascular diseases (Mahesh dave *et al.*, 2019). The World Health Organization (WHO) and the International Diabetes Federation (IDF) have defined criteria for the diagnosis of diabetes, with cutoff limits based on levels of glycemia associated with microvascular complications (in particular, retinopathy) and the population distribution of plasma glucose (WHO/IDF., 2006). Fasting plasma glucose 126 mg/L (7.0 mol/L) or 2-hour plasma glucose 200 mg/dl (11.1 mmol/L) during an oral glucose tolerance test have traditionally been used for diagnosis. More recently, the value of A1c for diagnostic purposes has been recognized with A1c $\geq 6.5\%$ as the cutoff point for a positive diagnosis (WHO., 2011). There were more males (58.6 %) than females (41.4 %) with T2DM in this study. Mean age of diabetic patients was 50.3 \pm 3.31 years (Age range 45 – 55 years). These values were similar to those reported by Kumar *et al.*, 2013. In our studied FBG level varies 71 mg/dl to 328 mg/dl with a mean level of 115.12 \pm 32.59 mg/dl and Postprandial glucose level varies 92 mg/dl to 422 mg/dl with a mean level of 191.70 mg/dl \pm 46.03 mg/dl. Values of HbA1c level was in range of 5.1 % - 14.9 % with a mean level of 8.27 \pm 1.57 %. Paulsen *et al.*, 1973 studied demonstrated similar type of results in their studies. Mean fasting blood glucose level in diabetic patients with good control was 104.09 mg/dl and level of HbA1c was 6.82%, while in fairly control, the FBG level was 161 mg/dl and level of HbA1c was 8.99% and in those with poor control, the FBG was 202.50 mg/dl and level of HbA1c was 11.74%. The P value (0.001) for FBG and HbA1c between



**Gopika et al.,**

those three groups of diabetic patients was highly significant. This shows that the level of HbA1c in diabetic patients is linearly correlated with the abnormal blood glucose level. Same has been reported by various workers including Gabbay, 1976 and Elkeles *et al.*, 1978. Kennedy *et al.*, 1979 found correlation between FBG and HbA1c levels were satisfactory while Nabarro *et al.*, 1979 found correlation between HbA1c and FBG were not satisfactory. However, in some individual cases, there was no correlation between HbA1c and FBG.

In our studied, serum cholesterol level varied from 119 mg/dl to 298 mg/dl with a mean level of 197.86 ± 22.14 mg/dl which was statistically significant. Diabetic cases studied by Dinesh Kumar *et al.*, 1967 also showed high serum cholesterol level 238.50 mg/dl in older untreated diabetics. Similar observations were also reported by Maleva., 1961, Sharma *et al.*, 1970. Nikkila *et al.*, 1978 found high serum cholesterol levels in poorly controlled diabetic males as well as in well controlled obese males. The increase in cholesterol level appears to be due to increased cholesterol synthesis during poor or no control of hyperglycaemic state, which returns to normal or near normal after good control of their diabetic state. Obesity is an additional cause of enhanced cholesterol production. In our studied, serum triglycerides level varied from 70 mg/dl to 192 mg/dl with a mean level of 131.34 ± 20.25 mg/dl which was statistically significant. Our finding was consistent with many studies. However, these levels were elevated in diabetics who were in poor control as compared to well controlled diabetics and also in obese male diabetics, although they were in good control. Akeel bai-Yaqobi *et al.*, 2011 showed higher level of triglyceride in diabetics. In our studied, serum HDL-cholesterol level varied from 20 mg/dl to 97 mg/dl with a mean level of 51.51 ± 8.87 mg/dl. The value of plasma HDL-cholesterol was significant low in diabetic subjects. This is in conformity with the studies of Lopes-Virella *et al.*, 1982. Various national and international epidemiological studies on lipid profile have also shown this pattern of dyslipidemia (Anjana *et al.*, 2011). No significant difference was observed in total cholesterol and absolute LDL levels in cases and controls in this study. Even if the absolute concentration of LDL cholesterol (LDL-c) is not significantly increased; there is typically a preponderance of smaller, denser LDL particles, which possibly increases atherogenicity (atherogenic dyslipidemia).

In our studied, there was statistically significant direct correlation between HbA1c levels and cholesterol, triglycerides while significant negative correlation was observed between HbA1c levels and plasma HDL-cholesterol levels. Peterson *et al.*, 1977 showed direct correlation between HbA1c and serum triglycerides and cholesterol levels. On the contrary Gonen *et al.*, 1977 did not demonstrate any correlation between HbA1c and serum cholesterol and triglyceride levels while Gabbay *et al.*, 1977 demonstrated direct correlation between HbA1c and serum cholesterol. Falko *et al.*, 1981 demonstrated significant inverse correlation between HbA1c and serum HDL-cholesterol level. Senthilkumar *et al.*, 2016 conducted a perspective study on 162 type 2 diabetes mellitus patients in Tamil Nadu. They found no significant correlation of HbA1c with TC, LDL, HDL and TG. In our studied there was statistically significant direct correlation between FBG level and total cholesterol level, triglycerides level, while significant negative correlation with was observed between FBG level and serum HDL cholesterol level. Samatha *et al.*, 2012 studied that negative correlation of FBG with HDL cholesterol level and a positive correlation of FBG with total cholesterol level and triglycerides level. On comparison we found that HbA1c was definitely a better marker of diabetic control as compared to FBG. While correlation of HbA1c to serum cholesterol was significant ($r= 0.38$, $P < 0.02$), it was just significant between FBG and serum cholesterol ($r= 0.53$, $P < 0.05$). Similarly, correlation between HbA1c to serum triglycerides was significant ($r= 0.09$, $P < 0.04$), it was just significant between FBG and serum triglycerides ($r= 0.22$, $P < 0.05$). HDL cholesterol correlates more significantly with FBG ($r= -0.08$, $P < 0.001$) than with HbA1c ($r= -0.04$, $P < 0.01$).

CONCLUSION

Diabetic dyslipidemia or atherogenic dyslipidemia is characterized by low HDL, high TGL and high small dense LDL. Early screening of diabetic patients for dyslipidemia and early intervention is required to minimize the risk of future cardiovascular mortality. Hence, we conclude that HbA1c level was increased in diabetics and it shows





Gopika et al.,

correlation with the status of control of diabetes. Diabetics have got increased level of serum cholesterol, triglycerides and decreased levels of serum HDL-cholesterol. HbA1c showed stronger correlation with serum cholesterol, triglycerides as compared to FBG. HDL-cholesterol showed more stronger correlation with FBG than HbA1c. Results suggest a high prevalence of dyslipidemia, which might be playing a major role in the development of cardiovascular diseases and cerebrovascular accidents among diabetic patients. The optimal care for diabetic patients should include routine monitoring of blood glucose and serum lipid profile. Efforts to achieve lifestyle changes, such as weight reduction, physical exercise and smoking cessation should be encouraged and initiated first and then followed by medication with lipid lowering drugs prescribed in evidence-based necessary conditions. The optimum treatment with proper antidiabetic drugs to obtain fair glycaemic control should go concomitantly with lipid lowering drugs as well as with taken dietary precautions. When those mentioned above are done, we might properly speak about the benefits that primary healthcare could ensure to diabetics by the advantage of monitoring patients more closely.

REFERENCES

1. Akeel bai-Yaqobi, Adnan al-Khafaji, Dheaa K. Alomar, Thi-qui medic singh, G and Kumar, A., *al journal (T.Q.M.J.)*; 52:39-44, 2011.
2. Anjana, R.M., Pradeepa, R., Deepa, M., Datta, M., Sudha, V and Unnikrishnan, R. Prevalence of diabetes and prediabetes (impaired fasting glucose and/or impaired glucose tolerance) in urban and rural India: phase I results of the Indian Council of Medical Research-India diabetes (ICMR-INDIAB) study. *Diabetologia*; 54:3022-7, 2011.
3. Arora, S., Ojha, S.K., Vohora, D Characterisation of Streptozotocin in induced diabetes mellitus in Swiss Albino mice, *Glo J of Pharmacol.*, **3(2)**: 81-84, 2009.
4. Aziz S, Hsiang YH. Comparative study of home blood glucose monitoring devices: Visidex, ChemstripbH, Glucometer, and Accu-Chek bG. *Diabetes Care*.;6:529-32, 1983.
5. Dinesh kumar and Gupta N.N. Serum cholesterol, phospholipids and beta lipoproteins in untreated diabetics. *J.A.P.I.*; 15:357, 1967.
6. Elkeles, R.S., Wu, J and Hambley, J. Glycosylated haemoglobin, blood glucose and HDL-cholesterol in insulin requiring diabetics. *Lancet*.; 2: 547, 1978.
7. Falko, J.M., O Dorisio, T.M and Cataland, S. Long term improvement of HDL-cholesterol and cholesterol/HDL-CH ratio in ambulatory type2 diabetics, treated using subcutaneous insulin pump. *Diabetes*.;30:280, 1981.
8. Gabbay, K.H. Glycosylated haemoglobin and diabetic control. (editorial) *New.Engl.J.Med.*; 295: 443, 1976.
9. Gabbay, K.H., Hasty, K., Breslow, J.L., Ellison, R.C., Bunn, H.F and Gallop, P.M. Glycosylated haemoglobin and long-term blood glucose control in diabetes mellitus. *J.Clin.endocr.meta.*; 44:859, 1977.
10. Gonen, B., Rubenstein, A.H., Rochman, H., Tancga, S.P and Horwitz, D.L. Glycosylated haemoglobin: an indicator of the metabolic control of diabetic patients. *Lancet*.; 2:734-70, 1977.
11. Ismail, M.Y. Clinical evaluation of antidiabetic activity of *Trigonella* seeds and *Aegle marmelos* Leaves, *WorldAppSci J.*, **7(10)**: 1231-1234, 2009.
12. Kennedy, L., Kandell, T.W and Merimee, T.J. Serum protein bound hexose in diabetes. The effect of glycaemic control. *Diabetes*.; 28:1006, 1979.
13. Kumar, A., Goel, M.K., Jain, R.B., Khanna, P and Chaudhary, V. India towards diabetes control: Key issues. *Australas Med J.*;6(10):524-31, 2013.
14. Lopes-Virella, M.F., Wohltmann, H.J., Loadholt, C.B., and Buse, M.G. Plasma lipids and lipoproteins in young insulin dependent diabetic patients. *Diabetologia*.;21:216-23, 1981.
15. Mahesh Dave, Ajay Kumar Gupta, Puneet patel and Heernath. Correlation between fasting blood glucose level, HbA1c Level and Serum lipid levels in Type 2 diabetes Mellitus patients. *International journal of Contemporary Medical Research*.; 6:G26-29, 2019.
16. Maleva, I.J. A study of protein fractions and blood lipoproteins in diabetes. *Abs. W. Med.*; 30:229, 1961.





Gopika et al.,

17. Nabarro, J.D.N., Mustaffa, B.E and Morris, D. Insulin deficient diabetes. *Diabetologia.*; 16:5, 1979.
18. Nikkila, E.A. and Gormilla P. Serum lipids and lipoproteins in insulin treated diabetes. Demonstrations of increased HDL-cholesterol concentration. *Diabetes.*; 27:1078-86, 1978.
19. Niederau CM, Reinauer H Glycohemoglobins In: *Thomas L, ed. Clinical Laboratory Diagnostics.* Use and assessment of clinical laboratory results. Frankfurt/Main: TH-Books Verlagsgesellschaft mbH.; 142-148, 1988.
20. Paulsen, E.P. Glycosylated haemoglobin in childhood diabetes. *Metabolism.*; 22: 269, 1973.
21. Peterson, C.M., Koenig, R.J., Jones, R.L., Saudek, C.D. and Cerami, A. Correlation of serum triglycerides levels and glycosylated haemoglobin concentration in diabetes mellitus. *Diabetes.*; 26:507-509, 1977.
22. Samatha, P., Venketeswarum and Siva Praboh. *Journal of clinical and diagnostic research.*; 4302:0012, 2012.
23. Sarat Chandra K, Bansal M, Nair T. Consensus statement on management of dyslipidemia in Indian subjects. *Indian Heart Journal.*; 66(Suppl 3):S1-S51, 2014.
24. Senthilkumar, N., Anadasayanam, A., Senthilvelu, S and Rashid, M. Correlation observation between HbA1c and Lipid profile in Type II Diabetes Mellitus Out-Patients. *International Journal of Pharma Research and Review.*; 5:9-20, 2016.
25. Sharma, D., Bansal, B.C and Prakash, C. Serum lipid studies in insulin dependent diabetes below the age of 30 years. *JIMA.*; 54:416, 1970.
26. Wild, S., Roglic, G., Green, A., Sicree, R and King, H. Global prevalence of diabetes: estimate for the year 2000 and projections for 2030. *Diabetes Care.*; 127(5):1047-1053, 2004.
27. World Health Organization (WHO). Use of glycated haemoglobin (HbA1c) in the diagnosis of diabetes mellitus. Available at: <http://www.who.int/diabetes/publications/report-HbA1c.pdf>. Accessed May 8, 2013, 2011.
28. World Health Organization/International Diabetes Federation (WHO/IDF). Definition and diagnosis of diabetes mellitus and intermediate hyperglycaemia. Available at: http://whqlibdoc.who.int/publications/2006/9241594934_eng.pdf. Accessed May 8, 2013, 2006.
29. Zimmet, P and Alberti, K.G. Global and societal implications of the diabetes epidemic, *Shaw J Nature.*; 414(6865):782-787, 2007.

S.No	Age Group (Years)	No. of. Patients	%
1	<35	30	3
2	>35-45	226	22.6
3	>45-55	449	44.9
4	>55-65	222	22.2
5	>65-75	62	6.2
6	>75	11	1.1

S.No	Degrees of Control	Normal	Under Control	Border Line	Unhealthy	
1	No. of. Cases	560	297	117	26	
2	FBG	MEAN	94.03	124.01	169.29	224.11
		SD	9.78	10.71	13.36	33.75
		SE	0.41	0.62	1.23	6.61
3	PPBG	MEAN	162.49	209.24	260.47	311.61
		SD	17.34	33.34	26.92	37.92
		SE	0.73	1.93	2.48	7.41
4	HbA1c	MEAN	7.26	8.88	10.66	12.25
		SD	0.61	1.15	0.89	0.83
		SE	0.25	0.06	0.08	0.16

Fasting Blood Glucose (FBG), Postprandial Glucose (PPBG), Glycosylated Haemoglobin (HbA1c).





Gopika et al.,

S. No	Degrees of Control	Normal	Under Control	Border Line	Unhealthy	
1	No. of. Cases	560	297	117	26	
2	TC	MEAN	191.71	198.79	217.19	232.8
		SD	20.62	17.02	20.73	27.81
		SE	0.87	0.98	1.91	5.45
3	TGL	MEAN	122.74	138.37	148.12	160.8
		SD	16.87	19.17	15.36	10.77
		SE	0.71	1.11	1.42	2.11
4	HDL - C	MEAN	52.64	50.55	49.18	48.42
		SD	9.39	7.75	8.83	4.85
		SE	0.39	0.44	0.81	0.95
5	LDL - C	MEAN	114.52	120.56	138.38	152.22
		SD	19.48	17.11	19.73	28.46
		SE	0.82	0.99	1.82	5.58

TC – Total Cholesterol, TGL – Triglycerides, HDL – C (High Density Lipoprotein) – Cholesterol, LDL – C (Low Density Lipoprotein) – Cholesterol.

S.No	Degrees of Control	Correlation Coefficient (r)	Significance (P value)
1	FBG and Cholesterol	0.538	< 0.05
2	FBG and Triglycerides	0.225	< 0.05
3	FBG and HDL- Cholesterol	-0.08	< 0.01
4	HbA1c and Cholesterol	0.383	< 0.02
5	HbA1c and Triglycerides	0.097	<0.04
6	HbA1c and HDL - Cholesterol	-0.04	<0.01





Application of Trigonometry to Science and Engineering

Sasmita Jena*

Centurion University of Technology and Management, Odisha, India.

Received: 06 Sep 2020

Revised: 08 Oct 2020

Accepted: 10 Nov 2020

*Address for Correspondence

Sasmita Jena

Centurion University of Technology and Management,
Odisha, India.

Email: sasmita.jena@cutm.ac.in



This is an Open Access Journal / article distributed under the terms of the **Creative Commons Attribution License** (CC BY-NC-ND 3.0) which permits unrestricted use, distribution, and reproduction in any medium, provided the original work is properly cited. All rights reserved.

ABSTRACT

Trigonometry is a very important subject that everyone understands from the student life. Trigonometry enables us to think differently to understand things. That's why trigonometry starts from the class ninth. This article describes how trigonometry is very useful in wide range in our real life applications. Its applications are used in Physics, Economics, Engineering, and in Business purposes in our daily life. Trigonometry is a science of triangles. Without Trigonometry, it is very difficult to solve the problems in Electrical and Electronics field. It is a useful subject because its applications are always used in Mechanical Engineering, Civil Engineering, and Electrical Engineering. It is also used in aviation, geography, flight engineering, satellite launching, criminology and archaeological studies. Its uses are also in the field of robotics technology and videogames. If trigonometry has so much uses in our day to day life, so how we neglect this topic. We should teach our students to learn trigonometry without hesitation.

Keywords: Trigonometry, Engineering, applications, Videogames, geographical

INTRODUCTION

Trigonometry is defined as the study of triangles. It involves the calculation of lengths, heights and angles of a triangle. Trigonometry has huge applications in our day to day life. Its functions are used in our daily life. Its functions are used in various field like starting from geography to astronomy. It is also used in satellite navigation system. For example it is used geography to calculate the distance between two landmarks and its uses are in astronomy to know the distance of nearby stars. The meaning of trigonometry is to simply calculate with triangles. It comes from the word "tri". Trigonometry is the study of relationships between base, perpendicular, hypotenuse and angles of right angled triangles. Trigonometry appeared during 3rd century BC. Trigonometric functions are used in different fields like architects, physicist, surveyors, astronauts, engineers, and crime scene investigators. Trigonometry is an important part of mathematics. It is a part of geometry. It has enormous application in the fields like electrical engineering, mechanical engineering, civil engineering, satellite launching, geographical fields and

28533



**Sasmita jena**

even in medical purposes. We can measure the angle, height, length and breadth of anything by calculation of trigonometric problems. Before going to the details of trigonometric functions, first find the answer a question that: Where is the trigonometry used first? Immediately we got answer that is science. Physics also uses a lot of concepts of trigonometry. Not only mathematics, physics but every branch of science and engineering uses trigonometry. Astronomy first uses trigonometry for navigation and construction of calendars. Geometry is around two thousand years old and trigonometry is based upon Geometry. We may not use directly the application of trigonometry in our day to day life but we use in different matters which we like a lot. Take music as an example, everyone knows music means sound that is waves which may not as like the sine or cosine graphs. Music system cannot able to listen or understand the rhythm as we people do. So, it acts graphically by its components through waves. So, it is necessary for sound engineers to know the fundamentals of trigonometry. By which music makes us calm, also relief from our busy and stressful life. That's why everyone should be thankful to trigonometry. Take another example, If the distance from where we observe the mountain and the angle of elevation are known, then we can easily calculate the height of the mountain using trigonometric ratio. Like that if one side and angle of depression from the top of the building are known then we can measure other sides of the building. Everyone saw the Mario game, Whenever we see it slides smoothly over the blocks of the road.

The player doesn't jump in the direction of Y-axis. The player faces the huddles on the root on which the player passes the road. In this game trigonometry is applied to jumping the huddles. Everyone knows the industry of game is totally depends on Information technology. Because of this software engineers use trigonometry for making any game. Civil engineers also use trigonometry for measuring the lands. In construction sites they use trigonometry for making the walls in paralleled or perpendicular. For installing ceramic tiles or roof inclination trigonometric ratio is used by the civil engineers. For any estimation regarding the height, the width and length of the constructed building and in many more works uses the application of trigonometry. Also uses trigonometry for measuring the loads of the structure, slopes of the rooftop, surfaces of grounds and many more things like, shading and angles of the lights. Flight engineers calculate the speed, distance and direction of the flight by using trigonometry. The wind plays a vital role in how and when plane will land wherever resolve. Using vectors to create a triangle using trigonometry to calculate. As for example, if a flight is travelling at 234 mph, 45 degree N of E, and there is a wind blowing due south at 20 mph. Trigonometry will assist to calculate the third side of the triangle, which will lead the flight in the right path, the flight will actually fly with force of wind which is added on to its rout.

Use of trigonometry in science

Trigonometry is much used in Physics. To find the component of vectors, to model the mechanics of wave and oscillations, the sum of strength of fields and in dot products and cross products. And also there is a lot of application of trigonometry in projectile motion. Trigonometry is also used in excavation of sites properly into equal areas of work. Using trigonometry in Archaeology, the archaeologists identify the various tools used by the civilization. Trigonometry can help them in these excavations. Trigonometry also helps them in measuring the distance from underground water system. Trigonometry is used in criminology. It helps for calculating a projectile's trajectory to estimate what caused a collision in car accident or how did an object fall down from somewhere or how a bullet shot in which angle. Trigonometry is used in marine biology too. Marine biologists use trigonometry to fix measurements. As for example to get how light aligns at different depths which affect the ability of algae for photosynthesis. To measure and understand sea animals and their behaviour marine biologists use mathematical models. To know the size of wild animals from long distance, marine biologists use trigonometry. To build and navigate marine vessels trigonometry is used in marine engineering. To be more specific trigonometry is used to design hump, which is a sloping surface to connect higher and lower level areas, it can be slope or even staircase depending on its application. To set direction such as East, West, North and South, trigonometry is used. It tells us in which direction, we take with compass to get or a straight direction. A location is pinpointed in order to use in navigation. It is used to get the distance of the shore from a point in the sea. To see the horizon, it is also used. Oceanography is another example which uses trigonometry for measuring the heights of the tides. Periodic functions are created using the functions of sine and cosine; by which we are able to understand waves. Physics uses calculus

28534



**Sasmita jena**

and basics of calculus are trigonometry. To roof a house, we use trigonometry functions. To make the roof inclined and height of roof building etc. Trigonometry is used in naval and aviation industries. To create maps trigonometry is very much used. In satellite system trigonometry has various types of applications. We know that trigonometry is the science of calculation of sides and angles and their relationships associated with an arbitrarily given triangles. It is originated from the Greek word "Trigon", which means a triangle. The subject was basically evolved to solve the problems of triangle and astronomy. Trigonometry is always used in Science, Engineering, Economics and Business applications. Music is composed of different frequencies and amplitudes and these are described using sine and cosine functions. TV and radio signals are described with sine and cosine functions. Medical equipment's use trigonometry functions to know the heart beat and breathing etc. We use trigonometric functions in heat equations to know how the things get hotter.

Use of trigonometry in engineering

Trigonometry is also used in fluid flow. Earth quake intensity is calculated using trigonometric functions. Trigonometric functions are used in optics and statics, motion of the tides and mechanical vibrations. Alternating current is represented by using trigonometric functions. Trigonometric functions used in Geometrical optics like lateral shift, normal shift, refraction through prism and refraction through lenses. It is used in physical optics like Theory of interference and polarization. In Electricity, trigonometric functions are used in Magnetic effect of current, mechanical effect of current, alternating current etc. Trigonometric functions are used in motion of two dimensional plain like if a particle is projected, then motion of the particle takes parabolic path, the height of the projectile, time of the flight can be expressed in trigonometric functions. It is applied in trigonometric functions in resolution of the vectors i.e. splitting of vector in to different components. Trigonometry is also used in robotics technology a lot. By the application trigonometry robots can do any of the works which is assigned. A robot works round a room, it's like using sensors and whether they are ultrasonic or detect light or even smells, the sensor do the calculation or measurement of the outside world into numbers and numbers means mathematics. As for example, for avoiding hitting something in its way, a robot records the numbers coming from the ultrasonic detectors, it's like a bat sending out a chirp, the signal that bounce off the obstacle coming back, and the robot measures the distance to the obstruction.

CONCLUSION

Now, we comprehend that, trigonometry is used in every branch of science and engineering like astronomy and architecture. Trigonometry help in the right positioning of cars, its sits, desks, benches, like so. Without climbing a tree, we are able to calculate the height of the tree with the use of trigonometric functions. Trigonometry is used everywhere in our daily life as well as research and scientific works. So if we leave trigonometry then we are facing a lots of problems for finding the exact angle and distance. Everyone knows trigonometry plays a vital role in our student as well as in professional, that's why trigonometry is compulsory in our school career. So give preference to study and practicing trigonometry.

REFERENCES

1. Keith Weber, Students' Understanding of Trigonometric Functions, Mathematics Education Research Journal, 2005, Vol. 17, No. 3, 91–112.
2. HülyaGür, Trigonometry Learning, New Horizons in Education, Vol.57, No.1, May 2009.
3. Suherman¹, Komarudin², Abdul Rosyid³, Sinta Aryanita⁴, Doni Asriyanto⁵, ThofanAradika Putra⁶, Tri Anggoro⁷, Improving Trigonometry Concept Through STEM (Science, Technology, Engineering, And Mathematics) Learning, 7Mathematics Education Department, UIN RadenIntan. Indonesia.
4. PetrGirg and LukášKotrla, p -Trigonometric and p -Hyperbolic Functions in Complex Domain, Abstract and Applied Analysis, Volume 2016, Article ID 3249439, 18 pages.





Sasmita jena

- 5. Er. NavinTalkokul, Research on the Trigonometry as a Main Function of Sine, Secant, Tangent and Formula of Tan and Cot are Inverse, International Journal of Mathematics Trends and Technology (IJMTT) – Volume 50 Number 3 October 2017.

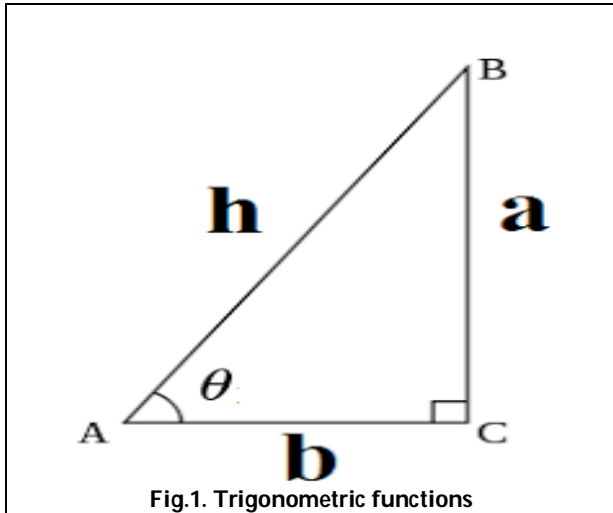


Fig.1. Trigonometric functions

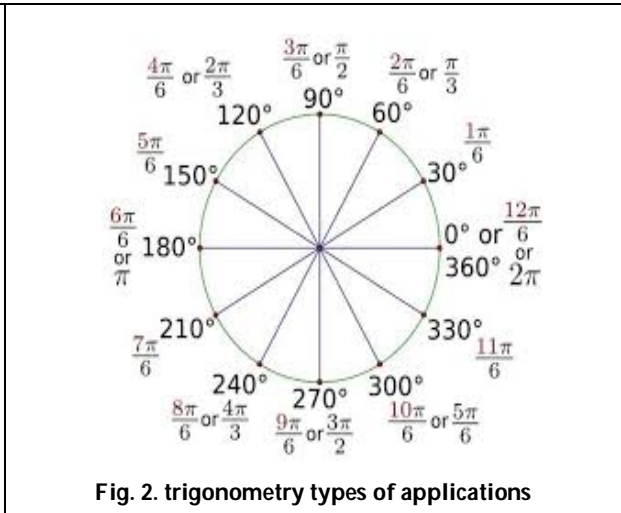


Fig. 2. trigonometry types of applications





Simulation of an Electrostatic Mirror

G. K. Sahu¹, P. K. Rath^{1*}, D. Das², H. Pai² and N. N. Deshmukh³

¹Centurion University of Technology and Management, Odisha, India.

²SINP, Kolkata India.

³School of Science, Auro University, Surat, India.

Received: 07 Sep 2020

Revised: 09 Oct 2020

Accepted: 11 Nov 2020

*Address for Correspondence

P. K. Rath

Centurion University of Technology and Management,

Odisha, India.

Email: prasanta.rath@cutm.ac.in



This is an Open Access Journal / article distributed under the terms of the **Creative Commons Attribution License** (CC BY-NC-ND 3.0) which permits unrestricted use, distribution, and reproduction in any medium, provided the original work is properly cited. All rights reserved.

ABSTRACT

The changing of ion /charge path is an important subject in the physics for most of the instrument which works on the basis charge detection and the motion of them in the different condition. The electrostatic mirror is one of the important kind which used in many instrument which detects the ions. The ES mirror orientation is very important. A Monte Carlo simulation has been done to understand the working of the electrostatic mirror.

Keywords: TOF, CF, MCP, mirror, efficiency

INTRODUCTION

The ion beam diagnostic plays an important role on the accelerator science. In addition with the beam diagnostic the ion detectors are also very important [1-3]. There are many detector in the market but some detector need to built or need to assemble using different components. There are many varieties are there out of which the electrostatic mirror (ES) based detectors are very important and interesting to study. When we say mirror it just work like mirror as the mirror reflects the light whatever fall on it the electrostatic mirror deflects the ion whatever fall on it. Most of the time the electrostatic mirror woks on the secondary electron which emits after a reaction or being generated purposely. Growing interest are there in electron energy spectra and energy which will be used as the secondary source of charges and in case of ion beam it is important as it allows energy selection while maintaining good image quality, like the mirror type. The electrostatic mirror becomes a critical part of the spectrometer if high spatial resolution and good image quality are required from the system. This paper contains a theoretical simulation of the effect of various parameters of such a mirror on its electron optical properties. As in our previous paper [4] we have mentions about the beam imaging device where we have used the mirror for the purpose of imaging.





PROCESS AND RESULTS

The electrostatic mirror is a metallic gridded made up of Be-Cu thin wire. A schematic has been shown in the Fig.1. One can see that the ES mirror will not work alone but in combination with the other components, it work integrally. One can see that there is a metal foil from which the secondary electron emits and these electron have the energy 30eV in the present case. These electron once come out from the foil they move in the beam direction and they strike the gridded ES mirror which has placed in the path of the beam/ion/secondary electron. The gap between the wires of the mirror is so high such that to the atoms /ion it feels like empty space but in between the space an electric potential has been applied and it is -120 V for the present simulation. The ES mirror has been placed on the path of the ion in 45 degree with the beam direction. Most of the time beam is not a spot it has some spreading in the spatial coordinated and in the present case it has taken a beam of 3 mm diameter having circular shape. When the secondary electron will hit the mirror they will see a -ve potential and the path of the electron will start to deflect toward the down direction. As a result the electron will bend 90degree down ward and the move towards the MCP. These MCP plates are very expensive and mounted perpendicular to the path of the scattered electron. A positive potential (+1000V) has been applied on the MCP plates. All the parts has been shown in Fig. 1. The simulation has been performed using random uniformly distributed ion beam in this case these are secondary electron and they move towards the mirror with mentioned potential. The path of the electron has considered in all direction but the straight path has been filtered out and allowed for further calculation. The randomly sampled electron within 3mm diameter has been moved towards the mirror and the time has been calculated in two parts. Part one is time from the foil to the mirror and part two is the time from mirror to MCP. As the distribution in the electron is 3mm one can expect a wide variation in time based on the path which it will take. But the it has been surprisingly that the time taken by the electron is same whatever path the electron will choose to reach MCP. The detail has been shown in Fig.2.

SUMMARY AND CONCLUSION

A clear picture with a Monte Carlo simulation has been performed and presented. It has been observed that no matter whatever the path electron will choose to reach the MCP from the foil under the influence of the potential ES it is always same. This type of device can be used for the TOF, DAQ system.

REFERENCES

1. P. K. Rath et.al. "A Suitable Random Number Generator (RNG) For computer simulations", IJONSs, Vol. 10, Issue. 60 page.20875(2020) (WoS)
2. P. K. Rath, et.al "Simulation Study of detection of ions/charge particles using Gas Detector" IJONS Vol.10, Issue.60, Page.20879 (2020) (WoS)
3. P. K. Rath, "Simulation Study of Collimators to use at low energy Facility" IJONS Vol.10, Issue.60, Page. 20409 (2020) (WoS)
4. P. K. Rath, et.al "Calculation of potential curve & cross section for compound nucleus ^{215}Rn " IJONS Vol.10, Issue.60, Page. 20960 (2020) (WoS)



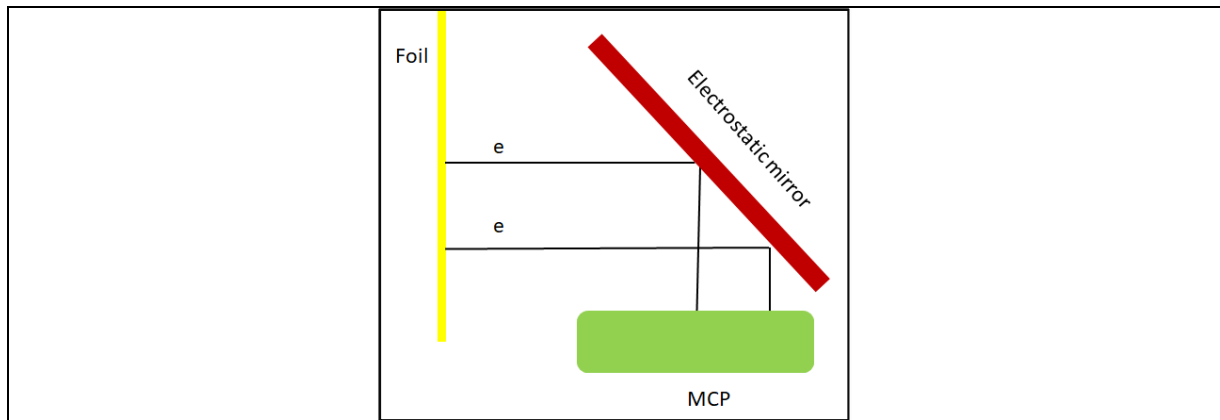


Fig 1 the schematic of the electrostatic mirror including the foil from where the secondary electron will emit and the mirror which will bend the path towards 90degree downward to MCP.

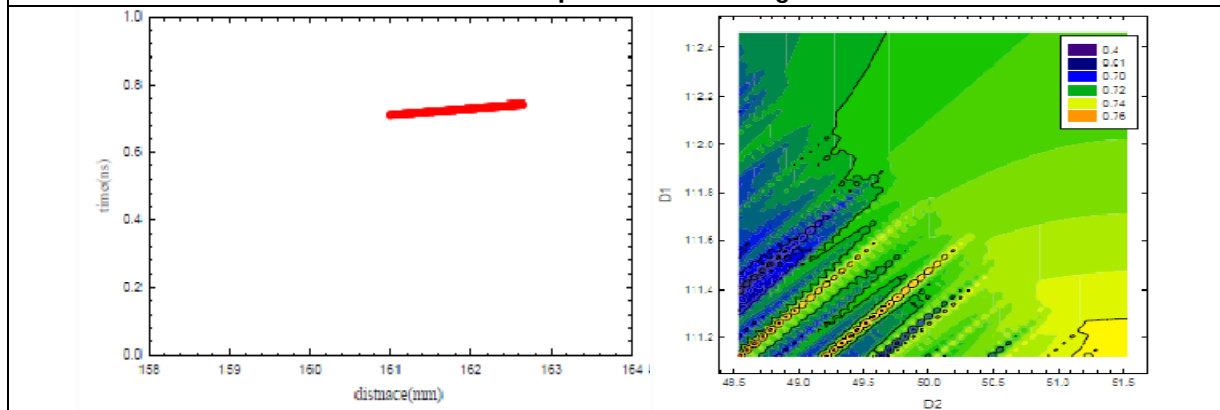


Fig. 2.(left) the result of the simulation of the ES. The spread in time is negligible (Right) the same thing has been shown in 2d map.





Biosynthesis and Characterization of Silver Nanoparticles from *Boerhavia diffusa* L. and their Anti-oxidant and Anti- cancer Activity in Human Cervical Cancer Cells

Delpiya. R¹, Priscilla Suresh^{2*} and Jasmine Maria James¹

¹Department of Zoology, Bishop Heber College (Autonomous), Tiruchirappalli, Tamil Nadu, India.

²Head and Assistant Professor, Department of Zoology, Bishop Heber College (Autonomous), Tiruchirappalli, Tamil Nadu, India.

Received: 13 Sep 2020

Revised: 16 Oct 2020

Accepted: 18 Nov 2020

*Address for Correspondence

Priscilla Suresh

Head and Assistant Professor,
Department of Zoology,
Bishop Heber College (Autonomous),
Tiruchirappalli, Tamil Nadu, India.
Email: priscisf@gmail.com



This is an Open Access Journal / article distributed under the terms of the **Creative Commons Attribution License** (CC BY-NC-ND 3.0) which permits unrestricted use, distribution, and reproduction in any medium, provided the original work is properly cited. All rights reserved.

ABSTRACT

Boerhavia diffusa L. is a herb used in Ayurveda and other traditional medicines for its antibacterial, diuretic and anti-inflammation properties. In the present study, we have synthesized the green silver Nanoparticle, from *B. diffusa* (Bd AgNPs) and studied their antioxidant and anticancer effect in cervical cancer cell lines. The Bd AgNPs were synthesized from *B. diffusa* aqueous and 0.02N AgNO₃ solutions. The synthesized Bd AgNPs particles were further characterized by UV- Vis spectrophotometer, XRD, FESEM, and EDAX. The cytotoxic effect of Bd AgNPs was studied in cervical cell line HeLa by MTT assay and their antioxidant activity by DPPH radical scavenging assay. Likewise investigated the anticancer properties by EtBr/AO staining method. We found that the formation of Bd AgNPs was monitored by UV- Vis spectroscopy at different ratio of *B. diffusa* aqueous extract and AgNO₃ solution. The shape and size of the Bd AgNPs were visualized by scanning electron microscopy. The result was further confirmed by X- ray powder diffraction (XRD), FESEM and EDAX. The developed Bd AgNPs were stable, almost spherical in shape with a size range 87.40 nm. The LC 50 dose of anticancer activity of Bd AgNPs was found to be 45.47 µg/ml (IC₅₀). Furthermore, the EtBr/ AO staining results showed that Bd AgNPs induced apoptosis in cervical cancer cells. In addition, Bd AgNPs showed 78.57 % scavenging activity by DPPH assay in a dose dependent. Manner taken together, these results showed that the biocompatible Bd AgNPs could be used for the treatment of cervical cancer. The results obtained from this study adds on to the evidences of the anti-cancer potential of Bd AgNPs in cervical cancer cells, further which can be developed as an anti-cancer drug.

Keywords: Bd AgNPs., HeLa cells, cervical cancer, DPPH., EtBr/ AO.





INTRODUCTION

Globally, cervical cancer is the chief cause of cancer-causing deaths in females after breast cancer. Indian scenario presents cervical cancer incidences to one fifth of the total cases reported globally (Rakhi Srivastava *et al.*, 2009). In medicine, nanoparticles are conjugated with drugs to increase the drug target specificity and enhanced drug delivery to increase the efficacy of the drug (Dipankar *et al.*, 2012). These nanoparticles are biodegradable, cost-effective way to process, that makes it a very attractive drug delivering system. They are being actively exploited for their anti-cancer properties. The advantages of using plant extracts, as drugs are that they are obtained naturally, easily absorbed by the cells and have less or no side effects. *B. diffusa* L. is an herb found in Ayurveda and other traditional medicines. The genus *Boerhavia* has several species and is distributed in the tropical, subtropical and temperate regions of the world (Heywood 1978). *B. diffusa* is a tropical crawling root plant, with bioactive compounds in both the leaves and roots. *B. diffusa* belongs to the family Nyctaginaceae. The major active principle present in the roots is alkaloid and is known as punarnavine. Pharmacological studies have demonstrated that punarnava possesses punarnavoside, which exhibits a wide range of properties diuretic (Gaitonde, *et al.*, 1974), antifibrinolytic (Jain and Khanna 1989), anticonvulsant (Adesina 1979), and antibacterial (Olukoya *et al.*, 1993). Scientific studies using the extract of this plant showed that it has got analgesic and anti-inflammatory property (Bhalla *et al.*, 1968, Hiruma-Lima *et al.*, 2000), hepato-protective activity (Rawat *et al.*, 1997), immunomodulatory activity (Mehrotra *et al.*, 2002) and anti-proliferative properties. Punarnavine, an alkaloid from *B. Diffusa* could enhance the immune response against the metastatic progression of B16F-10 melanoma cells in mice (Manu and Kuttan 2007). Whole plant extract of *B. Diffusa* has a radioprotective effect (Manu *et al.*, 2007). The aqueous methanol (3:7) extract of *B. Diffusa* was found to be effective in reducing the metastasis formation by B16F10 melanoma cells (Leyon *et al.*, 2005). In this study, we have biosynthesized, characterized and investigated the anticancer and antioxidant potential of silver nanoparticles of *B. diffusa* plant extract is inducing cytotoxicity in human cervical cancer (HeLa) cells.

MATERIALS AND METHODS

Cell culture

HeLa cells (Human cervical cancer, p-131) was purchased from NCCS, Pune, India. The cells were cultured in DMEM (Gibco, Invitrogen) supplemented 10% Foetal Bovine Serum (FBS) (Himedia), 100 u/ml penicillin and 100 µg/ml streptomycin, and maintained in an incubator under an atmosphere of 5% CO₂ at 37°C.

Plant collection

The plant material was collected from the Idukki District in Kerala and was authenticated by Dr. John Britto, Director, Rapinat Herbarium Trichy.

Extraction of plant powder

The collected plant material was washed well in the running tap water followed by a rinse in distilled water. The plants were shade dried, sliced into small pieces and ground well into a fine powder. The plant powder was stored safely away from light. The plant aqueous extract was prepared by dissolving 10 gm of fine powder of *B.diffusa* in 100 ml of distilled water and heated at 60 °C for 30 min. The mixture was filtered by filter paper and further filtered using Whatman filter paper.

Biosynthesis of *B. diffusa* silver nano particles (Bd AgNPs)

B. diffusa silver nano particles (Bd AgNPs) was synthesized using a different ratio of *B. diffusa* aqueous extract and 0.02 N AgNO₃ solvent. Five different ratios (5:5, 6:4, 7:3, 8:2, 9:1) was checked for the highest yield of Bd AgNPs. The best ratio (ratio 6.4) was selected and prepared in a large quantity. The synthesized Bd AgNPs was collected by centrifugation at 12,000 rpm for 15 min. The collected pellet was dried and used for further experiments.



**Delpiya et al.,****Characterization of the synthesized Bd AgNPs**

The optical property of green synthesized Bd AgNPs was determined by using UV-vis spectrophotometer (Perkin Elmer, Lambda 35, Germany). The samples used for analysis were diluted with 2 ml deionized water and subsequently measured by the UV-vis spectrum at regular different ratios (9:1, 7:3, 6:4, 5:5, 2:8) and time intervals (Raut Rajesh *et al*). The UV-vis spectrometric readings were recorded at a scanning speed of 200 to 1100 nm.

X-Ray Diffraction Analysis (XRD)

The phase variety and grain size of green synthesized silver nanoparticles were determined by using X-ray diffraction spectroscopy. The synthesized silver nanoparticles were studied with $\text{CuK}\alpha$ radiation at the voltage of 30 kV and current of 20 MA with the scan rate of 0.030 /s. Different phases present in the synthesized samples were determined by X'pert high score software with search and match facility.

Morphological studies of Bd AgNPs using FESEM and EDAX

The morphology of green synthesized Bd AgNPs was observed using Field Emission Scanning Electron Microscopic Studies (FESEM), and Energy Dispersive X-Ray Analysis (EDAX) confirmed the presence of silver.

Evaluation of anti-oxidant activity of the Bd AgNPs**DPPH free radical scavenging assay**

The total antioxidant potential of the *B. diffusa* sample was determined by DPPH assay by the method described by (Kitts *et al.*, 2000) with slight modifications. Briefly, 1ml of the DPPH working solution was mixed with 1 ml of nanoparticles dissolved in methanol. The mixture was kept for 30 min incubation in the dark at ambient temperature. The absorbance was measured at 520nm. The free radical scavenging property of DPPH was calculated according to the following equation.

$$[(\text{Abs Control}-\text{Abs sample}) / \text{Abs of control}] \times 100$$

Cytotoxicity potential of Bd AgNPs assessed using MTT assay

Cytotoxicity activity of plant-derived Bd AgNPs was carried out against A549 cell line at different concentrations of Bd AgNPs to determine the IC_{50} (50% growth inhibition) by MTT assay (Mosmann *et al* 1983). The percentage cell viability and IC_{50} value was calculated using Graph Pad Prism 6.0 software (USA).

EtBr /Ao Staining

AO and EtBr staining reveal the morphological changes of the cancer cell lines after treating with Bd AgNPs. The stained cells were characterized as early apoptotic (bright green fluorescence) and late apoptotic cells (reddish-orange fluorescence).

Statistical Analysis: The difference in estimated parameters between the groups was analyzed using one-way ANOVA with Bonferroni's test. Data expressed as mean \pm SD. All parameters were analyzed at 95% confidence intervals and a P value of <0.05 was considered to be statistically significant. Statistical analysis of the data was performed using Graph Pad Prism version 6.00 for Windows, GraphPad Software, San Diego California USA.

RESULTS**Characterization of Bd AgNPs using UV-visible spectroscopy analysis**

The Bd AgNPs results exhibited a broad-spectrum surface Plasmon absorption band width range between at 325 to 600 nm and absorption peak edge observed at 417 nm. The peaks obtained for different ratio concentrations of Bd AgNPs is given in tables 1 and Figures 1 (a): Blank, 1 (b): 9:1.





X-Ray Diffraction Pattern (XRD)

The X-ray diffraction patterns peak list of synthesized Ag with *B. diffusa* plant is given in Table 2 and shown in the Fig. 2. XRD peaks are angle at 38.26, 46.36, 64.61 and 77.50 corresponding to (111), (200), (220) and (311) HKL planes of Ag for the face-centred cubic silver was obtained as per the JCPDS card no. 89-3722. The average crystallite size was found to be 34 nm for Bd AgNPs.

Field Emission Scanning Electron Microscopic Studies (FESEM)

The morphology of synthesized Bd AgNPs are shown in Figure: 3 (a and b). The FESEM image showed that synthesized Bd AgNPs exhibited spherical with uniform grain boundaries and had an average particles size 30-40 nm

Energy Dispersive X-Ray Analysis (EDAX)

The results obtained showed that elemental Ag⁰ ion atomic percentages was observed at 100 % for Bd AgNPs and further, showed elemental constituents of silver (87.65 %), chlorine (6.49 %) and carbon (5.86 %). The principal sharp signal was observed at 3 keV for silver, which is distinctive for the absorption of crystalline nature of biosynthesized Bd AgNPs.

DPPH Radical Scavenging Activity

The DPPH scavenging assay exhibited effective inhibition activity of Bd AgNPs when compared with the standard. The Bd AgNPs exhibited increased inhibition with 78.57 % scavenging activity of DPPH (Figure 4). When adding Bd AgNPs in the DPPH solution, color change occurred, due to the scavenging ability of Bd AgNPs by donation of hydrogen atom to stabilize the DPPH molecule. This phenomenon was calorimetrically quantified at an absorbance of 517 nm (table 4).

Quantitative assessment of formation of formazan crystals in control cells and Bd AgNPs sample treated cells

Results of different concentrations of Bd AgNPs including 10 µg/ml to 100 µg/ml were shown in Fig. The formation of formazan crystals decreases when the concentration of Bd AgNPs increases in HeLa cells. The IC₅₀ values of Bd AgNPs on HeLa cell line was found to be 45.47 µg/ml (Figure 7 a). Bd AgNPs exerted high cytotoxicity in 100 µg/ml concentration against HeLa cell line with 64.12 % of cell growth inhibition (Figure 7 b). The results of MTT assay showed Bd AgNPs were effective in inhibiting the cervical cancer cells proliferation.

EtBr/AO Staining

Microscopic observations of the AO and EtBr stained cells revealed cell death and alteration in cellular morphology. Among the 100 cells scored for both treated and control, in treated cells, about 30% of cells were in early apoptotic, 63% cells were present in late apoptotic and 7% cells underwent necrosis when compared to the control samples that presented very low number of cells in early, late apoptotic and necrosis, 0.5%, 1.5%, and 0% respectively. These results, confirm that Bd AgNPs induced apoptosis in cervical cancer cell lines [Figure 8 and 9 (a), (b)].

Early apoptotic cells - No. of cells which appeared yellow-green fluorescence/100 cells

Late apoptotic cells - No. of cells which appeared orange nuclear fluorescence/100 cells

Necrotic cells- No. of cells which appeared orange-red fluorescence/100 cells

DISCUSSION

Evidences support claim that the roots and leaves of this plant have anti-inflammatory and anti-fibrinolytic properties (*et al.*). Available literature has been documented the anti-cancerous efficacy of ethanolic extract of *B. Diffusa* on human cervical cancer cell lines. Ethanolic extracts of *B. Diffusa* have shown chemotherapeutic effects on



**Delpiya et al.,**

Hela cells (Srivastava *et al* 2011). Manu et al has reported that *B. Diffusa* has shown anti metastatic colony forming efficacy in melanoma cells (B16F-10 cells) induced mice (Manu *et al* 2007). Silver nanoparticles biosynthesized under optimum conditions using *B. diffusa* bark extract in SEM analysis showed that the biosynthesized nanoparticles are spherical in nature and ranged from 30-50 nm in size. (Patil *et al.* 2012b). The EDAX spectrum illustrated the presence of strong metallic Ag signals. The results obtained showed that elemental Ag⁰ ion atomic percentages was observed at 100 % for Bd AgNPs and further, showed elemental constituents of silver (87.65 %), chlorine (6.49 %) and carbon (5.86 %). The principal sharp signal was observed at 3 keV for silver, which is distinctive for the absorption of crystalline nature of biosynthesized Bd AgNPs. Similar peak results were obtained from several studies (Muthukrishnan *et al.*, 2015; Kanipandian *et al.* 2014; Ramalingam *et al.*, 2014). In our study, the Bd AgNPs result exhibits a broad spectrum surface Plasmon absorption bandwidth range between 325 to 600 nm and absorption peak edge observed at 417 nm. These nanoparticles were found to have a crystalline structure with face centered cubic geometry. The Bd AgNPs exhibited increased inhibition with 78.57 % scavenging activity of DPPH (Figure 4). The results obtained from MTT assay showed that the green synthesized Bd AgNPs were effective in inhibiting the cervical cancer cells proliferation. The results of EtBr/AO assay confirm that Bd AgNPs induced apoptosis in cervical cancer cell lines.

CONCLUSION

The overall results obtained in this study have shown that the green synthesized Bd AgNPs have been effective in inhibiting the proliferation of (HeLa) cervical cancer cells as confirmed by AO/EtBr staining. Furthermore, Bd AgNPs have showed significant anti-oxidant potential, confirmed by the Bd AgNPs mediated reduction of DPPH. Therefore, we suggest that *B. diffusa* plant extract based AgNPs could be effectively used as an alternative novel treatment modality for cervical cancer. It's efficacy in *in vivo* and in other cancers will be evaluated in our further studies.

ACKNOWLEDGEMENT

Our thanks to HAIF – Bishop Heber College, Trichy for their technical support and St. Josephs College, Trichy for their help to identify the plant species.

REFERENCES

1. Kirtikar, K.R., and Basu, B.D (1956). In Indian Medicinal Plants. Ed. Uttar Pradesh, India.
2. Olukoya, D.K., Tdika, N. and Odugbemi, T (1993). Antibacterial activity of some medicinal plants from Nigeria. *Journal of Ethnopharmacology*, 39: 69-72.
3. Heywood, V.H (1978). Flowering Plants of the World. Oxford University Press, London, UK,
4. Gaitonde B. B., H. J. Kulkarni, and S.D. Nabar (1974). "Diuretic activity of punarnava (*Boerhaavia diffusa*)," *Bulletin of Haffkine Institute*, vol. 2, p. 24.
5. Jain G. K. and N. M. Khanna (1989). "Punarnavoside: a new antifibrinolytic agent from *Boerhaavia diffusa* Linn," *Indian Journal of Chemistry*, vol. 28, no. 2, pp. 163–166,
6. Adesina S. K., "Anticonvulsant properties of the roots of *Boerhaavia diffusa* (1979)." *Quarterly Journal of Crude Drug Research*, vol. 17, pp. 84–86.
7. Bhalla T. N., M. B. Gupta, P. K. Sheth, and K. P. Bhargava (1968). "Antiinflammatory activity of *Boerhaavia diffusa*," *Indian Journal of Physiology and Pharmacology*, vol. 12, p. 37.
8. Hiruma-Lima C. A., J. S. Gracioso, E. J. Bighetti, L. Germonsén Robineou, and A. R. Souza Brito (2000). "The juice of fresh leaves of *Boerhaavia diffusa* L. (Nyctaginaceae) markedly reduces pain in mice," *Journal of Ethnopharmacology*, vol. 7, pp. 267–274,.





Delpiya et al.,

9. Rawat A. K. S., S. Mehrotra, S. C. Tripathi, and U. Shome (1997). "Hepatoprotective activity of *Boerhaavia diffusa* L. roots a popular Indian ethnomedicine," *Journal of Ethnopharmacology*, vol. 56, no. 1, pp. 61–68.
10. Mehrotra S., K. P. Mishra, R. Maurya, R. C. Srimal, and V. K. Singh, (2002). "Immunomodulation by ethanolic extract of *Boerhaavia diffusa* roots," *International Immunopharmacology*, vol. 2, no. 7, pp. 987–996.
11. Lami N., S. Kadota, T. Kikuchi, and Y. Momose (1991). "Constituents of the roots of *Boerhaavia diffusa* L. III. Identification of Ca²⁺ channel antagonistic compound from the methanol extract," *Chemical & Pharmaceutical Bulletin*, vol. 39, pp. 1551–1555.
12. Borrelli F., V. Ascione, R. Capasso, A. A. Izzo, E. Fattorusso, and O. Tagliatalata-Scafati (2006). "Spasmolytic effects of nonprenylated rotenoid constituents of *Boerhaavia diffusa* roots," *Journal of Natural Products*, vol. 69, no. 6, pp. 903–906.
13. Leyon P. V., C. C. Lini, and G. Kuttan (2005). "Inhibitory effect of *Boerhaavia diffusa* on experimental metastasis by B16F10 melanoma in C57BL/6 mice," *Life Sciences*, vol. 76, no. 12, pp. 1339–1349.
14. Pandey R., R. Maurya, G. Singh, B. Sathiamoorthy, and S. Naik (2005). "Immunosuppressive properties of flavonoids isolated from *Boerhaavia diffusa* Linn.," *International Immunopharmacology*, vol. 5, no. 3, pp. 541–553.
15. Muthulingam M, K. Krishna Chaithanya *In vitro* anticancer activity of methanolic leaf extract of *Boerhaavia diffusa* Linn. against MCF-7 cell line (2018). *Drug Invention Today* | Vol 10 Special Issue 2.

Table 1: Absorption peaks of Bd AgNPs at various concentrations

Name	No	Peak (nm)	Peak (AU)
Blank	1	303.4	0.0316
Concentration at (9:1)	1	432.25	0.8595
Concentration at (7:3)	1	401.25	2.3813
	2	448.3	2.7506
Concentration at (6:4)	1	406.25	2.4859
	2	445.85	2.8588
Concentration at (5:5)	1	413.7	3.8946
	2	417.45	3.8579
Concentration at (2:8)	1	439.7	2.1968

Table 2: Peaks obtained for Bd AgNPs

Pos. [°2Th.]	Height [cts]	FWHM Left [°2Th.]	d-spacing [Å]	Rel. Int. [%]
28.0268	14.90	0.7872	3.18373	2.41
32.3710	49.81	0.1476	2.76572	8.04
38.2619	619.22	0.2952	2.35237	100.00
44.5101	226.48	0.3444	2.03558	36.57
46.3662	26.84	0.5904	1.95833	4.34
54.8603	7.33	1.1808	1.67352	1.18
57.5558	9.21	0.6888	1.60140	1.49
64.6102	165.66	0.2952	1.44255	26.75
77.5040	167.56	0.1968	1.23163	27.06





Delpiya et al.,

Table 3 (a): Spectrum processing

Peaks possibly omitted	1.251, 1.750, and 2.141 keV
Processing option	All elements analyzed (Normalised)
Number of iterations	1
Standard	Ag

Table 3(b): Elemental composition of Ag nanoparticles

Element	Weight%	Atomic%
Ag L	100.00	100.00
Total	100.00	

Table 4: Percentage antioxidant potential of Bd AgNPs assessed using DPPH assay.

S. No.	Concentration (In micro liter)	Control (OD at 517 nm)	Ascorbic acid (std) (OD at 517 nm)	% of antioxidant activity	Plant extract (OD at 517 nm)	% of antioxidant activity
1.	100	0.28	0.25	10.71	0.24	14.2
2.	200	0.28	0.22	21.43	0.21	25
3.	300	0.28	0.20	28.57	0.19	32.4
4.	400	0.28	0.13	53.57	0.11	60.71
5.	500	0.28	0.09	67.86	0.06	78.57

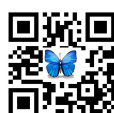
Table 5: Bar graph showing the Indexes of early, late apoptosis and necrosis of control and plant extract treated HeLa cells.

	Early apoptosis Index (%) (in duplicates)		Late apoptosis Index (%) (in duplicates)		Necrosis Index (%) (in duplicates)	
	1	0	2	1	0	0
Control	1	0	2	1	0	0
Treated with plant extract	28	32	66	60	8	6

(The bar graph was made by calculating 100 cells/Square and their mean value)

Table 6. Mean of early, late apoptotic and necrotic indexes (%)

	Early apoptosis Index (%)	Late apoptosis Index (%)	Necrosis Index (%)
Control	0.5	1.5	0
Treated	30	63	7



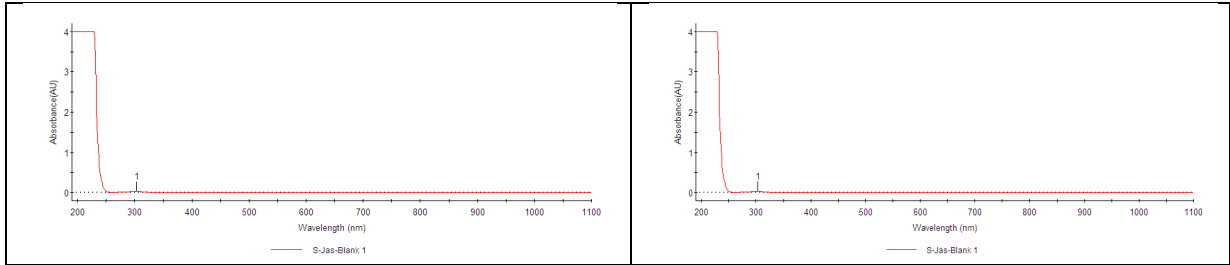


Figure: 1 (a) without plant extract (Blank)

Figure 1: (b) UV-Vis peak at the concentration- 9: 1

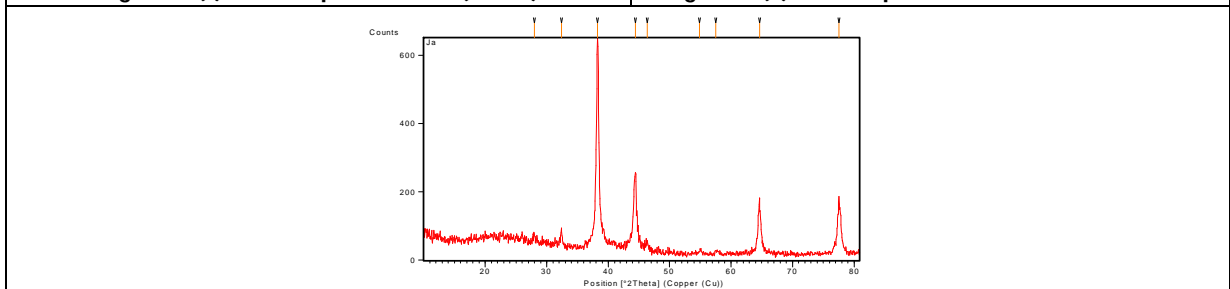


Figure 2: XRD spectra of synthesized Ag NPs

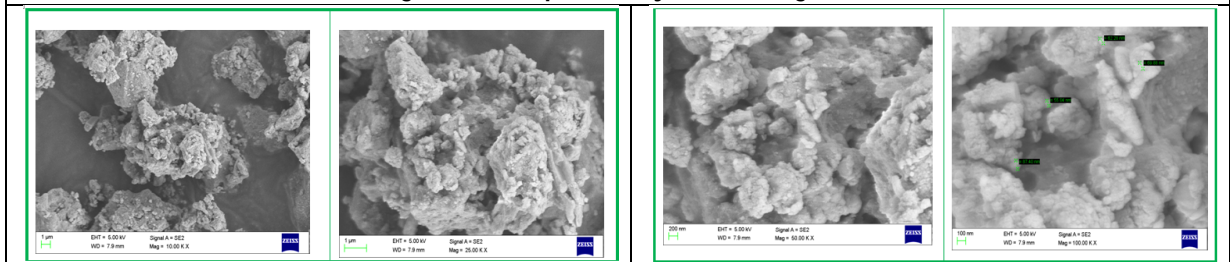


Figure 3 (a): FESEM image for Ag NPs at different magnifications (10X, 25X, 50X and 100X)

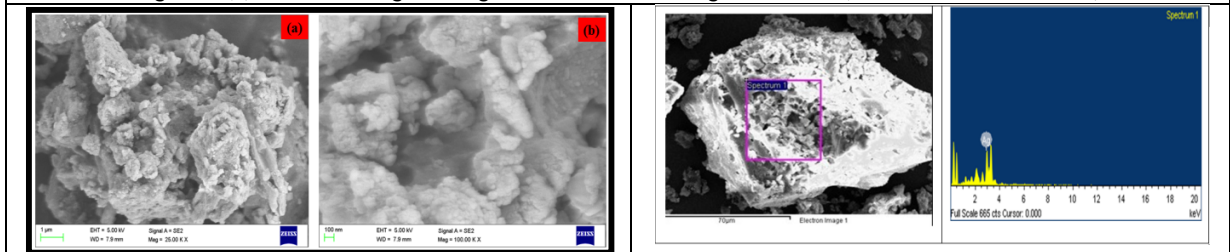


Figure 3 (b).FESEM image of lower and higher magnification image of Ag NPs

Figure 4 (a) EDAX spectra of Ag NPs

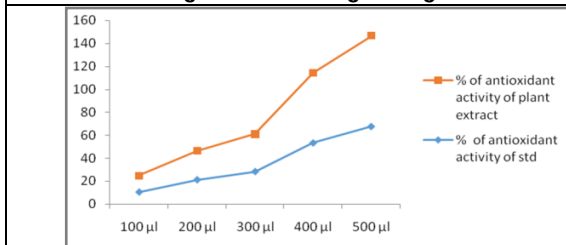


Figure 5: Antioxidant activity of Ag NPs at various concentrations

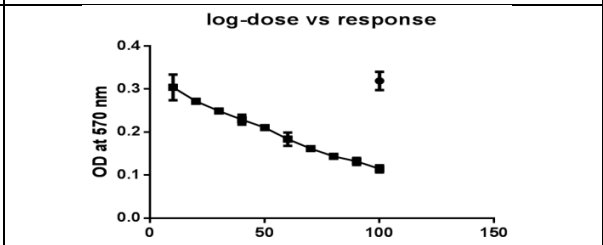


Figure 6 (a): OD at 570 nm





Delpiya et al.,

<p>Figure 6(b): Cell Viability (%)</p>	<p>Figures: 7(d) Control cells, 7(e) Bd AgNPs sample 100 µg/ml, 7(f) Bd AgNPs sample 70 µg/ml, 7(g) Bd AgNPs sample 50 µg/ml, 7(h) Bd AgNPs sample 30 µg/ml, 7(i). Bd AgNPs sample 10 µg/ml</p>												
<div style="text-align: center;"> <table border="1"> <caption>Data for Figure 8: AO/EtBr staining</caption> <thead> <tr> <th>Group</th> <th>Early apoptotic index %</th> <th>Late apoptotic index %</th> <th>Necrosis %</th> </tr> </thead> <tbody> <tr> <td>Control</td> <td>~1</td> <td>~2</td> <td>~0</td> </tr> <tr> <td>Treated with plant extract</td> <td>~30***</td> <td>~60***</td> <td>~10***</td> </tr> </tbody> </table> </div>		Group	Early apoptotic index %	Late apoptotic index %	Necrosis %	Control	~1	~2	~0	Treated with plant extract	~30***	~60***	~10***
Group	Early apoptotic index %	Late apoptotic index %	Necrosis %										
Control	~1	~2	~0										
Treated with plant extract	~30***	~60***	~10***										
<p style="text-align: center;">Figure 8:AO/EtBr staining</p>													
<p>Figure 9 (a) Control cells</p>	<p>Figure 9(b) Cells treated with 45.47 µg/ml of Bd AgNPs</p>												
<p style="text-align: center;">Figure 9: AO/EtBr staining</p>													





Phytochemical Constituents of *Hibiscus rosa-sinensis*, *Laurus nobilis* and *Psidium guajava* Leaves and their Antimicrobial Activity

Shalini Sehgal, Pragyan Khanna and Roshanlal Yadav*

Department of Food Technology, Bhaskaracharya College of Applied Sciences (University of Delhi), Dwarka, Delhi, India.

Received: 14 Aug 2020

Revised: 17 Sep 2020

Accepted: 20 Oct 2020

*Address for Correspondence

Roshanlal Yadav

Department of Food Technology,

Bhaskaracharya College of Applied Sciences (University of Delhi),

Dwarka, Delhi, India.

Email: roshanfst@gmail.com



This is an Open Access Journal / article distributed under the terms of the **Creative Commons Attribution License** (CC BY-NC-ND 3.0) which permits unrestricted use, distribution, and reproduction in any medium, provided the original work is properly cited. All rights reserved.

ABSTRACT

The growth of food poisoning pathogens as well as food spoilage is usually controlled by the use of chemical preservatives which cause an adverse effect on human health. Because of such apprehension, the requirement to find a safer, potentially effective and natural alternative is increased. Inside these texts, plant-based extracts have been used to estimate their phytoconstituents and antimicrobial activity. Tannins were the principal phytoconstituents which were detected in all the extracts. Antimicrobial activity of three plant extracts was investigated against *Escherichia coli* (MTCC 10312), *Bacillus subtilis* (MTCC 9003), *Pseudomonas aeruginosa* (MTCC 104) and *Staphylococcus aureus* (MTCC 106) by using agar disc diffusion technique. *Hibiscus rosa sinensis*, *Laurus nobilis* and *Psidium guajava* plant leaves showed antimicrobial activity (in respect to zone of inhibition) ranged from 8.33 to 13 mm, 8 to 13.16 mm and 7.83 to 15.33 mm respectively. The highly significant Pearson correlation indicated a symbiotic relationship among all the selected bacterial strains.

Keywords: Antimicrobial, Gram positive bacteria, Alkaloids , MIC , Plant extract, Phytoconstituent Tannins

INTRODUCTION

Now a days, more attention is been given to natural sources for managing and protection against food borne pathogens. Plant extracts containing phytochemicals can be explored for extending the shelf-life of food products and also helps in maintaining food safety. They can play a significant role in the inhibition of pathogens and the improvement of quality as well as yield of food without any adverse side effects. Food borne diseases including both types i.e. intoxication and infection are one of the most common causes of illness in developing countries [1]. Many research studies show that the food borne diseases are caused by the contamination of Gram-negative bacteria such



**Shalini Sehgal et al.,**

as *Pseudomonas aeruginosa* and *Escherichia coli* [2]. Gram-positive bacteria including *Bacillus subtilis* and *Staphylococcus aureus* have been implicated as the fundamental agents of food spoilage or food borne diseases [3]. As a result, the use of chemically synthesized agents in the preservation of foods was perceived to stop spoilage and food borne diseases which has become a safety concern for foods nowadays. Therefore, researchers started exploring the use of natural plant extracts as effective agent against microbial activities [4, 5]. Regardless, of the established effectiveness of the chemical preservatives in prevention and epidemic control of food poisoning diseases, their continuous intake has shown the accumulation of these chemical residues in feed and food chain, acquirement of microbial resistance to the applied chemicals and unfavorable side effects of these residues on human health [6, 7]. Due to these issues, a lots of efforts have been made to create potentially effective and health hazards free natural food preservatives. Within these contexts, various researches have carried out for the exploitation of plant extracts as antimicrobial agents and observed their role in preservation of different foods [8, 9]. It has been observed that the extracts obtained from different plants, measured as natural antimicrobial agents, also nutritionally safe and easily degradable [10, 11]. The antimicrobial activities of various plant extracts against some food poisoning bacteria have been studied by several researchers [12,13]. The antibacterial activity of ethanolic extracts of four plants i.e. *Cynodon dactylon*, *Achyranthes aspera*, *Tagetes patula* and *Lantana camara* was taken up and results showed that these plant extracts are more active against *S. aureus*, *Pseudomonas aeruginosa* and *Bacillus subtilis* with MIC's ranged from 25 to 125 mg/ml [14].

The plant *Hibiscus rosa sinensis* belongs to the family Malvaceae. It is widely grown as an ornamental plant in the tropical and subtropical parts of Asia including India. In recent studies, it was concluded that various phytoconstituents present in the plant leaves are responsible of their antimicrobial activity [15, 16]. A study found that leaves extract of *Hibiscus rosa sinensis* is responsible for antimicrobial properties against certain pathogens including *S. aureus*, *E. coli*, *Pseudomonas aeruginosa* and *Klebsiella pneumonia* and the author concluded that *S. aureus* has significant inhibition zones with diameters > 12 mm [17]. Similarly, the antimicrobial activity of *Hibiscus rosa sinensis* extracts was examined against Gram-negative and Gram-positive bacteria strains by measuring zone of inhibition, and the highest activity was measured against *Staphylococcus aureus* at very low concentration (2.5µg/ml) compared to *E.coli*, *Bacillus subtilis* [18]. *Laurus nobilis* or sweet bay belongs to the Lauraceae family and is grown as a high-value spice crop and as an ornamental plant in the region including Asia, Europe and America. Phytochemical analyses have revealed the presence of various compounds such as alkaloids, flavonoids, tannins, vitamins and minerals [19, 20]. Various researchers have found that the leaf extracts of *Laurus nobilis* contain high antibacterial and antifungal properties [21, 22]. The leaf extract was more effective against the growth of *Staphylococcus aureus*, *Pseudomonas aeruginosa* and *Escherichia coli* [23]. The *Psidium guajava*, commonly known as the guava is a small tree that belongs to the family Myrtaceae. It has great importance because of the availability of various phytochemicals such as alkaloids, flavonoids, carotenoids, and phenols. In a previous study, it was observed that guava leaves have high antibacterial activity in extracts that can inhibit the growth of *S. aureus* [24] The methanolic extract of leaves and bark of *Psidium guajava* has high antimicrobial activity which can inhibit the growth of *Bacillus* and *Salmonella* bacteria [25].

Most of the food borne diseases both intoxications as well as infections have been majorly linked with bacterial contaminations particularly with Gram-negative bacteria like *Escherichia coli* and *Pseudomonas aeruginosa* and Gram positive bacteria including *Staphylococcus aureus* and *Bacillus subtilis*. Researches regarding the efficiency of *Hibiscus rosa senensis*, *Laurus nobilis*, and *Psidium guajava* leaves against the etiological food spoilage bacteria are extremely modest in Asian areas. Consequently, the current study expected to evaluate the antibacterial activity of these plant extract against food poisoning or food spoilage organisms i.e. *Escherichia coli*, *Staphylococcus aureus*, *Bacillus subtilis* and *Pseudomonas aeruginosa* *in vitro*. The antimicrobial efficacy of any plant extract considerably depends upon the nature and type of phytochemicals present in that particular species. Consequently, phytochemical screening was also performed to determine their role in the establishment of antimicrobial activity.





MATERIALS AND METHOD

Bacterial culture and media

Bacterial strains i.e. *Escherichia coli* (10312), *Bacillus subtilis* (9003), *Pseudomonas aeruginosa* (104) and *Staphylococcus aureus* (106) were procured from Microbial Type Culture Collection and Gene Bank (MTCC) housed at the Institute of Microbial Technology (IMTECH), Chandigarh, India. The media used for their activation and maintenance were Nutrient Broth and Standard Plate Count Agar (PCA) purchased from Merck, India.

Collection of samples

Three different variety of leaves i.e. *Hibiscus rosa sinensis* (Hibiscus), *Laurus nobilis* (Bay) and *Psidium guajava* (Guava) were collected from the college premises of Bhaskaracharya College of Applied Sciences, New Delhi and they were confirmed by the Department of Botany, North Campus, University of Delhi, India.

Preparation of extract

All the three varieties of leaves were separately subjected to successive drying cycles in a microwave at a temperature of 110°C with 2450 MHz for their complete drying. The dried samples were then pulverized to fine powdered with the help of a warring blender. The extracts were prepared soaking the powder in 90 % ethanol in three different concentrations i.e. 3.5%, 4.5% and 5.5% [26]. The contents were then kept in dark for 24 h for the complete extraction of compounds into the solvent. The samples were filtered after 24 hours using whatman filter paper number 1 to obtain liquid ethanolic extracts.

Phytochemical screening

Qualitative phytochemical screening of ethanolic extracts (4.5%) was performed by the protocol [27, 28].

Tannins: The extract (0.5ml) was boiled with 10ml of distilled water in a test tube and then, few drops of 0.1% Ferric Chloride solution (FeCl_3) was added in the reaction mixture and the formation of blue-black precipitate indicated the presence of Tannins.

Saponins (Frothing test): With auto pipette 0.5ml of the extract was measured and it was added into a test tube containing 5ml of distilled water. The solution was shaken vigorously for about 2 min and observed for the stable persistent froth. The formation of stable foam indicates the presence of saponins.

Phylobatannins (Precipitate test): In a test tube 0.5ml of extract and 2 ml HCl (1%) were mixed and heated on hot plate. The formation of red precipitate indicated the presence of phylobatannins.

Carbohydrates (Molisch's test): For qualitative analysis of carbohydrates 0.5 ml of extract and 10 ml H_2O was mixed in a test tube and 2 drops 20% Ethanolic α -naphthol (Molisch's reagent) was added to the test tube followed by the addition of 2ml concentrated H_2SO_4 along the wall of test tube. The red-violet ring at the junction indicates the presence of carbohydrates.

Alkaloids (Wanger's test): Filtrates were treated with A few drops of Wanger's reagent (Iodine in Potassium Iodide) are mixed with 2ml of extract. The formation of brown/reddish precipitate indicates the presence of alkaloids.

Preparation of inoculum

The bacterial strains were activated using nutrient broth for 72 hours at 35°C. A loopful of activated culture from the mother stock solution was then inoculated into sterile nutrient broth blanks which were incubated for 24 hours at 37°C for further use.



**Shalini Sehgal et al.,****Antibacterial activity**

The agar disk diffusion method was used to estimate the antimicrobial activity. The method as described, was used with some minor modifications [29]. The plate count agar plates inoculated with the standardized inoculums of the selected test microorganisms were prepared. then, sterile filter paper discs about 6 mm in diameter loaded with the leaf extracts at varying concentrations (35mg/ml, 45mg/ml and 55mg/ml), were placed on the agar surface along with the control. In total 12 plates were prepared (one per sample of leaf extract per bacterial strain) which were then kept in an incubator at 37°C for 24 hours. After 24 hours, the zone of inhibition was noted and measured in millimeters. Each experiment was performed in triplicate and mean values were taken.

Minimum inhibitory concentration (MIC)

MIC is the lowest concentration of an antimicrobial compound that can inhibit the growth of a microorganism after incubation. The MIC for plant leaf extract was determined by noting down the lowest of the tested leaf extract concentrations which exhibited inhibitory activity [30]. The inhibitory activity was detected by the presence of a region of clearance (zone of inhibition) of a slightly lighter color with respect to that of the surrounding media (which supports the growth of bacteria). Similarly, the MIC was estimated for each of the leaf extracts against each of the tested bacterial strains based on the diameter of the zone of inhibition.

Statistical Analysis

The statistical analysis was performed by using SPSS 25. For each parameter, three independent determinations were made (n = 3), and the results were expressed as mean ± standard deviation (SD) at p < 0.05.

RESULTS**Phytochemical screening**

The phytochemical screening for tannins, saponins, phlobatannins, carbohydrate and alkaloids were carried out in all the three extracts of selected plant leaves i.e. *Hibiscus rosa sinensis*, *Laurus nobilis* and *Psidium guajava* (Table 1). During the qualitative analysis, it was found that except carbohydrate tannin was the major constituent that was present in all the samples. It was measured higher in *Laurus nobilis* and *Psidium guajava* leaves extract, whereas a moderate concentration was observed in *Hibiscus rosasinensis*. Among all the extracts *Psidium guajava* showed maximum number of phytochemicals, except phlobatannins all the tested constituents found present in the extract.

Antibacterial activity

The result presented in Table 2-4 showed that all leaves extracts used in this study exhibited a varying degree of antimicrobial activity against the tested gram-positive as well as gram-negative bacteria. Irrespective of their concentrations the leaves extracts of *Hibiscus rosasinensis* revealed highest zone of inhibition against *Staphylococcus aureus*, whereas it was measured lowest for *Escherichia coli* (p<0.05). Regardless of types of microorganism tested the highest zone of inhibition was measured at a concentration level of 55mg/ml. In *Laurus nobilis* a significantly high zone of inhibition was measured at a level of 55 mg/ml irrespective of tested microbial strains. Additionally, the maximum (11.88 mm) zone of inhibition was measured for *Staphylococcus aureus* and minimum (9.61 mm) was observed for *Escherichia coli* in spite of their different concentration level. In *Psidium guajava*, irrespective of tested microbial strain the zone of inhibition was found in order of 35mg/ml > 45 mg/ml > 55 mg/ml significantly maximum was reported as 13.62 mm and minimum was 10.83 mm. Regardless of concentration largest inhibition zone was showed by *Staphylococcus aureus* followed by *Bacillus subtilis*, *Escherichia coli* and *Pseudomonas aeruginosa*.

Minimum inhibitory concentration (MIC)

The lowest concentration of a chemical or extract, which prevents visible growth of a bacterium or bacteria is determined in terms of MIC and the result is presented in Table 5. The outcome of MIC showed that all the extracts



**Shalini Sehgal et al.,**

against all the tested microbial strains exhibit similar MIC value i.e. 35 mg/ml except *Hibiscus rosasensis* against microbial strain *Escherichia coli* MTCC 10312.

Pearson correlation

The result as presented in Table 6 showed a significant correlation among different tested microorganisms (*Escherichia coli*, *Bacillus subtilis*, *Pseudomonas aeruginosa* and *Staphylococcus aureus*) on their antimicrobial activity.

DISCUSSION

The antibacterial activities of *Hibiscus rosa sinensis*, *Laurus nobilis* and *Psidium guajava* leaves were carried out. All the extract showed an antibacterial (antimicrobial) activity against the human pathogens such as *Escherichia coli* (MTCC10312), *Bacillus subtilis* (MTCC 9003), *Pseudomonas aeruginosa* (MTCC 104) and *Staphylococcus aureus* (MTCC 106). The inhibition of bacterial growth in-vitro by the extracts of leaves could be due to the presence of some active compounds like tannin, saponin and alkaloids in the extracts. Leaves extract contain phenolics compounds like tannins that are very good antimicrobial agent (31). The higher antimicrobial activity of *Psidium guajava* leaves extract it might be due to the presence of higher number of phenolic compounds in it. The present investigation showed that tannin was only phenolic which was observed in all the extracts and this might be responsible for antimicrobial activity. It supports the earlier investigations which showed that the tannins isolated from the various extracts had remarkable toxic activity against bacteria and may assume pharmacological importance [32, 33, 34]. *Hibiscus rosa sensis* showed antimicrobial activity with respect to zone of inhibition and it was found in the range of 8.33 to 13 mm, similar observations were reported other researchers [16, 35]. The present study indicated that the *Hibiscus rosa sensis* extract was more effective against the growth of Gram-positive bacteria such as *Bacillus subtilis* (MTCC 9003) and *Staphylococcus aureus* (MTCC 106). as compared to Gram-negative bacteria. Gram-positive bacteria are usually more susceptible to the action of the extracts compared with the Gram-negative ones. This can be attributed to the presence of an additional outer membrane in Gram-negative bacteria, which may better protect the cytoplasmic membrane from the antimicrobial compounds [36]. The variation in MIC's of the different microorganisms could also be attributed to the differences in growth rate of the tested organisms, nutritional requirements, temperature and inoculum size [37]. It was found that the *Hibiscus rosa sensis* extract was more effective in controlling the growth of all tested microorganisms except *Escherichia coli* (MTCC 10312).

This study showed that *Laurus nobilis* extract at different concentrations was antibacterial against all the tested Gram-positive as well as Gram-negative bacterial strains. The overall zone of inhibition (mm) was directly proportional to the concentration of extract. A similar correlation between concentration and activity was reported. The zone of inhibition was in the range of 8 to 13.16 mm among all the tested microbial strains. The lowest was reported for *Escherichia coli* (MTCC 10312) whereas, highest was measured for *Staphylococcus aureus* (MTCC 106) [38]. The MIC results indicate that all the tested strains are inhibited at a similar minimum concentration. The results of this study show that all the extracts prepared from the leaves of *Psidium guajava* although having varying concentration showed inhibitory activity against all the tested Gram-positive and Gram-negative strains. Similar to *Hibiscus rosa sensis*, the extract of *Psidium guajava* also showed higher activity against the growth of Gram-positive bacteria as compared to Gram negative bacteria. It has been reported earlier that Gram-negative bacteria are usually more resistant to the plant-origin antimicrobials, compared to Gram-positive bacteria [36, 39]. The antimicrobial activity in respect to zone of inhibition was calculated and it was found in the range of 7.83 to 15.33 mm in concurrence with findings of Biswa et al.[24]. The extract which was effective against the growth of *Escherichia coli* (MTCC 10312) was also responsible for the reduction in the growth of other tested bacterial strains. The antibacterial activity of the extracts showed that the growth inhibition of *Bacillus subtilis* MTCC 9003 versus *Staphylococcus aureus* (MTCC 106) at significant level $p < 0.01$ and to *Pseudomonas aeruginosa* (MTCC 104) at significant level $p < 0.05$. All the three tested leaf extracts were having the antibacterial ability against the tested strains and therefore the potential to be used as biopreservatives after further studies.



**Shalini Sehgal et al.,**

CONCLUSION

The present work represents the phytochemical constituents and antimicrobial potential of *Hibiscus rosa senesis*, *Laurus nobilis*, and *Psidium guajava* leaf extracts. The results indicated that all the selected samples were effective as antibacterial agents against both Gram-positive as well as Gram-negative bacteria. The presence of phyto-constituents was responsible for their antibacterial property. The statistically significant differences between the different bacterial strains and the antimicrobial activity of three leaf extracts reveal that each extract has different potential to inhibit the growth of individual microbial strain. *Escherichia coli* (MTCC 1031) was found to be the most resistant whereas *Staphylococcus aureus* (MTCC 106) was the most sensitive bacterial strain. The present finding indicates that all the selected leaves can be a good source for natural antimicrobial agents against the spoilage caused by *Escherichia coli*, *Pseudomonas aeruginosa*, *Staphylococcus aureus* and *Bacillus subtilis*. Thus, this study provides scientific insight that these potentially effective extracts can be used as natural preventives to control food borne diseases and also in preservation of food products naturally by avoiding use of chemical antimicrobial agents. Use of these extracts as biopreservatives can also enhance the safety parameter of processed food.

ACKNOWLEDGEMENT

The authors want to acknowledge Bhaskaracharya College of Applied Sciences (University of Delhi) for providing facilities to conduct this research work.

REFERENCES

1. Mostafa AA, Al-Askar AA, Almaary KS, Dawoud TM, Sholkamy EN, Bakri MM (2018) Antimicrobial activity of some plant extracts against bacterial strains causing food poisoning diseases. Saudi J Biol Sci 25: 361-366
2. Pandey A, Singh P (2011) Antibacterial activity of *Syzygium aromaticum* (Clove) with metal ion effect against food borne pathogens. Asian J Plant Sci Res 1: 69-80
3. Logan NA (2012) Bacillus and relatives in foodborne illness. J Appl Microbiol 112: 417-429
4. Anand SP, Sati N (2013). Artificial preservatives and their harmful effects: looking toward nature for safer alternatives. Int J Pharm Sci Res 4: 2496
5. Moritz M, Geszke-Moritz M (2013)The newest achievements in synthesis, immobilization and practical applications of antibacterial nanoparticles. Chem Eng J 228: 596-613
6. Bialonska P, Ramnani SG, Kasimsetty KR, Muntha GR, Gibson D, Ferreira (2010) The influence of pomegranate by-product and punicalagins on selected groups of human intestinal microbiota. Int J Food Microbiol 140: 175-182
7. Rokka M, Jestoi M, Peltonen K (2013) Trace level determination of polyether ionophores in feed. Bio Med Res Int: 1-12
8. Gutierrez-del-Rio I, Fernandez J, Lombo F (2018). Plant nutraceuticals as antimicrobial agents in food preservation: Terpenoids, polyphenols and thiols. Int J Antimicrob Agents 52: 309-315
9. Sakarikou C, Kostoglou D, Simoes M, Giaouris E (2020). Exploitation of plant extracts and phytochemicals against resistant Salmonella spp. in biofilms. Food Res Int 128: 108806.
10. Seow YX, Yeo CR., Chung HL, Yuk HG (2014). Plant essential oils as active antimicrobial agents. Crit Rev Food Sci Nutr 54: 625-644
11. Vurro M, Miguel-Rojas C, Perez-de-Luque A (2019) Safe nanotechnologies for increasing the effectiveness of environmentally friendly natural agrochemicals. Pest Manag Sci 75: 2403-2412
12. Gonelimali FD, Lin J, Miao W, Xuan J, Charles F, Chen M, Hatab SR (2018) Antimicrobial properties and mechanism of action of some plant extracts against food pathogens and spoilage microorganisms. Front Microbiol 9: 1639
13. Mahboubi M (2020). Iranian medicinal plants as antimicrobial agents. J Microbiol Biotech Food Sci 9: 2388-2405.





Shalini Sehgal et al.,

14. Gupta RN, Kartik V, Manoj P, Singh PS, Alka G (2010) Antibacterial activities of ethanolic extracts of plants used in folk medicine. *Int J Res Ayurveda Pharm* 1: 529-535
15. Murugan T, Wins JA, Murugan M (2013) Antimicrobial activity and phytochemical constituents of leaf extracts of *Cassia auriculata*. *Indian J Pharm Sci* 75: 122-125
16. Sobhy EA, Abd Elaleem KG, Abd Elaleem HG (2017) Potential antibacterial activity of *Hibiscus rosa sinensis* linn flowers extracts. *Int J Cur. Microbiol App Sci* 6: 1066-1072
17. Al-Snafi AE (2018) Chemical constituents, pharmacological effects and therapeutic importance of *Hibiscus rosa-sinensis*- A review. *J Pharmacy* 8: 101-119
18. Fullerton M, Khatiwada J, Johnson JU, Davis S, Williams LL (2011) Determination of antimicrobial activity of sorrel (*Hibiscus sabdariffa*) on *Escherichia coli* O157:H7 isolated from food, veterinary, and clinical samples. *J Med Food* 14: 950-956
19. Loizzo M, Tundis R, Menichini F, Saab A, Satti G, Menichini F (2007) Cytotoxic activity of essential oils from Labiatae and Lauraceae families against in vitro human tumor models. *Anticancer Res* 27: 3293-3300
20. Abu-Dahab R, Kasabri V, Afifi F (2014) Evaluation of the volatile oil composition and antiproliferative activity of *Laurus nobilis* L. (Lauraceae) on breast cancer cell line models. *Rec Nat Prod* 8: 136-147
21. Fernandez-Andrade C, da Rosa M, Boufleuer E, Ferreira F, Iwanaga C, Gonçalves J, Cortez D, Martins C, Linde G, Simoes M, (2016) Chemical composition and antifungal activity of essential oil and fractions extracted from the leaves of *Laurus nobilis* L. cultivated in southern. *Brazil J Med Plants Res* 48: 865-871
22. Snuossi M, Trabelsi N, Ben Taleb S, Dehmeni A, Flamini G, de Feo V (2016) *Laurus nobilis*, *Zingiber officinale* and *Anethum graveolens* essential oils: Composition, antioxidant and antibacterial activities against bacteria isolated from fish and shellfish. *Molecules* 21: 1414
23. Fidan H, Stefanova G, Kostova I, Stankov S, Damyanova S, Stoyanova A, Zheljzkov VD (2019) Chemical composition and antimicrobial activity of *Laurus nobilis* L. essential oils from Bulgaria. *Molecules* 24: 804
24. Biswas B, Rogers K, McLaughlin F, Daniels D, Yadav A (2013) Antimicrobial activities of leaf extracts of guava (*Psidium guajava* L.) on two gram-negative and gram-positive bacteria. *Int J Microbiol* 2013: 7
25. Joseph B, Priya RM (2011) Phytochemical and biopharmaceutical aspects of *Psidium guajava* (L.) essential oil: A review. *Res J Med Plant* 5: 432-442
26. Alade RI, Irobi ON (1993) Antimicrobial activities of crude leaf extracts of *Acalypha wilkesiana*. *J Ethnopharmacol* 39: 171-174
27. Trease GE, Evans MD (1989) A text book of pharmacognosy, (13ed) Baillier, Tindal and Causse, London, pp 144-148
28. Odebiyi O, Sofowora EA (1978) Phytochemical screening of Nigerian medicinal plants. *L.Coydia* 41: 41-234
29. Seeley HW, Van Denmark PJ (1975) A laboratory manual of microbiology (2ed) D B Taraporewala Sons and Co, Bombay, pp. 55-80
30. Eloff JN (1998) A sensitive and quick microplate method to determine the minimal inhibitory concentration of plant extracts for bacteria. *Planta Medica* 64: 711-713
31. Scalbert AC (1991) Antimicrobial properties in tannins. *Phytochem* 30: 3875-3883
32. Sukumaran S, Kiruba S, Mahesh M, Nisha SR, Miller PZ, Ben CP, (2011) Phytochemical constituents and antibacterial efficacy of the flowers of *Peltophorum pterocarpum* (DC.) Baker ex Heyne. *Asian Pac J Trop Med* 4: 735-738
33. Kannathasan K, Senthilkumar A, Venkatesalu V (2011) In vitro antibacterial potential of some Vitex species against human pathogenic bacteria. *Asian Pac J Trop Med* 4: 645-648
34. Raja RDA, Jeeva S, Prakash JW, Antonisamy JM, Irudayaraj V (2011) Antibacterial activity of selected ethnomedicinal plants from South India. *Asian Pac J Trop Med* 4: 375-378
35. Ruban P, Gajalakshmi K (2012) In vitro antibacterial activity of *Hibiscus rosa-sinensis* flower extract against human pathogens. *Asian Pac J Trop Biomed* 2: 399-403
36. Tajkarimi MM, Ibrahim SA, Cliver DO (2010) Antimicrobial herb and spice compounds in food. *Food Control* 21: 1199-1218





Shalini Sehgal et al.,

37. Gaill W, Jon AW (1995) Antimicrobial susceptibility test dilution and disc diffusion methods. Manual of clinical microbiology (6ed) pp 1327-1333
38. Al-Ogaili N, Bilal R, Younis H, Khadim T (2020) The examination of the water concentrates of *Laurus nobilis* leaves antibacterial activity utilizing various strategies for extraction (in vitro). Int J Res Pharm Sci 11: 66-69
39. Rameshkumar KB, George V, Shiburaj S (2007) Chemical constituents and antibacterial activity of the leaf oil of cinnamomum chemungianum Mohan et Henry. J Essent Oil Res 19: 98-100

Table. 1. Qualitative analysis of Phytochemicals

Leaves (Samples)	Tannins	Saponins	Phlobatannins	Carbohydrates	Alkaloids
<i>Hibiscus rosa sinensis</i>	+	-	-	++	-
<i>Laurus nobilis</i>	++	-	-	+	-
<i>Psidium guajava</i>	++	+	-	++	+

+ Present in moderate concentration

++ Present in high concentration

- Absent

Table. 2. Antimicrobial activity of *Hibiscus rosa-sinensis*

Concentration	EC	BS	PA	SA	Total
	Zone of inhibition (mm)				
35 mg/ml	9.50 ± 0.50	10.50 ± 0.50	8.83 ± 0.76	10.50 ± 0.50	9.83 ± 0.89 ^a
45 mg/ml	8.33 ± 1.04	11.00 ± 0.50	10.83 ± 0.76	11.33 ± 0.58	10.38 ± 1.40 ^{ab}
55 mg/ml	9.00 ± 1.00	11.33 ± 0.58	11.00 ± 1.00	13.00 ± 1.00	11.08 ± 1.68 ^b
Total	8.94 ± 0.92 ^A	10.94 ± 0.58 ^{BC}	10.22 ± 1.27 ^B	11.61 ± 1.27 ^C	

All data are reported as mean ± SD (n=3)

Small and capital alphabets in superscripts indicate significant differences (p<0.05) among concentration and tested microbial strain respectively

EC= *Escherichia coli* MTCC 10312; BS= *Bacillus subtilis* MTCC 9003; PA= *Pseudomonas aeruginosa* MTCC 104; SA= *Staphylococcus aureus* MTCC 106

F-Statistics for tested microbial strain = 20.35 at df = 3, p=0.000

F-Statistics for concentrations = 8.18 at df = 2, p=0.000

F-Statistics for for tested microbial strain and concentrations = 3.50 at df = 6, p=0.000

Table. 3. Antimicrobial activity of *Laurus nobilis*

Concentration	EC	BS	PA	SA	Total
	Zone of inhibition (mm)				
35 mg/ml	8.83 ± 0.76	9.00 ± 1.00	8.00 ± 1.00	10.33 ± 1.04	9.04 ± 1.19 ^a
45 mg/ml	9.00 ± 1.00	10.33 ± 0.57	11.00 ± 0.50	12.16 ± 0.28	10.62 ± 1.31 ^b
55 mg/ml	11.00 ± 0.50	12.16 ± 0.28	12.83 ± 0.76	13.16 ± 0.28	12.29 ± 0.96 ^c
Total	9.61 ± 1.24 ^A	10.50 ± 1.50 ^{AB}	10.61 ± 2.21 ^B	11.88 ± 1.36 ^C	

All data are reported as mean ± SD (n=3)

Small and capital alphabets in superscripts indicate significant differences (p<0.05) among concentration and tested microbial strain respectively

EC= *Escherichia coli* MTCC 10312; BS= *Bacillus subtilis* MTCC 9003; PA= *Pseudomonas aeruginosa* MTCC 104; SA= *Staphylococcus aureus* MTCC 106

F-Statistics for tested microbial strain = 15.00 at df = 3, p=0.000

F-Statistics for concentrations = 60.05 at df = 2, p=0.000

F-Statistics for for tested microbial strain and concentrations = 2.72 at df = 6, p=0.037





Shalini Sehgal et al.,

Table.4. Antimicrobial activity of *Psidium guajava*

Concentration	EC	BS	PA	SA	Total
Zone of inhibition (mm)					
35 mg/ml	10.00 ± 1.00	12.33 ± 0.29	7.83 ± 0.29	13.17 ± 0.29	10.83 ± 2.23 ^a
45 mg/ml	10.50 ± 0.50	14.17 ± 0.29	10.00 ± 0.50	14.50 ± 0.50	12.29 ± 2.17 ^b
55 mg/ml	12.00 ± 0.50	15.33 ± 0.58	12.00 ± 0.50	15.17 ± 0.29	13.62 ± 1.75 ^c
Total	10.83 ± 1.09 ^B	13.94 ± 1.37 ^C	9.94 ± 1.84 ^A	14.28 ± 0.94 ^C	

All data are reported as mean ± SD (n=3)

Small and capital alphabets in superscripts indicate significant differences (p<0.05) among concentration and tested microbial strain respectively

EC= *Escherichia coli* MTCC 10312; BS= *Bacillus subtilis* MTCC 9003; PA= *Pseudomonas aeruginosa* MTCC 104; SA= *Staphylococcus aureus* MTCC 106

F-Statistics for tested microbial strain = 171.67 at df = 3, p=0.000

F-Statistics for concentrations = 93.58 at df = 2, p=0.000

F-Statistics for for tested microbial strain and concentrations = 3.81 at df = 6, p=0.008

Table. 5. Minimum Inhibitory Concentration (MIC) of different leaf extracts against different tested microbial strains

Test Microorganisms	<i>Hibiscus rosa-sensis</i>	<i>Laurus nobilis</i>	<i>Psidium guajava</i>
<i>Escherichia coli</i> MTCC 10312	45 mg/ml	35 mg/ml	35 mg/ml
<i>Bacillus subtilis</i> MTCC 9003	35 mg/ml	35 mg/ml	35 mg/ml
<i>Pseudomonas aeruginosa</i> MTCC 104	35 mg/ml	35 mg/ml	35 mg/ml
<i>Staphylococcus aureus</i> MTCC 106	35 mg/ml	35 mg/ml	35 mg/ml

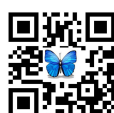
Table.6. Correlation between tested microbial strains

Pearson correlations				
	EC	BS	PA	SA
EC	1			
BS	0.766**	1		
PA	0.353	0.392*	1	
SA	0.625**	0.890**	0.492**	1

** Correlation is significant at the 0.01 level (2-tailed)

* Correlation is significant at the 0.05 level (2-tailed)

EC= *Escherichia coli* MTCC 10312; BS= *Bacillus subtilis* MTCC 9003; PA= *Pseudomonas aeruginosa* MTCC 104; SA= *Staphylococcus aureus* MTCC 106





A Review for the Neutron Production using Ion Beam from Accelerator

G. K. Sahu^{1*}, P. K. Rath¹, N. N. Deshmukh² and M. Mishra³

¹Centurion University of Technology and Management, Odisha, India.

²School of Science, Auro University, Surat, Gujarat, India.

³Saraswati Institute of IT and Management, Vikash group of Institution, Bhawanipatna, Kalahandi, Odisha, India.

Received: 12 Sep 2020

Revised: 14 Oct 2020

Accepted: 16 Nov 2020

*Address for Correspondence

G. K. Sahu

Centurion University of Technology and Management,
Odisha, India.

Email: gksahu@cutm.ac.in



This is an Open Access Journal / article distributed under the terms of the **Creative Commons Attribution License** (CC BY-NC-ND 3.0) which permits unrestricted use, distribution, and reproduction in any medium, provided the original work is properly cited. All rights reserved.

ABSTRACT

The production of neutron is very important. As the neutron are very danger due to the heavy mass and no charge so the generation of neutron with precise required energy is important from the experimental and safety point of view. There are many neutron generation method but here the best and suitable method has been presented including others.

Keywords: cross section, differential, associated particle method

INTRODUCTION

To study the neutrons and the neutron detectors, first we need to produce them [1-2]. There are traditionally two ways to produce them: neutron from the neutron sources & Using Accelerators. A neutron source is any device that emits neutrons, irrespective of the mechanism used to produce the neutrons. Neutron source devices are used in physics, engineering, medicine, nuclear weapons, petroleum exploration, biology, chemistry and nuclear power. Neutron source variables include the energy of the neutrons emitted by the source, the rate of neutrons emitted by the source, the size of the source, the cost of owning and maintaining the source. Certain isotopes undergo spontaneous fission (SF) with emission of neutrons. The most commonly used spontaneous fission source is the radioactive isotope californium-252 [3-5]. ²⁵²Cf and all other spontaneous fission neutron sources are produced by irradiating Uranium or another transuranic element in a nuclear reactor, where neutrons are absorbed in the starting material and its subsequent reaction products, transmuting the starting material into the SF isotope. The energy of the neutrons using ²⁵²Cf source are not very high and there is a broad distribution in the neutron energy but in many cases more precise energy information is important including the flux

28558





G. K. Sahu et al.,

value which is not possible by neutron sources. So the other method must have to be apply. The detail of the production of neutron using the other method and that is the accelerator based, which has been discussed.

Review and predictions

As mentioned above the neutrons are very important which need to produce them first and the neutron from the source is a good way to produce but the desired one for some special purposes are not available. The accelerator based is the other method which has been explained bellow. When the ions from the accelerator will hit a specific material they produce neutron including other particles. Like when alpha particles impinge upon any of several low atomic weight isotopes including isotopes of beryllium, carbon and oxygen. This nuclear reaction can be used to construct a neutron source by intermixing a radioisotope that emits alpha particles such radium, polonium or americium with a low atomic weight isotope, usually in the form of a mixture of powders of the two materials. The neutron energy i.e. the differential cross for the neutron emission from the charge particle reaction has been shown in the Fig.1. One can see from Fig.1 that the distribution is not symmetric in the lab, frame in center of mass it happens but in lab there are some specific angel where the emission rate is more. This indicate that to catch /generate maximum neutron one need to focus only on those angles where the emission possibility is more. Another important observation has also found that the neutron cross section using different accelerator based reaction has been shown in Fig.2. One can see from Fig.2 that the light atomic weight element are more use full but for some reaction the cross section is more and constant at high energy side where as for some reaction they are not. The best possible reaction is (d,d) as it works on the principle of the associated particle detection method. When the deuteron will strike the deuteron it will emit ^3He and neutron as the He is a charge particle, a charge particle detector can be used to catch it and the associated neutron can be used for some other purpose. The he will have the energy information so the neutron as well. Fig.2 clearly indicated the possible reaction for the neutron generation using accelerator using different reaction for different purpose.

SUMMARY AND CONCLUSION

A detail review and a clear picture has been provided for the neutron generation and the possible neutron sources. The accelerator based is one which can be controlled and can be used for the other purpose where the energy information is important and it involves the associated particle detection method.

REFERENCES

1. P. K. Rath et.al. "A Suitable Random Number Generator (RNG) For computer simulations", *IJONSs, Vol. 10, Issue.60 page.20875(2020) (WoS)*
2. P.K.Rath,et.al "Simulation Study of detection of ions/charge particles using Gas Detector" *IJONS Vol.10, Issue.60, Page.20879 (2020) (WoS)*
3. P. K. Rath, "Simulation Study of Collimators to use at low energy Facility" *IJONS Vol.10, Issue.60, Page. 20409 (2020) (WoS)*
4. P. K. Rath, et.al "Calculation of potential curve & cross section for compound nucleus ^{215}Rn " *IJONS Vol.10, Issue.60, Page. 20960 (2020) (WoS)*
5. G. K.Sahu, et.al "Study of Fission Fragment Mass Distribution of ^{252}Cf " *Indian Journal of Natural Sciences Vol.10, Issue.60, Page. 20954-20956 (2020) (WoS)*





G. K. Sahu et al.,

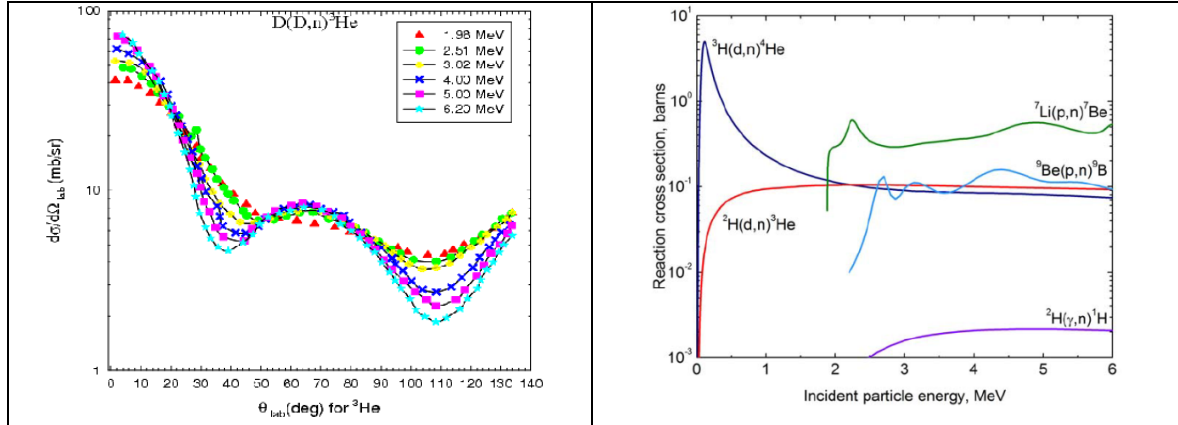


Fig. 1. The compiled differential cross section for the neutron using the (d, d) reaction. The distribution is not symmetric but peaks at some specific angles which has shown in the figure,

Fig. 2. The compiled cross section for the neutron generation from the various reaction and it has found that (d , d) is the best as it will give the energy gated neutron by associated particle detection method.





Comparative Study on Antibacterial Activity of Commercially Available Honey with Locally Obtained Honey

Kokila M¹, Ganesh P^{2*}, Parkavi S¹, Balalakshitha M¹ and Vigneshwari J¹

¹Ph.D Research Scholar, Department of Microbiology, Faculty of Science, Annamalai University, Annamalai Nagar, Chidambaram, Tamil Nadu, India.

²Assitant Professor, Department of Microbiology, Faculty of Science, Annamalai University, Annamalai Nagar, Chidambaram, Tamil Nadu, India.

Received: 13 Sep 2020

Revised: 15 Oct 2020

Accepted: 18 Nov 2020

*Address for Correspondence

Ganesh P

Assitant Professor, Department of Microbiology,

Faculty of Science, Annamalai University,

Annamalai Nagar, Chidambaram,

Tamil Nadu, India.

Email: drpg1974@gmail.com



This is an Open Access Journal / article distributed under the terms of the **Creative Commons Attribution License** (CC BY-NC-ND 3.0) which permits unrestricted use, distribution, and reproduction in any medium, provided the original work is properly cited. All rights reserved.

ABSTRACT

Honey is a natural sweet substance obtained from nectar by the secretion of the living parts of the plant that honey bees gather, turn, and mix to ripen and grow with various substances of their own. The honey samples used for the study are Dabur honey, Jiva honey, Lion honey, and one natural honey from a local area/supermarket in Chidambaram. The collected honey samples were tested for antimicrobial activity against different bacterial strains like *Staphylococcus lactis*, *Proteus Vulgaris*, *Bacillus cereus*, *Pseudomonas fluorescens*, and *Lactobacillus acidophilus* for inhibitory effect. The same bacterial strains were also used to check the inhibitory effect of conventional antibiotics like Gentamicin, ampicillin, ofloxacin, and ciprofloxacin. The antibiotic used also showed a high inhibitory effect against all tested bacteria. Among the antibiotics used, gentamicin showed a high inhibitory effect against *Proteus Vulgaris*. After gentamicin, ofloxacin showed antimicrobial activity against *Proteus Vulgaris* which is followed by ciprofloxacin against *Bacillus cereus* and *Staphylococcus lactis*. The ampicillin antibiotic showed minimum microbial activity against all the strains of bacteria. The entire tested honey sample showed antimicrobial activity against almost all the tested bacteria. Sample A (Dabur honey) showed maximum inhibitory effect against *Lactobacillus acidophilus*, *Bacillus cereus*, *Proteus Vulgaris*, and *Staphylococcus lactis* which is followed by sample C (Natural honey) and Sample B (Jiva honey). The maximum inhibitory effect was found in sample D (Lion honey) against all the tested bacteria. In the case of *Pseudomonas fluorescens*, Sample C showed maximum inhibitory effect followed by Sample A, B, and C.

Keywords: Natural Honey, Antibiotics, Antimicrobial activity.



**Kokila et al.,**

INTRODUCTION

Honey is a natural sweet substance obtained from nectar by the secretion of the living parts of the plant that honey bees gather, turn, and mix to ripen and grow with various substances of their own. Honey is widely used in traditional medicine throughout the world. However, it has limited use in modern medicine due to a lack of scientific support [1]. Honey is a mixture of sugar and other compounds concerning carbohydrates honey is mainly glucose (about 31.0%) and fructose (about 38.5%) as reported by the national honey board (2008) it is identical to the inverted sugar syrup produced which is approximately sucrose 5%, glucose 47%, and fructose 48%. Honey remaining carbohydrates include sucrose and maltose other complex carbohydrates [2,3]. The medicinal quality, taste, texture, color, the aroma of honey differs according to the geographical area and the species of plant from which it has been collected [4]. It is widely accepted that honey is beneficial. Honey is a very complex mixture containing several ingredients involved in "oxidant/antioxidant" physiological processes (hydrogen peroxide, nitrite, nitrate, glucose, glucose oxidase, iron, copper, chlorine, iodine, catalase, tyrosine, tryptophan, arginine, flavonoids, phenolics acid, Maillard reaction products, its pH is not stable. And till now, there was no standardized method to assess this property [5]. It has been observed that an alarming increase in the incidence of human infection is known to occur due to the rising prevalence of pathogenic microorganisms. The infectious disease accounts for about one half of death in tropical countries [6]. The antibacterial potency of honey has been attributed to its strong osmotic effect, naturally low pH, the ability to produce hydrogen peroxide which plays a key role in the antimicrobial activity of honey, and phytochemical factors [7]. The ancient Chinese and Sumerians provided the first written prescription relating to the medical use of honey, found as clay tablets, dating back to 2000 B.C as a medicine, Honey is being used in few hospitals in the present day, particularly in the clinical treatment of bedsores, ulcers, injuries, burns, and surgical wounds [8]. The antibacterial properties of honey can be especially useful against bacteria which have evolved resistance to many antibiotics e.g. *Staphylococcus aureus* which is a significant cause of wound sepsis in hospitals [9]. Honey is thus an ideal topical wound dressing agent in surgical infection, burns, and wounds infection [10]. Antibacterial properties of the honey spend up the growth of a new approach to heal the wound [11]. The bactericidal effect of honey is reported to be dependent on the concentration of honey used and the nature of the bacteria [12].

Objectives

- To Collect honey samples namely Dabur honey, Jiva honey, Lion honey, and one natural honey from the local area / supermarket in Chidambaram.
- To collect different strains of bacteria viz, *Staphylococcus lactis*, *Proteus vulgaris*, *Bacillus cereus*, *Pseudomonas fluorescens*, and *Lactobacillus acidophilus*.
- To test the efficacy of honey samples for the antibacterial activity by disc diffusion assay.

MATERIALS AND METHODS

Collection of Sample

The honey samples were used for this work were collected from a different location and designated as sample A (Dabur honey), Sample B (Jiva honey), Sample C (Lion honey), and Sample D (Natural honey) from a local area supermarket in Chidambaram.

Test of Organisms

The following test organisms bacterial culture were used *Staphylococcus lactis*, *Proteus vulgaris*, *Bacillus cereus*, *Pseudomonas fluorescens*, and *Lactobacillus acidophilus*. The organisms were obtained from the Department of Microbiology, Annamalai University.





Incubation

All the plates were incubated at 37°C. The plates were incubated in an upright position to promote air passage between the plates in stacks of no more than 5 plates. Care was taken to ensure adequate humidity. The time for the growth of bacteria strains was 24-28hrs.

Reading plates

After incubation of the plates, zones were examined. The diameters of the zones of inhibition were measured through a ruler who graduated to 0.5 mm of each zone was read twice (at right angles) and the average result was recorded to the nearest mm (averages of 0-5mm was rounded up).

Antibiotics used

The four different common antibiotics were used and their details are given in Fig- 1.

RESULTS

Antibacterial activity of conventional antibiotics

The antibacterial activity of conventional antibiotics has been found against all the tested bacteria. The inhibitory effect of antibiotics, Ampicillin maximum zone of inhibition (20mm) against *Staphylococcus lactis*, and minimum activity was recorded (13mm) against *Lactobacillus acidophilus*. The inhibitory effect of antibiotic Ofloxacin maximum zone of inhibition (31mm) against *Proteus vulgaris* and minimum activity was recorded (22mm) *Staphylococcus lactis*. The cipromycin antibiotic was found to have a similar amount of inhibitory effect against four bacteria viz *Staphylococcus lactis*, *Lactobacillus acidophilus*, *Bacillus cereus*, *Pseudomonas fluorescens* (30mm), and low for *Proteus vulgaris* (28mm). The antibiotic Gentamicin was found to have the highest inhibitory effect against *Proteus vulgaris* (32mm) and lowest activity against *Lactobacillus acidophilus* (20mm) (Table- 1).

Antibacterial activity of Honey samples

The tested honey samples were found to have antibacterial activity against all the bacterial strains that were used in antibiotics studies. *Lactobacillus acidophilus* organisms sample A was found to have the highest inhibitory effect of (15 mm) and sample D have a low inhibitory effect against *Proteus vulgaris* (13mm) and sample D have no inhibitory effect against *Staphylococcus lactis* and *Bacillus cereus* (16 and 13mm respectively) and sample D was found to have a low inhibitory effect against *Staphylococcus lactis* and *Bacillus cereus* (11 and 0.9 mm) respectively. For *Pseudomonas fluorescent* organisms sample A was found to have a high inhibitory effect of 12 mm and sample A was found to have a high inhibitory effect of 12 mm and sample D was found to have a high inhibitory effect of 12 mm and sample D was found to have no inhibitory effect against *Pseudomonas fluorescens* (Table-2).

DISCUSSION

Since ancient times honey has been used in many treatments as an effective remedy. The fact that honey has antibacterial properties was recognized for more than a century because it cures infections. It was found that the honey samples used in the present study have antibacterial properties that might be due to the presence of several phytochemical compounds and also several reason responsible for the inhibition of microbial growth and the present results were also parallel with the above finding.

CONCLUSION

The efficacy of honey samples is studied to the antibacterial effects against different bacteria strains such as *Staphylococcus lactis*, *Pseudomonas fluorescens*, *Bacillus cereus*, *Lactobacillus acidophilus*, and *Proteus vulgaris* showed





significant results. Among all the honey samples, sample A showed the highest inhibitory effect. Thus, the honey samples are can be used for the treatment of disease caused by the above bacterial strains.

ACKNOWLEDGMENT

I am a non-stipendiary research scholar. I wish to express sincere thanks to the authorities of Annamalai University for providing Lab facilities.

REFERENCES

1. Eman Haldwani M, Mohammed Shohayen M, Shaka, isdr. Honey surpass in their antibacterial activity local and imported honey available in Saudi markets against pathogenic and food spoilage bacteria. Australian Journal of basic applied sciences, 2011; 5(4): 187-191.
2. French VM, Cooper RA, Molan PC. The antibacterial activity of honey against coagulase-negative staphylococci. J Antimicrob Chemother 2005;56:228-231.
3. Cooper RA, Molan PC, Harding KG. Antibacterial activity of honey against strains of *S. aureus* from infected wounds. J Roy Soc Med, 1999;92:28-35.
4. Abdul Kareem Abd, HR, Ahmed AbuRaghif MR, Ihssan Salah Rabea. Antibacterial activity of Different types of Honey in Comparison to Ciprofloxacin against Multidrug Resistance *Pseudomonas aeruginosa* isolated from infected Burn. Kufa. Med. Journal, 2011; 14(1): 88-19.
5. Hayam M, Kameda M, Dalia Marzouk S. Antibacterial activity of Egyptian honey from different sources. International journal of microbiology research, 2011; 2(2): 149-155.
6. Logano-Chiu M, Nelson PW, Paetznick VL, Rex JH. Disk diffusion method for determining susceptibilities of *Candida* sp. to MK-0991. J Clin Microbiol. 1999;37:16-25.
7. Abhishek Chauhan, Vimlendu Pandey KM, Chacko RK, Khandal. Antibacterial activity of raw and processed honey. Electronic journal of biology, 2010; 5(3): 58-66.
8. Weston RJ, Mitchell KR, Allen KL. Antibacterial phenolic components of New Zealand honey. Food Chem 1999;64:295-301.
9. Ibrahim Khalil M, Abdul Motalib MD, Anisuzzaman, ASM, Animzzaman, Zakia sultana sathi, Hye, and Shahjahan M. Antibacterial activities of different brands of unifloral honey available in the northern region of Bangladesh. The science, 2001; 1(6): 389-392.
10. Mundo MM, Padilla-Zakour OI, Worobo RW. Growth inhibition of food-borne pathogens and food spoilage organisms by select raw honey. Int J Food Microbiol. 2004;94:1-8.
11. White JW, Subers MH, Schepartz AI. The identification of inhibin, the antibacterial factor in honey, as hydrogen peroxide and its origin in a honey glucose-oxidase system. Biochim Biophys Acta 1963;73:57-70.
12. Adeleke, OE, OlatinJO, Okepekepe. Comparative antibacterial activity of honey and gentamicin against *Escherichia coli* and *Pseudomonas aeruginosa*. Annals of burn and fire disasters, 2006; 19(4): 101-20.

Table. 1: Antibacterial activity of conventional antibiotics of tested bacteria

Bacteria tested	Zone of inhibition of Conventional antibiotics (mm)			
	Ampicillin	Ofloxacin	Cipromycin	Gentamicin
<i>Lactobacillus acidophilus</i>	13	25	30	20
<i>Proteus vulgaris</i>	19	31	28	32
<i>Staphylococcus lactis</i>	20	22	30	24
<i>Bacillus cereus</i>	16	30	30	24
<i>Pseudomonas fluorescens</i>	14	24	30	21





Kokila et al.,

Table 2: Antibacterial activity of honey samples on tested bacteria

Honey samples	<i>Lactobacillus acidophilus</i>	<i>Proteus Vulgaris</i>	<i>Staphylococcus lactis</i>	<i>Bacillus cereus</i>	<i>Pseudomonas fluorescens</i>
	Zone of inhibition (mm)				
Sample A	15	13	16	13	12
Sample B	11	9	12	11	10
Sample C	12	7	15	10	14
Sample D	7	No	11	8	No

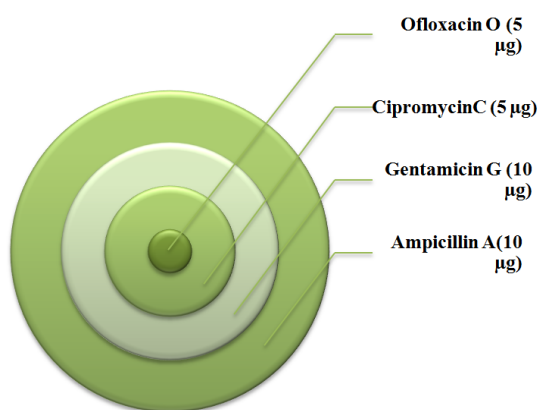


Fig - 1 Using Antibiotics





Thermal Behaviour, NLO Investigation and Antimicrobial Activity of L-Alanine doped Ethylene Diamine Tetra Acetate Composite Crystals

M. Joice Malini^{1,2*}, R. Kunjitham¹, M.K. Sangeetha² and S.Ramalingam³

¹Department of Chemistry, Poompuhar College (Autonomous), (Affiliated to Bharathidasan University, Tiruchirappalli), Melaiyur, Tamil Nadu, India.

²A.V.C. College of Engineering, Mayiladuthurai, Tamil Nadu, India.

³Department of Physics, A.V.C. College, Mayiladuthurai, Tamil Nadu, India

Received: 13 Aug 2020

Revised: 15 Sep 2020

Accepted: 17 Oct 2020

*Address for Correspondence

M. Joice Malini

Department of Chemistry, Poompuhar College (Autonomous),
(Affiliated to Bharathidasan University, Tiruchirappalli),
Melaiyur, Tamil Nadu, India
Email : msajce.mjoicemalini@gmail.com



This is an Open Access Journal / article distributed under the terms of the **Creative Commons Attribution License** (CC BY-NC-ND 3.0) which permits unrestricted use, distribution, and reproduction in any medium, provided the original work is properly cited. All rights reserved.

ABSTRACT

Optically transparent single crystal; L-Alanine doped EDTA is fruitfully grown using slow evaporation technique at room temperature. The grown crystals have been characterized morphologically, analyzed spectroscopically and thereby crystal and structural properties have been interpreted. The crystal parameters have been calculated from experimentally observed data and the calculated values proved orthorhombic crystal lattice formation. The variable refractive indices for different coordinates were measured and it ensured birefringence effect in the crystal. Thermal properties were studied from the data observed from TGA and DSC instruments and thermal stability of the sample was validated. The structural and morphological influence of L-Alanine on EDTA was analyzed by SEM. The partial organic compositions were identified from EDAX peaks and the percentage of organic elements in the crystal was traced. The NLO arrangement in the molecular configuration was mapped and SHG test was made to prove the NLO activity. The Micro dilution bioassay method described by ELOFF was followed to found the Minimum inhibitory concentration (MIC) of LAE for antibacterial activity.

Keywords: crystal growth, birefringence effect, NLO activity, TGA, DSC and MIC.

INTRODUCTION

The ideal organic crystal material could have potential applications in non-linear optical (NLO) devices and that should possess the combination of large non-linear figure of merit for frequency conversion, high laser damage threshold, fast optical response time, wide phase matchable angle, architectural flexibility for molecular design and

28566



**Joice Malini et al.,**

morphology, optical transparency and high mechanical strength [1-4]. Compared with inorganic NLO materials, organic composite materials confidently fulfill the requirements needed to acquire enriched NLO activity. By adopting suitable energetic compound to organic materials, the environmental stability, chemical and mechanical stability, laser damage thresholds and phase matching properties can be enhanced [5-7]. In this way, the fabrication of crystals with semi organic composite have some advantages such as higher second order optical non linearities, short transparency cut-off wavelength and stable physico-chemical performance over the traditional inorganic and organic crystals [8-9]. In order to get greater Second Harmonic Generation (SHG) efficiency, the organic compound requires highly Polarizable σ and π bonding molecular systems possessed asymmetric charge distribution [10-11]. Since there is a large demand for organic crystals in electronic industries in present time, it is required to synthesize new NLO materials and improve the properties of the existing materials. In this work, the growth and characterization of EDTA doped L-Alanine crystals by slow evaporation technique are reported, as no reports are available in literature. Hereafter, the grown semi organic crystals will be named as LAE (L-Alanine doped EDTA). In this work, the results of new L-Alanine EDTA crystals for the first time along with the characterization and analysis studies on Antibacterial activity.

Experimental Technique

The Selection of the solvent is an important step in the growth of crystals from solution by slow evaporation method. In this method, water is used as a solvent for dissolving organic substance. Commercially available annular grade L-alanine and disodium salt of EDTA were used in equal-molar ratio for the Crystal growth. Initially, the material was purified by repeated re crystallization then, the saturated solutions of L-alanine and EDTA at room temperature were prepared. Then the solution is filtered. The filtered solution was taken in a beaker which was sealed with small size hole to control the evaporation of the solvent. The well-defined crystals are obtained within a period of 15 days. White transparent single crystals of Pure L-Alanine and doped LAE crystals are harvested and are shown in within Table 1.

RESULTS AND DISCUSSION

Powder XRD analysis

The crystallinity nature of the studied organic composite was proved by obtained XRD spectrum with Cu K α ($\lambda = 1.5418 \text{ \AA}$) radiation. The sharp peak with maximum intensity showed the measure of better arrangement of interplanes of crystalline which explicit the optimized molecular configurational setup. The XRD pattern for showing different interplane reflections for LAE are shown in the Figure 1. According to the XRD peak assignment, the reflection-signals have been recorded at 21° , 28° , 29° , 34° , 38° , 46° and 55° for (001), (020), (002), (121), (220) and (301) miller indexed planes and they confirmed the orthorhombic crystal lattice existed in present crystal. In the case of organic composite, the peak intensity is usually weak and it always showed defective crystal formation and inactive crystallinity [12]. But, in this case, the peaks were observed with strong intensity that illustrates very good crystal arrangement. Due to this condition, the crystal was found to be formatted in good order and interplanes were spaced in good order. By the better configuration existed in organic crystal, the space group was clearly found to be $P2_1 P2_1 P2_1$ [13]. For understanding the crystal with expected dimensions, the crystal parameters were determined in order and they found to be $a=6.023 \text{ \AA}$, $b=12.343 \text{ \AA}$ and $c=5.784 \text{ \AA}$ and crystal dimension was $\alpha= \beta= \gamma=90^\circ$. All such parametric values proved orthorhombic structure of crystal. The volume of unit cell usually mention packing fraction capacity of crystals and it was found to be 430 \AA^3 which was moderate and able to make high dense packing in the crystal. The Birefringence effect was measured to be 0.188, it was moderately high to produce ordinary and extraordinary optical rays when it is hitting. The NLO efficiency was estimated with respect to SiO_2 and it was 0.6361. This was clearly showed the moderate NLO process taking place over the crystal material. The transmittance value was found to be $0.4500 - 2.317 \mu\text{m}$ for the present case. It belongs to beyond UV and within visible region of spectrum that denoted the optical response of the material. The complexity of crystal was calculated to be 381 which illustrates periodic network of atoms and bonds in molecular configuration and thereby unit cell of crystal. It was

28567



**Joice Malini et al.,**

more than enough to appraise lattice periodicity of present crystal. Here, from the parameter analysis, it was found that, though, the L-Alanine was doped with EDTA, the L-Alanine base lattice was maintained and EDTA was retained in such lattice.

Thermal Analysis

Thermo gravimetric (TGA) and differential scanning calorimetric (DSC) analyses were carried out, using universal V4-5A-TA instrument at a heating rate of 20°C/min, recorded in the same chart are shown in Figure 2. Thermo gravimetric analysis (TGA) usually carried out to record the weight of a substance as a function of temperature. In the present case, the TGA and DSC are carried out between 20°C and 800°C in an inert environment. The weight, particle size and the mode of preparation (the pre-history) of a sample, all govern the thermo gravimetric results. In practice, a small sample weight is desirable for thermo gravimetric results and hence the weight of the sample taken for investigation is 6.123mg. In TGA, the endothermic peak at around 250°C represents the melting point of the sample. In figure 6, there are four distinct weight losses was found above 250°C. At the first stage, about 91.44% of weight loss produced at 253.15°C, at the second stage, there is 59.83% of weight loss taking place at 284.59°C,. At the third stage, 40.01% of weight loss occurs at 294.16°C. In the final step, there is 20.02% of sample violated at 308.48°C, leaving about 0.8489% of the sample as end residue around 515.10°C. The exothermic process is nearly Coincide with the TGA weight loss prediction. The DSC is used to predict the phase transitions or chemical reactions can be followed by observation of the heat absorbed or liberated: Fusion, change in the crystalline state and other physical changes of the sample while heating give sharp endothermic peak. Dehydration is indicated by a broad endothermic peak. Certain chemical changes such as oxidative degradations are aided by exothermic peaks. The endothermic peak at 250°C is indicative of the melting point of the sample. From the above observation, it was clear that, the melting point of present crystal was found to be stabilized and elevated to high degree of temperature.

SEM observation

The surface of the present crystal was scanned at different magnification order and they are presented in Figure 3. Here, the crystal was customized by adopting L-Alanine organic molecule in EDTA molecular configuration and they crystallized by slow evaporation method. Different scanning pattern was registered in order to signify the smoothness of the surface and crystal grows ability. Here the Figure 3 (a) showed magnifications of 15kV and at a scale of 12.7µm where in which smoothed surfaces were found in the form of fine wire. In Figure 3(b), at magnifications of 15kV and at a scale of 63.6 µm, the joint network of fine wires. In Figure 3(c), at magnifications of 15kV and at a scale of 127 µm, well profound smoothness was found. In Figure 3(d), at magnifications of 15kV with scale of 25.4 µm, hairpin loop was appeared. From all SEM images, it was observed that, due to the addition of the doping species on dopant EDTA, the growth pattern is modified well and vertical and cross sectional layer growth is observed to be good and hence EDTA acts as a excellent growth catalyst.

EDAX examination

The partial energy distribution profile of present organic crystal composite was mapped from the EDAX spectrum and the dispersive elements are tabulated and are shown in Figure 4. The percentage of presence of organic elements is illustrated in same figure and also the atomic percentage was observed. The first organic element O was found to be 41.27 %, C was observed to be 34.63 % and N was calculated to be 14.90 %. All the organic elements are participated to customize the LAE crystal and it was verified with crystal parametric values. From the data, it was conferred that, the organic composite was pure and no contamination was found. Except Na, the crystal is needed not to be optimized and energy dispersion was appeared to be normal and equal distribution rate.

SHG Efficiency Measurement

The SHG property of LAE is determined by the modified version of powder technique by Kurtz and Perry. The microscopic origin of non-linearity in the NLO materials is due to the presence of delocalized π -electron systems, degenerate donor and acceptor groups, which enhance their asymmetric polarizability. Each type of constituent



**Joice Malini et al.,**

chemical bond is regarded as one part of the whole crystal that has contributions to the total non-linearity. The distribution of valence electrons of the metallic elements is an important factor that strongly affects the linear and nonlinear properties of each type of constituent chemical bond. The fundamental beam of 1064 nm from Q-switched Nd:YAG laser was used to test the SHG property of the grown crystal. The input pulse with energy 1.2mJ pulse and pulse width of 10 ns with a repetition rate of 10 Hz was used. The fundamental beam was filtered by using IR filter. A photo multiplier tube (Philips photonics) was used as detector of the optical output signal emitted by the sample. Potassium dihydrogen ortho phosphate (KDP) [50 mV] was used as the reference material. The second harmonic generation was confirmed by the emission of green light having the wavelength around 532 nm and the output is 60 mV and hereby the NLO efficiency was proved.

Antimicrobial Activity

Minimum inhibitory concentration (MIC) of compounds for antibacterial activity were determined using the micro dilution bioassay as described by ELOFF. Overnight cultures (incubated at 37°C in a water bath with an orbital shaker) of 1gm positive (*Staphylococcus aureus*, *Bacillus subtilis* and *Streptococcus pyogenes*) and 2gm negative (*Escherichia coli*, *Pseudomonas aeruginosa* and *Salmonella typhi*) bacterial strains were diluted with sterile Mueller-Hinton (MH) broth to give final inocula of approximately 10⁶ CFU/ml (colony forming units). The compound LAE was dissolved in water to known concentration 50mg/ml. 100micro litres of this sample was diluted two-fold with sterile distilled water in a 96 Well micro litre plate for each of the five bacterial strain. One hundred micro litres of each bacterial culture were added to each well. The plates were covered with parafilm and incubated at 37°C for 24hrs. Bacterial growth was indicated by adding 50µl of 0.2mg/ml p-iodonitrotetrazolium chloride (INT) with further incubation at 37°C for 2hrs. since the colourless tetrazolium salt is biologically reduced to a red product due to the presence of active organism, the MIC values were recorded as the concentration in the last well in which no colour change was observed after adding the INT indicator. Bacterial growth in the well was indicated by a redish pink colour. The assay was repeated twice with two replicates per assay (14) The results of this study revealed that the compound LAE exhibit antibacterial activity which might be helpful in preventing the progress of various diseases and can be used in alternative system of medicine. The antibacterial activity of LAE was more effective than the parent L-Alanine for some of the pathogens shown in the table (2).

CONCLUSION

L-Alanine was doped with EDTA and the corresponding crystal was grown using slow evaporation method. The crystal was found to be very acute and pure and the crystal physical-evaluation determined that the grown crystal was highly transparent and is able to act as NLO material. The XRD parameters were estimated and the respective data was calculated from the standard formula. The XRD morphological observation was made and calculated data confirms the orthorhombic lattice formation in the crystal and has taken the effect of NLO activity. The refractive indices for different coordinates ensured that, the entered optical energy was found to be boosted with higher order which was different in different crystal planes. In order to evaluate the NLO activity, the gain of amplification was measured and observed that the efficiency was comparatively high. The SEM images was examined with respect to step-up magnification process, the corresponding surface view of molecular arrangements have been identified. EDAX confirm the presence of the elements of LAE. The results of MIC study revealed that the compound LAE exhibit antibacterial activity.

REFERENCES

1. H. O. Marcy, L. F. Warren, M. S. Webb, C. A. Ebbers, S. P. Velsko, G. C. Kennedy and G. C. Catella, Applied Optics, Vol. 31, No. 24, 1992, pp. 5051-5060.
2. Y. J. Ding, X. Mu and X. Gu, Nonlinear Optical Physics and Material, Vol. 9, No. 1, 2000, p. 21.





Joice Malini et al.,

3. X. Q. Wang, D. Xu, D. R. Yuan, Y. P. Tian, W. T. Yu, S. Y. Sun, Z. H. Yang, Q. Fang, M. K. Lu, Y. X. Yan, F. Q. Meng, S. Y. Guo, G. H. Zhang and M. H. Jiang, Material Re-search Bulletin, Vol. 34, No. 12-13, 1999, pp. 2003-2011.
4. L. Li, Z. P. Wang, G. R. Tian, X. Y. Song and S. X. Sun, Journal of Crystal Growth, Vol. 310, No. 6, 2008, pp. 1202-1205.
5. G. Pasupathi and P. Philominathan, Material Letters, Vol. 62, No. 28, 2008, pp. 4386-4388
6. M. N. Bahat and S. M. Dharma Prakash, Journal of Crystal Growth, Vol. 236, No. 1-3, 2002, pp. 376-380.
7. X. Ren, D. L. Xu and D. F. Xue, Journal of Crystal Growth, Vol. 310, No. 7-9, 2008, pp. 2005-2009.
8. N. J. Long, "Organometallic Compounds for Nonlinear Optics, The Search for Enlightenment," Angewandte Chemie, Vol. 34, No. 1, 1995, pp. 21-38.
9. K. Y. Li, X. T. Wang, F. F. Zhang and D. F. Xue, Physical Review Letters, Vol. 100, No. 23, 2008, pp. 659-666.
10. D. F. Xue, L. J. Zou, L. Wang and X. X. Yan, Modern Physics Letters B, Vol. 23, No. 31-32, 2009, pp. 3761-3768.
11. P. Groth, "Chemische Krystallographie," Verlag Wilhelm Engelmann, Leipzig, Vol. 2, 1908, 362.
12. R. Krishnamurthy, Bincy Susan Samuel, G. Mani and R. Rajasekaran, Elixir Materials Science, 85, (2015), 34508-34511.
13. I. Cicilignatius, S. Rajathi, K. Kirubavathi, K. Selvaraju, Journal of optik, Vol.125, 2014, 4265-4269.
14. M.S. Kajamuhideena, K. Sethuramana, P. Sasikumarb, H. Shakila, Materials Science & Engineering B, 240, 106-115, 2019.

Table 1: Crystal parameters of L-Alanine doped EDTA

S. No.	Parameters	Values	Crystal view
1	Space group	P2 ₁ P2 ₁ P2 ₁	
2	Unit cell		
	A	6.023 Å	
	b	12.343 Å	
	c	5.784 Å	
3	$\alpha = \beta = \gamma$	90°	
4	Crystal type	Orthorhombic	
5	Refractive index		
	n₁	1.58	
	n₂	1.76	
	n₃	1.65	
6	Volume	430 Å ³	
7	Birefringence (Δn) Kλ/t	0.188	
8	NLO efficiency	0.6361 [1/1(SiO ₂)]	
9	Transmittance	0.4500 – 2.317 μ m	
10	complexity	381	

Table 2: MIC (μ g/ml) values of the pathogens against L-Alanine & LAE

Compound	<i>Bacillus subtilis</i>	<i>Staphylococcus aureus</i>	<i>Vibrio cholerae</i>	<i>Klebsiella</i>	<i>Escherichia coli</i>
L-Alanine	0.49	0.39	0.29	0.175	0.49
LAE	1.56	1.12	0.39	1.56	1.56





Joice Malini et al.,

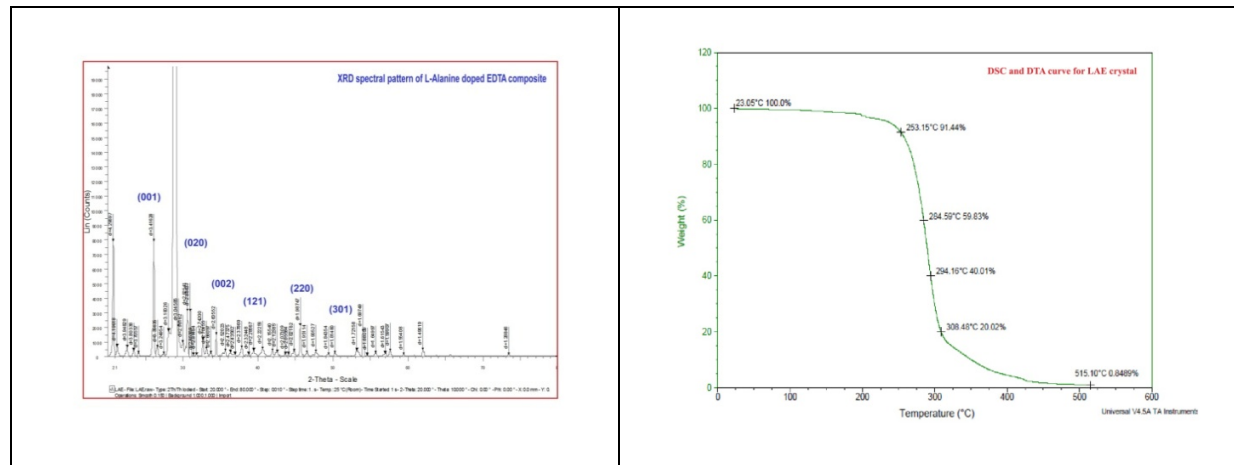


Figure 1: XRD spectral pattern of LAE crystal

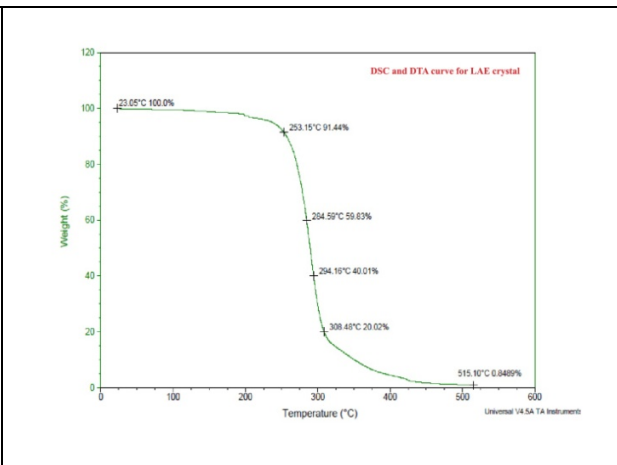


Figure 2: Thermal analysis curve

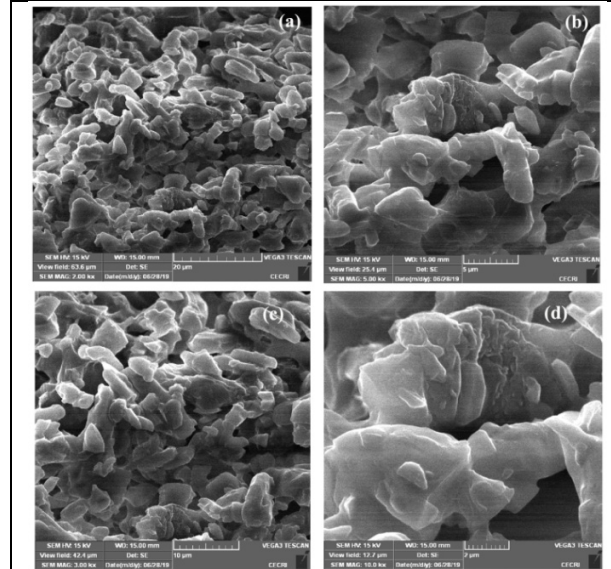


Figure 3: SEM images of LAE crystal

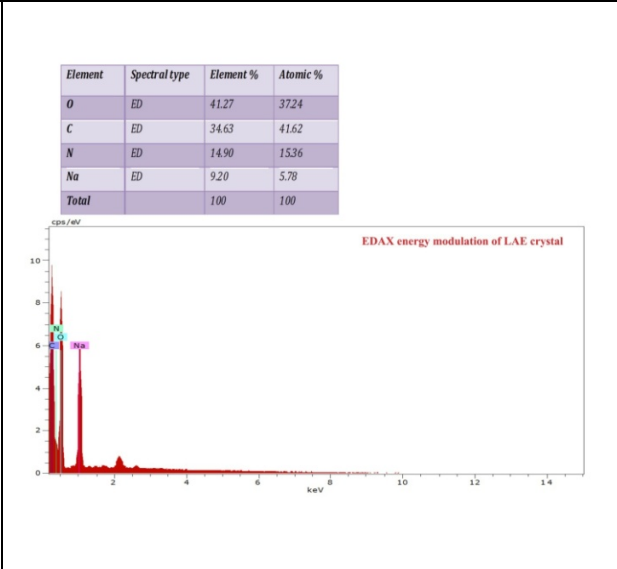


Figure 4: EDAX examination spectrum





Development and Validation of Simple RP-HPLC Method for the Estimation of Imatinib Mesylate

Senthil Kumar.V¹, Ajay Kumar.T.V², Krishnaprabha.N¹ and Parthasarathy.V^{1*}

¹Immunology Laboratory, Department of Pharmacy, Annamalai University, Annamalai Nagar, Tamil Nadu, India.

²Azidus Laboratories Ltd., Rathinamangalam, Vandalur, Chennai, Tamil Nadu, India.

Received: 13 Aug 2020

Revised: 15 Sep 2020

Accepted: 17 Oct 2020

*Address for Correspondence

V. Parthasarathy

Professor, Department of Pharmacy &
Director, Centre for Cell Biology and Drug Discovery
Annamalai University, Annamalai Nagar
Tamilnadu, India.
Email: vpartha@yahoo.com



This is an Open Access Journal / article distributed under the terms of the **Creative Commons Attribution License** (CC BY-NC-ND 3.0) which permits unrestricted use, distribution, and reproduction in any medium, provided the original work is properly cited. All rights reserved.

ABSTRACT

An accurate, simple, sensitive, precise, and rapid reverse phase high performance liquid chromatography (RP-HPLC) method for the analysis of Imatinib Mesylate was developed and validated. In this study various concentration of Imatinib Mesylate was prepared in phosphate buffer (pH 5.5) and analyzed using FLOWROSIL PAK C18 MG II 5 μ (250mm x 4.6mm) HPLC column (Shimadzu, Model: LC 2010 CHT, Japan) packed with porous spherical silica coated with a silicone polymer monolayer with octadecyl (C18) groups. The mobile phase used for the study was water : acetonitrile : methanol at the ratio of 300:200:500. To the mobile phase 3ml of glacial acetic acid was added and triethylamine was used to adjust the pH 5.5. The temperature of the column was maintained at 30°C and the flow rate of the column was adjusted to 0.5ml/min. The sample detection was carried out at 265 nm. The present study developed a simple, rapid, accurate, cost effective and superior method for the analysis of Imatinib Mesylate using RP-HPLC to overcome the problems associated with the existing reported methods.

Keywords: Breast Cancer, Imatinib Mesylate, RP-HPLC, Analysis.

INTRODUCTION

Cancer is an uncontrolled over proliferation of cells elsewhere in the body. Among the various types of cancers, the breast cancer is highly prevalent next to lung cancer and the incidence of breast cancer is more in underdeveloped regions of the world. Breast cancer occurs as a result of mutation in the genes like proto-oncogenes as well as tumor suppressor genes in a single clone of cells in the ductal and glandular regions of the breast. Although several drugs

28572





such as Raloxifene hydrochloride, Tamoxifen citrate, Abemaciclib, Paclitaxel, Everolimus, Imatinib, Alpelisib, Anastrozole, Pamidronate disodium and Aromasin are used for the prevention and treatment of breast cancer. A précised analytical technique is needed to maintain the appropriate therapeutic concentration for an effective therapy. The present study is aimed to develop a simple, accurate method to estimate the concentration of Imatinib Mesylate in body fluids and formulations. Imatinib Mesylate is chemically known as 4-[(4-methyl-1-piperazinyl)methyl]-N-[4-methyl-3-[[4-(3-pyridinyl)-2-pyrimidinyl] amino] phenyl]-benzamide methane sulfonate with the molecular formula, $C_{30}H_{35}N_7O_4S$ (Fig.1) and weight, 589.7gm/mol (Suresha et al., 2016). Imatinib Mesylate rationally designed to inhibit the Bcr-Abl tyrosine kinase (Druker et al., 1996; Buchdunger et al., 1996) as well as, c-Kit, platelet-derived growth factor receptor (PDGFR) tyrosine kinases (Druker et al., 2001; Demetri et al., 2002). Fig.1 The structure of Imatinib.

Imatinib Mesylate exerts its biological action by binding at the ATP site of tyrosine kinase (TK) enzyme and prevents phosphorylation of the proteins which is involved in signal transduction pathways. It is used for the treatment of chronic myelogenous leukaemia (CML) and gastro intestinal stromal tumours (GIST). The anticancer activity of Imatinib Mesylate is mediated through inhibiting cell proliferation and induce apoptosis (Druker et al., 1996; Beran et al., 1998; Gambacorti-Passerini et al., 1997; Deininger et al., 1997; Dan et al., 1998; Le Coutre et al., 1999; Druker et al., 2001). Sindhu et al (2015) developed a method for the estimation of Imatinib Mesylate in bulk and pharmaceutical dosage form. The separation was achieved on C18 G column (250x4.6 mm i.d, 5 μ m), using o-Phosphoric acid (0.1% v/v): Acetonitrile at the ratio of 70:30 v/v as mobile phase and the flow rate was 1.0 ml/min. Detection was carried out at 266 nm and the drug was eluted at the retention time of 3.25 min. The total run time was 5 minutes. Although the RT was short for this method but one of the solvents used for the preparation of mobile phase O-Phosphoric acid is a dense, corrosive and damp the column. Sathwik et al (2015) assessed the stability of Imatinib in water by performing the separation of Imatinib Mesylate using C18, 150x4.6 mm, 5 μ column in isocratic mode with the mobile phase containing a mixture of buffer: acetonitrile (72:28v/v). The flow rate of the mobile phase was 1.0 ml/min and the eluents were monitored at 265 nm. The authors found that the retention time of Imatinib Mesylate was 3.63 min. However, this method is not suitable for the analysis of Imatinib in formulations with various polymers. Kuna and co-workers (2018) developed a HPLC method for the determination of Imatinib Mesylate and its dimer impurity by using the column HiQSil C18 (250 mm x 4.6 mm, 5 μ m) with the mobile phase as methanol and acetate buffer pH 3.5 in the ratio of 80:20 v/v. The analysis was carried out at 273 nm. The flow rate of the mobile phase was 1.0 ml/min. and the retention time for the Imatinib Mesylate as well as dimer impurity was 8.060 and 11.398 respectively. This method has the limitation of longer retention time of 8.06 min for the analysis and consumes more mobile phase. Sandhya and co-workers (2013) reported a method of analysing the Imatinib Mesylate using Phenomenex column (4.6 mmx150 mm i.d) 5 μ column. The mobile phase used for the analysis was a mixture of Orthophosphoric acid buffer (pH 2.5): Methanol (50:50) and the detection was carried out at a wavelength of 263nm. The authors reported that the RP-HPLC method is a rapid and accurate for the estimation as well as validation of Imatinib Mesylate in tablet dosage format with the retention time of 2.2 min. Though the developed method has a short retention time but it has the limitation of using corrosive acidic orthophosphoric acid as a mobile phase. Kuna and co-researchers (2017) analysed the Imatinib Mesylate using HiQSil C18 (250 x 4.6 mm, 5 μ m) column with mobile phase containing methanol and acetate buffer pH 3.5 at the ratio of 80:20 v/v. The flow rate for the analysis was 1.0ml/min the eluent was monitored at 273nm. The authors found that the retention time for Imatinib Mesylate was 8.071 and its amine impurity as 4.958. Since, the retention time for the analysis was quite high, it requires proportionately high amount of mobile phase for the analysis and increases the cost of analysis. Shah and co-researchers (2017) carried out the analysis of Imatinib Mesylate by adopting RP-HPLC method using Eclipse XDB-C18 (150 mm x 4.6 mm), 5 μ analytical column as the stationary phase with isocratic elution of the mobile phase consisting of Sodium dihydrogen phosphate buffer (1.5g of Sodium dihydrogen phosphate into 500 ml of water and the pH was adjusted to 8.0 with Triethylamine) and the solvent mixture (200ml of methanol and 200ml of acetonitrile). Then the mobile phase was prepared by mixing dihydrogen phosphate buffer (pH8) and the solvent mixture at the ratio of 450:550 v/v. The flow rate of the analysis was 1.0 ml/min. The authors reported that the retention time of the Imatinib was 5.5 min. Hasin and co-workers (2017) developed a simple and sensitive HPLC method for the estimation of Imatinib Mesylate in



**Senthil Kumar et al.**

pure and in pharmaceutical dosage forms. A 4.6 mm x 150cm column packed with L1 (C18) was used and the mobile phase was a mixture of buffer: acetonitrile: methanol at the ratio of 50:25:25. The flow rate of the analysis was 1.1ml/min. and the effluent was monitored at 230nm. The authors reported that the retention time for the analysis was 5.784 min. and the system suitability parameters were within limit. In addition to these, Sahoo *et al* (2015) carried out a separation of Imatinib using C-18 column (Analytical technologies, 250mm x 4.6mm) with isocratic mode. The mobile phase for the study was acetonitrile: potassium dihydrogen phosphate buffer (pH 2.5) at the ratio of 30:70v/v with a flow rate of 0.8 ml/min. and the detection was carried out at 268 nm. The retention time of Imatinib was found to be 2.67 min. The authors developed a RP-HPLC method for the quantification of Imatinib in bulk and capsule dosage. Shah and co-workers (2015) performed a chromatographic elution of Imatinib Mesylate with C18 (5m Symmetry waters column, 150 mmx4.6 mm). The authors used gradient elution of mobile phase-A (A mixture of 500ml of pH 3.0 buffer solution and 500ml of methanol) and the mobile phase-B (A mixture of 40ml of pH 3.0 buffer solution and 960ml of methanol) at a flow rate of 1.0 ml/min. The detection was performed at 240 nm with the injection volume of 20 μ l and the run time of 65 min. From this study, the authors reported that the retention time of the Imatinib peak was observed at 21 min. Since the method has a longer retention time of 21 min, this method won't be considered as a simple method. Srirangam *et al* (2019) achieved a chromatographic separation on C18 column (250 mm x 4.6 mm i.e., 5 μ m) with a mobile phase composed of methanol: water:glacial acetic acid at a ratio of 65:35:0.03% v/v at a flow rate of 1.0 ml/min. The detection was carried out at 267 nm using photodiode array detector and the retention time of the elution was 5.02 min, with no interfering peak of excipients used for the preparation of dosage form. We the authors adopted various reported methods to estimate the concentration of Imatinib Mesylate in formulations and encountered many problems such as peak tailing and unable to get the sharp peak of chromatogram. Hence, the present study was undertaken to develop a simple, rapid, accurate, cost effective and superior method for the analysis of Imatinib Mesylate using RP-HPLC.

MATERIALS AND METHODS

Chemicals and reagents

Imatinib Mesylate was used as a drug candidate to develop a new RP-HPLC method. The solvents system used for the analysis was of HPLC grade. Acetonitrile was obtained from Sd Fine Chem. Ltd (India) and HPLC grade water was prepared using Milli Q Water (Merck). Imatinib Mesylate was a gift sample from Ranbaxy Laboratories Ltd, New Delhi.

Instrumentation

Imatinib Mesylate was analysed using HPLC column with FLOWROSIL PAK C18 MG II 5 μ (250mm x 4.6mm) (Shimadzu, Model: LC 2010 CHT, Japan), packed with porous spherical silica coated with a silicone polymer monolayer with octadecyl (C18) groups. The mobile phase used for the experiment was water: acetonitrile: methanol at the ratio of 300:200:500 and to this, 3ml of glacial acetic acid was added. Triethylamine was used to adjust the pH 5.5. The temperature of the column was maintained at 30°C and the flow rate of the column was adjusted to 0.5ml/min. The sample detection was carried out at 265 nm.

Method validation

The relative standard deviations (RSDs) of the area, tailing factor, and retention time were the chromatographic parameters selected for the present study to check the system suitability test.

Preparation of phosphate buffer pH 5.5

Accurately weighed 0.68gm of phosphate buffer (potassium dihydrogen ortho phosphate) and transferred into a 500ml volumetric flask. Added 400ml of Milli Q water, dissolved by sonication and the final volume was made up to 500ml using Milli Q water. The pH of the buffer solution was adjusted to 5 \pm 0.5 using ortho phosphoric acid (dilute). Filtered through membrane filter (0.45 μ m) prior to use.



**Senthil Kumar et al.****Preparation of standard solution of Imatinib**

Stock standard solution of Imatinib Mesylate was prepared by transferring 10mg of drug in to 10ml volumetric flask. Added 8ml of acetonitrile and sonicated for 5-10min. Finally, the volume was made up with acetonitrile to a final concentration of 1mg/ml. 10µm/ml of working standard solution was prepared by taking suitable aliquot from standard stock solution and the volume was made up with acetonitrile.

Statistical analysis of the study

The data were analysed using Microsoft excel.

RESULTS AND DISCUSSION**Linearity**

Stock solution of Imatinib Mesylate (1mg/ml) was suitably diluted with Acetonitrile to get the concentration in the linearity range of 50 to 400µg/ml (Table 1). A sample volume of 20µl was injected into the column. Chromatogram, peak area and retention times of each solution were recorded. Calibration curve of Imatinib Mesylate was prepared by plotting the concentration (µg/ml) in X-axis and average peak area in Y-axis (Table 1 and Figure 2). The HPLC chromatogram is given in Fig.3. The statistical analysis of linearity data was carried out to find out the slope intercept and correlation of coefficient and the R^2 for Imatinib was found to be 0.9994.

Table 1. Preparation of linearity of Imatinib Mesylate using RP-HPLC method. Where, various concentrations of Imatinib Mesylate and its corresponding peak area. Fig.2. Calibration curve of Imatinib Mesylate in phosphate buffer pH 5.5. The study was carried out using RP-HPLC method with C18 column at RT was about 5 minutes. Where, X axis denotes the concentration of Imatinib and the Y axis represents peak area. Fig.3. RP-HPLC profiles of various concentrations of Imatinib Mesylate. The analysis was carried out using HPLC column with FLOWROSIL PAK C18 MG II 5µ (250mm x 4.6mm) (Shimadzu, Model: LC 2010 CHT, Japan), packed with porous spherical silica coated with a silicone polymer monolayer with octadecyl (C18) groups. The mobile phase used for the experiment was water:acetonitrile:methanol at the ratio of 300:200:500 and to this 3ml of glacial acetic acid was added. Triethylamine was used to adjust the pH 5.5. The temperature of the column was maintained at 30°C and the flow rate of the column was adjusted to 0.5ml/min. The sample detection was carried out at 265 nm. Where, A, B,C and D represents the RP-HPLC profile of 50, 100, 200 and 400µg of Imatinib Mesylate respectively.

Relative standard deviation

To validate the newly developed RP-HPLC method for Imatinib Mesylate, the repeatability of the analysis was conducted with 300µg/ml concentration of drug. The RT and AUC of the study showed that the repeatability was within the permitted limit (Not more than 2%) Tab.2. Assessing the relative standard deviation of Imatinib Mesylate using RP-HPLC method.

CONCLUSION

The RP-HPLC method developed for the estimation of Imatinib Mesylate was very simple, rapid, accurate, precise, reproducible and cost effective. The mobile phase used for the present study was water acetonitrile :methanol in the ratio of 300:200:500 at the pH 5.5, which efficiently eluted the Imatinib Mesylate at the retention time of 5 minutes without any interference and tailing effect. In addition to these, the present RP-HPLC method has many advantages such as, the method requires only less amount of methanol for the preparation of mobile phase for RP-HPLC analysis as compared to other reported methods, which will reduce the risk of exposure to methanol and environmental damage. Hence, this new method would be suitable for the quantification of Imatinib Mesylate in pharmaceutical dosage forms as well as body fluids without interference.



**Senthil Kumar et al.****ABBREVIATIONS**

ACN: Acetonitrile
AUC: Area Under Curve
LOD/DL: Limit of Detection
LOQ/QL: Limit of Quantification
RP-HPLC: Reverse Phase High Performance Liquid Chromatography
RT: Retention Time
TKI: Tyrosine Kinase Inhibitor

ACKNOWLEDGEMENTS

The authors are grateful to the University Grants Commission (UGC), New Delhi for the financial support to Mr.V.Senthilkumar in the form of BSR fellowship to carry out this study. We also thank M/S Ranbaxy Ltd., New Delhi for providing the gift samples of Imatinib Mesylate and Mr.B.Tholkappian, Managing Director, Thorab Pharma and Research Laboratory, Puducherry, for extending the technical support including gift samples of Pharmaceutical excipients to carry out this research. Authors also express their sincere thanks to Mr. K. Maruthupandian and Mr.R.Paramguru, Managing Director, Ideal Analytical & Research Institute, Puducherry for extending their technical support to carry out this research.

CONFLICT OF INTEREST

The authors declare that they don't have conflict of interest.

REFERENCES

1. Suresha DN, Pramila T, Tamizh Mani T. Method development and validation of Imatinib Mesylate - Review. *International Journal of Pharmacy and Pharmaceutical analysis* 2016;01(03):01-11.
2. Druker BJ, Tamura S, Buchdunger E, Ohno S, Segal GM, Fanning S, Zimmerman J, Lydon NB. Effects of a selective inhibitor of the Abl tyrosine kinase on the growth of Bcr-Abl positive cells. *Nat Med* 1996;2:561-566.
3. Buchdunger E, Zimmermann J, Mett H, Meyer T, Müller M, Druker BJ, Lydon NB. Inhibition of the Abl protein-tyrosine kinase in vitro and in vivo by a 2-phenylaminopyrimidine derivative. *Cancer Res* 1996; 56:100-104.
4. Druker BJ, Talpaz M, Resta DJ, Bin Peng, Buchdunger E, Ford JM, Lydon, NB, Kantarjian H, Capdeville R, Ohno-Jones S, and Sawyers CL. Efficacy and Safety of a specific inhibitor of the BCR-ABL tyrosine kinase in chronic myeloid leukemia. *The New England Journal of Medicine*. 2001; 344:1031-1037. DOI: 10.1056/NEJM200104053441401.
5. Druker BJ, Sawyers CL, Kantarjian H, Resta DJ, Reese SF, Ford JM, Capdeville R, Talpaz M. Activity of a specific inhibitor of the BCR-ABL tyrosine kinase in the blast crisis of chronic myeloid leukemia and acute lymphoblastic leukemia with the Philadelphia chromosome. *N Engl J Med* 2001;344:1038-1042.
6. Demetri GD, von Mehren M, Blanke CD, Van den Abbeele AD, Eisenberg B, Roberts PJ, Heinrich MC, Tuveson DA, Singer S, Janicek M, Fletcher JA, Silverman SG, Silberman SL, Capdeville R, Kiese B, Peng B, Dimitrijevic S, Druker BJ, Corless C, Fletcher CDM, Joensuu H. Efficacy and safety of imatinibmesylate in advanced gastrointestinal stromal tumors. *N Engl J Med* 2002;347:472-480.DOI: 10.1056/NEJMoa020461.
7. Beran M, Cao X, Estrov Z, Jeha S, Jin G, O'Brien S, Talpaz M, Arlinghaus RB, Lydon NB, Kantarjian H. Selective inhibition of cell proliferation and BCR-ABL phosphorylation in acute lymphoblastic leukemia cells expressing Mr. 190,000 BCR-ABL protein by a tyrosinekinase inhibitor (CGP 57148). *Clin. Cancer Res.*1998;4,1661-1672.





Senthil Kumar et al.

8. Gambacorti-Passerini C, Le Coutre P, Mologni L, Fanelli M, Bertazzoli C, Marchesi E, Di Nicola M, Biondi A, Corneo GM, Belotti D, Pogliani E, Lydon NB. Inhibition of the ABL kinase activity blocks the proliferation of BCR/ABL⁺ leukemic cells and induces apoptosis. *Blood Cells Mol. Dis.* 1997;23(19):380–394.
9. Deininger, M. Goldman JM, Lydon N, Melo JV. The tyrosine kinase inhibitor CGP57148B selectively inhibits the growth of BCR–ABL-positive cells. *Blood* 1997;90, 3691–3698.
10. Dan S, Naito M, Tsuruo T. Selective induction of apoptosis in Philadelphia chromosome-positive chronic myelogenous leukemia cells by an inhibitor of BCR–ABL tyrosine kinase, CGP 57148. *Cell Death Differ* 1998; 5, 710–715.
11. Le Coutre P, Mologni L, Cleris L, Marchesi E, Buchdunger E, Giardini R, Formelli F, Cambacorti-Passerini, C. *In vivo* eradication of human BCR/ABL positive leukemia cells with an ABL kinase inhibitor. *J. Natl Cancer Inst.* 1999;91:163–168.
12. Sindhu SN, Rao YS, Kumar TH, Rao KVP. Method development and validation of RP-HPLC method for estimation of imatinib mesylate in pure and pharmaceutical dosage form. *Der Pharmacia Lettre* 2015;7(3):33-38.
13. Sathwik G, Dubey S, Prabitha P, Harish Kumar DR. Analytical method development and validation of solid dosage form of antineoplastic drug Imatinib Mesylate by RP HPLC. *International Journal of Pharma Sciences and Research (IJPSR)* 2015;6(4):697-705.
14. Kuna AK, Seru G, Radha GV. Method Development and validation for the estimation of Imatinib Mesylate and its dimer impurity in Pharmaceutical formulations by reverse-phase high performance liquid chromatography. *Asian J Pharm Clin Res* 2018;11(3): 136-139.
15. Sandhya P, Vishnu Priya P, Shyamala, Anjali Devi N, Sharma, JVC. Method development and validation of Imatinib Mesylate in Pharmaceutical dosage form by RP-HPLC. *World Journal of Pharmacy and pharmaceutical Sciences* 2013;3(1):682-688.
16. Kuna AK, Seru G, Radha GV. Analytical method development and validation for the estimation of Imatinib mesylate and its impurity in pharmaceutical formulation by RP-HPLC. *Int. J. Pharm. Sci. Rev. Res* 2017;42(2):113-118.
17. Shah P, Shah N, Shah R. Method development and validation of a stability indicating RP-HPLC method for assay determination of Imatinib in Imatinib Mesylate tablet dosage form. *International Journal of Pharmaceutical Sciences and Research* 2017;6(10):4453-4468.
18. Hasin F, Islam MT, Ahmad MF, Rakib MMH. Validation of assay method for the estimation of Imatinib Mesylate in table dosage form by HPLC. *European Journal of Biomedical and Pharmaceutical Sciences* 2017;4(7):74-81.
19. Sahoo NK, Sahu M, Alagarsamy V, Srividya B, Sahoo CK. Validation of assay indicating method development of Imatinib in bulk and its capsule dosage form by liquid chromatography. *Ann Chromatogr Sep Tech.* 2015;1(2):1010-1015.
20. Shah P, Shah R. A stability-indicating RP-HPLC method development and validation for the related substances determination of Imatinib process impurities and their degradation products in tablet dosage form. *International Journal of PharmTech Research* 2015;8(6):128-146.
21. Srirangam P, Patro VJ, Seru G. Development and validation of a sensitive RP-HPLC method for quantitative determination of Imatinib Mesylate in complex dosage forms like drug eluting coronary stents. *Journal of Pharmacy Research* 2019;13(1):15-19.

Table 1. Concentration of Imatinib Mesylate and their respective peak area.

Concentration of Imatinib Mesylate (µg/ml)	Peak Area
0	0
50	5,52,955
100	9,63,352
200	18,59,112
300	28,68,146
400	37,76,553

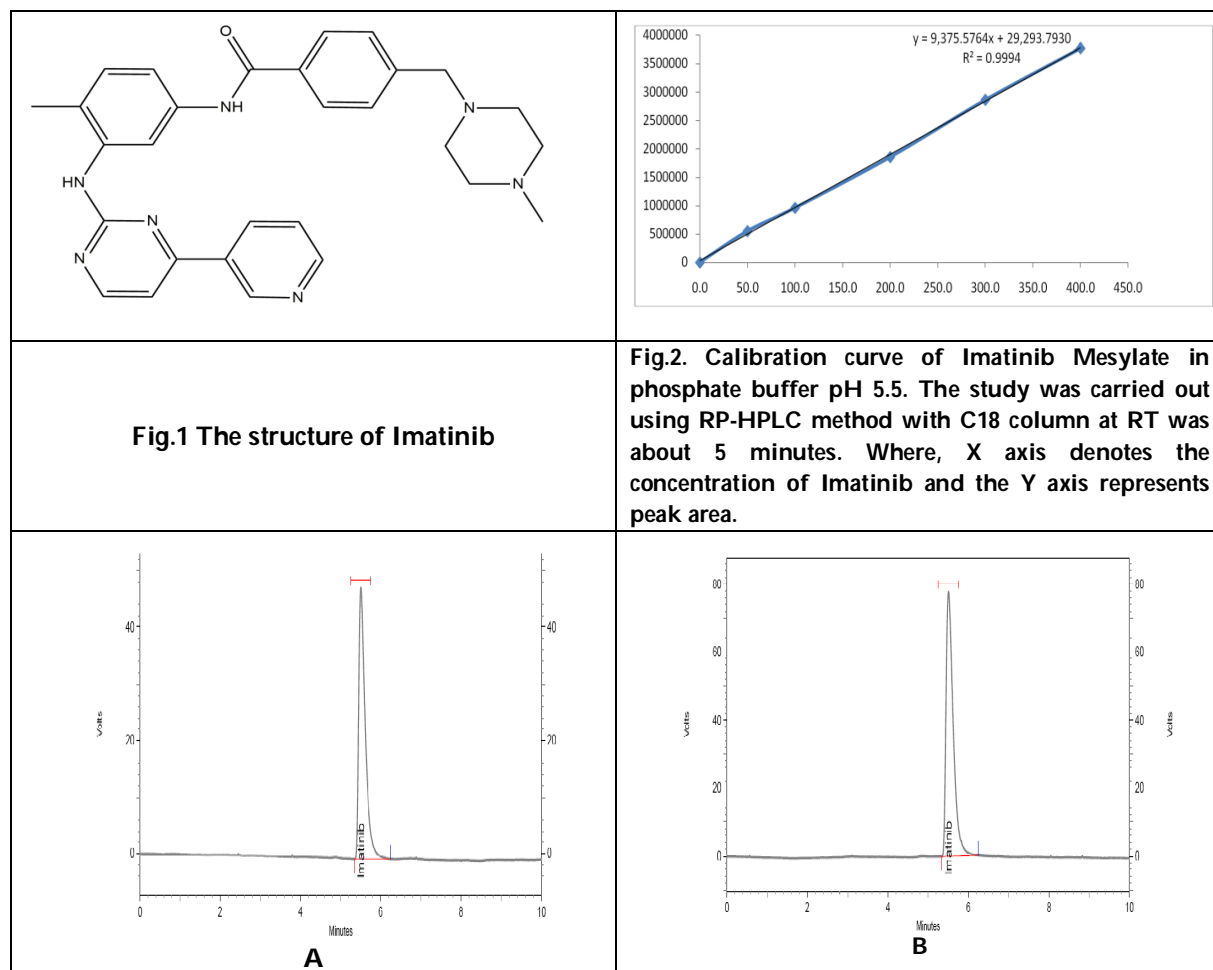




Senthil Kumar et al.

Table 2. Assessing the relative standard deviation of Imatinib Mesylate using RP-HPLC method

Concentration of Imatinib Mesylate (µg/ml)	Retention Time (Minutes)	Peak Area
300	5.589	2239119
300	5.587	2216284
300	5.594	2243058



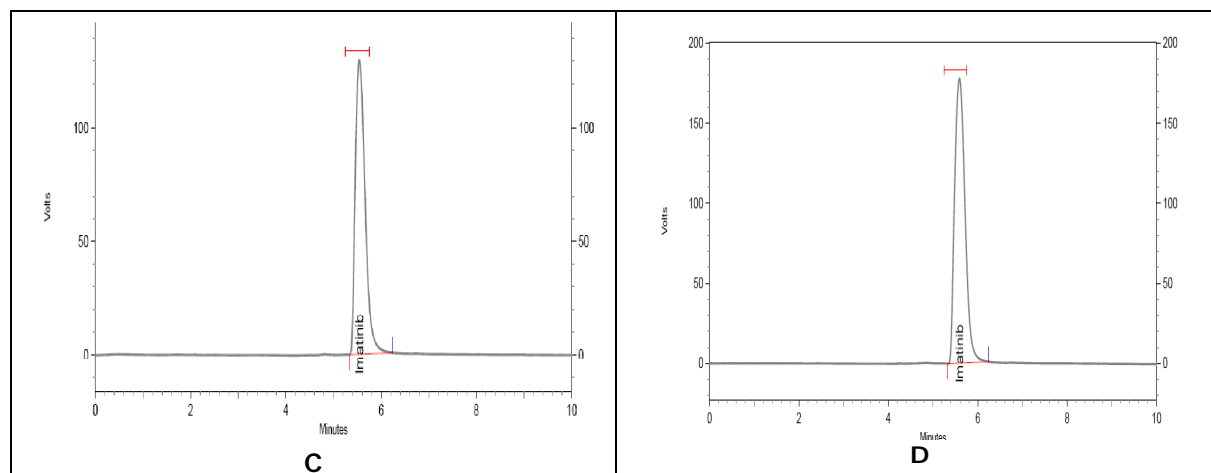
Senthil Kumar *et al.*

Fig.3. RP-HPLC profiles of various concentrations of Imatinib Mesylate. The analysis was carried out using HPLC column with FLOWROSIL PAK C18 MG II 5 μ (250mm x 4.6mm) (Make: Shimadzu, Model: LC 2010 CHT, Japan),packed with porous spherical silica coated with a silicone polymer monolayer with octadecyl (C18) groups. The mobile phase used for the experiment was water: acetonitrile: methanol at the ratio of 300:200:500 and to this 3ml of glacial acetic acid was added. Triethylamine was used to adjust the pH 5.5. The temperature of the column was maintained at 30°C and the flow rate of the column was adjusted to 0.5ml/min. The sample detection was carried out at 265 nm. Where, A, B,C and D represents the RP-HPLC profile of 50, 100, 200 and 400 μ g of Imatinib Mesylate respectively.





Clinical Profile and Outcome of Chronic Kidney Disease in a Tertiary Care Hospital, Salem

Nivetha S R, Balasubramanian Arul* and Ramalingam Kothai

Department of Pharmacy Practice, Vinayaka Mission's College of Pharmacy, Vinayaka Mission's Research Foundation (Deemed to be University), Salem, Tamil Nadu, India.

Received: 08 Sep 2020

Revised: 10 Oct 2020

Accepted: 12 Nov 2020

*Address for Correspondence

Balasubramanian Arul

Department of Pharmacy Practice,
Vinayaka Mission's College of Pharmacy,
Vinayaka Mission's Research Foundation (Deemed to be University),
Salem, Tamil Nadu, India.
Email: arul1971@yahoo.com



This is an Open Access Journal / article distributed under the terms of the **Creative Commons Attribution License** (CC BY-NC-ND 3.0) which permits unrestricted use, distribution, and reproduction in any medium, provided the original work is properly cited. All rights reserved.

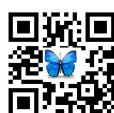
ABSTRACT

Chronic Kidney disease is a term that denotes the failure of the kidney to eliminate the toxins from the body. The main aim of the study is to establish the relationship between the staging of CKD with the duration of stay, co-morbidity conditions and compare the age group with clinical outcomes of CKD in a tertiary care hospital, Salem. Based on the study population, 33 % were female and 67 % were male patients with the average age of 61.66 ± 11.18 yrs. The number of days of hospitalization is increased in patients with ESRD. The major co-morbid condition observed on this study were hypertension and diabetes mellitus. Patients under the age group of 51-70 were observed under all 5 categories of clinical outcome of the CKD patients. ESRD is still prevalent in the patients with diabetes and hypertension being the common cause. Renal replacement therapy/dialysis is recommended.

Keywords: Chronic Kidney Disease, End stage renal disease (ESRD), staging of CKD, clinical outcome.

INTRODUCTION

Chronic renal failure (CRF) or chronic kidney disease (CKD) is defined as a long lasting improper functioning of kidney (or) serum creatinine level increased abnormally for more than 3 months or decreased glomerular filtration rate (GFR) of 60 ml per minute / $1.73m^2$. In United States; nearly 13% of the populations are affected by chronic kidney disease (CKD)[1,2]. The ratio of CKD will rise in elderly population with increasing numbers of patients affected with diabetes and hypertension. When there is increase in numbers of CKD patients, primary care practitioners will be confronted with management of the complex medical problems unique to patients with chronic renal impairment[3]. Chronic kidney disease may leads to severe complications such as drug toxicity, metabolic and



**Nivetha et al.,**

endocrine complications, increased risk for CVD, and several infections, frailty, and cognitive impairment. This may occur at any stage of CKD, leading to death. This can also occur due to adverse effects of interventions to prevent or treat the disease and associated comorbidity [4]. To facilitate assessment of CKD severity and, the National Kidney Foundation developed criteria, as part of its Kidney Disease Outcomes Quality Initiative (NKF KDOQI™), stratify CKD patients:

Stage 1: normal eGFR ≥ 90 mL/min per 1.73 m^2 and persistent albuminuria

Stage 2: eGFR between 60 to 89 mL/min per 1.73 m^2

Stage 3: eGFR between 30 to 59 mL/min per 1.73 m^2

Stage 4: eGFR between 15 to 29 mL/min per 1.73 m^2

Stage 5: eGFR of < 15 mL/min per 1.73 m^2 or end-stage renal disease[5]

Renal failure is typically detected by an elevated serum creatinine level. Problems observed in kidney failure include abnormal fluid levels in the body, increased acid levels, abnormal levels of potassium, calcium, phosphate, and (in the longer term) anemia as well as delayed healing in broken bones[6, 7]. Main risk factors for this CKD include diabetes, hypertension, blockages in the kidney, overuse of painkillers and allergic reactions to antibiotics, inflammation family history of kidney disease, premature birth, age and trauma/accident[6, 8]. CKD has been found to independently increase the risk of hypertension and other cardiovascular diseases, including heart attack, angina, coronary artery disease, stroke and heart failure[9]. Some established risk factors of CVD, such as obesity, abnormal lipid levels and diabetes, are also common among people with CKD. In addition, CKD complications, such as anemia and disturbed mineral metabolism, also contribute to increased risk of CVD[6, 10]. Shared risk factors of these diseases also promote co-occurrence of these diseases and strengthen the association between them[11].

MATERIALS AND METHODS

Study site: The proposed study was conducted at in-patient ward of Vinayaka Mission's Kirupanandha Variyar Medical College, Salem. It is a 560-bedded hospital providing tertiary level multi-super specialty care. It provides specialized services in pathology, microbiology, forensic medicines, community medicine, pediatrics, radiology, anaesthesiology, obstetrics & gynaecology, general medicine, general surgery, orthopedics, ophthalmology, ENT, accident & emergency care. Skin & STD.

Study design: Prospective Studies

Study duration: The study was conducted for a period of Nine months from September 2019 to May 2020.

Study Population: In this study a total of 100 patients were enrolled.

Study criteria: The patients visiting the nephrology in patient departments were enrolled in to the study after taking their consent and by considering following inclusion and exclusion criteria.

Inclusion Criteria

- Age > 30 years
- Patients of either sex
- Patients diagnosed as CKD
- Patients with other co-morbid conditions

Exclusion criteria

- Pregnant women
- Patients who are not diagnosed as CKD



**Nivetha et al.,****Data collection**

The data were collected from the patients who met the inclusion criteria. The relevant data of each patient were collected from the in-patient record. The demographic data (age, sex), the diagnosis by the treating nephrologists was obtained from the in-patient case records of each patient. Also, associated co-morbid conditions, risk factors identified for developing CKD were noted from the medical records. The details of the data collected were transferred into MS Office excel work sheet.

Study procedure

All patients admitted in the ward were reviewed and patients were enquired about their previous history of CKD. Patients with known complaint were interviewed for their past medication history and who met the study criteria were enrolled and their demographic details such as name, age, sex, weight, residential address, date of admission, reasons for admission, history of previous illness, family history, social history were collected. All the above mentioned data is entered in the patient profile form. Patients or their care takers are interviewed for source of treatment given previously.

Analysis of the clinical outcome of the patients with CKD

The clinical outcomes were observed to be fall under five categories. The categories are classified based on the clinical conditions of the patients which are mentioned on the discharge summary of the prescriptions.

Category 1: Requires follow up treatment

Here, the health condition of the patients are improved to greater extent and their eGFR rate were observed to reach the normal range therefore, these category patients requires only follow up treatment.

Category 2: Requires more attention and follow up treatment

Here, the clinical characteristics of the patients improved but does not reach the normal range. Therefore, these patients require more attention and follow up treatment.

Category 3: Undergone dialysis requires follow up treatment

Here, the clinical characteristics of the patients were observed to be very low on admission so these patients have to undergo dialysis. Even after the dialysis treatment their clinical characteristics has improved but does not reach the normal range.

Category 4: Undergone dialysis requires intensive care

In this category, the clinical characteristics of these patients were observed to be very low of admission so they have to undergo dialysis. After dialysis treatment, these patients do not show any improvement in their health condition therefore they require intensive care.

Category 5: Requires hemodialysis support upon discharge

This category of patients were observed to have their clinical characteristics below the normal range even after drug therapy therefore to improve their health condition hemodialysis can be perform.

RESULTS AND DISCUSSION

Gender wise distribution of the study population shows 33 % were female patients and 67 % were male patients. Here, male patients were observed to be more susceptible to CKD. This parameter correlates with the study conducted by PranaviDasari *et al.*, [12] which concludes that, out of their study population, 108 were male, 42 were female patients. The cases were analyzed on staging of CKD and duration of stay. The data were shown in table no.1. Overall patients under stage 3 stayed for nearly 4- 18 days, patients under stage 4 stayed for nearly 4-21 days and

28582



**Nivetha et al.,**

patients under ESRD stayed for 7-30 days. The average number of days of hospitalization was found to be 15.1 ± 6.58 days. These results shows that patients with ESRD were under hospitalization for more number of days when compared with the patients with Stage 3 and Stage 4. Several co morbidities were observed in CKD patients and the list is shown in table no.2. The patients with hypertension and diabetes mellitus were found to be large in number when compared with other co-morbidity conditions. These results are very similar to the study conducted by PranaviDasari *et al.*, [12] which concludes that that patients with hypertension and diabetes mellitus are in large number when compared to other diseases. The cases were analyzed based on the route of administration of the drug. 17.42% of the drugs are administered with intravenous administration and 82.57% of the drugs are administered with oral administration. These results shows that oral administration is the most prescribed route of administration. On the analysis, mode of treatment, 67% of the patients undergone drug therapy and 33% of patients were on dialysis treatment. The patients with dialysis treatment were observed to be less when compared to drug therapy.

The clinical outcome and age range of the CKD patients were analyzed. The data were shown in table 3. Out of this, 1% patient were found to be under the age group of 31-40 falls under the category 1 of the clinical outcome. 13% of patients were under the age group of 41-50, among which 4%, 1%, 3%, 5%, were under the categories of 2, 3, 4, 5. 39% of patients were under the age group of 51-60, among which 4%, 12%, 6%, 6%, 11% were under the categories of 1, 2, 3, 4, 5. 28% of patients were under the age group of 61-70, among which 2%, 12%, 4%, 5%, 5% were under the categories of 1, 2, 3, 4, 5. 12% of patients were under the age group of 71-80, among which 5%, 4%, 2%, 1% were under the categories of 2, 3, 4, 5. 7% of patients were under the age group of 81-90, among which 3%, 2%, 2% were under the categories of 2, 3, 5. Patients under the age group of 51-70 were observed under all 5 categories of clinical outcome of the CKD patients. These results shows that there should be a follow up treatment for all stages of CKD patients and also for the patients with low eGFR rate should be given dialysis. These results do not correlate with the study conducted by Su HooiTeo *et al.*, [13] in which they concluded that patient undergone dialysis are significantly associated with mortality.

CONCLUSION

During the study, male patients were observed to be more susceptible to CKD. With respect to age the patient with age in the range 51-60 are more prone to CKD than other age groups. The patients with ESRD were under hospitalization for more number of days when compared with Stage 3 and Stage 4. The major route of administration was found to be oral route. The patients undergone dialysis treatment were observed to be less when compared to drug therapy. Patients under the age group of 51-70 were observed under all 5 categories of clinical outcome of the CKD patients. In conclusion, the final stage of CKD presenting as ESRD is still prevalent in the patients with diabetes and hypertension being the common cause. Clinical presentation of the patients with CKD shows prognosis of CKD and the survival condition of the patients are highly risk. Therefore, renal replacement therapy/dialysis is recommended. The medical expenses for the renal replacement therapy/dialysis can be afforded and supported by the government, non-government and other health insurance companies.

ACKNOWLEDGEMENT

The authors are thankful to the authorities of Vinayaka Mission's Research Foundation (Deemed to be University), Salem for providing the facilities for carrying out this research.

REFERENCES

1. Coresh J, Selvin E, Stevens LA, Manzi J, Kusek JW, Eggers P, et al. Prevalence of chronic kidney disease in the United States. *JAMA*. 2007 Nov;298(17):2038–47.



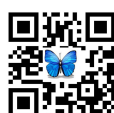


Nivetha et al.,

2. Divya M, Nivetha SR, Mohan L, Arul B, Kothai R. Drug-induced renal disorder-A Mini Review. *Int J Res Pharm Sci.* 2020;11(1):166–72.
3. Thomas R, Kanso A, Sedor JR. Chronic kidney disease and its complications. *Prim Care.* 2008 Jun;35(2):329–vii.
4. KDOQI, Foundation NK. KDOQI Clinical Practice Guidelines and Clinical Practice Recommendations for Anemia in Chronic Kidney Disease. *Am J Kidney Dis.* 2006 May;47(5 Suppl 3):S11-145.
5. Coresh J, Astor BC, Greene T, Eknoyan G, Levey AS. Prevalence of chronic kidney disease and decreased kidney function in the adult US population: Third National Health and Nutrition Examination Survey. *Am J Kidney Dis Off J Natl Kidney Found.* 2003 Jan;41(1):1–12.
6. Karthikeyan B, Sharma RK, Kaul A, Gupta A, Prasad N, Bhadauria DS. Clinical Characteristics, Patient and Technique Survival in Elderly Patients on Peritoneal Dialysis. *Indian J Nephrol.* 2019;29(5):334–9.
7. Li PK-T, Law MC, Chow KM, Leung C-B, Kwan BC-H, Chung KY, et al. Good patient and technique survival in elderly patients on continuous ambulatory peritoneal dialysis. *Perit Dial Int J Int Soc Perit Dial.* 2007 Jun;27 Suppl 2:S196-201.
8. Maitra S, Jassal S V, Shea J, Chu M, Bargman JM. Increased mortality of elderly female peritoneal dialysis patients with diabetes--a descriptive analysis. *Adv Perit Dial.* 2001;17:117–21.
9. Nivetha SR, Arul B, Kothai R. A review on diagnostic approaches and pharmacological regimen of chronic kidney disease. *J Nat Remedies.* 2020;21(4 S1):1–13.
10. Nivetha SR, Arul B, Kothai R. A Prospective Study of Clinical Characteristics of Chronic Kidney Diseases in a Tertiary Care Hospital, Salem. *Int J Pharm Res.* 2020;12(4):2946–50.
11. Sakacı T, Ahabap E, Koc Y, Basturk T, Ucar ZA, Sınangıl A, et al. Clinical outcomes and mortality in elderly peritoneal dialysis patients. *Clinics (Sao Paulo).* 2015/05/01. 2015 May;70(5):363–8.
12. Dasari P, Konuru V, Venisetty RK. Management of comorbidities in chronic kidney disease: A prospective observational study. *Int J Pharm Pharm Sci.* 2014 Mar;6:363–7.
13. Teo SH, Lee K-G, Koniman R, Tng ARK, Liew ZH, Naing TT, et al. A prospective study of clinical characteristics and outcomes of acute kidney injury in a tertiary care Centre. *BMC Nephrol.* 2019 Jul;20(1):282.

Table. 1. Analysis of the cases based on Staging of CKD and duration of stay

S. No	Staging of CKD	Duration of stay (in days)	No. of Patients	Total No. of Patients
1	Stage 3	4-6	2	9
		7-9	5	
		10-12	1	
		16-18	1	
2	Stage 4	4-6	6	27
		7-9	10	
		10-12	4	
		13-15	3	
		16-18	3	
3	ESRD	19-21	1	64
		7-9	2	
		10-12	10	
		13-15	7	
		16-18	14	
		19-21	13	
		22-24	8	
25-27	7			
		28-30	3	
		Grand Total		100





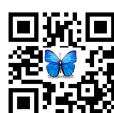
Nivetha et al.,

Table. 2. Analysis of the cases based on the comorbidity condition

S. No	Co- Morbid Conditions	No. of cases
1	HTN	17
2	HTN+ T2DM	32
3	HTN+CAD	14
4	HTN+T2DM+Anemia	3
5	HTN+T2DM+CAD	26
6	HTN+T2DM+COPD	7
7	Endometrial Cancer	1
	Grand Total	100

Table no: 3 Analysis of the clinical outcome of the patients with CKD

S. No	Age range	Clinical outcomes of the patients with CKD	No. of Patients	Total no. of Patients
1	31-40	Category-1 Requires follow up treatment	1	1
2	41-50	Category-2 Requires more attention and follow up treatment	4	13
		Category-3 Undergone dialysis requires follow up treatment	1	
		Category-4 Undergone dialysis requires intensive care	3	
		Category-5 Requires hemodialysis support upon discharge	5	
3	51-60	Category-1 Requires follow up treatment	4	39
		Category-2 Requires more attention and follow up treatment	12	
		Category-3 Undergone dialysis requires follow up treatment	6	
		Category-4 Undergone dialysis requires intensive care	6	
4	61-70	Category-5 Requires hemodialysis support upon discharge	11	28
		Category-1 Requires follow up treatment	2	
		Category-2 Requires more attention and follow up treatment	12	
		Category-3 Undergone dialysis requires follow up treatment	4	
5	71-80	Category-4 Undergone dialysis requires intensive care	5	12
		Category-5 Requires hemodialysis support upon discharge	1	
		Category-2 Requires more attention and follow up treatment	5	
		Category-3 Undergone dialysis requires follow up treatment	4	
6	81-90	Category-4 Undergone dialysis requires intensive care	2	7
		Category-5 Requires hemodialysis support upon discharge	1	
		Category-2 Requires more attention and follow up treatment	3	
		Grand Total		100





An Exploratory Journey from Artificial Intelligence to Augmented Intelligence – A Bird's Eye View of Few Contemporary Technologies

M S Chelva^{1*} and Jitendra Pramanik²

¹Associate Professor, Department of Electronics, Karnatak Arts Sciences and Commerce College, Bidar, Karnataka, India.

²Assistant Professor, Centurion University of Technology and Management, Odisha, India.

Received: 01 Aug 2020

Revised: 03 Sep 2020

Accepted: 05 Oct 2020

*Address for Correspondence

M S Chelva

Associate Professor,
Department of Electronics,
Karnatak Arts Sciences and Commerce College,
Bidar, Karnataka, India
Email : mschelva@gmail.com



This is an Open Access Journal / article distributed under the terms of the **Creative Commons Attribution License** (CC BY-NC-ND 3.0) which permits unrestricted use, distribution, and reproduction in any medium, provided the original work is properly cited. All rights reserved.

ABSTRACT

“AI winter” is over. The dream of intelligent technology-based world is going to become the reality. Multi facet rapid development of artificial intelligence (AI) is going to become the greatest change agent of coming time. Emergence of AI based technologies is sure going to bring out a great change in many dimensions in this world – at least the way we think of solutions to things, anything and everything. AI based innovative new solutions will profoundly change the human society and human life, in a way the entire modern world as a whole. AI is going to be the key change agent of the coming new millennium. This paper presents a review of some key technological breakthroughs that has paved the path from AI to AI, i.e., from artificial intelligence to augmented intelligence, touching machine learning, deep learning and Tens or Flow; the key areas of innovations of current time that has revolutionised the whole world.

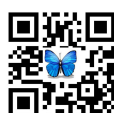
Keywords: Artificial Intelligence; Machine learning; Deep learning; Tens or Flow; Augmented Intelligence

INTRODUCTION

A Brief Historical Background of AI

Although the field of artificial intelligence (AI) has recently gained popularity among technocrats, the reality is AI is not a completely new concept. The idea of AI has been in the thoughts of human beings for centuries. The roots of AI can even be traced back to ancient mythologies. The history of AI is filled with many myths, stories and rumors. In 1956, an American computer and cognitive scientist named John Mc Carthy created the term "artificial intelligence" who was one of the founders of artificial intelligence as an independent discipline. But soon it was realised that

28586



**M S Chelva and Jitendra Pramanik**

achieving intelligence artificially was not so simple. Criticism against AI stopped US and British government to extend support and funding research and development in AI. Interest in the field of AI was dropped; making 1974 to 1980 became a period known as "AI winter." Subsequently, the situation improved and Japanese government started funding AI research which was again stopped by late 80s. AI had to face another major winter from 1987 to 1993 when again the government funding support was reduced.

In 1997, when the Deep Blue program defeated Gary Kasparov who was the world chess champion, it was considered a very big achievement. In 2011, the IBM's huge computer question-answering system (a mega expert system) Watson won the America's Favourite Quiz Show "Jeopardy!" by defeating the leading titleholders Brad Rutter and Ken Jennings. These are all attributed to the success of AI. Improvement in the electronics devices and rise in the availability of high performance modern computers during this time formed the key ingredients for AI's rapid success and development. The field of AI has passed through many ups and down before arriving at the stage what it is today. For the last many decades, human beings have imagined and dreamed of a technology-filled future. It appears, AI will make that dream come true with autonomous transportation, flying vehicles, clean and safe environment and a healthy, extended life. The rapid development of AI will greatly change the human society, lifestyle and change the world. In the subsequent sections of this paper, discussions on various contemporary technologies of AI are presented. Section 2 present a discussion on Machine Learning, Section 3 discusses Deep Learning, Section 4 discusses Tens or Flow, Section 5 discusses IBM Watson, Section 6 discusses Augmented Intelligence, Section 7 discusses Cognitive Security, Section 8 discusses Data Science and Section 9 discusses Data Analytics. Finally, Section 10 presents concluding remarks on the discussion of various AI based contemporary technologies and future perspective.

Machine Learning

The origins of machine learning started in 1950 when Alan Mathison Turing, an English computer scientist, mathematician and philosopher presented the "Turing Test" to demonstrate whether a computer has real intelligence. To pass the test, a computer must be able to fool a human into believing it is also human. In 1952, Arthur Lee Samuel, an American pioneer in the field of computer gaming and AI was the first person to create the term "machine learning" and wrote the first computer learning program. In 1957, Frank Rosenblatt, an American psychologist, was prominent for his contribution in the field of artificial intelligence for being the pioneer in designing the first neural network for computers (the perceptron) that was able to simulate the thought processes of the human brain.

What is Machine Learning?

- Machine Learning is a branch of AI where computer algorithms are used to independently learn from data and information.
- In machine learning, computers do not have to be explicitly programmed but can change and improve their algorithms by themselves.
- There are two types of learning algorithms which are commonly in use are:
 - Supervised Learning Algorithm, and
 - Unsupervised Learning Algorithm
- The third one is a combination of both, i.e., a Semi-supervised Learning Algorithm

Supervised Learning (Fig. – 1)

- Most of the practical machine learning algorithms are supervised learning, i.e., they are teacher based
- In supervised learning, we have some input variables (x) with an output variable (Y) and use an algorithm to learn a function f that maps the inputs to the output, i.e., $Y = f(x)$.



**M S Chelva and Jitendra Pramanik**

- The objective is to closely approximate the function (f) so accurately that by supplying new input data (x), we can predict the output variables (Y) for that data almost exactly.
- As the dataset controls the learning process just as a teacher, this algorithm is termed as supervised algorithm
- When the correct answer is supplied, the algorithm iteratively attempts to make right predictions from the training data. If the predication is incorrect, it is corrected by the teacher. When the algorithm attains an adequate level of performance (in terms of low error level), learning stops.
- Both regression and classification related problems are solved using supervised approach of learning

Unsupervised Learning (Fig. – 2)

- In many practical situations, we have only the input data (x) available without any information regarding the corresponding output for reference. Here we adopt unsupervised learning approach.
- The objective of unsupervised learning is to model the original structure or distribution in the supplied data with the hope to learn more about it.
- This is known as unsupervised learning as there is no source or teacher to supply the correct answer. The algorithm is left on its own to discover and present the interesting structure present in the data.
- Unsupervised learning can be further classified into two categories of problems:
 - Clustering problems and
 - Association problems.
- In clustering type problem, the natural groupings in the data are discovered, such as grouping of customers by their purchasing behavior.
- In association type problems, also known as association rule learning problems, our objective is to discover the rules that describe large portion of the data, such as people those who buy X are also inclined to buy Y

Semi-supervised Learning Algorithm (Fig. – 3)

- This situation arises when we have large amount of input data (X), out of which, few are labelled (Y), making the problem falling in between both supervised and unsupervised learning.
- One of the example of semi-supervised learning problem is an image collection few of them are labelled (e.g. grape, apple, pears) and the majority of the portioned are unlabelled.
- The semi supervised algorithm is mostly suitable for the majority of real world problems.
- This is because it is both time-consuming as well as costly to access to involve a domain expert to label the whole data. On the other hand, it is cheap to leave the data unlabelled and convenient to collect and store.
- In such cases, unsupervised learning method plays an important role to learn and discover the structure prevailing in the input data.
- A better approach, unsupervised learning can be adopted to make best guess prediction for the unlabelled data, and then input that data back into the supervised learning as training data to help the model make predictions on new unknown data.

Application of Machine Learning

Machine learning can be applied in varieties of fields such as

- Computer Vision,
- Speech Recognition,
- NLP,
- Web Search,
- Biotech,
- Risk Management,
- Cyber Security, and
- many others





Deep Learning

Deep learning has become a buzz word of today's world and is probably one of the hottest technical topics nowadays. Deep learning is the secret formula behind many exciting developments. Following subsections will present an overview of what deep learning is. In some sense of analogy, deep learning is nothing but an intellectual reformation of neural networks.

Background

Initially, computer scientist wanted to make machines think, learn and solve real-life problems like human beings. They tried to understand the biological functioning of human brain and identified the role of a key biological component in the brain, known as 'Neuron,' is responsible for the intelligence in accomplishing this. Motivated by this observation, they developed a concept artificial neuron for machines to solve problems. The attribute which differentiate deep learning from neural network is the deep learning uses multiple hidden layers for retrieving information from the data.

Biological Neuron (Fig.4)

Constituents of the biological neuron are

- Dendrite – treated as a link that transports data from outside to the input.
- Nucleus – that performs a mapping of the input information to the output and decides where the output needs to be delivered.
- Axon – a channel that carries the output signals. Axon ending or axon terminal forms the point of connecting to dendrites of other neurons.

Artificial Neuron (Fig.5)

Just like a neuron forms the basic element of the brain, an artificial neuron forms the basic element of the artificial neural network (ANN). The way a neuron generate an output by processing the input information, similarly, the neuron in ANN receive inputs, processes them and produces an output to become either input to other neurons for further processing or itself the final output.

Basic elements of artificial neuron are

- Input – links that convey the inputs to the Node
- Node – that perform the math function on the inputs and send the result on output link
- Output – a link that transports the output

Artificial Neural Network (ANN)(Fig.6)

ANN is the key conceptual element of deep learning. The objective of the ANN is to closely figure out the unknown mapping as a function from input to out. Neurons have weight on their inputs which is assigned on the basis of its relative importance to other inputs, and bias, which is another linear component, basically added to change the range of the weight multiplied input. Since a single neuron would not be able to do complex jobs, therefore, neurons are stacked on layers to perform complex tasks. In the simplest form, an ANN would have an input layer, a hidden layer and an output layer, each layer having multiple neurons, each neuron in a back-end layer being connected to each neuron in the layer in front of it, forming a network called fully connected network. ANN is the basic building block of machine learning. Deep learning has been around in history for a long time, which was helping machines to learn and solve problems. Non-availability of high performance computing infrastructure was the biggest hurdle in achieving desired performance of deep learning algorithm and was considered to be unusable on those days and thus was unpopular and remained in darkness for a long time. Availability of modern computing infrastructure and recent breakthrough in research has helped deep learning overcome most of the obstacles it had faced.





Application of Deep Learning

1. Deep learning algorithms are being used to object detection, and complex pattern recognition, adopt strategies for real time application
2. Asset managers are using deep learning to look for creditor's credibility from multiple data sources that are highly unstructured where regular statistical models fails to figure out credibility.
3. Fin Tech is extensively using deep learning for various predictive analyses.

Tens or Flow

In recent years, Tens or Flow has evolved as one of the best libraries developed by the Google Brain Trust as a powerful tool to integrate machine learning and deep learning into any production systems in variety of fields, including speech recognition, computer vision, robotics, information retrieval, natural language processing, geographic information extraction, etc. Following subsections will present an overview on what Tens or Flow is, its application, scope and future.

What is Tens or Flow?

- Tens or Flow is an API Library created by Google Brain for creating Deep Learning models.
- Deep Learning is a type of machine learning models that use multi-layer neural networks.
- Tens or Flow provides simple Python API to define a computational graph.
- Computational graph, such as back propagation ANN, comprising of nodes and edges, representing computations and connections between those computations respectively can be defined using Tens or Flow with flexibility.
- Tens or Flow API library helps in creating data graph flows for deep learning neural network model, where the graph consists of two units – a tensor and a node.
 - Tensor: A tensor is any multidimensional array.
 - Node: A node is a mathematical computation that is being worked at the moment.
- A data flow graph fundamentally maps the flow of information via the junctions between these two components. Once this graph is done, the model is executed and the output is computed.

Application of Tens or Flow

- Voice/Sound Recognition – a popular application that uses of Tens or Flow are the Sound and Voice related applications.
 - Voice recognition – mostly used in Io T, Automotive, Security and UX/UI (User Experience/ User Interface)
 - Voice search – mostly used in Telecoms, and Handset Manufacturers
 - Sentiment Analysis – mostly used in CRM (Customer Relationship Management)
 - Flaw Detection (engine noise) – mostly used in Automotive and Aviation

Augmented Intelligence

IBM demands to use AI for Augmented Intelligence (AI), rather than Artificial Intelligence (not AI). Augmented intelligence is an alternative form of artificial intelligence. We can think Augmented Intelligence as a reincarnation of Artificial Intelligence, a new conceptualization of Artificial Intelligence. AI in its new role is intended to assist human beings to boost their intelligence, but no way to replace human intelligence. For example, a traditional expert system, built on Artificial Intelligence is targeted to replace human intelligence. The word 'augmented' in AI, which means "to improve", emphasizes the role the human intelligence plays using machine learning and deep learning algorithms in various problem solving and prediction events.

Background

We're living in a world where technological evolution has outpaced that of human beings. Technological evolution is undergoing exponentially growth. Artificial Intelligence is empowering machines to exhibit intelligence in their





working. Now Artificial Intelligence is changing to Augmented Intelligence to help people to acquire world's best expertise available within short time. The fundamental difference between Artificial Intelligence and Augmented Intelligence lies in the fact how we apply the technology. In fact, augmented intelligence is an umbrella-term that covers concepts from many correlated domains. IBM has been research on AI technology for since more than last 50 years. In 2011, IBM's involvement came to limelight through success in Jeopardy! At IBM, the term "augmented intelligence" is used rather than "artificial intelligence" signifying attempt to enhance human expertise rather than replicate human intelligence. IBM calls their augmented intelligence approach as "cognitive computing." Few noteworthy areas of Augmented Intelligence by IBM includes: healthcare, social services, education, financial services, transportation, public safety, the environment, infrastructure, etc.

What is Augmented Intelligence?

Augmented intelligence is a combination of three key conceptual elements producing a result better than the composition of the components. The three components being:

1. machine learning,
2. human creation and
3. human intuition from meaningful user experience

IBM says augmented intelligence is a system that enhance human capabilities rather than a traditional artificial intelligence based systems that wants to reproduce the human intelligence.

Application of Augmented Intelligence

Augmented Intelligence has many real-life applications; few of which are cited below:

- **Speech Recognition:** Augmented intelligence in real life applications allows us to make use of images and video to recognize speech and interpret text.
- **Airline** – If a flight is delayed and the passenger id going to miss your connection, IBM Watson can help the flight attendants know which passengers are going to miss the connection and then send message to the passengers guiding where to go after landing with choices of next connections, thereby minimizing the time to run to the airport check-in desks and the luggage conveyer, making travel simpler and pleasurable.
- **Healthcare** – With IBM Watson, doctors can decide to attend the patient in traumatic care unit who is at the most serious state, suffering from terminal illness like cancer, leaving the rest of the patients under the control of a nurse. At the same time, Watson
- **Insurance** – Based on the person's driving habits, Watson can simplify the complexity in determining the premium amount and premium term (monthly or annually).

Future of Augmented Intelligence

Major players of Augmented Intelligence in future will Google, Amazon and IBM. The key dominating areas where Augmented Intelligence will find application are:

- Use of Augmented Intelligence for public benefits,
- Augmented Intelligence for social and economic applications,
- Emphasizing Augmented Intelligence in various streams of education to promote the technology,
- Addressing fundamental research gaps in Augmented Intelligence through research, and
- Multi-disciplinary research on Augmented Intelligence

CONCLUSION

In this paper, attempt has been made to present the study of multifarious application of artificial intelligence base tools and techniques in variety of fields and form. Although artificial intelligence has passed through a lot of ups and downs in its path of journey to the point what it is today, the future horizon of applications of artificial intelligence






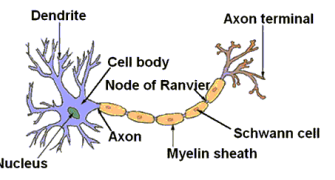
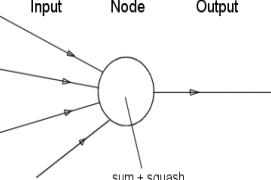
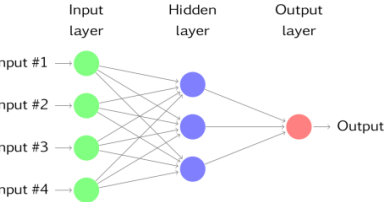


M S Chelva and Jitendra Pramanik

appears to be extremely vital for the benefit of humankind. A time will come when every application of technology in day-to-day life to mission-critical situations will incorporate artificial intelligence. This paper presents seven key tools, techniques and applications of artificial intelligence.

REFERENCES

1. Supervised and Unsupervised Machine Learning Algorithms, <https://machinelearningmastery.com/supervised-and-unsupervised-machine-learning-algorithms/>
2. Deep Learning for layman, <http://shakthydoss.com/technical/deep-learning-for-layman/>
3. Deep learning and neural networks, <https://theconversation.com/deep-learning-and-neural-networks-77259>
4. What is the difference between Data Science, Data Analysis, Big Data, Data Analytics, Data Mining and Machine Learning?, <https://onthe.io/learn/en/category/analytic/What-is-the-difference-between-Data-Science,-Data-Analysis,-Big-Data,-Data-Analytics,-Data-Mining-and-Machine-Learning%3F>
5. Why AI must be redefined as 'augmented intelligence', <https://venturebeat.com/2017/01/09/why-ai-must-be-redefined-as-augmented-intelligence/>
6. Augmented Intelligence: Response to - Request for Information, <http://research.ibm.com/cognitive-computing/ostp/rfi-response.shtml>
7. Cognitive security, <https://www-03.ibm.com/security/ca-en/cognitive/>
8. Connecting to the Future With Cognitive Security, <https://securityintelligence.com/connecting-to-the-future-with-cognitive-security/>
9. Why AI must be redefined as 'augmented intelligence', <https://venturebeat.com/2017/01/09/why-ai-must-be-redefined-as-augmented-intelligence/>

		
Figure 1. Supervised Learning	Figure 2. Unsupervised Learning	Figure 3. Semi-supervised Learning Algorithm
		
Figure 4. Biological Neuron	Figure 5. Artificial Neuron	Figure 5. Artificial Neural Network (ANN)





Acute and Subacute Toxicity Studies of Ethanolic Extract of Leaves of *Dichrostachys cinerea* Wight & Arn

R. Kothai¹, B. Arul^{1*} and E. Manivannan²

¹Department of Pharmacy Practice, Vinayaka Mission's College of Pharmacy, Vinayaka Mission's Research Foundation (Deemed to be University), Salem, Tamil Nadu, India.

²Department of Pharmacology, Vinayaka Mission's Kirupanandha Variyar Medical College and Hospitals, Vinayaka Mission's Research Foundation (Deemed to be University), Salem, Tamil Nadu, India.

Received: 07 Sep 2020

Revised: 09 Oct 2020

Accepted: 11 Nov 2020

*Address for Correspondence

B. Arul

Department of Pharmacy Practice, Vinayaka Mission's College of Pharmacy,
Vinayaka Mission's Research Foundation (Deemed to be University),
Salem, Tamil Nadu, India.
Email : arul1971@yahoo.com



This is an Open Access Journal / article distributed under the terms of the **Creative Commons Attribution License** (CC BY-NC-ND 3.0) which permits unrestricted use, distribution, and reproduction in any medium, provided the original work is properly cited. All rights reserved.

ABSTRACT

Dichrostachys cinerea Wight & Arn is a fast-growing, semi-deciduous tree commonly called the sickle bush. Traditionally, the plant possesses a wide spectrum of medicinal properties. The leaves, bark, and roots are used in the treatment of toothaches, elephantiasis, snakebites and scorpion stings, leprosy, dysentery, headaches, coughs, epilepsy, gonorrhoea, boils, and sore eyes. The present study was carried out to evaluate the safety of an ethanolic extract of leaves of *Dichrostachys cinerea*. The acute and subacute toxicity studies were performed as per OECD guidelines (Organisation for Economic Co-operation and Development) – Guidelines 423 and 407. For the acute toxicity study, the female mice were treated with a single oral dose of ethanolic extracts of leaves of *Dichrostachys cinerea* at 5, 50, 300 & 2000 mg /kg and observed for general toxicity and mortality for 14 days. In subacute studies, both male and female rats were treated with 100, 200 & 400 mg/kg orally for 28 days continuously. The animals were observed weekly for any changes in general behaviour, body weights, food intake, water intake, and signs of morbidity and mortality. The results of the present study demonstrated that the oral administration of this extract does not show any toxicity in both acute and subacute toxicity studies. Hence, it was concluded that the ethanolic extracts of leaves of *Dichrostachys cinerea* were safer and non-toxic to rats and further chronic studies are required to confirm its therapeutic efficacy in animals and humans.

Keywords: *Dichrostachys cinerea*, Acute toxicity, Sub-acute toxicity, Bio-chemical parameters, Haematological parameters.





INTRODUCTION

Plants play an important role in the development of new drugs. The use of plants based drugs for curing various ailments is as old as human civilization and is used in all cultures throughout history. The primitive man started to distinguish between useful and harmful are poisonous plants by trial and error. Natural products continue to play an important role in drug discovery programs of the pharmaceutical industry and other research organizations [1,2]. Many studies report that numerous active molecules were derived from plant products. Due to their diverse medicinal properties, it has created the belief that all plant products are safe [3]. Hence, a systematic study of medicinal plants for potential toxicity is a necessary step for the evaluation of their therapeutic effect. In this connection, many toxicological studies were conducted to evaluate the toxicity of medicinal plants and their products. *Dichrostachys cinerea* Wight & Arn is a fast-growing, semi-deciduous tree commonly called sickle bush that belongs to the family of Fabaceae. It is a natural multi-purpose tree, providing food, medicines, fuel, and various products and one among the most traditional medicinal plants of tropical countries. It is a much-branched thorny small tree, bark light-colored, Leaves are 2- pinnate, sometimes with red hairlets, especially near the base of pinnae and stipules 4-5 mm long. Flowers numerous, crowded in dense axillary, the lower red calyx 0.8mm long, corolla 2-2.5 mm long stamens of the perfect flower in the upper half of the spike yellow. Pods are glabrous, flat, subarticulated, dark brown, twisted up when ripe. Seeds are biconvex, elliptic to subcircular, having 6-10 seeds. Traditionally, the plant posses a wide spectrum of medicinal properties. the leaves, bark, and roots are used in the treatment of toothaches, elephantiasis, snakebites and scorpion stings, leprosy, dysentery, headaches, coughs, epilepsy, gonorrhoea, boils, and sore eyes. It can also be used as a contraceptive for women, as a laxative, and for massage of fractures. Currently, the plant has been reported for its antimicrobial [4-11], hepatoprotective [12], antiurolihiatic [13,14], analgesic & anti-pyretic [15-18], antihyperglycemic [19], antimalarial [20], antioxidant [21], anticonvulsant [22], antiviral & antispasmodic activities [23]. Despite these studies and the widespread use of this plant in traditional medicine, no works on the toxicological profile of extract from leaves have been reported. Thus, this study aims to evaluate the toxicological profile of the ethanolic extract of leaves of *Dichrostachys cinerea*.

MATERIALS AND METHODS

Plant material

The leaves of the plant, *Dichrostachys cinerea* was collected from the foothill of Yercaud, Salem, and from the tribal medical shops.in the month of October 2019. The collected plants (leaves) were identified and authenticated by the Botanical Survey of India, Tamilnadu, Agri University, Coimbatore, Tamilnadu. The herbarium specimen of the plant (AKDC-1) was maintained in the college museum. The plant parts were shade dried at room temperature for 10 days and coarsely powdered and passed through sieve No.60.

Preparation of extracts

About 500 g of dried leaves were coarsely powdered and subjected to continuous hot percolation with different solvents of increasing order of polarity such as pet ether, chloroform, acetone, ethanol, and aqueous [24,25]. The extracts were dried under the rotary evaporator and then tested for various phytochemical constituents like alkaloids, flavonoids, glycosides, phenols, saponins, sterols, tannins, proteins, and carbohydrates.

Animals

Healthy adult female Swiss albino mice and Wistar rats were used for the acute and subacute toxicity studies respectively. The animals were procured from CPCSEA listed suppliers of Sri venkateshwara Enterprises, Bangalore, India. Animals should be nulliparous and non-pregnant. The animals were kept in well-ventilated polypropylene cages at 12h light and 12 h dark schedule at 25°C and 55–65% humidity levels. The rats had been given a normal diet of pellets and free access to water. Each animal, at the commencement of the experiment, should be between 8 and 12 weeks old.





Preparation of animal

Healthy animals were randomly selected for the study and kept in their cages for at least 1 week prior to dosing to allow for acclimatization to the laboratory conditions. Before each test, the animals were fasted for at least 12h; the experimental protocols were subjected to the scrutiny of the Institutional Animals Ethical Committee (P.ceu/25/2019/IAEC/VMCP) and were cleared by the same. All experiments were performed during the morning according to CPCSEA guidelines for the care of laboratory animals and the ethical guideline for investigations of experimental pain in conscious animals. The standard orogastric cannula was used for oral drug administration in experimental animals.

Toxicity Studies

Acute and subacute toxicity studies were performed as per OECD (Organisation for Economic Co-operation and Development) – Guidelines 423 and 407 [26-28].

Acute oral toxicity studies

The acute toxicity studies were performed as per OECD guidelines 423. A total of 12 mice weighing between 25-30g were randomly divided into four groups of 3 mice each. Animals were fasted prior to dosing (food but not water was withheld over-night). Following the period of fasting, the bodyweight of the animals was measured and the ethanolic extract of leaves of *Dichrostachys cinerea* was administered orally to each group at single doses of 5, 50, 300, and 2000 mg/kg, respectively. The control groups received the same volume of distilled water. All the animals were individually observed periodically during the first 24h after administering the extracts and then once a day for 14 days. All the animals were then allowed free access to food and water and observed for signs of acute toxicity. It includes changes in body weight, food and water intake, skin and fur, eyes and mucous membranes, respiratory and circulatory systems, autonomic and central nervous systems, somatomotor activity, and behavior pattern. The number of deaths within this period was recorded. The urine analysis was performed to investigate any abnormalities in the excretion pattern after the exposure to the test drug for 14 days.

Subacute toxicity studies

The subacute toxicity studies were performed as per OECD guidelines 407. Rats weighing between 150-170g were divided into 3 groups of 10 rats each (5 male+ 5 female). All the animals were fasted over-night and after fasting, the bodyweight of the animals was measured. The ethanolic extract of leaves of *Dichrostachys cinerea* (ELDC) at the doses of 100, 200 and 400 mg/kg was administered orally to each group respectively. The control groups were treated with the same volume of distilled water. All the animals were individually observed periodically during the first 24h after administering the extracts and then once a day for 28 days. During the 28 days study, the body weights of all groups were measured once a week. Animals were also visually observed for mortality, changes in behavioural patterns, changes in physical appearance, and symptoms of illness.

Body weight

The individual weights of animals were determined shortly before the test substance was administered and at least weekly thereafter. Weight changes were calculated and recorded. At the end of the test surviving animals were again weighed.

Food and water intake

The food and water intake of each animal of both control and test groups was measured once per week throughout the study.

Urine analysis

The urine analysis was performed to investigate any abnormalities in the excretion pattern after the exposure with the test drug for 28 days.



**Kothai et al.**

On the 28th day, the animals were anesthetized with ether and the blood samples were collected by cardiac puncture for hematological and biochemical studies. After euthanasia, all the animals were sacrificed and the vital organs were removed. The weight of the organs was measured and subjected to necropsy and histopathological examination.

Statistical Analysis

The results were expressed as the mean \pm SEM and analyzed statistically by one-way ANOVA followed by Dunnett's t-test by using SPSS version 16. $P < 0.05$ compared to control was considered to be statistically significant.

RESULTS AND DISCUSSION

The purpose of this research is to give scientific validation to the plants by collect and extract plant materials and then to screen them for potential phytochemical and Toxicological aspects. several pharmacological studies have been reported with the leaves of this plant. But, there is no experimental evidence on its toxicity studies. Hence, the current research work focused on the evaluation of phytochemical and toxic effects of ethanolic extracts of leaves of *Dichrostachys cinerea*.

Phytochemical screening

The leaves of the plant *Dichrostachys cinerea* was collected from the foothill of Yercaud, Salem. The collected plants were identified and authenticated by a botanist. The leaves were shade dried at room temperature and coarsely powdered. The active principles present in the leaves were extracted by a continuous hot percolation method using various solvents and aqueous extract by cold maceration method. The active principles were identified by chemical tests, which showed the presence of various active principles such as Alkaloids, carbohydrates, gums and mucilages, phenolic compounds, proteins, and amino acids, flavonoids, phytosterols, tannins, and saponins.

Acute toxicity studies

Acute toxicity studies are performed to determine the short-term adverse effects of the drug when administered in a single dose orally. It also indicates the safety of the drug in-vivo. Acute toxicity study is generally carried out for the determination of LD50 value in experimental animals. The LD50 determination was done in mice as per OECD guidelines 423 and LD50 of the ethanolic extracts of leaves of *Dichrostachys cinerea* was found to be 2000 mg/kg and the ED50 values were 200 mg/kg, respectively.

Subacute toxicity studies

During the 28days study, there were no significant changes in the body weight, food, and water intake in all test groups animals were observed when compared to the control group. The body weight and daily food and water intake were not altered by the treatment with the test drug at various dose levels (low, medium, and high). The consequence of urine analysis does not show any abnormalities in the excretion pattern. The organs isolated from various groups did not reveal any abnormalities on gross examination. The weights of the important organs were listed in Table No.1 No statistically significant differences were observed in the weight of the liver, kidney, and heart, of all test groups when compared to the control group. At the end of the study period, no statistically significant differences were seen in the mean haemoglobin content, WBC, RBC, and differential cell counts of all test groups, when compared to the control group, as shown in Table No.2. At the end of the study period, no statistically significant differences were seen in the mean biochemical parameters were depicted in Table No.3. The histopathological studies with liver, stomach, spleen, kidney, heart, and lungs did not reveal any pathological changes and they were found to be normal as shown in Fig no.1-6. There were no significant changes in any liver function parameters, such as SGOT, SGPT, and ALP compared to the control. The normal levels of blood urea and serum creatinine indicate that the extracts did not interfere with renal function and that renal integrity was preserved [29]. Several researchers have reported that plant drugs are safe and effective in the treatment of incurable diseases



**Kothai et al.**

[30]. The present findings suggest that the tested extracts are non-toxic since no marked changes in hematological, biochemical, and histopathological parameters were observed.

DISCUSSION

Natural products play a major role in medicine because of their minimal side effects. Despite these, there is still a lack of scientific validation regarding the toxicological aspects of natural compounds. Hence, Scientific knowledge of toxicity studies is much needed. This will help us to identify the safe dose levels of the drug and also the therapeutic index of drugs [31]. In the present study, phytochemical screening of the ethanolic extracts of leaves of *Dichrostachys cinerea* showed the presence of various active principles such as Alkaloids, carbohydrates, gums, and mucilages, phenolic compounds, proteins, and amino acids, flavonoids, phytosterols, tannins, and saponins.

In acute toxicity studies, the animals showed no significant changes in behavior, breathing, cutaneous effects, sensory nervous system responses, or gastrointestinal effects during the observation period. No mortality or any toxic reaction was recorded in any of the four groups. Hence, it was safe up to 2000mg/kg. In subacute toxicity studies, the treatment of ELDC showed no significant changes in the weight of the body and organs. All the animals showed a gradual rise in body weight without much difference between both control and ELDC treated groups. The hematological parameters showed that the extract was not toxic to RBC and not altered its production and platelets. The hemopoietic pathway is one of the most vulnerable sites for toxic compounds and is a major physiological and pathological status measure in humans and animals [32]. Similarly, no changes were observed with WBC count and other factors. In addition, most of the biochemical parameters were not also altered by the ELDC treatment. It maintained the normal levels of liver enzymes, glucose, creatinine levels, which indicates the normal functioning of the liver and kidney. Thus, it also indicates that 28days of treatment does not alter the physiology of the liver, kidney, and metabolism of animals. The above results were further confirmed by the histopathological studies of the vital organs.

CONCLUSION

In conclusion, the oral administration of ethanolic extracts of leaves of *Dichrostachys cinerea* at the doses of 5,50, 300, 2000 mg/kg for a period of 14 days did not produce any short-term toxicological effects. Further, the oral administration of ELDC at the doses of 100, 200, and 400 mg/kg for a period of 28 days was found to be safe in both male and female rats. It didn't show any severe ELDC treatment-related toxicity. In the future, detailed chronic studies are essential to confirm the safety of this plant.

ACKNOWLEDGEMENT

The authors are thankful to the authorities of Vinayaka Mission's Research Foundation (Deemed to be University), Salem for providing the facilities for carrying out this research.

REFERENCES

1. Pal SK, Shukla Y. Herbal medicine: current status and the future. Asian Pac J Cancer Prev. 2003;4(4): 281-8.
2. J.B.Hudson. Plant Photosensitizes with antiviral properties. Antiviral Research.1989; 12: 55- 74.
3. Oliveira, A.K.M., Oliveira, N.A., Resende, U.M., Martins, P.F.R.B. Ethnobotany and traditional medicine of the inhabitants of the Pantanal Negro sub-region and the raizeiros of Miranda and Aquidauna, Mato Grosso do Sul, Brazil. Braz.J. Biol.2011; 71: 176–179.





Kothai et al.

4. Kolapo, A. L., Okunade, M. B., Adejumobi, J. A., & Ogundiya, M. O. In vitro antimicrobial activity and phytochemical composition of *Dichrostachys cinerea*. *Medicinal and Aromatic Plant Science and Biotechnology*.2008;2(2):131-133.
5. Jayakumari, S., & Rao, G. S. Antimicrobial activities of bark and root of *Dichrostachys cinerea* Linn. *Hamdard Medicus*.2009; 52(3): 34-36.
6. Bansa, A, Adeyemo, & S O. Evaluation of antibacterial properties of tannins isolated from *Dichrostachys cinerea*. *African Journal of Biotechnology*.2007;6(15): 1785–1787.
7. Neondo, J. O., Mbithe, C. M., Njenga, P. K., & Muthuri, C. W. Phytochemical characterization, antibacterial screening and toxicity evaluation of *Dichrostachys cinerea*. *Int J Med Plant Res*.2012; 1: 32-7.
8. Mudzengi, C. P., Murwira, A., Tivapasi, M., Murungweni, C., Burumu, J. V., & Halimani, T. Antibacterial activity of aqueous and methanol extracts of selected species used in livestock health management. *Pharmaceutical biology*.2017; 55(1): 1054-1060.
9. Shandukani, P. D., Tshidino, S. C., Masoko, P., & Moganedi, K. M. Antibacterial activity and in situ efficacy of *Bidens pilosa* Linn and *Dichrostachys cinerea* Wight and Arn extracts against common diarrhoea-causing waterborne bacteria. *BMC complementary and alternative medicine*.2018; 18(1), 171.
10. Eisa, M. M., Almagboul, A. Z., Omer, M. E. A., & Elegami, A. A. Antibacterial activity of *Dichrostachys cinerea*. *Fitoterapia*.2000; 71(3): 324-327.
11. Shandukani, P. D., Tshidino, S. C., Masoko, P., & Moganedi, K. M. Antibacterial activity and in situ efficacy of *Bidens pilosa* Linn and *Dichrostachys cinerea* Wight and Arn extracts against common diarrhoea-causing waterborne bacteria. *BMC complementary and alternative medicine*.2018; 18(1): 171.
12. Babu, P. S., Krishna, V., Maruthi, K. R., Shankarmurthy, K., & Babu, R. K. Evaluation of acute toxicity and hepatoprotective activity of the methanolic extract of *Dichrostachys cinerea* (Wight and Arn.) leaves. *Pharmacognosy research*.2011;3(1): 40.
13. Jayakumari, S., Anbu, J., & Ravichandran, V. Antiulcerogenic activity of *Dichrostachys cinerea* (L.) Wight & Arn root extract. *Journal of Pharmacy Research*. 2011;4 (4): 1206-1208.
14. Lakshmi, T., & Devaraj, E. Antiulcerogenic activity of phytochemical extracts: A review. *Journal of Advanced Pharmacy Education & Research* .2017; 7(3):200-203.
15. AbouZeid, A. H., Hifnawy, M. S., Mohammed, R. S., & Sleem, A. A. Lipoidal Contents, Analgesic and Antipyretic Activities of the Aerial Parts of *Dichrostachys cinerea* L. *Journal of Herbs, Spices & Medicinal Plants*.2015; 21(2):118-128.
16. Agbonlahor, O., Godswill, N., & Ozolua, R. Analgesic and anti-inflammatory effects of the aqueous leaf extract of *Dichrostachys cinerea*. *Journal of Applied Sciences and Environmental Management*.2017; 21(5): 821-825.
17. Aworet Samseny, R. R., Kiessoun, K., Sophie, A. A., Madingou, N. K., & Datte, J. Y. *Dichrostachys cinerea* (Wight and Arn., Mimosaceae) potential on anti-inflammatory activity and protection, in anaphylactic in conscious guinea-pig. *Int J Pharmacogn Phytochem*.2011; 29: 1189-94.
18. Susithra, E., & Jayakumari, S. Analgesic and anti-inflammatory activities of *Dichrostachys cinerea* (L.) Wight and Arn. *Drug Invention Today*.2018;10(3).361-66
19. Bolleddu, R., Venkatesh, S., Hazra, K., Rao, M. M., & Shyamsunder, R. Anatomical and antihyperglycemic activity of *Dichrostachys cinerea* roots. *Medical Journal of Dr. DY Patil Vidyapeeth*.2020; 13(3): 258.
20. Kweyamba, P. A., Zofou, D., Efang, N., Assob, J. C. N., Kitau, J., & Nyindo, M. In vitro and in vivo studies on anti-malarial activity of *Commiphora africana* and *Dichrostachys cinerea* used by the Maasai in Arusha region, Tanzania. *Malaria journal*.2019;18(1): 119.
21. Bolleddu, R., Venkatesh, S., Rao, M. M., & Shyamsunder, R. Investigation of the pharmacognostical, phytochemical, and antioxidant studies of various fractions of *Dichrostachys cinerea* root. *Journal of Nature and Science of Medicine*.2019;2(3): 141
22. Abou AH, Hifnawy MS, Mohammed RS, & Amany A. Sleem. (2014). Volatiles Constituents and Anticonvulsant Activity of the Aerial Parts of *Dichrostachys cinerea* L. *Scientific Journal of October 6 University*.2014; 2(2): 196-200.





Kothai et al.

23. El-Sharawy, R. T., Elkhateeb, A., Marzouk, M. M., Abd El-Latif, R. R., Abdelrazig, S. E., & El-Ansari, M. A. (2017). Antiviral and antiparasitic activities of clovamide: the major constituent of *Dichrostachys cinerea* (L.) Wight and Arn. *Journal of Applied Pharmaceutical Science*.2017; 7(9): 219-223.
24. Arul B, Kothai R, Sureshkumar K, Christina AJM. Anti-Inflammatory Activity of *Coldenia procumbens* Linn. *Pak J Pharm Sci [Internet]*. 2005;18(3):17–20.
25. Arul B, Kothai R, Jacob P, Sangameswaran K, Sureshkumar K. Anti-inflammatory activity of *Sapindus trifoliatus* Linn. *J Herb Pharmacother*. 2004;4(4):43–50.
26. OECD. OECD guideline for testing of Animals. 2008. 2 p.
27. OECD. Test No. 407: Repeated Dose 28-day Oral Toxicity Study in Rodents [Internet]. 2008. 13 p.
28. Manivannan. E., Kothai. R., Arul. B. Acute and subacute (28-Day) toxicity assessment of Ethanol extract of seeds of *Asteracanthalongifolia* Nees (Linn). *International Journal of Pharmaceutical Research*. 2020; (12)4: 2936-40.
29. Diallo A, Eklu-Gadegkeku K, Agbonon A, Akilokou K, Creppy EE, Gbeassor M. Acute and sub-chronic (28-day) oral toxicity studies of hydroalcohol leaf extract of *Ageratum conyzoides* L (Asteraceae). *Trop J Pharm Res* 2010; 9(5): 463-7.
30. G M Mohana Rao, Venkateswararao, A K S Rawat, P Pushpangadan, A Shirwaikar. Antioxidant and antihepatotoxic activities of *Hemidesmus indicus* R. Br., *ActaPharmacTurc*, 2005; 47, 73-78.
31. Adaramoye OA, Osaimoje DO, Akinsanya AM, Nnejicm, Fafunso MA, Ademowo OG. Changes in antioxidant status and biochemical indices after acute administration of artemether, artemether-lumefantrine and halofantrine in rats. *Basic Clin Pharmacol Toxicol* 2008; 102(4): 412-8.
32. Diallo A, Eklu-Gadegkeku K, Agbonon A, Aklikokou K, Creppy EE, Gbeassor M. Acute and subchronic (28-day) oral toxicity studies of hydroalcoholic extract of *Lanneakerstingii* Engl. and K. Krause (Anacardiaceae) stem bark. *J Pharmacol Toxicol* 2010; 5(7): 343-9.

Table No.1. Weight of isolated organs of rats after 28 days exposure to test and control groups

S.No	Group	Treatment	Dose mg/kg	Liver (g)	Kidney (g)	Heart (g)
1	I	Control	-	7.300±0.052	1.100±0.037	0.555±0.006
2	II	ELDC	100	7.320±0.093 ^{ns}	0.992±0.035 ^{ns}	0.558±0.004 ^{ns}
3	III	ELDC	200	7.217±0.048 ^{ns}	1.020±0.009 ^{ns}	0.588±0.006 ^{ns}
4	IV	ELDC	400	7.267±0.049 ^{ns}	1.027±0.006 ^{ns}	0.602±0.006 ^{ns}

Values were expressed as Mean ± SEM of 6 rats in each group. The differences in mean weight of organs in extract treated groups were not significantly different from control group at the end of study (28 days).

Table no. 2. Effect of ethanolic extracts of leaves of *Dichrostachys cinerea* on haematological parameters in sub-acute toxicity studies.

Group	Treatment	Dose mg/kg	Hb (g/dl)	RBC (million/mm ³)	WBC (1000/mm ³)	Differential count				
						Neutrophils %	Eosinophils %	Basophils %	Lymphocytes %	Monocytes %
I	Control	-	13.17±0.31	9.32±0.21	10.33±0.50	26.33±0.33	2.73±0.08	0.17±0.005	76.33±0.49	2.67±0.21
II	ELDC	100	14.00±0.37 ^{ns}	8.73±0.39 ^{ns}	9.33±0.42 ^{ns}	25.00±0.26 ^{ns}	2.12±0.06 ^{ns}	0.16±0.009 ^{ns}	76.17±0.40 ^{ns}	3.00±0.45 ^{ns}
III	ELDC	200	14.17±0.31 ^{ns}	8.58±0.27 ^{ns}	9.83±0.40 ^{ns}	26.33±0.21 ^{ns}	2.32±0.09 ^{ns}	0.17±0.006 ^{ns}	76.67±0.33 ^{ns}	2.83±0.31 ^{ns}
IV	ELDC	400	14.33±0.33 ^{ns}	8.85±0.35 ^{ns}	9.50±0.22 ^{ns}	25.33±0.67 ^{ns}	2.50±0.05 ^{ns}	0.17±0.006 ^{ns}	74.50±0.34 ^{ns}	2.67±0.33 ^{ns}

Values were expressed as Mean ± SEM of 6 rats in each group.

The mean values observed in Hb, RBC, WBC and Differential cell count of extract treated groups were not significantly different from control group at the end of study (28 days).

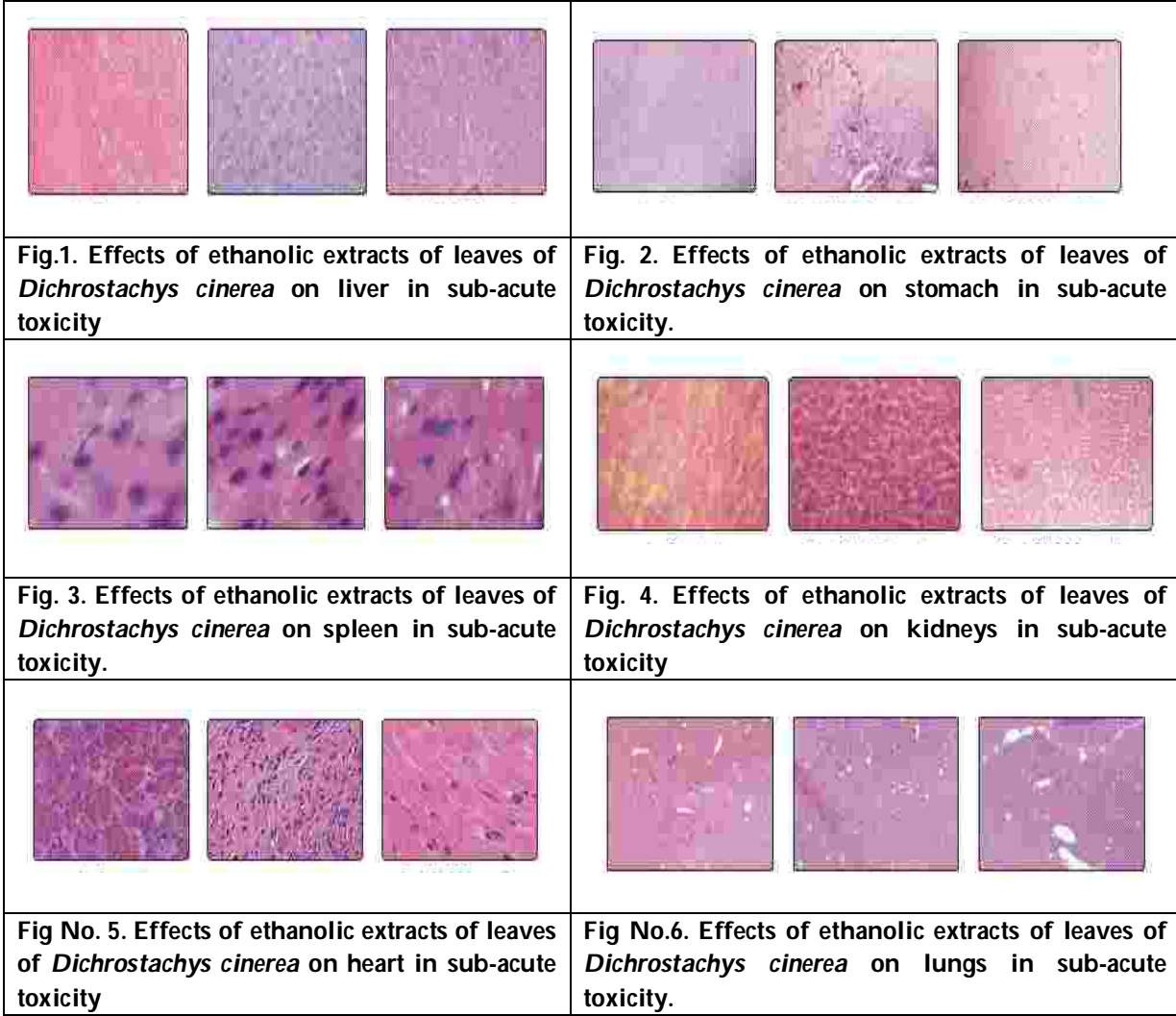




Kothai et al.

Table no.3. Effect of ethanolic extracts of leaves of *Dichrostachys cinerea* on biochemical parameters in sub-acute toxicity studies.

Group	Treatment	Dose (mg/kg)	SGOT (U/L)	SGPT (U/L)	ALP (U/L)	Total Protein (g/dl)	Total cholesterol (mg/dl)	Total bilirubin (mg/dl)
I	Control	-	191.83±1.28	80.33±0.67	230.50±0.56	7.23±0.03	121.33±0.42	0.50±0.004
II	ELDC	100	190.50±0.76 ^{ns}	79.83±0.70 ^{ns}	235.67±0.42 ^{ns}	7.04±0.04 ^{ns}	122.67±0.42 ^{ns}	0.45±0.019 ^{ns}
III	ELDC	200	190.33±0.80 ^{ns}	81.00±0.37 ^{ns}	236.17±0.48 ^{ns}	7.10±0.07 ^{ns}	122.67±0.33 ^{ns}	0.45±0.015 ^{ns}
IV	ELDC	400	190.33±0.67 ^{ns}	81.33±0.33 ^{ns}	233.33±0.80 ^{ns}	7.13±0.03 ^{ns}	121.50±0.43 ^{ns}	0.44±0.011 ^{ns}





Spatiotemporal Variation of Air Pollutants during COVID–19 Lockdown Over Andhra Pradesh, India

M.C.Ajay Kumar¹, P. Vinay Kumar¹ and P. Venkateswara Rao^{2*}

¹Department of Physics, Aurora's Technological and Research Institute, Parvathapur Hyderabad, India.

²Department of Physics, Vasavi College of Engineering, Ibrahimbagh, Hyderabad, India.

Received: 09 Sep 2020

Revised: 11 Oct 2020

Accepted: 12 Nov 2020

*Address for Correspondence

P. Venkateswara Rao

Department of Physics,

Vasavi College of Engineering, Ibrahimbagh,

Hyderabad, India.

Email: dr.pvr@staff.vce.ac.in



This is an Open Access Journal / article distributed under the terms of the **Creative Commons Attribution License** (CC BY-NC-ND 3.0) which permits unrestricted use, distribution, and reproduction in any medium, provided the original work is properly cited. All rights reserved.

ABSTRACT

The unexpected pandemic COVID – 19 disrupted the lives and livelihoods of individuals across the globe. Major negative effects are reported on socio and economic issues; however positive effects have also been reported with respect to air quality. A nationwide lockdown was imposed in India initially for three weeks from 24th March to 14th April 2020, which was later extended upto 31st May 2020 in three phases (15th April –3rd May; 4th – 17th May 2020 and 18th – 31st May 2020). During this lockdown all anthropogenic activities that include transportation, industrial and other human activities which contribute to air pollution ceased. In the present study we examine the effect of lockdown on air quality on four major cities: Rajamahendravaram (RJM), Amaravathi (AMV), Visakhapatnam (VSP) and Tirupati (TPT) in Andhra Pradesh (India). The variations in the concentration of major air pollutants (PM_{2.5}, PM₁₀, NO₂ and O₃) were analysed during pre-lockdown and different phases of lockdown. The detailed study showed maximum dip in the second and third phase due to strict implementations of lockdown. The results revealed that from 1st March to 21st March 2020, the mean concentrations of air pollutants (PM_{2.5}, PM₁₀, NO₂ and O₃), averaged over these four stations, was found to be 26 µg/m³, 57 µg/m³, 20.15 µg/m³ and 31.73 µg/m³ respectively and they subsequently decreased by 53%, 50%, 32.6% and 0.63% during second and third phases of the lockdown. Analysis of Variance (ANOVA) showed a strong spatial variation in NO₂ and O₃ across the stations ($p < 0.05$). These findings are sparsely reported in the study area and it provides an opportunity to estimate the levels of pollution due to human anthropogenic activities, which is not possible to guess under normal conditions. The present study helps the policy makers and scientists to frame the policies so that there will be certain reduction in air pollution even under normal conditions based on these findings.

Keywords: Air pollution, COVID–19, air quality, pandemic, lockdown





Ajay Kumar et al.,

INTRODUCTION

The novel coronavirus disease COVID-19 is a pneumonia caused by severe acute respiratory syndrome coronavirus 2 (SARS-CoV-2). This novel coronavirus was first reported in December, 2019 in Wuhan, the capital of China's Hubei Province. Since then, it has spread rapidly to several countries and has been declared a pandemic by the World Health Organization (WHO) on March 11th, 2020. More than 59, 34,936 cases have been confirmed globally, with 3, 67,166 deaths, and have been reported till 31st May 2020 according to [1]. The rapid spreading of the virus across the globe may be due to International travel [2]. Since 30th January 2020, after the first case was reported in India, the number of cases caused by COVID – 19 has increased gradually till the second week of March due to foreign returns and also due to persons contact with them. Later, after 15th March, the number of daily cases increased sharply as a result the government proposed nationwide lockdown from 24th March 2020 after a 12 hour Janatha Curfew on 21st March 2020. From 24th March 2020, more than 1.38 billion Indian residents were forced to shut their activities to break the chain of transmission of COVID –19 outbreak. In order to combat the pandemic and restrict the further spread of the virus from one source to another, multiple interventions, including lock down, have been implemented. In India, lockdown was implemented in 4 phases; First phase from 24th March – 14th April 2020, Second phase 15th April – 3rd May 2020, Third phase 4th – 17th May 2020 and Fourth phase from 18th – 31st May 2020. Even though lockdown started from March 24th, in reality it took a few days to implement strictly. In the third phase of lockdown the government announced certain relaxations and classified all districts into four different zones namely RED, ORANGE, GREEN and CONTAINMENT. Subsequently, the guidelines for lockdown 4.0 allowed shops and markets except those in malls to open with staggered timings. E- Commerce companies were also permitted to deliver all goods. Many more relaxations were made in the industrial sector and inter – state travel was permitted in phase four. Later, the government on 30th May announced the guidelines for Unlock 1.0 followed by 2.0, 3.0 and 4.0, under which the restrictions imposed under the COVID-19-induced lockdown were relaxed gradually.

The immediate consequence of this lockdown is economic dip, both globally and nationwide, which may take years to return at par with the previous conditions. In the positive sense this lockdown has benefited the environment in terms of air and water quality improvement and decline in noise pollution level [3-5]. The air quality of seven cities of Rajasthan showed a trend of decrease in concentration of all the pollutants (except ozone) during lockdown period as compared to that of before lockdown period [6]. Reference [7] examined the impact of the lockdown on tropospheric NO₂ concentrations using satellite based ozone monitoring instrument sensor data and showed a decline of 12.1% during four weeks of lockdown and an increase of 0.8% in NO₂ concentration was observed for the same period in 2019. The reduced concentration was attributed to restricted anthropogenic activities during the lockdown. Reference [8] also found reduction in PM_{2.5}, PM₁₀ and NO₂ for six mega cities during the lockdown period. This lockdown provides a unique opportunity to the scientific community to study the relation between baseline air quality and natural process. Several researchers throughout the world reported the difference in air quality before and during lockdown. All reports reveal a clear decline in air pollutant concentrations in India and other countries [9-15]. Many of these reports focused on metropolitan cities. In our present study we consider four developing cities (Rajamahendravaram, Amaravathi, Visakhapatnam and Tirupati) in the budding state of Andhra Pradesh and studied the effect of lockdown on air quality.

Area of study

Rajamahendravaram (RJM), with a population of about 5.4 Lakhs, lies on the left bank of the river Godavari. It is the Divisional Headquarters of East Godavari District. This city witnessed a lot of development after the reorganization of Andhra Pradesh State in 2014. It is one of the major business centres and it is the industrial hub with two thermal power stations, paper mills and petrochemical industries. It is the headquarters for the ONGC and GAIL in KG Basin. Amaravathi (AMV) is also a town on the bank of Krishna River in Guntur District with a population around 1 lakh. It is the capital of Andhra Pradesh with a huge construction activity due to developments in academic,



**Ajay Kumar et al.,**

educational, residential, business sectors in the last few years. Visakhapatnam (VSP), often known as a bowl area for assessment of environmental related issues, lies between Eastern Ghats and the cost of the Bay of Bengal [16]. It is the one of the four smart cities of Andhra Pradesh selected under smart cities mission, presently witnessing a boom of industrialization and urbanization and a consequent explosion of population. It is the most populous city, crossing 2 million mark, in the state and was ranked 122 in the list of fastest – growing cities in the world. The IT industry in VSP witnessed many national and multi international firms in recent years. The Jawaharlal Nehru Pharma City (JNPC) developed at Parawada in Visakhapatnam has major pharma companies. The city is host of many other industries like Steel Plant, Hindustan Petroleum Corporation (HPCL), Hindustan Shipyard, Simhadri Thermal Power Station etc. Tirupati (TPT) is the seventh most urban agglomerated city in Chittoor District, referred as “Temple Town” with a population around 6.8 Lakhs. TirumalaVenkateswara Temple is the most notable temple for being the world's richest Vaishnavite temple of Lord Venkateswara. Besides this, there are many other temples in the city. It lies at the foot of Eastern Ghats, attracts a large number of pilgrims every year.

METHODOLOGY

The effect of lockdown on air quality of four selected cities in Andhra Pradesh (RJM, AMV, VSP and TPT) has been reviewed for two time periods: before lockdown from 1st March to 21st March 2020 and during lockdown from 24th March to 31st May 2020 (covering all phases of lockdown). Under the National Ambient Monitoring Program, the Central Pollution Control Board (CPCB) operates continuous monitoring stations across India and assesses the air quality by measuring the concentrations of major air pollutants. An hourly data of air pollutants such as PM_{2.5}, PM₁₀, Ozone (O₃) and Nitrogen dioxide (NO₂) for four stations in Andhra Pradesh were downloaded from Continuous Ambient Air Quality Monitoring Stations (CAAQMS) website (<https://cpcb.nic.in/automatic-monitoring-data/>) from 1st March to 31st May 2020 and it was used in our present study. In addition to the above data, we also considered two more years of data (2018–2019) for the annual study (for the same period). In order to assess the effect of lockdown quantitatively (both spatially and temporally) we used the Rate of Change (ROC) and Analysis of Variance (ANOVA) one way test in our study. The details of the stations and their significance are mentioned in Table 1.

RESULTS AND DISCUSSION

Overview of Air Pollutant Concentrations on Four Stations in Andhra Pradesh

Daily mean variation in the levels of air pollutants PM_{2.5}, PM₁₀, NO₂ and O₃ (8 h) during the study period covering pre-lockdown and different phases of lockdown across the stations are shown in Figure 1(a–d). In order to study the trend of these concentrations, over all these stations, a quadratic fit has been plotted for the study period 2020 (red) and also for previous years' average (2018–2019, black). A significant decline in the concentration of all pollutants except O₃ was observed over Andhra Pradesh during the first three phases of the lockdown. While, the concentration values were found to increase in phase four. The trends of PM_{2.5}, PM₁₀ and NO₂ clearly indicate that the values in the current year are much less than the previous years during the lockdown period. However, the trend of O₃ concentration was not showing much variation with the previous years. The average concentration of PM_{2.5}, PM₁₀, NO₂ and O₃ over Andhra Pradesh were 26 µg/m³, 57 µg/m³, 20.15 µg/m³ and 31.73 µg/m³ during pre-lockdown. Similarly the corresponding values during the lockdown period (first three phases) are 15.29 µg/m³, 40.68 µg/m³, 11.22 µg/m³ and 33.48 µg/m³. The phase wise city lockdowns have shown a substantial improvement in the air quality due to restrictions on human, vehicular and industrial activities. These observations made us assess the temporal and spatial variations of air pollutants to understand the benefits of lockdowns over Andhra Pradesh.

Temporal Variation of Air Pollutants across Different Stations

Figure 2 shows the temporal characteristics of PM_{2.5}, PM₁₀ (a–d) and NO₂, O₃ (e–h) for the four stations during the study period. In RJM station the daily mean concentrations of PM_{2.5}, PM₁₀, NO₂ and O₃ ranges from 12.16 – 43.64

28603



**Ajay Kumar et al.,**

$\mu\text{g}/\text{m}^3$; 32.81 – 90.42 $\mu\text{g}/\text{m}^3$; 13.4 – 22.54 $\mu\text{g}/\text{m}^3$ and 20.4 – 99.97 $\mu\text{g}/\text{m}^3$ respectively during the pre-lockdown phase. Similarly during the first three lockdown phases the corresponding ranges are 3.48 – 30.33 $\mu\text{g}/\text{m}^3$; 19.7 – 60.25 $\mu\text{g}/\text{m}^3$; 4.22 – 11.46 $\mu\text{g}/\text{m}^3$ and 17.2 – 74.85 $\mu\text{g}/\text{m}^3$ respectively. In AMV station the daily mean concentrations of $\text{PM}_{2.5}$, PM_{10} , NO_2 and O_3 ranges from 10.37 – 39.94 $\mu\text{g}/\text{m}^3$; 18.84 – 64.32 $\mu\text{g}/\text{m}^3$; 5.08 – 12.48 $\mu\text{g}/\text{m}^3$ and 19.19 – 52.04 $\mu\text{g}/\text{m}^3$ respectively during the pre-lockdown phase. Similarly during the first three lockdown phases the corresponding ranges are 7.42 – 35.38 $\mu\text{g}/\text{m}^3$; 11.00 – 66.93 $\mu\text{g}/\text{m}^3$; 3.49 – 14.25 $\mu\text{g}/\text{m}^3$ and 12.79 – 44.61 $\mu\text{g}/\text{m}^3$ respectively. In VSP station the daily mean concentrations of $\text{PM}_{2.5}$, PM_{10} , NO_2 and O_3 ranges from 14.23 – 66.51 $\mu\text{g}/\text{m}^3$; 38.06 – 153.21 $\mu\text{g}/\text{m}^3$; 15.14 – 52.92 $\mu\text{g}/\text{m}^3$ and 11.08 – 39.79 $\mu\text{g}/\text{m}^3$ respectively during the pre-lockdown phase. Similarly during the first three lockdown phases the corresponding ranges are 2 – 40 $\mu\text{g}/\text{m}^3$; 18 – 97 $\mu\text{g}/\text{m}^3$; 10.43 – 36.38 $\mu\text{g}/\text{m}^3$ and 6.57 – 58.27 $\mu\text{g}/\text{m}^3$ respectively. In TPT station the daily mean concentrations of $\text{PM}_{2.5}$, PM_{10} , NO_2 and O_3 ranges from 18.63 – 50.04 $\mu\text{g}/\text{m}^3$; 33.96 – 87 $\mu\text{g}/\text{m}^3$; 4.77 – 48.69 $\mu\text{g}/\text{m}^3$ and 19.31 – 59.52 $\mu\text{g}/\text{m}^3$ respectively during the pre-lockdown phase. Similarly during the first three lockdown phases the corresponding ranges are 3.42 – 30.65 $\mu\text{g}/\text{m}^3$; 17.5 – 65 $\mu\text{g}/\text{m}^3$; 3.96 – 12 $\mu\text{g}/\text{m}^3$ and 29 – 74 $\mu\text{g}/\text{m}^3$ respectively. During the fourth phase of lockdown, the concentrations values of air pollutants are in the same range as that of the pre-lockdown phase across all the stations.

The daily mean concentrations of $\text{PM}_{2.5}$, PM_{10} , NO_2 and O_3 are well below the National Ambient Air Quality (NAAQ) standards during the study period across all stations except in VSP, where the $\text{PM}_{2.5}$ and PM_{10} values exceed NAAQ standards. The effect of lockdown over VSP showed a significant decline in the concentration of $\text{PM}_{2.5}$ and PM_{10} falling below the NAAQ standard. However, the mean concentrations are well above the WHO standards. In order to study the variation of pollutant levels ($\text{PM}_{2.5}$, PM_{10} , NO_2 and O_3) across all stations for pre and lockdown phases, the hourly data was averaged accordingly and the results are depicted in Figure 3. On an average, across all the stations, concentration levels of $\text{PM}_{2.5}$, PM_{10} and NO_2 shows a gradual decrease during the first three lockdown phases when compared to pre-lockdown except O_3 . The $\text{PM}_{2.5}$ (PM_{10}) concentration shows a significant dip in second (2.0) and third (3.0) lockdown phases with average concentration values 12 $\mu\text{g}/\text{m}^3$ (38.5 $\mu\text{g}/\text{m}^3$) when compared to corresponding pre-lockdown concentrations 26 $\mu\text{g}/\text{m}^3$ (57 $\mu\text{g}/\text{m}^3$) across all the stations. The NO_2 concentration levels varied across the stations during (pre) lockdown phases from 5.5 to 19.9 $\mu\text{g}/\text{m}^3$ (8.1 to 31.9 $\mu\text{g}/\text{m}^3$) with maximum at VSP and minimum at AMV. The O_3 concentrations during pre-lockdown are found to be 44 $\mu\text{g}/\text{m}^3$, 30.8 $\mu\text{g}/\text{m}^3$, 16.4 $\mu\text{g}/\text{m}^3$ and 35.7 $\mu\text{g}/\text{m}^3$ in RJM, AMV, VSP and TPT respectively. A reasonable dip was observed during second and third lockdown phases in RJM (4.5 $\mu\text{g}/\text{m}^3$) and AMV (5.2 $\mu\text{g}/\text{m}^3$). However, a marginal and considerable increase in O_3 concentrations was observed in VSP (0.6 $\mu\text{g}/\text{m}^3$) and AMV (8.3 $\mu\text{g}/\text{m}^3$). The concentration differences during the lockdown period (averaged over second and third phases) is compared with the average of previous 2018–2019 of corresponding periods in Figure 4. The mean concentration levels of air pollutants in 2020 are found to be very less when compared with averages concentrations of previous years in all stations except for O_3 at VSP and TPT where the difference is less.

Rate of Change (ROC) in Concentrations

The rates of change in concentrations of air pollutants were calculated for different phases of lockdown with respect to pre-lockdown and are shown in Table 2. A significant difference was found in each city. The overall concentrations of air pollutants except O_3 showed a clear decline in all phases when compared with pre-lockdown across all stations with maximum dip in second and third phases of lockdown. However, in case of O_3 a marginal decline was seen in RJM and AMV and in other two stations VSP and TPT the O_3 values were found to increase. From Table 2 the second and third phases have shown maximum dip, hence we considered second and third phases as complete lockdown periods for calculating rate of change of concentrations with respect to pre-lockdown. Figure 5 shows the percentage changes of concentrations, averaged over second and third phases of lockdown with respect to pre-lockdown. The analysis shows significant declination in $\text{PM}_{2.5}$ concentrations at RJM (67.05%) followed by VSP (61%), TPT (55%) and AMV (26.5%). The major sources of $\text{PM}_{2.5}$ are road dust, vehicle emissions and industrial processes [17]. This reduction in $\text{PM}_{2.5}$ clearly indicates the effect of lockdown related to the cessation of transportation and industrial activities. The concentration of PM_{10} showed a noticeable change with maximum reduction of 43.14% in TPT. The percentage change of NO_2 was observed to be different across stations with a



**Ajay Kumar et al.,**

maximum decline of ~ 69% at TPT and minimum of 31.48% at AMV. TPT, popularly known as the spiritual capital of Andhra Pradesh has tourism as the major industry and is surrounded with many hotels. The city has heavy traffic, in conjunction with poor quality roads and maximum daily floating pilgrims. The means of transport is mainly through public diesel vehicles. The vehicle travels on paved and unpaved roads, construction activities, industrial processes and vehicle emission are the main sources of PM₁₀ and NO₂ [18]. Since the above activities were shut down completely during lockdown, results in maximum reduction of PM₁₀ and NO₂ concentration at TPT were recorded, when compared to other stations. Reference [19] reported a similar decline in Sale' city during the lockdown period for PM₁₀ and NO₂ with percentage 75% and 96% respectively. The concentration of O₃ showed a noticeable change in TPT and VSP with a percentage increase of 3.66% and 23.25%, whereas a marginal decline was found in RJM (10.23%) and AMV (16.72%) respectively.

The observed increase in O₃ concentration during lockdown period could be due to solar radiation and decrease in NO₂ owing to the favorability of photochemical reaction [20]. Short term meteorological parameters may also influence the variation in O₃. These results revealed a substantial improvement in the air quality over the study area during lockdown. Reference [21] has observed a substantial improvement of air quality in China during the lockdown period with a reduction in PM_{2.5} (37%), PM₁₀ (33.7%), NO₂ (55.6%) and an enhancement in O₃. Further, we calculated ROC in air pollutant concentrations averaged over second and third lockdown periods of 2020 following the average of 2018 – 2019 for corresponding periods across all the stations. The results shown in Figure 6 indicate a clear declination in all parameters across the stations. The PM_{2.5} concentration in RJM and VSP decreases shapely by 67% and 60% respectively. The overall concentration of PM₁₀ in all four stations is reduced by 50%. A sharp decrease in NO₂ concentration was observed at TPT and minimum reduction at VSP. The changes in O₃ concentration are marginal fall at VSP and TPT, whereas RJM and AMV showed a reasonable reduction in O₃ concentration. These variations in the concentrations can be attributed to the restrictions imposed during lockdown in 2020 and local meteorological conditions. Reference [22] reported a significant decline (25.5%) in NO₂ during COVID – 19 Pandemic compared to historical years.

Spatial Variation of Air Pollutants

Figure 7 and 8 gives the levels of air pollutant concentrations for different stations during the study period. The central box comprises values of 25 and 75 percentiles, and whiskers show the range of values falling within 1.5 times the interquartile range beyond the box. The solid lines within the box represent the median values. The outliers defined as data points beyond the inner fence, are represented with '+' symbols. The median values of air pollutant concentrations in second and third phases of the lockdown are found to be minimum at all stations. A remarkable decrease of concentration was observed across all the stations during the second and third phases of lockdown. The PM_{2.5} and PM₁₀ showed a very weak spatial dependence during the study period. However, in case of NO₂ and O₃ a strong spatial dependence is observed. Another interesting fact that can be observed is that the O₃ values during lockdown phase are found to be higher than pre-lockdown phase. In the case of TPT, a substantial difference in NO₂, was observed between the two study periods when compared to other stations. Further, ANOVA one way test was used on daily concentration data (averaged over second and third lockdown phase) to provide a comprehensive picture of spatial variations in air pollutant concentrations. The analysis shows a significant spatial difference ($p < 0.05$) in PM_{2.5} concentration between RJM, TPT and RJM, AMV. The mean concentrations of PM₁₀ and NO₂ at VSP have a significantly different value when compared to other stations ($p < 0.05$). However, a significant spatial difference ($p < 0.05$) was observed in O₃ concentrations across the stations except between RJM and TPT ($p > 0.05$). To assess the differences in air pollutant levels associated with spatial and temporal factors we used ANOVA one way test on lockdown year 2020 (averaged over second and third lockdown phase) with the average of previous 2018–2019 of corresponding periods. The median values of air pollutant concentrations during the lockdown period (averaged over second and third phases) are compared with the average of previous 2018–2019 of corresponding periods in Figure 9. The central box comprises values of 25 and 75 percentiles, and whiskers show the range of values falling within 1.5 times the interquartile range beyond the box. The solid lines within the box represent the median values. The outliers defined as data points beyond the inner fence, are represented with '+' symbols. The Figure

28605



**Ajay Kumar et al.,**

shows a substantial spatial difference in NO₂ and O₃. However, such spatial difference was not seen in case of PM_{2.5} and PM₁₀. Another noticeable observation is that the median of NO₂ concentration reduced sharply at TPT in 2020 when compared to previous years' average. The test results reveal that the p values < 0.05 which are considered statistically significant were observed across all the stations indicating a significant difference in spatial and temporal variations.

CONCLUSIONS

It is inevitable that this short term reduction in air pollution due to COVID – 19 pandemic will be reversed when the crisis ends and conditions return to normal. This study covered a short time frame to assess the effect of COVID– 19 on air quality over four stations in Andhra Pradesh. During lockdown, all the activities, that includes industrial, transportation, tourism, construction and many other human actions are put on hold or minimized resulting in a reduction in air pollution. Our results showed an overall significant declination in air pollutant concentrations across all stations during different phases of lockdown. The average reduction in concentrations of PM_{2.5}, PM₁₀, NO₂ and O₃ were 53%, 50%, 32.6% and 0.63% during the second and third phases of the lockdown when compared to pre–lockdown. The daily mean concentrations of air pollutants (averaged over four stations) except O₃ of current year are subsidized when compared to the previous year (averaged over 2018–2019) concentration values, but there is no much variation in case of O₃. In depth study showed a clear reduction in the concentrations of air pollutants in the second and third phase of lockdown when compared to other phases indicates that the relaxations implemented on human and industrial activities during different phases of lockdown affected the air pollution. The mean concentrations (averaged over second and third phase of lockdown) of 2020 across all stations are comparatively less when compared to the corresponding averages of previous year (2018–2019). The analysis shows a significant percentage change in air pollutant concentration except O₃ during the second and third phase of lockdown when compared to pre lockdown. The O₃ concentration showed a reasonable enhancement at VSP and TPT and marginal decline at RJM and AMV. A remarkable reduction of concentration was observed across all stations during the second and third phase of lockdowns. In general, PM_{2.5} and PM₁₀ showed weak spatial difference and NO₂ and O₃ showed strong spatial difference across stations. Further analysis of temporal variations across the stations of the current year with the average of previous years showed a significant difference in the concentrations. The COVID–19 pandemic teaches a lesson to all and gives a chance to rebuild our environment. The results obtained in our study can be attributed in general to the shutdown of anthropogenic activities due to forced lockdown. The weather and meteorological conditions may also be a part of the coronavirus outbreak besides the social factors. So, still there is a scope to study and assess the effect of lockdown in detail by considering these meteorological factors. To protect the environment in future, the present study helps the policy makers and scientists to frame the policies so that there will be certain reduction in air pollution even under normal conditions based on scientific evidence.

ACKNOWLEDGEMENTS

The authors acknowledge Andhra Pradesh State Pollution Control Board (APSPCB) and Central Pollution Control Board (CPCB) for making the data available to users. The authors would like to thank the management of Vasavi College of Engineering, Hyderabad, India and Aurora's Technological and Research Institute, Hyderabad, India for their active support and encouragement.

REFERENCES

1. WHO. 2020, Coronavirus disease (COVID–19) Situation Report – 132, Available at: https://www.who.int/docs/default-source/coronaviruse/situation-reports/20200531-covid-19-sitrep-132.pdf?sfvrsn=d9c2eaeef_2.
2. II Bogoch, A Watts, A Thomas–Bachli, C Huber, MUG Kraemer and K Khan. Pneumonia of unknown aetiology in Wuhan, China: Potential for international spread via commercial air travel. J. Travel Med., 2020; 27: taaa008. <https://doi.org/10.1093/jtm/taaa008>.



**Ajay Kumar et al.,**

3. I Mandal and S Pal. COVID–19 pandemic persuaded lockdown effects on environment over stone quarrying and crushing areas. *Science of the Total Environment*, 2020; 139281.
4. MH Masum and SK Pal. Statistical evaluation of selected air quality parameters influenced by COVID–19 lockdown. *Global J. Environ. Sci. Manage.*, 2020; 6(SI):85–94.
5. H Bherwani, M Nair, K Musugu, S Gautam, A Gupta, A Kapley and R Kumar. Valuation of air pollution externalities: comparative assessment of economic damage and emission reduction under COVID–19 lockdown. *Air Qual. Atmos. Health*, 2020; 13, 683 –694.
6. M Sharma, S Jain and BY Lamba. Epigrammatic study on the effect of lockdown amid Covid–19 pandemic on air quality of most polluted cities of Rajasthan (India). *Air Qual. Atmos. Health*, 2020; 13, 1157–1165. <https://doi.org/10.1007/s11869-020-00879-7>.
7. A Biswal, T Singh, V Singh, K Ravindra and S Mor. COVID–19 lockdown and its impact on tropospheric NO₂ concentrations over India using satellite–based data, *HELIYON*, 2020; <https://doi.org/10.1016/j.heliyon.2020.e04764>.
8. Sarvan Kumar. Effect of meteorological parameters on spread of COVID–19 in India and air quality during lockdown. *Science of the Total Environment*, 2020; 745, 141021, <https://doi.org/10.1016/j.scitotenv.2020.14102>.
9. VR Polisetty, MC Ajay Kumar and P Vinay Kumar. Effect of lockdown on air pollutants during COVID–19, over Hyderabad. *Indian Journal of Science and Technology*, 2020; 13 (32), 3339–3348. <https://doi.org/10.17485/IJST/v13i32.1411>.
10. G He, Y Pan and T Tanaka. The short–term impacts of COVID–19 lockdown on urban air pollution in China. *Nature Sustainability*. 2020; <https://doi.org/10.1038/s41893-020-0581-y>.
11. T Le, Y Wang, L Liu, J Yang, LY Yung, G Li, et al. Unexpected air pollution with marked emission reductions during the COVID–19 outbreak in China. *Science*, 2020; 369(6504):702–706. <https://doi.org/10.1126/science.abb7431>.
12. P Vinay Kumar, MC Ajay Kumar and P VenkateswaraRao. Changes in PM₁₀, NO_x and SO₂ concentrations during COVID – 19 Lockdown over Hyderabad. *Science and Engineering Journal*, 2020; 24 (8), 366–374.
13. P Sicard, A De Marco, E Agathokleous, Z Feng, X Xu, E Paoletti and V Calatayud. Amplified ozone pollution in cities during the COVID–19 lockdown. *Science of the Total Environment*, 2020; 139542.
14. S Sharma, M Zhang, Anshika, J Gao, H Zhang and SH Kota. Effect of restricted emissions during COVID–19 on air quality in India. *Science of the Total Environment*, 2020; 728(1). <https://doi.org/10.1016/j.scitotenv.2020.138878>.
15. SK Dhaka, VK Chetna, V Panwar, AP Dimri, N Singh, et al. PM_{2.5} diminution and haze events over Delhi during the COVID–19 lockdown period: an interplay between the baseline pollution and meteorology. *Scientific Reports*, 2020; 10(1). <https://doi.org/10.1038/s41598-020-70179-8>.
16. J Srinivas and AV Purushotham. Determination of air quality index status in industrial areas of Visakhapatnam, India. *Res. J. Eng. Sci.* 2013; 2 (6), 13e24.
17. M Sharma and O Dikshit. 2016, Comprehensive study on air pollution and greenhouse gases (GHGs) in Delhi. A report submitted to the Government of NCT Delhi and DPCC Delhi, 1–334.
18. R Yadav, LK Sahu, SNA Jaaffrey and G Beig. Temporal variation of Particulate Matter (PM) and potential sources at an urban site of Udaipur in Western India. *Aerosol Air Qual. Res.* 2014; 14(6):1613–1629.
19. A Otmani, A Benchrif, M Tahri, M Bounakhla, EM Chakir, et al. Impact of Covid–19 lockdown on PM₁₀, SO₂ and NO₂ concentrations in Salé City (Morocco). *Science of the Total Environment*, 2020; <https://doi.org/10.1016/j.scitotenv.2020.139541>.
20. AM Shrestha, UB Shrestha, R Sharma, S Bhattarai, HNT Tran and M Rupakheti. Lockdown caused by COVID–19 pandemic reduces air pollution in cities worldwide. *Science of the Total Environment*, 2020; 730:139086. <https://doi.org/10.1016/j.scitotenv.2020.139086>.
21. H Zheng, S Kong, N Chen, et al. Significant changes in the chemical compositions and sources of PM_{2.5} in Wuhan since the city lockdown as COVID–19, *Science of the Total Environment*, 2020; 739, 140000. <https://doi.org/10.1016/j.scitotenv.2020.140000>.
22. JD Berman and K Ebusu. Changes in U.S. air pollution during the COVID–19 pandemic. *Science of the Total Environment*, 2020; DOI:10.1016/j.scitotenv.2020.139864.





Ajay Kumar et al.,

Table 1: Details of Station

Station	Latitude and Longitude	Height above Sea level	Significance
Rajamahendravaram (RJM)	17 N, 81.8 E	14m	Residential, Industrial, Urban City on the river bank of Godavari
Amaravathi (AMV)	16.5 N, 80.5 E	25m	Residential, Town, on the river bank of Krishna
Visakhapatnam (VSP)	17.6 N, 83.2 E	45m	Industrial, Residential, Smart, city, surrounded by Eastern Ghats and Bay of Bengal
Tirupati (TPT)	13.6 N, 79.4 E	156m	Industrial, Residential urban city surrounded by Eastern Ghats

Table 2. The Rates of Change (ROC) in concentrations of air pollutant for different phases of lockdown with respect to pre-lockdown.

Station	Parameter (µg/m ³)	Pre-lockdown	Lockdown n 1.0	Lockdown n 2.0	Lockdown n 3.0	Lockdown n 4.0	ROC of Lockdown n 1.0 (%)	ROC of Lockdown n 2.0 (%)	ROC of Lockdown n 3.0 (%)	ROC of Lockdown n 4.0 (%)
RJY	PM _{2.5}	22.7	20.9	7.66	7.3	26.4	-7.93	-66.26	-67.84	16.30
AMV		21.5	22.6	15.7	16.1	25.2	5.12	-26.98	-25.12	17.21
VSP		31.1	22.6	13.7	10.3	25.2	-27.33	-55.95	-66.88	-18.97
TPT		28.6	21.1	16	9.5	24.4	-26.22	-44.06	-66.78	-14.69
RJY	PM ₁₀	53.3	43.5	25.1	36.9	74.1	-18.39	-52.91	-30.77	39.02
AMV		37.6	45.5	37.1	38.4	73.2	21.01	-1.33	2.13	94.68
VSP		81.3	61.4	53.4	44.8	93.6	-24.48	-34.32	-44.90	15.13
TPT		56.1	38.2	31.2	32.6	64.5	-31.91	-44.39	-41.89	14.97
RJY	NO ₂	16.1	7.35	6.71	7.97	10.6	-54.35	-58.32	-50.50	-34.16
AMV		8.1	4.63	4.92	6.18	8.01	-42.84	-39.26	-23.70	-1.11
VSP		31.9	29	25	14.8	30	-9.09	-21.63	-53.61	-5.96
TPT		24.5	12.89	7.64	7.56	9.47	-47.39	-68.82	-69.14	-61.35
RJY	O ₃	44	45.1	39.9	39.1	63.4	2.50	-9.32	-11.14	44.09
AMV		30.8	31.2	29.1	22.2	37.4	1.30	-5.52	-27.92	21.43
VSP		16.4	22.3	18	16	26.1	35.98	9.76	-2.44	59.15
TPT		35.7	50.8	47.9	40.1	63	42.30	34.17	12.32	76.47





Ajay Kumar et al.,

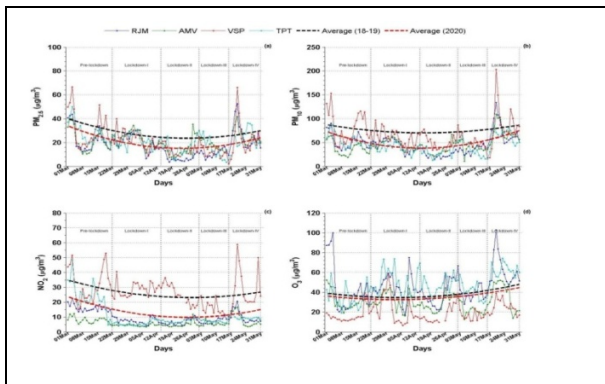


Fig 1. Daily mean variation of PM_{2.5}, PM₁₀, NO₂ and O₃ (8 h) across four stations from 1st March to 31st May 2020 with a quadratic fit for the study period (red) and also for previous years' average (2018–2019, black).

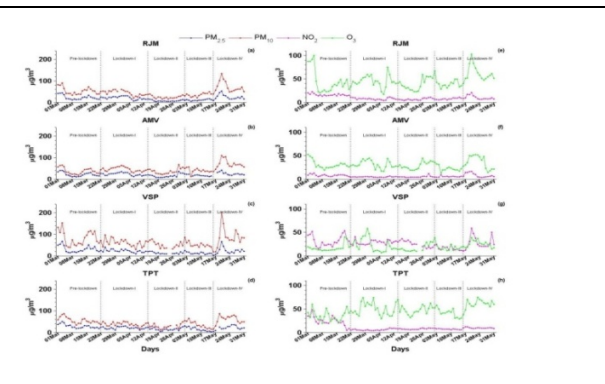


Fig 2. Station-wise variations of PM_{2.5}, PM₁₀, NO₂ and O₃ (8 h) from 1st March to 31st May 2020

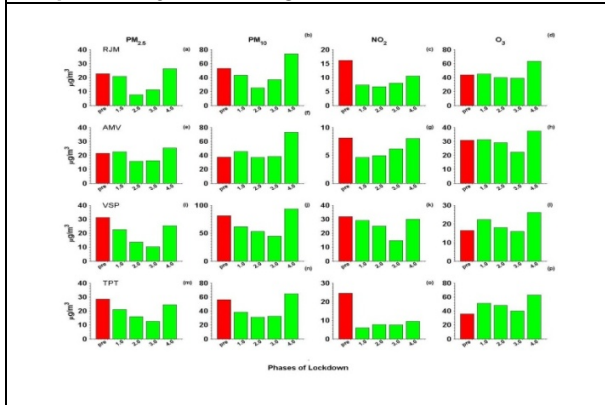


Fig 3. Air pollutant concentration levels: PM_{2.5} (a-d); PM₁₀ (e-h); NO₂ (j-l) and O₃ (o-p) in Four Stations averaged over pre-lockdown and different phases of lockdown.

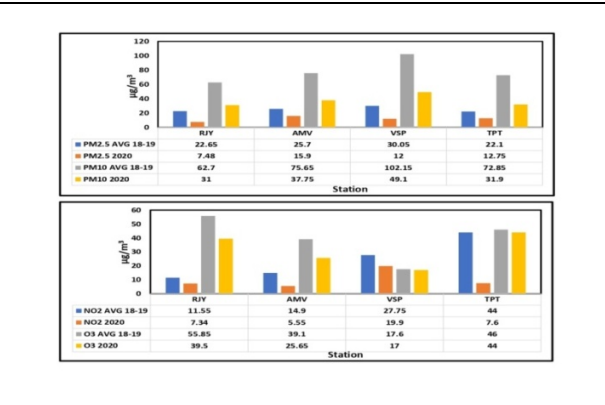


Fig 4. Comparison of pollutant concentrations between lockdown phases (averaged over second and third phases) and average of previous years (2018–2019) of corresponding periods for different stations.

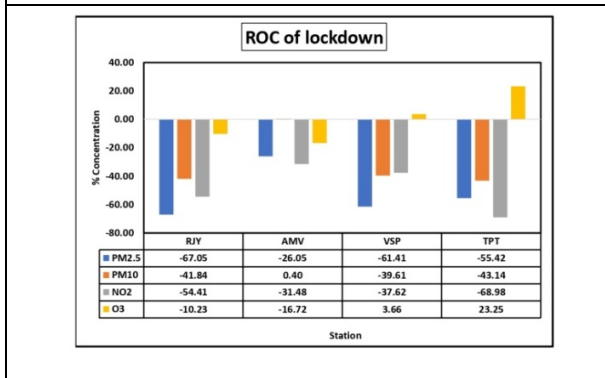


Fig 5. The percentage changes of concentrations, averaged over second and third phases of lockdown with respect to pre-lockdown.

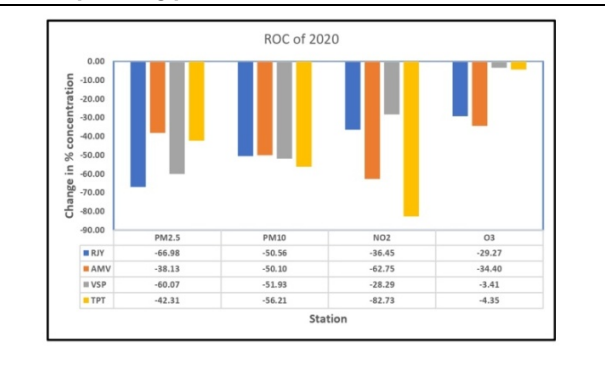


Fig 6. ROC in air pollutant concentrations averaged over second and third lockdown periods of 2020 following the average of 2018 - 2019 for corresponding periods across all the stations.





Ajay Kumar et al.,

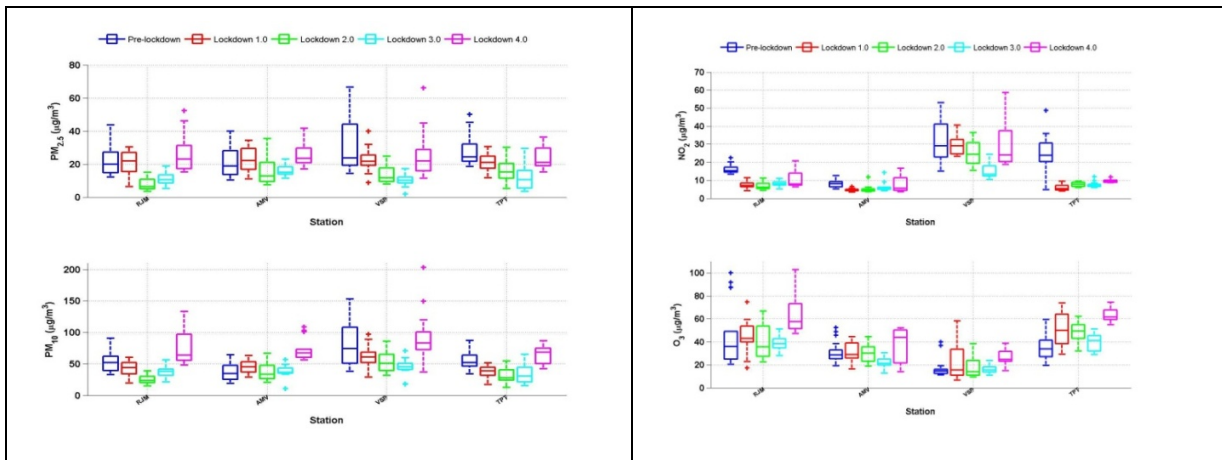


Fig 7.The levels of PM concentration for different stations during study period with median values (solid line within box), 25 and 75 percentiles and whiskers. The outliers are represented with '+' symbols.

Fig 8.Same as Figure 7 but for NO₂ and O₃.

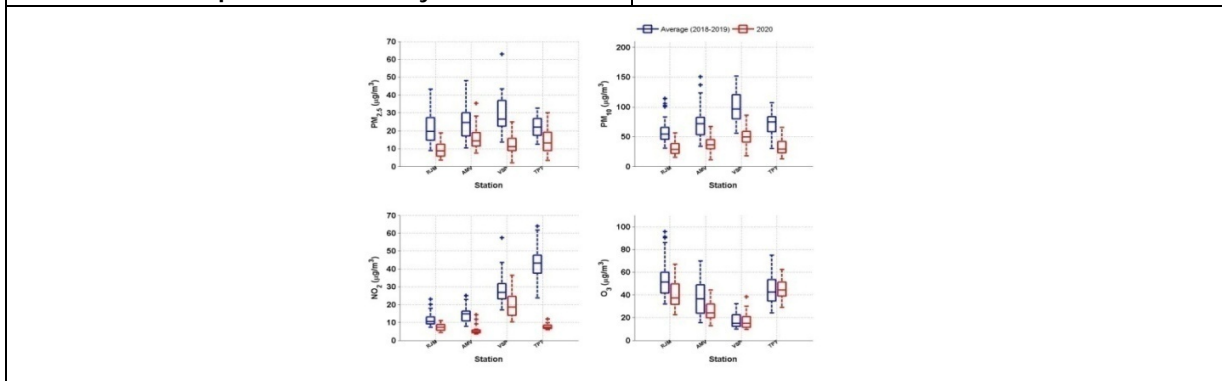


Fig 9. The levels of air pollutant concentrations during the lockdown period (averaged over second and third phases) are compared with the average of previous 2018–2019 of corresponding periods with median values (solid line within box), 25 and 75 percentiles and whiskers. The outliers are represented with '+' symbols.

